SYNTHESIS, CHARACTERIZATION AND BIOLOGICAL APPLICATIONS OF SOME ACETYLPYRIDINE, ACETOPHENONE DERIVATIVES AND THEIR METAL COMPLEXES

NURA SULEIMAN GWARAM

FACULTY OF SCIENCE
DEPARTMENT OF CHEMISTRY
UNIVERSITY OF MALAYA

2014

SYNTHESIS, CHARACTERIZATION AND BIOLOGICAL APPLICATIONS OF SOME ACETYLPYRIDINE, ACETOPHENONE DERIVATIVES AND THEIR METAL COMPLEXES

NURA SULEIMAN GWARAM

A THESIS SUBMITTED IN FULFILLMENT OF THE REQUIREMENT FOR THE DEGREE OF DOCTOR OF PHILOSOPHY

DEPARTMENT OF CHEMISTRY
FACULTY OF SCIENCE
UNIVERSITY OF MALAYA
KUALA LUMPUR

2014

UNIVERSITI MALAYA

ORIGINAL LITERARY WORK DECLARATION

Name of Candidate: Nura Suleiman Gwaram

Registartion/Matric No: SHC100019

Name of Degree: Doctor of Philosophy

Title of the project paper / Research Report / Dissertation /Thesis ("this Work): Synthesis, characterization and biological applications of some acetylpyridine, acetophenone derivatives

Field of Study: Inorganic Chemistry (Aspect: Synthesis & Biological applications)

I do solemnly and sincerely declare that:

1. I am the sole author/writer of this work;
2. This work is original;
3. Any use of any work in which copyright exists was done by way of fair dealing and for permitted purposes and any excerpt or extract from, or reference to or reproduction or any copyright work has been disclosed expressly and sufficiently and the title of the work and its authorship have been acknowledged in this work;
4. I do not have any actual knowledge nor do I ought reasonably to know that making of this work constitutes an infringement of any copyright work;
5. I hereby assign all and every rights in the copyright to this work to the University of Malaya ("UM"), who henceforth shall be owner of the copyright in this work and that any reproduction or use in any form or by any means whatsoever is prohibited without the written consent of UM having been first and obtained;
6. I am fully aware that if in the course of making this work I have infringed any copyright whether intentionally or otherwise, I may be subject to legal action or any other action as may be determined by UM.

Candidates Signature: Date

Subscribed and solemnly declared before,

Witness's Signature: Date

Name: Prof. Hapipah Mohd Ali

Designation: Supervisor

Dedication

This thesis is dedicated to my late Father, who passed away on 6th August, 2008. He is indeed a Father; his memory is still fresh in my mind may his gentle soul rest in perfect peace amen.

Acknowledgement

All praise and adoration is due to Allah the most beneficent the most merciful. The Creator and Sustainer of the universe, who is similar to nothing and nothing is comparable to Him.

Apart from the efforts of me, the success of this thesis depends largely on the encouragement and guidelines of many others. I take this opportunity to express my gratitude to the people who have been instrumental in the successful completion of this thesis.

I would like to express my deepest appreciation to all those who directly or indirectly provided me in one way or another, the possibility to complete this thesis report. A special gratitude I give to my supervisors Prof. Dr. Hapipah Mohd Ali and Prof. Dr. Mahmood Ameen Abdulla who's their contributions, suggestions and encouragement, helped me to coordinate my project.

My thanks and appreciations also go to my Lab mates, colleagues and friends both at Department of Chemistry and Faculty of Medicine, University of Malaya, as well as all other Staffs and technicians for their support both known and unknown to me and people who have willingly helped me out with their abilities.

Furthermore I would also like to thank Umaru Musa Y'ar'adua University (UMYU) for the opportunity given to me to further my studies. I am grateful for the time and support both morally and financially which was vital for the success of my research project.

Lastly, an appreciation to my family and my beloved wife, for their love, kindness and patience shown during the time it has taken me to finalize this task. Thank you

Abstract

A series of compounds derived from 2-acetylpyridne or acetophenones with morpholine, piperazine and piperidine moeity were synthesized and structurally characterized. The compounds were analysed for *in silico, in vitro* and *in vivo* biological applications (anti-cancer, anti-bacteria, anti-Alzheimer and anti-ulcer). They were first screened for *in vitro* anti-bacterial activity against *Methicillin-resistant Staphylococcus aureus* (MRSA), *Acinetobacter baumanni* (AC), *Klebsiella pneumonie* (KB) and *Pseudomonas aeruginosa* (PA) using the disc diffusion and micro broth dilution assays. Based on the overall results, they showed the highest activities against MRSA while a weak antibacterial activity was observed against *A. baumanii* and *P. Aeruginosa*. Another second series of 2-acetypyridine and acetophenone derivatives of gallic hydrazide-derivatives were synthesized and examined for their antioxidant activities and *in vitro* and *in silico* acetylcholinesterase inhibition. The ferric reducing antioxidant power (FRAP) and 2,2-diphenyl-1-picrylhydrazyl (DPPH) assays revealed that all the compounds have strong antioxidant activities.

Molecular docking simulation of the ligand-enzyme suggested that they positioned in the enzyme's (acetylcholinesterase) active-site gorge. This work warrants further preclinical studies to assess the potential for these novel compounds for the treatment of Alzheimer Disease. Furthermore, some copper(II) and zinc(II) complexes were investigated for *in vivo* gastroprotective effects against ethanol-induced superficial hemorrhagic mucosal lesions in rats. Rats were divided into 7 groups. Groups 1 and 2 were orally administered with Tween 20 (10% v/v). Group 3 was orally administered with 20 mg/kg omeprazole/cimetidine (10% Tween 20). Groups 4–7 received 10, 20, 40, and 80 mg/kg of the complex (10% Tween 20), respectively. Tween 20 (10% v/v) was given orally to group

1 and absolute ethanol was given orally to groups 2–7, respectively. Rats were sacrificed after 1 h. Group 2 exhibited severe superficial hemorrhagic mucosal lesions. This study describes a model to produce extensive gastric necrosis in rats by induction with absolute ethanol. The administration of complexes at 1hour before induction with absolute ethanol reduced or totally eliminated lesions.

Abstrak

Satu siri sebatian yang diperolehi daripada 2 acetylpyridne atau acetophenones dengan morpholine, piperazine dan piperidine moeity telah disintesis dan struktur ciri-ciri. Sebatian dianalisis untuk *dalam silico, in vitro* dan *in vivo* aplikasi biologi (Anti-kanser, anti-bakteria, Anti-Alzheimer dan Anti-ulser). y ini telah mula ditayangkan *dalam vitro* Satu aktiviti nti-bakteria terhadap *Methicillin tahan Staphylococcus aureus* (MRSA), *Acinetobacter baumanni* (AC), *Klebsiella pneumonie* (KB) dan *Pseudomonas aeruginosa* (PA) menggunakan penyebaran cakera dan pencairan sup mikro ujian. Berdasarkan keputusan keseluruhan, y menunjukkan aktiviti yang tinggi terhadap MRSA manakala aktiviti antibakteria lemah diperhatikan terhadap *A. baumanii* dan *P. aeruginosa.* Satu lagi siri kedua 2-acetypyridine dan derivatif acetophenone daripada Gallic hydrazide-deriv atives telah disintesis dan diperiksa untuk aktiviti antioksidan dan *in vitro dan in silico* perencatan acetylcholinesterase. The kuasa penurunan ferik (FRAP) dan 2,2-Diphenyl-1-picrylhydrazyl (DPPH) ujian menunjukkan bahawa semua bahan mempunyai aktiviti antioksidan yang kuat. Simulasi dok Molekul es kompleks ligan-enzim mencadangkan bahawa y diletakkan dalam (acetylcholinesterase) yang aktif tapak gaung enzim ini. Th adalah waran kerja lagi kajian pra-klinikal untuk menilai berpotensi untuk sebatian novel untuk rawatan A lzheimer D isease. Tambahan pula, beberapa kuprum (II) dan zink (II) kompleks telah disiasat *dalam* kesan gastroprotective *vivo* terhadap etanol yang disebabkan luka-luka mukosa berdarah cetek pada tikus. Tikus telah dibahagikan kepada 7 kumpulan. Kumpulan 1 dan 2 telah secara lisan ditadbir dengan Tween 20 (10% v / v). Kumpulan 3 telah secara lisan ditadbir dengan 20 mg / kg omeprazole / cimetidine (10% Tween 20). Kumpulan 4-7 menerima 10, 20, 40, dan 80 mg / kg kompleks (10% Tween 20), masing-masing. Tween 20 (10% v / v) telah diberikan secara lisan kepada kumpulan 1 dan mutlak

etanol telah diberikan secara lisan kepada kumpulan 2-7, masing-masing. Tikus dikorbankan selepas 1 h. Kumpulan 2 dipamerkan teruk cetek luka-luka mukosa berdarah. Kajian ini menerangkan model untuk menghasilkan gastrik luas nekrosis pada tikus secara aruhan dengan etanol mutlak. Pentadbiran es kompleks pada 1 jam sebelum induksi dengan etanol mutlak dikurangkan atau benar-benar dihapuskan luka-luka.

Keywords: M kompleks etal; kristalografi sinar-X; A nti-bakteria; perencatan sakit; Satu kajian nti-kanser; M dok olecular; ulser gastrik dan mekanisme.

Table of content

List of Figures

List of Tables

List of abbreviations

Å	Angstrom
NCI	National Cancer Institute
DCB	Division of Cancer Biology
STN	Scientific & Technical Information Network
CHN	Carbon, Hydrogen and Nitrogen
FT-IR	Fourier transforms infrared spectroscopy
UV-Vis	Ultraviolet–visible spectroscopy
FT-NMR	Fourier-Transform Nuclear Magnetic Resonance
MRSA	*Methicillin resistant Staphylococcus aureus*
PA	*Pseudomonas aeruginosa*
AC	*Acinetobacter baumannii*
VRE	*Vancomycin resistant enterococci*
HCl	Hydrochloric acid
KBr	Potassium bromide
NaI	Sodium iodide
NaSCN	Sodium thiocyanate
MHz	Megahertz
DMSO	Dimethyl sulfoxide
TMS	Trimethylsilane
LMCT	Ligand to metal charge transfer
NBT	Nitro-blue tetrazolium
EDTA	Ethylenediaminetetraacetic acid
SOD	Superoxide dismutase
GSH	Reduced glutathione
DTNB	5,5-dithio-bis(2-nitrobenzoic acid)
MDA	Malondialdehyde
FRAP	Ferric Reduction Antioxidant Power
TPTZ	2, 4, 6-tripyridyl-s-triazine
DPPH	1,1-Diphenyl-2-picrylhydrazyl
MTT	3-(4,5-dimethylthiazol-2-yl)-2,5-diphenyltetrazolium]bromide
MIC	Minimum inhibition concentration
MBC	Minimal bactericidal concentration

1. Introduction

1.1 Imine formation in ketones - the general picture

The electrophilic carbon atoms of ketones can be targets of nucleophilic attack by amines. The end result of this reaction is a compound in which the C=O double bond is replaced by a C=N double bond. Mechanistically, the formation of an imine involves two steps. First, the amine nitrogen acts as a nucleophile, attacking the carbonyl carbon. This is closely analogous to hemiacetal and hemiketal formation. Based on knowledge for the mechanism of acetal and ketal formation, you might expect that the next step would be attack by a second amine to form a compound with a carbon bound to two amine groups – the nitrogen version of a ketal. Instead, what happens next is that the nitrogen is deprotonated, and the electrons from this N-H bond 'push' the oxygen off of the carbon, leaving us with a C=N double bond (an imine) and a displaced water molecule.

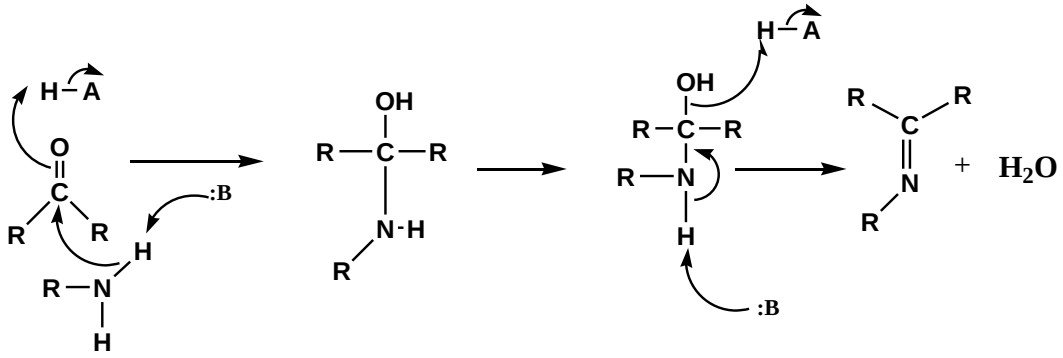

Figure 1.1: The formation of ketimine

The formation of ketimine (Figure 1.1) is an equilibrium system. The reaction is normally conducted under slightly acidic conditions *ca*. pH 4.5. The reaction begins with a nucleophilic attack at the carbonyl carbon of the ketone by the lone pair on the N atom of the incoming primary amine. A proton is moved from the positively charged nitrogen to the negatively charged oxygen producing a neutral carbinolamine. The OH group is then protonated by the acid, forming OH_2^+, which is a better leaving group than the OH group.

This dehydration step leads to the formation of an iminium ion. The next step is the deprotonation of the nitrogen of the iminium ion by water and the formation of the final product, an imine. As the formation of water is one of the driving forces of the reaction, its removal should push the reaction to the right and maximize yields.

Imines derived ligands have played significant important roles in chemistry; because they are potentially capable of forming stable complexes with metal ions (Souza, 1985). Many complexes derived from ketones show excellent activity in various reactions at high temperature (>100 °C) and in the presence of moisture.

In the field of coordination chemistry, ketimines of the general type [Figure 1.2a] and Figure 1.2b] that the intramolecular hydrogen bonds between the (O) and the (N) atoms plays a significant role in the formation of metal complexes, the Schiff base compounds show photochromism and thermochromism in the solid state by proton transfer from the hydroxyl (O) to the ketimine (N) atoms (Elerman, 2002).

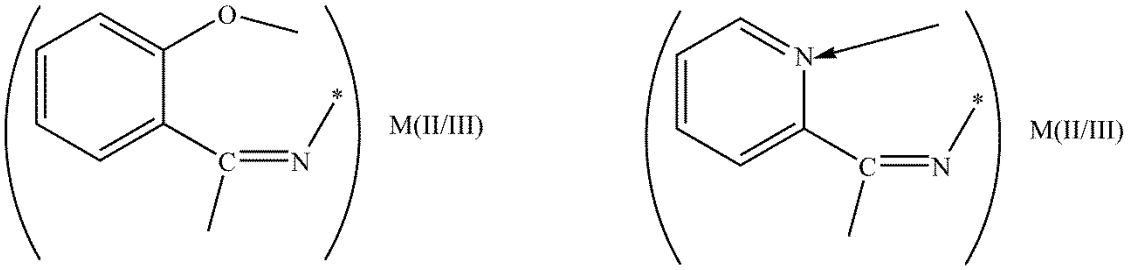

a b

Figure 1.2: Ketimine complexes of acetophenone and acetylpyridine

Condensation between ketones and amines in different reaction conditions has been realized, and in different solvents. The formations of ketones derived Schiff bases (ketimines) have been successful in the presence of dehydrating agents. Acid salts (usually $MgSO_4$ or Na_2SO_4) are commonly employed as dehydrating agents. Primary alcohols such

as ethanol have been widely used as a solvent for the preparation of ketimines. They have been purified by crystallization methods because separation of Schiff bases using silica gel can cause some degree of decomposition, through hydrolysis. If the compounds are insoluble in hexane or cyclohexane, they can be purified by stirring the crude reaction in a mixture of solvents, sometimes adding a small portion of relatively polar solvent e.g diethyl ether and dichloromethane, in order to eliminate impurities. In general, Schiff bases are stable solids and can be stored without many precautions (Cozzi, 2004).

1.2 Biological activities of ketimines and their metal complexes

In the area of bioinorganic chemistry the interest in the complexes lies in that they provide synthetic models for the metal-containing sites in metalloproteins/enzymes and also contributed enormously to the development of medicinal chemistry, radio immunotherapy, cancer diagnosis and treatment of tumor (Quiroga, 2004). In addition, some of the complexes containing N and O donor atoms are effective as stereospecific catalysts for oxidation (Kureshy, 1999) reduction (Aoyama, 1986), biocidal activity (Sengupta, 2001) and other transformations of organic and inorganic chemistry.

It is known that the existence of metal ions bonded to biologically active compounds may enhance their activities (Prakash, 2010). They showed great diversity in their varied biological activities as anticonvulsant (Sridhar, 2002), antifungal (Bharti, 2010; Kalagouda, 2006; Cukurovali, 2006; Tansir, 2008 and Manabu, 1990), anti-HIV (Pandeya, 1999), antiviral and anticancer (Zhang, 2009) antimicrobial (Mandal, 2011, Yusnita, J., *et. al.* 2009, Pignatello, 1994; Ceyhan, 2011; Tajudeen, 2009; Bagihalli, 2008) and antibacterial (Ispir, 2008) agents.

Morpholine is an extremely versatile chemical with many important applications. The physiological activity of the morpholine nucleus is attested by the number of pharmaceutical applications which have been found for it. A platinum(II) complexes involving chelating diamine 2-morpholinoethylamine as the carrier ligand were reported by the direct reaction between cis-[Pt(MPEA)I2] and the disilver salt of corresponding dicarboxylic acid. The cytotoxicity of the complexes was evaluated in the human lung cancer cell lines A549 and A549/ATCC. The 2-morpholinoethylaminoplatinum(II) complexes with dicarboxylates did not show any significant cytotoxicity, but cis-[Pt(MPEA)Cl_2] was more active than carboplatin against both the sensitive and resistant cells, and had less cross-resistance activities with cisplatin.

Jian-Ying Miao (2011) reported two new mononuclear bromido-coordinated zinc and copper complexes, from 2-[2-(1-pyridin-2- ylethylideneamino)ethylamino]ethanol and *N'*-(1-pyridin-2- ylethylidene)ethane-1,2-diamine, synthesized and structurally characterized by IR spectra and X-ray crystallography. The Zn atom is five-coordinate in a trigonal-bipyramidal geometry, and the Cu atom is five coordinate in a square pyramidal geometry. Both Schiff bases coordinate to the metal atoms through the pyridine N, imine N and amine N atoms.

Over the long period of time, many reports on homogeneous and heterogeneous catalysis of Schiff base ligands and their complexes has been done, and reported by (Naeimi, 2007 and Lippard and Berg, 1994). Recently Zhong-Lu You (2010) reported a synthesis, characterization and urease inhibitory activity of oxovanadium(V) complexes with analogous salicylaldehydes derived Schiff bases. The structure–activity relationship indicates that the shorter the terminal groups of the Schiff base ligands are, the stronger the urease inhibitory activities of the oxovanadium(V) complexes. Considering that the

oxovanadium complexes have interesting biological activities and have been widely used in medicine (Chohan, 2010), the complexes may be used in the treatment of infections caused by urease producing bacteria.

1.3 Summarized biological information of some compounds used in this thesis

(1) 2-Acetylpyridine was one of a group of pyridine derivatives screened for mutagenicity and carcinogenicity data to identify candidate chemicals for genetic toxicity testing in the National Cancer Institute, Division of Cancer Biology's (NCI/DCB's) Short-term Testing Program. Very limited toxicological information was found on 2-acetylpyridine.

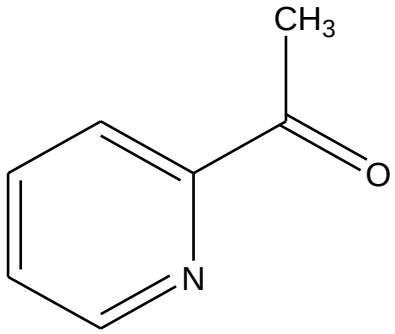

Figure 1.3: Structure of 2-acetylpyridine

2-acetylpyridine (Figure 1.3) has been detected as a flavor or aroma constituent of various consumed food products; some sources include peppermint and spearmint oils, coriander oil, licorice extract, heated corn oil, roasted sesame seed oil, and beer and whiskey, in which pyridines are especially associated with off-flavor (STN International, 1996). 2-Acetylpyridine has been identified as a volatile Maillard reaction product thermally generated and released during corn flour extrusion cooking (Nair, 1994). 2-Acetylpyridine can be prepared by the catalytic air oxidation of 2-ethylpyridine in the liquid phase (Goe, 1982). Two other preparative methods are described in the recent chemical literature as follows:

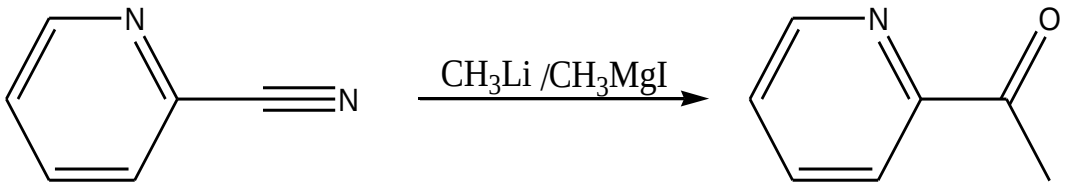

2-cyanopyridine 2-acetylpyridine

Grignard reaction of 2-cyanopyridine with organolithium (CH_3Li) or alkylmagnesium halide (CH_3MgI) (Kim, 1993) oxidation of ethylpyridine using *tert*.-butylhydroperoxide and a chromium zinc hydrotalcite-like catalyst (Choudary, 1996).

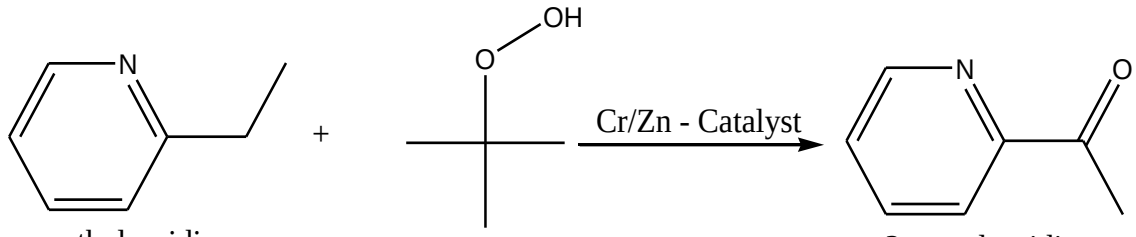

ethylpyridine tert.-butylhydroperoxide 2-acetylpyridine

(2) Morpholine undergoes most chemical reactions typical for other secondary amines, though the presence of the ether oxygen withdraws electron density from the nitrogen, rendering it less nucleophilic (and less basic) than structurally similar secondary amines such as piperidine. For this reason, it forms stable chloramines (Lindsay, 1993). It is commonly used to generate enamines (Noyori, 1988). A number of morpholine derivatives have been described as analgesics and local anesthetics.

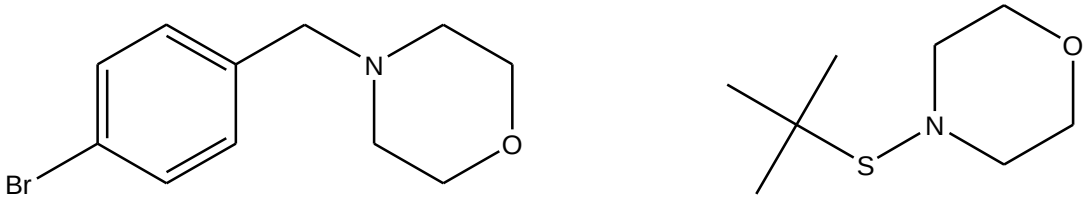

Figure 1.4(a): 4-(4- Bromobenzyl) morpholine (b) 4-tbutylmercaptomorpholine

4-(4- Bromobenzyl) morpholine (Figure 1.4a), for instance, is reported to be only 25% as toxic as procaine, but almost equal to it in activity. Other pharmaceutical fields in which morpholine have found application includes choleretics, antispasmodics, analeptics, and antimalarials. In addition to its use as a corrosion inhibitor, 4-tbutylmercaptomorpholine has been employed as an antioxidant for lubricating oils. Di-4-morpholinyl monosulfide has been claimed as a lubricating oil stabilizer, and multifunctional oil additives that possess antioxidant properties and can be prepared from wax-phenols, formaldehyde, and morpholine.

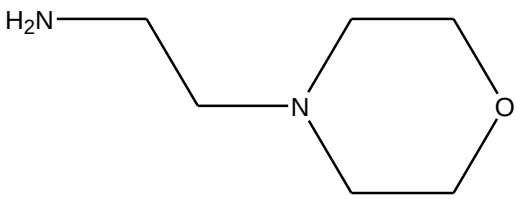

Figure 1.5: Structure of 2-Morpholin-4-yl-ethylamine

(3) Piperidine is a widely used secondary amine. It is widely used to convert ketones to enamines (Vinayak, 1990) Enamines derived from piperidine can be used in the Stork enamine alkylation reaction (March's, 2001) Piperidine is also commonly used in chemical degradation reactions, such as the sequencing of DNA in the cleavage of particular modified nucleotides.

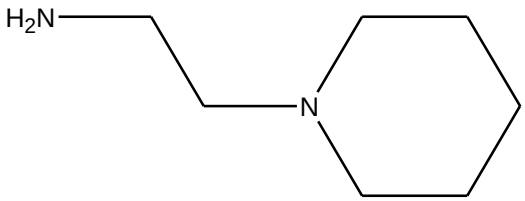

Figure 1.6: structure of 2-Piperidin-1-yl-ethylamine

(4) Piperazine is an organic compound that consists of a six-membered ring containing two opposing nitrogen atoms Piperazine was introduced to medicine as a solvent for uric acid. When taken into the body the drug is partly oxidized and partly eliminated unchanged. Outside the body, piperazine has a remarkable power to dissolve uric acid and producing a soluble urate, but in clinical experience it has not proved equally successful (Noyori, 1988; Klaus, 2003).

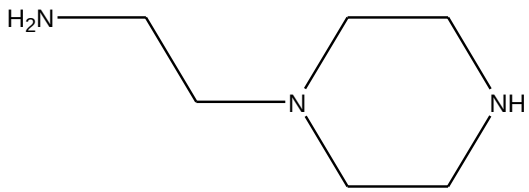

Figure 1.6: Structure of 2-Piperazin-1-yl-ethylamine

1.3 SUMMARY OF PROPOSED LIGANDS IN THIS RESEARCH

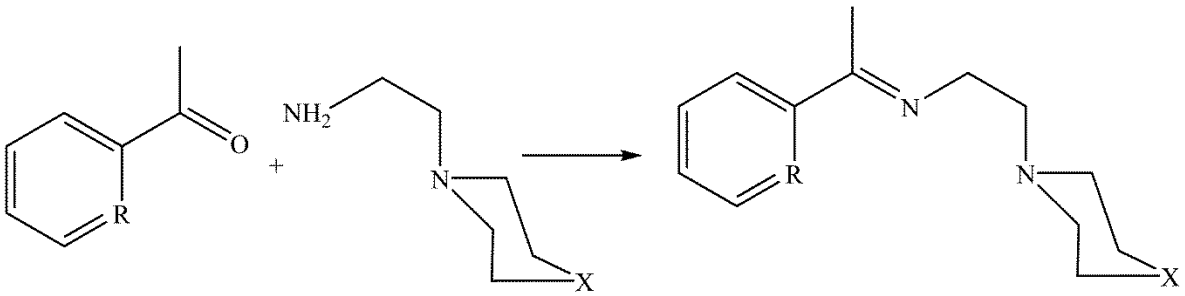

Where
X = O (Morpholine); X = CH_2 (piperidine); X = NH (Piperazine)
R = N(2-acetylpyridine); R = C-OH(2-hydroxacetophenone)

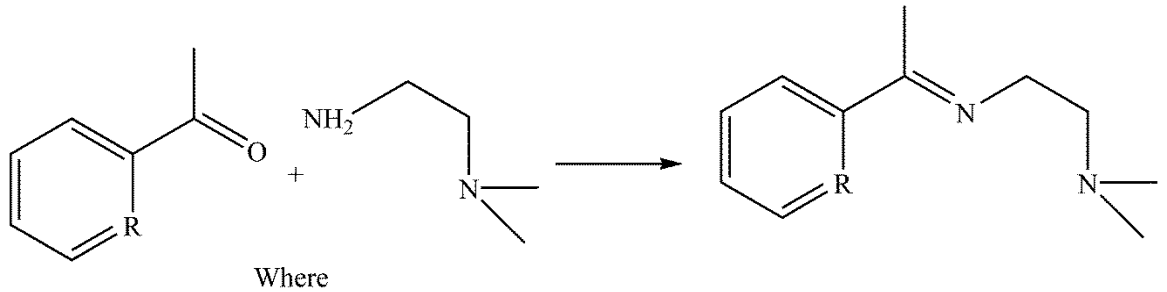

Where
R = N (2-acetylpyridine); R = C-OH (2-hydroxacetophenone)

1.4 SUMMARY OF PROPOSED COMPLEXES IN THIS RESEARCH

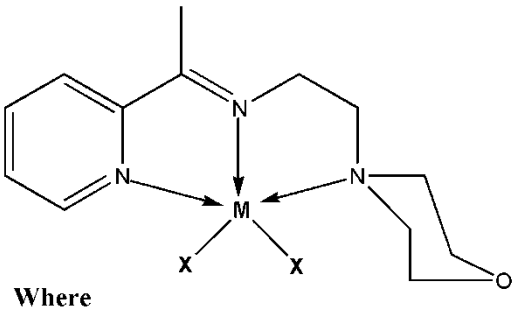

Where

M = Cd^{2+}, Co^{2+}, Cu^{2-}, Mn^{2-}, Ni^{2+} and Zn^{2-}

X = Br^-, Cl^-, I^-, N_3^- and SCN^-

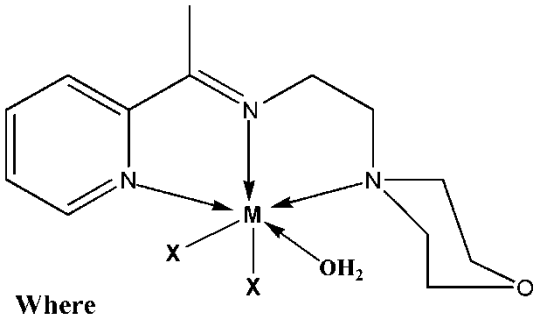

Where

M = Cd^{2-}, Co^{2-}, Mn^{2+} and Ni^{2+}

X = N_3^- and SCN^-

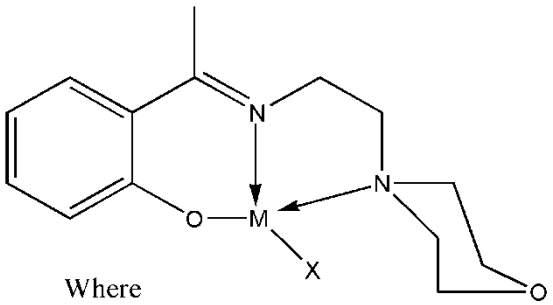

Where

M = Cu^{2+}, Mn^{2+}, Ni^{2+} and Zn^{2-}

X = Br^-, Cl^-

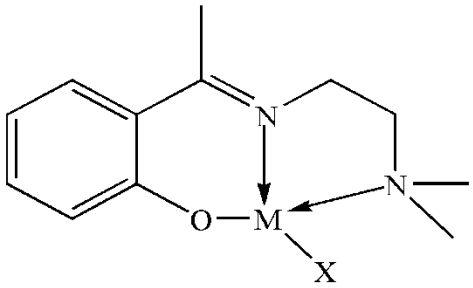

Where
M = Cu, Mn, Ni or Zn
X = Cl^- or Br^-

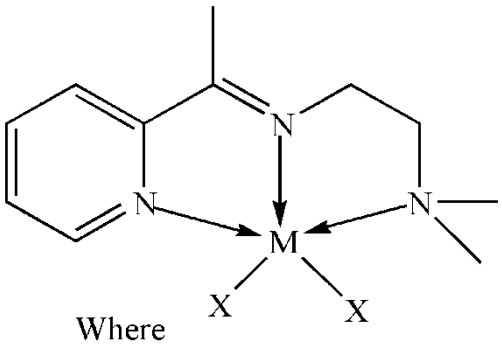

Where
M = Cu, Mn, Ni, or Zn
X = Br^-,Cl^- or NCS^-

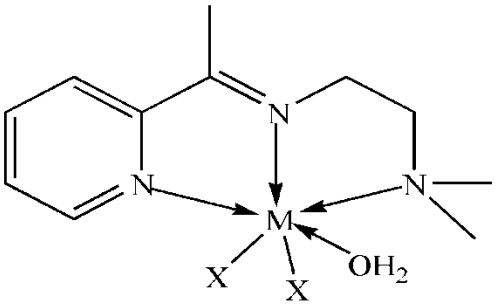

Where
M = Cu, Mn, Ni, or Zn
X = Br^-,Cl^- or NCS^-

1.5 OBJECTIVES OF THIS RESEARCH THESIS

- This research aims at synthesizing ligands derived from condensation reactions of 2-acetylpyridine or acetophenone derivatives with different types of amines [4- (2-aminoethyl) morpholine, 4-(2-aminoethyl) piperazine, 4-(2-aminoethyl) piperidine, N,N-dimethylethylenediamine, gallic hydrazide and benzene sulfanohydrazide]
- The synthesized ligands will be reacted with different kind of transition metal ions [Mn, Co, Ni, Cu, Zn and Cd their (acetates, halides, thiocyanates and azides)] derivatives to form different complexes of different geometries.
- Also both the synthesized ligands and their corresponding metal complexes will then be structurally characterized by using spectroscopic techniques (CHN, FT-IR, UV-Visible, FT-NMR) and singe crystal X-ray crystallography.
- Lastly the synthesized and fully characterized compounds will be analyzed for their biological applications which include *in vitro* anti-oxidants, both *in vitro* and *in silico* anti-Alzheimer, *in vitro* anti-bacterial studies against *methicillin resistant Staphylococcus aureus* (MRSA), *Pseudomonas aeruginosa* (PA), *Acinetobacter baumannii* (AC), and *vancomycin resistant enterococci* (VRE) and *in vitro* anti-cancer as well as *in vivo* anti-ulcer activities.

2.0 EXPERIMENTAL

Reagents

4-(2-aminoethyl)piperidine, 4-(2-aminoethyl)morpholine, 4-(2-aminoethyl)piperazine, N,N-dimethylethyldiamine, 2-acetylpyridne, 2-hydroxyacetophenone, manganese(II) acetate, manganese(II) chloride, cobalt(II) acetate, nickel(II) acetate, nickel(II) chloride, copper(II) acetate, copper(I) bromide, copper(II) chloride, zinc(II) acetate, zinc(II) chloride, cadmium(II) acetate, cadmium(II) chloride, ammonium thiocyanate, Sodium thiocyanate, sodium azide, sodium iodide, hydrochloric acid, glacial acetic acid, triethylamine, absolute ethanol (99.8%), ethanol (95%), dimethylsulphoxide, deuterated dimethylsulphoxide, acetonitrile and tween 20 that have been used in this research were reagent-grade quality and purchased from Sigma, Fluka or Merck. TagametTM 200 mg (cimetidine) and omeprazole were purchased from Caring Pharmacy.

2.1 SYNTHESIS OF IMINE LIGANDS

2.1.1 Preparation of 2-morpholino-N-(1-(pyridin-2-yl)ethylidene)ethanamine (LMA)

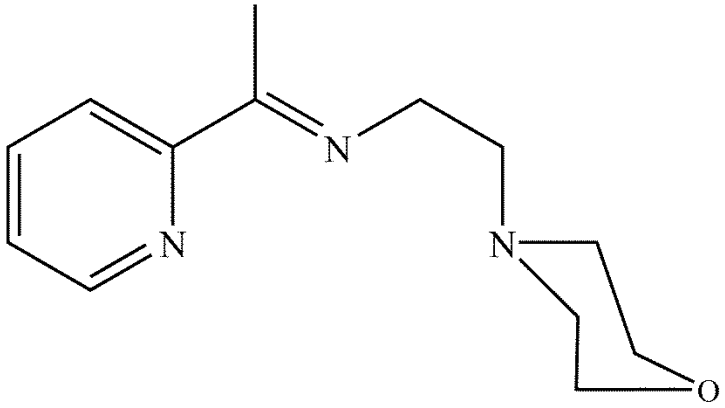

A mixture of 4-(2-aminoethyl)morpholine (0.65 g, 5 mmol) and 2-acetylpyridine (0.61 g, 5 mmol) in ethanol (50 ml) was refluxed for 2 h followed by addition of a few drops of glacial acetic acid to adjust the pH. An oily solution was formed. The solid product was dissolved in methanol and heated to 60 °C. After evaporation of the solvent under reduced pressure, an orange colored solid was formed. This ligand was characterized by using elemental analysis, IR, NMR and UV/Vis-spectroscopy.

2.1.2 Preparation of 2-(1-(2-morpholinoethylimino)ethyl)phenol (LMH)

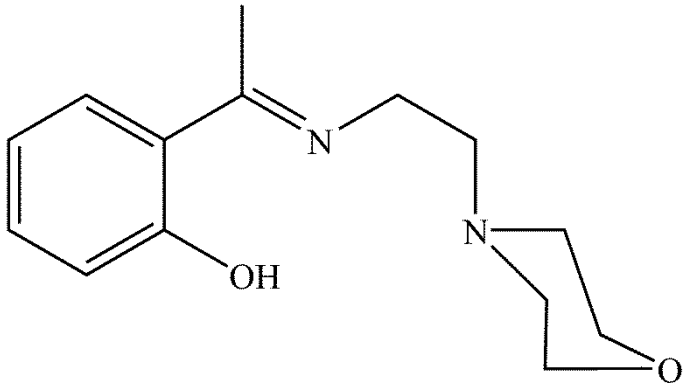

The ligand was obtained from the condensation reaction of 2-hydroxyacetophenone with 4-(2-aminoethyl) morpholine in the presence of a few drops of glacial acetic acid to adjust the pH. An oily solution was formed. The solid product was dissolved in methanol and heated to 60 °C. After evaporation of the solvent under reduced pressure, a yellowish colored solid was formed. This ligand was characterized by elemental analysis, IR, NMR and UV/Vis-spectroscopy.

2.1.3 Preparation of 2-(piperazin-1-yl)-N-(1-(pyridin-2-yl)ethylidene)ethanamine (LPA)

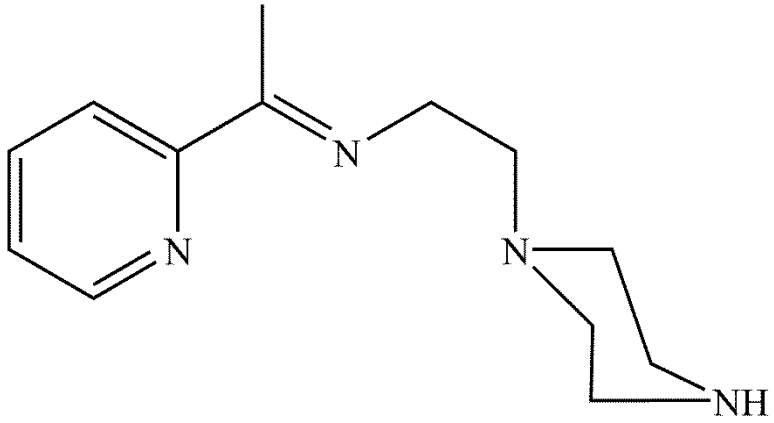

A mixture of 4-(2-aminoethyl)piperazine (0.65 g, 5 mmol) and 2-acetylpyridine (0.61 g, 5 mmol) in ethanol (50 ml) at a temperature of 75–85 °C was refluxed for three hours followed by addition of a few drops of glacial acetic acid to adjust the pH. Same procedure as **LMA** was applied in the isolation of this Schiff base.

2.1.4 Preparation of 2-(piperidin-1-yl)-N-(1-(pyridin-2-yl)ethylidene)ethanamine (LPiA)

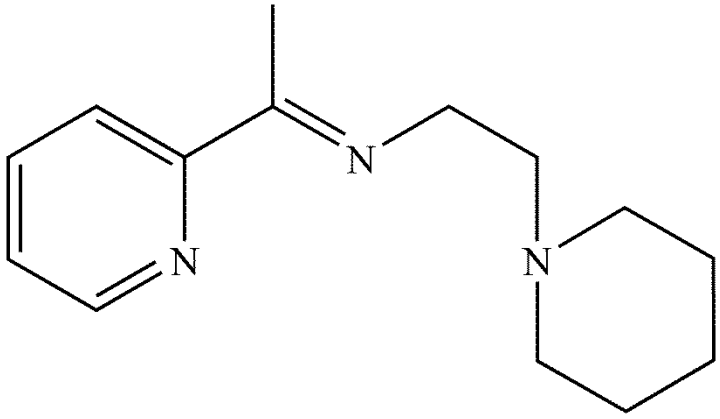

A mixture of 4-(2-aminoethyl)piperidine (0.65 g, 5 mmol) and 2-acetylpyridine (0.61 g, 5 mmol) in ethanol (50 ml) was refluxed for 2 h followed by addition of few drops of glacial acetic acid to adjust the pH. After evaporating all the solvent to dryness using rotary evaporator, a yellowish orange colored solid was formed.

2.1.5 Preparation of N1,N1-dimethyl-N2-(1-(pyridin-2-yl)ethylidene)ethane-1,2-diamine (LNA)

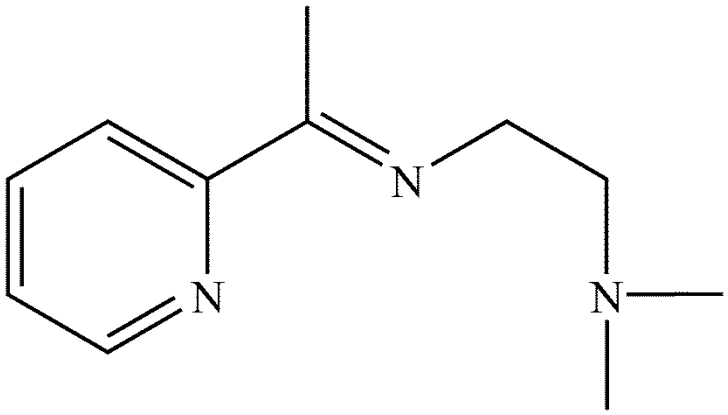

An accurately measured amount 2-acetylpyridine (0.61 g, 5 mmol) and *N*,*N*-dimethylethyldiamine (0.44 g, 5 mmol) in ethanol (25 mL) at a temperature of 75–85 °C was refluxed for three hours. The progress of the reaction was monitored by using thinlayer chromatography (TLC), eluent ethylacetate:Hexane in a ratio (1:4), and confirmed by one spot different from the starting maerials. After the reaction reached completion the solvent was evaporated to dryness and the solid obtained was isolated and washed several time with ethanol.

2.1.6 Preparation of 2-(1-(2-(dimethylamino)ethylimino)ethyl)phenol (LNH)

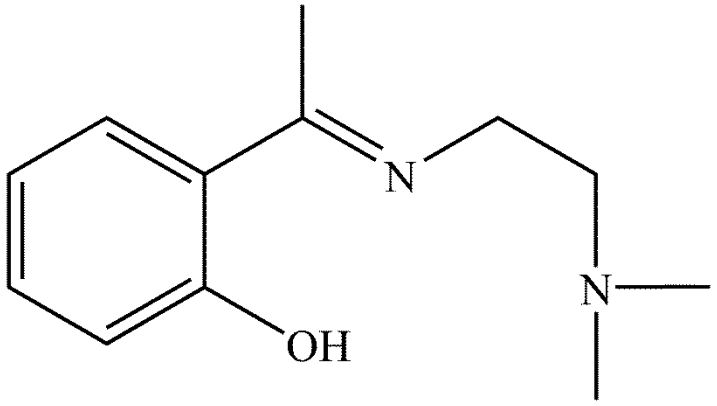

A measured amount of 2-hydroxyacetophenone (0.61 g, 5 mmol) and *N*,*N*-dimethylethyldiamine (0.44 g, 5 mmol) in ethanol (25 mL) at a temperature of 75–85 °C was heated under refluxfor three hours, to give a yellowish-orange solution. After the reaction reached completion the solvent was evaporated to dryness using a rotary evaporaor and the solid obtained was isolated washed several time with methanol to obtain a pure product.

2.2 SYNTHESIS OF METAL COMPLEXES

2.2.1 Preparation of Dichlorido{2-morpholino-N-[1-(2-pyridyl)ethylidene] ethanaminek^{3}N,N',N''}manganese(II) [Mn(LMA)Cl2]

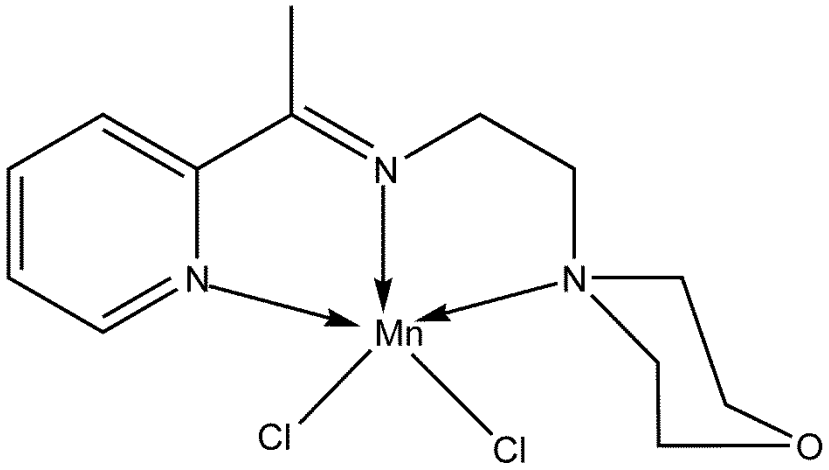

A mixture of 2-acetylpyridine (0.2 g, 1.65 mmol) and 4-(2-aminoethyl)morpholine (0.21 g, 1.65 mmol in ethanol (20 ml) was heated under reflux for 2 hr followed by addition of a solution of manganese(II) chloride (0.206 g, 1.65 mmol) in a minimum amount of water. The resulting solution was heated under reflux for 30 min, and then set aside at room temperature. The crystals of the manganese(II) complex were obtained after a few days.

2.2.2 Preparation of Aqua{2-(morpholin-4-yl)-N-[1-(2-pyridyl)ethylidene]ethanamine k^3N,N',N''} bis(thiocyanato-k^N)- manganese(II) [$Mn(LMA)(NCS)_2(H_2O)$]

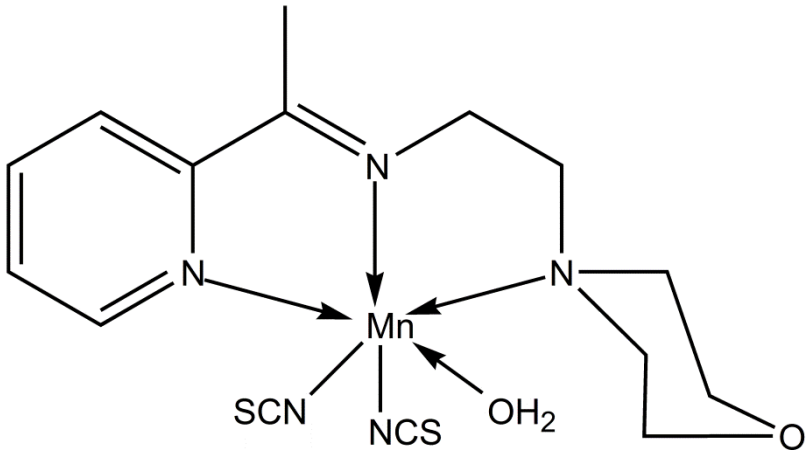

A mixture of 2-acetylpyridine (0.20 g, 1.65 mmol) and 4-(2-aminoethyl)morpholine (0.21 g, 1.65 mmol) in ethanol (20 ml) was heated under reflux for 2 hr followed by addition of a solution of manganese(II) acetate tetrahydrate (0.41 g, 1.65 mmol) and ammonium thiocyanate (0.13 g, 1.65 mmol) in a minimum amount of ethanol. The resulting solution was heated under reflux for 30 min, and then left at room temperature. The crystals of the title complex were obtained in a week.

2.2.3 Preparation of Dichlorido{2-morpholino-N-[1-(2-pyridyl)ethylidene] ethanaminekκ^3 N,N',N''} cobalt(II) [Co(LMA)Cl$_2$]

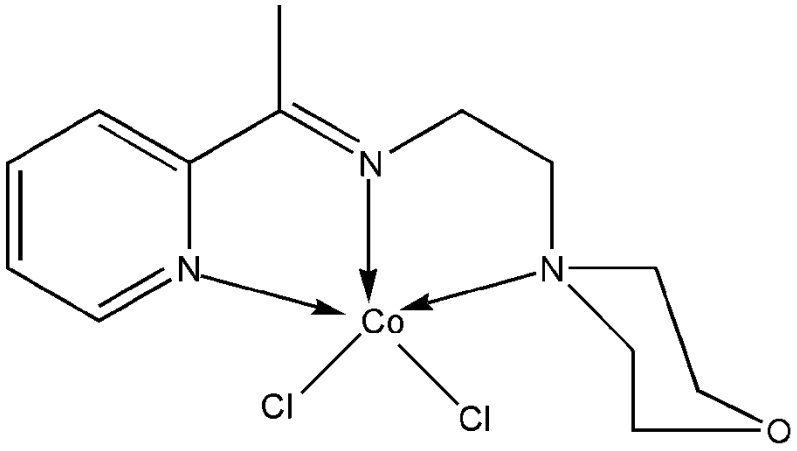

A mixture of 2-acetylpyridine (0.20 g, 1.65 mmol) and 4-(2-aminoethyl)morpholine (0.21 g, 1.65 mmol) in ethanol (20 ml), was refluxed. After 2 hr a solution of cobalt(II) chloride anhydrous (0.21 g, 1.65 mmol) in a minimum amount of water was added. The resulting solution was refluxed for 30 min, and then left at room temperature. The crystals of the title complex were obtained in a few days.

2.2.4 Preparation of Cobalt(III)tris(azido-κN){2-Morpholino-N-[1-(2-pyridyl)ethylidene] ethanamine-κ^3N,N',N''} [Co(LMA)(N_3)$_3$]

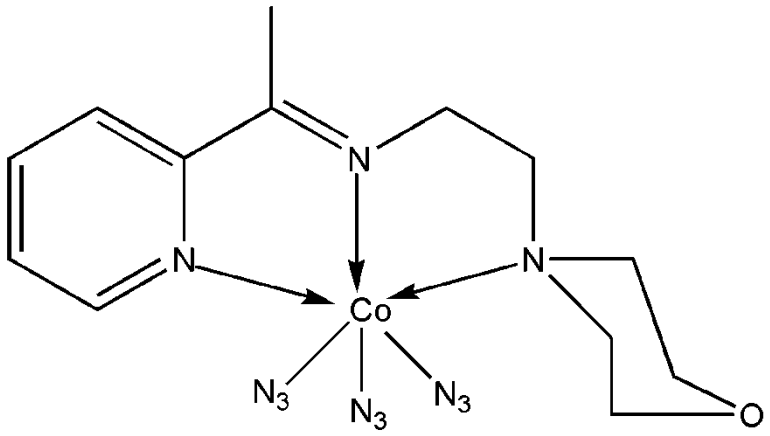

A mixture of 2-acetylpyridine (0.20 g, 1.65 mmol) and 4-(2-aminoethyl)morpholine (0.21 g, 1.65 mmol) in ethanol (20 ml) was refluxed for 2 hr followed by addition of a solution of cobalt(II) acetate tetrahydrate (0.41 g, 1.65 mmol) and sodium azide(0.22 g, 3.30 mmol) in a minimum amount of water. The resulting solution was refluxed for 30 min, and then left at room temperature. The crystals of the title complex were obtained in a few days; the resulting pure crystal was filtered off, washed with cold ethanol and dried under vacuum over silica gel.

2.2.5 Preparation of Aqua{2-morpholino-N-[1-(2-pyridyl)- ethylidene]ethanamine-k3N,N',N''-bis(thiocyanato-kN)cobalt(II) [Co(LMA)(NCS)$_2$(H$_2$O)]

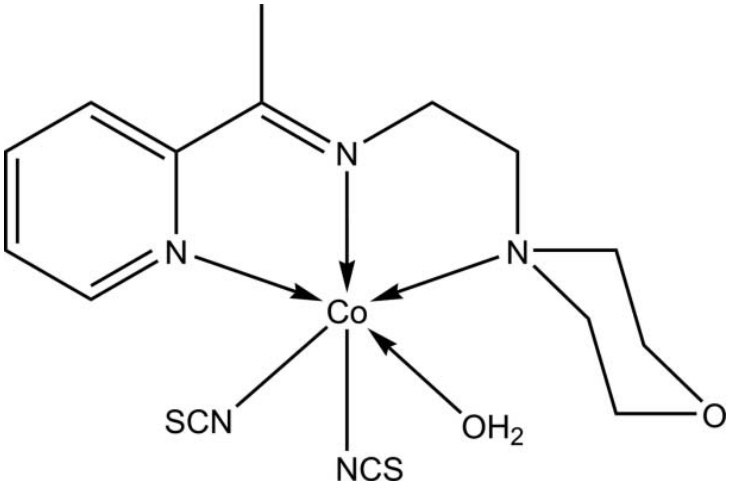

A mixture of 2-acetylpyridine (0.20 g, 1.65 mmol) and 4-(2-aminoethyl)morpholine (0.21 g, 1.65 mmol) in ethanol (20 ml) was heated under reflux for 2 hr followed by addition of a solution of cobalt(II) acetate tetrahydrate (0.41 g, 1.65 mmol) and sodium thiocyanete (0.134 g, 1.65 mmol) in a minimum amount of water. The resulting solution was heated under reflux for 30 min, then left at room temperature. The crystals of the title complex were obtained in a few days.

2.2.6 Preparation of Aqua{2-morpholino-N-[1-(2-pyridyl)-ethylidene]ethanamine-k3N,N',N"}-bis(thiocyanato-kN)nickel(II) [Ni(LMA)(NCS)$_2$(H$_2$O)]

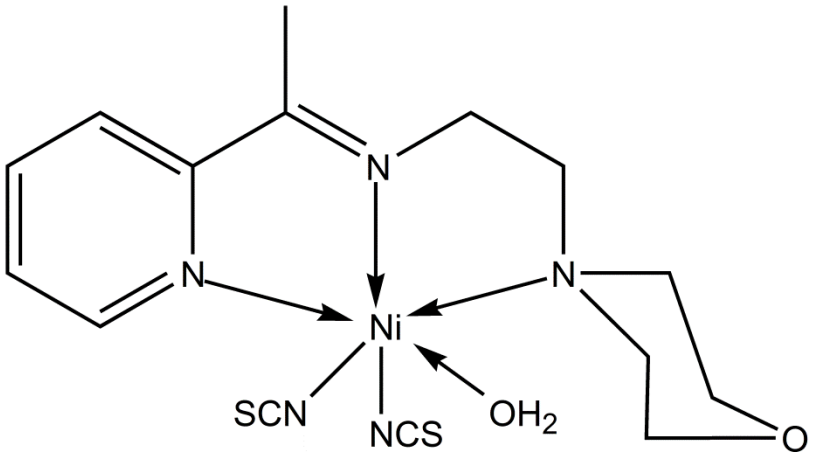

A mixture of 2-acetylpyridine (0.20 g, 1.65 mmol) and 4-(2-aminoethyl)morpholine (0.21 g, 1.65 mmol) in ethanol (20 ml) was heated under reflux for 2 hr followed by addition of a solution of nickel(II) acetate tetrahydrate (0.41 g, 1.65 mmol) and sodium thiocyanate (0.134 g, 1.65 mmol) in a minimum amount of water. The resulting solution was heated under reflux for 30 min, then left at room temperature. The crystals of the title complex were obtained in a week.

2.2.7 Nickel(II)poly(azido-κN){2-Morpholino-N-[1-(2-pyridyl)ethylidene] ethanamine-κ3N,N',N''} [$Ni_2(LMA)_2(N_3)_2(H_2O)_2$]

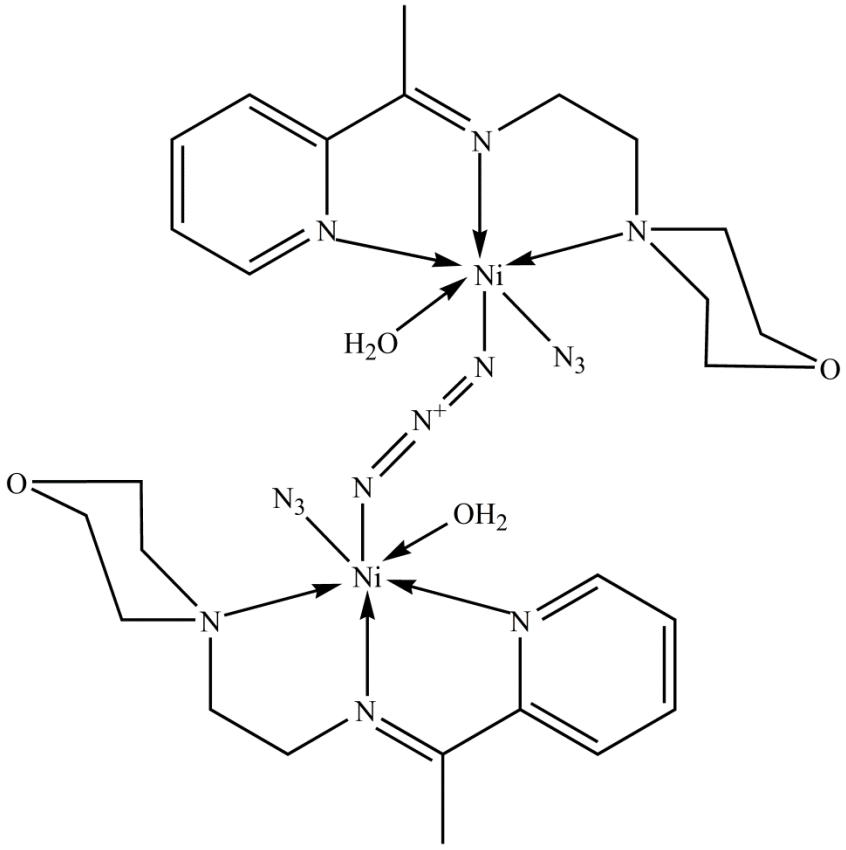

A mixture of 2-acetylpyridine (0.20 g, 1.65 mmol) and 4-(2-aminoethyl)morpholine (0.21 g, 1.65 mmol) in ethanol (20 ml) was refluxed for 2 hr followed by addition of a solution of nickel(II) acetate tetrahydrate (0.41 g, 1.65 mmol) and sodium azide (0.22 g, 3.30 mmol) in a minimum amount of water. The resulting solution was heated under reflux for 30 min, and then left at room temperature. The crystals of the title complex were obtained in a week; the resulting pure crystal was filtered off, washed with cold ethanol and dried over silica gel.

2.2.8 Preparation of Dichlorido{2-(morpholin-4-yl)-N-[1-(pyridin-2-yl)ethylidene]ethanaminek^{3}N,N',N''}copper(II) monohydrate [Cu(LMA)Cl_2 .H_2O]

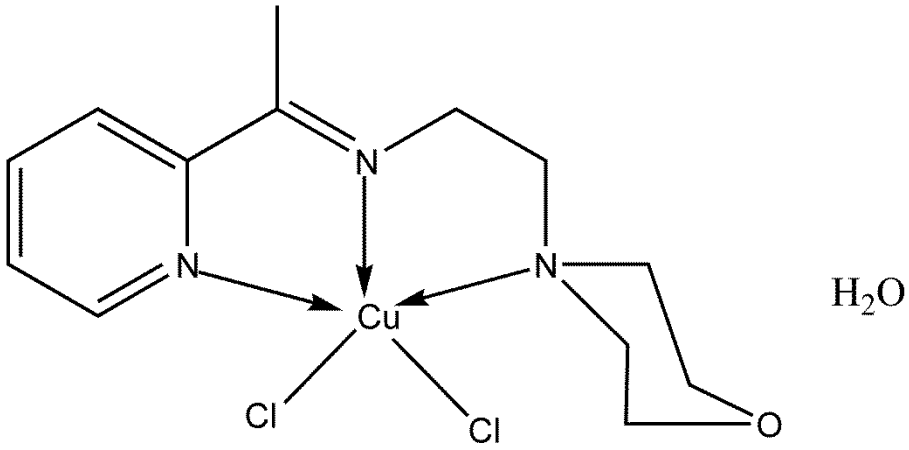

A mixture of 2-acetylpyridine (0.20 g, 1.65 mmol) and 4-(2-aminoethyl)morpholine (0.21 g, 1.65 mmol) in ethanol (20 ml) was refluxed. After 2 hr a solution of copper(II) chloride dihydrate (0.28 g, 1.65 mmol) in a minimum amount of ethanol was added and the resulting solution was heated under reflux for 30 min, then set aside at room temperature. The crystals of the title complex were obtained after a few days.

2.2.9 Preparation of {2-Morpholino-N-[1-(2-pyridyl)ethylidene]ethanamine-k^{3}N,N',N''} bis(thiocyanato-kN)copper(II) [Cu(LMA)(NCS)$_2$]

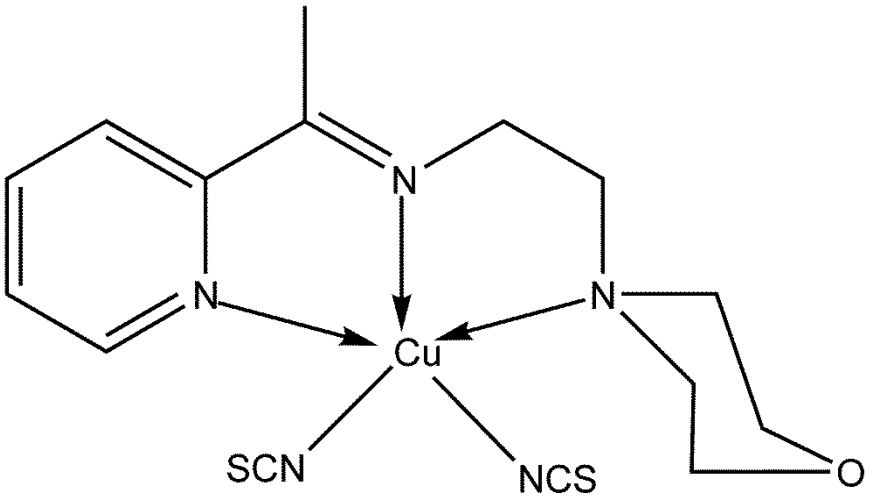

A mixture of 2-acetylpyridine (0.20 g, 1.65 mmol) and 4-(2-aminoethyl)morpholine (0.21 g, 1.65 mmol) in ethanol (20 ml) was refluxed for 2 hr followed by addition of a solution of copper(II) acetate monohydrate (0.33 g, 1.65 mmol) and sodium thiocyanate (0.134 g, 1.65 mmol) in a minimum amount of ethanol. The resulting solution was heated under reflux for 30 min, and then left at room temperature. The crystals of the title complex were obtained in a week.

2.2.10 Preparation of Dibromido{2-morpholino-N-[1-(2-pyridyl)ethylidene] ethanaminek^{3}N,N',N''} zinc(II) [Zn(LMA)Br$_2$]

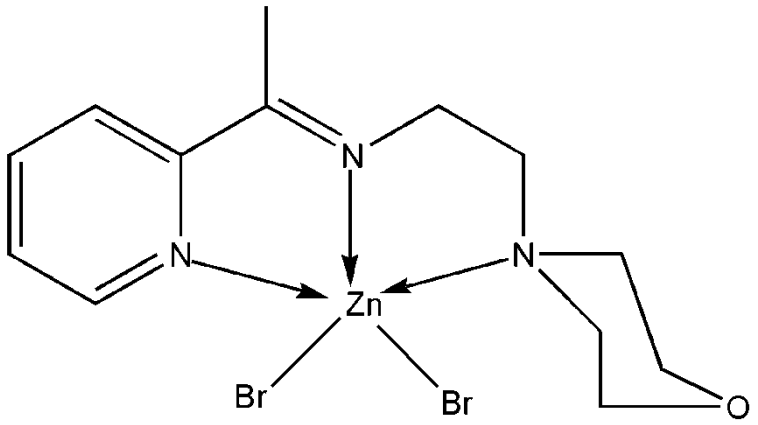

A mixture of 2-acetylpyridine (0.20 g, 1.65 mmol) and 4-(2-aminoethyl) morpholine (0.21 g, 1.65 mmol) in ethanol (20 ml) was heated under reflux. After 2 hr a solution of zinc (II) acetate dihydrate (0.36 g, 1.65 mmol) and potassium bromide (0.196 g, 1.65 mmol) in a minimum amount of water was added.. The mixture was refluxed for 2-3 hours resulting in the formation of small precipitate. More precipitate was obtained by removal of some solvent by distillation. The product was collected by filtration, washed several times with ethanol until a milky colored compound is obtained.

2.2.11 Preparation of Dichlorido{2-morpholino-N-[1-(2-pyridyl)ethylidene] ethanaminek^3 N,N',N''}zinc(II) [Zn(LMA)Cl$_2$]

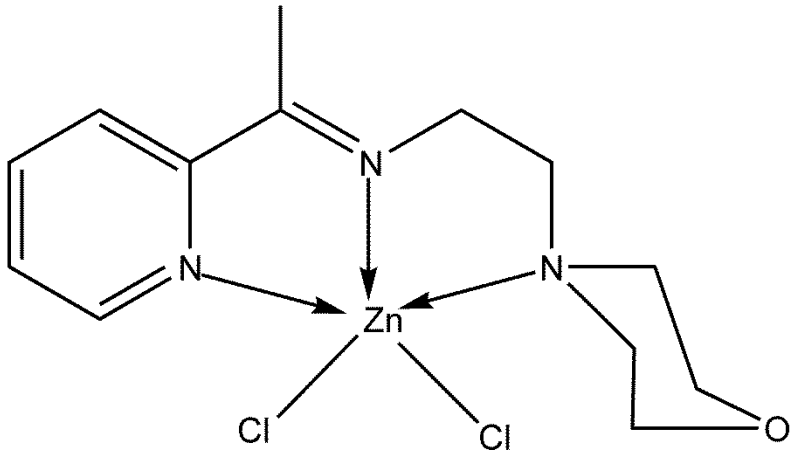

A mixture of 2-acetylpyridine (0.20 g, 1.65 mmol) and 4-(2-aminoethyl)morpholine (0.21 g, 1.65 mmol) in the presence of a few drops of HCl (37%) in ethanol (20 ml) was heated under reflux. After two hours, a solution of zinc(II) acetate dihydrate (0.36 g, 1.65 mmol) in a minimum amount of water was added and the resulting solution was refluxed for 30 min, then set aside at room temperature. The crystals of the title complex were obtained after a few days.

2.2.12 Preparation of Diiodido{2-(morpholin-4-yl)-N-[1-(2-pyridyl)ethylidene] ethanaminek^3 N,N',N''}zinc [Zn(LMA)I_2]

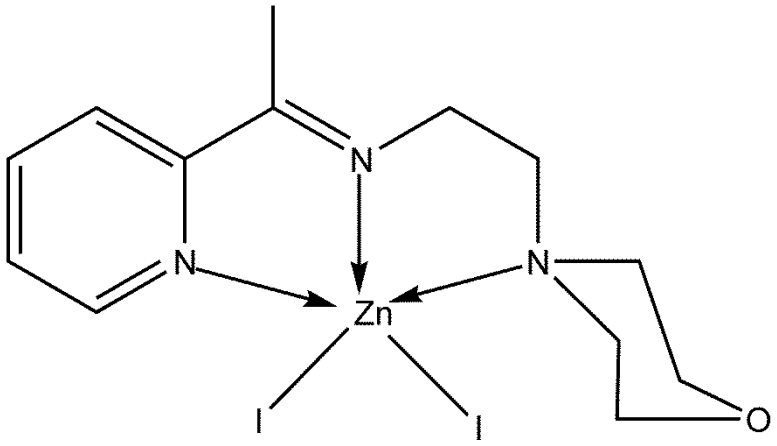

A mixture of 2-acetylpyridine (0.20 g, 1.65 mmol) and 4-(2-aminoethyl)morpholine (0.21 g, 1.65 mmol) in ethanol (20 ml) was heated under reflux for two hours, followed by addition of a solution of zinc(II) acetate dihydrate (0.36 g, 1.65 mmol) and potassium iodide (0.54 g, 3.3 mmol) in a minimum amount of water. The resulting solution was heated under reflux for 30 min and then left at room temperature. Brown crystals of the title complex were obtained in a few days.

2.2.13 Preparation of {2-Morpholino-N-[1-(2-pyridyl)-ethylidene]ethanamine-k^3N,N',N"} bis(thiocyanato-k^N)zinc(II) [Zn(LMA)(NCS)$_2$]

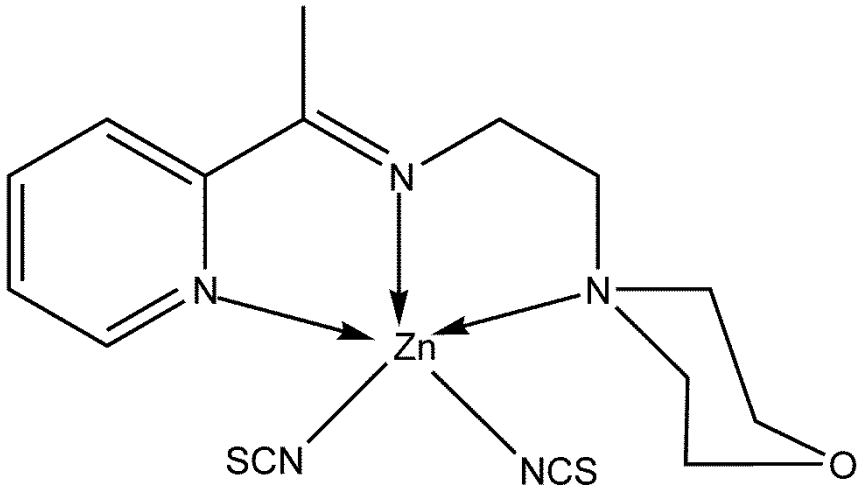

A mixture of 2-acetylpyridine (0.20 g, 1.65 mmol) and 4-(2-aminoethyl)morpholine (0.21 g, 1.65 mmol) in ethanol (20 ml) was heated under reflux for 2 hr followed by addition of a solution of zinc(II) acetate dihydrate (0.36 g, 1.65 mmol) and sodium thiocyanate (0.134 g, 1.65 mmol) in a minimum amount of water. The resulting solution was heated under reflux for 30 min, then left at room temperature. The crystals of the title complex were obtained in a few days.

2.2.15 Preparation of 2-Morpholino-N-[1-(2-pyridyl)ethylidene]ethanamine-κ^3N,N',N''-bis(azido-κ^N)zinc(II) [Zn(LMA)(N_3)$_2$]

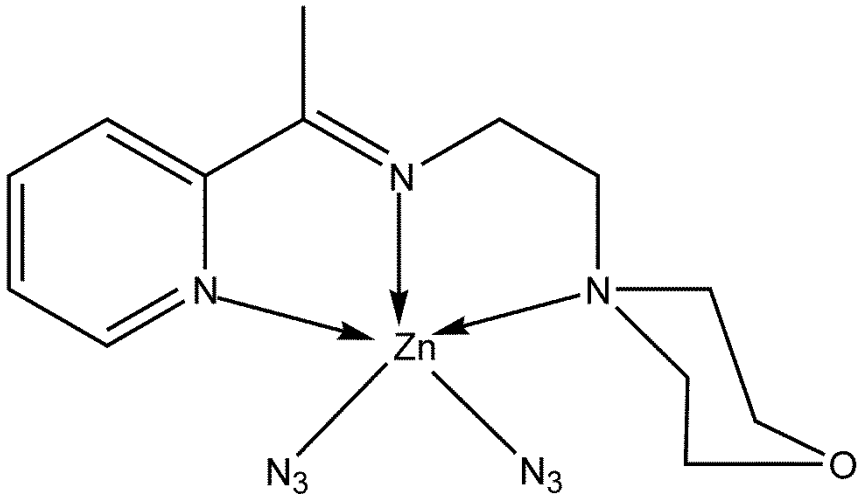

A mixture of 2-acetylpyridine (0.20 g, 1.65 mmol) and 4-(2-aminoethyl)morpholine (0.21 g, 1.65 mmol) in ethanol (20 ml) was heated under reflux for 2 hr followed by addition of a solution of zinc(II) acetate dihydrate (0.36 g, 1.65 mmol) and sodium azide 0.22 g, 3.30 mmol) in a minimum amount of water. The resulting solution was heated under reflux for 30 min, and then left at room temperature. The crystals of the title complex were obtained in a few days; the resulting pure crystal was filtered off, washed with cold ethanol and dried over silica gel.

2.2.16 Preparation of Dibromido{2-(morpholin-4-yl)-N-[1-(2-pyridyl)ethylidene] ethanaminek^{3}N,N',N''}cadmium [Cd(LMA)Br$_2$]

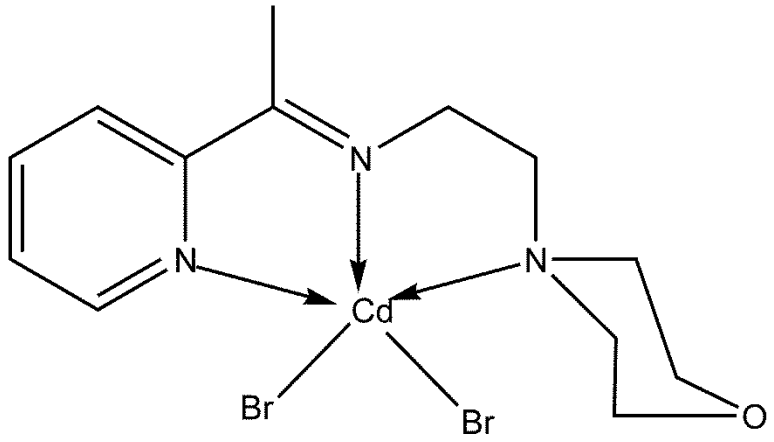

A mixture of 2-acetylpyridine (0.20 g, 1.65 mmol) and 4-(2-aminoethyl)morpholine (0.21 g, 1.65 mmol) in ethanol (20 ml) was heated under reflux. After 2 hr a solution of cadmium(II) acetate dihydrate (0.44 g, 1.65 mmol) and potassium bromide (0.196 g, 1.65 mmol) in a minimum amount of water was added. The resulting solution was heated under reflux for 30 min, and then left at room temperature. The crystals of the title complex were obtained in a few days.

2.2.17 Preparation of Dichlorido{2-morpholino-N-[1-(2-pyridyl)ethylidene] ethanamine-k^{3}N,N',N''}-cadmium [Cd(LMA)Cl$_2$]

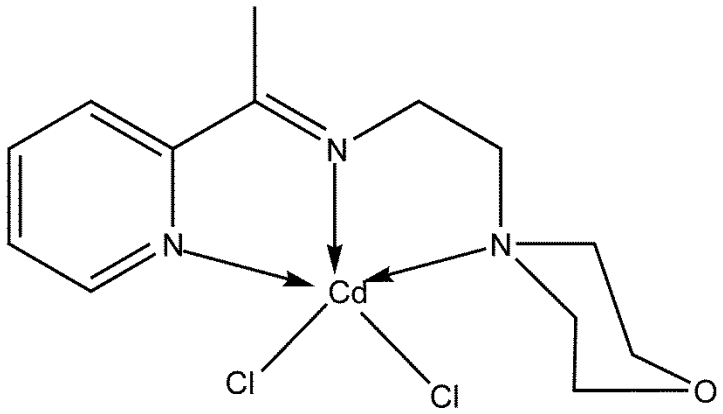

A mixture of 4-(2-aminoethyl)morpholine (0.65 g, 5 mmol) and 2-acetylpyridine (0.61 g, 5 mmol) in ethanol (50 ml) was heated under reflux for 2 h followed by addition of a solution of cadmium(II) chloride (0.92 g, 5 mmol) in a minimum amount of water. The resulting solution was heated under reflux for 30 min, then evaporated partially and set aside at room temperature. The crystals of the cadmium(II) complex were obtained after a week.

2.2.18 Preparation of Aqua{2-morpholino-N-[1-(2-pyridyl)- ethylidene]ethanamine-k^3N,N',N''}-bis(thiocyanato-k^N)cadmium(II) [Cd(LMA)$(N_3)_2(H_2O)$]

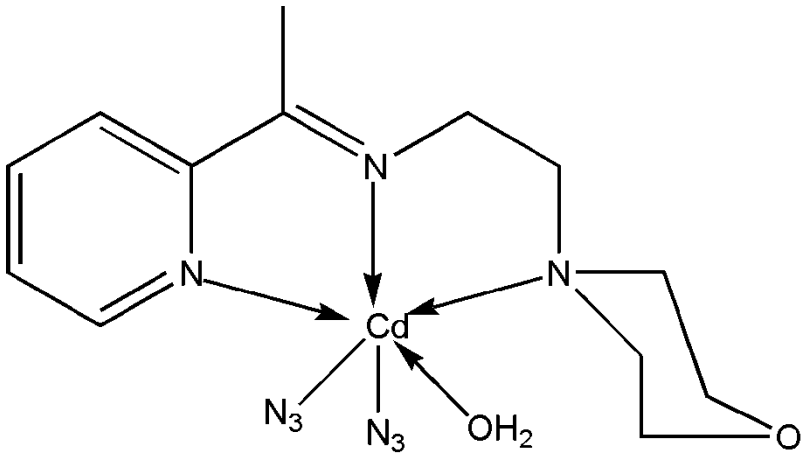

A mixture of 2-acetylpyridine (0.20 g, 1.65 mmol) and 4-(2-aminoethyl)morpholine (0.21 g, 1.65 mmol) in ethanol (20 ml) was heated under reflux for 2 hr followed by addition of a solution of cadmium(II) acetate dihydrate (0.44 g, 1.65 mmol) and sodium azide (0.22 g, 3.30 mmol) in a minimum amount of water. The resulting solution was heated under reflux for 30 min, and then left at room temperature. The crystals of the title complex were obtained in a few days; the resulting pure crystal was filtered off, washed with cold ethanol and dried over silica gel.

2.2.19 Preparation of Di-l-thiocyanato-k^{2N}:S;k2S:N-bis({2-morpholino-N-[1-(2-pyridyl) ethylidene]ethanamine-k^{3} N,N',N''}(thiocyanatojN)cadmium) [$Cd_2(LMA)_2(NCS)_4$]

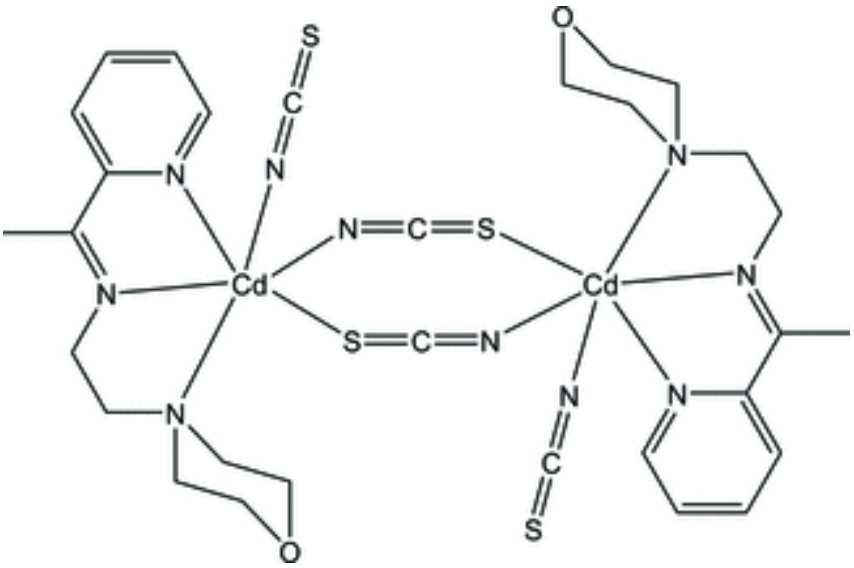

A mixture of 2-acetylpyridine (0.20 g, 1.65 mmol) and 4-(2-aminoethyl)morpholine (0.21 g, 1.65 mmol) in ethanol (20 ml) was heated under reflux for 2 hr followed by addition of a solution of cadmium(II) acetate dihydrate (0.44 g, 1.65 mmol) and sodium thiocyanate (0.268 g, 3.30 mmol) in a minimum amount of water. The resulting solution was heated under reflux for 30 min, and then left at room temperature. The crystals of the title complex were obtained in a week.

2.2.20 Preparation of 2-(1-(2-morpholinoethylimino)ethyl)phenoxy)manganese(II) bromide [Mn(LMH)Cl]

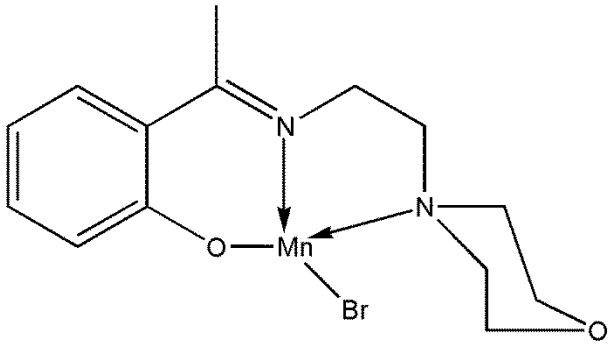

The title compound was obtained through the reaction of 2-hydroxyacetophenone (0.5 g, 3.7 mmol) and 4-(2-aminoethyl)morpholine (0.48 g, 3.7 mmol) in ethanol (20 ml), manganese(II) acetate tetrahydrate (0.41 g, 1.65 mmol), potassium bromide (0.22 g, 1.85 mmol) in a minimum amount of water (Gwaram, 2012)

2.2.21 Preparation of 2-(1-(2-morpholinoethylimino)ethyl)phenoxy)manganese(II) chloride [Mn(LMH)Cl]

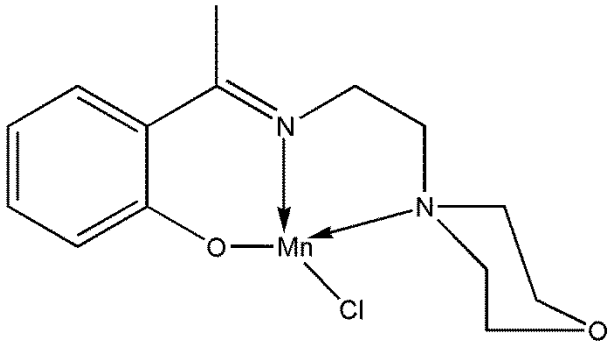

The title compound was obtained through the reaction of 2-hydroxyacetophenone (0.5 g, 3.7 mmol) and 4-(2-aminoethyl)morpholine (0.48 g, 3.7 mmol) in ethanol (20 ml), manganese(II) chloride (0.24 g, 1.85 mmol) in a minimum amount of water.

2.2.22 Preparation of 2-(1-(2-morpholinoethylimino)ethyl)phenoxy)nickel(II) bromide [Ni(LMH)Br]

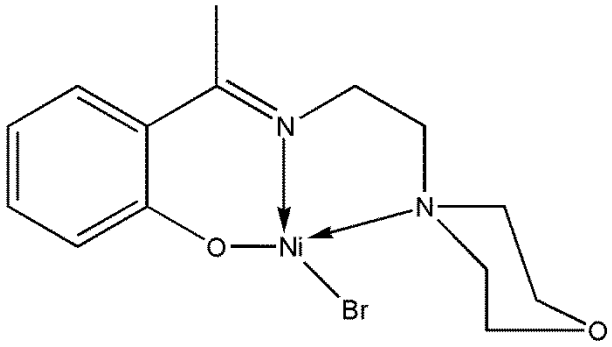

The title compound was obtained through the reaction of 2-hydroxyacetophenone (0.5 g, 3.7 mmol) and 4-(2-aminoethyl)morpholine (0.48 g, 3.7 mmol) in ethanol (20 ml), nickel(II) acetate dihydrate (0.6 g, 3.7 mmol), potassium bromide (0.22 g, 1.85 mmol) in a minimum amount of water.

2.2.23 Preparation of 2-(1-(2-morpholinoethylimino)ethyl)phenoxy)nickel(II) chloride [Ni(LMH)Cl]

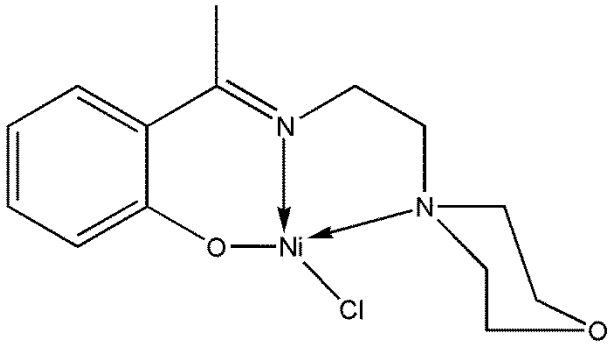

The title compound was obtained through the reaction of 2-hydroxyacetophenone (0.5 g, 3.7 mmol) and 4-(2-aminoethyl)morpholine (0.48 g, 3.7 mmol) in ethanol (20 ml), nickel(II) chloride (0.24g, 1.85mmol) in a minimum amount of ethanol.

2.2.24 Preparation of Bromido(2-{1-[(2-morpholinoethyl)-imino]ethyl}phenolato-κ^3N,N',O) copper(II) [Cu(LMH)Br]

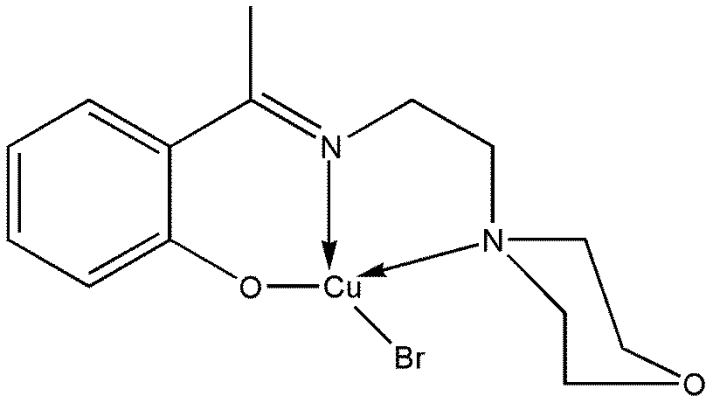

The title compound was obtained through the reaction of 2-hydroxyacetophenone (0.5 g, 3.7 mmol) and 4-(2-aminoethyl)morpholine (0.48 g, 3.7 mmol) in ethanol (20 ml), copper(II) chloride dihydrate (0.63 g, 3.7 mmol), potassium bromide (0.22 g, 1.85 mmol) in a minimum amount of water.

2.2.25 Preparation of Chlorido(2-{1-[(2-morpholinoethyl)-imino]ethyl}phenolato-κ^3N,N',O)-copper(II) [Cu(LMH)Cl]

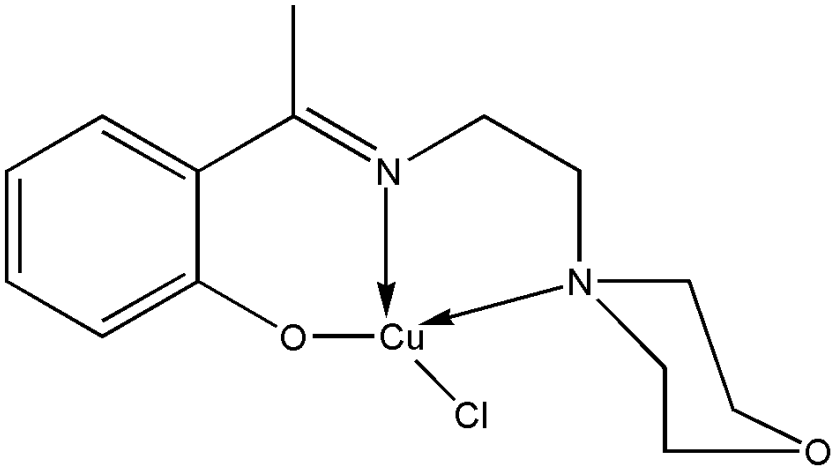

A mixture of 2-hydroxyacetophenone (0.5 g, 3.7 mmol) and 4-(2-aminoethyl)morpholine (0.48 g, 3.7 mmol) in ethanol (20 ml), copper(II) chloride dihydrate (0.63 g, 3.7 mmol) in a minimum amount of ethanol. The resulting solution was refluxed for 30 min, and then left at room temperature. The crystals of the title complex were obtained after a few days.

2.2.26 Preparation of 2-(1-(2-morpholinoethylimino)ethyl)phenoxy)zinc(II) bromide [Zn(LMH)Br]

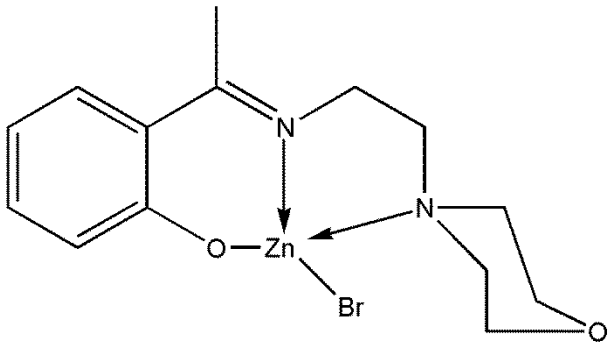

The title compound was obtained through the reaction of 2-hydroxyacetophenone (0.5 g, 3.7 mmol) and 4-(2-aminoethyl)morpholine (0.48 g, 3.7 mmol) in ethanol (20 ml), zinc(II) acetate dihydrate (0.6 g, 3.7 mmol), potassium bromide (0.22 g, 1.85 mmol) in a minimum amount of water.

2.2.27 Preparation of 2-(1-(2-morpholinoethylimino)ethyl)phenoxy)zinc(II) chloride [Zn(LMH)Cl]

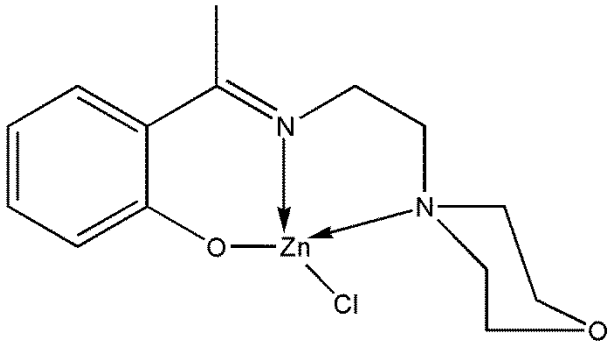

The title compound was obtained through the reaction of 2-hydroxyacetophenone (0.5 g, 3.7 mmol) and 4-(2-aminoethyl)morpholine (0.48 g, 3.7 mmol) in ethanol (20 ml), zinc(II) chloride (0.35g, 1.85 mmol) in a minimum amount of ethanol.

2.2.28 Preparation of Hexachloridobis{l2-2-(piperazin-1-yl)-N-[1-(2-pyridyl)ethylidene] ethanamine}-trizinc dihydrate $[Zn_3(LPA)_2(Cl)_6]$

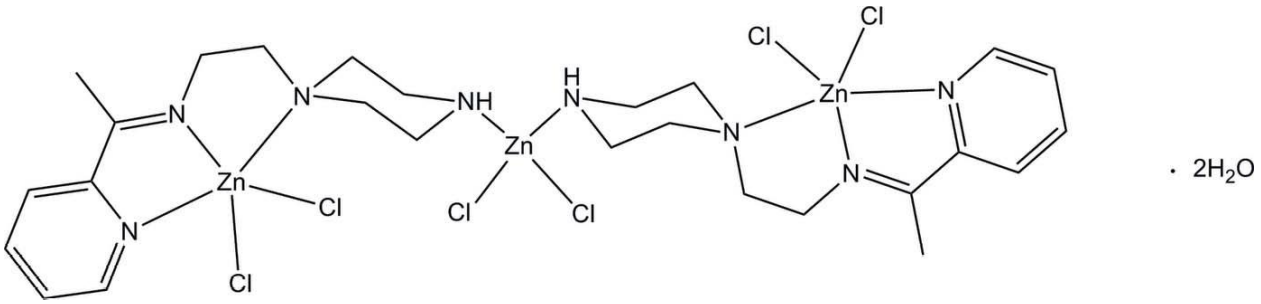

A mixture of 4-(2-aminoethyl) piperazine (0.2 g, 1.55 mmol) and 2-acetylpyridine (0.19 g, 1.55 mmol) in ethanol (20 ml) was heated under reflux for 2 h and then an ethanolic solution of zinc (II) chloride (0.21 g, 1.55 mmol) was added. The resulting solution was heated under reflux for 30 min and then set aside at room temperature for a few days whereupon the prismatic crystals of the title compound were obtained.

2.2.29 Preparation of Octachloridobis[l2-2-(piperazin-1-yl)-N-1-(2-pyridyl)ethylidene ethanamine-bis-4-(2-aminoethyl)piperazine]-tetracadminic $[Cd_4(LPA)_2(PA)_2(Cl)_8]$

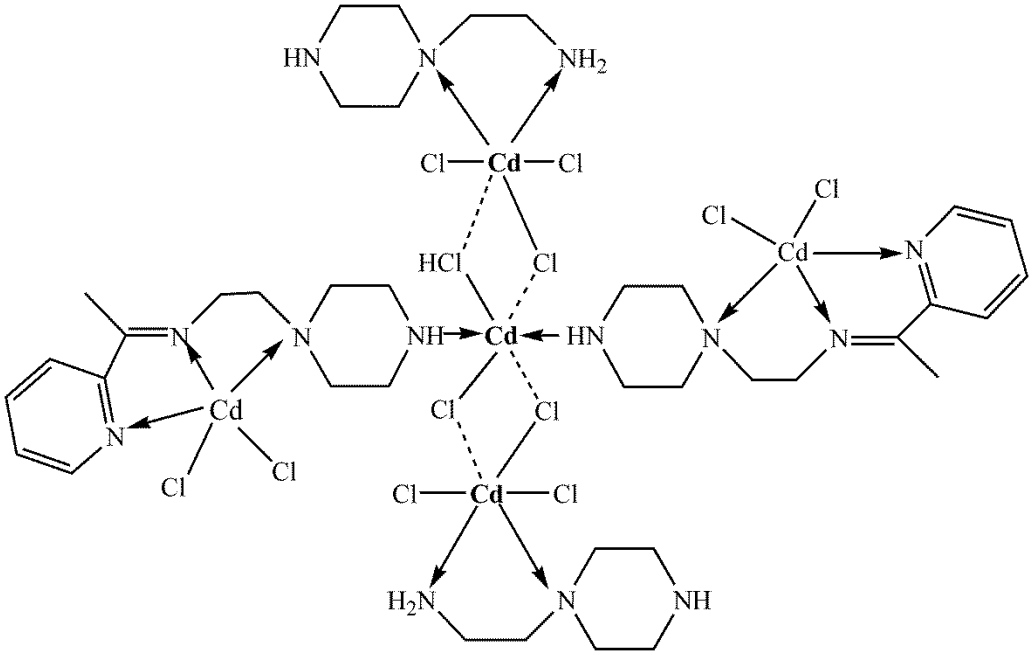

A mixture of 4-(2-aminoethyl)piperazine (0.65 g, 5 mmol) and 2-acetylpyridine (0.61 g, 5 mmol) in ethanol (50 ml) was heated under reflux for 2 h followed by addition of a solution of cadmium(II) chloride (0.92 g, 5 mmol) in a minimum amount of water was added. The resulting solution was heated under reflux for 30 min and then set aside at room temperature for one week where upon the tiny crystals of the chlorine bridged polymerized compound were obtained.

2.2.30 Preparation of Dichlorido{2-piperidino-N-[1-(2-pyridyl)ethylidene]ethanamine κ^3N,N',N''} zinc(II) [Zn(LPiA)Cl_2]

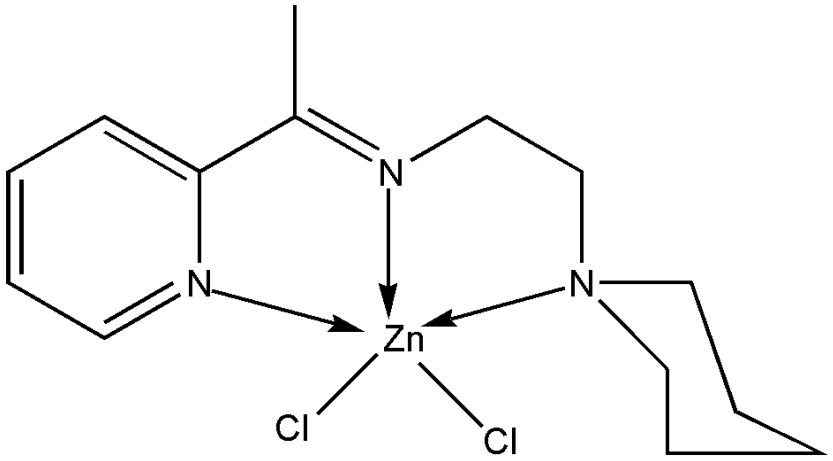

A mixture of 2-acetylpyridine (0.20 g, 1.65 mmol) and 4-(2-aminoethyl)piperidine (0.21 g, 1.65 mmol) in the presence of a few drops of HCl (37%) in ethanol (20 ml) was refluxed. After 2 hr a solution of zinc(II) acetate dihydrate (0.36 g, 1.65 mmol) in a minimum amount of water was added and the resulting solution was refluxed for 30 min, then set aside at room temperature. The crystals of the title complex were obtained after a few days.

2.2.31 Preparation of {2-piperido-N-[1-(2-pyridyl)-ethylidene]ethanamine-κ^3N,N',N''} bis(thiocyanato-k^N)zinc(II)] [Zn(LPiA)(NCS)$_2$]

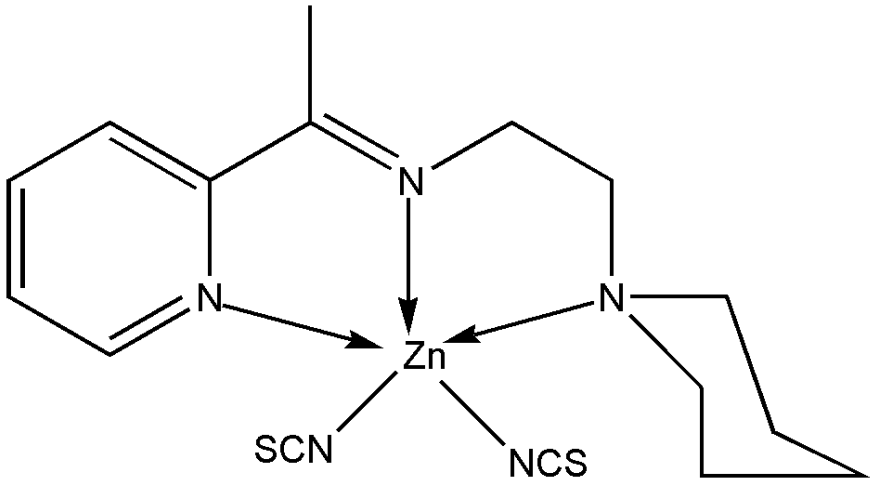

A mixture of 2-acetylpyridine (0.20 g, 1.65 mmol) and 4-(2-aminoethyl)piperidine (0.21 g, 1.65 mmol) in ethanol (20 ml) was heated under reflux for 2 hr followed by addition of a solution of zinc(II) acetate dihydrate (0.36 g, 1.65 mmol) and sodium thiocyanate (0.134 g, 1.65 mmol) in a minimum amount of water. The resulting solution was heated under reflux for 30 min, and then left at room temperature. The crystals of the title complex were obtained in a few days

2.2.32 Preparation of Dichlorido{N,N-dimethyl-N0-[1-(2-pyridyl)ethylidene]ethane-1,2-diaminek^3 N,N',N''}manganese(II) [Mn(LNA)Cl_2]

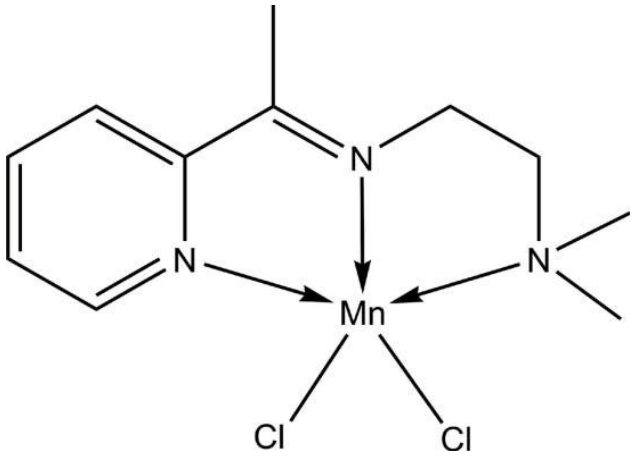

A mixture of 2-acetylpyridine (0.61 g, 5 mmol) and *N,N*-dimethylethyldiamine (0.44 g, 5 mmol) in ethanol (50 ml) was heated under reflux for 2 hr followed by addition of a solution of manganese(II) chloride (0.63 g, 5 mmol) in a minimum amount of water. The resulting solution was heated under reflux for 30 min, then set aside at room temperature. The crystals of the title compound were obtained after a few days.

2.2.33 Preparation of Aqua{N,N-dimethyl-N'-[1-(2-pyridyl)-ethylidene]ethane-1,2-diaminek^{3}N,N',N"}bis(thiocyanato-k^{N})nickel(II) [Ni(LNA)(NCS)2(H_2O)]

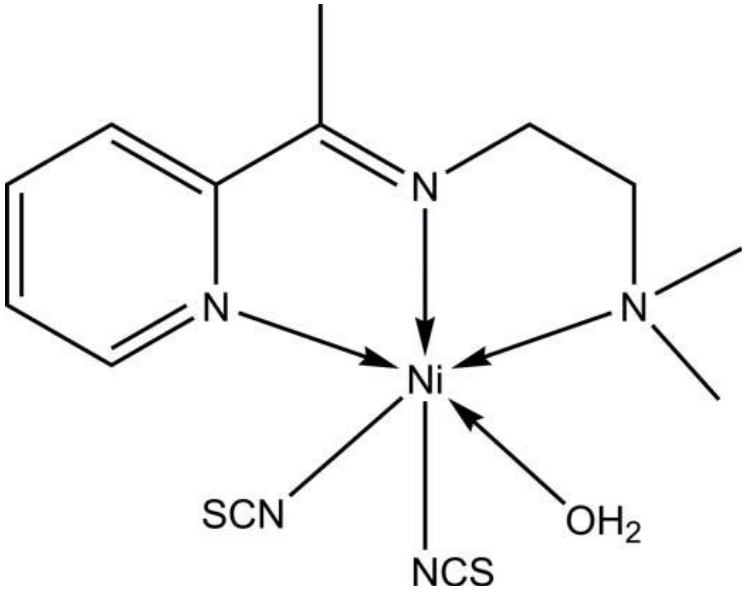

A mixture of 2-acetylpyridine (0.2 g, 1.65 mmol) and *N*,*N*-dimethylethyldiamine (0.15 g, 1.65 mmol) in ethanol (20 ml) was heated under reflux for 2 h followed by addition of a solution of nickel(II) acetate tetrahydrate (0.41 g, 1.65 mmol) and sodium thiocyanate (0.27 g, 3.3 mmol) in a minimum amount of water. The resulting solution was heated under reflux for 30 min, then set aside at room temperature. Brown crystals of the title compound were obtained by slow evaporation of the resulting reaction mixture.

2.2.34 Peparation of {N,N-Dimethyl-N'-[1-(2-pyridyl)ethylidene] ethane-1,2-diamine-k^3N,N',N''}- bis(thiocyanato-k^N)copper(II) [Cu(LNA)(NCS)$_2$]

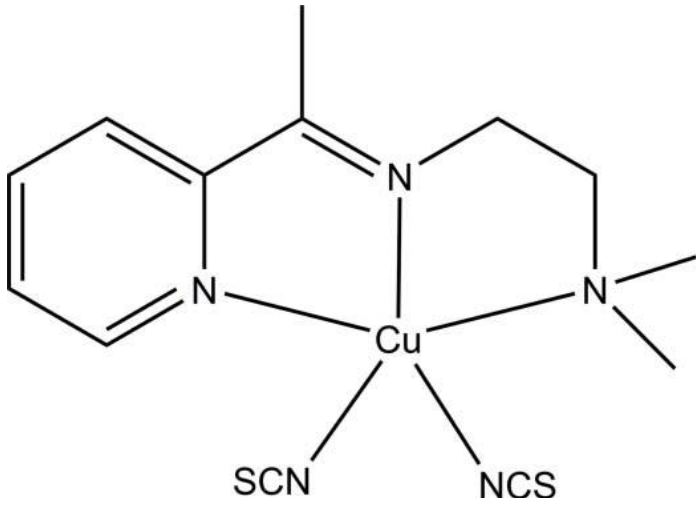

A mixture of 2-acetylpyridine (0.2 g, 1.65 mmol) and *N*,*N*-dimethylethyldiamine (0.15 g, 1.65 mmol) in ethanol (20 ml) was heated under reflux. After 2 hr a solution of copper(II) chloride dihydrate (0.28 g, 1.65 mmol) and sodium thiocyanate (0.27 g, 3.3 mmol) in a minimum amount of water was added. The resulting solution was heated under reflux for an hour, then left at room temperature. The green crystals of the title compound were obtained in a few days.

2.2.35 Preparation of Dichlorido{N,N-dimethyl-N0-[1-(2-pyridyl)ethylidene]ethane-1,2-diaminek^{3}N,N',N''}zinc [Zn(LNA)Cl_2]

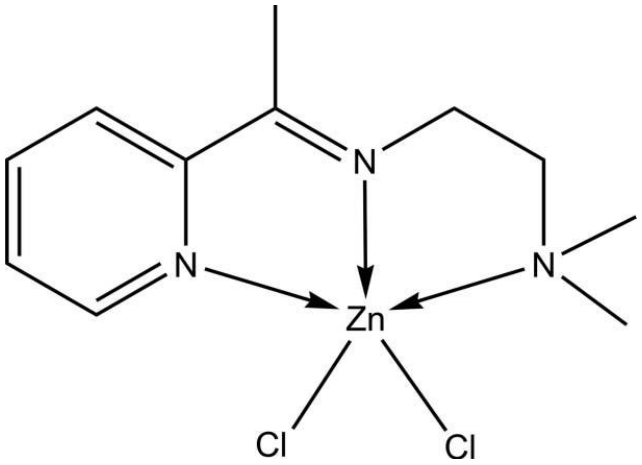

A mixture of 2-acetylpyridine (0.20 g, 1.65 mmol) and *N*,*N*-dimethylethyldiamine (0.15 g, 1.65 mmol) in ethanol (20 ml) was heated under reflux for 2 hr followed by addition of a solution of zinc(II) chloride (0.225 g, 1.65 mmol) in the minimum amount of water. The resulting solution was heated under reflux for 30 min, and then set aside at room temperature. The colorless crystals of the title compound were obtained in a few days.

2.2.36 N,N-Dimethyl-N'-[1-(2-pyridyl)ethylidene]ethane-1,2-diamine-k^{3}N,N',N''}bis (thiocyanate)zinc(II) [Zn(LNA)(NCS)$_2$]

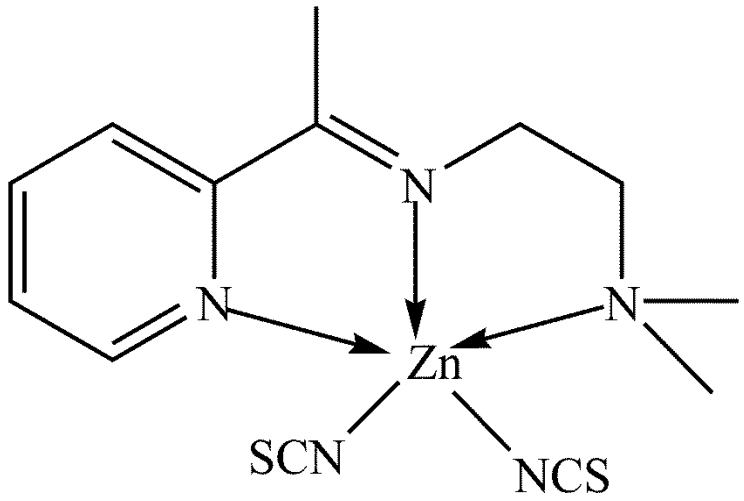

A mixture of 2-acetylpyridine (0.61 g, 5 mmol) and *N,N*-dimethylethyldiamine (0.44 g, 5 mmol) in ethanol (50 mL) was heated under reflux for 2 h followed by addition of a solution of Zinc (II) acetate (0.92 g, 5 mmol) and sodium thiocyanate (0.406 g, 5 mmol) in a minimum amount of water. The mixture was heated under reflux for 2–3 h resulting in the formation of a white precipitate. More precipitate was obtained by removal of some solvent. The product was collected by filtration, washed several times with ethanol until a white colored compound is obtained. It was re-crystallized from the same solvent (ethanol), filtered to remove the suspended impurities. Yield = 72%.

2.2.37 Preparation of Dichlorido{N,N-dimethyl-N0-[1-(pyridin-2-yl)ethylidene]ethane-1,2-diaminek^3N,N',N''}cadmium [Cd(LNA)Cl_2]

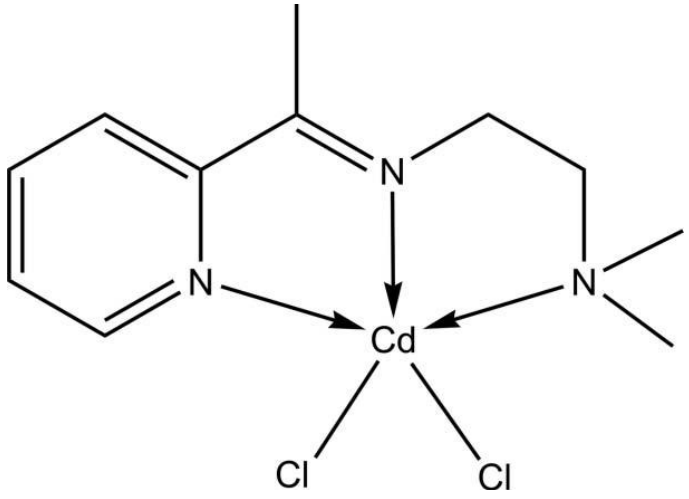

A mixture of 2-acetylpyridine (0.61 g, 5 mmol) and *N*,*N*-dimethylethyldiamine (0.44 g, 5 mmol) in ethanol (50 ml) was heated under reflux for 2 hr followed by addition of a solution of cadmium(II) chloride (0.92 g, 5 mmol) in a minimum amount of water. The resulting solution was heated under reflux for 30 min, then set aside at room temperature. The colorless crystals of the title compound were obtained after a few days.

2.2.38 Preparation of catena-Poly[[{N,N-dimethyl-N'-[1-(pyridin-2-yl)ethylidene]ethane-1,2-diamine-k^{3}N,N',N''}(thiocyanato-k^N)-cadmium]-l-thiocyanato-k2S:N] [Cdn(LNA)n(NCS)n]n

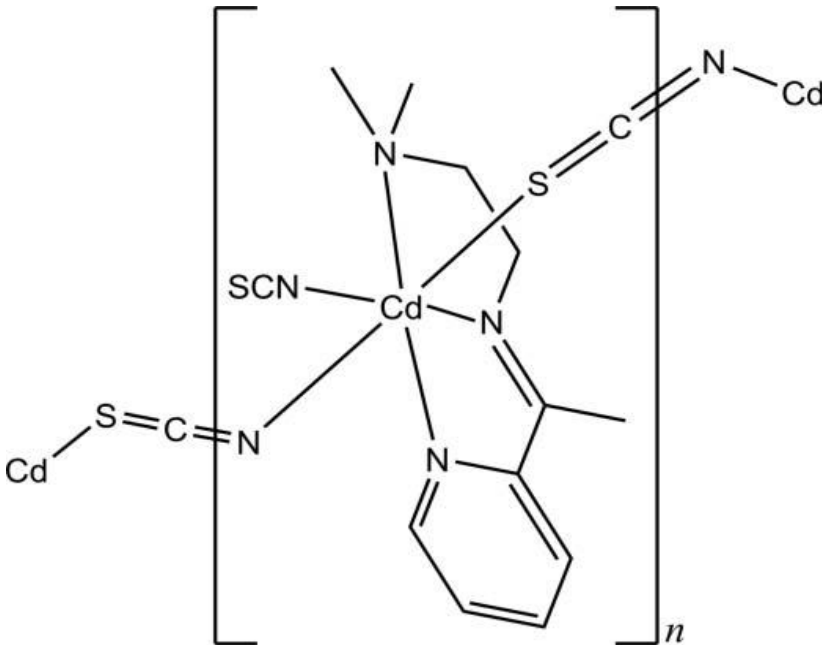

A mixture of 2-acetylpyridine (0.2 g, 1.65 mmol) and *N*,*N*-dimethylethyldiamine (0.15 g, 1.65 mmol) in ethanol (20 ml) was heated under reflux for 2 hr followed by addition of a solution of cadmium(II) acetate dihydrate (0.44 g, 1.65 mmol) and sodium thiocyanate (0.27 g, 3.3 mmol) in a minimum amount of water. The resulting solution was heated under reflux for 30 min, then set aside at room temperature. The crystals of the title compound were obtained in a few days.

2.2.39 Preparation of Bis(l-2-{1-[2-(dimethylamino)ethylimino] ethyl}phenolato)bis [bromido copper(II) monohydrate [$Cu_2(LNH)2Br_2$]

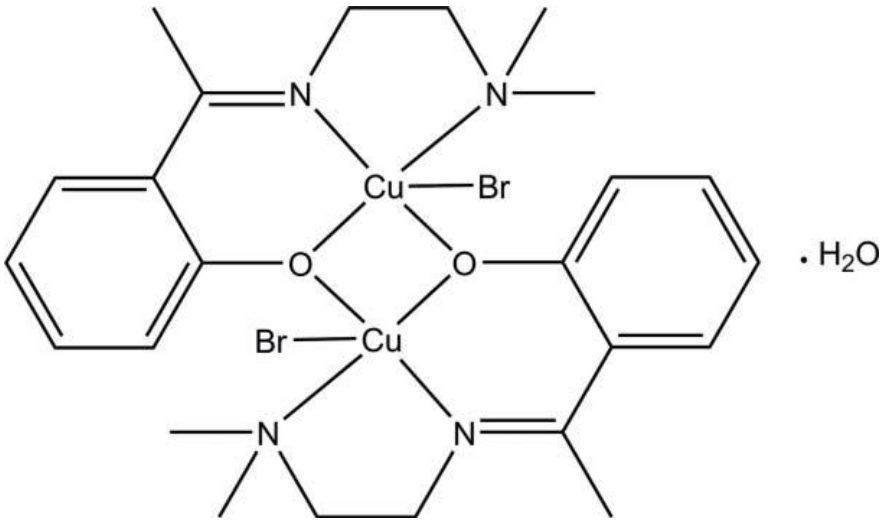

A solution of 2-hydroxyacetophenone (0.20 g, 1.65 mmol) and *N*,*N*-dimethylethyldiamine (0.14 g, 1.65 mmol) in ethanol (20 ml) was stirred at reflux for 2 hr. Then, a solution of copper (I) bromide (0.21 g, 1.65 mmol) in a minimum amount of ethanol was added. The resulting mixture was heated under reflux for 30 min, and then left at room temperature. The crystals of the title complex were obtained in a few days.

2.3 SYNTHESIS OF SECOND SERIES OF HYDRAZONE COMPOUNDS

2.3.1 Preparation of N-(1-(5-Bromo-2-hydroxyphenyl)-ethylidene)-3,4,5-trihydroxybenzo hydrazide

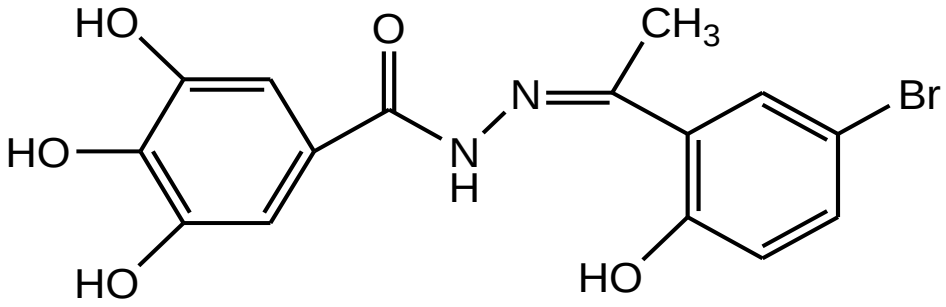

Molecular Weight: 381.18

Gallic hydrazide (1.84 g, 0.01 M) in (20 mL) ethanol was added to an ethanolic solution (20 mL) of 5-bromo-2-hydroxyacetophenone (2.15 g, 0.01 M respectively). The mixture was stirred for 2–3 h whereupon the color of the solution turned yellowish. The pH was adjusted by adding a few drops of dilute HCl. The reaction was continued for another hour resulting in the formation of a yellow precipitate. More precipitate was obtained when reducing the solvent by distillation. The product was collected by filtration, washed several times with ethanol and dried in an oven. (Yield 75%),

2.3.2 Preparation of N-(1-(5-Chloro-2-hydroxyphenyl)-ethylidene)-3,4,5-trihydroxybenzo hydrazide

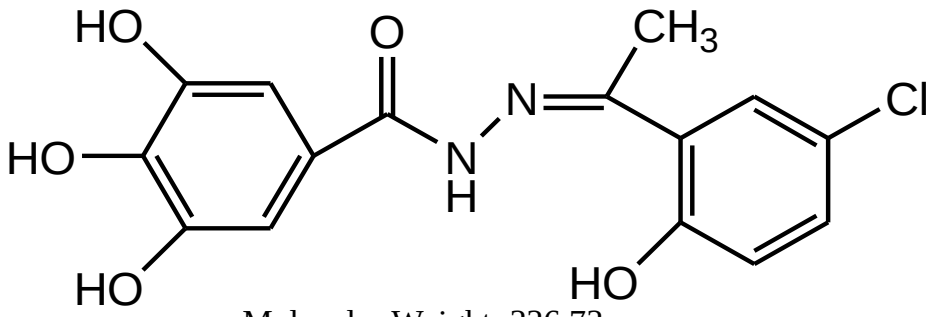

Molecular Weight: 336.73

An accurately weighed amount of gallic hydrazide (1.84 g, 0.01 M) in ethanol (20 mL) was added to the same ethanolic solution (20 mL) of 5-chloro-2-hydroxyacetophenone (2.15 g, 0.01 M), and the mixture was stirred for 2–3 h as the color of the solution turned yellowish. The pH was adjusted by adding few drops of dilute HCl. The reaction was continued for another 1 h to give a yellow precipitate. More precipitate was obtained after reducing the solvent by distillation. The product was collected by filtration, washed several times with ethanol and dried in an oven. (Yield 75%)

2.3.3 Preparation of N-(1-(2-Hydroxy-5-methoxyphenyl)-ethylidene)-3,4,5-trihydroxybenzo hydrazide

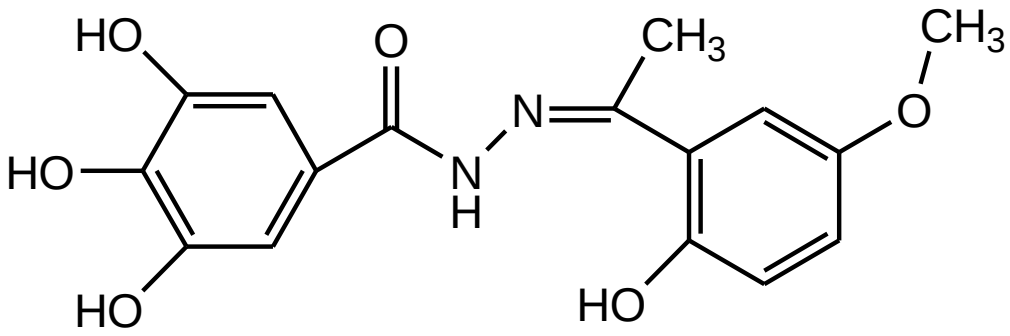

Molecular Weight: 332.31

An ethanolic solution (20 mL) of gallic hydrazide (1.84 g, 0.01 M) was added to an ethanolic solution (20 mL) of 2-hydroxy-5-methoxyacetophenone (1.06 g, 0.01 M) in 1:1 ratio. The mixture was refluxed for 2–3 h resulting in the formation of a slightly yellow precipitate. More precipitate was obtained by removal of some solvent by distillation. The product was collected by filtration, washed several times with ethanol until a milky colored compound is obtained. The ligand was re-crystallized by using the same solvent (ethanol), filtered to remove the suspended impurities and a single crystal was obtained suitable for X-ray analysis. (Yield = 65%)

2.3.4 Preparation of 3,4,5-Trihydroxybenzoic Acid [1-Pyridylethylidene] Hydrazide

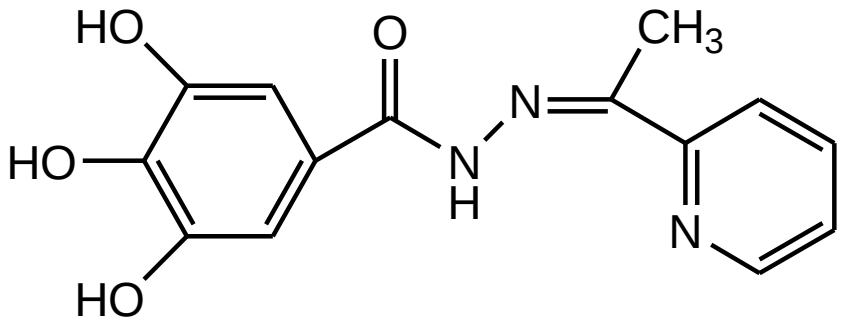

Molecular Weight: 287.27

A stoichiometric amount of gallic hydrazide (1.84 g, 0.01 M) in ethanol (20 mL) was added to a solution (20 mL) of 2-acetylpyridine (1.21 mL, 0.01 mmol) and the mixture was refluxed on a water bath for 2–3 h, resulting in the formation of a small amount of white precipitate. More precipitate was obtained after evaporating the solvent by distillation. The product was then collected by filtration, washed several times with ethanol until white powder product was formed. The white powder ligand was recrystallized by using DMF to obtained single crystals for X-ray structural determination. (Yield = 65%)

2.3.5 Preparation of N'-(1-(6-Acetylpyridin-2-yl)ethylidene)-3,4,5-trihydroxybenzo hydrazide

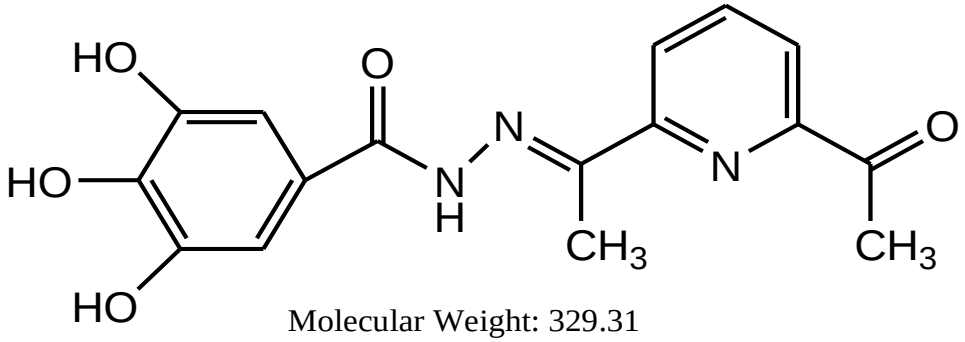

Molecular Weight: 329.31

A weighed amount of gallic hydrazide (1.84 g, 0.01 M) in (20 mL) ethanol was added to the same volume (20 mL) of ethanolic solution of 2,6-diacetylpyridine (1.63 g, 0.01 M). The mixture was stirred for 2–3 h while the color of the solution turned yellowish. The pH was adjusted by adding few drops of dilute HCl. The reaction was continued for another one hour resulting in the formation of a yellow precipitate. The product was collected by filtration, washed several times with ethanol and dried in an oven. (Yield 90%)

2.3.6 Preparation of 2'-[1-(2-hydroxyphenyl) ethylidene] benzenesulfanohydrazide

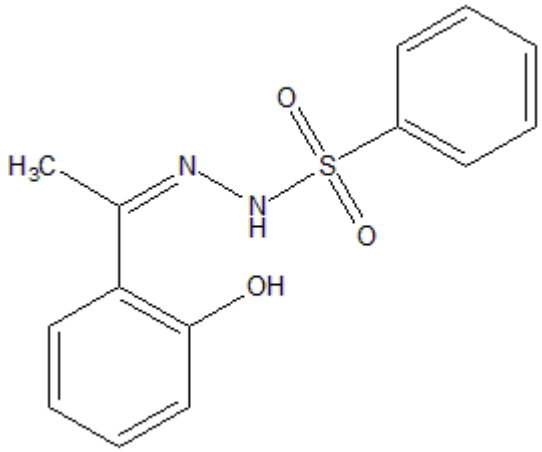

Benzenesulfanohydrazide (0.690 g, 0.0035mol) was accurately weighed on a digital balance in a 100 ml beaker and dissolved in 50 mL acidified ethanol (95;5, ethanol:acetic acid); 2-hydroxyacetophenone (0.60 g, 0.0035 mol) was also dissolved in another sample of acidified ethanol (50 mL). The two solutions were mixed together in a 500 mL flat bottom flask which was then clamped on a water bath and refluxed on a magnetic hot plate for 2 h while stirring. The resulting yellow precipitate was filtered into a conical flask and re-crystallized in ethanol to yield pale yellow crystals.

2.3.7 Synthesis of 2'- (5-chloro -2-hydroxy benzylidene) benzenesulfanohydrazide

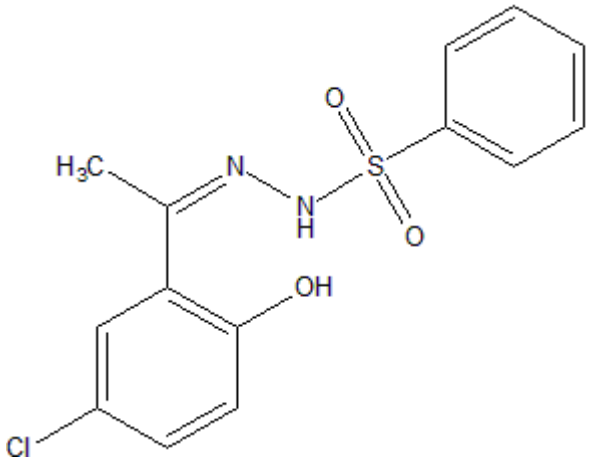

Benzenesulfanohydrazide (0.690 g, 0.0035mol) was accurately weighed on a digital balance in a 100 ml beaker and dissolved in 50 mL acidified ethanol (95;5, ethanol:acetic acid); 5'-chloro-2'-hydroxyacetophenone (0.60 g, 0.0035 mol) was also dissolved in another sample of acidified ethanol (50 mL). The two solutions were mixed together in a 500 mL flat bottom flask which was then clamped on a water bath and refluxed on a magnetic hot plate for 2 h while stirring. The resulting yellow precipitate was filtered into a conical flask and re-crystallized in ethanol to yield pale yellow crystals.

2.3.8 Synthesis of Zinc(II) complex of 2'-[1-(2-hydroxyphenyl) ethylidene] benzenesulfanohydrazide

A solution of zinc(II) acetate (0.15 g, 0.0006 mole) in basified ethanol (50 ml) was mixed with a (50 ml) ethanolic solution of 20-[1-(2-hydroxyphenyl) ethylidene] benzenesulfonyl hydrazide (0.35 g, 0.0012 mol) at a 1:2 M ratio. The mixture was stirred and refluxed for 5 h. Dark brown solid was formed. Yield =65%

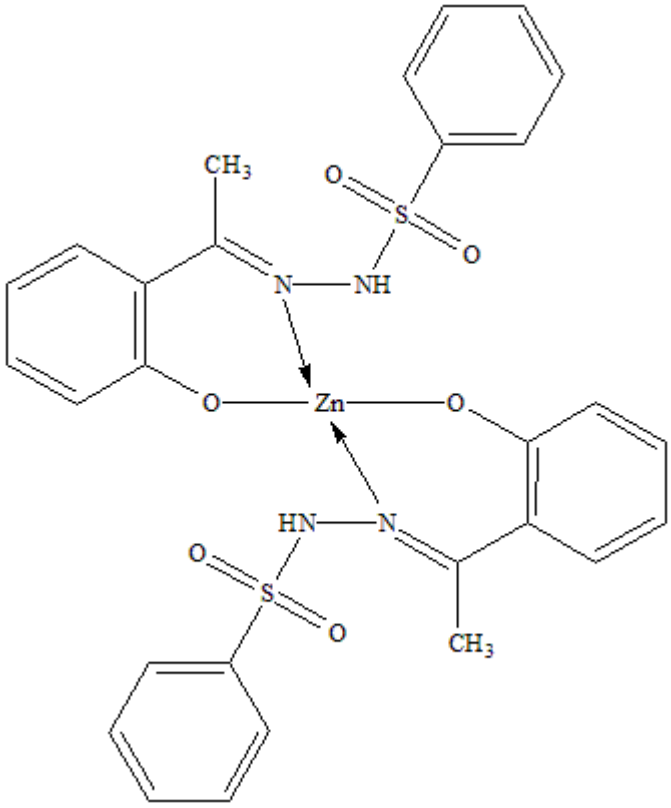

RESULTS AND DISCUSSION

3.0 General characterization of Synthesized Compounds

This part of the research thesis comprises of six types of ligands divided into two series which showed different modes of coordination. The first series of ligands involved an *N,N',N''*-donor Schiff base ligands from the reaction of 2-acetylpridine with four different amines: 4-(2-aminoethyl)morpholine (**LMA**), 4-(2-aminoethyl)piperazine (**LPA**), 4-(2-aminoethyl)piperidine (**LPiA**) and *N,N'*-dimethylethylenediane (**LNA**). The second series are *N,N',O*-donor Schiff bases from the condensation reaction of 2-hydroxyacetophenone with two amines *viz:* 4-(2-aminoethyl)morpholine (**LMH**), and *N,N'*-dimethylethylenediane (**LNH**). The ligands were reacted with most of the transition metal acetates in presence of Cl^-, Br^-, I^- and SCN^- ions derived from hydrochloric acid (HCl), potassium bromide (KBr), sodium iodide (NaI) and sodium thiocyanate (NaSCN) respectively. For the set of the complexes, the respective ligands were mixed in different ratios in ethanol and refluxed for 2-3hours. In most of the complexes an *in situ* method was used in which the ligands were not isolated and the ethanolic solutions of metal acetates and chlorides with different salts were used. The ligands and complexes were characterized by elemental analysis, spectroscopic techniques such as IR, NMR, UV/Visible and X-Ray crystallography.

3.1 Physico-Chemical properties of the compounds

Table 3.1: Physical properties for 2-morpholino-N-(1-(pyridin-2-yl)ethylidene)ethanamine (LMA) and metal complexes.

Compound	Mol.W. (g/mol)	Melting Point	Yield (%)	Color	Elemental Percentage (%) Calculated (Found)		
					C	H	N
LMA (Liq)	233.31	-	62	Orange	66.92	8.21	18.01
$[Mn(LMA)Cl_2]$	359.15	>350	82	Brown	43.47(43.74)	5.33(5.34)	11.70(11.70)
$[Mn(LMA)(NCS)_2.H_2O]$	422.43	>380	86	Reddish	42.65(42.64)	5.01(5.05)	16.58(16.58)
$[Co(LMA)Cl_2]$	363.15	>370	60	Brownish	43.00(43.10)	5.27(5.44)	11.57(12.07)
$[Co(LMA)(N_3)_3]$	418.30	>400	95	Brown	41.85(40.65)	5.67(5.60)	28.16(28.32)
$[Co(LMA)(NCS)_2.H_2O]$	426.42	>400	78	Pink	42.25(42.55)	4.96(5.06)	16.42(16.42)
$[Ni(LMA)NCS_2.H_2O]$	426.18	>400	80	Green	42.27(42.31)	4.97(4.98)	16.43(16.43)
$[Cu(LMA)Cl_2]$	367.76	>360	90	Greenish	42.46(42.19)	5.21(5.11)	11.43(11.39)
$[Cu(LMA)(NCS)_2.H_2O]$	413.02	>365	82	Blue	43.62(43.61)	4.64(4.64)	16.96(16.99)
$[Zn(LMA)Br_2]$	458.51	>400	85	Milky	30.89(30.79)	3.79(3.49)	8.31(8.28)
$[Zn(LMA)Cl_2]$	369.61	>370	90	White	42.24(42.24)	5.18(5.18)	11.37(11.37)
$[Zn(LMA)I_2]$	552.51	>400	55	Brown	28.26(29.26)	3.47(3.67)	7.61(7.51)
$[Zn(LMA)(NCS)_2]$	414.86	>375	81	White	43.43(43.45)	4.62(4.62)	16.88(16.54)
$[Zn(LMA)(N_3)_2]$	382.74	>355	88	White	40.80(40.88)	5.00(5.10)	32.94(32.98)
$[Cd(LMA)Br_2]$	416.63	>400	81	White	37.48(37.28)	4.60(4.45)	10.09(10.19)
$[Cd(LMA)Cl_2]$	505.53	>400	76	Milky	34.85(34.92)	4.27(4.17)	9.38(9.77)
$[Cd(LMA)(N_3)_2.H_2O]$	447.78	>375	90	White	34.87(34.88)	4.73(4.74)	28.15(28.17)

Table 3.2: Physical properties for 2-(1-(2-morpholinoethylimino)ethyl)phenol (LMH) and metal complexes.

Compound	**Mol. Weight (g/mol)**	**Melting Point(^{o}C)**	**Yield (%)**	**Color**	**Elemental Percentage (%) Theory (Experimental)**		
					C	H	N
LMH (Liq.)	248.15		55	Yellow	67.71	8.12	11.28
[Mn(LMH)Br]	382.15	>400	65	Brown	44.00(43.97)	5.01(5.17)	7.33(7.40)
[Mn(LMH)Cl]	337.70	>385	73	Reddis	49.79(48.99)	5.67(5.54)	8.30(8.40)
[Ni(LMH)Br]	385.91	>400	68	Greeni	43.57(44.00)	4.96(5.01)	7.26(7.28)
[Ni(LMH)Cl]	341.46	>365	76	Green	49.24(49.25)	5.61(5.63)	8.20(8.50)
[Cu(LMH)Br]	390.76	>360	78	Brown	43.03(43.19)	4.90(4.11)	7.17(7.29)
[Cu(LMH)Cl]	346.31	>350	83	Blue	48.55(48.49)	5.53(5.71)	8.09(8.39)
[Zn(LMH)Br]	392.61	>355	87	Milky	42.83(42.94)	4.88(4.88)	7.14(7.24)
[Zn(LMH)Cl]	348.16	>400	82	White	48.30(48.48)	5.50(5.79)	8.05(8.98)
LPA (Liq.)	232.17	-	40.3	Orange	67.21	8.68	24.12
$[Zn_3(LPA)_2Cl_4]$	891.55	>400	68	White	35.03(35.21)	4.75(4.88)	12.57(12.60)
LPiA (Liq.)	231.34	-	49	Orange			
$[Zn(LPiA)Cl_2]$	367.63	>360	75	White	45.74(45.75)	5.76(5.81)	11.43(11.46)
[Zn(LPiA)(NCS)		>365	69	Yellow			

Table 3.3: Physical properties for *N1,N1*-dimethyl-*N2*-(1-(pyridin-2-yl)ethylidene)ethane-1,2-diamine (LNA) and complexes

Compound	**Mol. Weight (g/mol)**	**Melting Point**	**Yield (%)**	**Color**	**Elemental Percentage (%) Theory (Experimental)**		
					C	H	N
LNA (Liq.)	191.27		54	Orange	69.87	8.80	13.58
$[Mn(LNA)Cl_2]$	327.57	>350	82	White	40.33(40.63)	5.23(5.43)	12.83(13.03)
$[Cu(LNA)(NCS)_2]$	372.83	>385	68	White	35.27(35.17)	4.57(4.67)	11.22(11.21)
$[Zn(LNA)Cl_2]$	370.98	>400	62	Green	42.09(41.99)	4.62(4.62)	18.88(18.87)
$[Zn(LNA)(NCS)_2]$	384.15	>375	72	Green	40.65(40.85)	4.99(5.00)	18.23(18.82)
$[Zn(LNA)(N_3)_2]$	458.50	>350	61	White	-	-	-
$[Cd(LNA)Cl_2]$	374.59	>400	74	White	35.27(35.36)	4.57(4.64)	11.22(11.22)
$[Cd(LNA)(NCS)_2]$	317.12	>350	84	Brown	41.66(41.68)	5.40(5.41)	13.25(13.25)

Table 3.4: Physical properties for 2-(1-(2-(dimethylamino)ethylimino)ethyl)phenol (LNH) and complexes

Compound	**Mol.Weight (g/mol)**	**Melting Point (^oC)**	**Yield (%)**	**Color**	**Elemental Percentage (%) Theory (Experimental)**		
					C	H	N
LNH (Liq.)	206.28	-	59	Yellow	69.87	8.80	13.58
[Mn(LNH)Br]	340.12	>400	65	Brown	42.38(42.97)	5.04(5.17)	8.24(8.40)
[Mn(LNH)Cl]	295.67	>385	73	Reddish	48.75(48.99)	5.80(5.84)	9.47(9.50)
[Ni(LNH)Br]	343.87	>400	68	Brown	41.91(42.00)	4.98(5.01)	8.15(8.28)
[Ni(LNH)Cl]	299.42	>365	76	Green	48.14(49.25)	5.72(5.73)	9.36(9.50)
$[Cu_2(LNH)_2Br_2]$	715.47	>400	85	Blue	40.29(40.88)	5.07(5.20)	7.83(7.93)
[Cu(LNH)Br]	348.73	>360	80	Brown	41.33(42.19)	4.91(4.91)	8.03(8.29)
[Cu(LNH)Cl]	304.28	>360	72	Green	47.37(48.19)	5.63(6.11)	9.21(9.39)
[Zn(LNH)Br]	350.57	>355	87	Yellow	41.11(42.94)	4.89(4.98)	7.99(7.99)

In summary Tables 3.1, 3.2, 3.3 and and 3.4 above presented physical properties of the synthesized compounds which includes; molecular weight, melting points, percentage yield, colors and elemental analysis data for ligands and their respective metal complexes. The calculated values for the elemental analysis (CHN analysis) are in a good agreement with the experimental value found.

3.2 Infrared Spectral analysis for the compounds

Aromatic compounds show useful characteristic infrared bands in five regions of the mid-infrared spectrum. The v(C–H) stretching bands of aromatic compounds appear in the 3100–3000 cm^{-1} range, so making them easy to differentiate from those produced by aliphatic v(C–H) groups which appear below 3000 cm^{-1}. In the 2000–1700 cm^{-1} regions, a series of weak combination and overtone bands appear and the pattern of the overtone bands reflects the substitution pattern of the benzene ring. Skeletal vibrations, representing v(C=C) stretching, absorb in the 1650–1430 cm^{-1} range. The v(C–H) bending bands appear in the regions 1275–1000 cm^{-1} (in-plane bending) and 900–690 cm^{-1} (out-of plane bending). The bands of the out-of-plane bending vibrations of aromatic compounds are strong and characteristic of the number of hydrogen in the ring, and hence can be used to give the substitution pattern.

The IR spectra of transition metal complexes were recorded in 4000–400 cm^{-1} range. The characteristic IR stretching frequencies of the metal complexes along with their proposed assignments are summarized in Table 3.5 below. There are similarities in the IR spectrum of the metal complexes to each other, except for some slight variations in the shifts and intensities of few vibration peaks caused by different metal(II) ions, indicating that the metal complexes had similar structure. However, there were some significant differences between the metal(II) halides complexes and that of the azides and thiocyanate complexes, as expected.

Table 3.5. Some of the important IR bands in (cm^{-1}) for 2-morpholino-N-(1-(pyridin-2-yl)ethylidene)ethanamine (LMA) and metal complexes.

Compound	**ν(C-H)**	**ν(NCS/N_3)**	**ν(C=N)**	**ν(C-C)**	**ν(C-N)**	**ν(M-N)**
LMA	2972	-	1642	1451	1113	-
[Mn(LMA)Cl_2]	2938	-	1650	1464	1109	555
[Mn(LMA)$(NCS)_2H_2O$]	2974	2082	1651	1442	1165	568
[Co(LMA)Br_2]	3033	-	1654	1438	1121	557
[Co(LMA)Cl_2]	3106	-	1652	1441	1107	516
[Co(LMA)$(N_3)_3$]	2944	1992	1646	1428	1112	572
[Co(LMA)$(NCS)_2H_2O$]	2880	2071	1650	1435	1110	563
[Ni(LMA)NCS_2 H_2O]	2880	2082	1652	1441	1107	516
[Cu(LMA)Br_2]	2980	-	1652	1441	1107	516
[Cu(LMA)Cl_2]	2949	-	1655	1443	1144	577
[Cu(LMA)N_3]	2979	2066	1659	1446.	1145	573
[Cu(LMA)$(NCS)_2H_2O$]	2964	2086	1656	1444	1115	523
[Zn(LMA)Br_2]	2959	-	1649	1439	1114	561
[Zn(LMA)Cl_2]	3069	-	1654	1438	1121	557
[Zn(LMA)I_2]	2956	-	1652	1433	1119	558
[Zn(LMA)$(NCS)_2$]	2874	2070	1654	1433	1118	566
[Zn(LMA)$(N_3)_2$]	2965	2069	1657	1461	1114	565
[Cd(LMA)Br_2]	2957	-	1652	1433	1119	558
[Cd(LMA)Cl_2]	2962	-	1650	1458	1115	556
[Cd(LMA)$(N_3)_2H_2O$]	2951	2045	1649	1438	1110	552

The IR spectra of LMA ligand and series of complexes (Figure 3.2.1 - 3.2.4) and Table 3.5 possess characteristic absorption bands in the region of 1665-1640 cm^{-1} which is attributed to the ν(C=N) stretching vibration of the Schiff base imino functional group (Yusnita, 2009; Raman and Khan, 2011). The characteristics frequencies appeared in the spectra of all complexes in the region of 3110-2874 cm^{-1} assignable to ν(C-H/NH) group. The ν(OH) stretching frequency appeared in the spectra of the ligand as broad bands in wave number of 3340cm^{-1}. This is due to the presence of water molecules, located outside the coordination sphere (Maeda, 1999). For thiocyanates and azide complexes chemical shifts were observed in the region of 2090-1990 attributable to metal coordination (Banerjee and Chattopadhyay, 2005). The spectra for the complex showed ν(M–N) bands at a lower wavelength in the range of 580-515 cm^{-1} (Mohamed, 2009; Shahabadi, 2010).

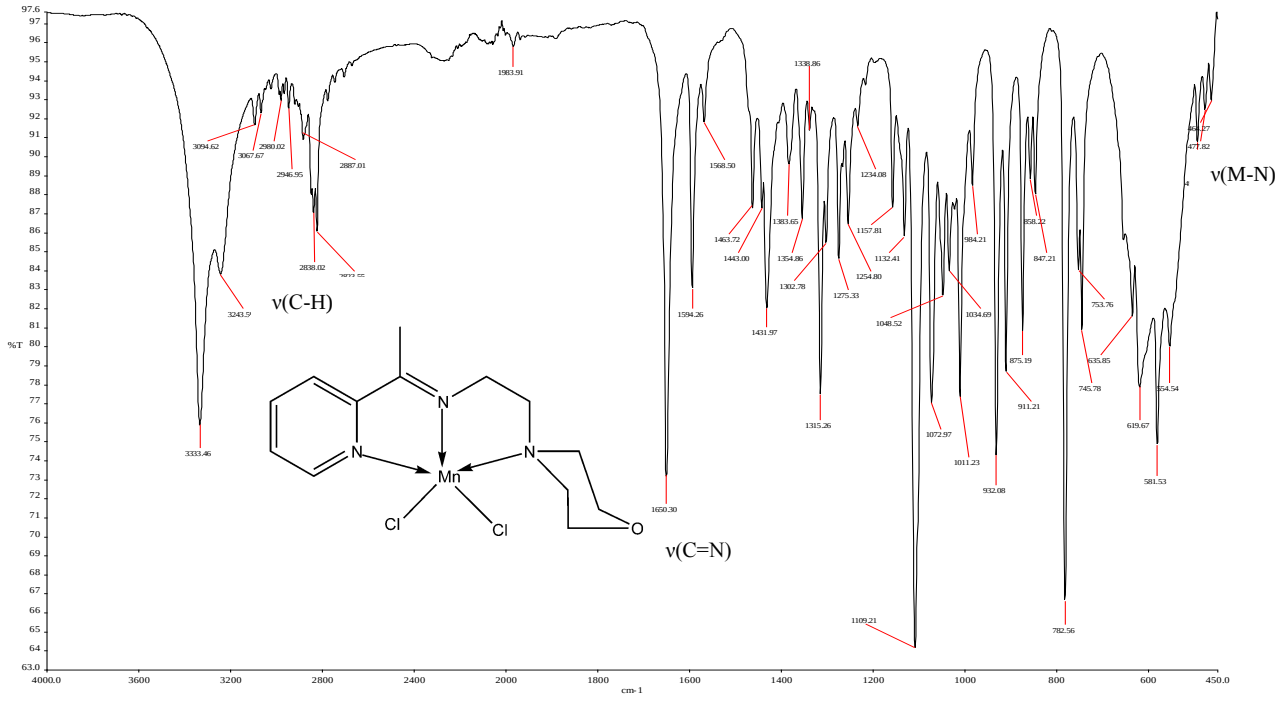

Figure 3.2.1: IR spectra of [Mn(LMA)Cl2]

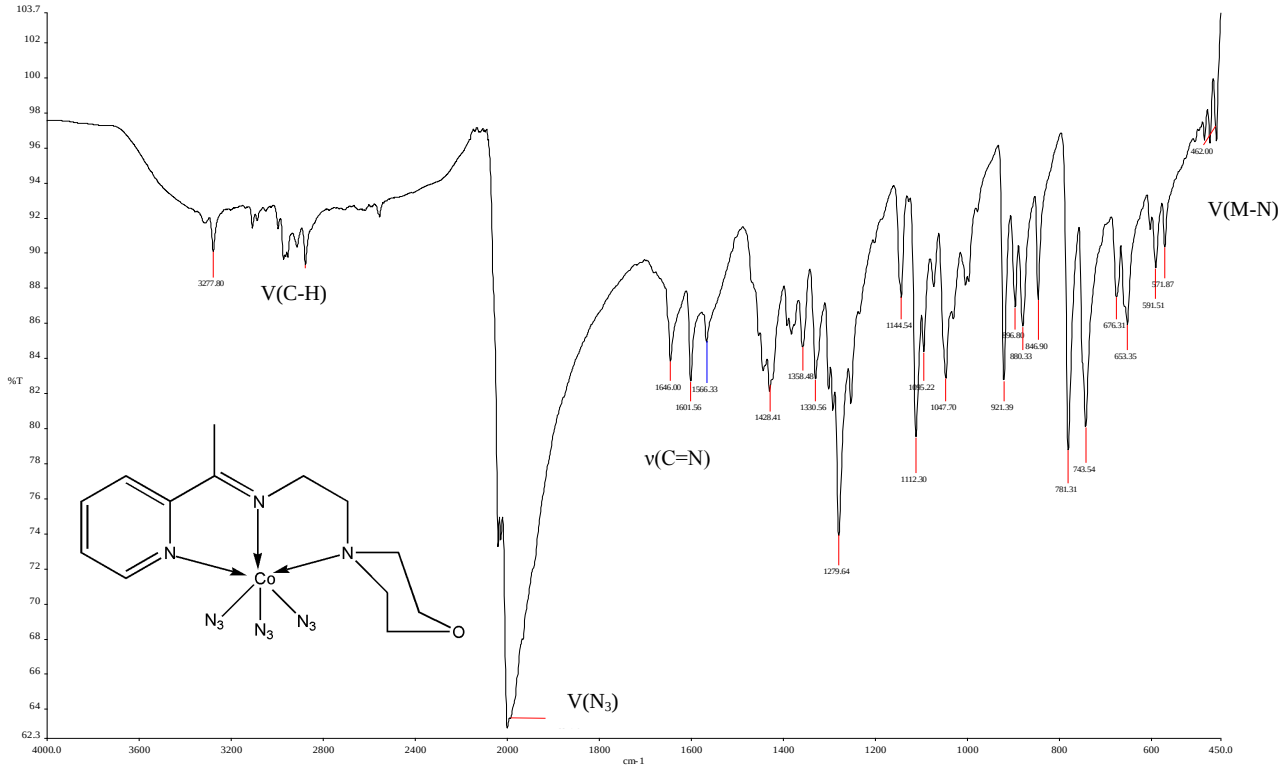

Figure 3.2.2: IR spectra of $[Co(LMA)(N_3)_3]$

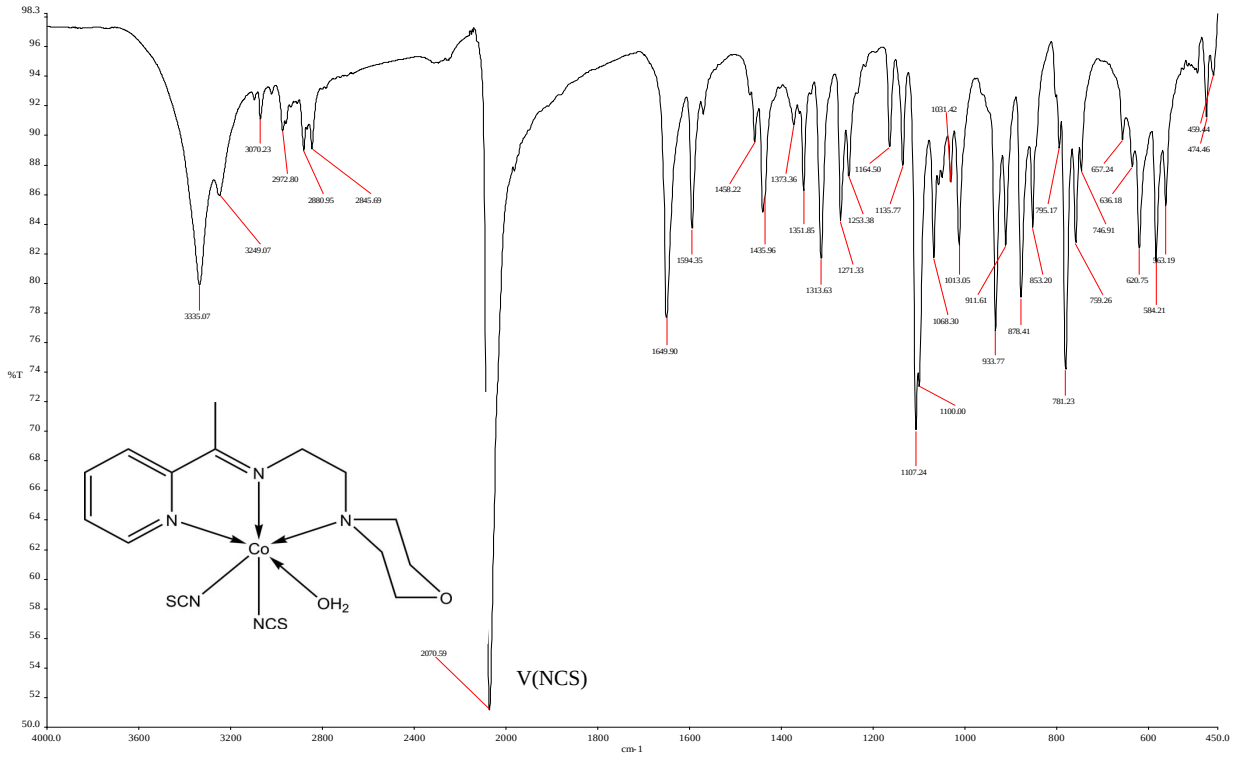

Figure 3.2.3: IR spectra of $[Co(LMA)(NCS)_2H_2O]$

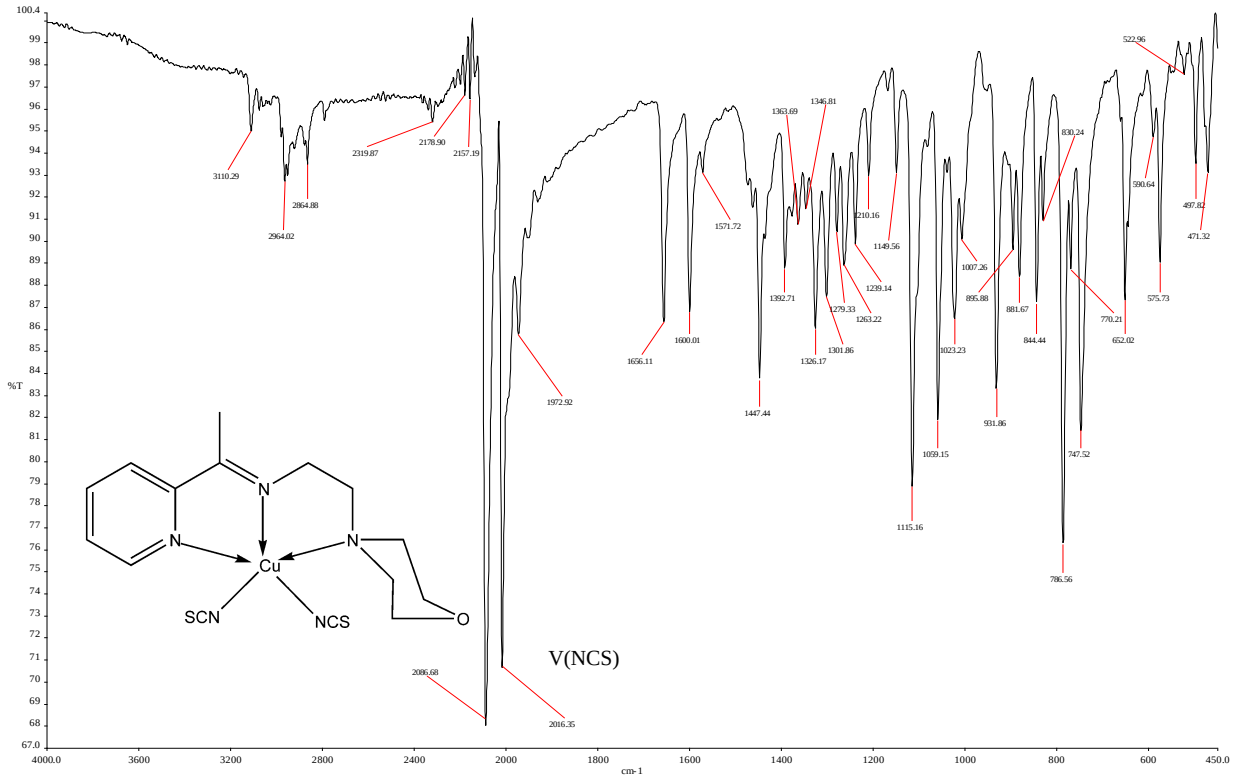

Figure 3.2.4: IR spectra of $[Cu(LMA)(NCS)_2]$

Table 3.6: Some of the important IR bands (cm^{-1}) for 2-(1-(2-morpholinoethylimino)ethyl)phenol (LMH) and metal complexes.

Compound	**ν(C-H)**	**ν(C=N)**	**ν(C-C)**	**ν(C-N)**	**ν(M-N)**	**ν(M-O)**
LMH	2952	1611	1448	1113	-	-
[Mn(LMH)Br]	2838	1650	1464	1109	555	462
[Mn(LMH)Cl]	2974	1651	1442	1165	522	461
[Ni(LMH)Br]	2980	1597	1441	1157	516	492
[Ni(LMH)Cl]	2943	1605	1436	1102	518	474
[Cu(LMH)Br]	3109	1664	1428	1125	531	473
[Cu(LMH)Cl]	2972	1580	1432	1113	526	493
[Zn(LMH)Br]	3076	1654	1438	1121	557	454
[Zn(LMH)Cl]	2984	1654	1438	1115	541	453

The IR spectra of the free ligand (**LMH**) and corresponding complexes exhibit various bands in the **400-4000** cm^{-1} region (Figure 3.2.6 and 3.27). The ν(O-H) stretching frequency of the free ligand is found in the 3397.19 cm^{-1} region as expected (Figure 3.2.5). The coordination of the ligand to the metal center could be determined by comparing the IR spectra of the metal complexes with their respective ligands and are mainly elucidated by the disappearance of hydroxyl group of the ligand (O-H) and the formation of new metal-oxygen (M-O) and metal-nitrogen (M-N) bands. Nonetheless, the assignment of ν(M-O) and ν(M-N) bands at the lower region seems to be due to the interference with the vibration signals of the ligand.

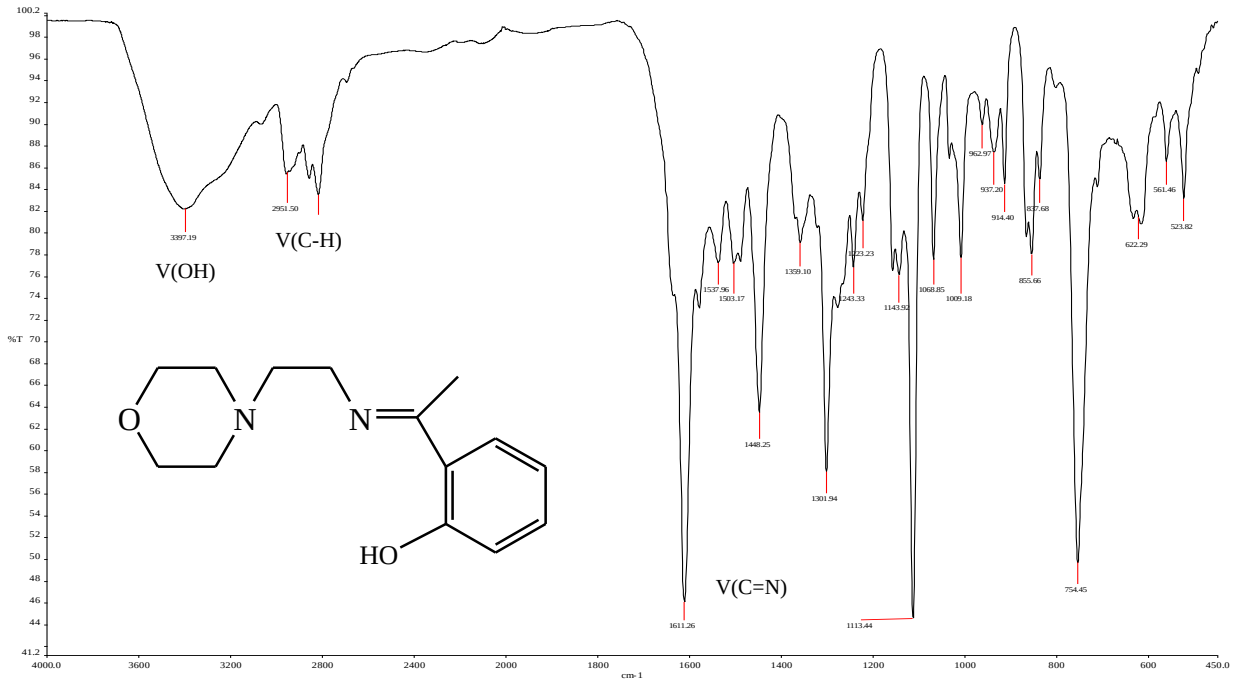

Figure 3.2.5: IR spectra of LMH

The band at 1611cm^{-1} is attributed to the ν(C=N). Upon chelation, a shift to a different wave number in the region of 1664-1580cm^{-1}, indicates a change in the bond order due to coordination of the metal atom to the azomethine nitrogen lone pair. This small shift of ν(C=N) was also reported in the previous studies (Leovac, 2008). We considered differences caused by the difference of the strength of the ν(M-O) and ν(M-N) bonding in the various complexes. In the complexes, the closed-shell metal ions react primarily with the negatively charged oxygen; the ν(M-O) bonding plays a more important role than the ν(M-N) bonding. On the other hand, transition metal ions in group complexes react primarily with the covalent nitrogen, the ν(M-N) bonding is stronger than the ν(M-O) bonding. That is, the ν(M-N) bonding plays a more important role in the complexes. These results are in agreement with Pearson's soft-hard acid-base theory.

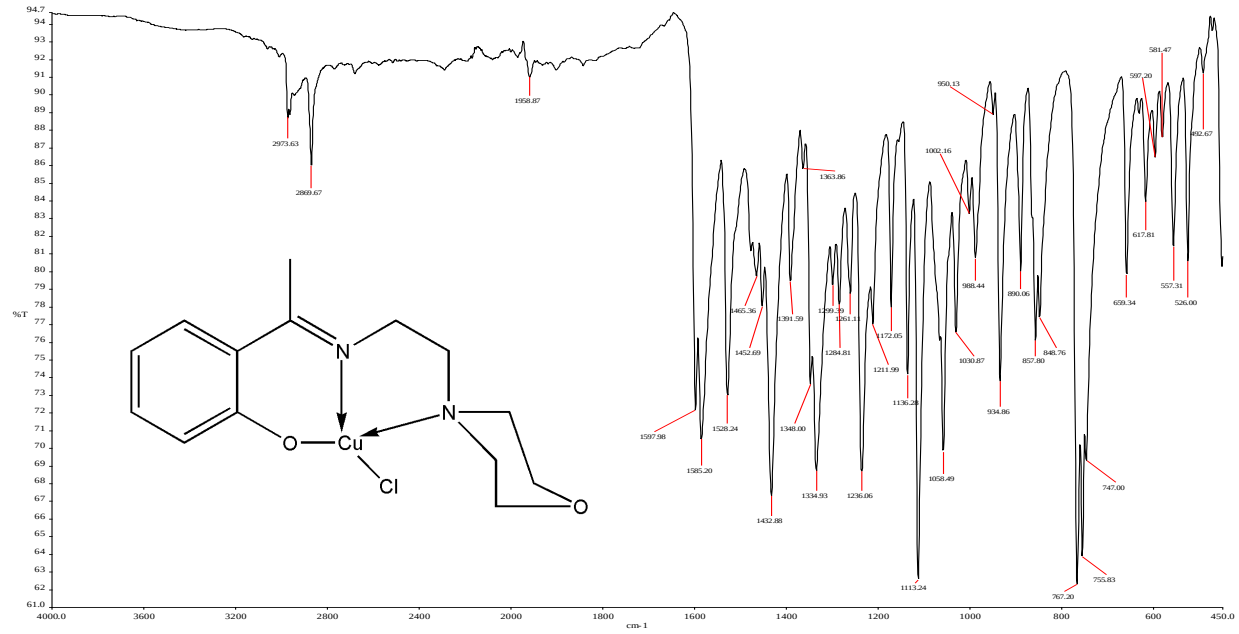

Figure 3.2.6: IR spectra of [Cu(LMH)Cl]

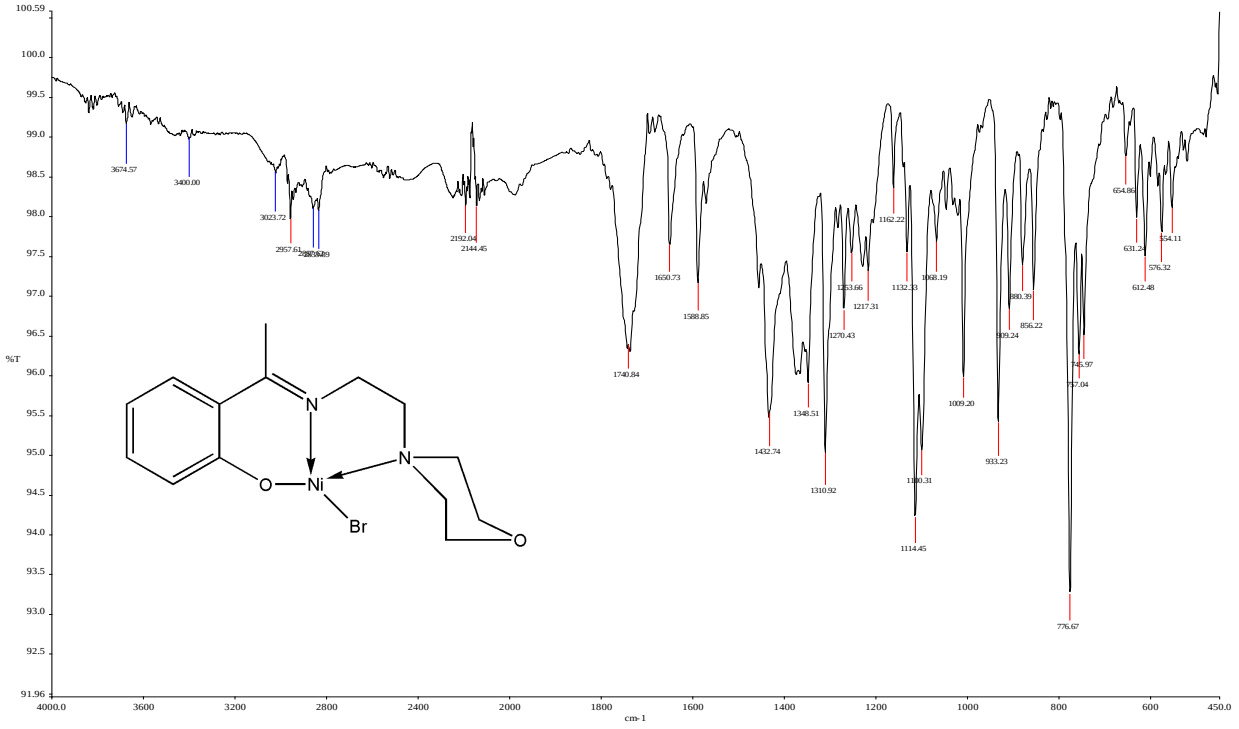

Figure 3.2.7: IR spectra of [Ni(LMH)Br]

Table 3.7: Some of the important IR bands for 2-(piperazin-1-yl)-N-(1-(pyridin-2-yl)ethylidene)ethanamine (LPA)

Compound	**ν(C-H)**	**V(NCS)**	**ν(C=N)**	**ν(C-C)**	**ν(C-N)**	**ν(M-N)**
LPA	2945		1640	1437	1132	-
$[Zn_3(LPA)_2Cl_6]$	2953		1654	1439	1130	576
$[Cd_4(LPA)_2(PA)_2(Cl)_8$	3221		1654	1438	1121	556

The IR spectra of (**LPA**) ligand and series of complexes (Figure Appendix) possess very strong characteristic absorption bands in the region of 1660-1640 cm^{-1} which is attributed to the ν(C=N) stretching vibration of the Schiff base imino functional group. The characteristics frequencies appeared in the spectra of all complexes at region of 3220-2950 cm^{-1} assignable to ν(C-H/NH) group. The spectra for the complex showed ν(M–N) bands at a lower wavelength in the range of 570-550 cm^{-1} (Mohamed, 2009; Shahabadi, 2010).

Table 3.8: Some of the important IR bands for 2-(piperidin-1-yl)-*N*-(1-(pyridin-2-yl)ethylidene)ethanamine (LPiA) with their metal complexes.

Compound	**ν(C-H)**	**V(NCS)**	**ν(C=N)**	**ν(C-C)**	**ν(C-N)**	**ν(M-N)**
LPiA	2736	-	1638	1458	1116	-
$[Zn(LPiA)Cl_2]$	2958	2080	1626	1449	1120	566
$[Zn(LPiA)(NCS)_2]$	3223	2079	1624	1438	1121	556

In the IR spectrum (of **LPiA)** and series of complexes (Figure 3.2.8 and 3.2.9) possess the medium and sharp bands at 2.30 cm^{-1} assigned to thev(N-H) stretching vibration; however, the strong absorption bands at 1640-1660 cm^{-1} in the complexes are assigned to the stretching vibration of the azomethine groups (Yusnita, 2009) The intense absorptions at 550 cm^{-1} and 580 cm^{-1} for are assigned to the stretching vibration of the ν(M-N) groups (Mohamed , 2009; Shahabadi, 2010).

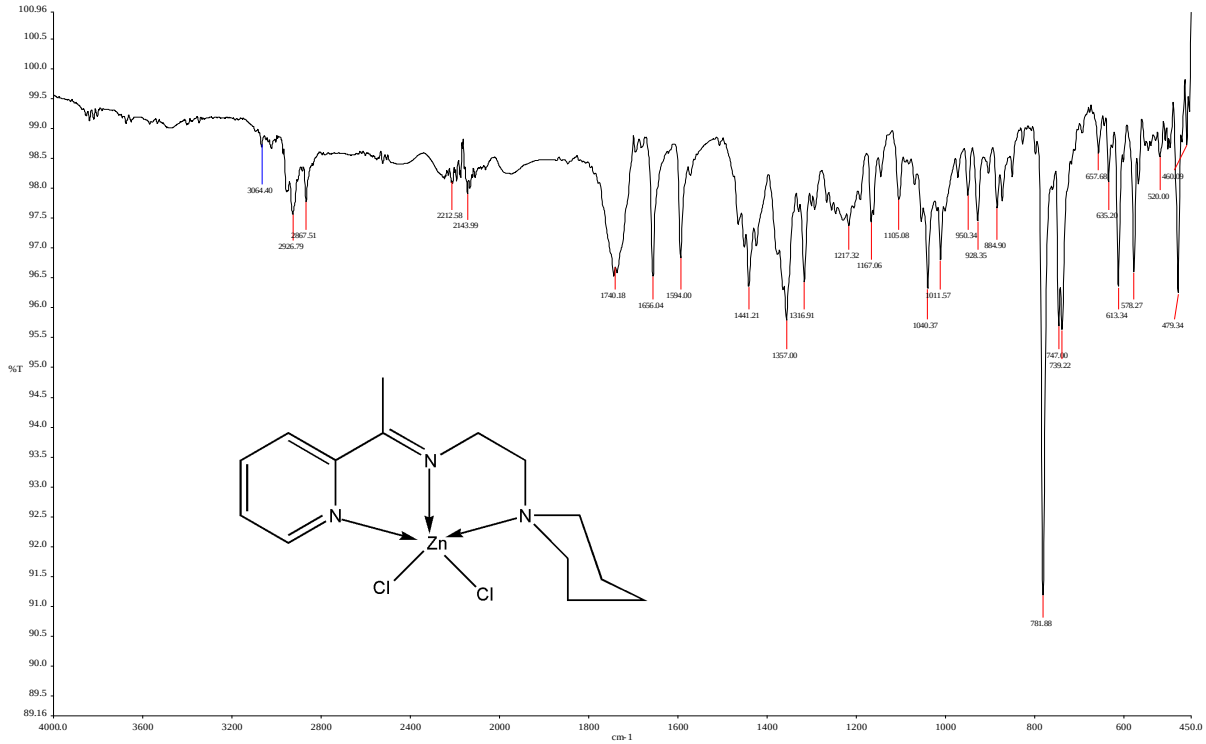

Figure 3.2.8: IR spectra of [Zn(LPiA)Cl2]

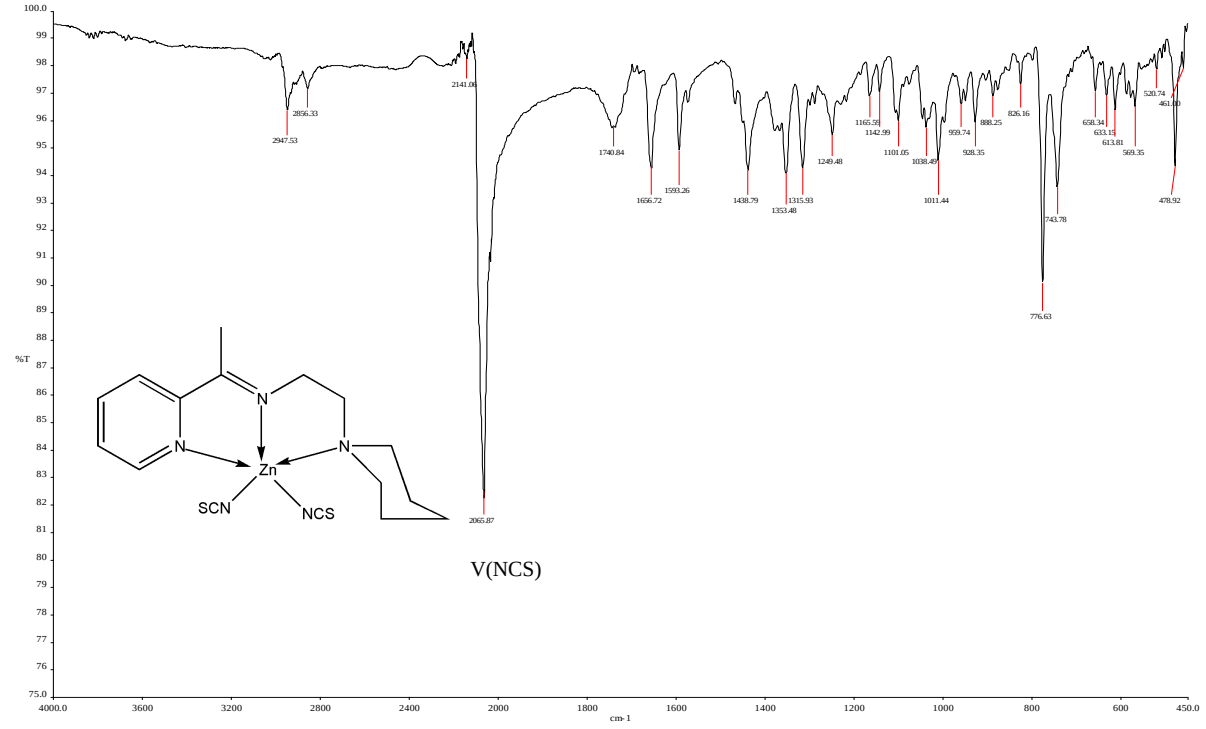

Figure 3.2.9: IR spectra of [Zn(LPiA)(NCS)2]

Table 3.9: Some of the important IR bands for *N1,N1*-dimethyl-*N2*-(1-(pyridin-2-yl)ethylidene)ethane-1,2-diamine (LNA) and metal complexes.

Compound	**ν(C-H)**	**ν(NCS/N_3)**	**ν(C=N)**	**ν(C-C)**	**ν(C-N)**	**ν(M-N)**
LNA	2946	-	1639	1435	1103	-
[Mn(LNA)Cl_2]	2838,	-	1650	1464	1109	554
[Ni(LNA)$(NCS)_2H_2O$]	2880	2082	1652	1441	1107	515
[Cu(LNA)$(NCS)_2$]	2979	2066	1659	1446	1144	573
[Zn(LNA)Cl_2]	2852	-	1661	1443	1139	575
[Zn(LNA)$(NCS)_2$]	2849	2070	1655	1438	1139	577
[Cd(LNA)$(NCS)_2$]n	2863	2116	1661	1436	1160	559

The characteristic IR stretching frequencies of the ligand (**LNA**) (Figure 3.2.10) showed bands at 2946cm^{-1} assignable to v(C-H) group. The strong band of the azomethine group v(C=N) occurred at range of 1642 cm^{-1}. In the spectra of the complexes (Figure 3.2.11 - 13), v(C=N) band signal shifted to the different frequencies indicating that the coordination of the ligand to metal ion occurs through nitrogen atom of the imine group (Li, 2011). The IR spectrum of the metal complexes are similar to each other, except for some slight variations in the shifts and intensities of few vibration peaks caused by different metal(II) ions, indicating that the metal complexes had similar structure.

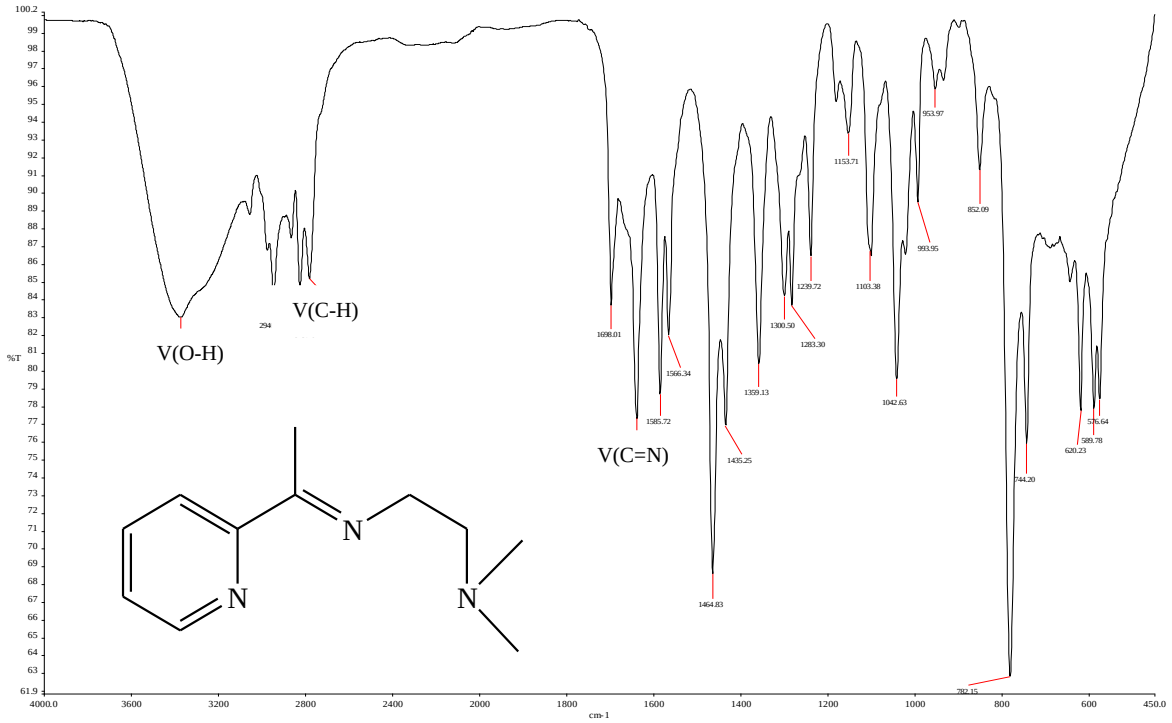

Figure 3.2.10: IR spectra of LNA

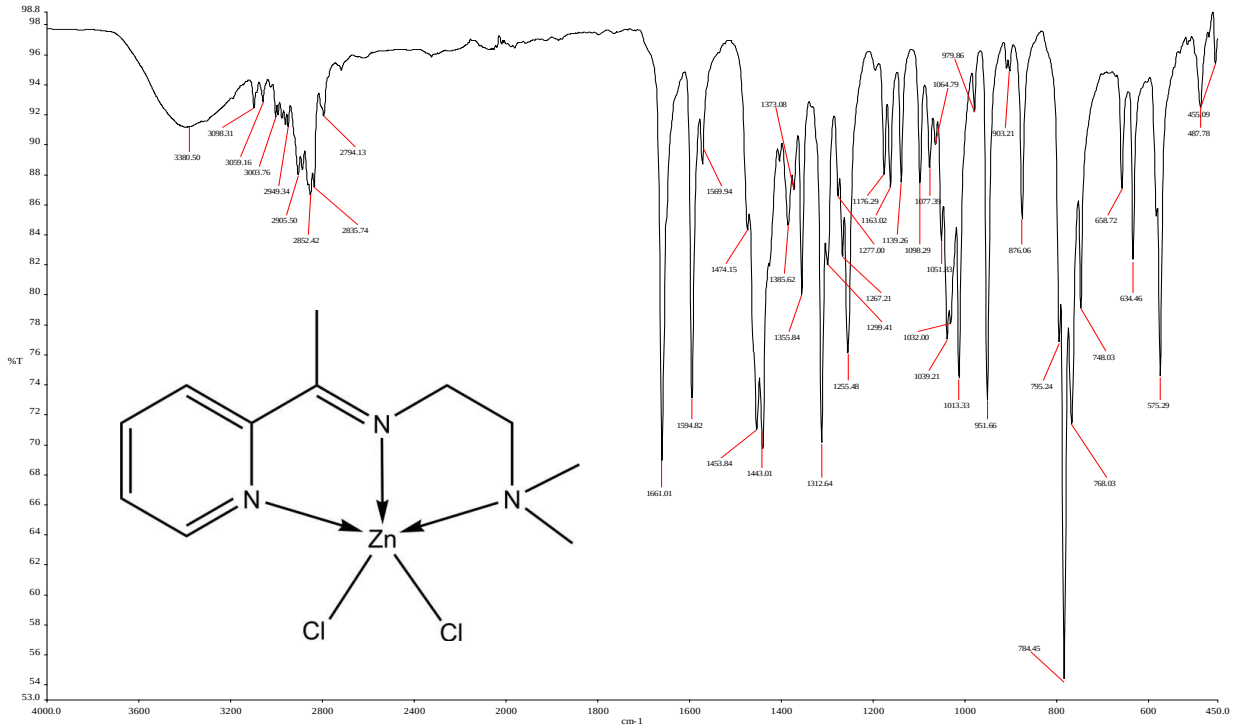

Figure 3.2.11: IR spectra of $[Zn(LNA)Cl_2]$

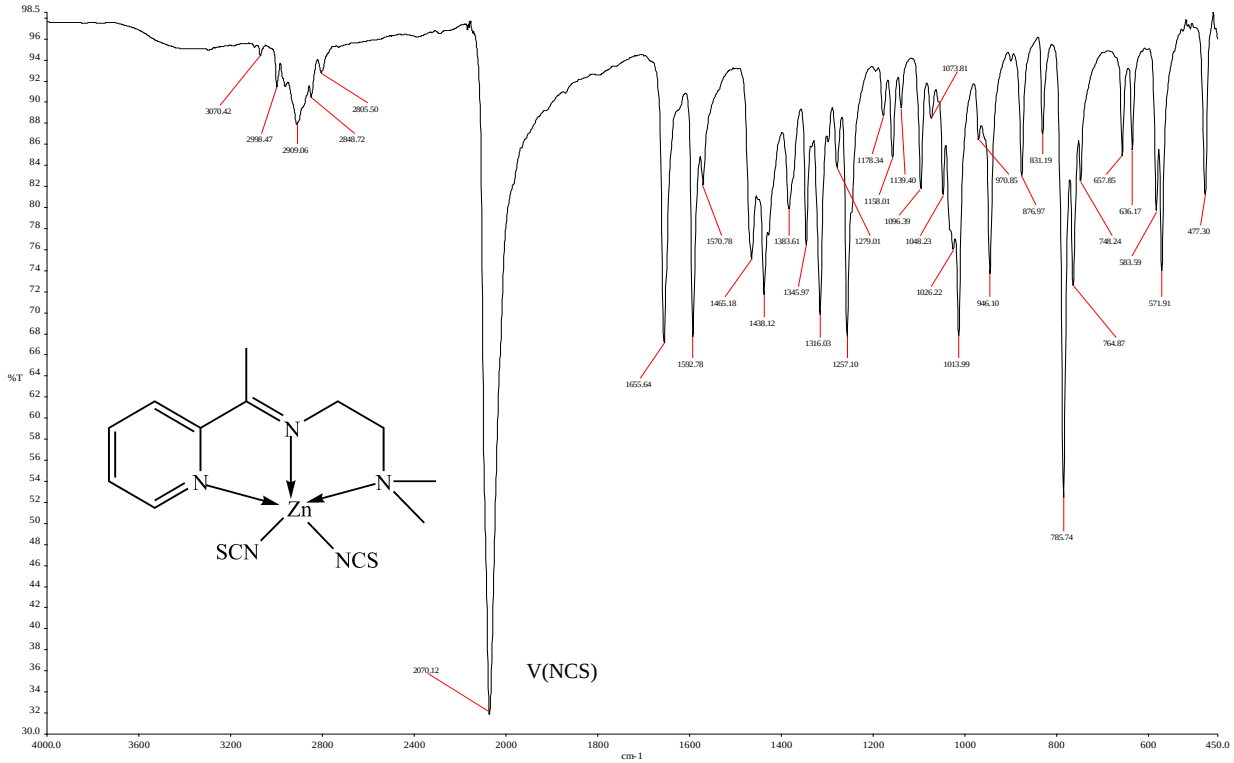

Figure 3.2.12: IR spectra of $[Zn(LNA)(NCS)_2]$

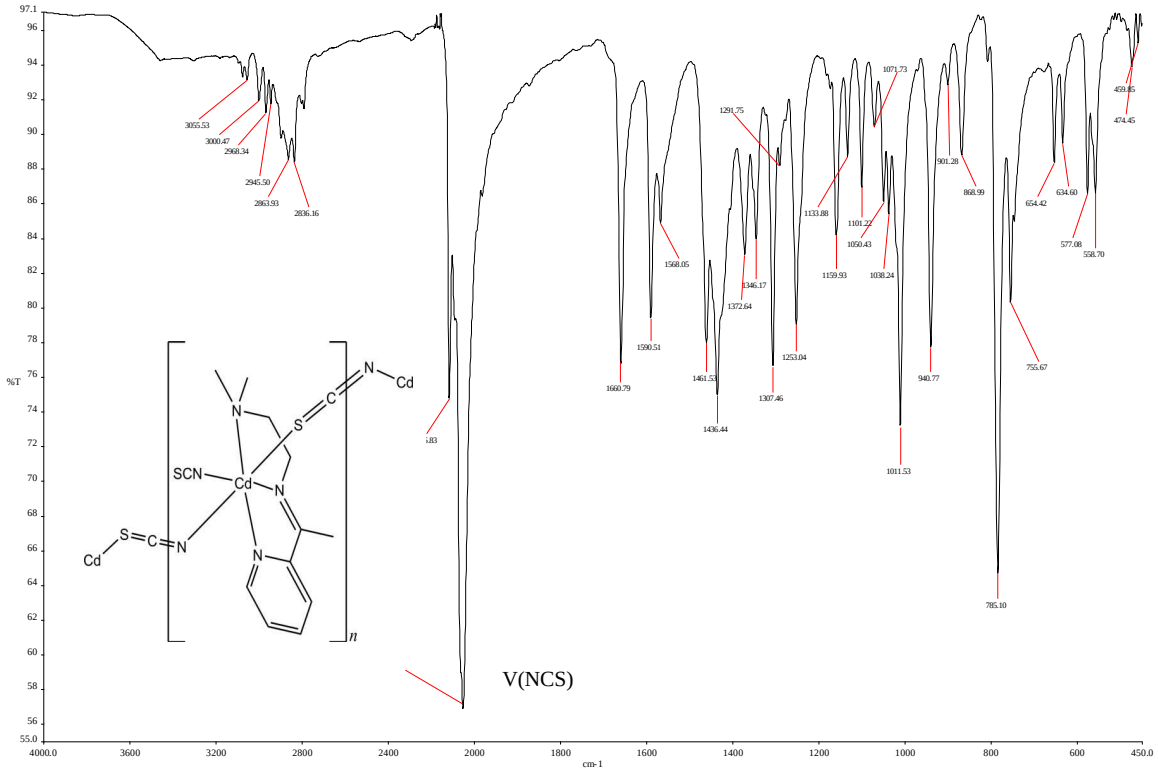

Figure 3.2.13: IR spectra of Preparation of [Cd(LNA)(NCS)2]n

The complex shows characteristic intense IR band for thiocyanate anion at 2093 cm^{-1} (Banerjee, 2005 and Chattopadhyay 2005). The bands in the region 560–505 cm^{-1} are assigned to the ν(M-N) vibrations (Deoghoria, 2004; Shahabadi, 2010 and Lakshmi, 2011). The presences of hydrates were characterized by the exhibition of bands in the range of 650–700 cm^{-1} (Chan et al., 1995).

Table 3.10: Some of the important IR bands for 2-(1-(2-(dimethylamino)ethylimino)ethyl)phenol (LNH) and metal complexes.

Compound	**ν(C-H)**	**ν(C=N)**	**ν(C-C)**	**ν(C-N)**	**ν(M-N)**	**ν(M-O)**
LNH	2944	1642	1445	1183	-	
[Mn(LNH)Br]	3107	1650	1443	1109	524	461
[Mn(LNH)Cl]	3103	1651	1449	1105	528	461
[Ni(LNH)Br]	3058	1597	1471	1116	505	422
[Ni(LNH)Cl]	3050	1605	1474	1112	508	423
[Cu(LNH)Br]	2943	1605	1436	1102	518	423
[Cu(LNH)Cl]	3105	1579	1432	1113	526	492
[Zn(LNH)Br]	3070	1650	1428	1121	557	451
[Zn(LNH)Cl]	3105	1654	1435	1119	531	433

The IR spectra of the free ligand (LNH) and corresponding complexes exhibit various bands in the 400-4000 cm^{-1} region. The ν(O-H) stretching frequency of the free ligand is found in the 3524.15 cm^{-1} region as expected (Figure 3.2.14).

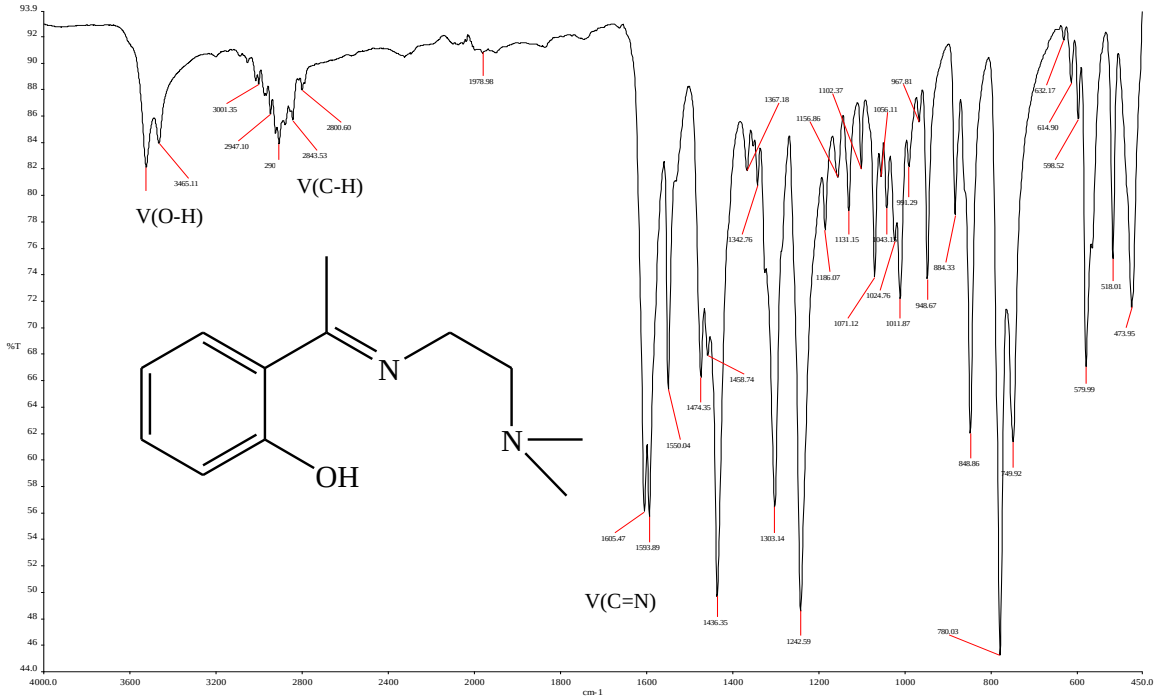

Figure 3.2.14: IR spectra of LNH

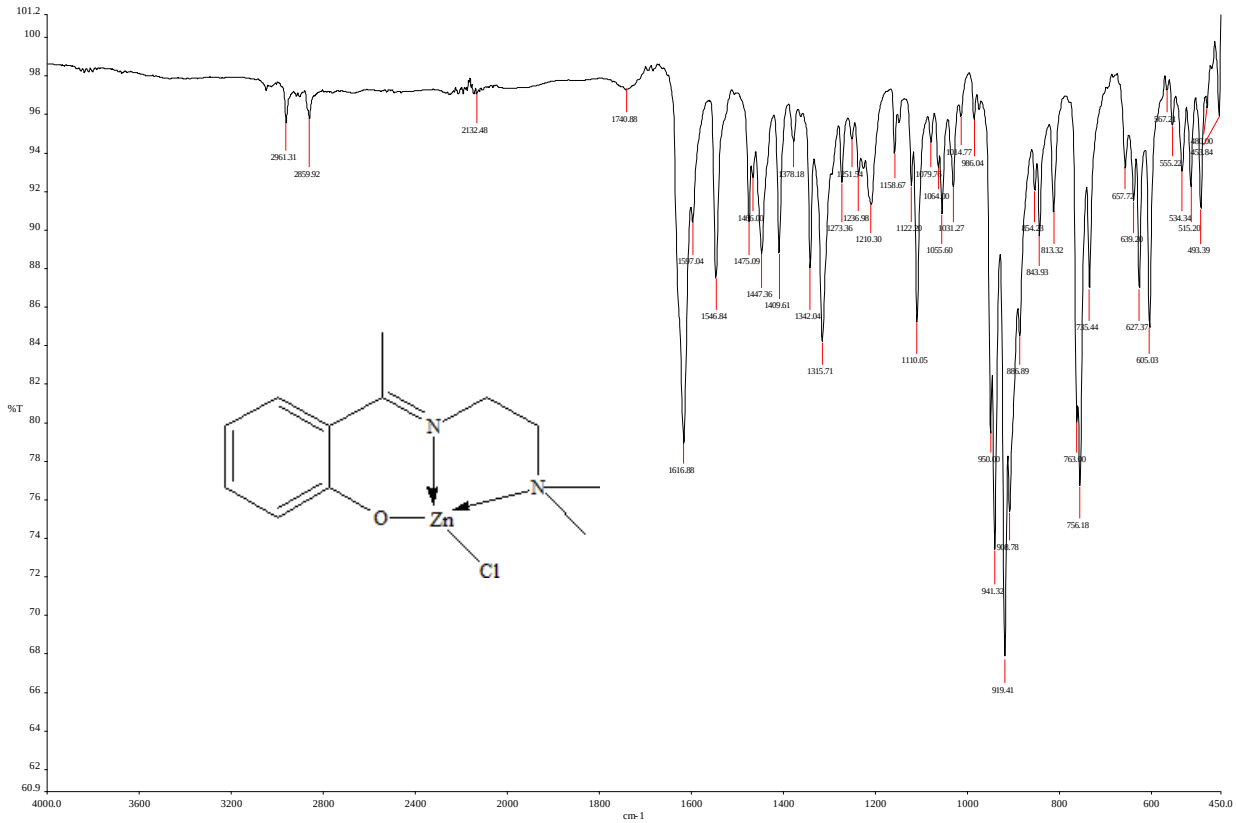

Figure 3.2.15: IR spectra of [Zn(LNH)Cl]

The sharpness of the signals reveals that no intramolecular or intermolecular hydrogen bonding interaction occurs (Pouralimardan, 2007). In the spectra of the complexes, v(C=N) band signal shifted to the different frequencies ranging from 1650 cm^{-1} to 1575 cm^{-1} indicating that the coordination of the ligand to metal ion occurs through nitrogen atom of the imine group. Two new weak bands appears at lower frequencies range of 505 cm^{-1} and 560 cm^{-1} assigned to v(M-N) (Bagihalli, 2008), are observed in metal complexes spectra also v(M-O) bands in the range of 490 cm^{-1}- 420 cm^{-1} are observed in metal complexes spectra but not in the spectra of the ligand which is consistent with the formation of the desired metal complexes. Nonetheless, the assignment of v(M-O) and v(M-N) bands at the lower region seems to be due to the interference with the vibration signals of the ligand.

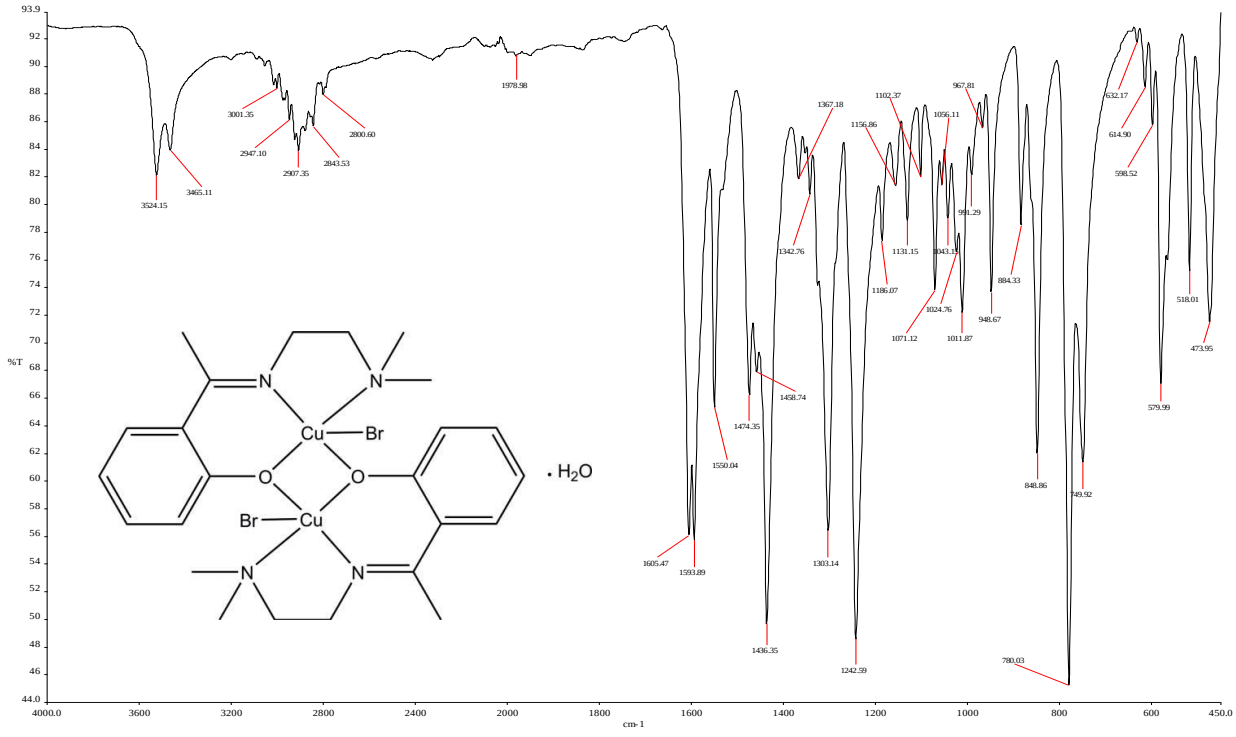

Figure 3.2.16: IR spectra of Preparation of $[Cu_2(LNH)_2Br_2]$

In general the difference just noted suggests that a fundamental difference in the structure of some sort may exist between the two groups of complexes. We considered differences caused by the difference of the strength of the v(M-O) and v(M-N) bonding in the various complexes. In the complexes like (Figure 3.2.15), the metal ions react primarily with the negatively charged oxygen; the v(M-O) bonding plays a more important role than the M-N bonding. On the other hand, transition metal ions in group complexes (Figure 3.2.16) react primarily with the covalent nitrogen, the v(M-N) bonding is stronger than the v(M-O) bonding. That is, the v(M-N) bonding plays a more important role in the complexes. These results are in agreement with Pearson's soft-hard acid-base theory.

3.3 ^{1}H-NMR Spectral analysis of the compounds

The ^{1}H and ^{13}C NMR spectra of the ligand and complexes (Figure 3.3.1-3.3.8) were recorded using a Bruker Apex 600MHz; FT-NMR spectrometers chemical shifts are given in δ values (ppm) using TMS as the internal standard. Deuterated dimethylsulphoxide (DMSO-d_6) was used as solvent.

Table 3.11: 1H-NMR- Spectra for 2-morpholino-N-(1-(pyridin-2-yl)ethylidene)ethanamine (LMA) and metal complexes.

Compound	^{1}H-NMR (600 MHz, δ, DMSO-d_6)				
	(H^1 - H^3) Ar-H	H^4	H^5	H^6	H^7
LMA	8.59 - 7.73	3.92	3.83	2.81	2.61
[Zn(LMA)Br_2]	8.78 - 7.89	3.89	3.85	2.91	2.62
[Zn(LMA)Cl_2]	8.70 - 7.86	3.92	3.84	2.82	2.61
[Zn(LMA)I_2]	8.70 - 7.85	3.92	3.84	2.82	2.61
[Zn(LMA)$(N_3)_2$]	8.69 - 7.93	3.70	3.68	2.76	2.62
[Zn(LMA)$(NCS)_2$]	8.69 - 7.96	3.85	3.81	2.80	2.61
[Cd(LMA)Br_2]	8.76 - 7.87	3.87	3.83	2.89	2.66
[Cd(LMA)Cl_2]	8.69 - 7.85	3.93	3.73	2.82	2.55
[Cd(LMA)$(N_3)_2H_2O$]	8.68 - 7.85	3.79	3.74	2.79	2.53
[$Cd_2(LMA)_2(NCS)_4$]	8.81 - 7.87	3.81	3.70	2.80	2.51

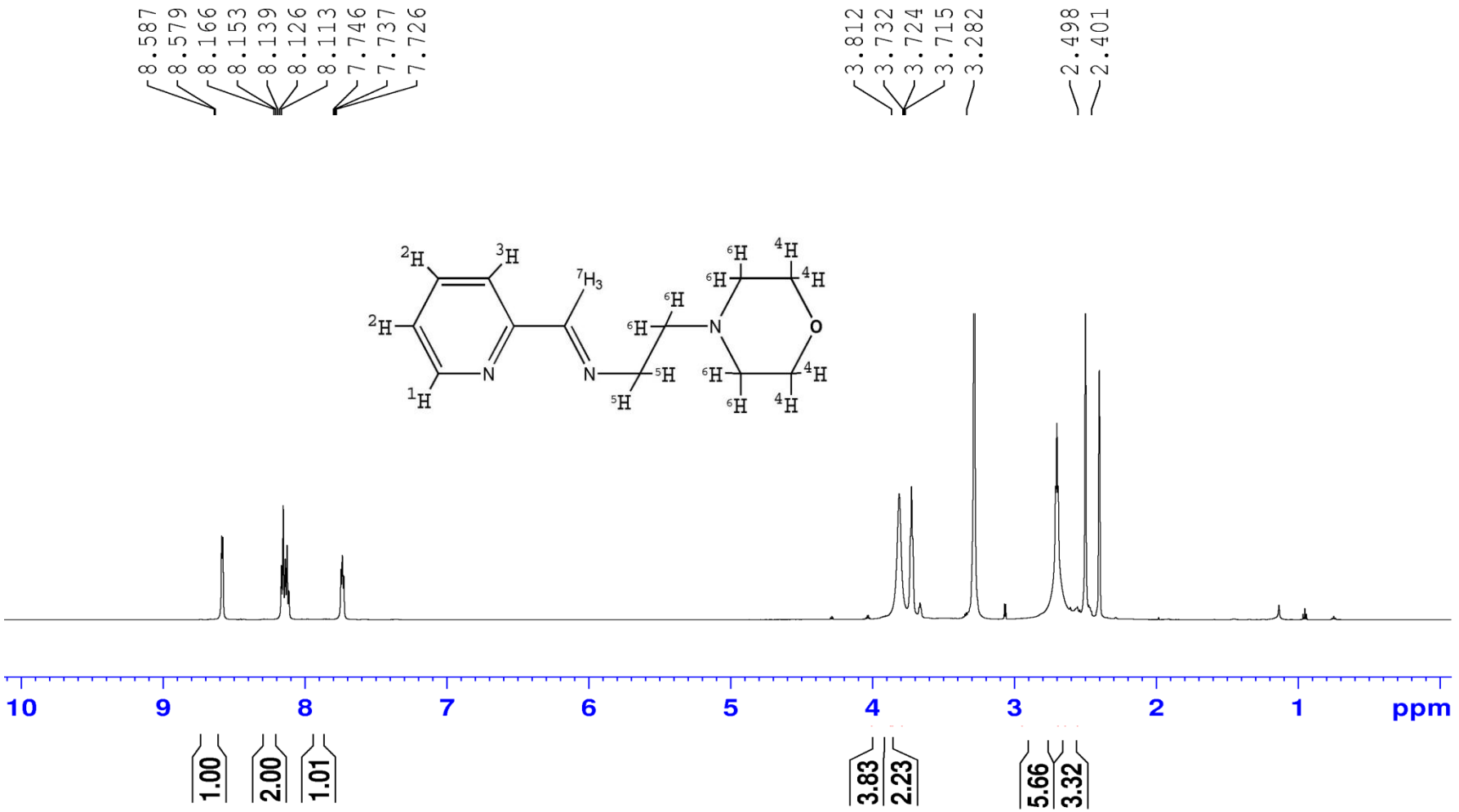

Figure 3.3.1: 1H-NMR spectra of LMA

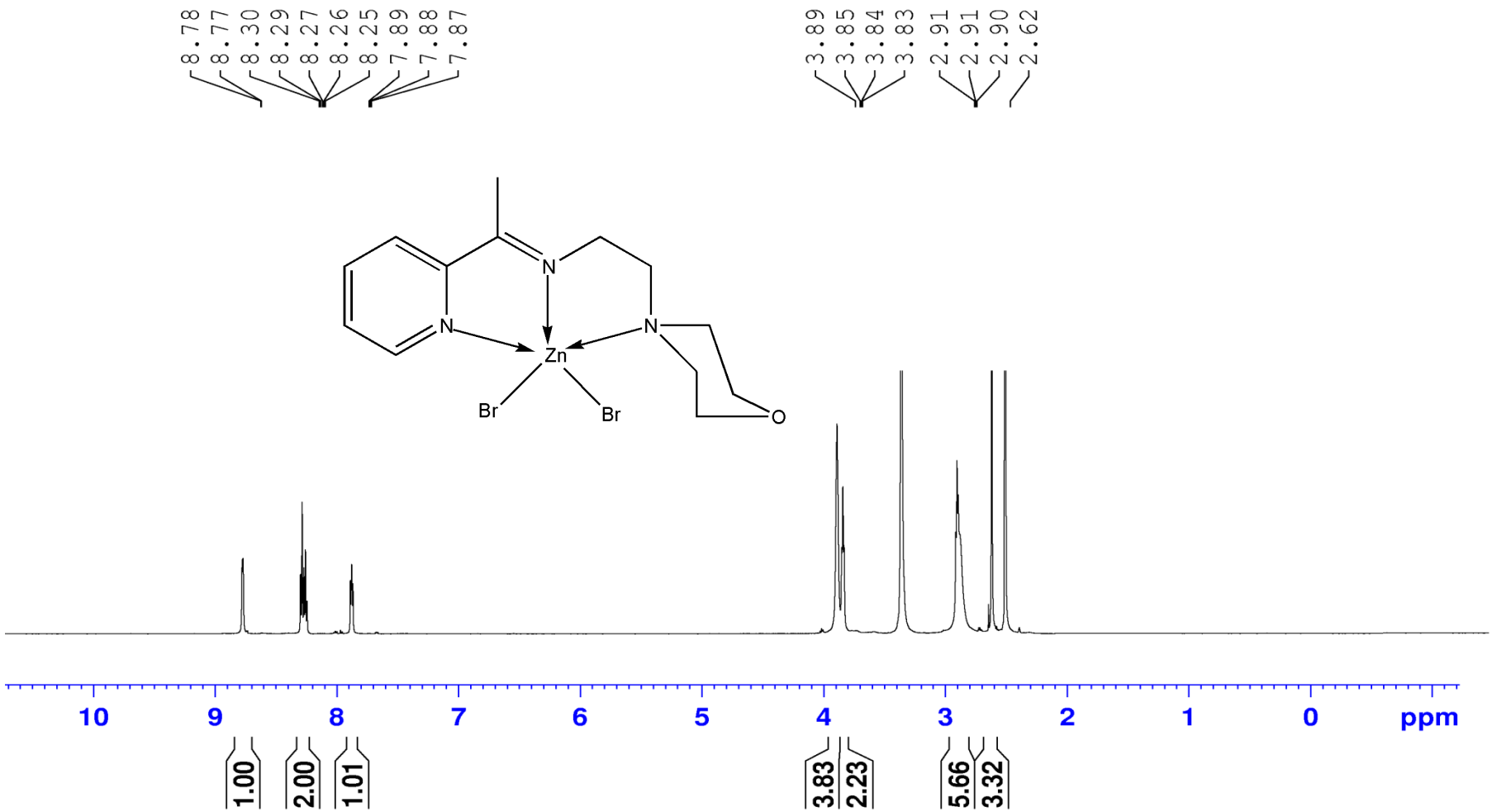

Figure 3.3.2: 1H-NMR spectra of [Zn(LMA)Br2]

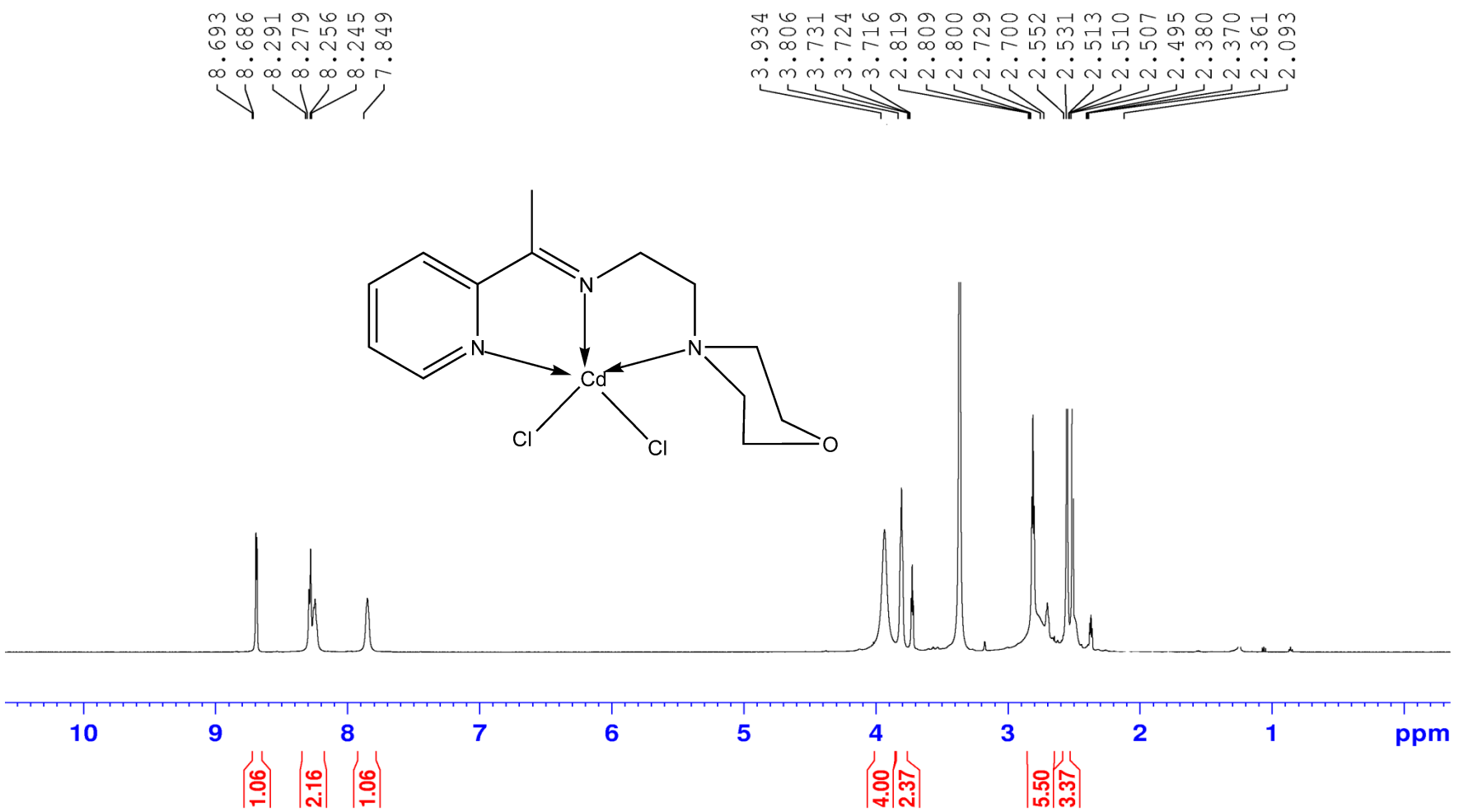

Figure 3.3.3: 1H-NMR spectra of [Cd(LMA)Cl_2]

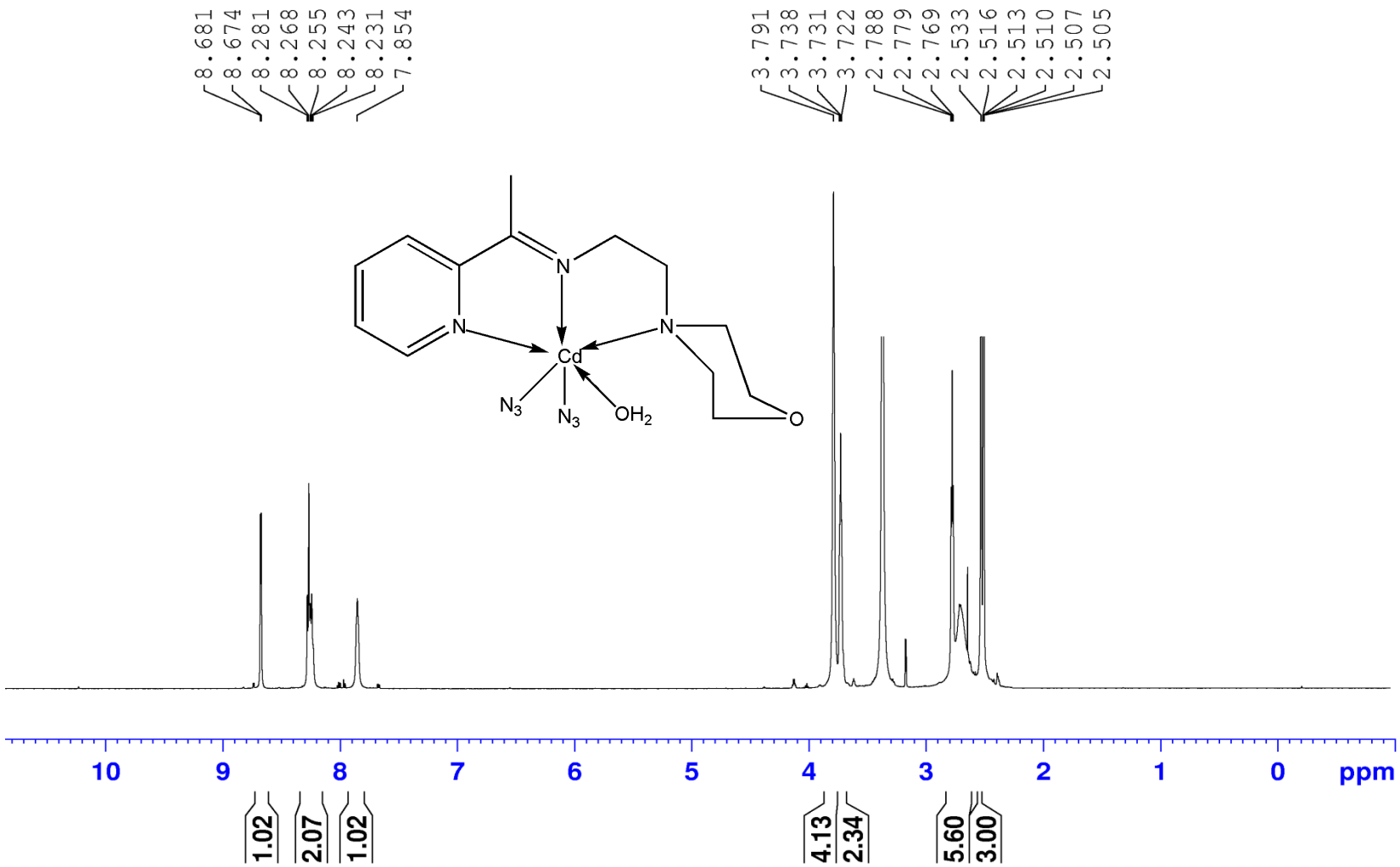

Figure 3.3.4: 1H-NMR spectra of [Cd(LMA)(N_3)2(H_2O)]

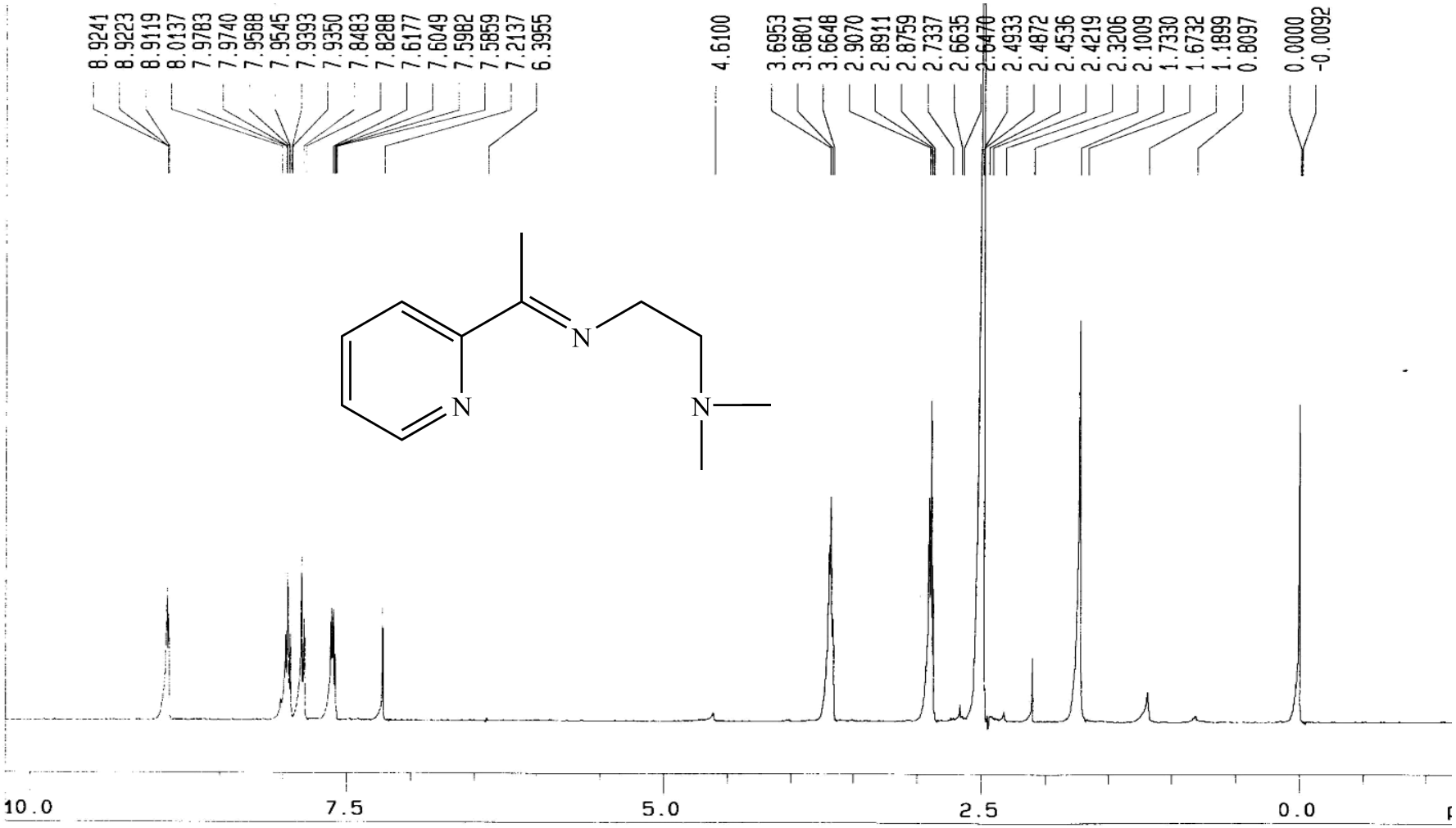

Figure 3.3.5: 1H-NMR spectra of LNA

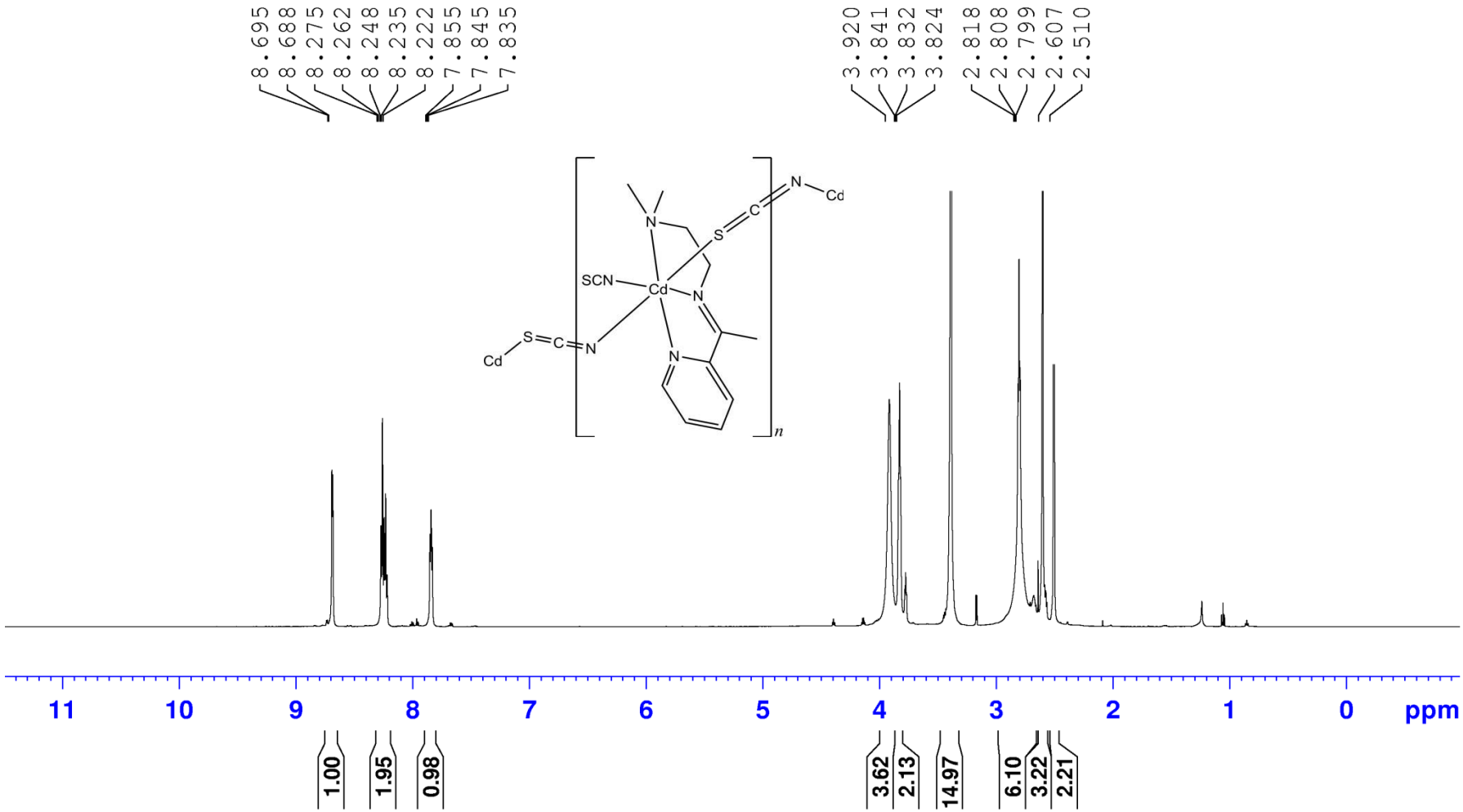

Figure 3.3.6: 1H-NMR spectra of [Cd(LNA)(SCN)2]n and n=Polymer

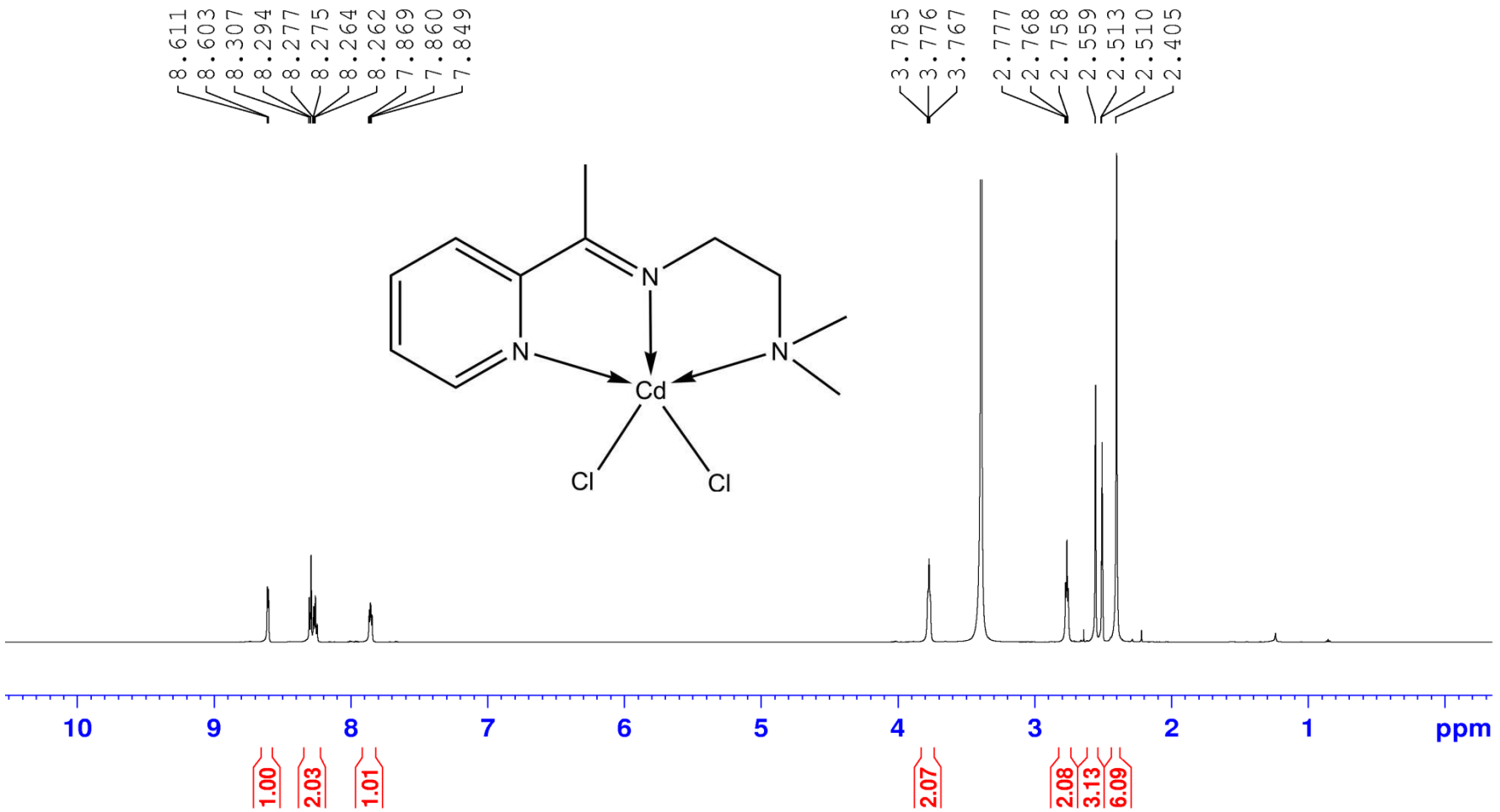

Figure 3.3.7: 1H-NMR spectra of [Cd(LNA)Cl2]

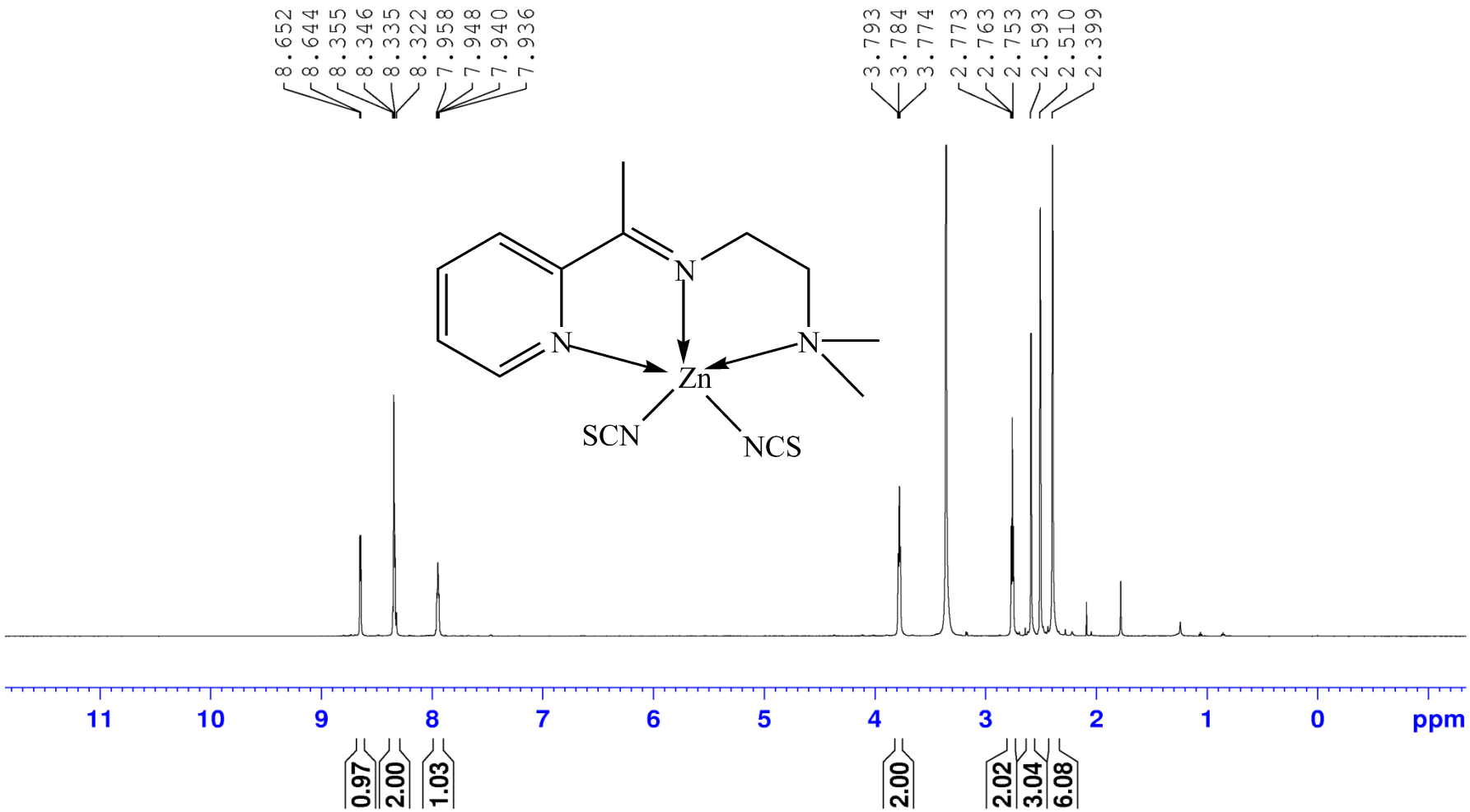

Figure 3.3.8: 1H-NMR spectra of [Zn(LNA)$(SCN)_2$]

3.4 ^{13}Carbon NMR spectra of the ligands and complexes

In the ^{13}C NMR spectra of the metal complexes, the signal at region of 165.00 ppm-170.00 can be assigned to the azomethine (C=N) carbon atoms for complexes (Shahabadi *et. al.*, 2010). Aromatic ring carbon atoms of the ligands were determined in the region of 120.00-160.00 ppm (Ali *et. al.,* 2008).

Table 3.12: ^{13}C-NMR- Spectra for 2-morpholino-N-(1-(pyridin-2-yl)ethylidene)ethanamine (LMA) and metal complexes.

Compound	^{13}C-NMR (600 MHz, δ, DMSO-d_6)						
	C^1	(C^2 - C^6) Ar-C	C^7	C^8	C^9	C^{10}	C^{11}
LMA	168.54	148.46 - 123.81	63.45	56.09	53.68	44.22	15.83
$[Zn(LMA)Br_2]$	168.38	146.49 - 124.05	62.88	54.55	52.09	44.12	15.86
$[Zn(LMA)Cl_2]$	168.54	148.46 - 123.81	63.45	56.09	52.67	44.22	15.82
$[Zn(LMA)I_2]$	165.22	149.58 - 124.85	65.99	58.62	53.99	-	15.85
$[Zn(LMA)(N_3)_2]$	169.11	148.63 - 124.52	63.90	57.30	53.42	53.11	15.86
$[Zn(LMA)(NCS)_2]$	168.42	147.85 - 124.47	63.72	56.93	53.07	43.79	15.77
$[Cd(LMA)Br_2]$	169.18	149.22 - 124.55	65.36	63.94	57.35	53.14	15.91
$[Cd(LMA)Cl_2]$	166.90	149.13 - 124.42	64.65	53.49	36.00	30.67	15.95
$[Cd(LMA)(N_3)_2H_2O]$	164.66	149.02 -	65.43	58.06	53.44	44.46	15.29
$[Cd_2(LMA)_2(NCS)_4]$	165.80	149.24 - 127.68	64.76	53.44	44.36	21.98	15.77

FT-NMR for the coordinated complexes have been summarized in Table 3.1.1 and 3.12. The proton NMR chemical shift in the region 8.70-7.80 ppm, were observed for zinc complexes respectively and they were assigned to the aromatic ring protons (Ali *et. al.,* 2008). The other single peaks appeared in the region 2.60 ppm-2.90 ppm respectively were

attributed to δ(CH_3) indicating the methyl on the carbonyl group in the complexes (Ali *et. al.,* 2008). In the ^{13}C NMR spectra of the metal complexes, the signal at region of 165.00 ppm-170.00 can be assigned to the azomethine (C=N) carbon atoms for complexes. Aromatic ring carbon atoms of the ligands were determined in the region of 120.00-160.00 ppm (Ali *et. al.,* 2008).

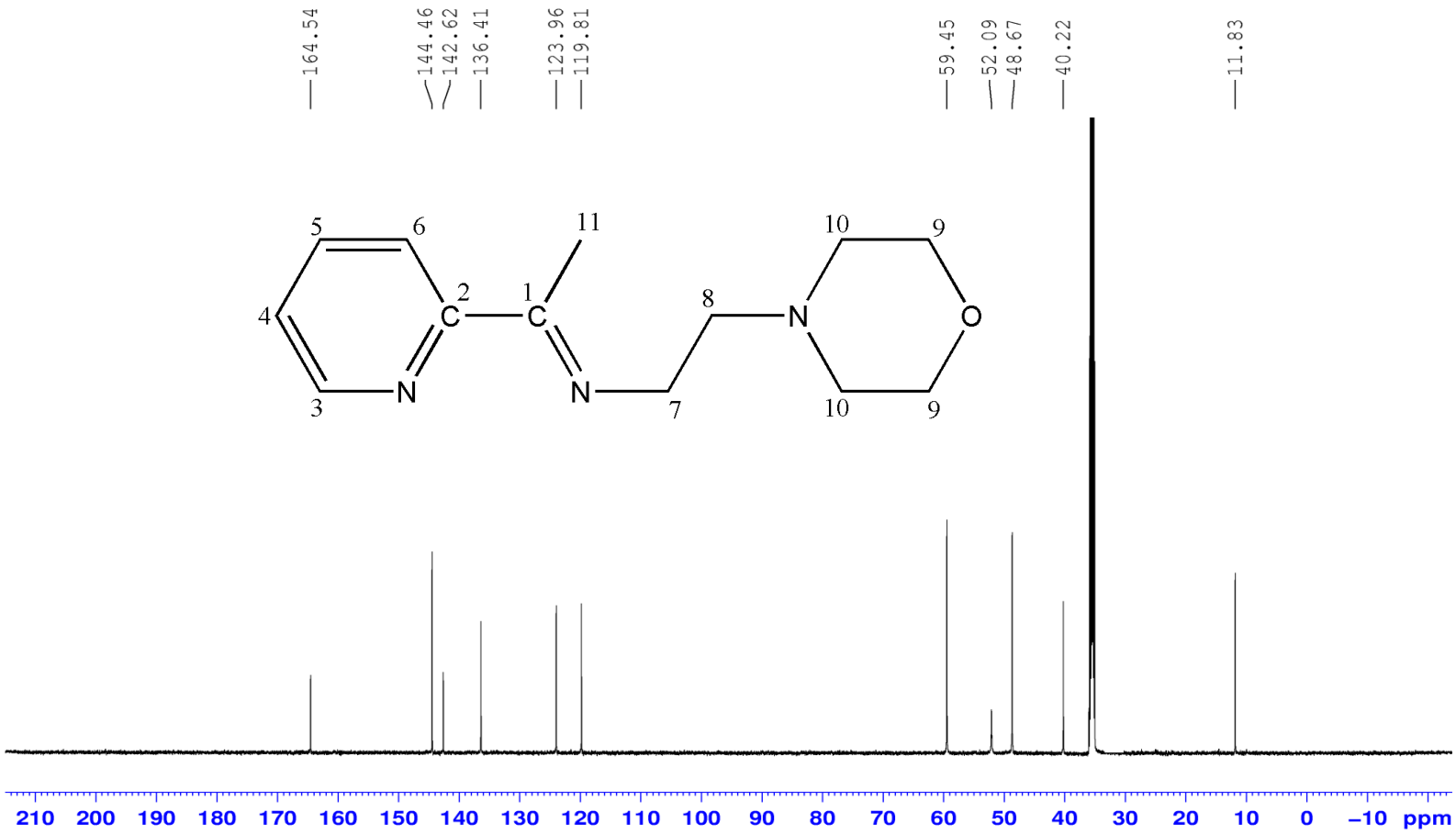

Figure 3.4.1: 13C-NMR spectra of LMA

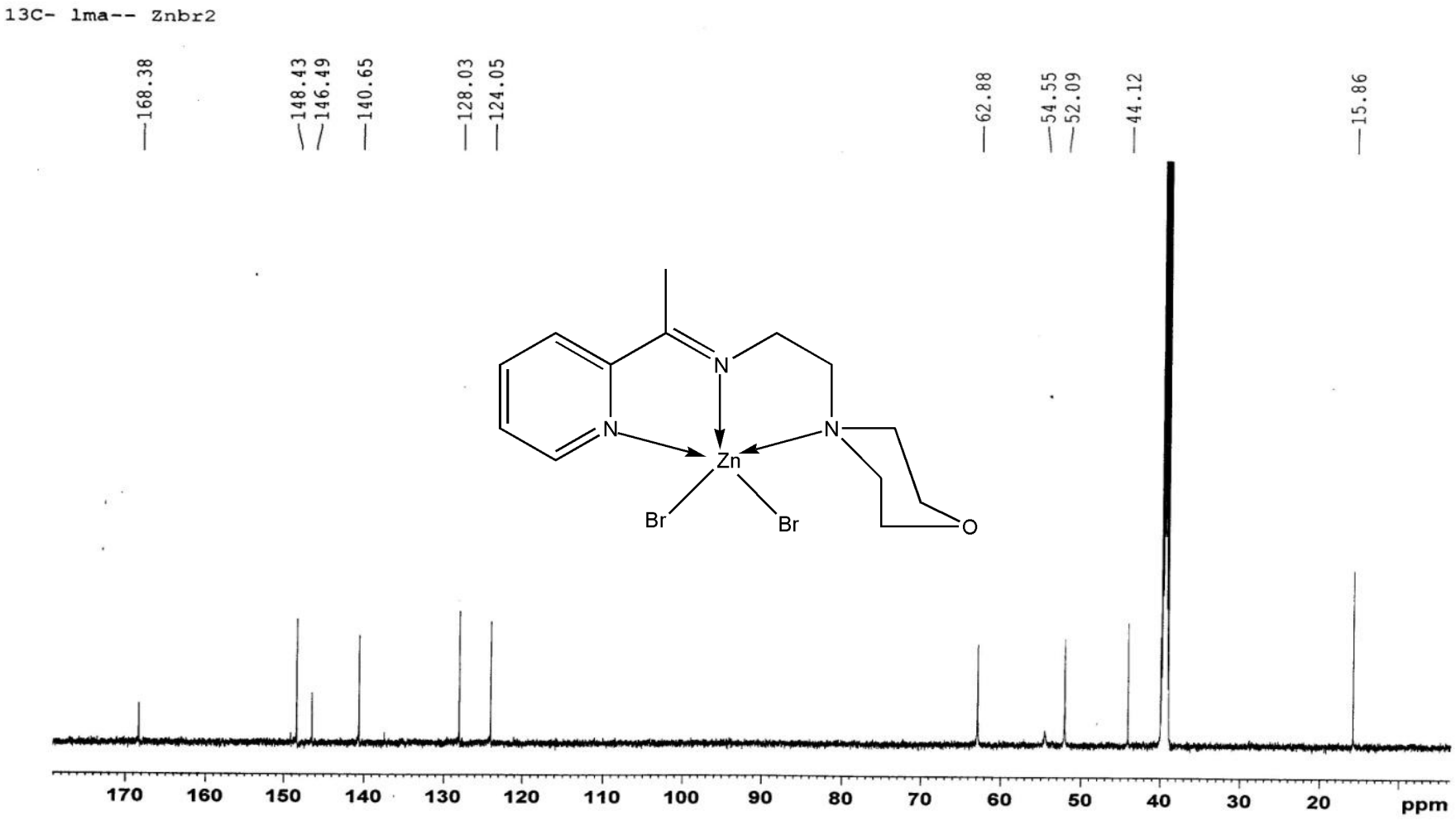

Figure 3.4.2: 13C-NMR spectra of Preparation of [Zn(LMA)Br2]

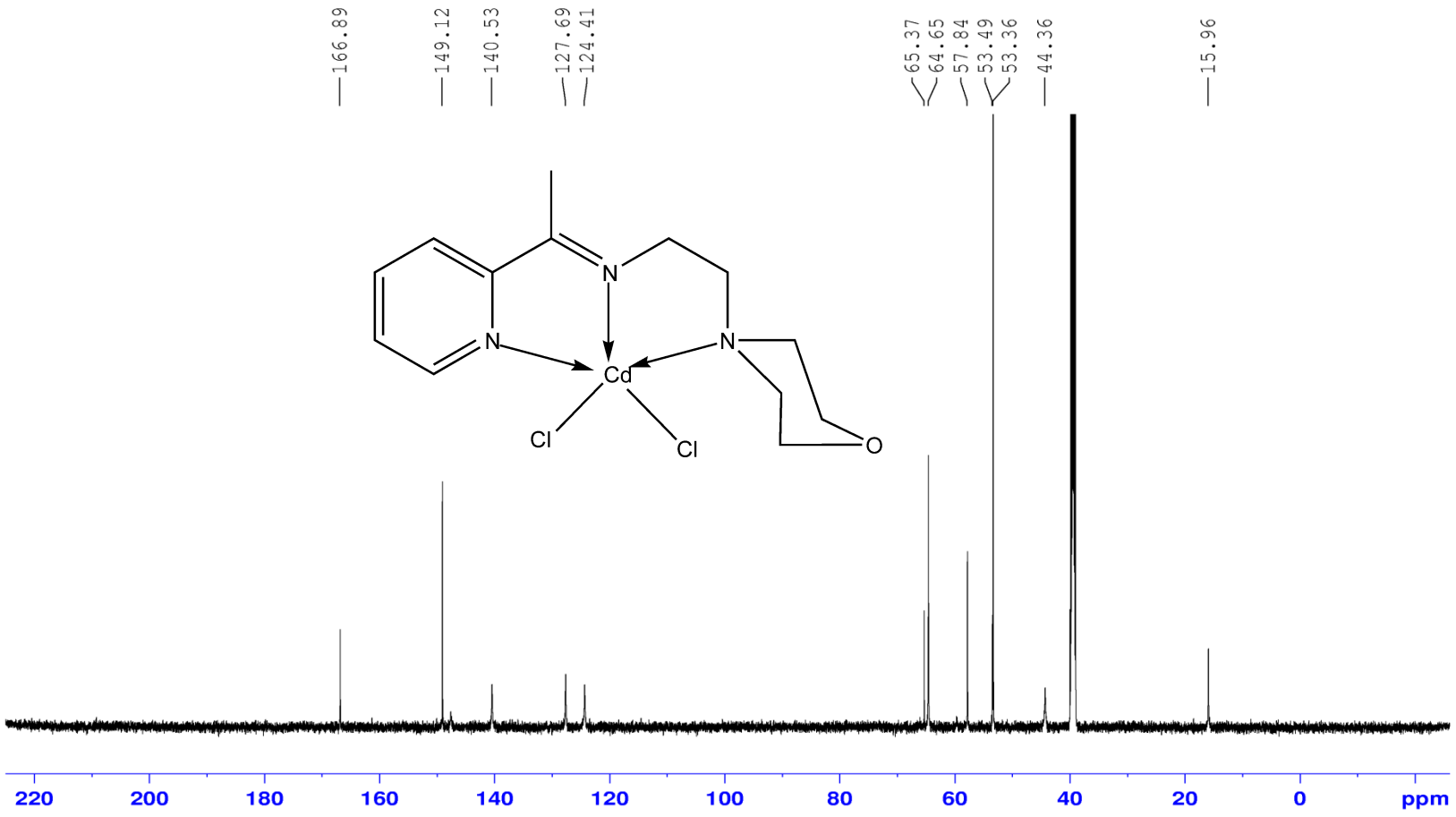

Figure 3.4.3: 13C-NMR spectra of [Cd(LMA)Cl_2]

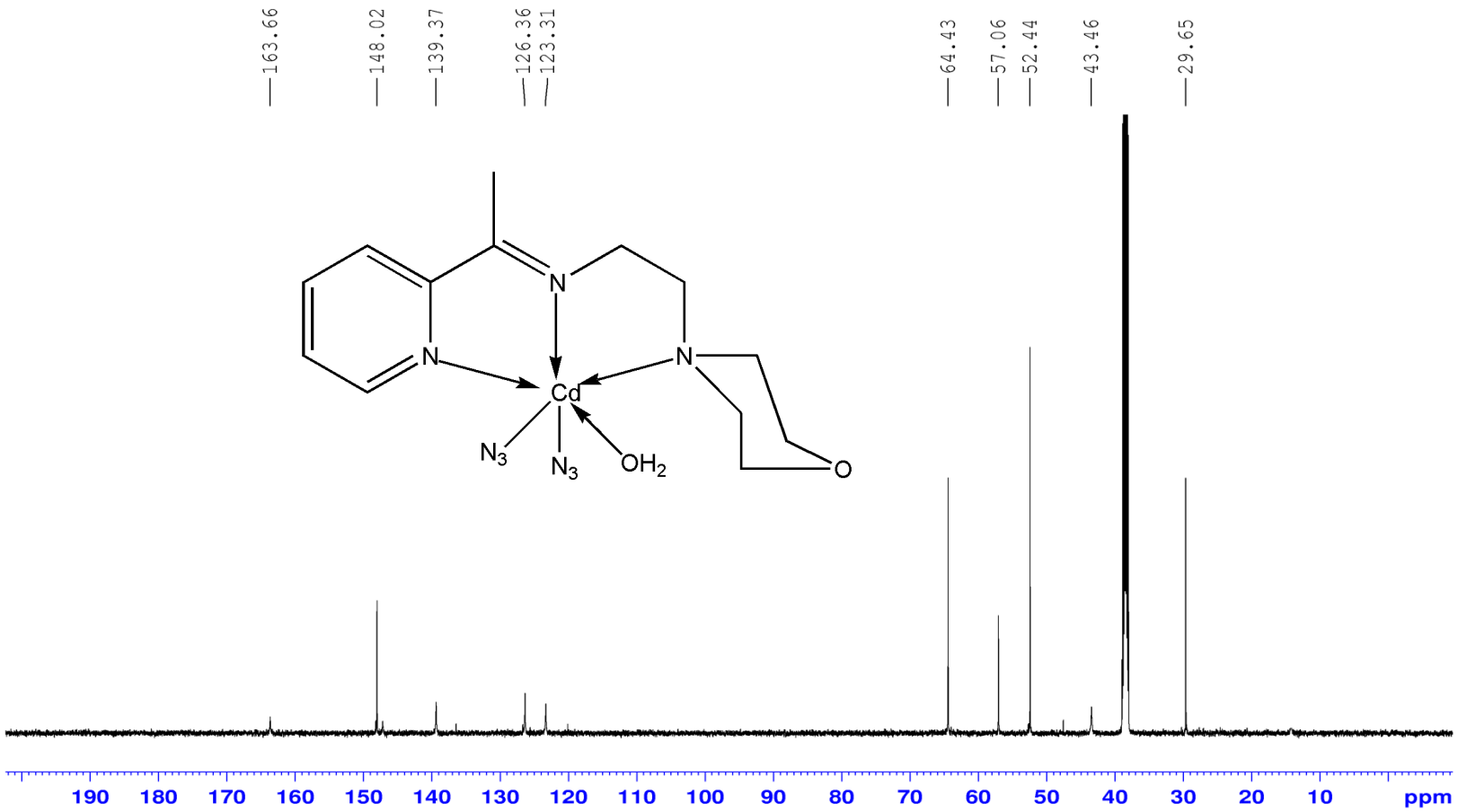

Figure 3.4.4: 13C-NMR spectra of [Cd(LMA)(N_3)2(H_2O)]

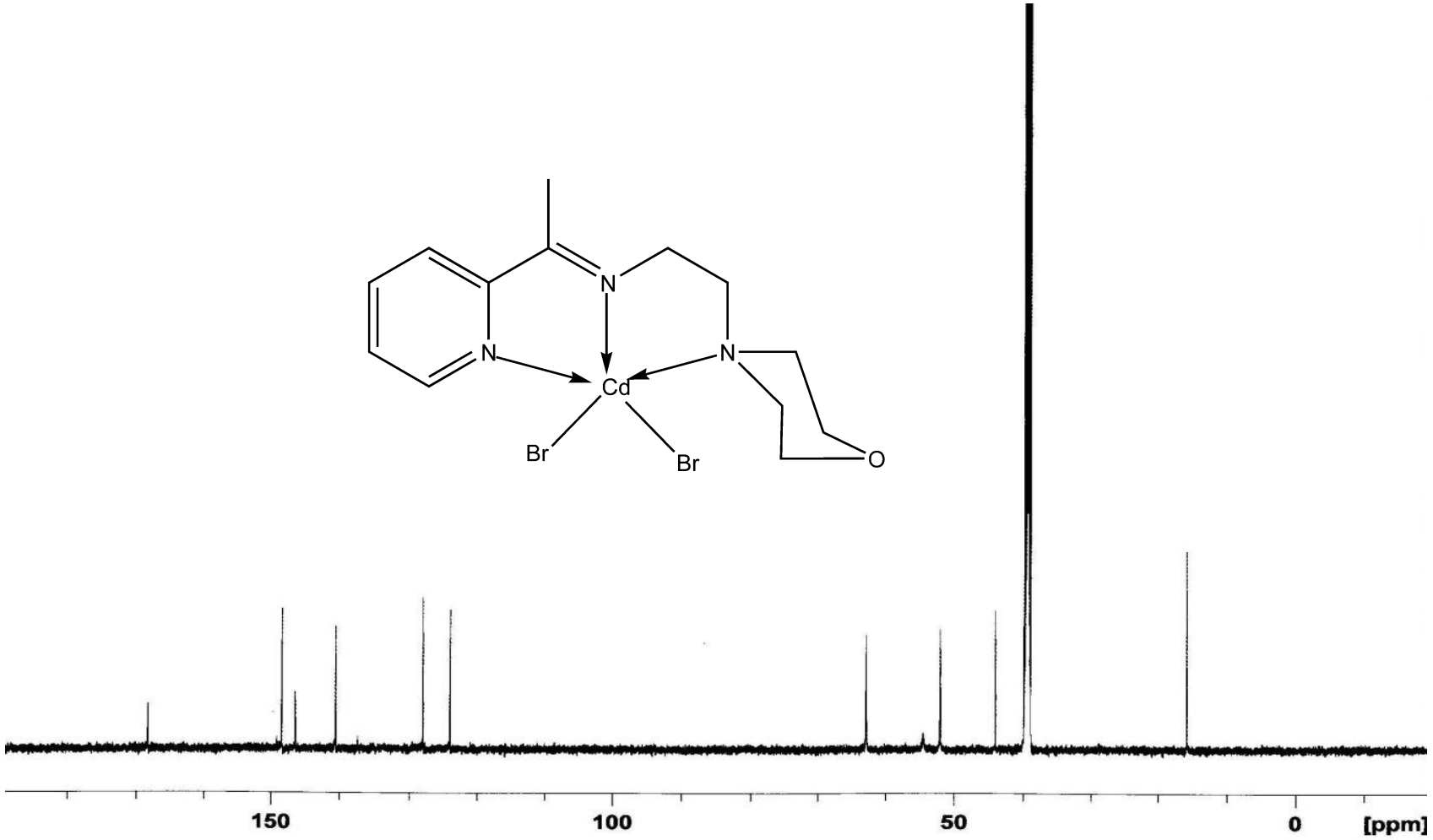

Figure 3.4.5: 13C-NMR spectra of [Cd(LMA)Br_2]

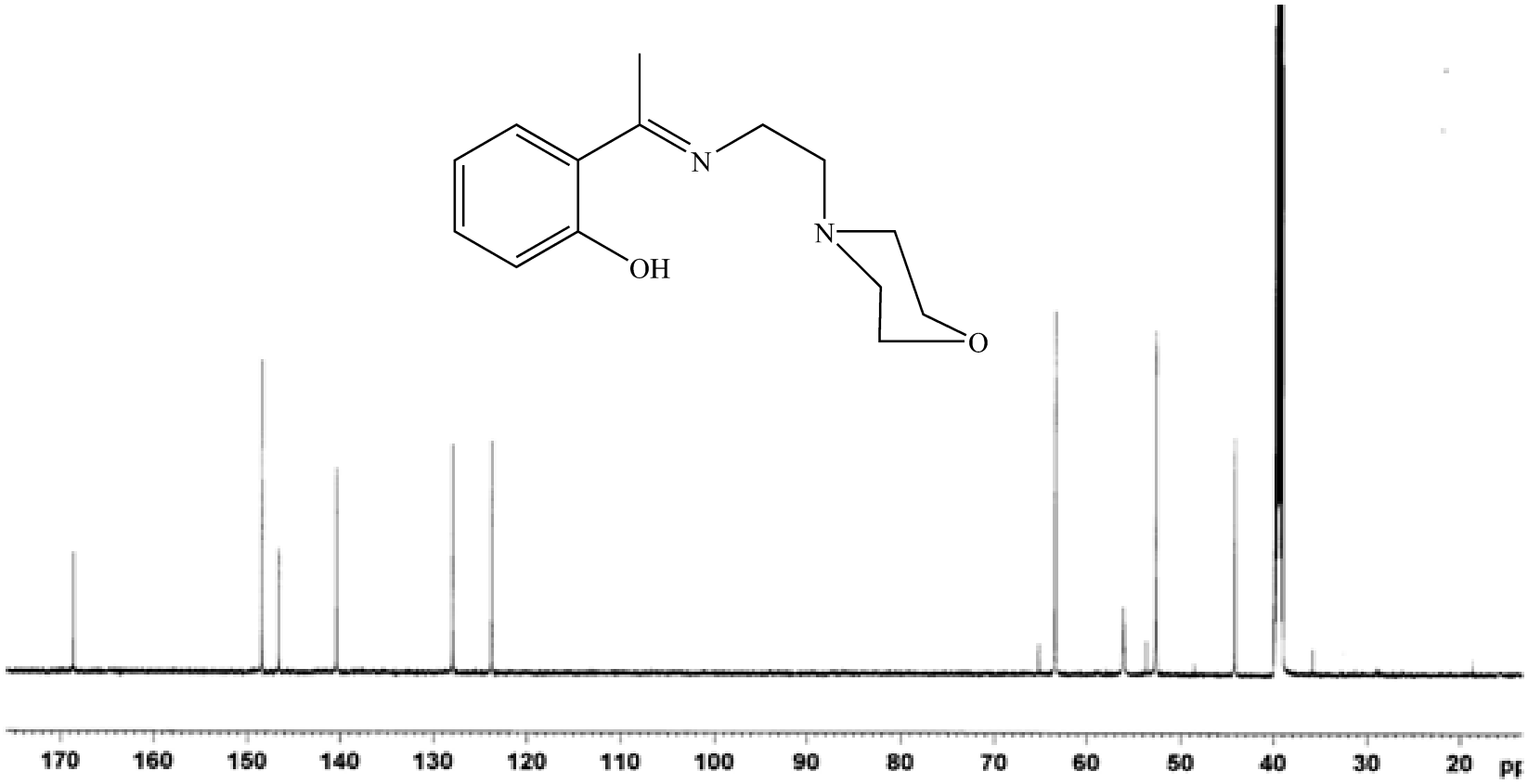

Figure 3.4.6: 13C-NMR spectra of LMH

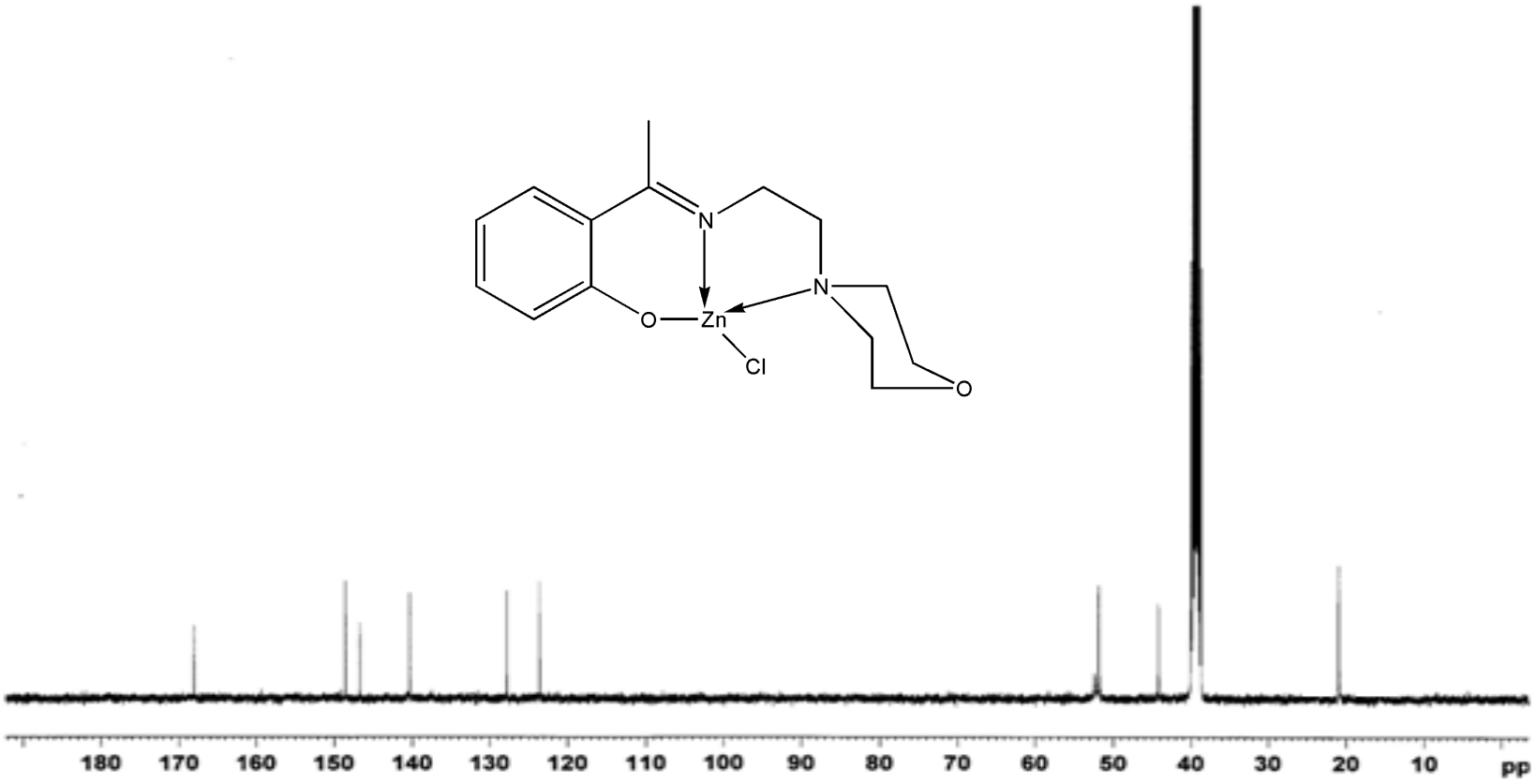

Figure 3.4.7: 13C-NMR spectra of [Zn(LMH)Cl]

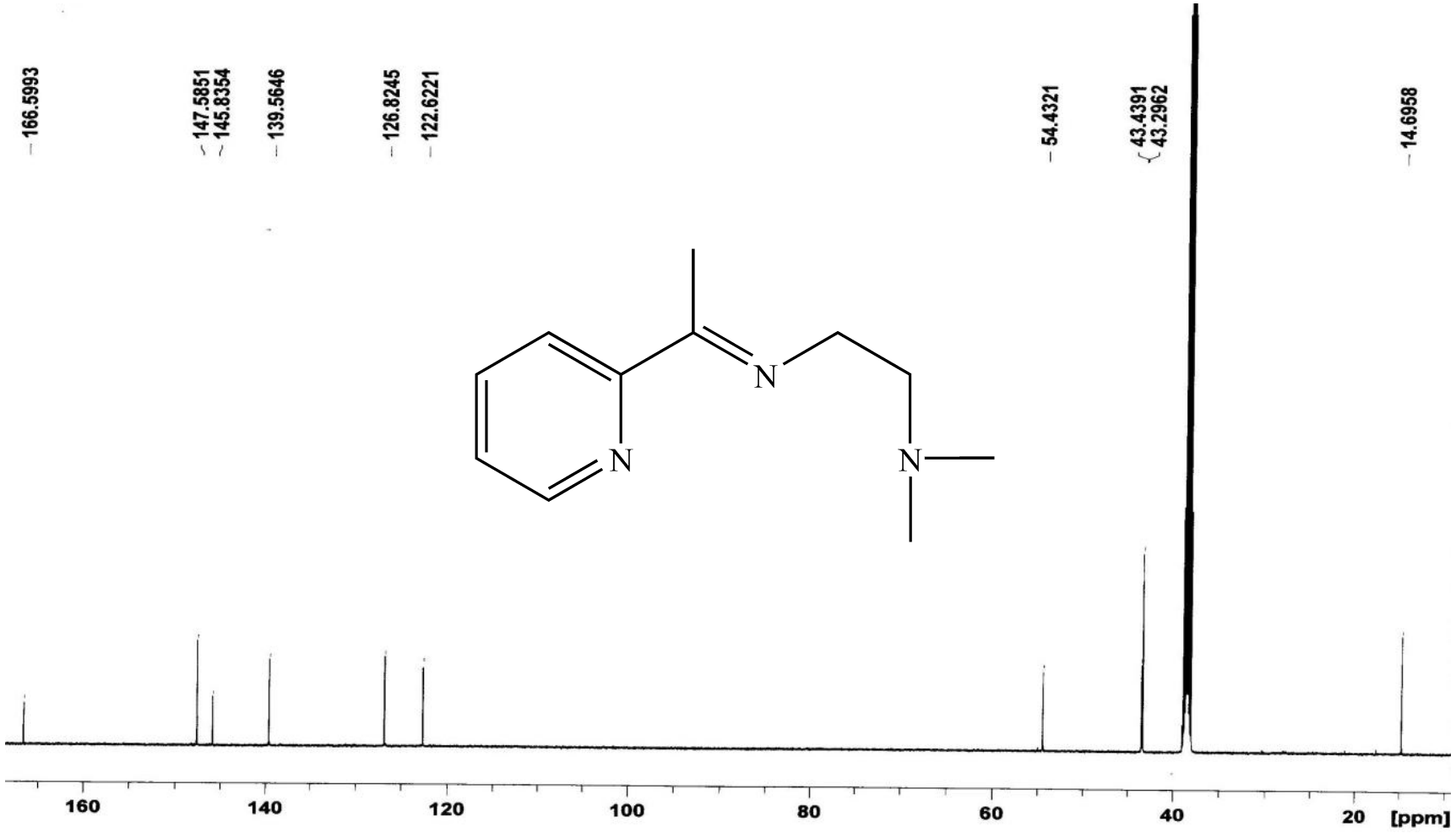

Figure 3.4.8: 13C-NMR spectra of LNA

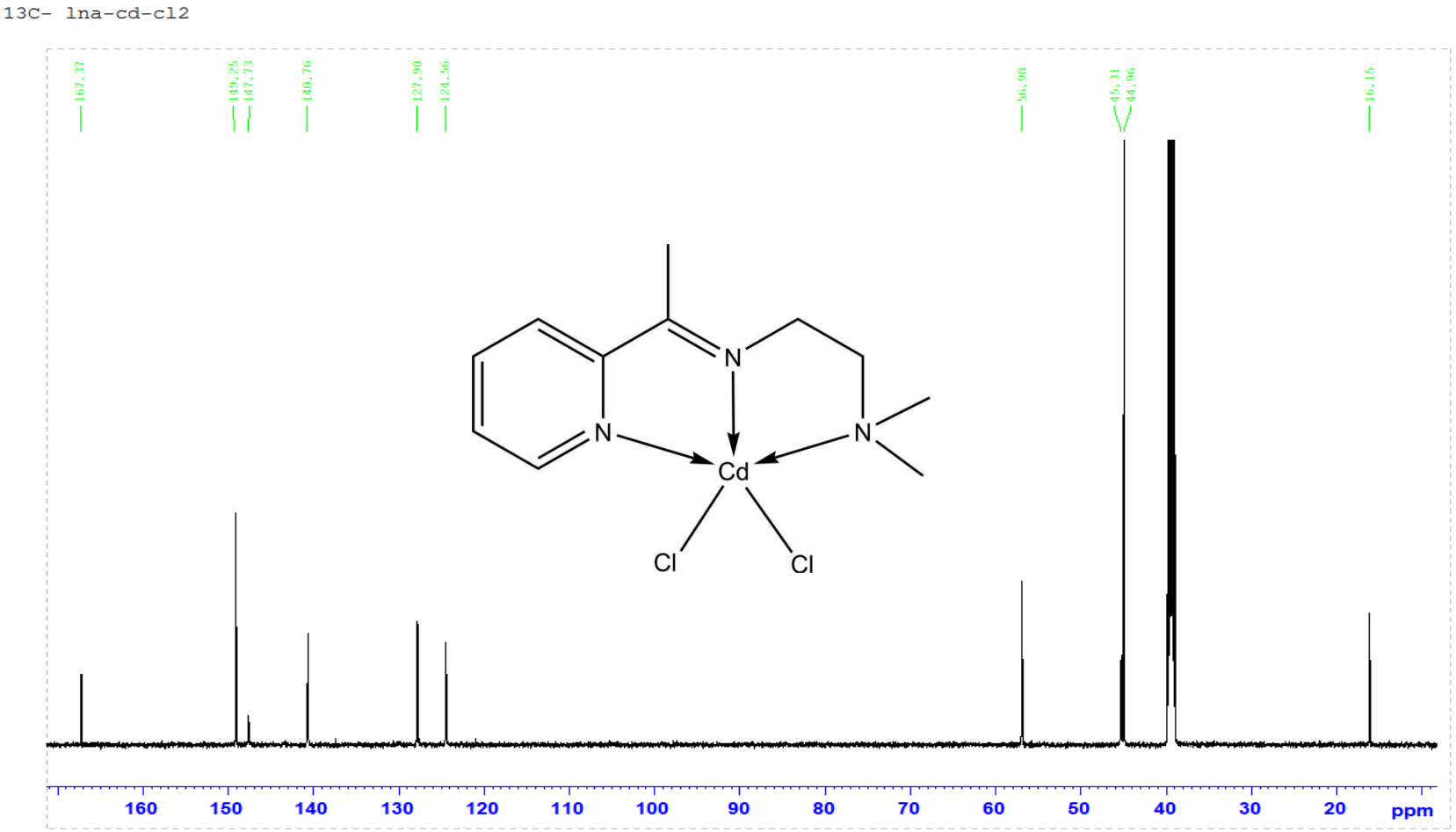

Figure 3.4.9: 13C-NMR spectra of [Cd(LNA)Cl_2]

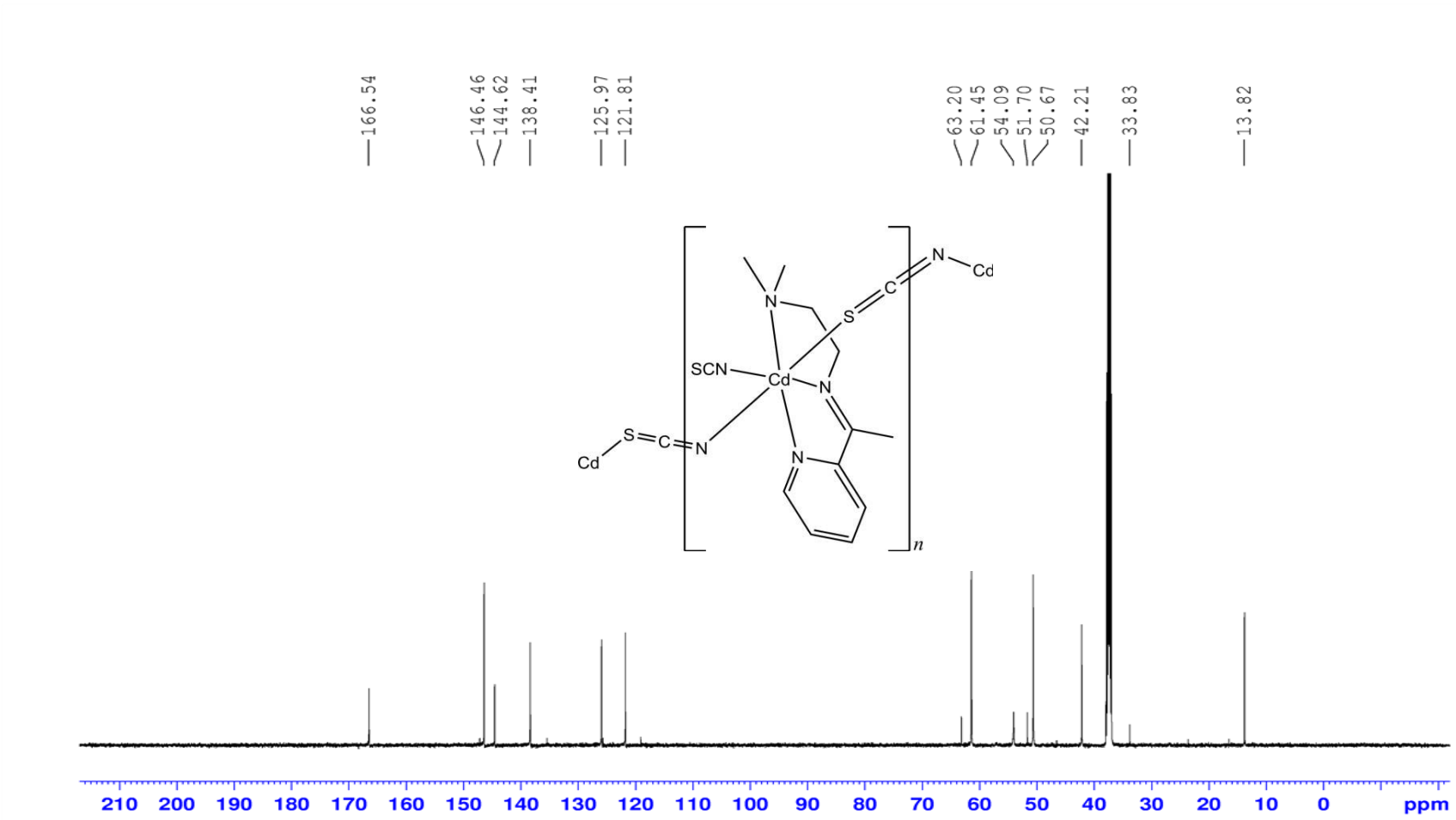

Figure 3.4.10: 13C-NMR spectra of [Cd(LNA)$(SCN)_2$]n

3.5 UV-Visible spectroscopy

The isolated benzene ring exhibits three characteristic absorptions all assigned to $n \rightarrow \pi^*$ type transitions. The substitutions on the ring by auxochromes and chromophores shift this band to the red. The band occurring for the ligands assigned as $n \rightarrow \pi^*$ transition involving molecular orbitals of the C=N chromophore and the benzene. The remainder of the observed bands in all the ligands are assigned as $n \rightarrow \pi^*$ type transitions involving molecular orbitals located essentially on the phenolic chromophore. Electron donating group on the aromatic ring generally caused a bathochromic shift in all the observed bands.

The electronic spectra for the free ligands were obtained and showed absorption band in two distinct regions. The first region is characteristic for the electronic inter-ligand $\pi \rightarrow \pi^*$ transitions (Chen, 2010), while the second characteristic wavelength is the inter ligand $n \rightarrow \pi$ transition of the C=C and C=N chromophores (Creaven, 2010). Another distinct region in the complexes is the characteristic for the charge transfer from metal to ligand (C.T.M→L) or ligand to metal charge transfer (LMCT) from the nitrogen atom to the transition metal centre (Ali, 2008). The last distinct region is the characteristic for inter metal d→d* transition (Ali, 2008).

Table 3.13 (a): UV-Visible spectroscopy for 2-morpholino-*N*-(1-(pyridin-2-yl) ethylidene) ethanamine (LMA) with its manganese and cobalt metal complexes.

Compound	Wavelength (nm)			
	λmax	Absorb.	εmax($Lmol^{-1}cm^{-1}$)	Assignment
LMA	488	0.250	500.00	n→ π*
[Mn(LMA)Cl2]	272	2.591	5182.00	C.T. M → L
	603	0.065	130.00	$^6A_1 \rightarrow {}^4E_{(D)}$
	813	0.094	188.00	
[Mn(LMA)(NCS)2H2O]				
	486	3.470	82.14	$^6A_{1g} \rightarrow {}^4A_{1g(E)}$
	327	23.724	561.61	$^6A_{1g} \rightarrow {}^4T_{2g(E)}$
	641	15.397	364.49	$^6A_{1g} \rightarrow {}^4T_{1g(E)}$
[Co(LMA)Br2]				
	356	0.258	516.00	$^4T_{1g(F)} \rightarrow {}^4A_{2g(F)(v2)}$
	603	0.095	190.00	$^4T_{1g(F)} \rightarrow {}^4T_{1g(D)\,(v3)}$
	821	0.103	206.00	$^4T_{1g(F)} \rightarrow {}^4T_{2g(F)\,(v1)}$
[Co(LMA)Cl2]	275	20.096	553.00	$^4T_{1g(F)} \rightarrow {}^4A_{2g(F)\,(v2)}$
	309	18.730	525.73	
	525	3.072	84.59	$^4T_{1g(F)} \rightarrow {}^4T_{1g(D)\,(v3)}$
	569	2.765	76.14	
	635	3.063	84.35	$^4T_{1g(F)} \rightarrow {}^4T_{2g(F)\,(v1)}$
[Co(LMA)(N3)3]	395	3.135	6270.00	$^1A_{1g} \rightarrow {}^3A_{1g;}$
	416	3.311	6622.00	$^1A_{1g} \rightarrow {}^3T_{2g;}$
	596	1.434	2868.00	$^1A_{ig} \rightarrow {}^5T_{2g}$
[Co(LMA)(NCS)2H2O]	286	0.106	212.00	$^4T_{1g(F)} \rightarrow {}^4A_{2g(F)\,(v2)}$
	658	0.127	254.00	$^4T_{1g(F)} \rightarrow {}^4T_{1g(P)\,(v3)}$
	668	0.127	254.00	
	803	0.106	212.00	$^4T_{1g(F)} \rightarrow {}^4T_{2g(F)\,(v1)}$

Another factor to be considered in the assignment of these transitions for the free ligand is its absence in the spectrum of the corresponding metal(II) complexes as shown in Table 3.13 (a-c). The $n \rightarrow \pi^*$ type transition due the C=N chromophore shifts to different energies on complexation. In general, the $A+X^*$ type transition due to the aromatic ring undergoes a similar smaller shift. The deconvolution of the visible portion of the optical absorption spectrum yields extra peaks.

The electronic spectra of Mn^{2+} ion d^5 complex $Mn(LMA)Cl_2$ exhibited bands at 272, 603 and 813 corresponding to $^6A_1 \rightarrow {}^4E_{(D)}$ in distorted square bipyramidal geometry. $Mn(LMA)(NCS)_2(H_2O)$ with a transitions of $^6A_1 \rightarrow {}^4E_{(D)}$ and $^6A_1 \rightarrow {}^4T_{2(D)}$ can be attributed to the band at 203, 486, 327, and 641 nm indicates that they have tetrahedral geometries.

The Co(II) ion with its d^7 configuration for $Co(LMA)Cl_2$ and $Co(LMA)Br_2$ exhibits absorption bands at 275, 309, 525, 569, 635 and 240, 356, 603, 821 nm respectively assigned to the transition $^4T_{1g(F)} \rightarrow {}^4T_{2g(P)}$ (V3), $^4T_{lg(F)} \rightarrow {}^4A_{2g(F)(V2)}$ and $^4T_{1g(F)} \rightarrow {}^4T_{2g(F)}$ (V1) in octahedral geometry (Carlin 1968). The Co(II) complex in $[Co(LMA)(NCS)_2(H_2O)]$ exhibited bands at 286, 658, 668, 803 which is attributed to the electronic transitions of $^4T_{1g(F)} \rightarrow {}^4A_{2g(F)}$, $^4T_{1g(F)} \rightarrow {}^4T_{1g(P)}$. These transitions correspond to Co(II) as a distorted octahedral complex. The *d-d* peaks on the spectrum (Figure 3.5.4) are transitions for the d^6 cobalt(III) complex in $[Co(LMA)(N_3)_3]$ bands at 240, 395, 416, 596 nm attributable to $^1A_{1g} \rightarrow {}^3A_{1g}$; $^1A_{ig} \rightarrow {}^3T_{2g}$ and $^1A_{ig} \rightarrow {}^5T_{2g}$ Judging by the Tanabe-Sugano diagram for d^6 complexes, the ground state 5D would be split into a $^5T_{2g}$ and a ^5E_g. The stronger of the two peaks is most likely the transition between these two states. The weaker peak may be a spin-forbidden transition, which cannot be accurately predicted. The complex is most likely weak field, with four unpaired electrons.

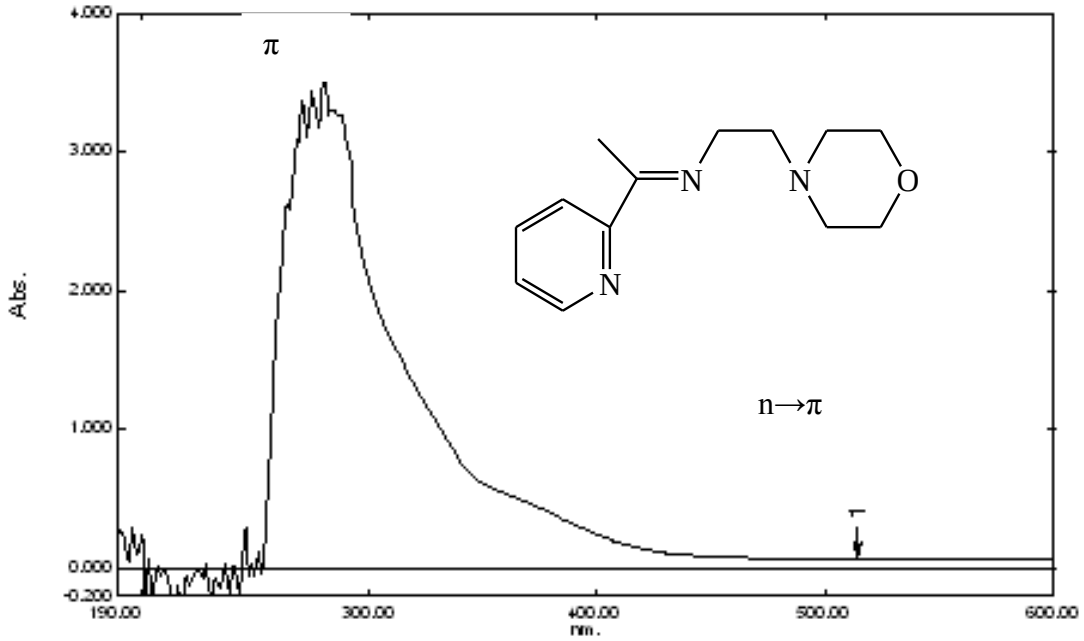

Figure 3.5.1: UV-Visible spectrao of [LMA]

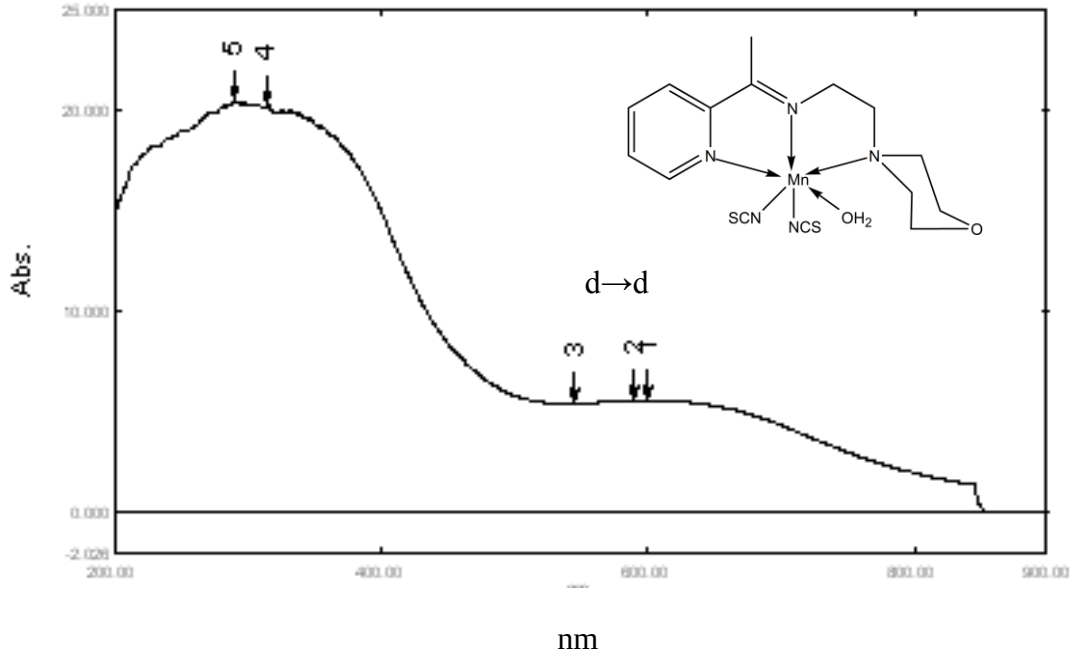

Figure 3.5.2: UV-Visible spectra of $[Mn(LMA)(NCS)_2H_2O]$

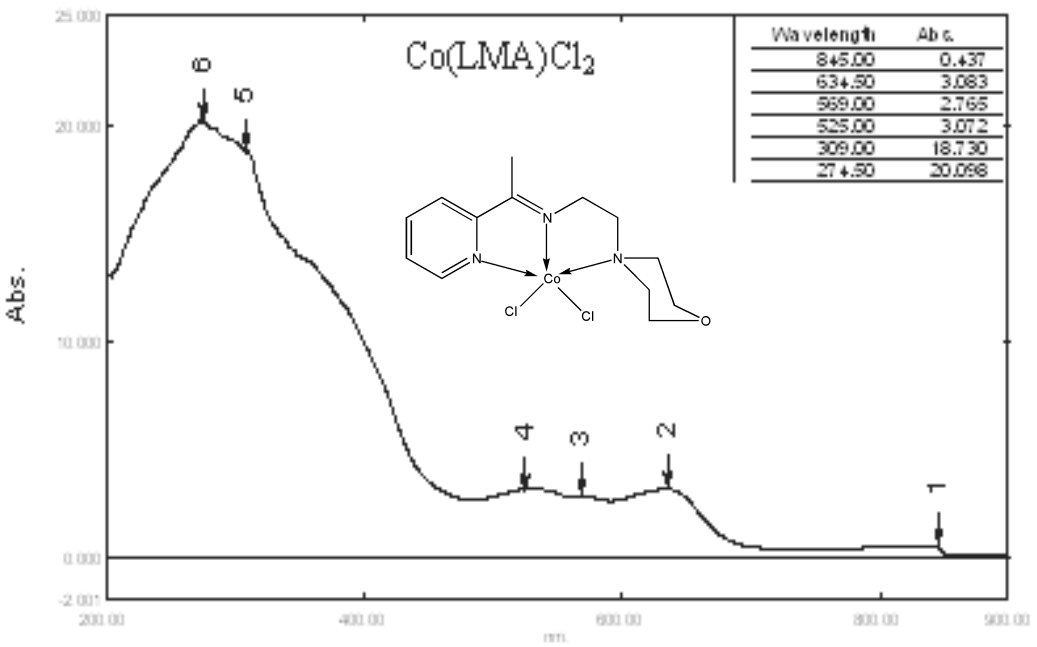

Figure 3.5.3: UV-Visible spectra of [Co(LMA)Cl_2]

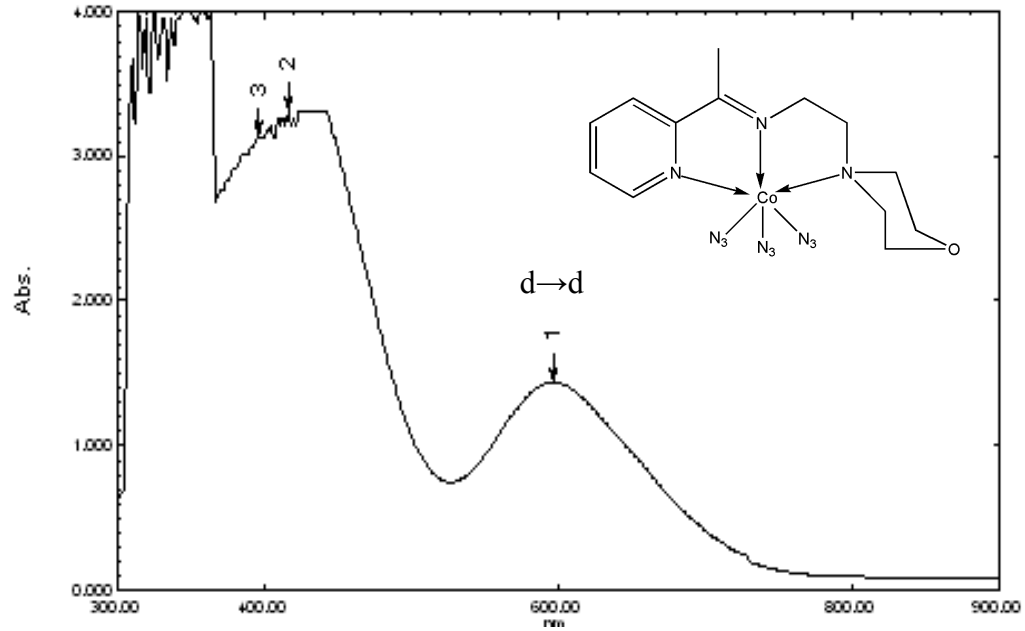

Figure 3.5.4: UV-Visible spectra of Co(LMA)N_3

Table 3.13 (b): UV-Visible spectroscopy for 2-morpholino-N-(1-(pyridin-2-yl)ethylidene) ethanamine (LMA) with its nickel and copper metal complexes.

Compound	Wavelength (nm)			
	λmax	Absorb.	εmax($Lmol^{-1}cm^{-1}$)	Assignment
LMA	488	0.250	500.00	$n \rightarrow \pi^*$
[Ni(LMA)N3]Polymer	279	3.215	6430.00	$^3A_{2g(F)} \rightarrow {}^3T_{2g(F)}$
	307	1.372	2744.00	$^3A_{2g(F)} \rightarrow {}^3T_{1g(P)}$
	628	0.116	232.00	
	712	0.114	228.00	$^3A_{2g(F)} \rightarrow {}^3T_{1g(P)}$
[Ni(LMA)(NCS)2H2O]	276	18.978	445.30	
	301	19.021	446.31	$^3A_{2g(F)} \rightarrow {}^3T_{1g(P)}$
	323	19.361	454.29	$^3A_{2g(F)} \rightarrow {}^3T_{1g(F)}$
	578	4.166	97.75	$^3A_{2g(F)} \rightarrow {}^3T_{2g(P)}$
[Cu(LMA)Br2]	275	19.406	424.96	C.T. M → L
	316	19.916	436.12	
	375	17.925	392.52	$^2E_{g(D)} \rightarrow {}^2T_{g(D)}$
	636	13.800	302.19	$^2E_{g2(D)} \rightarrow {}^2b_{1g(D)(\nu 1)}$
[Cu(LMA)Cl2]	288	14.596	396.88	C.T. M → L
	309	14.441	392.67	C.T. M → L
	337	14.206	386.28	$^2A_{1g(D)} \rightarrow {}^2B_{1g(D)(\nu 3)}$
	645	2.889	78.56	$^2E_{g(D)} \rightarrow {}^2B_{1g(D)(\nu 1)}$
[Cu(LMA)(N3)2]	279	16.245	426.49	C.T. M → L
	316	16.293	427.75	C.T. M → L
	689	16.355	429.38	$^2E_{g2(D)} \rightarrow {}^2B_{1g(D)(\nu 2)}$
	707	16.469	432.37	$^2E_{g2(D)} \rightarrow {}^2B_{1g(D)(\nu 1)}$
	722	16.386	430.19	
[Cu(LMA)(NCS)2]	290	20.401	493.95	C.T. M → L
	315	20.227	489.734	C.T. M → L
	544	5.435	131.59	$^2B_{2g(D)} \rightarrow {}^2B_{1g(D)}$
	591	5.527	133.82	
	601	5.550	134.38	$^2E_{2g(D)} \rightarrow {}^2B_{1g(D)(\nu 1)}$

Nickel(II), which has d^8 configuration, commonly exhibits octahedral, square planar and tetrahedral coordination geometries. Octahedral geometry generally occurs for nickel(II) with a coordination number of six. The electronic spectra of Ni(II) complexes [Ni(LMA)$(N_3)_3$] showed d-d transitions in the region of 279, 307, 628 and 712. These are assigned to the transitions $^3T_{1(F)} \rightarrow {}^3A_{2(F),}$ $^3T_{1(F)} \rightarrow {}^3T_{1(P)}$ and $^3T_{1(F)} \rightarrow {}^3T_{2(F)}$ consistent with distorted octahedral geometry (Cotton and Wilkinson 1998). The electronic spectra of Ni(II) complex [Ni(L2)$(NCS)_2(H_2O)$] shows an absorption band at 276, 301, 323 and 578 corresponding to the transitions $^3A_{2g(F)} \rightarrow {}^3T_{2g(F),}$ $^3A_{2g(F)} \rightarrow {}^3T_{1g(F)}$ and $^3A_{2g(F)} \rightarrow {}^3T_{1(P)}$ respectively. These assignments correspond for Ni(II) as an octahedral complex with the coordinated water molecule complete the geometry (Lever, 1968).

Cu(II) is usually found in tetragonal coordination environment, with four short equatorial bonds and one or two axially elongated bonds due to the Jahn-Teller effect, though some four coordinate tetrahedral and planar complexes are known.

The spectrum of Cu(II) complexes Cu(LMA)Cl_2 and Cu(LMA)Br_2 showed bands in the visible region at 288, 309, 337, 645 nm and 275, 316, 375, 636nm respectively. These are assigned to the transitions $^2B_{1g} \rightarrow {}^2B_{2g}$, $^2B_{1g} \rightarrow {}^2A_{1g}$ and $^2B_{1g} \rightarrow {}^2E_g$ respectively consistent with distorted square planar geometry (Shayma, 2010). Also spectra of Cu(LMA)$(NCS)_2$ complex exhibits three broad bands in the region of 290, 315, 544, 591 and 601, likewise Cu(LMA)$(N3)_2$ complex exhibits bands at 279, 316, 689, 707 and 722 all corresponding to the d-d transitions $^2B_1 \rightarrow {}^2A_1$, $^2B_1 \rightarrow {}^2B_2$ and $^2B_1 \rightarrow {}^2E$ (Shayma Shaker, 2009). Therefore, these transitions confirmed that the Cu(II) complex has a distorted octahedral geometry.

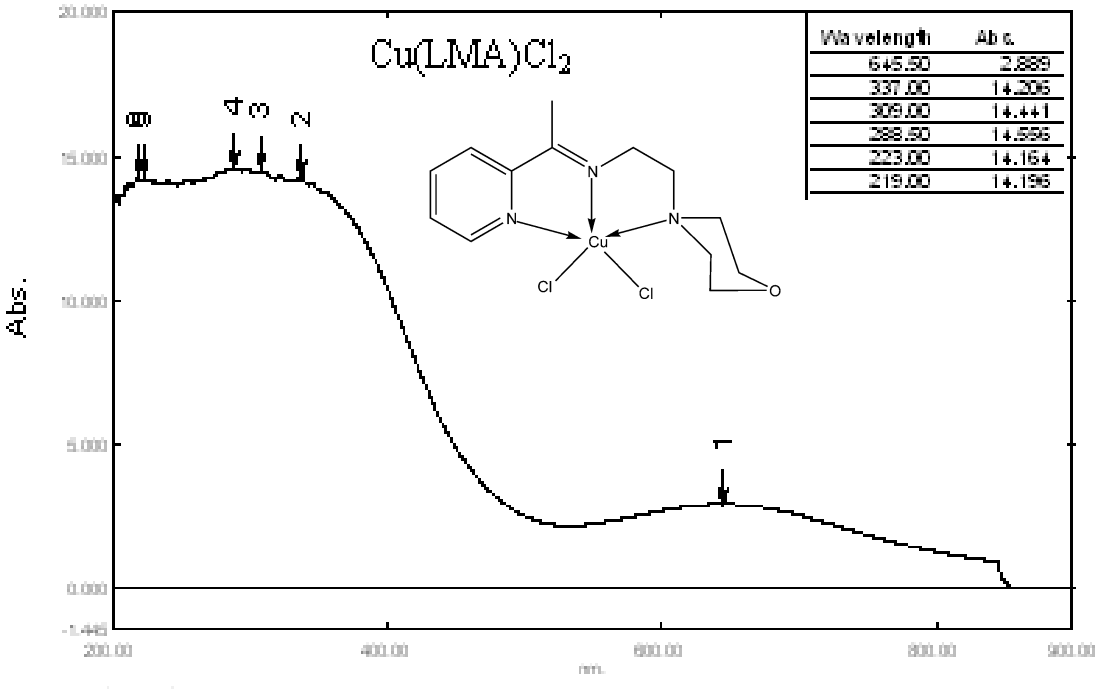

Figure 3.5.5: UV-Visible spectra of [Cu(LMA)Cl_2]

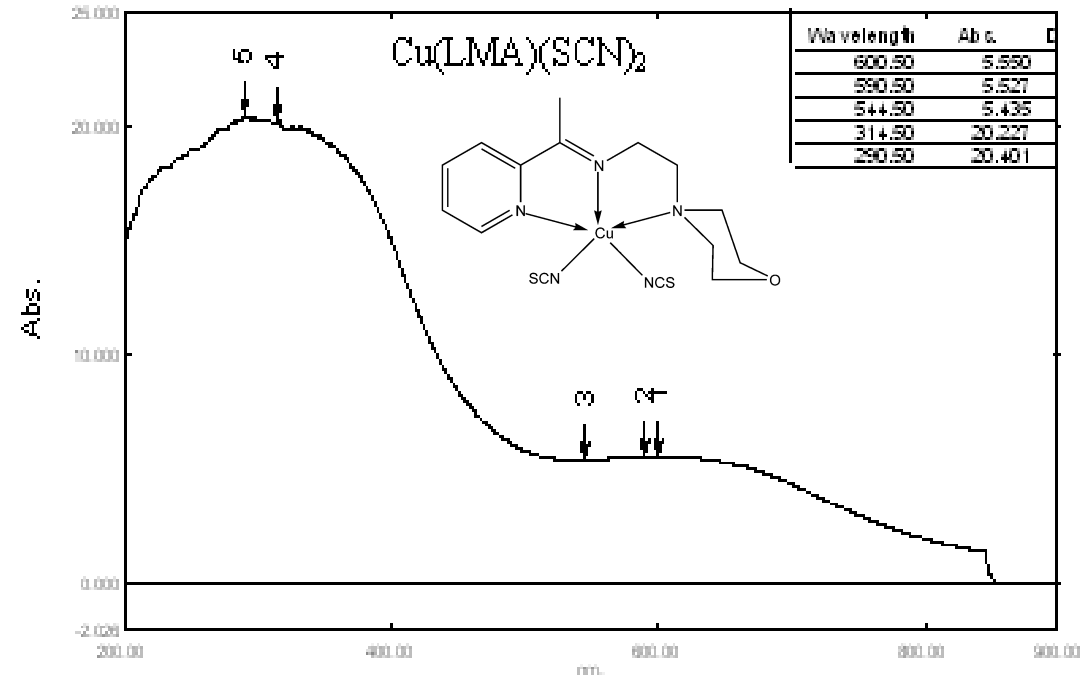

Figure 3.5.6: UV-Visible spectra of [Cu(LMA)$(NCS)_2$]

Table 3.13 (c): UV-Visible spectroscopy for 2-morpholino-N-(1-(pyridin-2-yl)ethylidene) ethanamine (LMA) with its zinc and cadmium metal complexes.

Compound	Wavelength (nm)			
	λmax	Absorb.	εmax($Lmol^{-1}$ cm^{-1})	Assignment
LMA	488	0.250	500.00	n→ π*
[Zn(LMA)Br2]	272	18.145	395.74	π→ π*
	312	16.115	351.46	C.T. M → L
[Zn(LMA)Cl2]	279	16.570	448.31	π→ π*
	476	0.094	2.54	C.T. M → L
[Zn(LMA)I2]				
	274	8.570	155.11	C.T. M → L
[Zn(LMA)(N3)2]	289	3.402	6804.00	π→ π*
	492	0.079	158.00	C.T. M → L
[Zn(LMA)(NCS)2]	271	17.324	417.59	π→ π*
	315	15.661	377.50	C.T. M → L
	506	0.116	2.79	C.T. M → L
[Cd(LMA)Br2]	275	3.436	6872.00	π→ π*
	291	3.524	7048.00	C.T. M → L
[Cd(LMA)Cl2]	279	2.364	4728.00	π→ π*
	403	0.095	19.10	C.T. M → L
[Cd(LMA)(N3)2]	272	16.437	367.08	π→ π*
	793	0.464	10.36	C.T. M → L
[Cd2(LMA)2(NCS)4]	277	3.436	6872.00	π→ π*
	288	3.524	7048	C.T. M → L

Lastly the electronic spectra for Zn(II) and Cd(II) complexes with an electronic configuration of d^{10} did not presented any *d-d* transitions. Instead the absorption bands observed were due to charge transfer transitions which suffered from blue shift with hyper chromic effect (Shayma, 2009). Coordination of the free ligand to Zn(II) and Cd(II) ions, is supported by the appearance of three main bands. Both π →π* and n→π* transition bands experience bathochromic shift and appear at the shorter wavelength of 220-250 nm and

280-370 nm respectively. The exhibition of the new LMCT band centered at 3920-580 nm is associated with the (LMCT) charge transfer in the spectra of metal complexes supported the formation of the zinc(II) and cadmium(II) complexes. All these absorptions for the free ligands and their corresponding metal complexes have been fully assigned in [Table 3.1.3 (c)].

In summary the difference observed in the visible spectra of the copper(II), cobalt(II/III), manganese(II) and nickel(II) complexes when compared with the spectra of the corresponding free ligand is the appearance of a broad low-intensities band in the ranges of 200-850 nm. This band is attributed to the *d-d* transitions of the metal(II/III) ions. These bands are of low molar absorptivity, E, being Laporte "forbidden" transition. Another important characteristic is the absence of the $n \rightarrow \pi^*$ band. The formation of the metal nitrogen bond stabilizes the electron pair on the nitrogen atoms, i.e., the energy of the nonbonding *n* orbital is lowered and the transition occurs at a lower wavelength. The absorption peak from approximately 400 nm to 600 nm means that the compound absorbs light in the violet-blue-green range. The sum of the non-absorbed, or reflected, wavelengths gives the products different colors.

Table 3.14: UV-Visible spectroscopy for 2-(1-(2-morpholinoethylimino)ethyl)phenol (LMH) and metal complexes.

Compound	**Wavelength (nm)**			
	λ_{max}	Absorb.	ε_{max} ($Lmol^{-1}cm^{-1}$)	Assignment
LMH	321	2.817	5634.00	$n \rightarrow \pi^*$
	396	0.749	1498.00	$n \rightarrow \pi^*$
[Mn(LMH)Br]				
	307	1.068	2136.00	$^6A_1 \rightarrow {}^4E_{(D)}$
	712	0.112	224.00	$^6A_1 \rightarrow {}^4T_{2(D)}$
[Mn(LMH)Cl]	277	2.672	5344.00	
	307	1.068	2056.00	$^6A_1 \rightarrow {}^4E_{(D)}$
	628	0.114	228.00	$^6A_1 \rightarrow {}^4T_{2(D)}$
	728	0.126	252.00	
	745	0.078	156.00	
[Ni(LMH)Br]				
	372	2.635	5270.00	$^3T_{1(F)} \rightarrow {}^3A_{2(F)}$
	597	0.332	664.00	$^3T_{1(F)} \rightarrow {}^3T_{1(P)}$
	778	0.063	126.00	$^3T_{1(F)} \rightarrow {}^3T_{2(F)}$
[Ni(LMH)Cl]				
	574	0.374	748.00	$^3T_{1(F)} \rightarrow {}^3T_{1(P)}$
	845	0.224	448.00	$^3T_{1(F)} \rightarrow {}^3T_{2(F)}$
[Cu(LMH)Br]				
	403	3.215	6430.00	$^1A_{1g} \rightarrow {}^1B_{1g}$
	596	0.734	1468.00	$^1A_{1g} \rightarrow {}^1A_{2g}$
	778	0.090	180.00	$^1A_{1g} \rightarrow {}^1E_g$
[Cu(LMH)Cl]	279	1.551	3102.00	
	358	1.470	2942.00	$^1A_{1g} \rightarrow {}^1B_{1g}$
	594	0.231	462.00	$^1A_{1g} \rightarrow {}^1A_{2g}$
	726	0.162	324.00	$^1A_{1g} \rightarrow {}^1E_g$
	744	0.110	220.00	
[Zn(LMH)Br]				
	307	1.068	2136.00	C.T. M → L
[Zn(LMH)Cl]				
	322	0.645	1290.00	C.T. M → L

The electronic spectra for the free ligands were obtained and showed absorption band in two distinct regions. The first region is characteristic for the electronic inter-ligand $\pi \rightarrow \pi^*$ transitions (Chen, 2010) while the second characteristic wavelength is the second inter ligand $n \rightarrow \pi$ transition of the C=C and C=N chromophores (Creaven, 2010). The electronic spectra of Mn(LMH)Cl and Mn(LMH)Br indicate that they have tetrahedral geometries. The $^6A_1 \rightarrow {}^4E(D)$ and $^6A_1 \rightarrow {}^4T_2(D)$ can attributed to the band at 307, 628, 745 and 307, 712 nm respectively (Shayma, 2010).

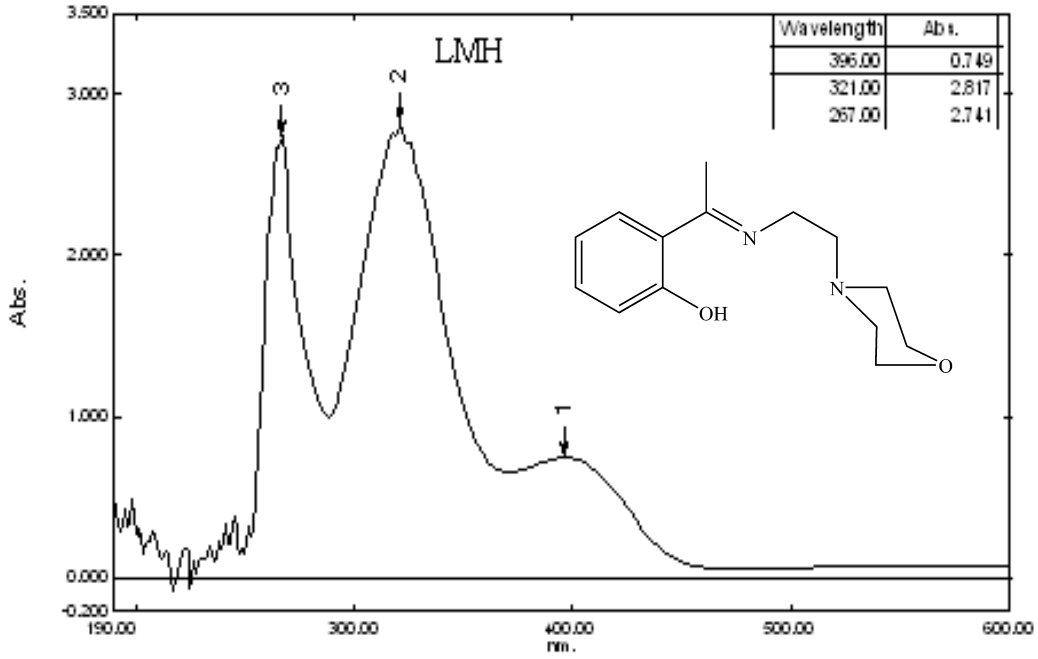

Figure 3.5.7: UV-Visible spectra of LMH

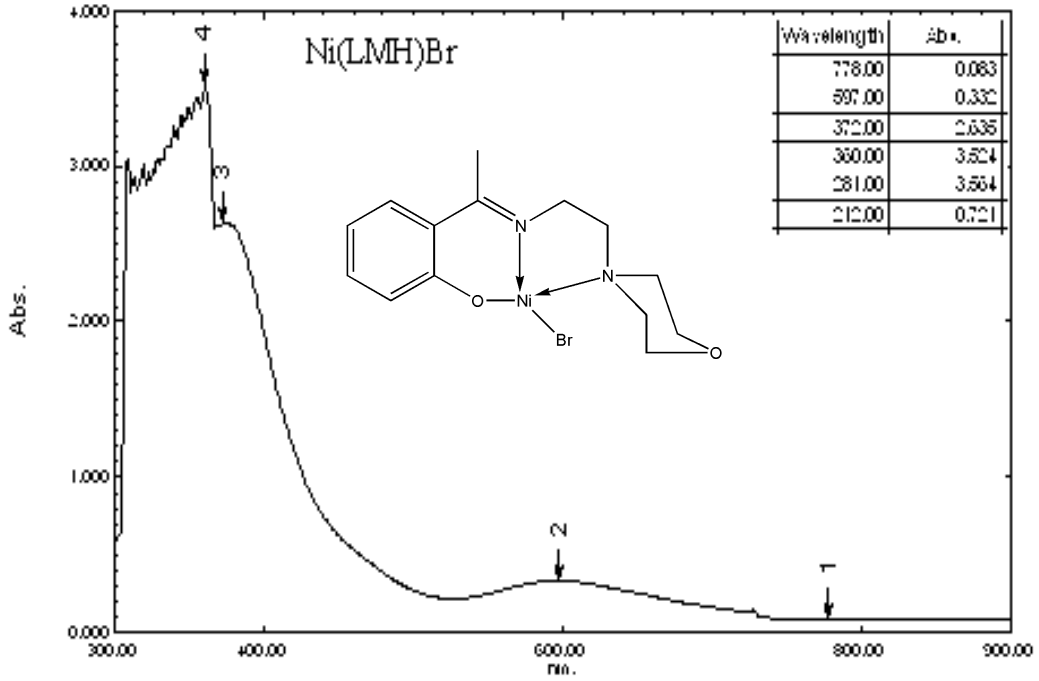

Figure 3.5.8: UV-Visible spectra of [Ni(LMA)Br]

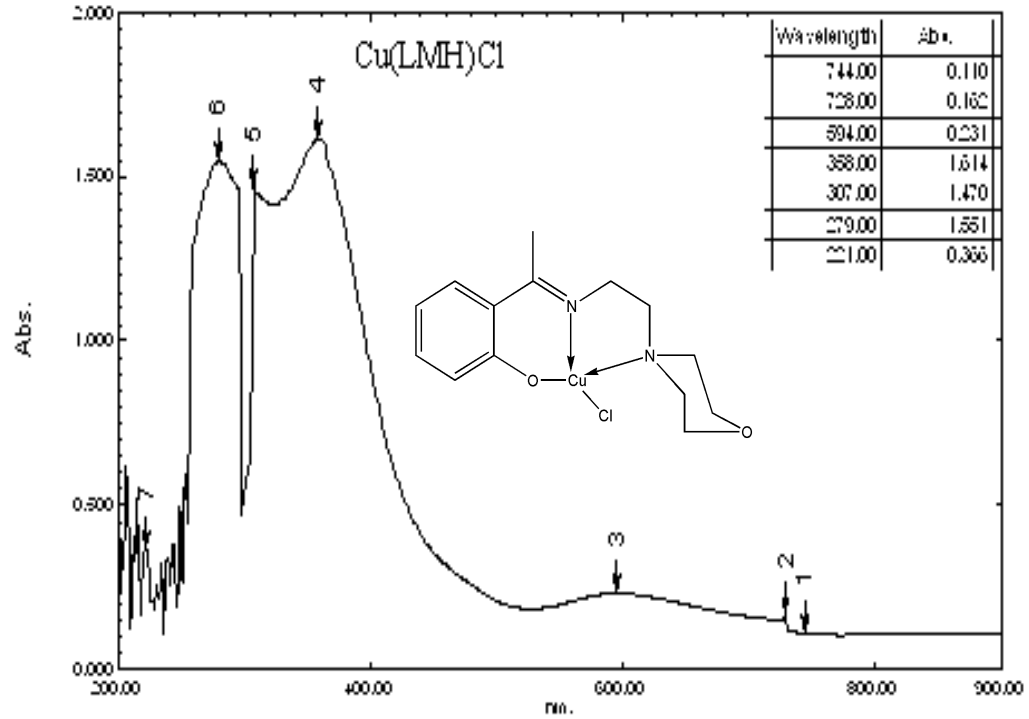

Figure 3.5.9: UV-Visible spectra of [Cu(LMA)Cl]

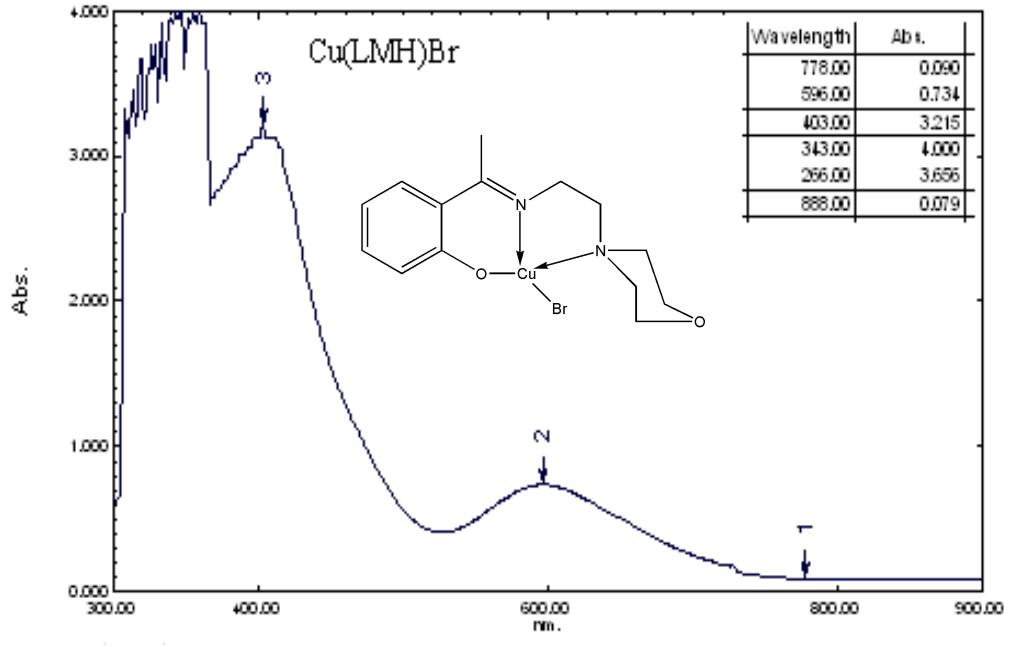

Figure 3.5.10: UV-Visible spectra of [Cu(LMA)Br]

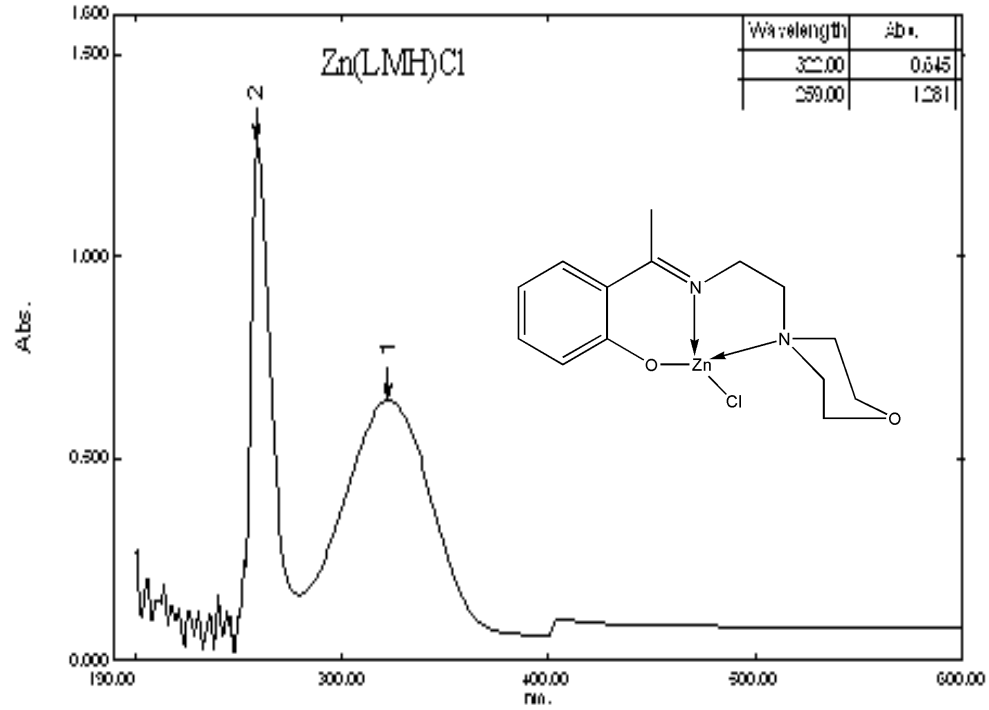

Figure 3.5.11: UV-Visible spectra of [Zn(LMA)Cl]

The electronic spectra of Ni(II) complexes Ni(LMH)Cl and Ni(LMH)Br showed *d-d* transitions in the region of 265, 574, 845 and 261, 372, 597, 778nm respectively. These are assigned to the transitions $^3T_{1(F)} \rightarrow {}^3A_{2(F),}$ $^3T_{1(F)} \rightarrow {}^3T_{1(P)}$ and $^3T_{1(F)} \rightarrow {}^3T_{2(F)}$ consistent with tetrahedral geometry (Shayma Shaker 2010; Cotton and Wilkinson 1998).

The spectrum of Cu(II) complexes Cu(LMH)Cl and Cu(LMH)Br showed three bands in the visible region at 594, 726, 744 nm and 403, 596, 778 respectively. These are assigned to the transitions $^1A_{1g} \rightarrow {}^1B_{1g;}$ $^1A_{1g} \rightarrow {}^1A_{2g;}$ $^1A_{1g} \rightarrow {}^1E_g$ respectively consistent with distorted square planar geometry (Shaker, 2010). Lastly the electronic spectra for Zn(II) and Cd(II) complexes with an electronic configuration of d^{10} did not presented any (d-d) transitions. Instead the absorption bands observed were due to charge transfer transitions which suffered from blue shift with hyper chromic effect (Shayma, 2009). All these absorptions for the free ligands and their corresponding metal complexes have been fully assigned in (Table 3.14).

Table 3.15: UV-Visible spectroscopy for *N1,N1*-dimethyl-*N2*-(1-(pyridin-2-yl)ethylidene)ethane-1,2-diamine (LNA) and metal complexes.

Compound	**Parameters**			
	λ_{max}	Absorb.	ε_{max} ($Lmol^{-1}$ cm^{-1})	Assignment
LNA				
	487	0.058	116.00	n→ π*
$[Mn(LNA)Cl_2]$	272	2.591	5182.00	C.T. M → L
	603	0.065	130.00	$^6A_1g \rightarrow {}^4A_1g$
	813	0.094	188.00	$^6A_1g \rightarrow {}^4Eg, {}^4A_1g$
$[Ni(LNA)(NCS)_2H_2O]$	270	2.061	4042.00	$^3A_2g_{(F)} \rightarrow {}^3T_1g_{(P)}$
	364	0.900	1800.00	$^3A_2g_{(F)} \rightarrow {}^3T_1g_{(F)}$
	807	0.109	218.00	$^3A_2g_{(F)} \rightarrow {}^3T_2g_{(F)}$
$[Cu(LNA)(NCS)_2]$	281	2.696	5392.00	C.T. M → L
	643	0.125	250.00	$^2E_{2g(D)} \rightarrow {}^2B_{1g(D)}$
$[Zn(LNA)Cl_2]$				
	284	3.675	7350.00	C.T. M → L
	603	0.084	168.00	C.T. M → L
$[Zn(LNA)(NCS)_2]$	280	2.285	4570.00	π→ π*
	606	0.064	128.00	C.T. M → L
$[Cd(LNA)Cl_2]$				
	279	0.285	570.00	C.T. M → L
	407	0.089	178.00	C.T. M → L
$[Cd(LNA)(NCS)_2]n$	280	2.767	5534.00	π→ π*
	467	0.055	110.00	C.T. M → L

The electronic spectra of Mn^{2+} ion $Mn(LNA)Cl_2$ exhibited bands at 272, 603 and 813 corresponding to $^6A_1 \rightarrow {}^4E(D)$ in distorted square bipyramidal geometry. $Mn(LMA)(NCS)_2(H_2O)$ with a transitions of $^6A_1 \rightarrow {}^4E(D)$ and $^6A_1 \rightarrow {}^4T_2(D)$ can be attributed to the band at 203, 486, 327, and 641 nm indicates that they have tetrahedral geometries. The electronic spectra of Ni(II) complexes $Ni(LMA)(NCS)_2$ showed d-d transitions in the region of 270, 364 and 807. These are assigned to the transitions $^3A_2g_{(F)} \rightarrow {}^3T_1g_{(P),}$ $^3A_2g_{(F)} \rightarrow {}^3T_1g_{(F)}$ and $^3A_2g_{(F)} \rightarrow {}^3T_2g_{(F)}$ consistent with distorted octahedral geometry (Lever, 1968). The spectrum of Cu(II) complex $Cu(LNA)(NCS)_2$ complex exhibits broad bands in the region of 28190 and 643 corresponding to the d-d transition $^2e_2g_{(D)} \rightarrow {}^2b_1g_{(D)}$. Therefore, these transitions confirmed that the Cu(II) complex has a distorted square pyramidal geometry.

Coordination of the free ligand to Zn(II) and Cd(II) ions, is supported by the appearance of three main bands. Both $\pi \rightarrow \pi^*$ and $n \rightarrow \pi^*$ transition bands experience bathochromic shift and appear at the shorter wavelength of 220-250 nm and 280-370 nm respectively. The exhibition of the new LMCT band centered at 392-580 nm is associated with the (LMCT) charge transfer in the spectra of metal complexes supported the formation of the Zinc(II) and Cadmium(II) complexes. All these absorptions for the free ligands and their corresponding metal complexes have been fully assigned in (Table 3.15).

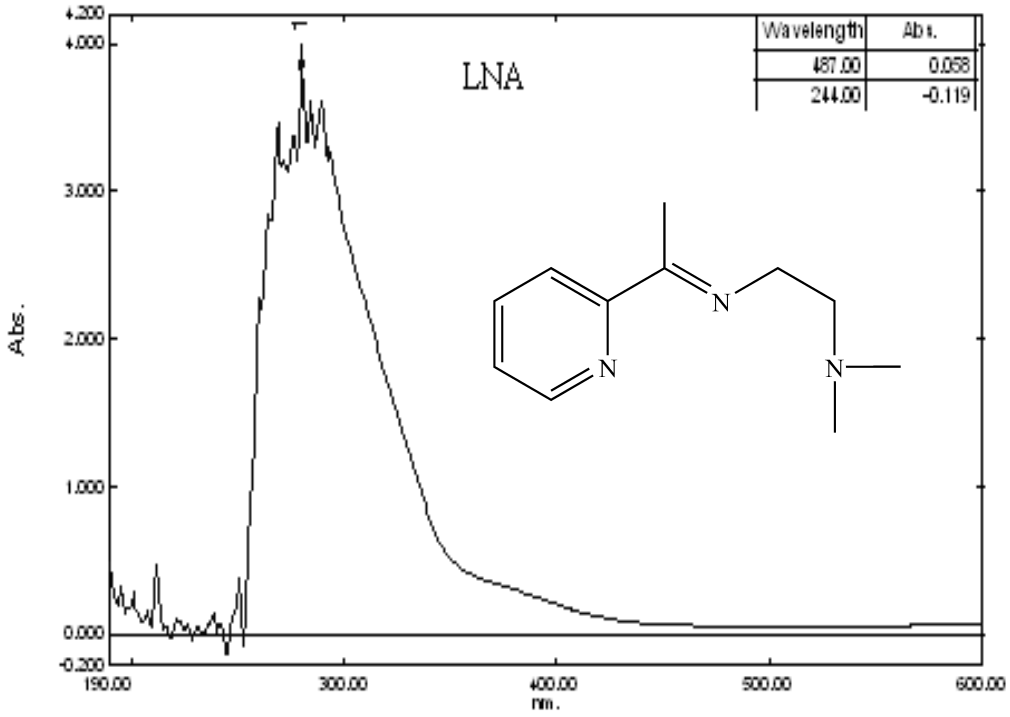

Figure 3.5.12: UV-Visible spectra of (LNA)

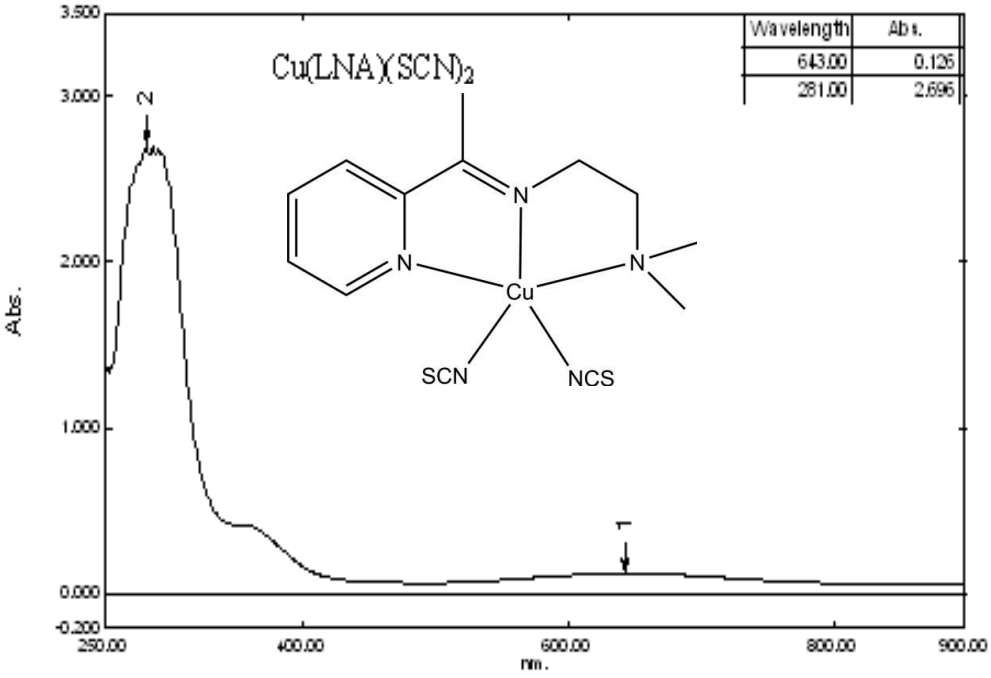

Figure 3.5.13: UV-Visible spectra of [Cu(LNA)(NCS)2]

Table 3.16: UV-Visible spectroscopy for 2-(1-(2-(dimethylamino)ethylimino)ethyl)phenol (LNH) and metal complexes.

Compound	λ_{max}	Absorb.	ε_{max} ($Lmol^{-1}$ cm^{-1})	**Assignment**
LNH	272	3.612	7224.00	$\pi \rightarrow \pi^*$
	364	1.823	3646.00	$n \rightarrow \pi^*$
$[Cu_2(LNH)_2Br_2]$				
	276	3.612	7224.00	C.T. M → L
	307	1.379	2758.00	C.T. M → L
	364	2.107	4214.00	$^2B_2g_{(D)} \rightarrow {}^2B_1g_{(D)}$
	606	0.166	332.00	
	726	0.147	294.00	$^2E_2g_{(D)} \rightarrow {}^2B_1g_{(D)}$
	743	0.095	190.00	
	778	0.090	180.00	

The electronic spectrum of $Cu_2(LNH)_2Br_2$ presented bands in the region of 276, 307, 364, 606, 726, 743 and 778 which correspond to the transition of $^2B_2g_{(D)} \rightarrow {}^2B_1g_{(D)}$ and $^2E_2g_{(D)} \rightarrow {}^2B_1g_{(D)}$. All these absorptions for the free ligand and corresponding metal complex have been fully assigned in (Table 3.16).

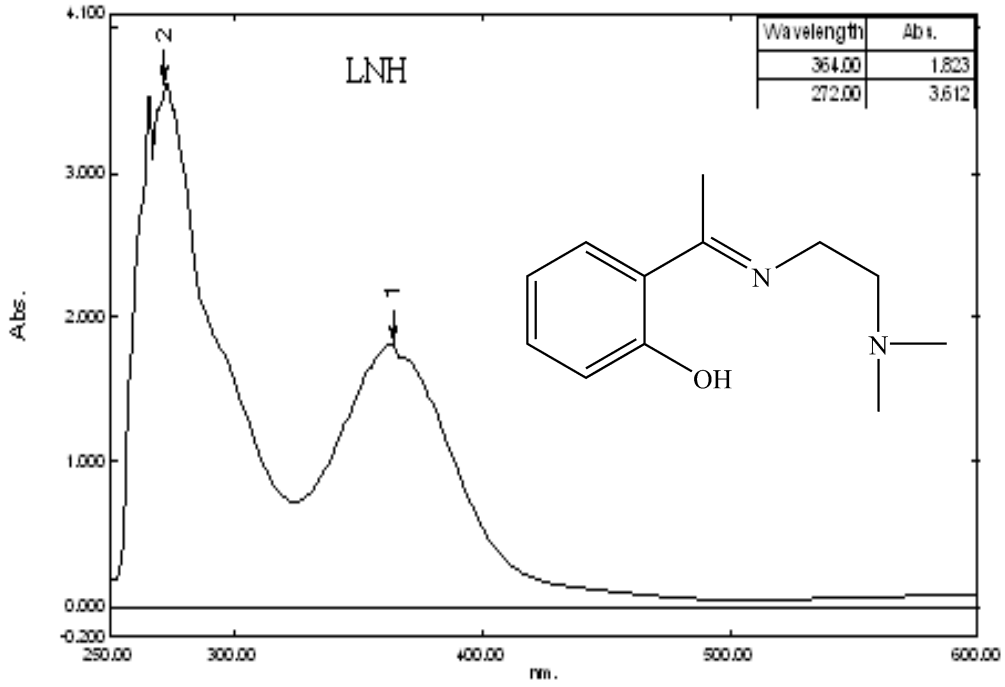

Figure 3.5.14: UV-Visible spectra of LNH

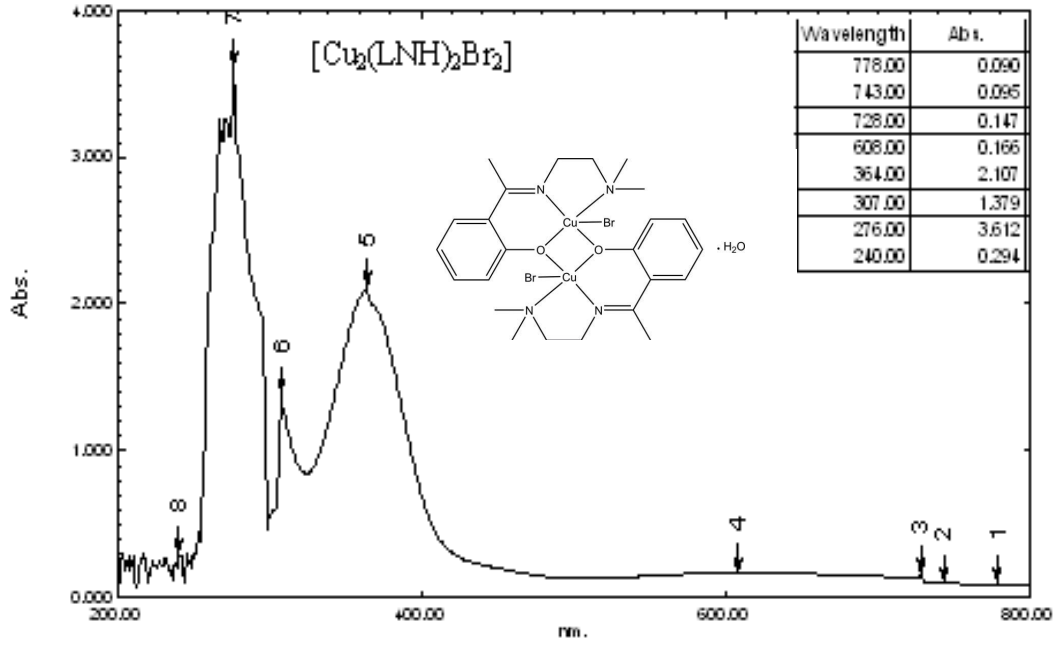

Figure 3.5.15: UV-Visible spectra of $[Cu_2(LNH)_2Br_2. H_2O]$

3.6 X-ray crystallographic structures of the complexes

3.6.1 Dichlorido{2-morpholino-N-[1-(2-pyridyl)ethylidene] ethanamineκ ^{3}N,N',N''}Mn(II)

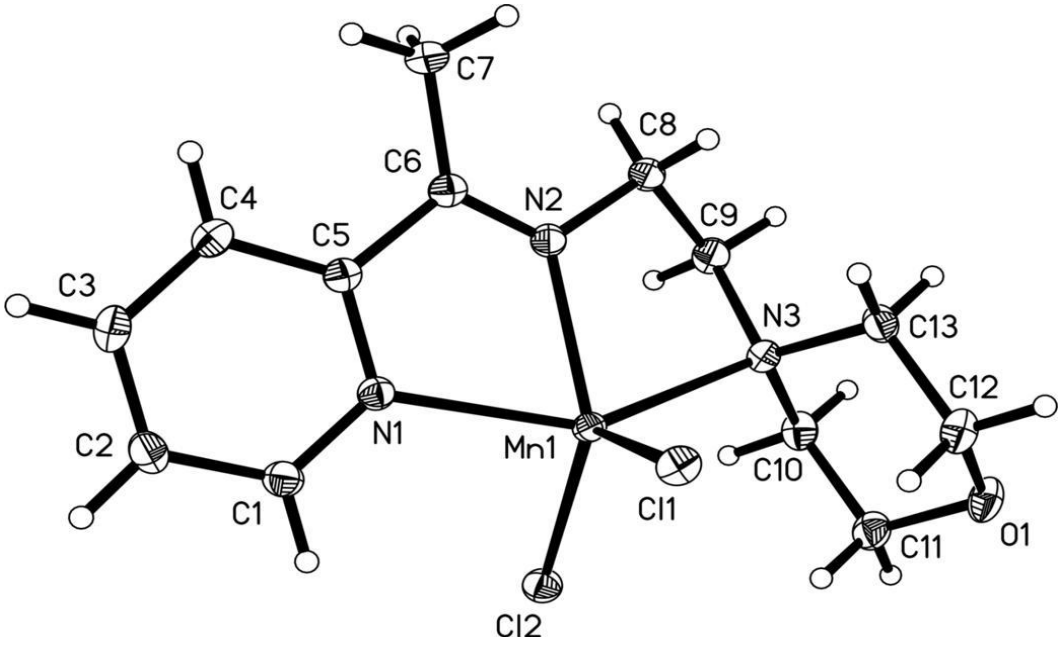

Figure 3.6.1: Crystal structure for [Mn(LMA)Cl_2]

The brown colored crystal compound is isostructure to the recently reported Cd(II) complex (Ikmal Hisham, 2010). The Mn(II) ion is five-coordinated by the Schiff base 2-morpholino-*N*-[1-(2-pyridyl)ethylidene]ethanamine and two Cl atoms in a distorted square-pyramidal environment (τ = 0.22). The Mn-Cl and Mn-N bond lengths in the present structure is similar to those in [$MnCl_2(C_{24}H_{25}N_3)$], the structurally closest Mn(II) complex (Schmiege, 2007). In the crystal structure, intermolecular C-H···Cl hydrogen bonds link the adjacent molecules into a three-dimensional network. An intramolecular C-H···Cl hydrogen bonding has also been observed.

In summary, the Mn(II) ion is pentacoordinated in a distorted square-pyramidal geometry. The coordination environment is defined by the *N,N',N''*-tridentate Schiff base ligand and one Cl atom in the basal positions and one Cl atom in the apical position.

3.6.2 Aqua{2-morpholino-N-[1-(2-pyridyl)-ethylidene]ethanamine-κ^3N,N',N''}-bis (thiocyanato-κ^N)manganese(II)

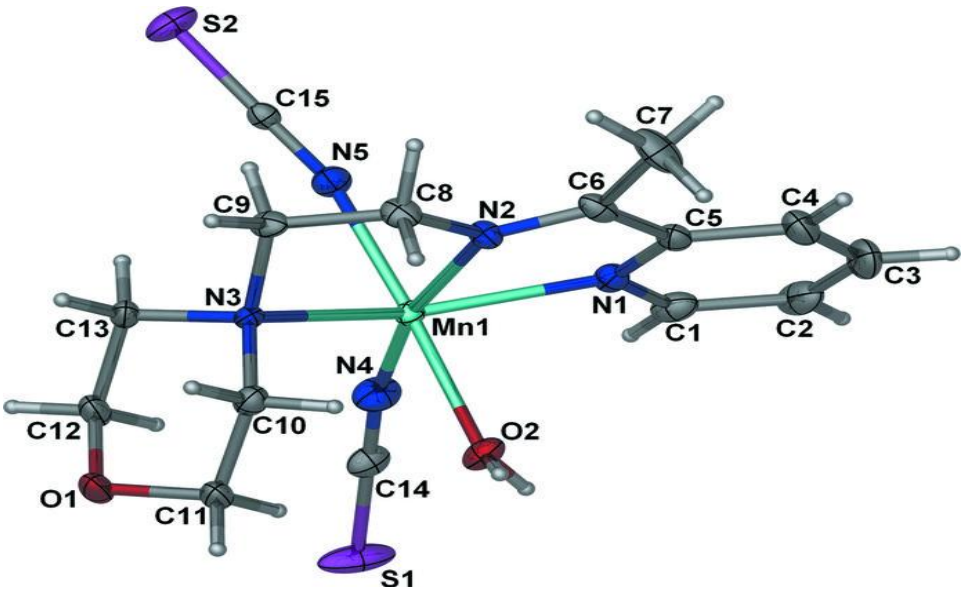

Figure 3.6.2: Crystal structure for [Mn(LMA)$(NCS)_2(H_2O)$]

The crystal of the title compound is iso structural with the previously reported Co(II) complex (Gwaram, 2011). The metal center is coordinated by the *N,N',N''*-tridentate Schiff base, two *N*-donor thiocyanates and one water O atom in a distorted octahedral geometry. In the crystal, the molecules are linked through O-H···O and O-H···S hydrogen bonds into layers parallel to the *ac* plane and these are connected into a three-dimensional network *via* C-H···S interactions. Moreover, intramolecular C-H···O hydrogen bonding is observed.

In summary, the Schiff base acts as an *N,N',N''*-tridentate ligand, forming two five-membered chelating rings with the Mn(II) atom. The distorted octahedral geometry around the metal atom is completed by two *cis*-positioned *N*-bound thiocyanate ligands and one water molecule. In the crystal, adjacent molecules are linked through O-H---O, O-H---S and C-H---S hydrogen bonds into a three-dimensional supra-molecular structure (Figure 3.6.3). An intramolecular C-H---O hydrogen bond also occurs.

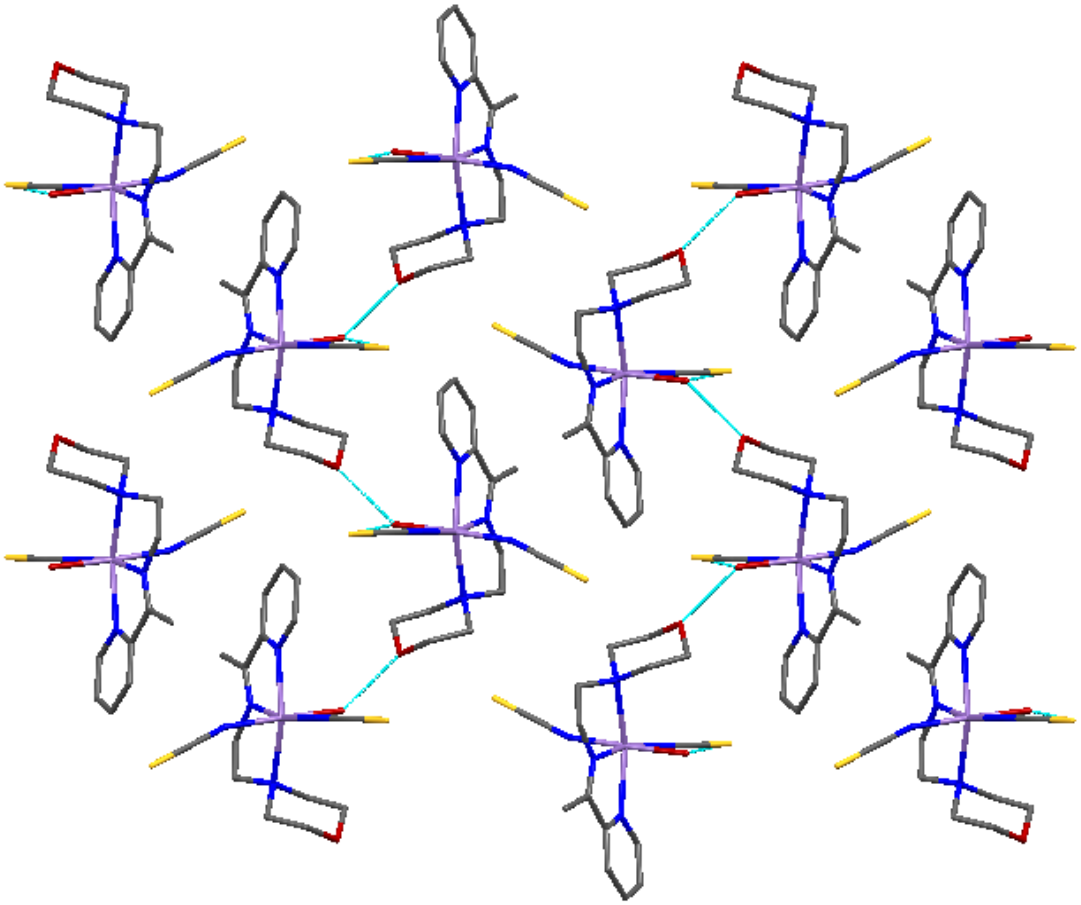

Figure 3.6.3: Packing structure for [Mn(LMA)$(NCS)_2(H_2O)$]

Table 3.17: Crystal data and structure refinement for [Mn(LMA)Cl2] & $[Mn(LMA)(NCS)_2(H_2O)]$ complexes

Identification code	**$[Mn(LMA)Cl_2]$**	**$[Mn(LMA)(NCS).H_2O]$**
Empirical formula	$C_{13}H_{19}Cl_2MnN_3O$	$C_{15}H_{21}MnN_5O_2S_2$
Formula weight	359.15	422.43
Temperature/K	373(2)	373(2)
Crystal system	monoclinic	monoclinic
Space group	$P2_1/n$	$P2_1/c$
a/Å	9.6117(6)	7.1837(13)
b/Å	13.8507(8)	22.408(4)
c/Å	12.1330(7)	12.112(2)
α/°	90.00	90.00
β/°	106.7380(10)	91.149(3)
γ/°	90.00	90.00
Volume/$Å^3$	1546.82(16)	1949.3(6)
Z	4	4
$\rho_{calc}mg/mm^3$	1.542	1.439
m/mm^{-1}	1.197	0.910
F(000)	740.0	876.0
Crystal size/mm^3	0.40 × 0.35 × 0.25	0.19 × 0.16 × 0.08
2Θ range for data collection	4.58 to 55°	3.64 to 54.58°
Index ranges	$-12 \le h \le 12, -16 \le k \le 17, -$	$-9 \le h \le 9, -28 \le k \le 15, -13$
Reflections collected	15613	12085
Independent reflections	3543[R(int) = 0.0188]	4358[R(int) = 0.0403]
Data/restraints/parameters	3543/0/182	4358/2/233
Goodness-of-fit on F^2	1.108	1.040
Final R indexes [I>=2σ (I)]	$R_1 = 0.0195, wR_2 = 0.0520$	$R_1 = 0.0378, wR_2 = 0.0842$
Final R indexes [all data]	$R_1 = 0.0206, wR_2 = 0.0526$	$R_1 = 0.0602, wR_2 = 0.0964$
Largest diff. peak/hole/e $Å^{-3}$	0.33/-0.23	0.38/-0.47

3.6.3 Dichlorido{2-morpholino-N-[1-(2-pyridyl)ethylidene]ethanamineκ^3N,N',N''} cobalt(II)

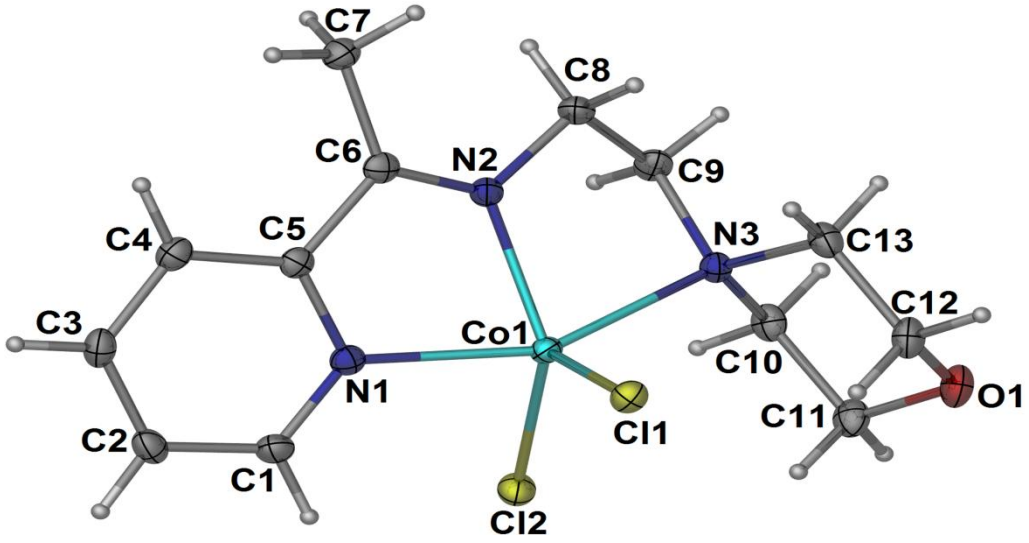

Figure 3.6.4: Crystal structure for [Co(LMA)Cl_2]

The reddish brown colored crystal compound is isostructural to the Mn(II) complex (Ikmal Hisham, 2010). The Co(II) ion is five-coordinated by the Schiff base 2-morpholino-*N*-[1-(2-pyridyl)ethylidene]ethanamine and two Cl atoms in a distorted square-pyramidal environment ($\tau = 0.21$). The Co-Cl and Co-N bond lengths in the present structure is similar to those in [$MnCl_2(C_{24}H_{25}N_3)$], the structurally closest Mn(II) complex (Schmiege, 2007). In the crystal structure, intermolecular C-H···Cl hydrogen bonds link the adjacent molecules into a three-dimensional network. An intramolecular C-H···Cl hydrogen bonding has also been observed.

In summary, the Co(II) ion is pentacoordinated in a distorted square-pyramidal geometry. The coordination environment is defined by the *N,N',N''*-tridentate Schiff base ligand and two Cl atoms that completed the five coordinated geometry.

3.6.4. Aqua{2-morpholino-N-[1-(2-pyridyl)-ethylidene]ethanamine-κ^3N,N',N''}-bis (thiocyanato-κ^N)cobalt(II)

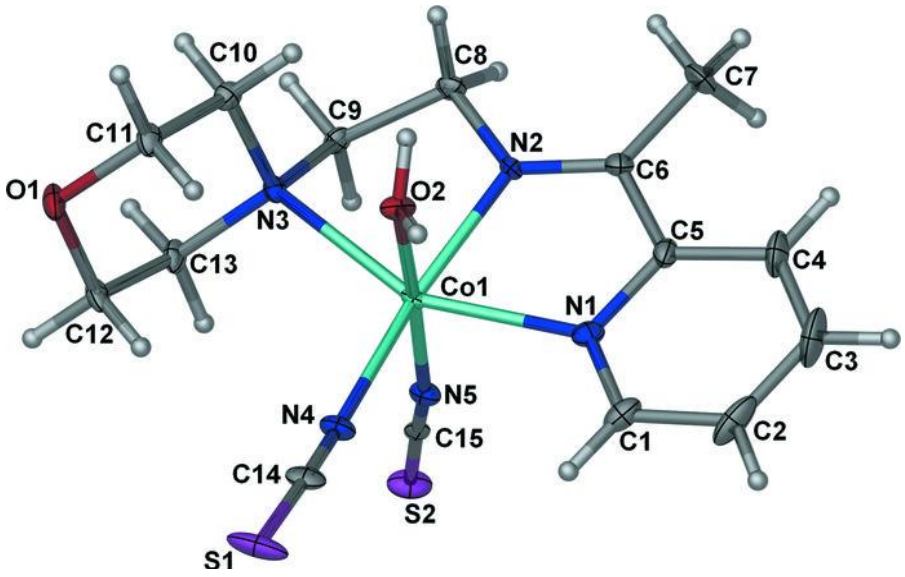

Figure 3.6.5: Crystal structure for $[Co(LMA)(NCS)_2(H_2O)]$

The crystal structure of the Co(II) complex is isostructural with the previously reported Ni(II) complex (Gwaram, 2011). The Schiff base, prepared *in situ*, acts as an *N,N',N''*-tridentate ligand towards the Co(II) ion to form two five membered chelate rings with the metal atom. Two *cis*-located isothiocyanate and one water molecule complete a distorted octahedral geometry around the Co(II) center. A similar arrangement was observed in a related Co(II) complex (Sun, 2007). In the crystal, the adjacent molecules are connected *via* O-H···O, O-H···S, C-H···S hydrogen bonds into infinite layers parallel to the *ac* plane. The layers are further linked into a three-dimensional polymeric structure through an S···S interaction [3.5546 (18) Å] between S1 and S2 of the symmetry related molecule at *–x+1*, *y* - 1/2, -*z* + 3/2.

In summary, the Co(II) ion is six-coordinated by the *N,N',N''*-tridentate Schiff base, the N atoms of two thiocyanate ligands and one water molecule in a distorted octahedral geometry. Intramolecular C-H---N and C-H---O hydrogen bonds occur (Figure 3.6.6).

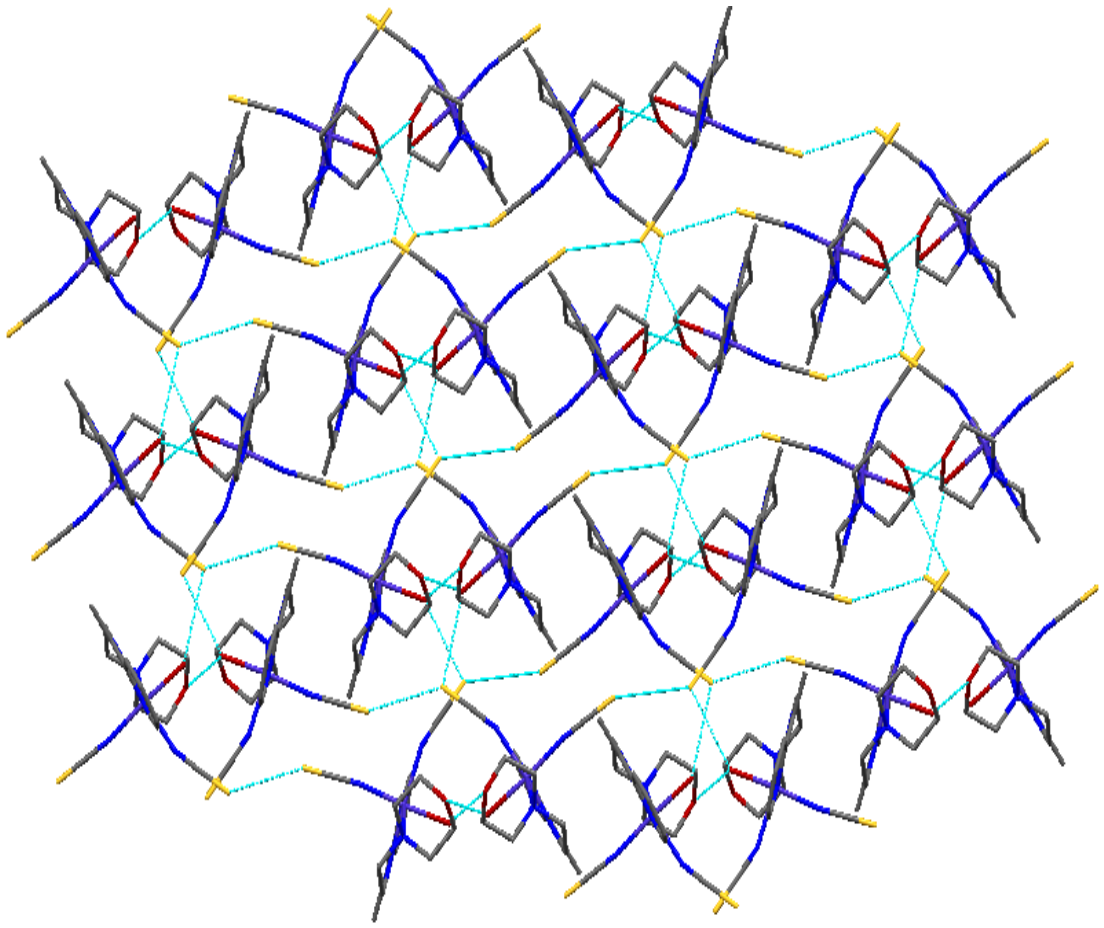

Figure 3.6.6: Packing Structure $Co(LMA)(NCS)_2(H_2O)$ along c-axis

3.6.4 Cobalt(III)tris(azido-κ^N){2-Morpholino-N-[1-(2-pyridyl)ethylidene]ethanamine-κ^3N,N',N''}

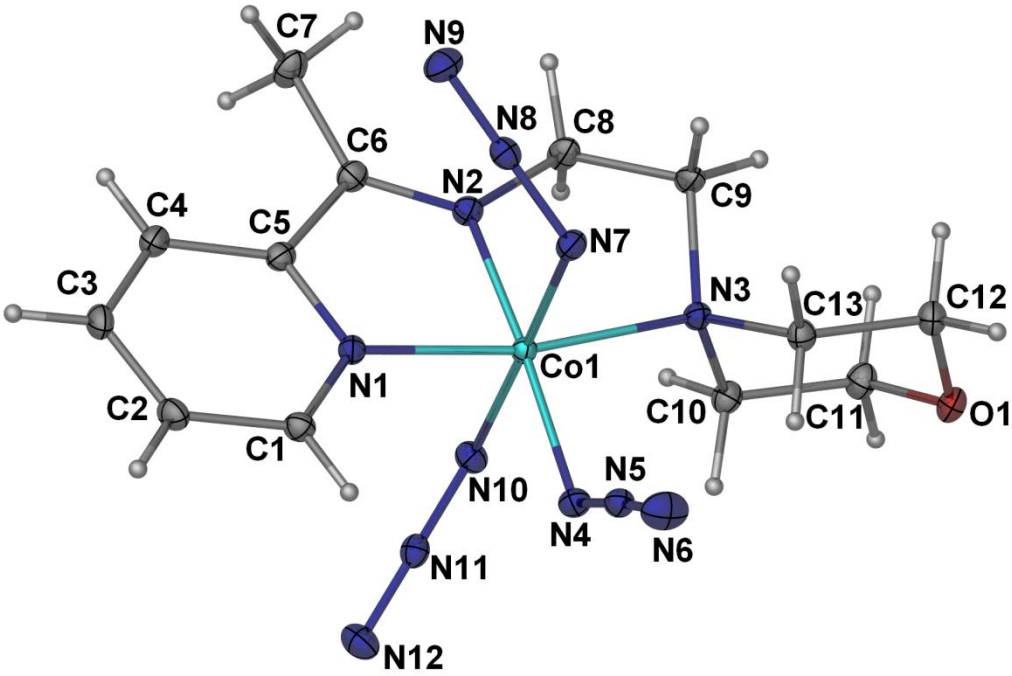

Figure 3.6.7: Crystal structure for $[Co(LMA)(N_3)_3]$

The crystal structure of Co(III) compound as depicted in (Figure 3.6.7) and selected bond lengths and angles are listed in Table 3.19. In the compound, the Schiff base molecule acts as an *N,N',N''*-tridentate ligand to form two five-membered chelate rings with the Co(III) atom. Three meridionally arranged nitrogen atoms from three azide ligands complete a distorted octahedral geometry around the metal center. The distortion from an ideal octahedron is evident from the cisoid [82.45(5)-96.03(5)^0] and transoid [168.62(5)-177.62(5)^0] angles. The azide groups are almost linear [175.65(15)-179.22(14)^0] whereas the Co-*N-N-N* linkages are significantly bent [114.33(9)-123.13(9)^0]. The Co-N bond lengths are similar to those observed in a similar structure (Rahman, 2005).

Table 3.18: Crystal data and structure refinement for cobalt complexes

Identification code	**[Co(LMA)Cl_2]**	**[Co(LMA)(NCS)]**	**[Co(LMA)$(N_3)_3$]**
Empirical formula	$C_{13}H_{19}Cl_2CoN_3O$	$C_{16}H_{21}ClCoN_5O_2S_2$	$C_{13}H_{19}CoN_{12}O$
Formula weight	363.14	438.43	418.33
Temperature/K	373(2)	373(2)	373(2)
Crystal system	monoclinic	monoclinic	monoclinic
Space group	$P2_1/n$	$P2_1/c$	$P2_1/c$
a/Å	9.6620(5)	7.1554(3)	10.0164(2)
b/Å	13.6941(7)	22.1870(10)	12.6221(3)
c/Å	11.9927(6)	12.1297(5)	13.7134(3)
α/°	90.00	90.00	90.00
β/°	107.0790(10)	91.115(3)	91.1770(10)
γ/°	90.00	90.00	90.00
Volume/$Å^3$	1516.81(13)	1925.31(14)	1733.39(7)
Z	4	4	4
ρ_{calc}mg/mm^3	1.590	1.513	1.603
m/mm^{-1}	1.482	1.129	1.024
F(000)	748.0	908.0	864.0
Crystal size/mm^3	0.32 × 0.25 × 0.15	0.18 × 0.10 × 0.08	0.27 × 0.21 × 0.18
2Θ range for data collection	4.64 to 54°	3.68 to 51.98°	4.06 to 54°
Index ranges	$-12 \le h \le 11$, $-16 \le k \le 17$, $-12 \le l \le 15$	$-8 \le h \le 8$, $-27 \le k \le 26$, $-14 \le l \le 14$	$-12 \le h \le 12$, $-16 \le k \le 15$, $-17 \le l \le 17$
Reflections collected	7632	11529	15495
Independent reflections	3291[R(int) = 0.0229]	3782[R(int) = 0.0622]	3783[R(int) = 0.0199]
Data/restraints/parameters	3291/0/182	3782/2/233	3783/0/245
Goodness-of-fit on F^2	1.028	1.049	1.102
Final R indexes [I>=2σ (I)]	R_1 = 0.0277, wR_2 = 0.0584	R_1 = 0.0579, wR_2 = 0.1352	R_1 = 0.0223, wR_2 = 0.0545
Final R indexes [all data]	R_1 = 0.0350, wR_2 = 0.0613	R_1 = 0.0842, wR_2 = 0.1480	R_1 = 0.0253, wR_2 = 0.0557
Largest diff. peak/hole / e $Å^{-3}$	0.32/-0.23	0.87/-0.60	0.34/-0.28

3.6.5 Aqua{2-morpholino-N-[1-(2-pyridyl)-ethylidene]ethanamine-κ3N,N',N''}-bis (thiocyanato-κN)nickel(II)

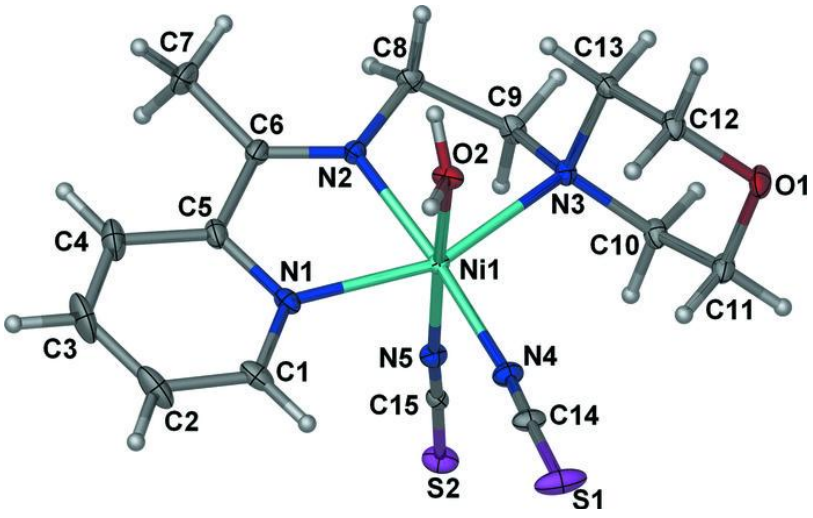

Figure 3.6.8: Crystal structure for $[Ni(LMA)(NCS)_2(H_2O)]$

The mixed-ligand nickel(II) complex was obtained by following a similar synthetic procedure as for its analogous copper(II) complex (Gwaram, 2011). However, compared to the square-pyramidal environment around the Cu(II) ion, afforded by the tridentate Schiff base and the *N* atoms of two SCN^-, the Ni(II) ion is coordinated by one additional water ligand to have an octahedral geometry.

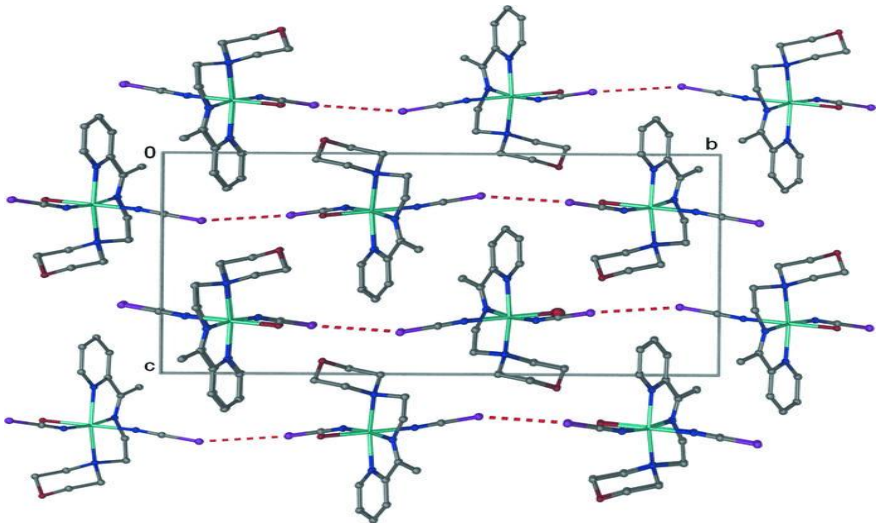

Figure 3.6.9: Packing structure for $[Ni(LMA)(NCS)_2(H_2O)]$

The Ni-N and Ni-O bond lengths in this complex are comparable to those in the similar structures (Chiumia, 1999; Zhao, 2008). In the crystal, the adjacent molecules are linked together through O-H···S, O-H···O and C-H···S hydrogen bonds into layers parallel to the *ac* plane (Figure 3.6.9). An S···S interaction [3.5276 (7) Å] between S1 and S2 of the symmetry related molecule at *-x, y* + 1/2, *-z* + 3/2, connects the layers into a three-dimensional network. Intramolecular C-H···N and C-H···O hydrogen bonding are also observed.

In summary, the Ni(II) ion is six-coordinated by the *N,N',N''*-tridentate Schiff base, the *N* atoms of two thiocyanate ligands and one water *O* atom in a distorted octahedral geometry.

3.6.6 Nickel(II)poly(azido-κ^N){2-Morpholino-N-[1-(2-pyridyl)ethylidene] ethanamine-κ^3N,N',N''} [$Ni_2(LMA)2(N_3)_2(H_2O)_2$]

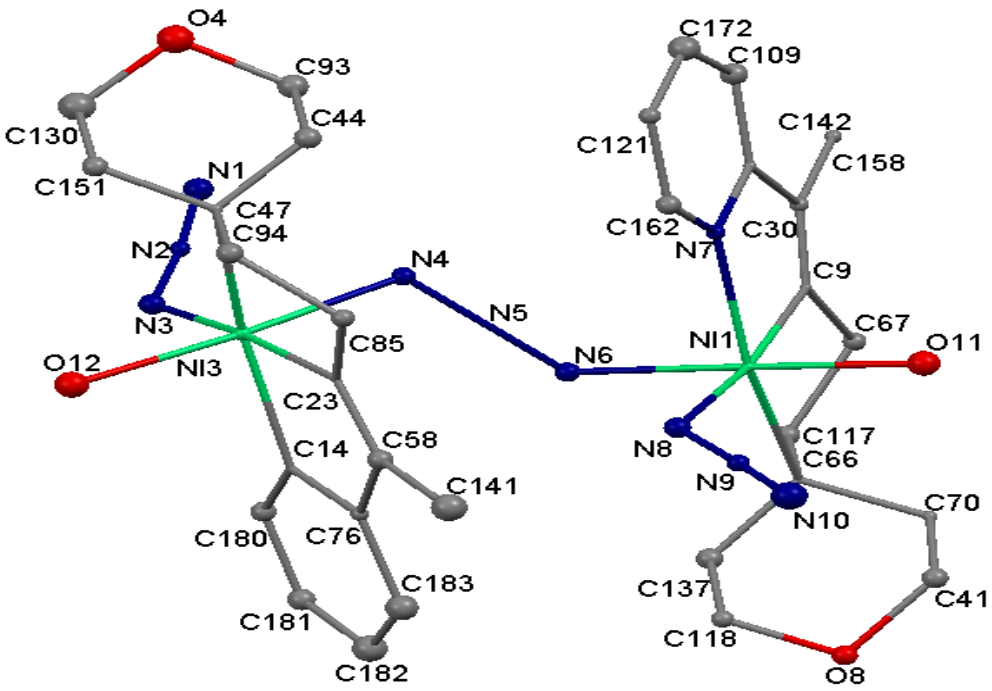

Figure 3.6.10: Crystal structure for $[Ni_2(LMA)_2(N_3)_2(H_2O)_2]$

In the compound, the Ni(II) atom is octahedrally coordinated by the *N,N',N''*-tridentate Schiff base ligand and one terminal azide N atom. In the crystal, adjacent Ni(II) ions are linked by the azide *N:N*-bridges into polymeric chains along the c axis.

The azide ions act as either bridging or terminal ligands. However, different from the doubly bridged dimeric structure of the former, in the present structure the bridging azide ligands singly bridge the adjacent metal centers into infinite chains along the *c* axis. Within this coordination polymer, Two azide *N:N*-bridges, one terminal azide *N* atom and the Ni(II) ion is coordinated by one additional water ligand to have an octahedral geometry.

Table 3.19: Crystal data and structure refinement for [Ni(LMA)(NCS)(H_2O)] and [Ni_2($LMA)_2$(N_3)2(H_2O)$_2$] complexes

Identification code	**[Ni(LMA)(NCS)(H_2O)]**	**[Ni_2($LMA)_2$(N_3)$_2$(H_2O)$_2$]**
Empirical formula	$C_{15}H_{21}N_5NiO_2S_2$	$C_{13}HN_9ONi$
Formula weight	426.20	357.94
Temperature/K	373(2)	373(2)
Crystal system	monoclinic	triclinic
Space group	$P2_1/c$	P1
a/Å	7.18810(10)	10.4169(4)
b/Å	21.9708(3)	15.0746(6)
c/Å	12.1438(2)	20.7751(9)
α/°	90.00	90.00
β/°	91.4120(10)	90.00
γ/°	90.00	90.00
Volume/$Å^3$	1917.27(5)	3262.3(2)
Z	4	8
ρ_{calc}mg/mm^3	1.477	1.458
m/mm^{-1}	1.248	1.209
F(000)	888.0	1424.0
Crystal size/mm^3	0.35 × 0.32 × 0.22	0.19 × 0.11 × 0.05
2Θ range for data collection	5 to 50.5°	1.96 to 60.08°
Index ranges	-8 ≤ h ≤ 8, -26 ≤ k ≤ 26, -14 ≤ l ≤ 14	-14 ≤ h ≤ 14, -20 ≤ k ≤ 20, -29 ≤ l ≤ 28
Reflections collected	14240	34671
Independent reflections	3474[R(int) = 0.0228]	30044[R(int) = 0.0553]
Data/restraints/parameters	3474/4/233	30044/3/753
Goodness-of-fit on F^2	1.093	1.828
Final R indexes [I>=2σ (I)]	R_1 = 0.0254, wR_2 = 0.0568	R_1 = 0.1362, wR_2 = 0.3318
Final R indexes [all data]	R_1 = 0.0288, wR_2 = 0.0582	R_1 = 0.1667, wR_2 = 0.3515
Largest diff. peak/hole /e $Å^{-3}$	0.45/-0.36	8.48/-2.13

3.6.7. Dichlorido{2-(morpholin-4-yl)-N-[1-(pyridin-2-yl)ethylidene]ethanamineκ^3, N',N''} copper(II)monohydrate

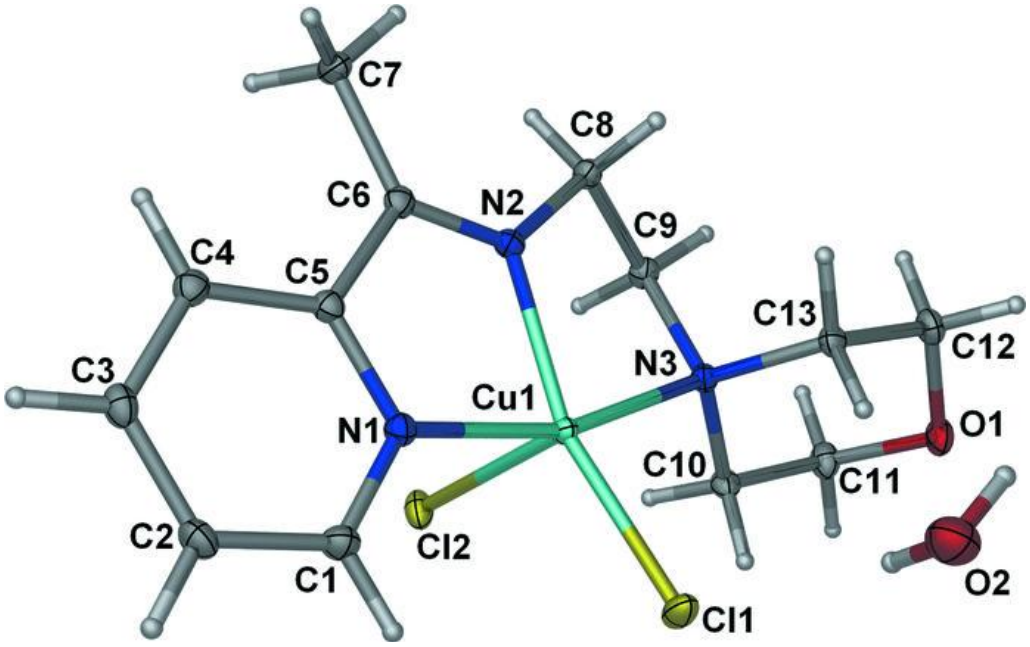

Figure 3.6.11: Crystal structure for [Cu(LMA)Cl_2 .H_2O]

The asymmetric unit of the title compound consists of a copper(II) complex and one molecule of water. Like the $CdCl_2$ complex of the Schiff base, 2-morpholino-*N*-[1-(2-pyridyl)ethylidene]ethanamine, (Ikmal Hisham, 2010) the metal ion in the present structure is five-coordinated by the *N,N',N''*-tridentate Schiff base ligand and two Cl atoms in a distorted square-pyramidal geometry, the τ value (Addison, 1984) being 0.15. The Cu-Cl and Cu-*N* inter atomic distances are comparable to the values reported in the literature (Saleh Salga, 2010; Wang, 2009). In the crystal, the adjacent metal complexes and water molecules are linked into a three-dimensional network *via* O-H···Cl, C-H···Cl and C-H···O interactions. In addition, intramolecular C-H···Cl hydrogen bonding is observed.

In summary the crystal system of the complex, tridentate Schiff base ligand and the two Cl atoms complete distorted square-pyramidal coordination geometry around the Cu(II) ion in

which the three *N* atoms and one Cl atom are located in the basal plane and the other Cl atom is at the apical position. In the crystal, O-H---Cl hydrogen bonds link the complex molecules and the uncoordinated water molecules into infinite chains along the *a*-axis. The chains are further connected into a three-dimensional network via C-H---O and C-H---Cl interactions.

3.6.8 2-Morpholino-N-[1-(2-pyridyl)ethylidene]ethanamine-κ^{3},N',N''-bis(thiocyanato-κ^{N}) copper(II)

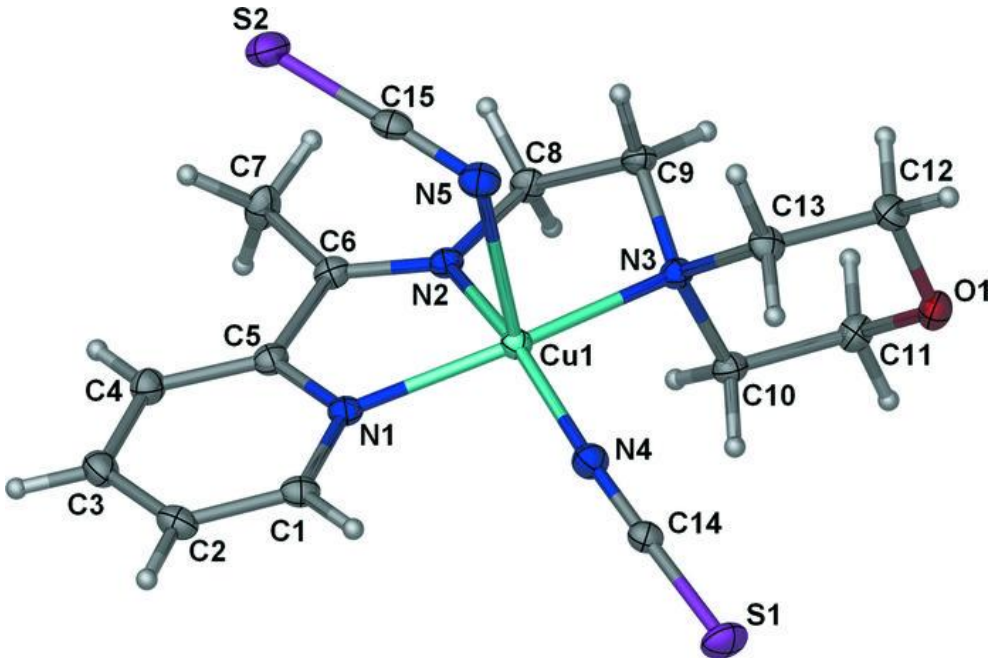

Figure 3.6.12: Crystal structure for [Cu(LMA)$(NCS)_2$]

The title compound is a mixed-ligand copper(II) complex with isothiocyanate and the Schiff base 2-morpholino-*N*-[1-(2-pyridyl)ethylidene]ethanamine. The geometry of the complex is slightly distorted square-pyramidal ($\tau = 0.05$) with the *N,N',N''*-tridentate Schiff base and one NCS ligand at the basal positions, while the apical position is occupied by a second NCS ligand. This arrangement has been observed in some other mixed-ligand copper(II) complexes (Drew, 2009; You, 2006; Yue, 2005). In the crystal structure, the C-

H···N, C-H···O and C-H···S interactions within the range for normal hydrogen bonds link the adjacent molecules into layers parallel to the *ac* plane (Fig. 2). An intramolecular C-H···N hydrogen bonding is also observed. Moreover, the aromatic rings of each two molecules related by the symmetry -*x* + 2, -*y*, -*z* + 1, are arranged in an anti parallel manner with centroid-centroid separation of 3.9412 (9) Å, indicative of a weak π–π interaction.

In summary, the Cu(II) ion is five-coordinated by the *N,N',N''*-tridentate Schiff base and the N atoms of two isothiocyanate ligands in a square pyramidal geometry. In the crystal, C-H---N, C-H---O and C-H---S interactions link adjacent molecules into layers parallel to the ac plane.

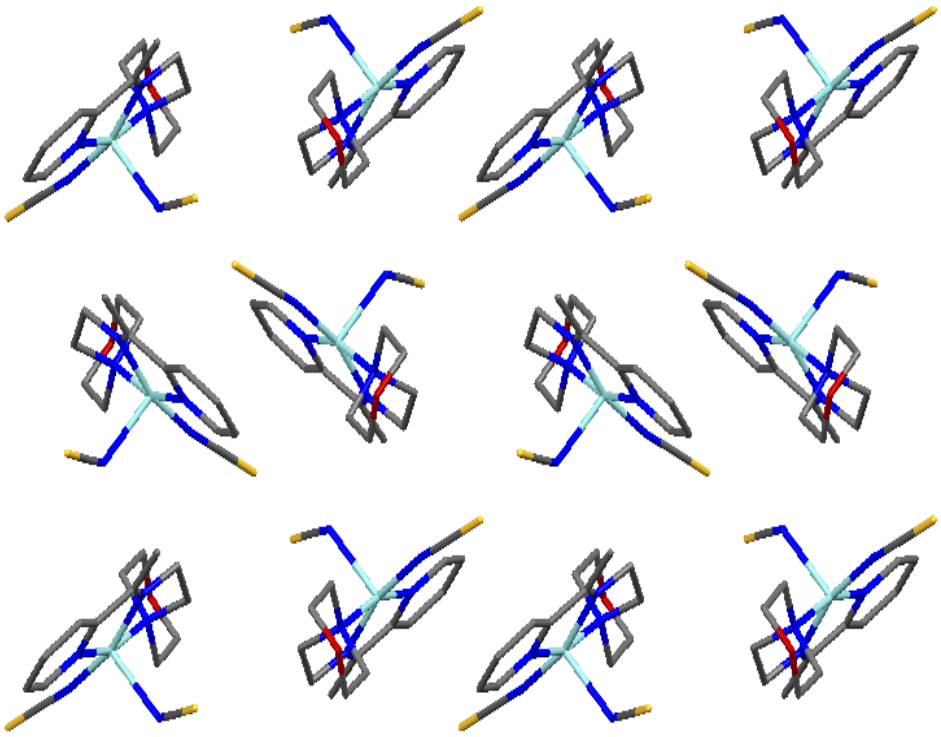

Figure 3.6.13: Packing structure for along c-axis for [Cu(LMA)$(NCS)_2$]

Table 3.20: Crystal data and structure refinement for $[Cu(LMA)(NCS)_2]$

Identification code	$[Cu(LMA)(NCS)_2]$
Empirical formula	$C_{15}H_{19}CuN_5Os_2$
Formula weight	413.01
Temperature/K	373(2)
Crystal system	monoclinic
Space group	$P2_1/c$
a/Å	10.69120(10)
b/Å	14.0350(2)
c/Å	12.2530(2)
α/°	90.00
β/°	92.2030(10)
γ/°	90.00
Volume/$Å^3$	1837.22(4)
Z	4
$\rho_{calc}mg/mm^3$	1.493
m/mm^{-1}	1.428
F(000)	852.0
Crystal size/mm^3	0.41 × 0.39 × 0.08
2Θ range for data collection	4.42 to 54°
Index ranges	$-13 \leq h \leq 13, -17 \leq k \leq 17, -15 \leq l \leq 15$
Reflections collected	16491
Independent reflections	4007[R(int) = 0.0242]
Data/restraints/parameters	4007/2/218
Goodness-of-fit on F^2	1.078
Final R indexes [I>=2σ (I)]	$R_1 = 0.0234$, $wR_2 = 0.0592$
Final R indexes [all data]	$R_1 = 0.0271$, $wR_2 = 0.0607$
Largest diff. peak/hole / e $Å^{-3}$	0.37/-0.26

3.6.9 Dibromido{2-morpholino-N-[1-(2-pyridyl)ethylidene]ethanaminekκ^3,N,N',N''} zinc(II)

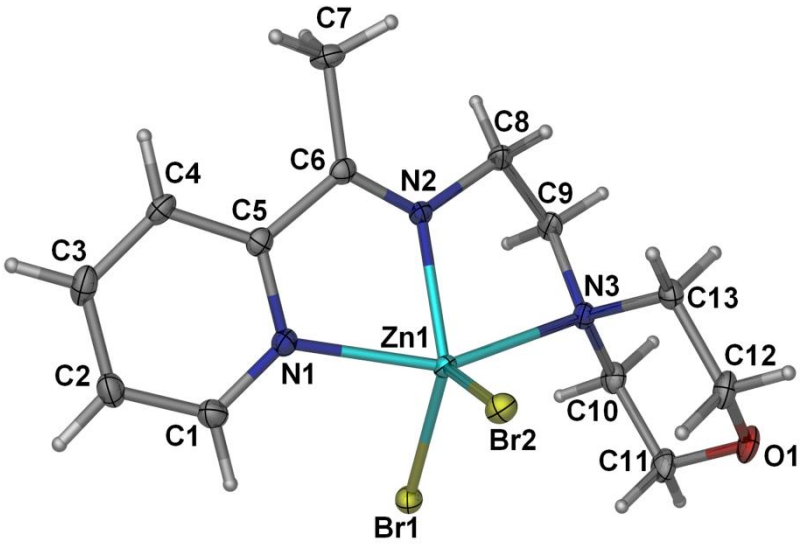

Figure 3.6.14: Crystal structure for [Zn(LMA)Br_2]

The compound [Zn(LMA)Br_2] was obtained upon the reaction of 2-morpholino-N-[1-(2-pyridyl) ethylidene]ethanamine with Zn(II) ion in the presence of potassium bromide. Similar to the structure of the analogous $ZnCl_2$ complex (Hisham, 2011), the metal center is five-coordinated by the *N*,*N*',*N*''-tridentate Schiff base ligand and two halogen atoms. The geometry of the complexes can be determined by using the index $\tau = (\beta-\alpha)/60$, where β is the largest angle and α is the second one around the metal center. For an ideal square-pyramid τ is 0, while it is 1 in a perfect trigonal-bipyramid (Addison, 1984). The τ value in the present structure is calculated to be 0.30, indicative of a distorted square-pyramidal geometry. The Zn-Br and Zn-*N* bond lengths in the complex are in agreement with the values reported in the literature (You, 2006; Zakrzewski, 1970).

In summary, the Zn(II) ion in the compound, is five-coordinated by the *N,N',N''*-tridentate Schiff base ligand and two Br atoms in a distorted square-pyramidal geometry. The three Zn-*N* bond lengths are given as Zn(1)-*N*(1) 2.243(3), Zn(1)-*N*(2) 2.076(2), Zn(1)-*N*(3) 2.331(2), and two Zn–Br bond lengths are Zn(1)-Br(1) 2.4036(4) (18), Zn(1)-Br(2) 2.4172(4). In the crystal, intermolecular C---H...Br hydrogen bonds link the adjacent molecules into infinite chains along the crystallographic axis. An intramolecular C---H...Br interaction is also observed.

3.6.10 Dichlorido{2-morpholino-N-[1-(2-pyridyl)ethylidene]ethanamineκ^3N,N',N''} zinc(II)

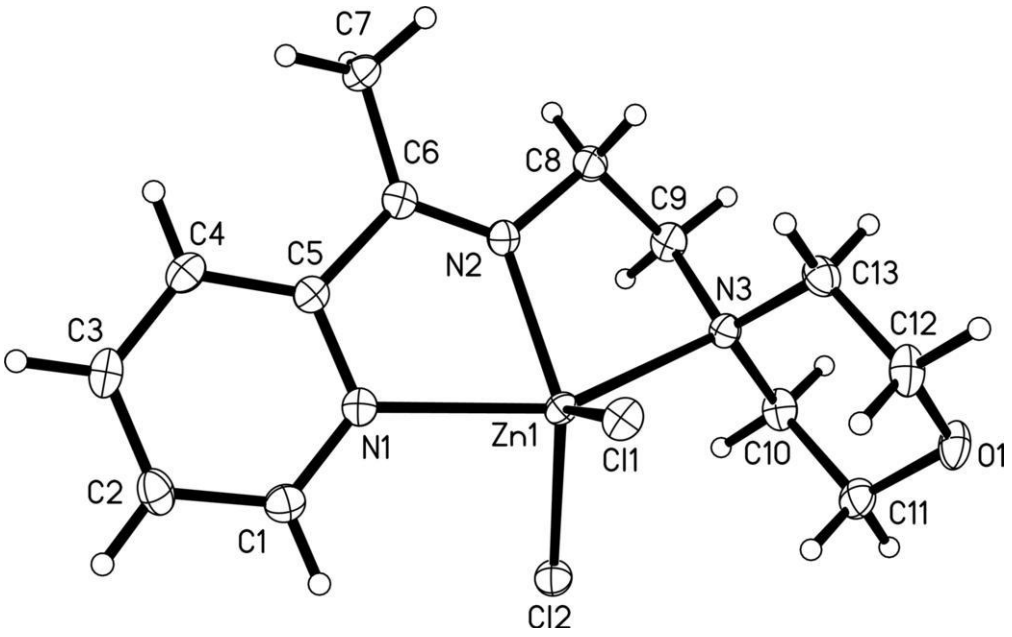

Figure 3.6.15: Crystal structure for [Zn(LMA)Cl_2]

The title compound is isostructural with the analogous Cd(II) complex (Ikmal Hisham, 2010). The Schiff base, 2-morpholino- *N*-[1-(2-pyridyl)ethylidene]ethanamine and two Cl atoms coordinate the Zn(II) ion in a distorted square-pyramidal geometry (τ = 0.22). The Zn-Cl and Zn-*N* bond lengths in the structure are in agreement with the values reported in the literature (Chattopadhyay, 2009; Sun, 2005). In the crystal structure, intermolecular C-

H···Cl hydrogen bonding and long range C-H···O and C-H···Cl interactions link the adjacent molecules into a three-dimensional network. An intramolecular C-H···Cl hydrogen bonding has also been observed.

In summary, the Schiff base ligand acts as an *N,N',N''*-tridentate chelating agent, making two five-membered rings with the Zn(II) ion. The metal atom is five-coordinated by the Schiff base ligand and two Cl atoms in a distorted square-pyramidal geometry.

3.6.11 Diiodido{2-(morpholin-4-yl)-N-[1-(2-pyridyl)ethylidene]ethanamineκ^3N,N',N''} zinc(II)

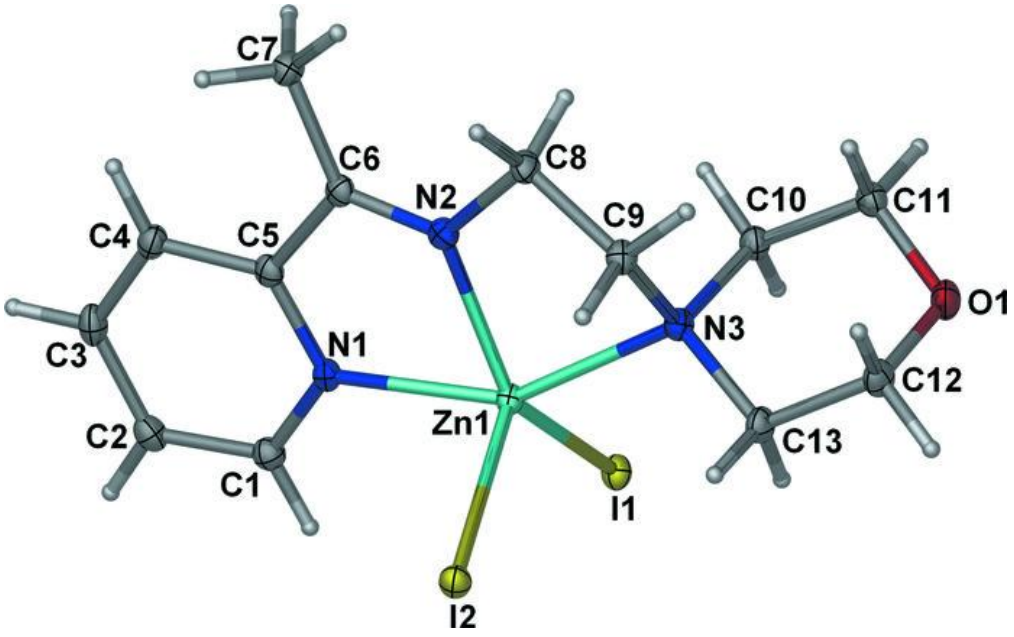

Figure 3.6.16: Crystal structure for [Zn(LMA)I2]

The above compound was obtained *via* the complexation of Zn(II) ion with the *in situ* prepared Schiff base, 2-morpholino-*N*-[1-(2-pyridyl)ethylidene]ethanamine, and two iodide ions. Similar to what was observed in an analogous $ZnCl_2$ complex (Ikmal Hisham, 2011), the Schiff base acts as an *N,N',N''*-tridentate chelate ligand, along with two halide ligands, make a distorted square-pyramidal geometry around the metal ion τ = 0.24, (Addison, 1984). The Zn-*I* and Zn-*N* interatomic distances (Table 1) are comparable to the values

reported for similar structures (Drew & Hollis, 1978; Yousefi, 2010). In the crystal, a pair of the molecules, related by a symmetry operation -*x* + 1, -*y* + 2, -*z* + 2, are linked through C-H···O hydrogen bonds into a centrosymmetric dimer (Table).

In summary, the compound, the Zn(II) ion is five coordinated in a distorted square-pyramidal geometry, in which the basal plane is defined by three N atoms from the Schiff base ligand and one iodide ion. A second iodide ligand, situated in the apical position, completes the coordination geometry.

2.6.12 2-Morpholino-N-[1-(2-pyridyl)-ethylidene]ethanamine-κ^3N,N',N''-bis(thiocyanato-κ^N) zinc(II)

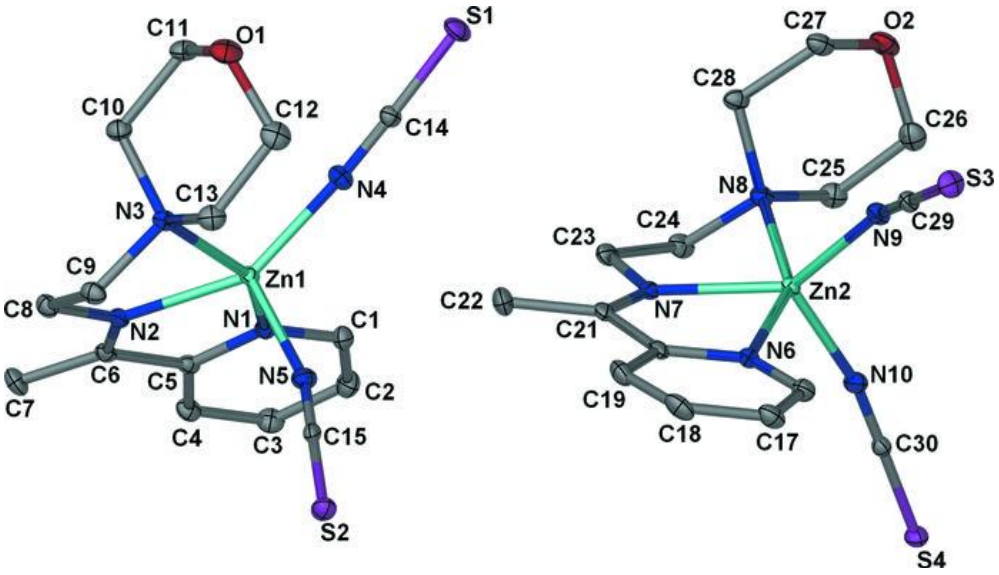

Figure 3.6.17: Crystal structure for $[Zn(LMA)(NCS)_2]$

Owing to the presence of several donor atoms and the flexibility of the morpholine ring, this Schiff base can, in principle, show ambidentate coordination behavior toward metal ions. On the other hand, thiocyanate is known to bind metal ions in different modes: *N*-donor, *S*-donor or *N:S*-bridging mode. The title compound is a mixed-ligand zinc(II) complex with the two ambidentate ligands. In the crystal, two geometrically slightly

different molecules exist. The weighted root mean square (r.m.s.) fit for the superposition of the non-H atoms in both molecules is 1.5267 Å. The Schiff base ligand in the molecules acts as an *N,N',N''*-tridentate chelate, along with the *N* atoms of two isothiocyanate ligands this makes pentacoordinated zinc(II) complexes. Similar coordination environment has been reported in related mixed-ligand zinc(II) complexes (Cai, 2009; Chen, 2005). The geometry of the two present complexes can be determined by using the index $\tau = (\beta-\alpha)/60$, where β is the largest angle and α is the second one around the metal center. For an ideal square-pyramid τ is 0, while it is 1 in a perfect trigonal-bipyramid (Addison, 1984). The τ values in the two molecules are 0.14 for the Zn1 complex and 0.33 for the Zn2 complex, indicating distorted square-pyramidal geometries. The NCS groups are almost linear [178.3 (2)° and 179.9 (3)° in the Zn1 complex; 179.1 (2)° and 179.1 (2)° in the Zn2 complex], whereas the Zn-*N*-CS linkages are somewhat bent [158.34 (19)° and 165.19 (18)° in the Zn1 complex; 145.54 (17)° and 169.54 (18)° in the Zn2 complex]. The morpholine rings in both molecules adopt a chair conformation. The crystal structure is stabilized by intermolecular C-H···S and an intramolecular C-H···N hydrogen bond (Table).

In summary, the asymmetric unit of the title compound contains two crystallographically independent molecules. In each molecule, the Zn(II) ion is five-coordinated by the *N,N',N''*-tridentate Schiff base and the N atoms of two thiocyanate ligands in a distorted square-pyramidal geometry. The two molecules differ mainly in the deviations from the ideal geometry, with τ values of 0.14 and 0.33. In the crystal, intermolecular C-H---S hydrogen bonds are observed. An intramolecular C-H---N hydrogen bond occurs in one of the independent molecules.

3.6.13 2-Morpholino-N-[1-(2-pyridyl)ethylidene]ethanamine-κ^3N,N',N''}bis(azido-κ^N)zinc(II)

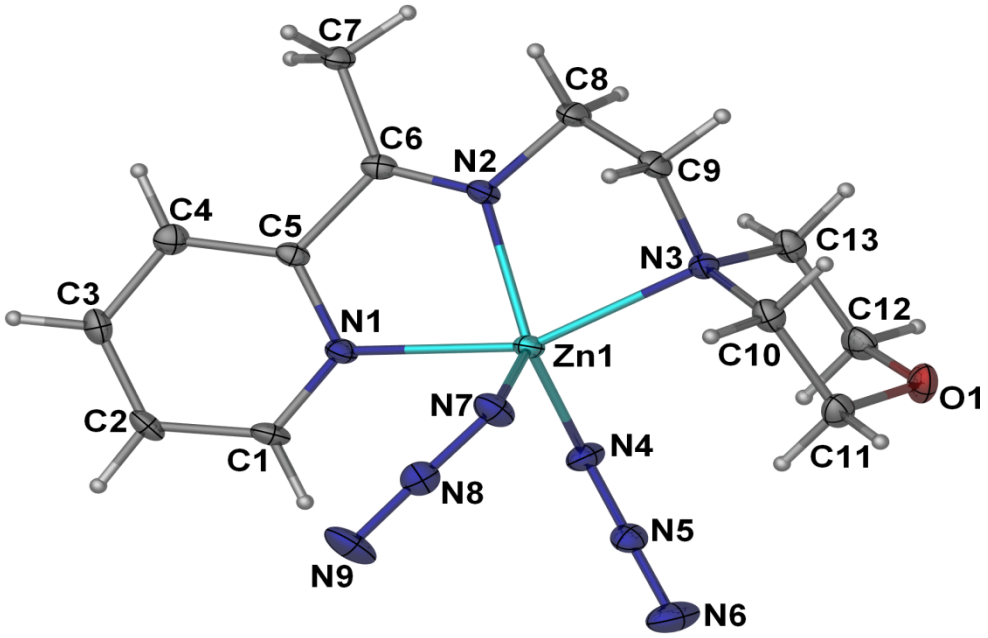

Figure 3.6.18: Crystal structure for $[Zn(LMA)(N_3)_2]$

The compound above is a square-pyramidal zinc(II) complex in which the metal center is coordinated by the *N,N',N''*-tridentate Schiff base and the *N* atoms of two azide ligands. The $CH_2N(CH_3)_2$ fragment is disordered over two sets of sites in a 0.53(4):0.471 (4) ratio. Like the structure of the zinc(II) thiocyanate complexes of similar Schiff bases (Cai, 2009); Chen, 2005), the present structure is a mononuclear square-pyramidal metal complex, the τ value being 0.35. In contrast, the cadmium(II) thiocyanate complex of the same Schiff base (Gwaram, 2011), showed a polymeric structure wherein the metal centers are linked by the *N:N*-bridging azide ligands. In the crystal structure of the title compound, C---H...N interactions connect a pair of molecules, related by symmetry −x+1, −y, −z, around a center of inversion. The zinc atom is bonded to three donor nitrogen atoms of the ligand and two azides bonded through the nitrogen atoms ending.

Table 3.21: Crystal data and structure refinement for zinc(II) complexes

Identification code	**[Zn(LMA)Br_2]**	**[Zn(LMA)Cl_2]**	**[Zn(LMA)I_2]**
Empirical formula	$C_{13}H_{19}Br_2N_3OZn$	$C_{13}H_{19}Cl_2N_3OZn$	$C_{13}H_{19}I_2N_3OZn$
Formula weight	458.50	369.58	552.48
Temperature/K	373(2)	373(2)	373(2)
Crystal system	monoclinic	monoclinic	triclinic
Space group	$P2_1/n$	$P2_1/n$	P-1
a/Å	9.8290(2)	9.5737(12)	8.8874(3)
b/Å	14.0218(2)	13.7064(17)	10.3117(4)
c/Å	12.1371(2)	12.0766(15)	10.3643(4)
α/°	90.00	90.00	68.881(2)
β/°	106.9180(10)	106.643(2)	81.959(2)
γ/°	90.00	90.00	66.399(2)
Volume/$Å^3$	1600.35(5)	1518.3(3)	811.91(5)
Z	4	4	2
$\rho_{calc}mg/mm^3$	1.903	1.617	2.260
m/mm^{-1}	6.527	1.968	5.314
F(000)	904.0	760.0	524.0
Crystal size/mm^3	0.33 × 0.25 × 0.11	0.35 × 0.21 × 0.05	0.17 × 0.13 × 0.09
2Θ range for data collection	4.56 to 54°	4.6 to 52°	4.22 to 53.98°
Index ranges	$-12 \le h \le 12$, $-17 \le k \le 17$, $-14 \le l \le 15$	$-11 \le h \le 11$, $-16 \le k \le 16$, $-14 \le l \le 14$	$-11 \le h \le 11$, $-13 \le k \le 13$, $-13 \le l \le 13$
Reflections collected	12535	13693	7292
Independent reflections	3496[R(int) = 0.0351]	2979[R(int) = 0.0474]	3517[R(int) = 0.0128]
Data/restraints/parameters	3496/0/182	2979/0/182	3517/0/182
Goodness-of-fit on F^2	1.028	1.080	1.048
Final R indexes [I>=2σ (I)]	R_1 = 0.0271, wR_2 = 0.0595	R_1 = 0.0336, wR_2 = 0.0866	R_1 = 0.0182, wR_2 = 0.0438
Final R indexes [all data]	R_1 = 0.0360, wR_2 = 0.0624	R_1 = 0.0411, wR_2 = 0.0912	R_1 = 0.0205, wR_2 = 0.0451
Largest diff. peak/hole / e $Å^{-3}$	0.68/-0.47	1.03/-0.39	0.85/-1.23

Table 3.22: Crystal data and structure refinement for zinc(II) complexes

Identification code	**[Zn(LMA)(NCS)]**	**[Zn(LMA)(N_3)$_2$]**
Empirical formula	$C_{15}H_{19}N_5Os_2Zn$	$C_{13}H_{19}N_9OZn$
Formula weight	414.84	382.74
Temperature/K	373(2)	373(2)
Crystal system	triclinic	monoclinic
Space group	P-1	$P2_1/c$
a/Å	9.9203(2)	10.7118(19)
b/Å	13.5659(2)	9.2241(16)
c/Å	14.6957(2)	17.110(3)
α/°	112.7020(10)	90.00
β/°	91.4710(10)	105.719(2)
γ/°	94.3560(10)	90.00
Volume/Å^3	1815.97(5)	1627.4(5)
Z	4	4
ρ_{calc}mg/mm^3	1.517	1.562
m/mm^{-1}	1.594	1.531
F(000)	856.0	792.0
Crystal size/mm^3	0.42 × 0.33 × 0.25	0.25 × 0.06 × 0.05
2Θ range for data collection	4.12 to 52°	4.94 to 52.82°
Index ranges	-12 ≤ h ≤ 12, -16 ≤ k ≤ 16, -	-13 ≤ h ≤ 13, -11 ≤ k ≤ 11, -
Reflections collected	15354	8625
Independent reflections	7118[R(int) = 0.0203]	3323[R(int) = 0.0582]
Data/restraints/parameters	7118/5/435	3323/0/218
Goodness-of-fit on F^2	1.042	1.011
Final R indexes [I>=2σ (I)]	R_1 = 0.0278, wR_2 = 0.0756	R_1 = 0.0459, wR_2 = 0.0870
Final R indexes [all data]	R_1 = 0.0345, wR_2 = 0.0797	$C_{13}H_{19}N_9OZn$
Largest diff. peak/hole/e Å^{-3}	0.62/-0.30	382.74

3.6.14 Dibromido{2-morpholino-N-[1-(2-pyridyl)ethylidene]ethanamine-κ^3N,N',N''}-cadmium

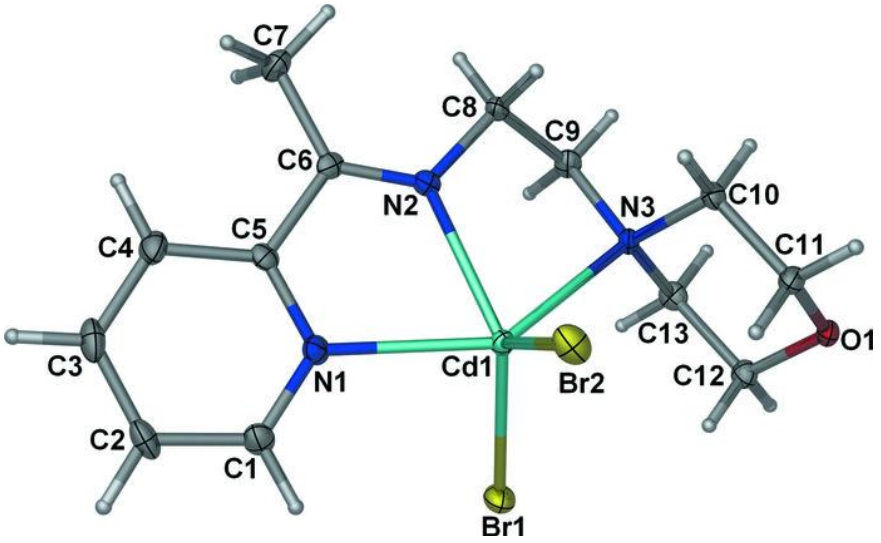

Figure 3.6.19: Crystal structure for [Cd(LMA)Br_2]

The white colored crystal compound [Cd(LMA)Br_2] was obtained upon the reaction of 2-morpholino-*N*-[1-(2-pyridyl)ethylidene]ethanamine with Cd(II) ion in the presence of potassium bromide. Similar to the structure of the analogous $CdCl_2$ complex (Ikmal Hisham, 2010), the metal center is five-coordinated by the *N,N',N''*-tridentate Schiff base ligand and two halogen atoms. The geometry of the complexes can be determined by using the index $\tau = (\beta-\alpha)/60$, where β is the largest angle and α is the second one around the metal center. For an ideal square-pyramid τ is 0, while it is 1 in a perfect trigonal-bipyramid (Addison, 1984). The τ value in the present structure is calculated to be 0.18, indicative of a distorted square-pyramidal geometry. The Cd-Br bond lengths in the complex are in agreement with the values reported in the literature (Bermejo, 1999; Bermejo, 2003). In the crystal, the adjacent molecules are connected together *via* C-H···O and C-H···Br hydrogen bonds, forming infinite layers parallel to the *ab* plane. Moreover an intramolecular C-H···Br occurs. The Cd(II) ion, is five-coordinated by the *N,N',N''*-tridentate Schiff base ligand and two Br atoms in a distorted square-pyramidal geometry.

3.6.15 Dichlorido{2-morpholino-N-[1-(2-pyridyl)ethylidene]ethanamine-κ^3N,N',N''}-cadmium

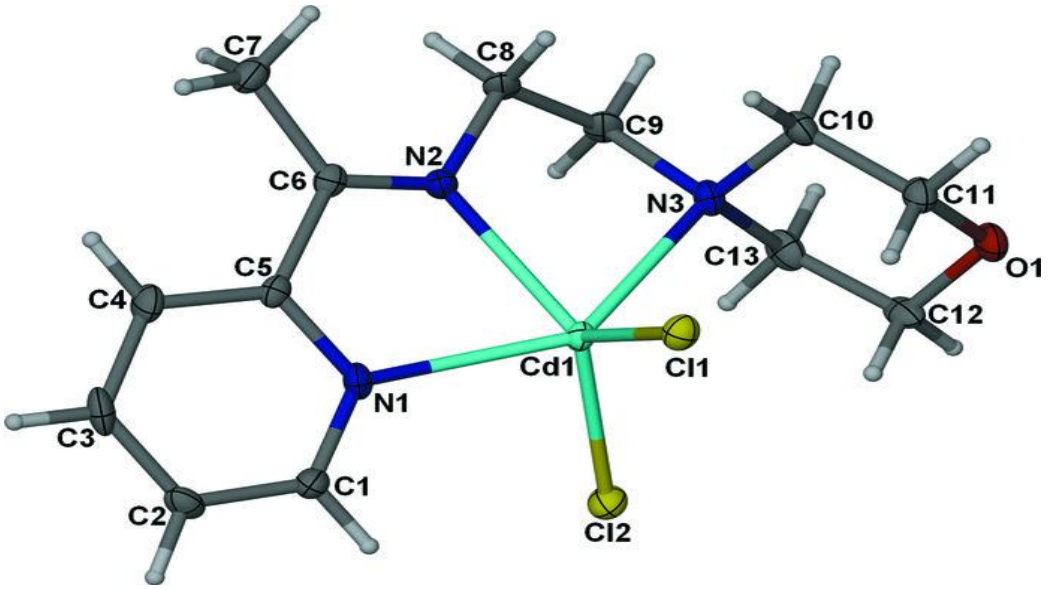

Figure 3.6.20: Crystal structure for [Cd(LMA)Cl_2]

The crystal of this compound has been obtained *via* the complexation of cadmium(II) chloride by the *N,N',N''*-tridentate ligand, 2-morpholino-*N*-[1-(2-pyridyl)ethylidene]ethanamine, which had itself been prepared from the condensation of 4-(2-aminoethyl)morpholine and 2-acetylpyridine. The geometry of the complex can be defined as distorted square-pyramidal (τ = 0.18) with one of the chloride ligands in the apical position. Like the similar structures reported in the literature (Ikmal Hisham, 2009; Cai, 2009), the morpholine ring in the present complex adopts a chair conformation. In the crystal structure, the molecules are linked together through C-H···Cl interactions into a three dimensional network.

In summary, the Cd(II) ion is five-coordinate, with the *N,N',N''*-tridentate Schiff base ligand 2-morpholino-*N*-[1-(2-pyridyl)ethylidene]ethanamine and two Cl atoms in a distorted square-pyramidal geometry.

3.6.16 Di-l-thiocyanato-j2N:S;k2 S:N-bis ({2-morpholino-N-[1-(2-pyridyl)ethylidene]-Ethanamine-k^{3}N,N',N"} (thiocyanatokN)cadmium) Aqua{2-Morpholino-N-[1-(2-pyridyl)ethylidene] ethanamine-κ^{3}N,N',N"} bis(azido-κ^N) cadmium(II)

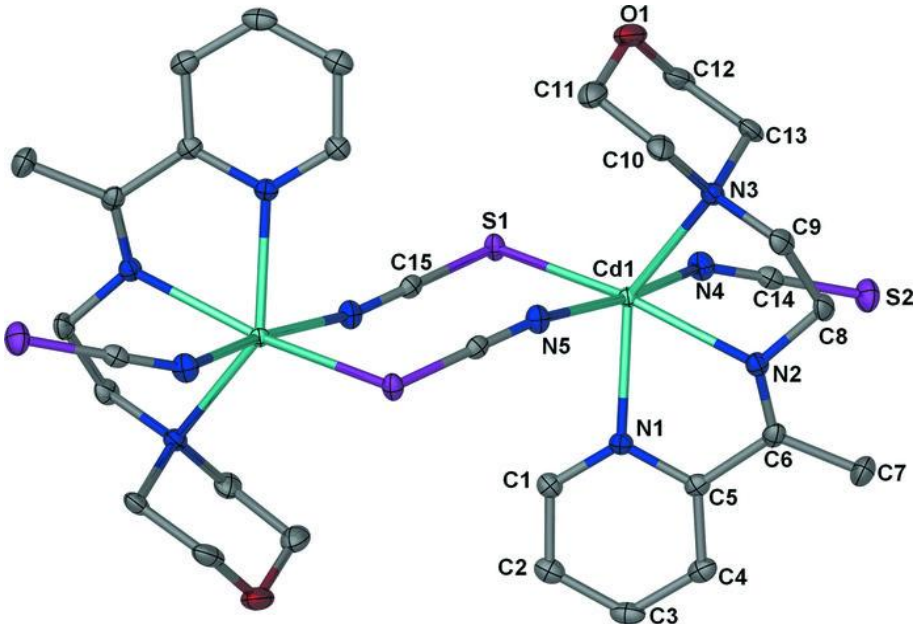

Figure 3.6.21: Crystal structure for $[Cd_2(LMA)_2(NCS)_4]$

In the title complex, $[Cd_2(LMA)_2(NCS)_4]$, the two Cd(II) ions are bridged by a pair of thiocyanate N:S-bridging ligands around an inversion center. One terminal thiocyanate N atom and one *N,N',N"*-tridentate Schiff base ligand complete a distorted Cd*N*5*S* octahedral geometry about each Cd^{II} atom. In the crystal, the Schiff base aromatic rings of adjacent molecules are arranged above each other into infinite chains along the a-axis with alternate centroid–centroid separations of 3.5299 (13) and 3.7857 (13) A ° . For the structure of the Cu(II) complex with the same Schiff base and thiocyanate, see: (Gwaram, 2011). For the structures of similar cadmium complexes, see: (Banerjee, 2005); You, 2006).

In summary, the title compound is a mixed-ligand cadmium(II) complex with thiocyanate and the Schiff base 2-morpholino-*N*-[1-(2-pyridyl)ethylidene]ethanamine. Unlike the mononuclear square-pyramidal structure of the analogous copper(II) complex (Suleiman,

2011), the present structure represents a dinuclear metal complex with a distorted octahedral geometry around the cadmium atoms. Each two Cd(II) centers are linked by a pair of thiocyanate *N:S* bridges around an inversion center to form an eight-membered $Cd_2(\mu 2\text{-}NCS)_2$ ring. The resulting ring has a chair conformation, the displacement of Cd1 out of the $(NCS)_2$ plane being 0.635 (2) Å. Within this double bridged dimer, the Cd···Cd distance [5.9380 (3) Å] is similar to those observed in the related complexes (Banerjee, 2005; You, 2006). The distorted octahedral geometry about the metal cadmium is completed by one terminal thiocyanate N atom and one *N,N',N''*-tridentate Schiff base ligand. In the crystal, the molecules are connected into infinite chains along the *a* axis *via* π-π interactions formed by the Schiff base aromatic ring and its symmetry related counterparts at (-*x* + 1, -*y*, -*z* and –*x* + 2, -*y*, -*z*) with centroid separations of 3.5299 (13) Å and 3.7857 (13) Å respectively.

3.6.17 Structure of Aqua{2-morpholino-N-[1-(2-pyridyl)- ethylidene]ethanamine-k^3N,N',N''}bis(thiocyanato-k^N)cadmium(II) [Cd(LMA)$(N_3)_2(H_2O)$]

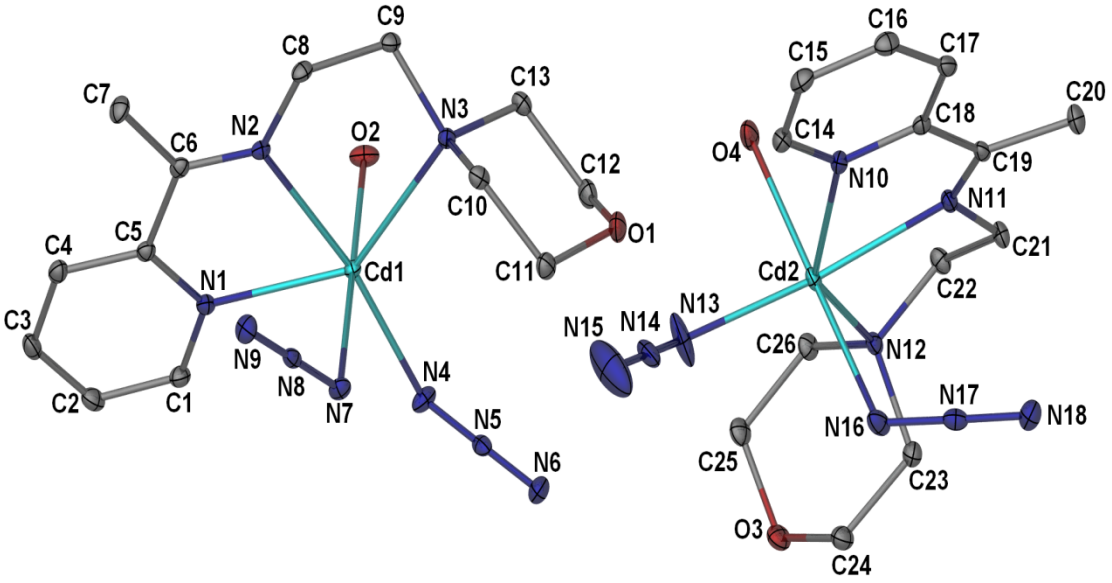

Figure 3.6.22: Crystal structure for [Cd(LMA)$(N_3)_2(H_2O)$]

In the compound, the Cd(II) atom is octahedrally coordinated by the *N,N',N''*-tridentate Schiff base ligand and two terminal azide N atom. The adjacent Cd(II) ions are coordinated by one additional water ligand to have complete distorted octahedral geometry.

3.6.18 Chlorido(2-{1-[(2-morpholinoethyl)-imino]ethyl}phenolato-κ^3N,N',O)-copper(II)

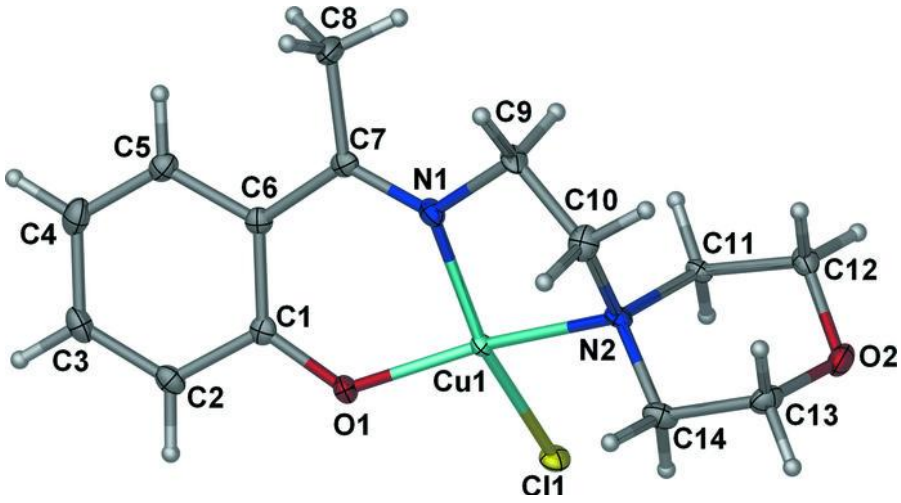

Figure 3.6.23: Crystal structure for [Cu(LMH)Cl]

The title compound was obtained through the reaction of the Schiff base ligand, prepared *in situ*, with copper(II) chloride. Upon complexation, the Schiff base loses its phenolic hydrogen to chelate the Cu(II) ion as an anionic tridentates ligand. One chloride atom completes the distorted square-planar geometry of the complex. The deviation from the regular geometry is evident from the disposition of the metal atom 0.0494 (15) Å out of the *N1-N2*-O1-Cl1 coordination plane.

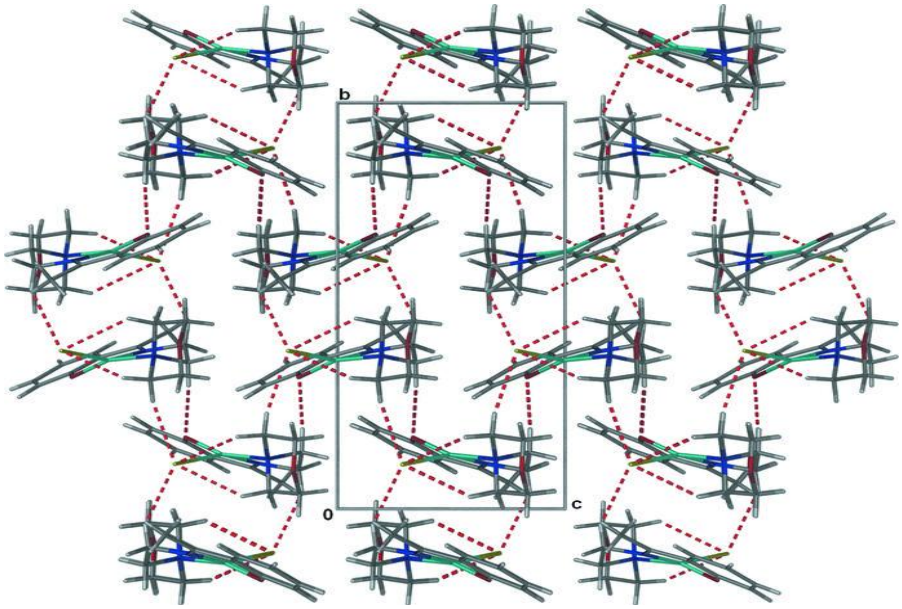

Figure 3.6.24: Packing structure for [Cu(LMH)Cl]

The Cu-*N*, Cu-*O* and Cu-Cl bond lengths in the present complex are comparable with those in similar structures (Elias, 1982; Ikmal Hisham, 2009; Wang & You, 2007). In the crystal, C-H···Cl and C-H···O interactions within the range for normal hydrogen bonds, link adjacent molecules into two-dimensional networks parallel to the *bc* plane (Figure 3.6.23). In addition, intramolecular C-H···Cl hydrogen bonds occurs.

In summary, the Cu(II) ion is four-coordinated by one deprotonated *N,N',O*-tridentate Schiff base and one chloride ion in a distorted square-planar geometry.

3.6.19 Hexachloridobis{-2-2-(piperazin-1-yl)-N-[1-(2-pyridyl)ethylidene]ethanamine}-trizinc dihydrate

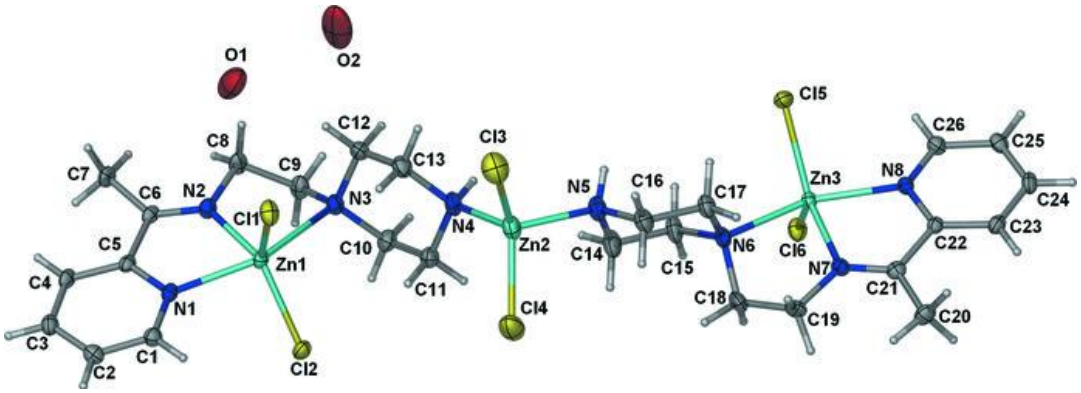

Figure 3.6.25: Crystal structure for $[Zn_3(LPA)_2Cl_6].2H_2O$

It has been shown that ligands having piperazine ring, depending on the ring conformation (chair or boat), may display ambidentate ligation behavior (Mukhopadhyay, 2003; Xu, 2008). The title compound was obtained upon the reaction of the *in situ* prepared Schiff base, 2-piperazino-*N*-[1-(2-pyridyl)ethylidene]ethanamine, with zinc(II) chloride. As shown in Fig. 3.6.25, the compound contains three unique metal centers. One Schiff base ligand chelates each of the two terminal zinc atoms *via* three *N* atoms. The piperazine rings assume chair conformations and their nitrogen atoms, N_4 and N_5, which stay away from chelation, are coordinated to the central zinc atom. Within the resulting trinuclear zinc complex, the metal atoms are separated by 5.8498 (7) Å (Zn1···Zn2) and 7.0153 (7) Å (Zn2···Zn3).

The coordination environment around each metal center is completed by two Cl atoms, resulting in a tetrahedral geometry for the central Zn(II) ion and square-pyramidal geometries for the terminal zinc atoms τ = 0.39 and 0.26 for Zn1 and Zn3 centers, respectively, (Addison, 1984). The crystal structure contains intra- and intermolecular C-

H···Cl interactions. The latter connect the adjacent metal complexes into a three-dimensional network. The complex is N-H···O and C-H···O hydrogen bonded to two molecules of water, one of which being disordered between two sites.

In summary, the trinuclear title compound, each terminal Zn(II) atom is coordinated by an N_3 donor set from the Schiff base ligands and two Cl atoms in a distorted square-pyramidal geometry. The central Zn(II) atom is tetrahedrally coordinated by two piperazine N atoms from two Schiff base ligands and two Cl atoms. The piperazine rings adopt chair conformations.

3.6.20 Octachloridobis[l2-2-(piperazin-1-yl)-N-1-(2-pyridyl)ethylidene ethanamine-bis-4-(2-aminoethyl)piperazine]-tetracadminic $Cd_4(LPA)_2(PA)_2(Cl)_8$]

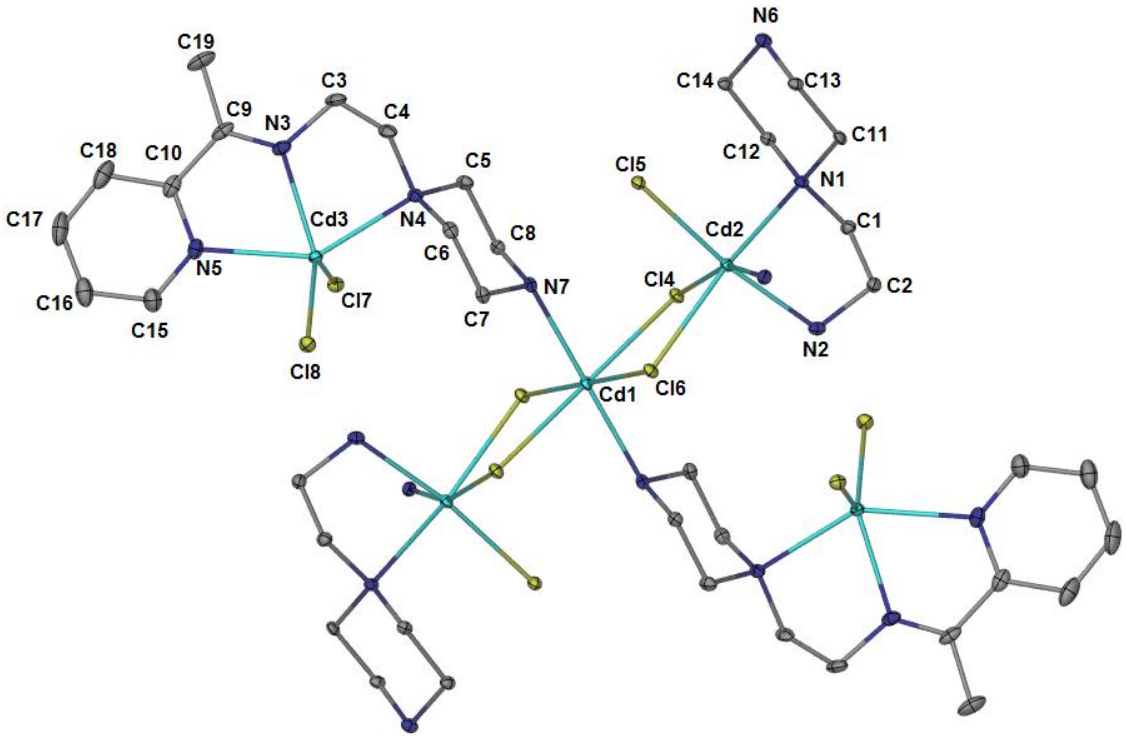

Figure 3.6.26: Crystal structure for $Cd_4(LPA)_2(PA)_2(Cl)_8$]

In the crystal system of the complex, Cd(II) ion in the adjacent ligands is five-coordinate, with the *N,N',N''*-tridentate Schiff base ligand 2-piperazino-*N*-[1-(2-pyridyl)ethylidene]

ethanamine and two Cl atoms in a distorted square-pyramidal geometry.

Also the Cl and Cd(II) atoms are located on a twofold rotation axis and the Cd(II) atom is octahedrally coordinated by two *N,N'*-bidentate 2-(piperazino-4-yl)ethanamine ligands and two *trans*-located Cl atoms. The chloride ions act as either bridging or terminal ligands.The piperazine rings adopt chair conformations. However, different from the doubly bridged dimeric structure of the former, in the present structure the bridging chlorine ligands doubly bridged the adjacent metal centers into chains along the axis. Within this coordination polymer, the central Cd(II) atom is octahedrally coordinated by two piperazine N atoms from two Schiff base ligands and four Cl atoms from the two *N,N'*-bidentate 2-(piperazino-4-yl)ethanamine ligands.

3.6.21 Dichlorido-2-(piperidin-1-yl)-N-[1-(2-pyridyl)ethylidene]ethanamineκ^3N,N',N''}zinc(II)

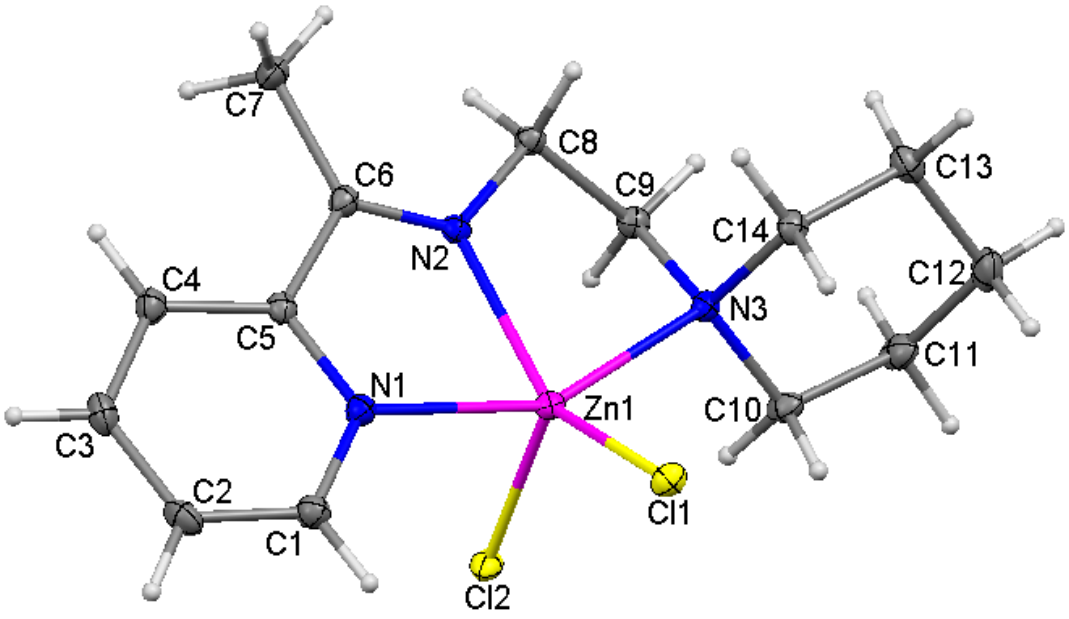

Figure 3.6.27: Crystal structure for [Zn(LPipA)Cl_2]

The crystal of this compound has been obtained *via* the complexation of zinc(II) chloride by the *N,N',N''*-tridentate ligand, 2-piperodino-*N*-[1-(2-pyridyl)ethylidene]ethanamine,

which had itself been prepared from the condensation of 4-(2-aminoethyl)piperidine and 2-acetylpyridine. Schiff base, 2-piperidino-*N*-[1-(2-pyridyl)ethylidene]ethanamine and two Cl atoms coordinate the Zn(II) ion in a distorted square-pyramidal geometry (τ = 0.22). The Zn-Cl and Zn-*N* bond lengths in the structure are in agreement with the values reported in the literature (Chattopadhyay, 2009; Sun, 2005) with one of the chloride ligands in the apical position. Like the similar structures reported in the literature (Ikmal Hisham, 2009; Cai, 2009), the morpholine ring in the present complex adopts a chair conformation.

In the crystal structure, intermolecular C-H···Cl hydrogen bonding and long range C-H···O and C-H···Cl interactions link the adjacent molecules into a three-dimensional network. An intramolecular C-H···Cl hydrogen bonding has also been observed.

3.6.22 Dithiocyanate-2-(piperidin-1-yl)-N-[1-(2-pyridyl)ethylidene]ethanamineκ^3N,N',N''} zinc(II)

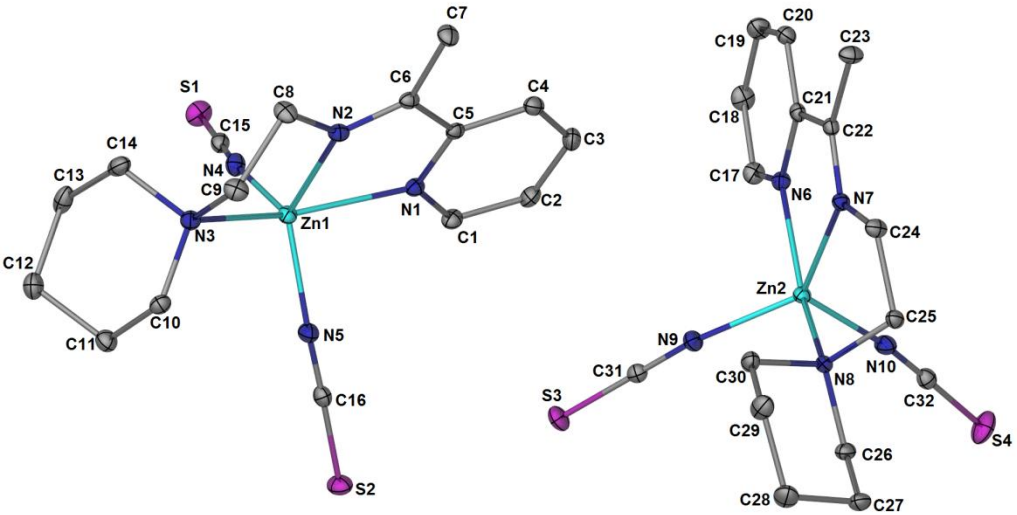

Figure 3.6.28: Crystal structure for [Zn(LPipA)(NCS)]

Thiocyanate is known to bind metal ions in different modes: *N*-donor, *S*-donor or *N:S*-bridging mode. The title compound is a mixed-ligand zinc(II) complex with the two ambidentate ligands. In the crystal, two geometrically slightly different molecules exist.

The asymmetric unit of the title compound, contains two independent penta coordinate Zn(II) complex molecules. In each molecule, the metal atom is coordinated by an *N,N',N''*-tridenate Schiff base and two N-bound thiocyanate ligands in a distorted square-pyramidal geometry. The two molecules differ little in their geometry, but more in their intermolecular interactions. In the crystal, adjacent molecules are connected via C-H---N interactions into a three dimensional supra molecular structure. The network is supplemented by π–π* interactions formed between the aromatic rings of pairs of the symmetry-related molecules.

3.6.23 Dichlorido{N,N-dimethyl-N'-[1-(2-pyridyl)ethylidene]ethane-1,2-diamineκ^3 N,N',N''} manganese(II)

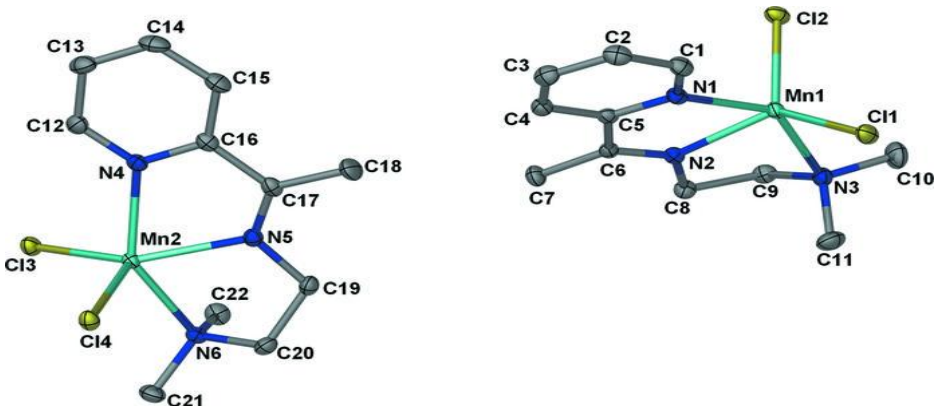

Figure 3.6.29: Crystal structure for [Mn(LNA)Cl_2]

The title compound was obtained upon complexation of the Schiff base, *N*,*N*-dimethyl-*N'*-[methyl(2- pyridyl)methylene]ethane-1,2-diamine, with $MnCl_2$. Similar to its analogous copper(II) complex (Saleh Salga, 2010), the metal center is five-coordinated by the *N*,*N'*,*N''*-tridentate Schiff base and two Cl atoms. Two geometrically different molecules exist in the crystal structure. In both molecules, the Mn(II) ions are in a square-pyramidal coordination environment with different degrees of distortion from the ideal geometry as revealed by the τ values of 0.101 for Mn1 complex and 0.035 for Mn2 complex. The weighted r.m.s. fit for the superposition of the non-H atoms in both molecules is 0.0868 Å.

The Mn-Cl and Mn-N bond lengths in the two molecules are comparable with those in the related structures (Gibson, 2003; Reardon, 2002). In the crystal, the adjacent molecules are connected *via* C-H···Cl hydrogen bonds into a three-dimensional polymeric structure. The crystal structure contains void spaces with the size of 54.00 Å-3 within which there is no evidence for included solvent.

In summary, the asymmetric unit of the compound contains two crystallographically independent molecules with slightly different geometries. In each molecule, the Mn(II) ion is five coordinated by the *N,N',N''*- tridentate Schiff base and two Cl atoms in a distorted square pyramidal geometry.

3.6.24 Aqua{N,N-dimethyl-N'-[1-(2-pyridyl)-ethylidene]ethane-1,2-diamineκ^3N,N',N''} bis (thiocyanato-κ^N)nickel(II)

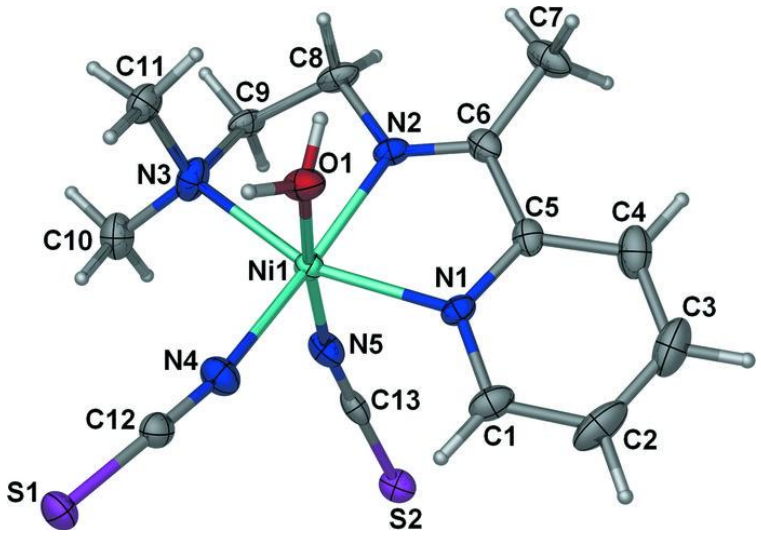

Figure 3.6.30: Crystal structure for [Ni(LNA)$(NCS)_2(H_2O)$]

The title mixed-ligand complex was obtained *via* the treatment of nickel(II) ion with the Schiff base *N,N*-dimethyl-*N'*- [methyl(2-pyridyl)methylene]ethane-1,2-diamine, prepared *in situ*, and the thiocyanate salt. The Schiff base acts as an *N,N',N''*-tridentate chelate and the

two thiocyanate ions behave in an *N*-donor fashion towards the Ni(II) ion. The geometry around the metal center is completed by one water O atom. This arrangement is similar to what was observed in the nickel(II) thiocyanate complex of a similar Schiff base (Gwaram, 2011). In contrast, the metal ions in the nickel(II) thiocyanate complex of *N*,*N*-dimethyl-*N*′-(2-pyridylmethylene)ethane-1,2-diamine (Diao, 2007) and *N*,*N*-diethyl- *N*′-[methyl(2-pyridyl)methylene]ethane-1,2-diamine (Bhowmik, 2010) are doubly bridged into dimers by *N*:*S*-bridging thiocyanate ligands.

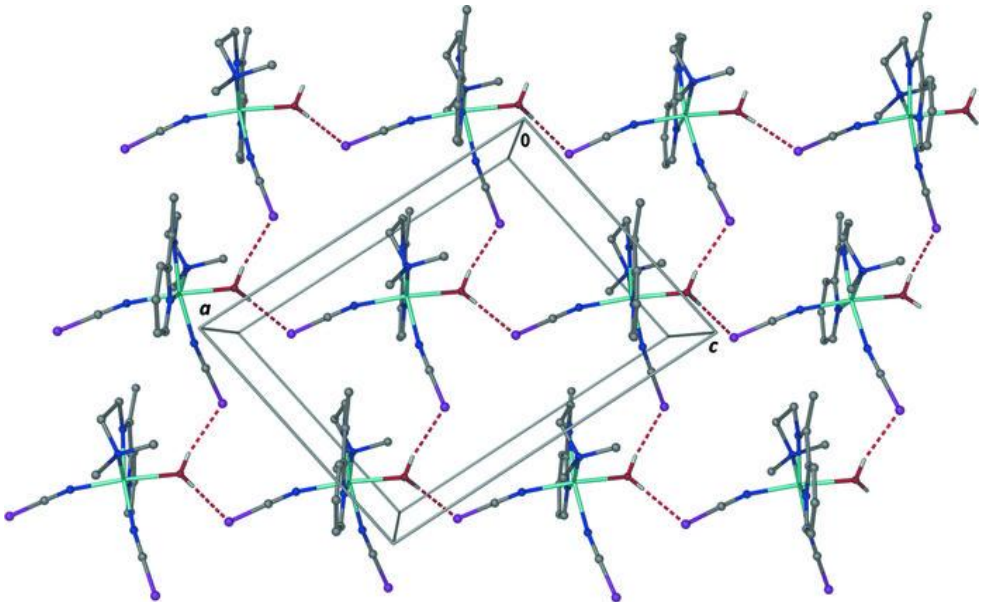

Figure 3.6.31: Packing crystal structure for [Ni(LNA)$(NCS)_2(H_2O)$]

In the present structure, the adjacent molecules are connected into 2-D arrays in *ac* plane *via* O-H···S interactions (Figure 3.6.31). A C-H···π interaction connects the layers into a three-dimensional structure.

In summary, the Ni(II) ion is six-coordinated by the *N,N',N*″-tridentate Schiff base *N* atoms, two *cis*-positioned N-bound isothiocyanate groups and one water molecule. In the crystal, O-H---S hydrogen bonds link adjacent molecules into infinite layers parallel to the ac plane. The layers are further connected into a three dimensional network via C-H---

interactions. The-CH_2-N(CH_3)$_2$ fragment is disordered over two sets of sites in a 0.556 (5):0.444 (5) ratio.

3.6.24 N,N-Dimethyl-N'-[1-(2-pyridyl)ethylidene]ethane-1,2-diamine-κ^3N,N',N''}bis (thiocyanato-κ^N)copper(II)

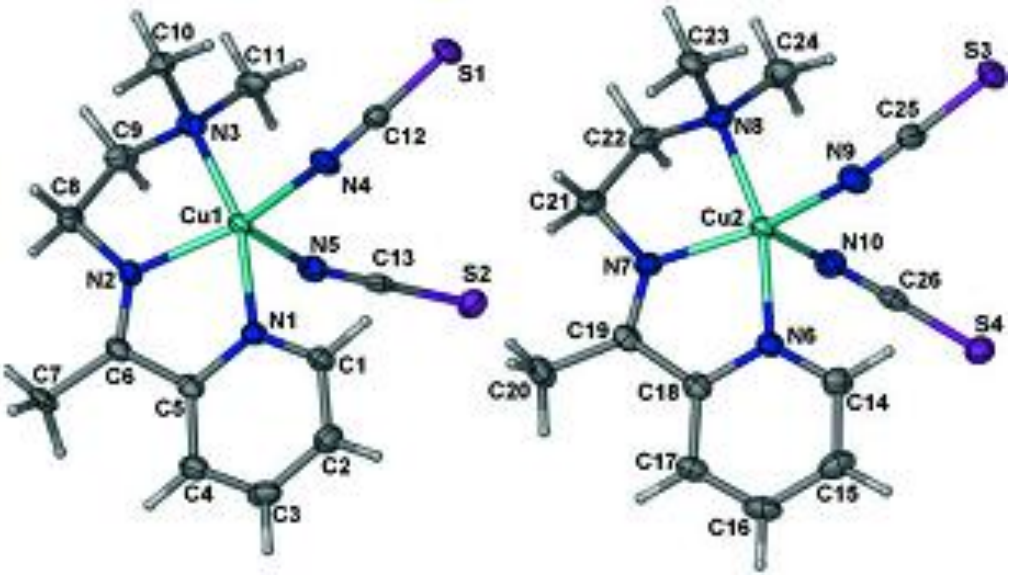

Figure 3.6.32: Crystal structure for [Cu(LNA)(NCS)$_2$]

The title compound was obtained upon the reaction of the Schiff base, *N*,*N*-dimethyl-*N'*-[methyl(2-pyridyl)methylene]ethane-1,2-diamine, with Cu(II) ion in the presence of thiocyanate anion. There are two geometrically slightly different molecules in crystal structure. The weighted r.m.s. fit for the superposition of the non-H atoms in both molecules is 0.296 Å. Each metal ion is five-coordinated by the three *N* atoms from the Schiff base and two *N*-donor thiocyanate ligands. Similar arrangements are observed in the structures of related mixed-ligand copper(II) complexes (Xue, 2010; Yue, 2005). Different from those, in the cadmium(II) thiocyanate complex of the same Schiff base (Gwaram, 2011), *N:S* bridging thiocyanates connect the metal ions into an octahedral polymeric structure. The Addison τ values (Addison, 1984) of 0.13 for Cu1 complex and

0.14 for Cu2 complex (τ = 0 for an ideal square pyramid and τ = 1 for an ideal trigonal bipyramid) imply distorted square-pyramidal geometries of the molecules. In the crystal, the adjacent molecules are bonded *via* C-H···S and C-H···N interactions into layers parallel to the *ac* plane. Moreover, intramolecular C-H···N hydrogen bonding occurs.

In summary, asymmetric unit of the title compound consists of two crystallographically independent molecules. In each molecule, the Cu(II) ion is five-coordinated in a distorted square-pyramidal geometry wherein the basal plane is defined by the *N,N',N''*-tridentate Schiff base and one N-bound thiocyanate ligand. The second N-donor thiocyanate group, located at the apical site, completes the coordination environment.

3.6.25 Dibromido{N,N-dimethyl-N'-[1-(2-pyridyl)ethylidene]ethane-1,2-diamineκ^3 N,N',N''}zinc

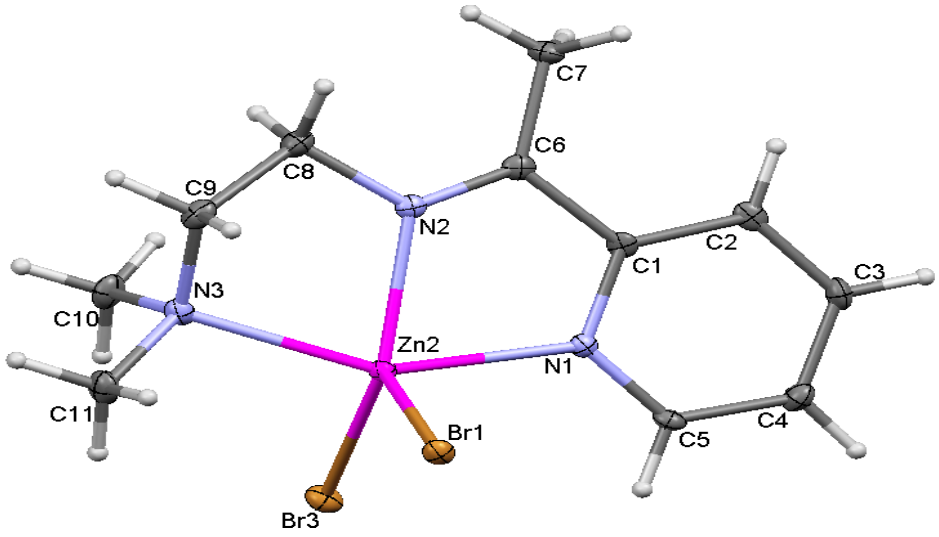

Figure 3.6.33: Crystal structure for [Zn(LNA)Br_2]

The zinc(II) ion is penta-coordinated by the *N,N',N''*-tridentate Schiff base ligand and two Br atoms in a distorted square-pyramidal geometry, the τ value (Addison, 1984) being 0.17. This arrangement is similar to what was observed in the structure of [$ZnBr_2(C_{10}H_{15}N_3)$], the closest analogous cadmium complex (Bian, 2003). In the crystal, pairs of the molecules,

related by symmetry *-x, -y, -z* + 1, are bonded into centrosymmetric dimers *via* C7-H7B···Br_2 interaction.

3.6.26 Dichlorido{N,N-dimethyl-N'-[1-(2-pyridyl)ethylidene]ethane-1,2-diamineκ^3 N,N',N''}zinc

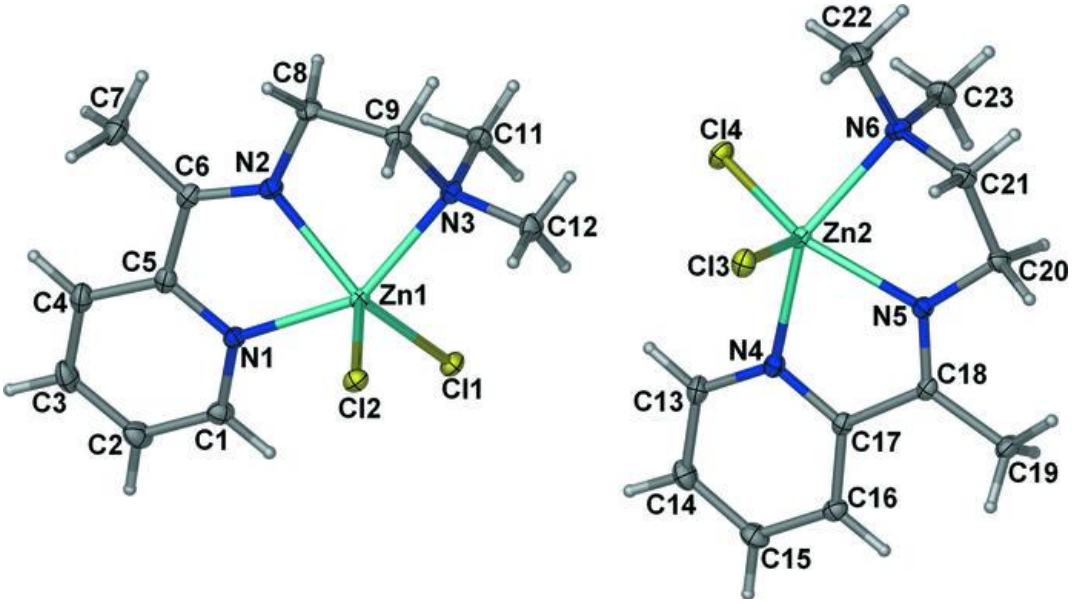

Figure 3.6.34: Crystal structure for [Zn(LNA)Cl_2]

The crystal structure of the title Zn(II) complex is isomorphous with that of the Mn(II) analogue (Ikmal Hisham, 2011). The asymmetric unit consists of two geometrically slightly different molecules; the weighted r.m.s. fit for the superposition of the non-H atoms in both molecules (after inversion) being 0.078 Å. The metal centers are five-coordinate in distorted square-pyramidal geometries, the apical positions being occupied by a chlorine atom. The Addison τ values (Addison, 1984) for Zn1 and Zn2 molecules are 0.103 and 0.168, respectively. The Zn-Cl and Zn-*N* bond lengths are comparable to those reported for similar complexes (Gourbatsis, 1999, Sun, 2005). In the crystal, the molecules are linked through C-H···Cl interactions into a three-dimensional polymeric structure and this is consolidated by π–π interactions formed between pairs of molecules [*Cg*1···*Cg*1i = 3.6255

(10) Å; *Cg*2···*Cg*2ii = 3.7073 (10) Å, where *Cg*1 and *Cg*2, are the centroids of the rings *N1*/C_1-C_5 and *N4*/C_{12}-C_{16}, for i: -*x*, -*y* + 1, -*z*; ii: -*x* + 1, -*y* + 1, -*z* + 1]. The lattice contains void spaces with the size of 52 $Å^3$ within which there is no evidence for included solvent. In summary, the asymmetric unit of the title compound, contains two independent *penta* coordinate Zn(II) complex molecules. In each molecule, the metal atom is coordinated by an *N,N',N''*-tridenate Schiff base and two Cl atoms in a distorted square-pyramidal geometry. The two molecules differ little in their geometry, but more in their intermolecular interactions. In the crystal, adjacent molecules are connected via C-H---Cl interactions into a three dimensional supra molecular structure. The network is supplemented by π–π* interactions formed between the aromatic rings of pairs of the symmetry-related molecules [centroid-centroid distances = 3.6255 (10) and 3.7073 (10) Å]. The crystal lattice contains void spaces with a size of 52 $Å^3$.

3.6.27 N,N-Dimethyl-N'-[1-(2-pyridyl)ethylidene]ethane-1,2-diamine-κ^3N,N',N''-bis (thiocyanato-κ^N)zinc(II)

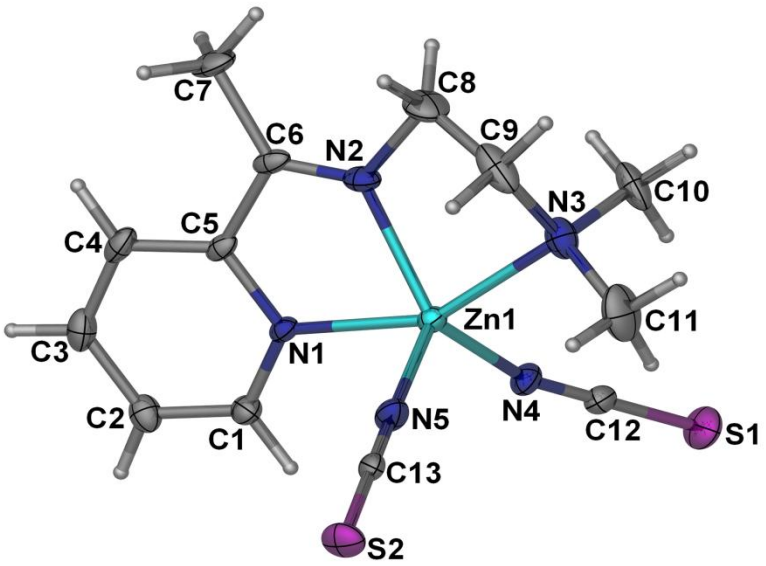

Figure 3.6.35: Crystal structure for [Zn(LNA)$(NCS)_2$]

The compound $Zn(LMA)(NCS)_2$, is a mixed-ligand Zn(II) complex with the *in situ* prepared Schiff base and thiocyanate ligands. Like the structure of the zinc(II) thiocyanate complexes of similar Schiff bases (Gwaram, 2011 and Ikmal, 2011), the present structure is a mononuclear square-pyramidal metal complex, the τ value being 0.35 (Addison,, 1984). In contrast, the cadmium(II) thiocyanate complex of the same Schiff base (Gwaram, 2011), showed a polymeric structure wherein the metal centers are linked by the N:S-bridging thiocyanate ligands. In the crystal structure of the title compound, C---H...S interactions connect a pair of molecules, related by symmetry -x+1, -y, -z, around a center of inversion.

In summary, the zinc atom is bonded to three donor nitrogen atoms of the ligand and two thiocyanates both bonded through the nitrogen atoms. The five Zn–*N* bond lengths as apparent from figure 3.6.35 are given as Zn(1)-*N*(1) 2.1752(18), Zn(1)-*N*(2) 2.0752(18), Zn(1)-*N*(3) 2.217(2), Zn(1)-*N*(4) 1.9681(18), Zn(1)-*N*(5) 1.9698(19). The compound, $[Zn(NCS)_2(C_{11}H_{17}N_3)]$, is a square-pyramidal zinc(II) complex in which the metal center is coordinated by the *N,N′,N″*-tridentate Schiff base and the *N* atoms of two thiocyanate ligands. In the crystal structure, pairs of molecules are connected into centrosymmetric dimer. The $CH_2N(CH_3)_2$ fragment is disordered over two sets of sites in a 0.529 (4):0.471 (4) ratio.

3.6.28 Dichlorido{N,N-dimethyl-N'-[1-(pyridin-2-yl)ethylidene]ethane-1,2-diamineκ^3 N,N',N''}cadmium(II)

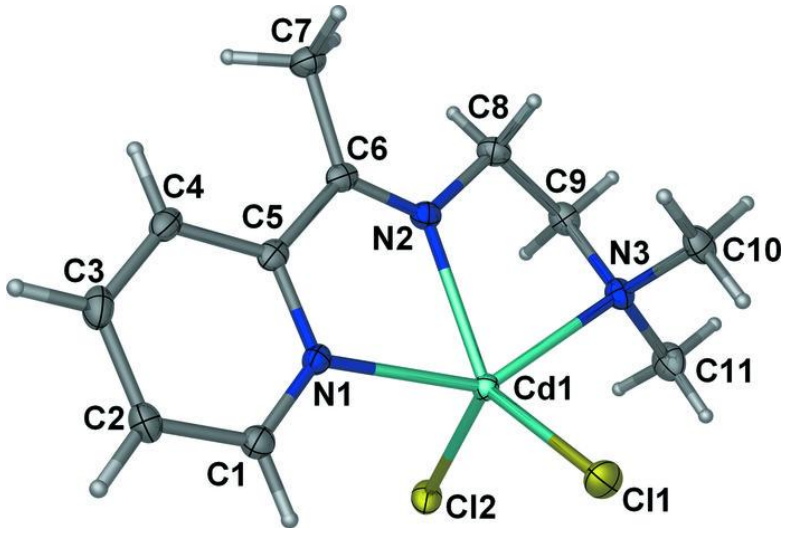

Figure 3.6.36: Crystal structure for [Cd(LNA)Cl_2]

The title compound was obtained *via* the complexation of $CdCl_2$ by *N,N*-dimethyl-*N'*-[methyl(2-pyridyl)methylene]ethane-1,2-diamine. Similar to the structure of the analogous copper(II) complex (Saleh Salga, 2010), the cadmium(II) ion is penta-coordinated by the *N,N',N''*-tridentate Schiff base ligand and two Cl atoms in a distorted square-pyramidal geometry, the τ value (Addison, 1984) being 0.17. This arrangement is similar to what was observed in the structure of [$CdCl_2(C_{10}H_{15}N_3)$], the closest analogous cadmium complex (Bian, 2003). In the crystal, pairs of the molecules, related by symmetry *-x*, *-y*, *-z* + 1, are bonded into centrosymmetric dimers *via* C7-H7B···Cl2 interaction.

In summary, the Schiff base acts as an *N,N',N''*-tridentate ligand towards the Cd(II) ion. Two Cl atoms complete a distorted square-pyramidal geometry around the metal atom.

3.6.29 Catena-Poly[[{N,N-dimethyl-N'-[1-(pyridin-2-yl)ethylidene]ethane-1,2-diamine-κ^3N,N',N''} (thiocyanato-κ^N)-cadmium]-l-thiocyanato-κ2S:N]

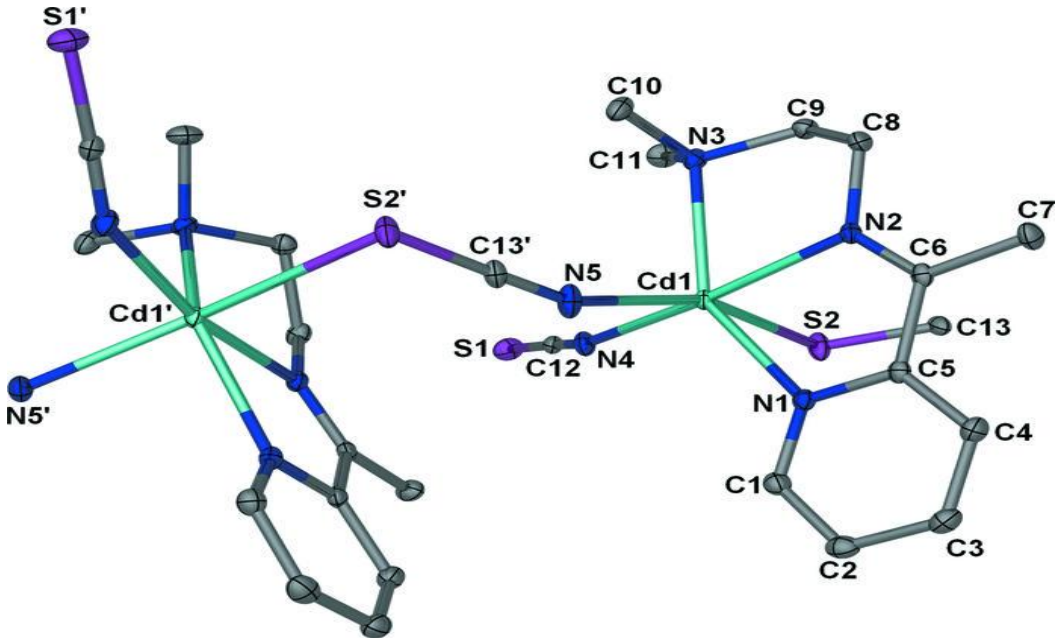

Figure 3.6.37: Crystal structure for [Cd(LNA)$(NCS)_2$]n

Thiocyanate anion is known to bind the cadmium ion in different modes: terminal *N*-bound, terminal *S*-bound (Nfor, 2006) or *N:S*-bridging ligand. As a bridging ligand, it may give rise to a singly bridged (Bose *et al.* 2004), doubly bridged or triply bridged (Chen, 2002) cadmium complex. The title compound is a mixed-ligand cadmium complex with thiocyanate and the Schiff base *N*,*N*-dimethyl-*N'*-[methyl(2-pyridyl)methylene]ethane-1,2-diamine. Similar to what was observed in the cadmium thiocyanate adduct of the similar Schiff base, *N*,*N*-diethyl-*N'*-[methyl(2-pyridyl)methylene]ethane-1,2-diamine (Banerjee, 2005), the thiocyanate ions act as either bridging or terminal ligands. However, different from the doubly bridged dimeric structure of the former, in the present structure the bridging thiocyanate ligands singly bridge the adjacent metal centers, related by symmetry *x*, –*y*+1/2, *z* - 1/2, into infinite chains along the *c* axis. Within this coordination polymer, the Cd(II) ions are separated by the distance of 8.0234 (9) Å. Two thiocyanate *N:S*-bridges,

one terminal thiocyanate N atom and the *N,N',N''*-tridentate Schiff base make a distorted octahedral geometry around the Cd(II) atoms.

In summary, the Cd(II) atom is octahedrally coordinated by the *N,N',N''*-tridentate Schiff base ligand and one terminal thiocyanate N atom. Two trans- N:S-bridging thiocyanates complete the N5*S* donor set around the Cd atom. In the crystal, adjacent Cd(II) ions are linked by the thiocyanate *N:S*-bridges into polymeric chains along the c axis.

3.6.30 Bis(l-2-{1-[2-(dimethylamino)ethylimino]ethyl}phenolato)bis[bromidocopper(II)] monohydrate

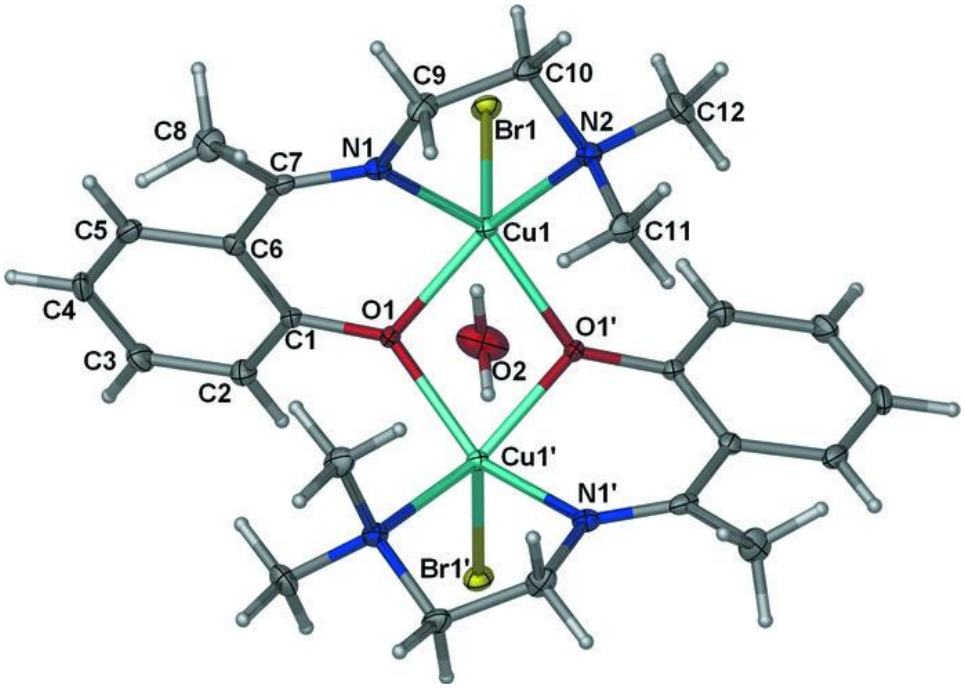

Figure 3.6.38: Crystal structure for $[Cu_2(LNH)_2Br_2]H_2O$

The title dimeric copper(II) complex was synthesized through the reaction of the *in situ* prepared Schiff base, *N,N*-dimethyl- *N'*-[methyl(2-phenolyl)methylene]ethane-1,2-diamine, with copper(I) bromide. Under the reaction conditions, the Cu(I)ion was oxidized to Cu(II) and chelated by the deprotonated *N,N',O*-tridentate Schiff base. Pairs of metal centers are doubly bridged *via* the phenoxide *O* atoms around centers of inversion. Within the formed

dimer, the Cu···.Cu distance [2.9935 (8) Å] is comparable to those reported for similar structures (Li, 2000; Rigamonti, 2008; Suo, 2008). The square-pyramidal geometry (τ = 0.11, Addison, 1984) around each Cu(II) ion is completed by one apically positioned Br atom. The dimeric complex is cocrystallized with one molecule of water whose oxygen atom is situated on a 2-fold rotational axis. In the crystal, the water molecules link the dimers into infinite chains along the *b* axis *via* O-H···Br and-H···O interactions.

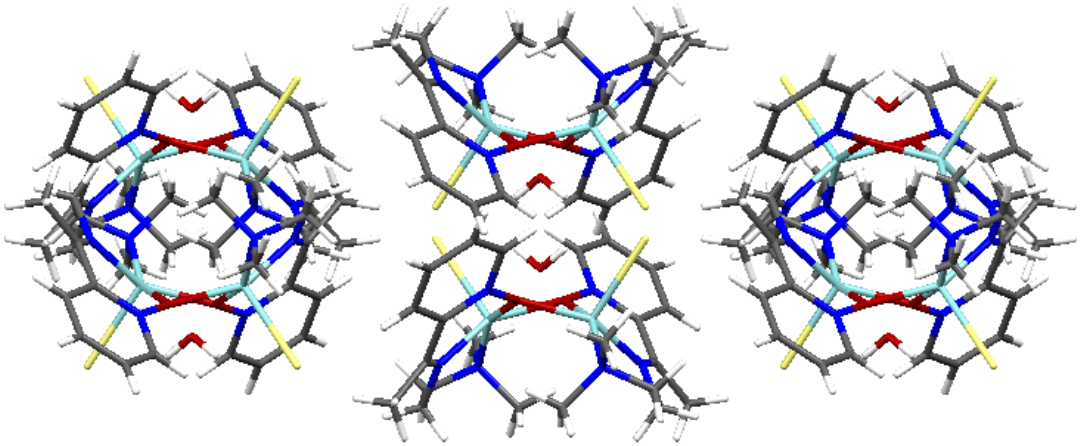

In the centrosymmetric dinuclear copper(II) title complex, each Cu(II) ion is five coordinated in a square-pyramidal geometry by the *N*,*NO*,O-tridentate Schiff base, one Br atom and the bridging *O* atom of the centrosymmetrically related Schiff base. In the crystal, the water molecules link the complex molecules into infinite chains along the *b*-axis via O-H---Br and C-H---O hydrogen bonds.

BIOLOGICAL APPLICATIONS

4. Experimental

4.1 Anti ulcer Activities

Omeprazole: In this research, omeprazole obtained from the University of Malaya Medical Centre (UMMC) Pharmacy was used as the reference anti-ulcer drug. The drug was dissolved in 10% Tween 20 (Merck Schuchardt OHG, 85662 Hohenbrunn, Germany). A 10% v/v dilution of Tween 20 was used as the vehicle for rat dosing (5 ml/kg) and administered orally to the rats in doses of 20 mg/kg body weight (5 ml/kg) according to (Mahmood 2010).

4.1.1 Acute toxicity testing and experimental animals

Adult, healthy male and female Sprague-Dawley rats (6-8 weeks old) were obtained from the Animal House, Faculty of Medicine, University of Malaya, Kuala Lumpur (Ethics No. PM/27/07/2010/MAA (R)). The rats weighed between 150-180 g. The animals were given standard rat pellets and tap water *Ad libitum*. The acute toxicity study was used to determine a safe dose for the zinc(II) complex. Thirty-six rats (18 males and 18 females) were divided equally into three groups that were administered the vehicle only (10% Tween 20) and 1 or 2 g/kg of the prepared compound. The animals were fasted overnight (with water) prior to dosing, and food was withheld for a further 3 to 4 hours after dosing. The animals were observed for 0.5, 2, 4, 8, 24 and 48 hours after administration for the onset of clinical or toxicological symptoms. Mortality, if any, was observed over a period of two weeks. The animals were sacrificed on day fifteen. The histology, hematological and serum biochemical parameters were determined according to the Guideline for testing (OECD, 2005). This study was approved by the ethics committee for animal experimentation, Faculty of Medicine, University of Malaya, Malaysia. All of the animals received humane

care according to the criteria outlined in the "Guide for the Care and Use of Laboratory Animals" prepared by the National Academy of Sciences and published by the National Institutes of Health.

4.1.2 Ethanol-induced gastric ulcer formation

Prior to the experiment, the rats were fasted for 24 hours according to our published method (Mahmood, 2010). And they were allowed free access to drinking water until 2 hours before the experiment. Gastric ulcer formation was induced by orogastric intubation of absolute ethanol (5 ml/kg) as described by (Abdulla 2010). Both the negative control rats (Group 1) and the ulcer control rats (Group 2) were orally administered 10% Tween 20 (5 ml/kg). The reference group (Group 3) received oral doses of 20 mg/kg omeprazole in 10% Tween 20 (5 ml/kg) as a positive control. The experimental groups were orally administered the zinc(II) compound dissolved in 10% Tween 20 (5 ml/kg) at 50 and 100 mg/kg (Groups 4 and 5, respectively). One hour after this pretreatment, (Group 1) were orally administered distilled water in 5 ml/kg 10% Tween 20, whereas (Group2, 3, and 4) were orally administered absolute ethanol (5 ml/kg) to induce gastric ulcer formation. The rats were euthanized sixty minutes later (Mahmood, 2010) with an overdose of xylazine and ketamine anesthesia, and their stomachs were immediately excised.

4.1.3 Gastric wall mucus determination

The glandular segments of the stomach were removed, weighed and assessed for gastric wall mucus content. Each segment was transferred immediately into a 1% Alcian blue solution (in sucrose solution buffered with sodium acetate at pH 5), and the excess dye was removed with a sucrose solution rinse. The dye complexed with the gastric wall mucus was extracted with a magnesium chloride solution. A 4-ml aliquot of the blue extract was then shaken with an equal volume of diethyl ether. The resulting emulsion was centrifuged, and

the absorbance of the aqueous layer was recorded at 580 nm. The quantity of Alcian blue extracted per gram of glandular tissue (net) was then calculated.

4.1.4 Gross gastric lesion evaluation

Ulcers of the gastric mucosa appear as elongated bands of hemorrhagic lesions parallel to the long axis of the stomach. The gastric mucosa of each rat was thus examined for damage. The length and width of the ulcer (mm) were measured with a planimeter (10 × 10 mm^2 = ulcer area) under a dissecting microscope (1.8x). The ulcerated area was measured by counting the number of small squares (2 mm × 2 mm) covering the length and width of each ulcer band. The sum of the areas of all lesions for each stomach was applied in the calculation of the ulcer area (UA), wherein the total number of small squares × 4 × 1.8 = UA (mm^2) according to (Zahra et al. 2009). The inhibition percentage (I%) was calculated using the following formula according to (Abdulla, 2010).

$$(I\%) = [(UA_{control} - UA_{treated}) \div UA_{control}] \times 100\%.$$

4.1.5 Histological evaluation of the gastric lesions

The gastric wall specimens were fixed in 10% buffered formalin and processed in a paraffin tissue-processing machine (Leica, Germany). Sections of the stomach were prepared at a thickness of 5 µm and stained with hematoxylin and eosin for histological evaluation (Behmer, 1976).

4.1.7 Preparation of the homogenates

The gastric tissue was washed thoroughly with ice-cold saline. A 10% (w/v) homogenate was prepared using a Teflon homogenizer (Polytron, Heidolph RZR 1, Germany) in ice-

cold 50 mM phosphate buffer pH 7.4 containing mammalian protease inhibitor cocktail. The homogenate was centrifuged at 10,000 g for 30 min at 4°C. The supernatant was used in the assays for antioxidant activity/level and lipid peroxidation.

4.1.8 The measurement of superoxide dismutase (SOD) activity

SOD activity was measured according to (Sun, 1988). The activity of the enzyme was evaluated by measuring its capacity to inhibit the photochemical reduction of nitro-blue tetrazolium (NBT). In this assay, the photochemical reduction of riboflavin generates O^{2-} that reduces the NBT to produce formazan salt, which absorbs light at a wavelength of 560 nm. In the presence of SOD, the reduction of the NBT is inhibited because the enzyme converts the superoxide radical to peroxide. The results are expressed as the quantity of SOD necessary to inhibit the rate of reduction of the NBT by 50% in units of the enzyme per gram of protein. The homogenates (10% of the tissue in phosphate buffer) were centrifuged (10 min, 3,600 rpm, 4°C), and the supernatant was removed and centrifuged a second time (20 min, 12,000 rpm, 4 °C). The resulting supernatant was assayed. In a dark chamber, 1 mL of the reactant (50 mM phosphate buffer, 100 nM EDTA and 13 mM l-methionine, pH 7.8) was mixed with 30 μL of the sample, 150 μL of 75 μM NBT and 300 μL of 2 μM riboflavin. The tubes containing the resulting solution were exposed to fluorescent light bulbs (15 W) for 15 minutes and then read using a spectrophotometer at 560 nm.

4.1.9 The measurement of reduced glutathione

To assess changes in the amount of gastric mucosal GSH, which is a non-protein sulfhydryl compound, the GSH content was measured according to (Sedlak and Lindsay 1968). The glandular segment from each stomach was homogenized in an ice-cold solution of 0.02 M

EDTA (at 10%). Aliquots (400 μL) of the tissue homogenate were mixed with 320 μL of distilled water and 80 μL of 50% (w/v) trichloroacetic acid in glass tubes and centrifuged at 3,000 rpm for 15 min. Subsequently, the supernatants (400 μL) were mixed with 800 μL Tris buffer (0.4 M, pH 8.9), and 5,5-dithio-bis(2-nitrobenzoic acid) (DTNB; 0.01 M) was added to the mixture. After the reaction mixture was shaken for 3 minutes, its absorbance was measured at 412 nm within 5 minutes of the addition of DTNB against a blank with no homogenate. The absorbance values were extrapolated from a glutathione standard curve, and the GSH content was expressed in μg GSH/g of protein. The protein concentration was measured using the Bradford method (Varley, 1980).

4.1.10 The measurement of membrane lipid peroxidation

The rate of lipoperoxidation in the gastric mucous membrane was estimated by measuring the malondialdehyde (MDA) content with the thiobarbituric acid reactive substances (TBARS) test. The stomachs were washed with buffered saline to minimize the effect of hemoglobin on the free radicals and to remove the blood adhered to the mucous membrane. The stomachs were homogenized with 10% of the tissue in potassium phosphate buffer. A 250-μL aliquot of the homogenate was removed and stored at 37°C for 1 hour, after which 400 μL of 35% perchloric acid was added, and the mixture was centrifuged at 14,000 rpm for 20 minutes at 4°C. The supernatant was removed, mixed with 400 μL of 0.6% thiobarbituric acid and incubated at 95–100 °C for 1 hour. After cooling, the absorbance was measured at 532 nm. A standard curve was generated using 1,1,3,3-tetrametoxy propane. The results were expressed as nM of MDA/mg of protein. The concentration of the proteins was measured using the Bradford method (Bradford, 1976). The measurement of the total protein content in the stomach samples after ethanol-induced lesion formation was based on the interaction of the Coomassie Blue G250 dye with protein.

At the pH of the reaction, the interaction between proteins of high molecular weight and the dye causes a shift in the dye to the anionic form, which absorbs strongly at 595 nm. Solutions containing an albumin standard, distilled water, buffer and each sample were added to the wells. For sample preparation, 2 µL of a sample and 38 µL of buffer were added to each well. Then, 200 µL of Bradford's solution (diluted 5×) was added to each well. After 5 minutes, a reading was obtained at a wavelength of 595 nm.

4.2 *IN VITRO* ANTIOXIDANT ACTIVITY

4.2.1 Ferric Reduction Antioxidant Power (FRAP) assay

The determination of the total antioxidant activity (FRAP assay) of the compounds is a modified method of (Choi, 2002). The stock solutions included 300 mM acetate buffer (3.1 g $C_2H_3NaO_2 \cdot 3H_2O$ and 16 ml $C_2H_4O_2$), pH 3.6, 10 mM TPTZ (2, 4, 6-tripyridyl-s-triazine) solution in 40 mMHCl, and 20 mM $FeCl_3 \cdot {}_6H_2O$ solution. The fresh working solution was prepared by mixing 25 ml acetate buffer, 2.5 ml TPTZ, and 2.5 ml $FeCl_3 \cdot {}_6H_2O$. The temperature of the solution was raised to 37 °C before use. CLG (10 µL) was allowed to react with 300 µl of the FRAP solution in the dark. Readings of the colored product (ferrous tripyridyltriazine complex) were taken at 593 nm. The standard curve was linear between 100 and 1000 µM $FeSO_4$. Results are expressed in µM Fe (II)/g dry mass and compared with that of ascorbic acid and BHT.

4.2.2 DPPH (1,1-Diphenyl-2-picrylhydrazyl) radical scavenging activity

The scavenging activity of the compounds on DPPH was determined using the method described in (Benzie, 1999). Compounds were tested at final concentrations ranging from 0-25µg/mL in methanol. One milliliter of 0.3 mM DPPH ethanol solution was added to 2.5 mL of sample solution of different concentrations to make the test solutions; while 1 mL of methanol was added to 2.5 mL of samples to make the blank solutions. The negative

control (blank) consisted of 1 mL DPPH solution plus 2.5 mL of methanol. These solutions were allowed to react at room temperature for 30 minutes in the dark. The absorbance values were measured at 518 nm and converted into percentage antioxidant activity according to the equation: % Inhibition = $[(A_B-A_A)/A_B]$ X 100.

Where: A_B: absorption of blank sample; A_A: absorption of tested samples. The IC_{50} as well as the kinetics of DPPH scavenging activity was determined. Ascorbic acid was used as a positive control in this assay.

4.3 *IN VITRO* ANTI-CANCER STUDIES

4.3.1 MTT - Culture of cells and cytotoxicity assay

The MCF-7 cells (human breast cancer cells) were seeded into 96 well plates at an initial cell density of approximately $5x10^5$ cells cm^{-3}. After 24 hours incubation for cell attachment and growth, the medium was removed and replaced with fresh medium containing varying concentrations of the compounds. The compounds added were first dissolved in DMSO at the required concentration. Subsequent 6 desirable concentrations was prepared using growth medium. Control wells received only DMSO. Each concentration of the compound under study was assayed in six replicates. The assay was terminated after 48 hours incubation period. Again, the medium was removed and cell viability was determined after further 4 hours with 5 mg cm-3 MTT [3-(4,5-dimethylthiazol-2-yl)-2,5-diphenyltetrazolium]bromide; also named thiazol blue. DMSO was then added per well and the dissolving formazan precipitate was read by using Elisa plate reader, Dynatech MR5000 at 570 nm. Comparison was made with positive control tamoxifen.

4.3.2 Soft-agar Colony Formation Assay (Clonogenic Assay)

A two-layer technique was used, with a base layer consisting of 1% agar (Promega), and a

second layer containing cells with 0.7% agar. The base agar containing 1% agar was melted in a microwave oven and cooled to 40˚C in a water bath. 2X RPMI 1640 with 20% FCS were warmed at 40˚C in a water-bath and for 30 minutes. Then, equal volumes of the two solutions were mixed to obtain 0.5% agar and 1X RPMI 1640 with 10% FCS. After that, 1.5 ml of mixed solutions was added to a petri dish (35 mm). The second layer, the top agar containing 0.7% agar, was melted in a microwave oven and cooled to 40˚C in a water-bath. Also, 2X RPMI 1640 with 20% FCS were heated at the same temperature.

Cells were trypsinised and counted to a ratio of 5×10^3 cells per plate. Then, 3 ml of 2X RPMI 1640 (20% FCS) and 3 ml of 0.7% agar were added to a centrifuge tube and mixed gently, after which 1.5 ml was added to each petri dish (35 mm) that was covered with base agar. Incubated assays were performed at 37˚C with 5% CO_2 in a humidified incubator for 9 days. After that, plates were stained with 0.5 ml of 0.005% crystal violet for approximately 2 hrs; then colonies were counted using an inverted microscope Nikon Eclipse Ti camera. Also, the cloning efficiency was calculated as the number of colonies divided by the number of cells added to each plate.

4.3.3 DNA Fragmentation Assays

DNA fragmentation assay was performed using the Suicide Track™ DNA Ladder Isolation Kit (Calbiochem, CA), according to manufacturer's instructions. Briefly, 1×10^6 MCF-7 cells were cultured in a T-25 flask and treated with different concentration of compounds for 24 hours. Floating and trypsinized-adherent of treated and untreated cells were collected by centrifuging at 1500 × g for 5 min. Cell pellets were then resuspended in 500 µl of extraction buffer following incubation on 4°C for 30 min. The suspensions were then centrifuged at 16, 000 × g for 5 min at room temperature. The resulting supernatant were transferred to a clean tube, followed by the addition of 20 µl of RNase A solution and

incubated at 37°C for 1 h. DNA isolation buffer was added and further incubated at 50°C for overnight. Then, 2 µl of Pellet Paint® Co-precipitant was added to the suspension together with 60 µl of 3 M sodium acetate and 662 µl of 2-propanol. Samples were mixed by inversion for 2 min and then centrifuged at 16, 000 × g for 5 min. The resulting pellets were washed with 500 µl of 70% and 100% ethanol, respectively. The small apoptotic DNA fragments were separated from intact chromatin and were then air-dried and resuspended in 50 µl of resuspension buffer (10 mM Tris, 1 mM EDTA). Finally, purified fragments were analyzed on a 1.5% (w/v) agarose gel electrophoresis and stained with 0.5 µg/ml ethidium bromide. Fragmentation of DNA was observed under UV illumination and visualized using a gel documentation system (UVP Biospectrum HR410). Positive control was supplied by Calbiochem which consist of 1×10^6 HL-60 cells treated with 0.5 mg/ml Actinomycin D for 19 h.

4.4 *IN VITRO* ANTI-MICROBIAL STUDIES

4.4.1 Antimicrobial Testing

The synthesized compounds were first screened for potential antibacterial activity by testing against two randomly selected strains from each bacterial species, using disc diffusion assay (CLSI, 2011). Briefly, a loopful of an overnight bacterial culture of each strain was suspended in sterile 0.85% saline (BDH) to the concentration of approximately "10^8" cfu/ml (equivalent to 0.5 Mc Farland units) before inoculated evenly on the entire surface of Mueller Hinton agar (Oxoid) with a sterile cotton swab. Sterilized paper discs (Thermo Fisher, 6mm diameter), impregnated with 30 µg of respective synthetic Schiff compound, and was placed on the inoculated agar plate. DMSO disc was used as a negative control in the test. The diameter of inhibition zone around the impregnated paper disc was measured after 18 hour of incubation at 37˚C. All tests were performed in duplicate.

Synthetic Schiff compounds, in which inhibition zone was observed in any one of the four species tested, were selected for MIC and MBC determination with broth micro-dilution assay. Only compounds with MIC and MBC value lesser than "10 µg/mL," is considered potentially active against the corresponded bacterial species; and further tested against the entire collection of the corresponded bacterial species with disc diffusion assay. This was to determine the variation in the susceptibility responses to the tested compound within the bacterial species tested. The two selected strains for each species in the initial screening were: MRSA 0804-25 and MRSA 0807-7 for MRSA; AC 0612-7 and AC 0903-21 for *A. baumannii*; KB 71 and KB 83 for *K. pneumonia*; and PA45 and PA104 for *P. aeruginosa*.

4.4.2 MIC determination

Minimum inhibition concentration (MIC) was determined with 96-well broth micro-dilution assay. The inoculum was prepared by suspending an overnight culture in a sterile 0.85% saline (BDH) to approximate 10^8 cfu/ml (equivalent to 0.5 McFarland units) and further diluted in cation adjusted Mueller Hinton broth (CMHB; BD) to the concentration of 10^6 cfu/ml. Two-fold serial dilutions of the tested compound were prepared in CMHB across the 96-well microtiter plate with the highest concentration starting from 750 ppm (750 µl/ml) in duplicate rows. The prepared suspension of the bacteria was added to each well except the negative control wells of the microtitre plate in a 1:1 ratio with final bacteria concentration of approximately "5 x 10^5" cfu/ml. The inoculated microtitre plates were incubated at 37˚C for 24 hour.

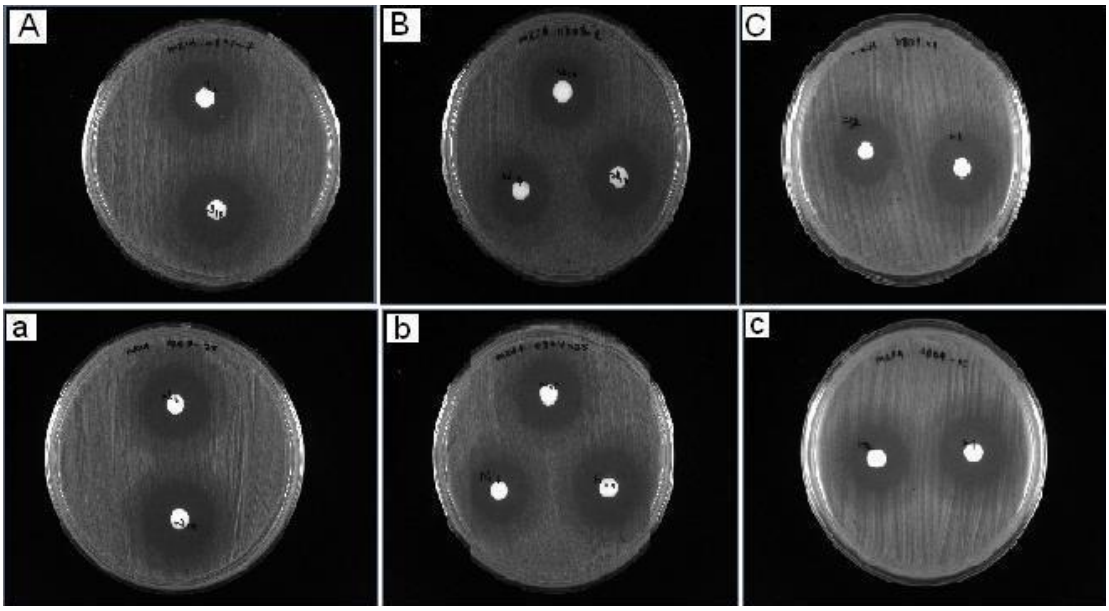

Figure 4.4.2.1: Photograph showing the antibacterial (MRSA 0804-25-A,B,C) and (MRSA 0807-7- a,b,c) screening

The MIC was determined as the lowest concentration of the test compound that exhibits no visible growth. A further confirmative test was done by adding 30 µl of MTT dye (Sigma) to each well. Wells with color changes within 30 - 60 minutes incubation at room temperature were scored as positive growth. The lowest concentration of the tested compound that exhibits no color changes (yellow) is determined as the MIC value.

4.4.3 MBC determination

Before MTT dye was added to each well, 0.1ml was removed from each turbid well and inoculated onto Mueller Hinton agar (MHA) plate. It was then incubated at 37°C for 24 hour before result was read. The minimal bactericidal concentration (MBC) was determined as the lowest concentration of the tested compound that exhibits no viable microorganism growth on the MHA plate. The antimicrobial compound is regarded as bactericidal if the MBC is not more than four times the MIC.

4.5 ANTIBACTERIAL EVALUATION

Nosocomial infections caused by multidrug resistant bacteria are an increasing medical problem worldwide, particularly among immunocompromised patients and those hospitalized in intensive care units. Both Gram positive and Gram negative bacteria have developed high level resistance to multiple classes of antibacterial agents. These include methicillin resistant *Staphylococcus aureus* (MRSA), *Pseudomonas aeruginosa*, *Acinetobacter baumannii*, *Escherichia coli* and vancomycin resistant enterococci (VRE) (Guidos, 2010). Few available drugs such as linezolid and some newer glycopeptides, and tigecycline are active against MRSA and VRE, but their success rates are variable (Esposito, 2007). As such, there is a need to explore other sources of effective antibacterial compounds to augment the limited choice of drugs for therapeutic treatment.

A series of Schiff bases derived from 2-acetylpyridne and their metal complexes were were screened for anti-bacterial activity against Methicillin-resistant *Staphylococcus aureus* (MRSA), *Acinetobacter baumanni* (AC), *Klebsiella pneumonie* (KB) and *Pseudomonas aeruginosa* (PA) using the disc diffusion and micro broth dilution assays. Based on the overall results, the complexes showed the highest activities against MRSA while a weak antibacterial activity was observed against *A. baumanii* and *P. Aeruginosa*, while no activity was observed in *K. pneumonie*.

Scheme 1. Reaction pathway for the coordinated complexes.

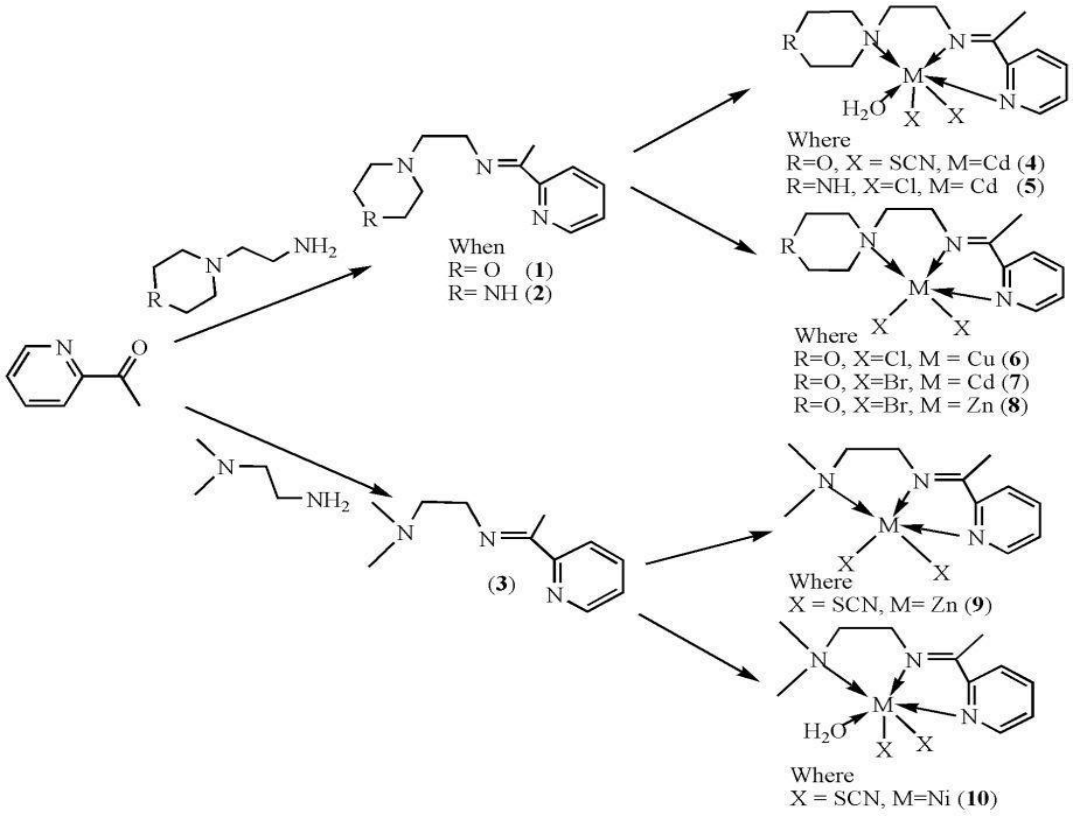

Pharmacology: *Bacterial Strains:* The antibacterial activities of the investigated compounds were tested against a panel of multi-drug resistant nosocomial bacterial pathogens, consisted of ten (10) isolates of methicillin-resistant *Staphylococcus aureus (MRSA)–MRSA 0804-25*, *MRSA 0805-21*, *MRSA 0806-1*, *MRSA 0807-1*, *MRSA 0807-7*, *MRSA 0807-19*, *MRSA 0808-35*, *MRSA 0809-15*, *MRSA 0809-24*, *MRSA 0809-38*; two (2) isolates of *Acinetobacter baumannii(AC)–AC 0612-7*, *AC 0903-21*, two (2) isolates of *Klebsiella pneumonia (KB)–KB 71*, *KB 83*, and two (2) isolates of *Pseudomonas aeruginosa (PA)–P. aeruginosa*. All tested bacterial strains of *MRSA* were of clinical origin and have shown resistance to at least four antibiotics. For each bacterial species, six to ten strains were included in the antibacterial study to capture possible drug resistance variation within species. All bacterial strains that used in this study were obtained from the bacteria

culture collection of Biomedical Science Laboratory, Institute of Graduate Studies University of Malaya, Kuala Lumpur, Malaysia.

4.6 RESULTS AND DISCUSSION

Antibacterial Activity Results: A total of ten Schiff-base compounds were synthesized and screened for potential antibacterial activity against the emerging multi-drug resistance nosocomial bacterial pathogens in hospital settings, namely, methicillin-resistant *Staphylococcus aureus, A. baumanii, K. pneumonia* and *P. aeroginosa*. In the first level antibacterial screening with the disc diffusion assay, all compounds under study were tested against eight clinical strains, two from each bacterial species. Inhibition zones were observed in the Schiff base compounds. However, no inhibition zone was observed in any of the compounds tested against *K. pneumonia* (Table 4.1). All compounds were strongly inhibitive against MRSA, while they showed weak antibacterial activity against *A. baumanii* and *P. aeroginosa* in the disc diffusion test (Table 4.1). This higher antimicrobial activity of the metal complexes **4**–**10**, compared with that of Schiff base ligands **1**–**3**, is perhaps due to the change in structure as a result of coordination, as chelating tends to make metal complexes act as more powerful and potent bacteriostatic agents, thus inhibiting the growth of the microorganisms (Chohan, 2006 & Chohan, 2003). These seven compounds were then analyzed further for the MIC and MBC value using broth micro-dilution assay (Table 4.2). The result from broth micro-dilution assay was in total analogue to the disk diffusion screening. The test showed that, all of the seven compounds were most active against MRSA, with MIC value ranged from 0.7–2.9 µg/mL; MBC value ranged from 2.9–46.9 µg/mL (Table 4.2). Both *A. baumanii* and *P. aeroginosa* were resistant to the tested compounds at concentration lower than 93.8 and 187.0 µg/mL, respectively (Table 4.2). Therefore, it was concluded that these seven compounds were highly inhibitive only against

the Gram positive bacterium MRSA. Further antibacterial tests were conducted against eight clinical strains of multi-drug resistant MRSA (Table 4.3) showing varying responses towards the seven selected Schiff-based compounds in the disc diffusion assay (scheme 1), however, they demonstrated twenty percent of resistance rate (two strains out of ten were resistant to the seven tested compounds). The broth micro-dilution assay resulted in similar findings, in which all, but MRSA 0807-1 and MRSA 0808-35, were inhibited at MIC ranging from "1.5 to 11.7" µg/mL. Both, MRSA 0807-1 and MRSA 0808-35, were only inhibited at MIC ranging from "209.7 to 419.4" µg/mL. (Table 4.4) presented the antibiogram of ten clinical strains of MRSA used in this antibacterial analysis with some known antibacterial drugs in which MRSA either showed resistant (R), susceptible (S) or intermediate resistant (I) towards them.

Table 4.1: First level antibacterial screening Disc diffusion assay.

Compound	MRSA 0804-25	MRSA 0807-7	AC 0612-7	AC 0903-21	KB 71	KB 83	PA 45	PA 104
1	6	6	0	0	0	0	5	6
2	5	5	0	0	0	0	5	5
3	0	0	0	0	0	0	0	0
4	21	22	7	7	0	0	8	8
5	24	23	9	8	0	0	11	19
6	22	23	9	8	0	0	10	10
7	23	22	10	10	0	0	8	8
8	21	20	10	9	0	0	9	9
9	23	23	9	8	0	0	10	9
10	22	22	7	7	0	0	10	9
Control (DMSO)	0	0	0	0	0	0	0	0

Table 4.2: Second level antibacterial screening.

Minimum inhibitory concentration (MIC; µg/mL)/minimum bactericidal concentration (MBC; µg/mL)								
	MRSA 0804-25	**MRSA 0807-7**	**AC 0612-7**	**AC 0903-21**	**KB 71**	**KB 83**	**PA 45**	**PA 104**
1-3	n.d.	n.d.	n.d.	n.d.	n.d.	n.d.	n.d.	n.d.
4	0.7/2.9	1.5/2.9	93.8/750	93.8/750	375/750	375/750	187.5/750	187.5/750
5	0.7/2.9	0.7/2.9	93.8/750	93.8/750	187.5/750	187.5/750	187.5/750	187.5/750
6	1.5/5.9	1.5/5.9	93.8/375	93.8/375	375/750	375/750	187.5/750	187.5/750
7	1.5/5.9	1.5/5.9	93.8/375	93.8/375	187.5/750	187.5/750	187.5/750	187.5/750
8	1.5/5.9	1.5/2.9	93.8/750	93.8/750	375/750	375/750	187.5/750	187.5/750
9	1.5/5.9	1.5/23.4	187.5/750	187.5/750	375/750	375/750	187.5/750	187.5/750
10	2.9/46.9	2.9/46.9	187.5/750	187.5/750	375/750	375/750	187.5/750	187.5/750
DMSO	375/>375	375/>375	375/>375	375/>375	375/>375	375/>375	375/>375	375/>375

n.d. = not determined.

Table 4.3: Varying responses of the eight MRSA clinical strains towards the seven selected Schiff-base complexes in the disc diffusion assay.

Compounds	**MRSA 0805-21**	**MRSA 0806-1**	**MRSA 0807-1**	**MRSA 0807-19**	**MRSA 0808-35**	**MRSA 0809-15**	**MRSA 0809-25**	**MRSA 0809-38**
4	23	24	0	23	0	22	22	21
5	23	24	0	25	0	23	23	23
6	24	22	0	22	0	21	21	22
7	24	20	0	21	0	19	20	20
8	25	23	0	24	0	21	21	22
9	23	23	0	22	0	23	24	23
10	22	22	0	22	0	22	22	22
(DMSO)	0	0	0	0	0	0	0	0

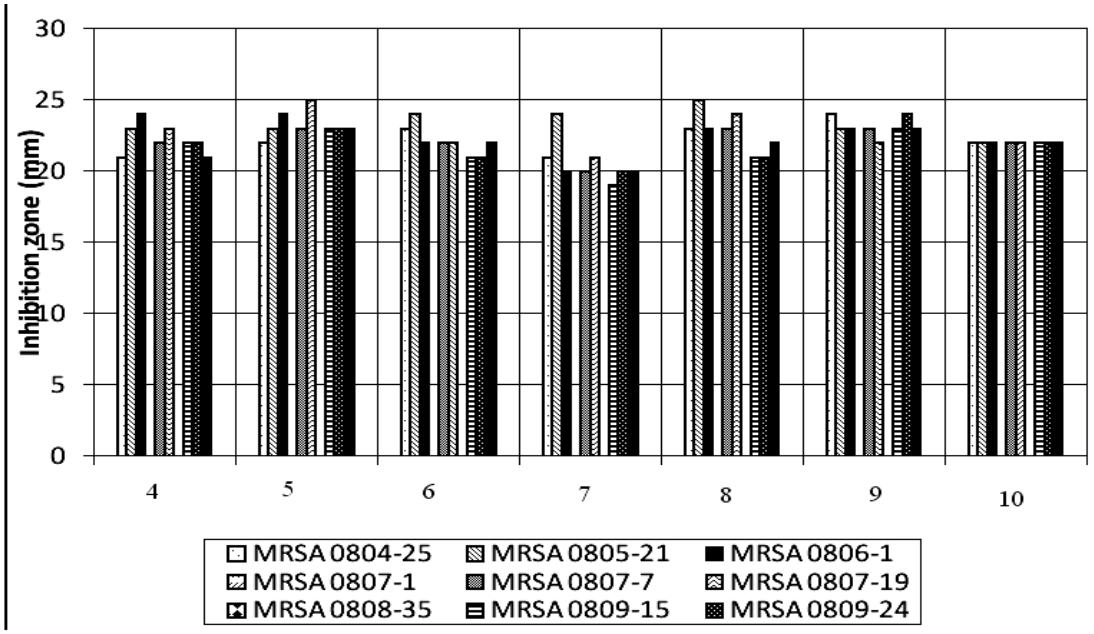

Figure 4.6.1: Histogram for the 10 MRSA clinical strains of Schiff-base complexes.

Table 4.4: Antibiogram of the ten clinical strains of MRSA used in the antibacterial analysis.

Strain No	E	CN	LZD	MUP	RD	DA	TEC	CIP	NET	TE	VA	FD	OX	SXT
MRSA 0805-21	R	R	S	S	S	S	S	R	R	R	S	S	R	R
MRSA 0806-1	R	R	S	S	S	S	S	R	R	R	S	S	R	R
MRSA 0807-1	R	R	S	S	S	S	S	R	R	R	S	S	R	R
MRSA 0807-19	R	R	S	S	S	S	S	R	I	S	S	S	R	S
MRSA 0808-35	R	R	S	S	S	S	S	I	I	R	S	S	R	R
MRSA 0809-15	R	R	S	S	S	S	S	R	R	R	S	S	R	R
MRSA 0809-24	R	R	S	S	S	S	S	R	R	R	S	S	R	R
MRSA 0809-38	R	R	S	S	S	S	S	R	R	R	S	S	R	S
MRSA 0807-7	R	R	S	S	S	S	S	R	I	R	S	S	R	R
MRSA 0804-25	R	R	S	S	S	S	S	R	S	S	S	S	R	S

E = erythromycin; GN = gentamycin; LZD-linozolid acid; MUP = muciprocin; RD- rifampicin; DA = clindamycin; TEC = teicoplanin; CIP = ciproflozaxin; NET = netilmycin; TE = tetracycline; VA = vancomycin; FD = fusicidic acid; OX = oxacilin; SXT = Trimethoprim-sulfamethaxazole; R = resistant; S = sensitive; I = intermediate resistant.

4.7 ANTICANCER STUDIES

Schiff base compounds derived from morpholine are completely stable in biological systems, allowing rigorous long-term applications as they constitute a radical re-design of DNA (Summerton., 2007); these important factors are considered in designing this morpholine derived ligands and their metal complexes for their potential antibacterial and anticancer applications. First row transition metals play major roles in various biological activities because of the exceptionally wide range of reactivity available and have been particularly attractive (Petrovic., 1996). In this part, metal complexes of some newly synthesized *N,N'N"* and *N'N"O* donor Schiff base ligands from the reaction of 4-(2-aminoethyl)morpholine with either 2-acetylpyridine or 2-hydroxyacetophenone in presence of Cl^-, N_3^-, and SCN^- ions (scheme 1), were examined for potential anti-cancer applications.

4.7.1: RESULTS AND DISCUSSION

MTT assay: MTT assay was used to determine the metal complexes cytotoxicity against human breast cancer cells MCF-7. This assay served as an index used to determine cytotoxicity of the metal complex to stimulate or inhibit cell viability and growth by detecting the reduction of tetrazolium salt to blue formazan by mitochondrial enzyme activity of succinate dehydrogenase in living cells. MCF-7 cells were treated with varying concentrations of the complexes for 48 h, and the cells viabilities were measured by MTT assay. The metal complexes were found to inhibit the growth of MCF-7 cells in a dose-dependent manner (Table 4.5). The free ligand MTT assay showed no significant inhibition activities at a concentration even higher than the complex which confirmed that chelation of ligand with metal ions was significance for the activity of this novel compounds.

Table 4.5: EC50 values in µg/ml of the tested compounds on WRL68 and MCF-7 cell lines

		EC50 µg/ml				EC50 ug/ml	
	Cpd.	**WRL68**	**MCF-7**		**Cpd.**	**WRL68**	**MCF-7**
1	L1	n.d.	n.d.	**10**	L2	n.d.	n.d.
2	Cu(L1)Cl	41.15	37.58	**11**	$Cu(L2)Cl_2$	47.80	64.24
3	Cu(L1)Br	23.28	4.25	**12**	$Cu(L2)Br_2$	31.09	57.18
4	Zn(L1)Br	52.26	33.09	**13**	$Cu(L2)(N_3)_2$	3.84	2.51
5	Zn(L1)Cl	32.69	10.94	**14**	$Mn(L2)Cl_2$	34.29	>100
6	Ni(L1)Cl	13.05	8.15	**15**	$Mn(L2)(SCN)_2$	30.25	26.45
7	Ni(L1)Br	64.53	27.64	**16**	$Ni(L2)(SCN)_2$	2.68	1.82
8	Mn(L1)Cl	44.25	24.54	**17**	$Zn(L2)I_2$	39.25	34.55
9	Mn(L1)Br	4.65	5.93	**18**	Cisplatin	-	2.50

Clonogenic assay: Clonogenic assay is used f or studying the effectiveness of specific agents on the survival and proliferation of cells. In this study we determine the effectiveness for the cytotoxicity of Cobalt(III) compound to inhibit growth of MCF-7 cells. Cells were trypsinised and counted to a ratio of 5×10^3 cells per plate. The number of cells that formed colony was reduced after exposure to the Cobalt compound at concentrations of 2.80, 3.72 and 4.53 µg/ml as compared to the untreated MCF-7 (control) (Figure 4.7.1). No colony was observed at the concentration of higher than 8.56 µg/ml, indicating the Cobalt(III) compound showed toxicity and inhibited the proliferation of MCF-7 cell. Toxicity of compound was further supported by clonogenic efficiency (CE) which is the number of colonies divided by the number of cells added to each plate (Table 4.6). This result is consistent with the result of the MTT assay (IC_{50}).

Table 4.6: MTT assay for cobalt(III) complex

Compound	Concentrations (µg/ml-IC_{50})	Number of Cells/Plat	Number of Apoptotic colonies	Total colony number before treatment	CE*
Co(III)	2.80±0.02	5×10^3	250	500	0.050
Co(III)	3.72±0.05	5×10^3	290	500	0.042
Co(III)	4.53±0.03	5×10^3	340	500	0.032
Co(III)	8.56±0.02	5×10^3	500	500	0
Co(III)	12.45±0.03	5×10^3	500	500	0
Control	-	5×10^3	10	500	0.098

Where **CE***= Colonogenic efficiency

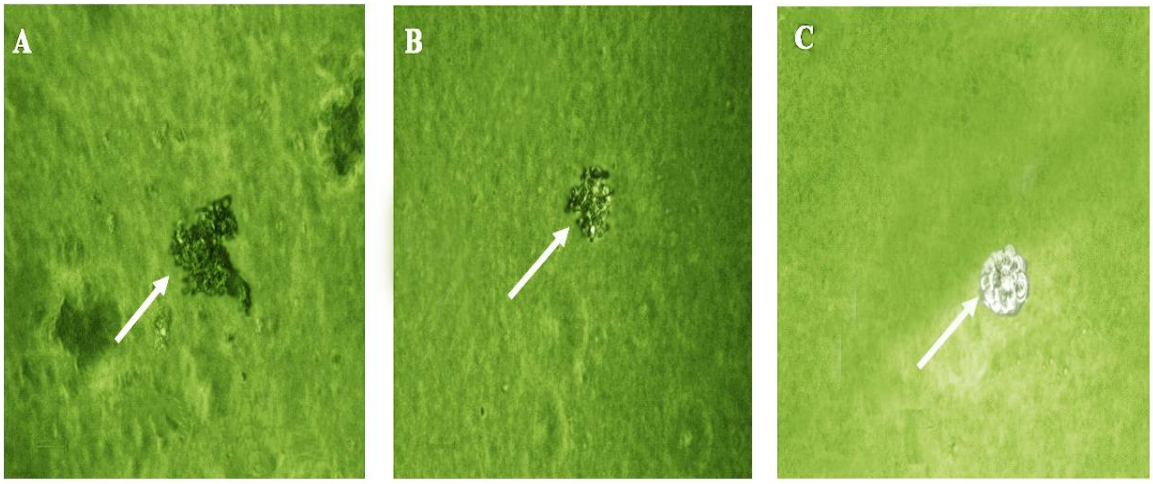

Figure 4.7.1: Clonogenic assay by treatment of the Cobalt(III) on MCF-7 cell lines at 14 days after seeding. Panels A and B represent *in vitro* growth inhibition of MCF-7 by Cobalt(III) at concentrations of 2.80±0.02 and 3.72±0.05 µg/ml. White arrows indicate reduced apoptotic colonies. Panel C shows untreated MCF-7 as control. The colonies which is defined to consist of at least 50 cells were counted and photographed. Magnification 20×.

Multiparameter cytotoxicity analysis: The multiparameter cytotoxicity analysis identifies the changes in nuclear morphology, size, and membrane permeability status, cytochrome C level and mitochondrial damage caused by compound toxicity. In this study, treated MCF-7 cells with Cobalt(III) compound induced reduction of nuclear morphology size, cell density and increased cell membrane permeability, which highlights better activity than Tamoxifen (standard drug). However, cytochrome C release by Tamoxifen was rather higher than by the Cobalt compound (Figure 4.7.2). The decline in mitochondrial membrane together with simultaneous nuclear fragmentation, increased cell permeability and cytochrome C release confirmed the mode of cell death as apoptosis (S. Syam, 2012).

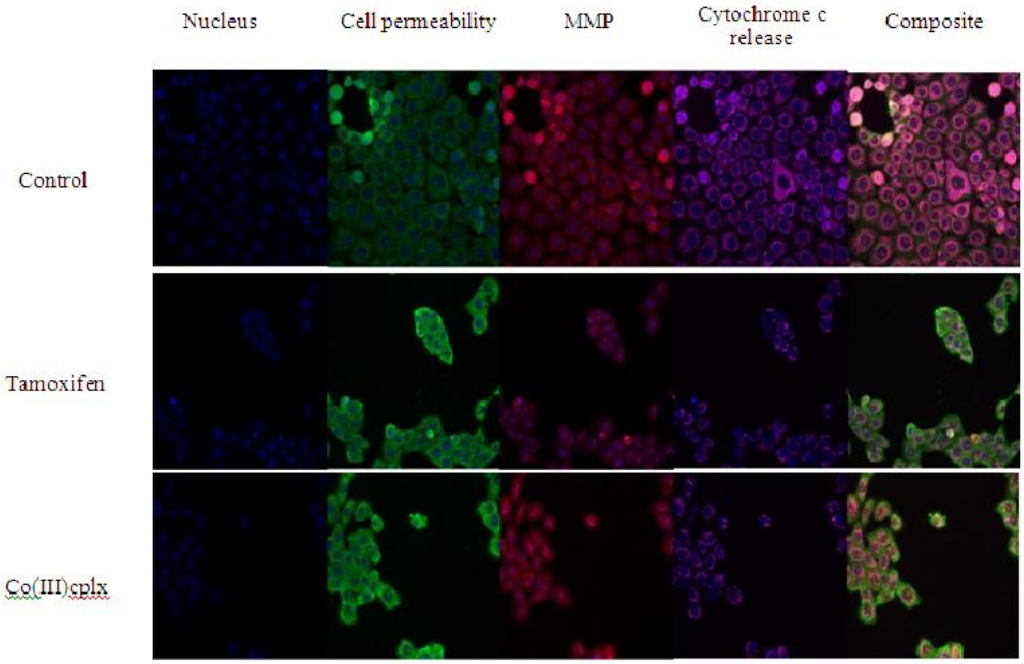

Figure 4.7.2: Multiparameter cytotoxicity analysis

The nuclear morphological changes of treated MCF-7 cells using Hoechst 33342 staining were examined to show nuclear condensation and fragmentation for 48 hrs, which is the hallmark for apoptosis. Our results were in agreement with previous studies which showed that the treated cells that underwent apoptosis exhibited characteristic morphological

changes, such as cell shrinkage, membrane blebbing, chromatin condensation, and nuclear fragmentation (Kerr., 1991). Mitochondrial membrane potential, which is important for ATP formation and cell survival, showed a significant reduction of fluorescence intensity (Figure 4.7.3) on treated MCF-7 cells with Cobalt(III) compound for 48 hrs. In particular, Cobalt(III) compound disrupted mitochondrial membrane potentials in MCF-7 cells, indicating increased mitochondrial membrane permeability (Figures 4.7.3). The cell permeability was also increased subsequently upon treatment with the compound. An apoptotic stimulus which triggers the release of cytochrome C from the mitochondria into the cytosol by binding to Apaf-1, plays an important role in apoptosis (Liu. 2011). Cobalt(III) compound significantly triggered the MCF-7 cells to translocate the cytochrome C from the mitochondria into the cytosol during apoptosis. In this study, cytochrome C was released even at the concentration of 2 µg/ml. These effects occurred more rapidly, and followed a dose-response pattern.

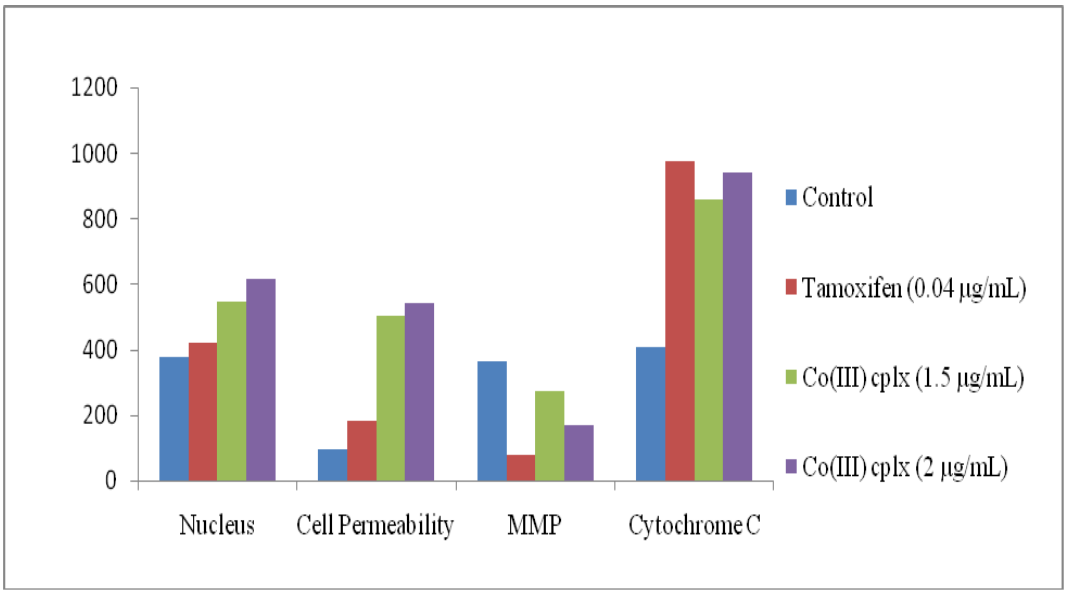

Figure 4.7.3: Graph of Multiparameter cytotoxicity analysis

DNA Fragmentation Assays: Apoptotic DNA fragmentation is a key feature of apoptosis, a type of programmed cell death (Syam, 2011). Apoptosis is characterized by the activation of endogenous endonucleases with subsequent cleavage of chromatin DNA into internucleosomal fragments. Degradation of nuclear DNA into nucleosomal units is one of the hallmarks of apoptotic cell death (Figure 4.7.4). It occurs in response to various apoptotic stimuli in a wide variety of cell types. The enzyme responsible for apoptotic DNA fragmentation is the Caspase-Activated DNase (CAD) that is normally inhibited by the Inhibitor of Caspase Activated DNase (ICAD). However, during apoptosis, the apoptotic effector caspase, caspase-3, cleaves ICAD and thus causes CAD to become activated. At 2 µg/ml concentration the Cobalt(II) compound was capable in producing DNA ladder, the ladder formation increased with increase in concentration of the compound used.

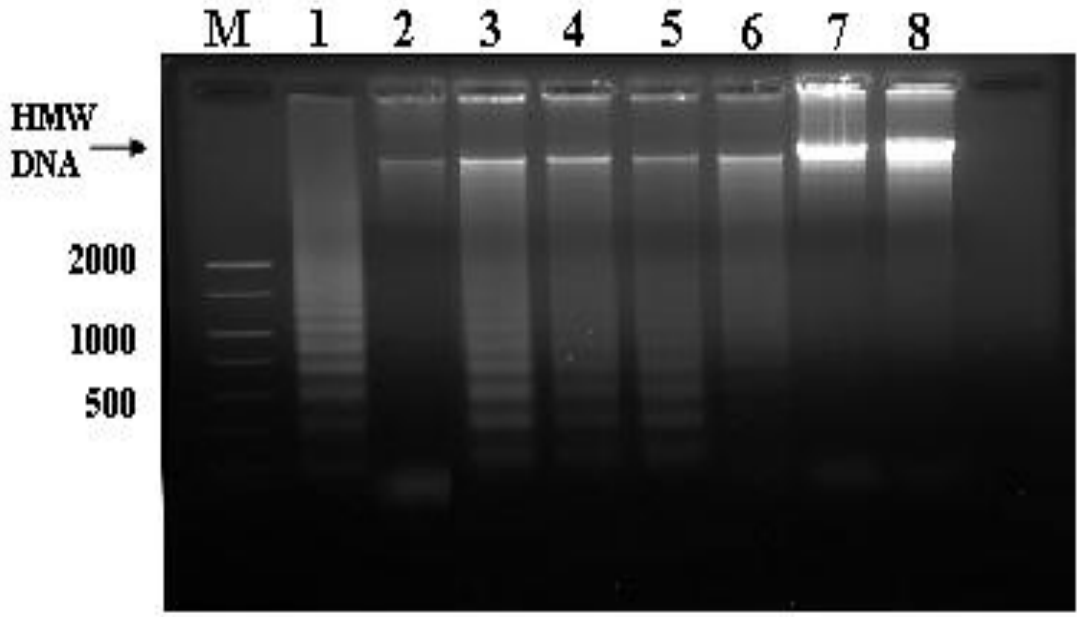

Figure 4.7.4: Apoptotic DNA fragmentation showing degradation of nuclear DNA into nucleosomal units

Roles of caspase-3 in compound-induced apoptosis in MCF-7 cells: To further confirm the Cobalt compound induced apoptosis in MCF-7 cells, we performed calorimetric measurement of the caspase activity and mechanisms involved after treatment with 1.5, 3 and 4.5 µg/ml Cobalt compound for 48 h. The activity of caspase-3 increased remarkably in MCF-7 cells after administration of cobalt compound via the intrinsic mitochondrial apoptotic pathway in caspase-3 activity, which confirmed the apoptosis of MCF-7 cells induced by Cobalt compound (Figure 4.7.5). The importance of caspase-3 is well discussed elsewhere (Porter, 1999) as it has a role in DNA fragmentation and other morphological changes in relation to apoptosis.

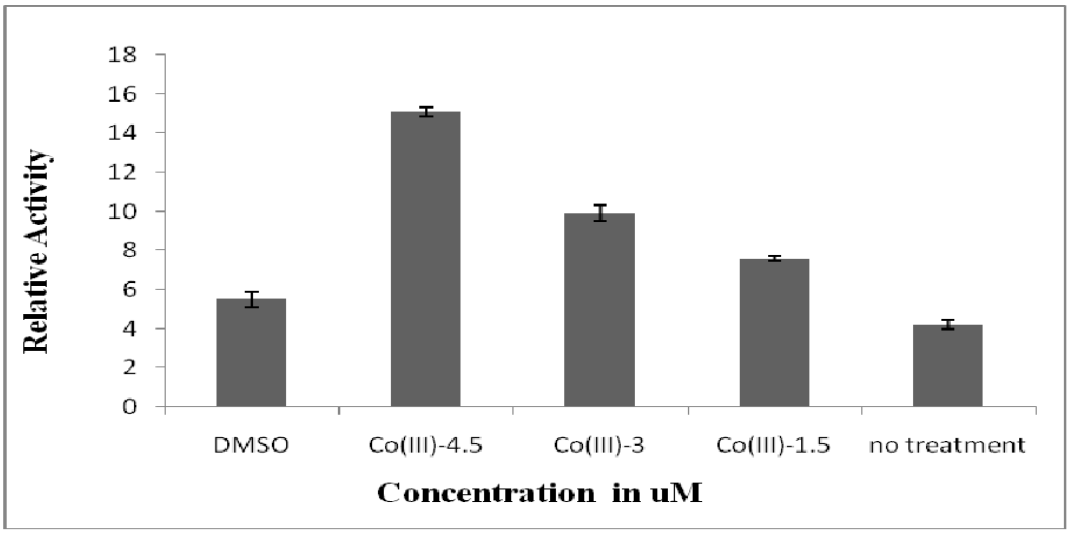

Figure 4.7.5: Histology of the Result of caspase-3 relative activity vs concentration in uM

Molecular Docking: Caspase-3 (pdb id: 1PAU) is a member of the cysteine-aspartic acid protease (caspase) family (Alnemri., 1996). Sequential activation of caspase-3 plays a central role in the execution-phase of cell apoptosis. The catalytic site of caspase-3 involves the sulfohydryl group of Cys-285 and the imidazole ring of His-237. His-237 stabilizes the carbonyl group of the key aspartate residue, while Cys-285 attacks to ultimately cleave the

peptide bond. Cys-285 and Gly-238 also function to stabilize the tetrahedral transition state of the substrate-enzyme complex through hydrogen bonding (Lavrik., 2005).

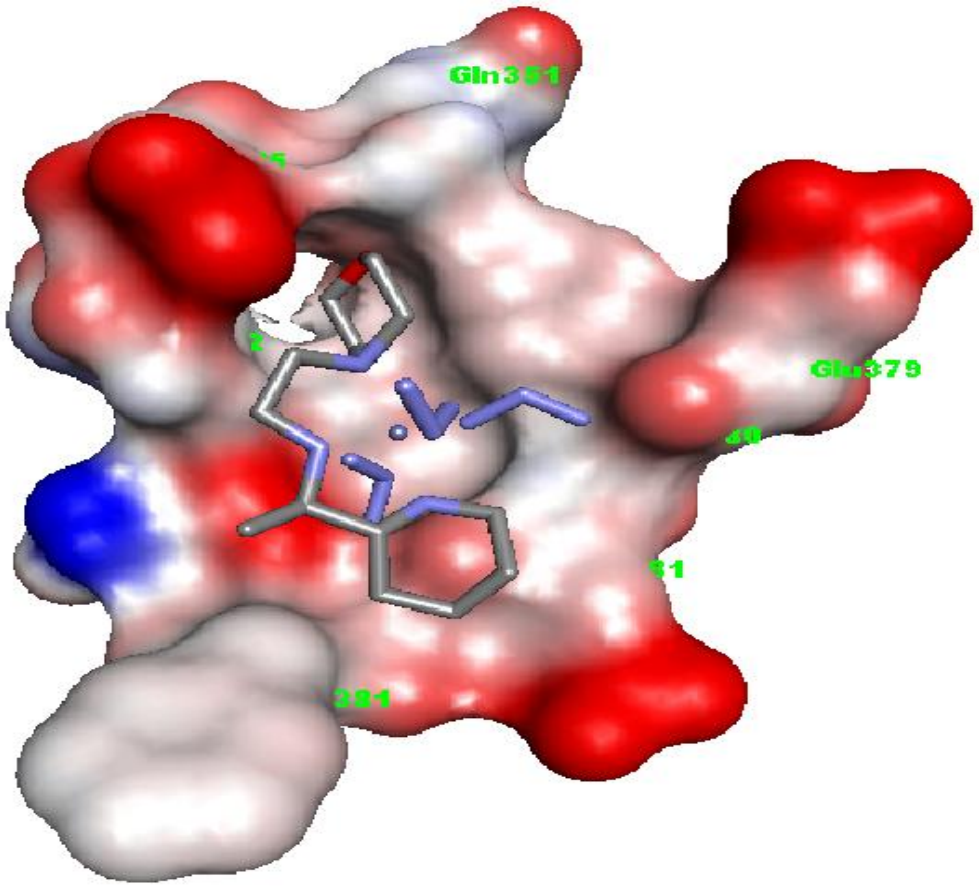

Figure 4.7.6 (a) Surface Connolly representation of the molecular model of the complex formed between cobalt(III) and Caspase-3 (1PAU) (at the binding site).

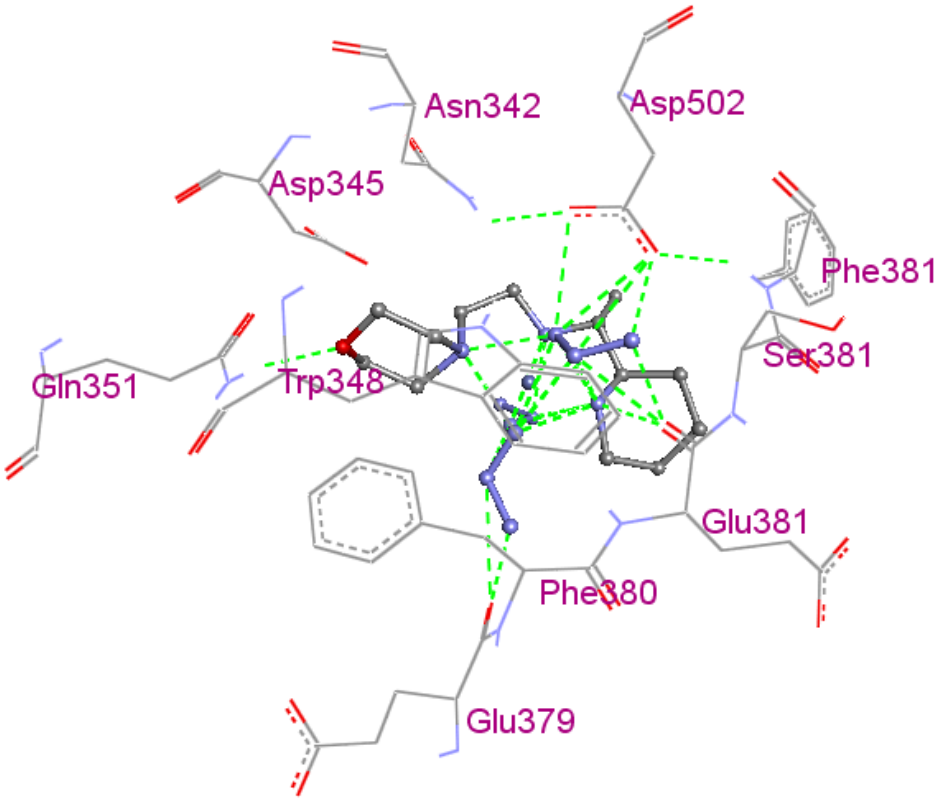

Figure 4.7.6 (b). 3D representation of the ligand-enzyme binding interactions. Cobalt(III) compound is represented as balls and sticks, the surrounding residues as sticks and hydrogen bonds as green dashed lines.

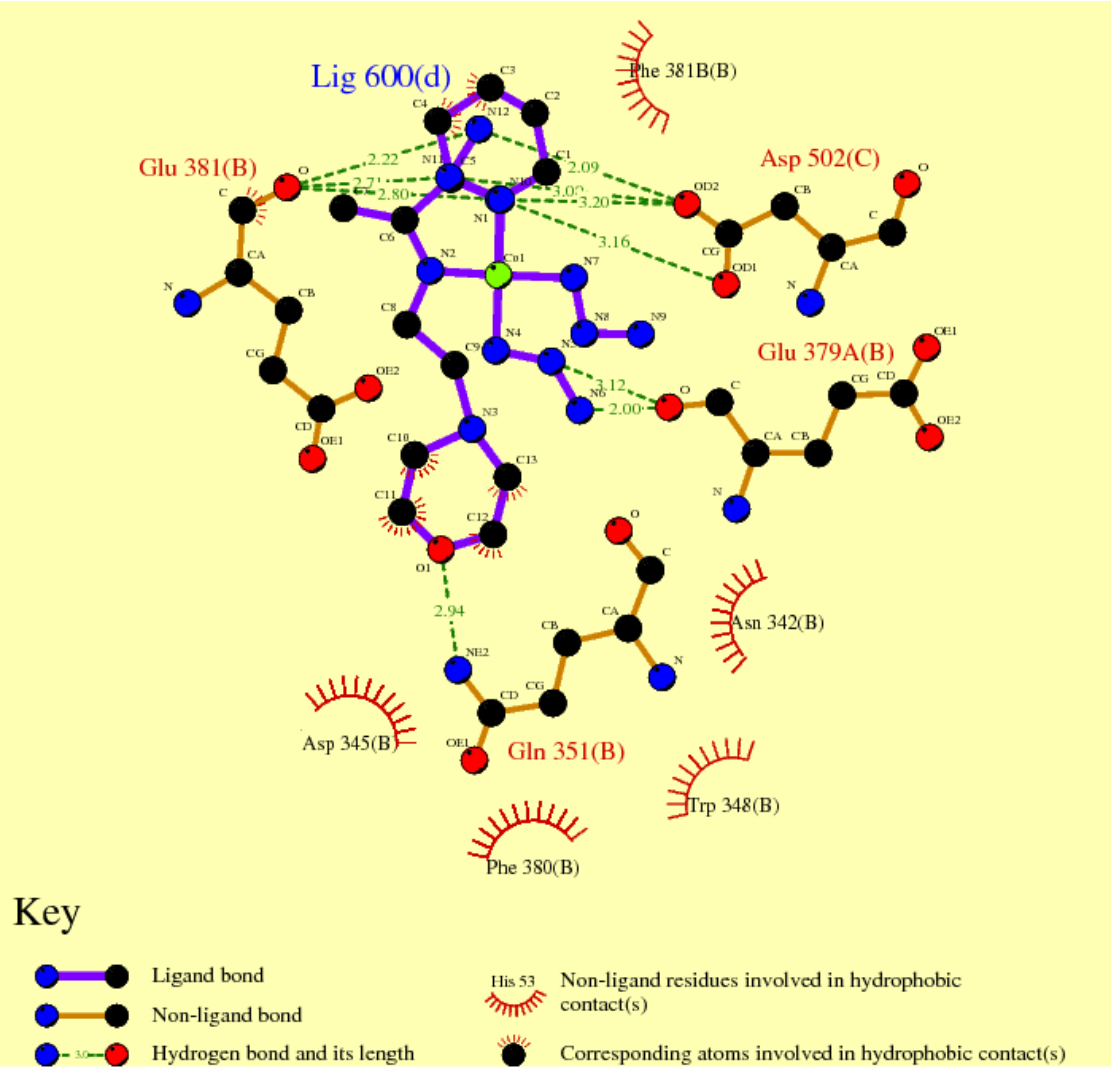

Figure 4.7.6 (c). 2D schematic representation of the hydrogen bonding and hydrophobic interactions between the Cobalt(III) compound and the residues at the binding site of Caspase-3.

The residues involved in the interactions of Cobalt(III) compound are Asn 342, Asp 345, Asp 502, Gln 351, Glu 379, Glu 380, Glu 381, Phe 380, Phe 381, Ser 381, and Trp 348 [Figure 4.7.6 (a)]. The complex formed between cobalt(III) compound and caspase-3 showed that the ligand does not bind to the active-site gorge. And the caspase-3 zymogen (pdb id: 1PAU) has virtually no activity until it is cleaved by an initiator caspase after apoptotic signaling events have occurred (Walters., 2009), therefore, the introduction of cobalt(III) compound can activate caspase-3 initiator into cells targeted for apoptosis (Katunuma, 2001). This extrinsic activation then triggers the hallmark caspase cascade characteristic of the apoptotic pathway, in which caspase-3 plays a dominant role (Perry., 1997). The decline in mitochondrial membrane potential leads to release of cytochrome C (both confirmed by high content screening) and this could eventually lead to caspase-3 activation and hence apoptosis. Thus it is not the cobalt(III) compound that directly binds to capsase-3 which resulted the increase in caspase-3 after the treatment, rather, the mitochondria mediated apoptotic signaling cascade which leads to the increase in level (Syam, 2012, Narula, 1999). In intrinsic activation, cytochrome C from the mitochondria works in combination with ATP to process procaspase-3 (Katunuma., 2001; Porter., 1999, Li, 2004). A closer inspection of the interactions [Figure 4.7.6 (b)] showed the presence of hydrogen bond between the oxygen attached to the morpholine group with Gln 351 (B), π-π and cation-π stacking involving between nitrogen atoms from the azide groups and Glu 379(A), Glu 381(B), Phe 380, Ser 381 and Asp 502(C). Furthermore, hydrophobic interactions [Figure 4.7.6(c)] between ligand and caspase-3 residues [Phe 380, Asp 345 (B), Phe380 (B), Trp 348 (B) and Asn 342(B)] was observed which enables the morpholine oxygen to form a hydrogen bond with Gln 351(B) and azide groups to form a cluster of networking hydrogen bonds with Gln351(B).

4.8 ANTI-ALZHEIMER AND ANTI-OXIDANT ACTIVITIES

Over view: The chemistry of hydrazones is an intensive area of study and numerous Schiff base ligands and their complexes of this type have been synthesized and their biological applications reported (da Silva, 2011, Creaven, 2010, Ceyhan, 2011, Qiao, 2011 and Xu, 2008). The major antioxidants currently used in foods are monohydroxy or polyhydroxy phenol compounds with various ring substitutions. These compounds have low activation energy for hydrogen donation (Rice-Evans., 1999). Alzheimer's disease (AD) is the most common form of dementia among older people and the pathogenesis of this disease is associated with oxidative stress. Acetylcholinesterase inhibitors with antioxidant activities are considered potential treatments for AD. Some novel ketone derivatives of gallic hydrazide-derived Schiff bases were synthesized and examined for their antioxidant activities and *in vitro* and *in silico* acetyl cholinesterase inhibition. The compounds were characterized using spectroscopy and X-ray crystallography. Mainly from *in vitro* studies, polyphenols have been reported to have antioxidant (Clemetso., 1966, Sun-Waterhouse, 2009), anti-cancer (Kuhn, 2005 and Samoylenko., 2011) and cardioprotecive activities (Claudine, 2005)

Researchers have recently investigated the potential health benefits of polyphenols in organic product (Bourn, 2002). Increased consumption of polyphenols has been associated with a reduced risk of cardiovascular disease and possibly cancer and stroke. Laboratory findings have shown that oxidative stress may play an important role to the pathogenesis of AD. Therefore, the risk of AD disease might be decreased by intake of antioxidants that neutralize the unfavorable effects of oxidative stress (Arts, 2005). The present work reports the synthesis, characterization, antioxidants activities and X-ray crystal structures of Schiff bases derived from the condensation reaction of gallic hydrazide with pyridine and

acetophenone derivatives, together with their acetylcholinesterase inhibition and antioxidant activity (Scheme 1).

Scheme 1. Reaction pathways.

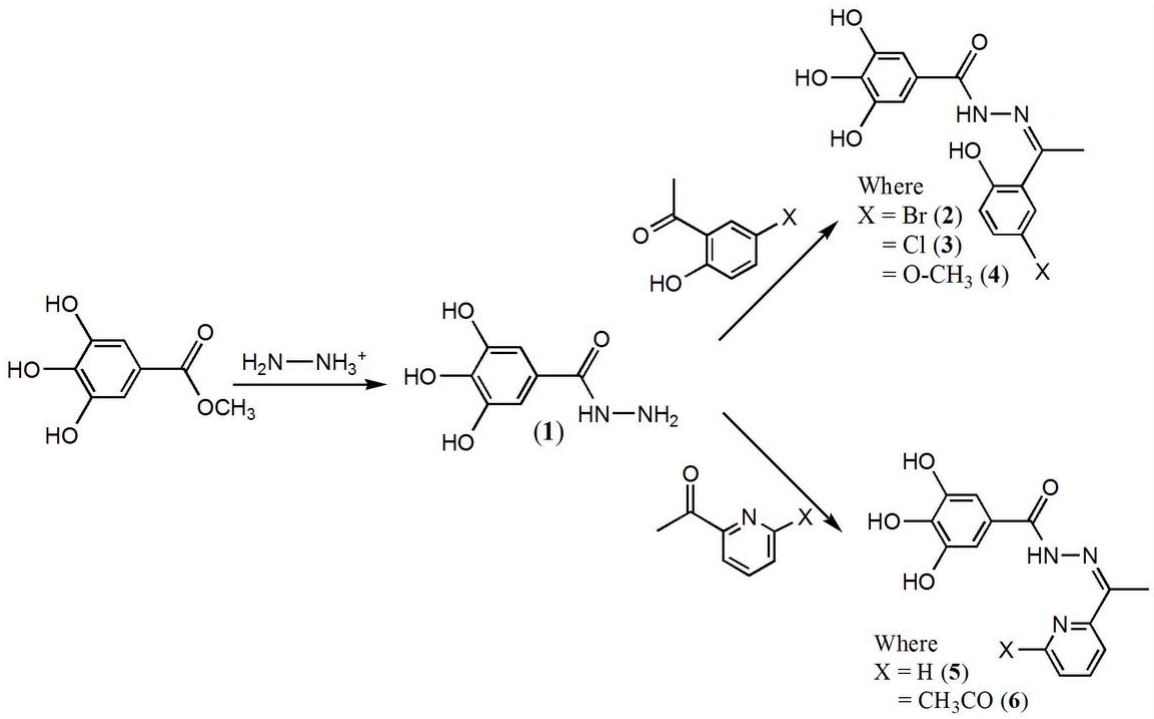

4.8.0: Synthesis of Gallic Hydrazide (1)

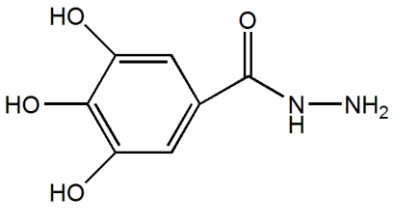

Molecular Weight: 184.15

(Yield 70%), melting point = 290 °C, elemental analysis theory: C (45.6%); H (4.3%); N (15.2%); found: C (45.2%); H (5.04%); N (15.04%), %, FT-IR spectra (KBr); 3,429 cm^{-1} (νAr-OH), 3,299 cm^{-1} (νN-H), 1,654 cm^{-1} (νC=O), 1,344cm^{-1} (νC-O), 1,103 cm^{-1} (νN-N), ^{1}H-NMR (DMSO-d_6): 9.35 ppm [δ(Ar-OH), 1H s], 9.13 ppm, 9.05 ppm [δ(Ar-OH), 2H, d], 8.65 ppm [δ(NH), 1H, brd], 6.79 ppm, 6.82 ppm [δ(Ar-H), 2H s], 4.37 ppm [δ(NH_2), 2H s].

^{13}C-NMR (DMSO-d_6): 166.39 ppm [δ(CONH), 1C], 145.37 ppm [δ(aromatic), 1C-OH], 136.10, 136.42 ppm [δ(aromatic), 2C-OH], 124.00 ppm [δ(aromatic), 1C], 106.43 ppm [δ(aromatic), 2C = C] ppm.

4.8.1 N-(1-(5-Bromo-2-hydroxyphenyl)-ethylidene)-3,4,5-trihydroxybenzohydrazide (2)

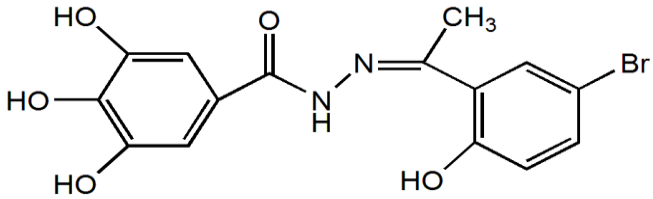

Molecular Weight: 381.18

(Yield 75%), elemental analysis: theory C (47.50); H (3.89); N (7.32); found C (47.26); H (3.44); N (7.35); IR spectra (KBr); 3,558 cm^{-1} (νAr-OH), 3,235 cm^{-1} (νN-H), 1,604 cm^{-1} (νC=N), 1,658 cm^{-1} (νC=O), 1,242 cm^{-1} (νC-O), 953 cm^{-1} (νN-N), ^{1}H-NMR (DMSO-d_6): 13.57 ppm [δ(OH), 1H, s], 11.10 ppm [δ(OH), 1H, s], 9.05 ppm [δ(OH), 2H, brd], 6.79–7.73 ppm [δ(aromatic), 5H, m], 4.34 ppm [δ(NH), 1H, s], 1.24 ppm [δ(-CH3), 3H, s]. ^{13}C-NMR (DMSO-d_6): 166.39 ppm [δ(C=N)], 164.43 ppm [δ(C=O)], 145.53 ppm, 145.36 ppm [δ(aromatic), 2C-OH], 137.41 ppm [δ(aromatic), 1C-OH], 137.40, 136.10 ppm, [δ(aromatic), 2C], 130.31 ppm [δ(aromatic), 1C], 123.51 ppm, 122.35 ppm, 121.52 ppm, 119.50 ppm [δ(aromatic), 4C], 107.54 ppm, 106.42 ppm [δ(aromatic), 2C=C], 13.92 ppm [δ(CH_3)] ppm.

4.8.2 N-(1-(5-Chloro-2-hydroxyphenyl)-ethylidene)-3,4,5-trihydroxybenzohydrazide (3)

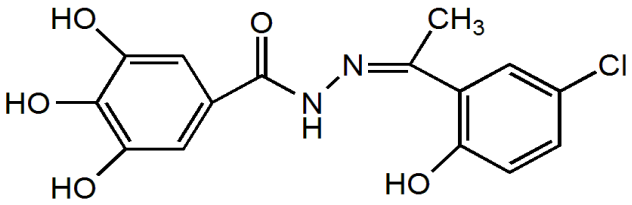

Molecular Weight: 336.73

(Yield 75%) respectively, elemental analysis: theory C (53.50); H (3.89); N (8.32); found C

(53.39); H (3.76); N (8.33); IR spectra (KBr); 3,568 cm^{-1} (νAr-OH), 3,225 cm^{-1} (νN-H), 1,638 cm^{-1} (νC=O), 1,604 cm^{-1} (νC=N), 1,212 cm^{-1} (νC-O), 953 cm^{-1} (νN-N). ^{1}H-NMR (DMSO-d_6): 11.14 ppm [δ(OH), 1H, s], 11.13 ppm [δ(OH), 1H, s], 9.30 ppm [δ(OH), 2H, brd], 7.66 ppm [δ(NH), 1H, s], 7.37–6.93 ppm [δ(aromatic), 3H, m], 6.983 ppm, 6.976 ppm [δ(aromatic), 2H str d], 2.12 ppm [δ(-CH3), 3H, s]. ^{13}C-NMR (DMSO-d_6): 166.94 ppm [δ(C=N)], 164.84 ppm [δ(C=O)], 157.94 ppm [δ(aromatic) 1C], 146.10 ppm, 145.93 ppm [δ(aromatic), 2C-OH], 137.97 ppm [δ (aromatic), 1C-OH], 128.10 ppm, 124.08 ppm, 122.92 ppm, 122.53 ppm, 121.48 ppm, 119.58 ppm [δ(aromatic), 6C], 108.10 ppm, 106.98 ppm [δ(aromatic), 2C=C], 14.48 ppm [δ(CH_3)] ppm.

4.8.3 N-(1-(2-Hydroxy-5-methoxyphenyl)-ethylidene)-3,4,5-trihydroxybenzohydrazide (4)

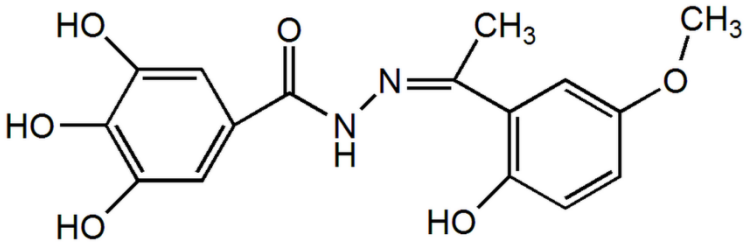

Molecular Weight: 332.31

(Yield = 65%), elemental analysis: theory C (57.83); H (4.85); N (8.43); found C (58.30); H (4.51); N (8.71); IR spectra (KBr); 3,467 cm^{-1} (νAr-OH), 3,308 cm^{-1} (νN-H), 1,650 cm^{-1} (νC=O), 1,623 cm^{-1} (νC=N), 1,282 cm^{-1} (νC-O), 944 cm^{-1} (νN-N), ^{1}H-NMR (DMSO-d_6): 12.89 ppm [δ(OH)], 10.98 ppm [δ(OH), 1H, s], 9.28 ppm [δ(OH), 2H, brd], 8.90 ppm [δ(NH)], 7.11 ppm [δ(aromatic), 2H str s], 7.11–6.83 ppm [δ(aromatic), 3H, m], 3.75 ppm [δ(O-CH_3), 3H, s], 1.24 ppm [δ(-CH3), 3H, s]. ^{13}C-NMR (DMSO-d_6): 152.58 ppm [δ(C=N)], 151.36 ppm [δ(C=O)], 145.52 ppm [δ(aromatic), 2C-OH], 137.27 ppm [δ(aromatic), 1C-OH], 122.70 ppm, 122.61 ppm, 117.77 ppm, 117.39 ppm, 119.49 ppm [δ(aromatic), 5C], 107.44 ppm [δ(aromatic), 2C=C], 55.54 ppm [δ(O-CH3)], 13.94 ppm [δ(CH_3)] ppm.

4.8.4: 3,4,5-Trihydroxybenzoic Acid [1-Pyridylethylidene] Hydrazide (5)

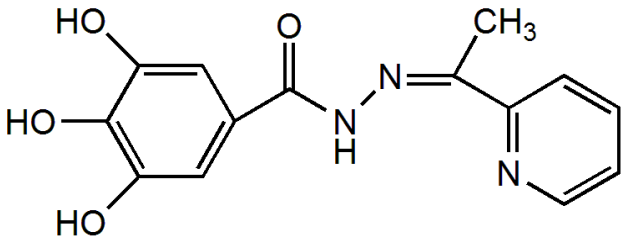

Molecular Weight: 287.27

(Yield = 65%), melting point = 253 °C, elemental analysis: theory: C (58.53%); H (4.56%); N (14.63%); found: C (57.99%); H (4.56%); N (14.06%), IR spectra (KBr); 3,399 cm^{-1} (νAr-OH), 3,351 cm^{-1} (νN-H), 1,621 cm^{-1} (νC=N), 1,618 cm^{-1} (νC=O), 1,560 cm^{-1} (νC=N)Py, 1,281 cm^{-1} (νC-O), 1,032 cm^{-1} (νN-N), ^{1}H-NMR (DMSO-d_6): 9.38 ppm [δ(OH), 1H, s], 9.21 ppm, 9.11 ppm [δ(OH), 2H, brd], 8.14–8.07 ppm [δ(aromatic), 2H m], 7.87–7.70 ppm [δ(aromatic), 2H m], 7.63 ppm [δ(NH), 1H, s, brd], 6.92 ppm [δ(aromatic), 2H str s], 1.24 ppm [δ(-CH3), 3H, s]. ^{13}C-NMR (DMSO-d_6): 162.47 ppm [δ(C=N)], 155.25 ppm [δ(C=O)], 148.54 ppm [δ(aromatic), pyridine], 145.85 ppm [δ (aromatic), 2C-OH], 138.70 ppm [δ(aromatic), 1C-OH], 136.52 ppm [δ(aromatic), pyridine], 124.57 ppm [δ(aromatic), 1C], 123.95 ppm, 122.90 ppm [δ(aromatic), pyridine], 107.55 ppm, 106.35 ppm [δ (aromatic), 2C=C], 22.10 ppm [δ(CH_3)] ppm.

4.8.5: N'-(1-(6-Acetylpyridin-2-yl)ethylidene)-3,4,5-trihydroxybenzohydrazide (6)

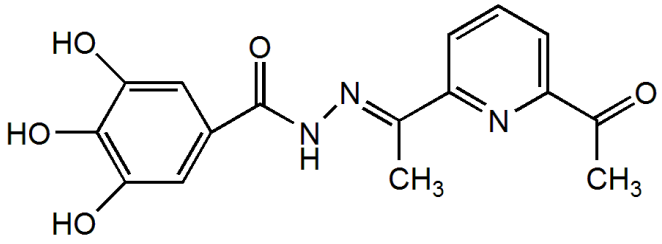

Molecular Weight: 329.31

(Yield 90%), elemental analysis: theory C (58.36); H (4.59); N (12.76); found: C (57.99); H (4.89); N (13.11); IR spectra (KBr); 3,448 cm^{-1} (νAr-OH), 3,239 cm^{-1} (νN-H), 1,674 cm^{-1}

(νC=O), 1,610 cm^{-1} (νC=N), 1,511 cm^{-1} (νC-N)py, 1,265 cm^{-1} (νC-O), 955cm^{-1} (νN-N). ^{1}H-NMR (DMSO-d_6): 9.29 ppm [δ(OH), 1H, s], 8.26 ppm, 8.28 ppm [δ(OH), 2H, brd], 8.14–8.03 ppm [δ(aromatic), 2H m], 8.01–7.90 ppm [δ(aromatic), 2H m] 6.89 ppm [δ(aromatic), 2H str s], 4.3 ppm [δ(NH), 1H, s], 1.19 ppm [δ(-CH3), 3H, s]. ^{13}C-NMR (DMSO-d_6): 166.38 ppm [δ(C=N)], 164.34 ppm [δ(C=O)], 151.97 ppm [δ(aromatic), pyridine], 145.37 ppm [δ(aromatic), 2C-OH], 137.87 ppm [δ(aromatic) 1C-OH], 136.13 ppm [δ(aromatic), pyridine], 123.87 ppm [δ(aromatic), 1C], 123.51 ppm [δ(aromatic), 2C=C], 121.13 ppm, 120.26 ppm [δ(aromatic), pyridine], 199.24 ppm, 106.45 ppm [δ(C=OCH3)], 25.50 ppm [δ(CH_3-C=O)], 18.52 ppm [δ(CH_3)] ppm.

Anti-AChE Assay: The anti-cholinesterase activities of the compounds were evaluated by Ellmann's method with slight modifications, using acetylthiocholine as a substrate (Guilhermino, 1996) and 5,5'-dithiobis[2-nitrobenzoic acid](DTNB). Sodium phosphate buffer (pH 8.0, 110 μL) was added into the 96 wells followed by sample solution (20 μL), DTNB (0.126 mM, 50 μL) and AChE enzyme (0.6 U/mL, 20 μL). The mixture was incubated for 50 minutes at 37 °C. The reaction was then initiated by the addition of acetylthiocholine iodide (0.120 mM, 50 μL). The hydrolysis of acetylthiocholine was monitored by the formation of yellow 5-thio-2-nitrobenzoate anion as the result of the reaction of DTNB with thiocholine, released by the enzymatic hydrolysis of acetylthiocholine, at a wavelength of 412 nm every 30 s for 25 minutes using a 96-well microplate plate reader (TECAN Infinite M200, Mannedorf, Switzerland). Test compounds were dissolved in analytical grade DMSO. Tacrine and propidium iodide were used as reference standards (Laskwoski., 2001). The reactions were performed in triplicate and monitored with a spectrophotometer. The percent inhibition of the enzyme activity due to the presence of increasing test compound concentration was obtained from the expression;

100 − (*vi/vo* × *100*), where *vi* is the initial rate calculated in the presence of inhibitors and *vo* is the enzyme activity.

4.9 RESULTS AND DISCUSSION

Chemistry: The reaction of gallic hydrazide (**1**) with selected hydroxyacetophenones and pyridine derivatives resulted in the formation of the corresponding polyphenolic compounds: *N*-(1-(5-Bromo-2-hydroxyphenyl)-ethylidene)-3,4,5-trihydroxybenzohydrazide (**2**); *N*-(1-(5-Chloro-2-hydroxyphenyl)-ethylidene)-3,4,5-trihydroxybenzohydrazide (**3**); *N*-(1-(2-Hydroxy-5-methoxyphenyl)-ethylidene)-3,4,5-trihydroxybenzohydrazide (**4**); 3,4,5-Trihydroxybenzoic acid [1-pyridylethylidene] hydrazide (**5**); 3,4,5-Trihydroxybenzoic acid [1-(4-acetyl-pyridin-2-yl)-ethylidene] hydrazide (**6**) (Scheme 1). Their NMR, IR and UV-visible spectra were all consistent with the proposed structures.

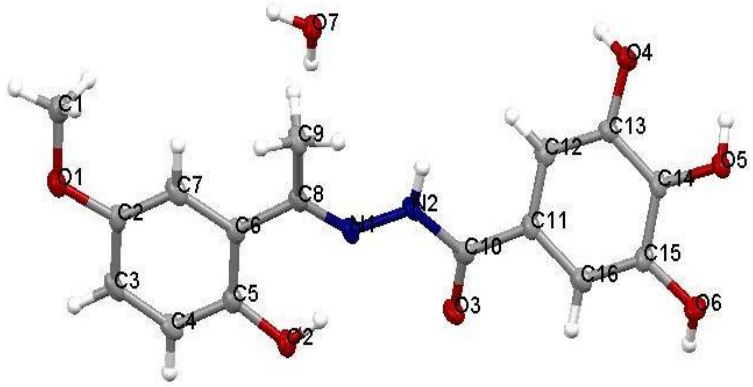

Figure 4.9.1. ORTEP-type view of the crystal structure of compound 4 showing the labeling scheme. Thermal ellipsoids are drawn at the 50% probability level.

Anti-AChE Assay: The inhibitory activities of compounds **1–6** on human acetyl cholinesterase were in the range of 16–77% at 100 μM (see Table 4.7) and thus comparable to those of the standard drugs tacrine and propidium.

Table 4.7: Human AChE inhibitory effects and anti-oxidant activities for compounds **1–6.**

Cpd	**Molecular weight**	**AChE Inhibition (%)**	**DPPH (IC_{50}, µg/mL)**	**FRAP value (Mean ± SD)**
1	184.15	38.0 ± 1.3	1.210 ± 0.002	81,633.30 ± 0.075
2	381.18	77.0 ± 1.8	1.140 ± 0.001	62,200.00 ± 0.083
3	336.73	68.9 ± 1.8	1.400 ± 0.002	35,740.00 ± 0.011
4	332.31	48.5 ± 2.5	1.220 ± 0.001	30,080.00 ± 0.054
5	287.27	16.4 ± 1.4	1.460 ± 0.001	22,946.70 ± 0.004
6	329.31	71.5 ± 1.7	2.300 ± 0.001	23,340.00 ± 0.021
Propidium	-	54.5 ± 1.6	-	-
Tacrine	-	51.2 ± 1.6	-	-
Asc. acid	-	-	2.260 ± 0.001	19,400.00 ± 0.007
BHT	-	-	-	187.3 ± 2.6

1: Gallic hydrazide; **2**: *N*-(1-(5-Bromo-2-hydroxyphenyl)-ethylidene)-3,4,5-trihydroxybenzohydrazide; **3**: *N*-(1-(5-Chloro-2-hydroxyphenyl)-ethylidene)-3,4,5-trihydroxybenzohydrazide; **4**: *N*-(1-(2-Hydroxy-5-methoxyphenyl)-ethylidene)-3,4,5-trihydroxybenzohydrazide; **5**: 3,4,5-Trihydroxybenzoic acid [1-pyridylethylidene] hydrazide, **6**: 3,4,5-Trihydroxybenzoic acid [1-(4-acetyl-pyridin-2-yl)-ethylidene] hydrazide; BHT: Butylated hydroxytoluene.

Compounds **2**, **3** and **6** showed the highest activities. This indicates that introduction of chlorine or bromine atom at position 5 of the acetophenone moiety significantly enhances the inhibition activity. This might be ascribed to the electron donating properties of the halogens by resonance, making the lone pair electrons more available to a plausible electron transfer. The activity of **6** could be attributed to the presence of the acetyl group on the pyridine ring making the lone pair electron on the pyridine nitrogen atom available for electron transfer, also increasing of bond dissociation enthalpy (BDE) values in phenolic structure contain substituent of electron withdrawing groups such as COR, COOR, CN (Heider, 2006) could discourage the abstraction of hydrogen. O-H bond dissociation enthalpy (BDE) is a theoretical parameter successfully used to measure the H-atom-donating ability of various antioxidants. Similar results have been reported by Kadoma (Kadoma., 2007).

Molecular Docking: The crystal structure of hAChE (in complex with fasciculin-2) (pdb id: 1B41) shows that the enzyme possesses a deep narrow gorge which penetrates halfway into the enzyme, where the catalytic site resides (Kadoma., 2007). The binding site of AChE consists of five subsites: a peripheral anionic site (PAS), an acyl binding pocket (ABP), the esteratic site (ES), an oxyanion hole (OH) and an anionic subsite (AS).

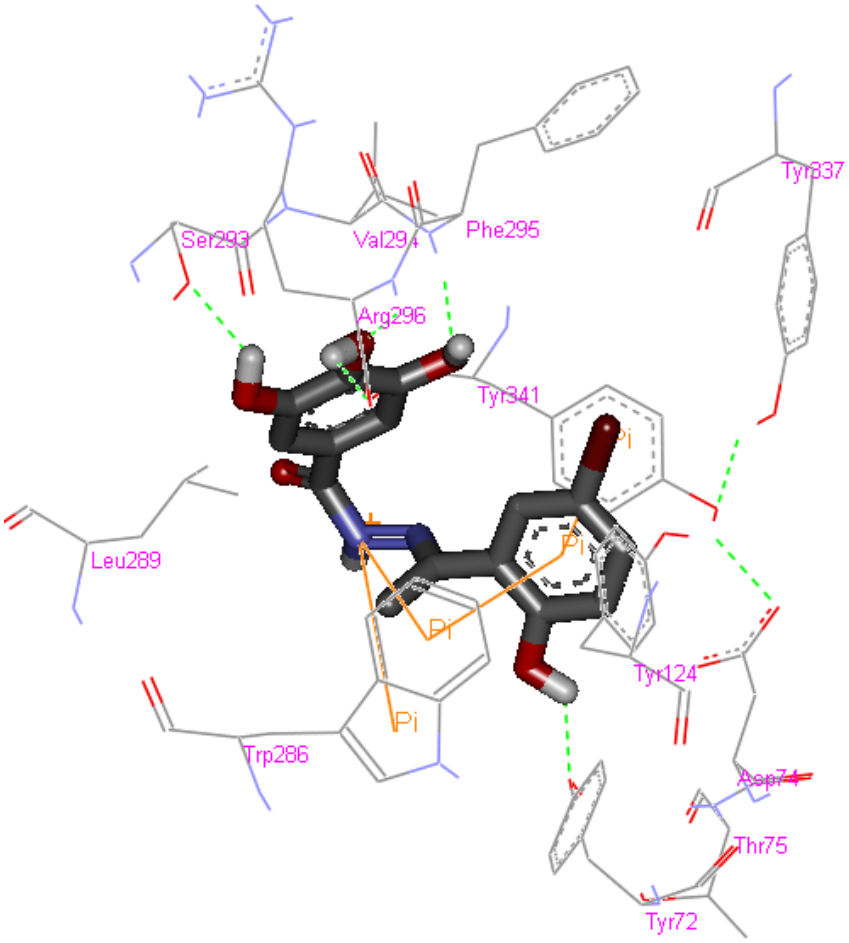

Figure 4.9.2(a): Representations of the molecular model of the complex formed between compound 2 and hAChE. 3D representation of the ligand-enzyme binding interactions. Compound **2** is represented as a dark grey sticks and hydrogen bonds as green dashed lines

Figure. *Cont.*

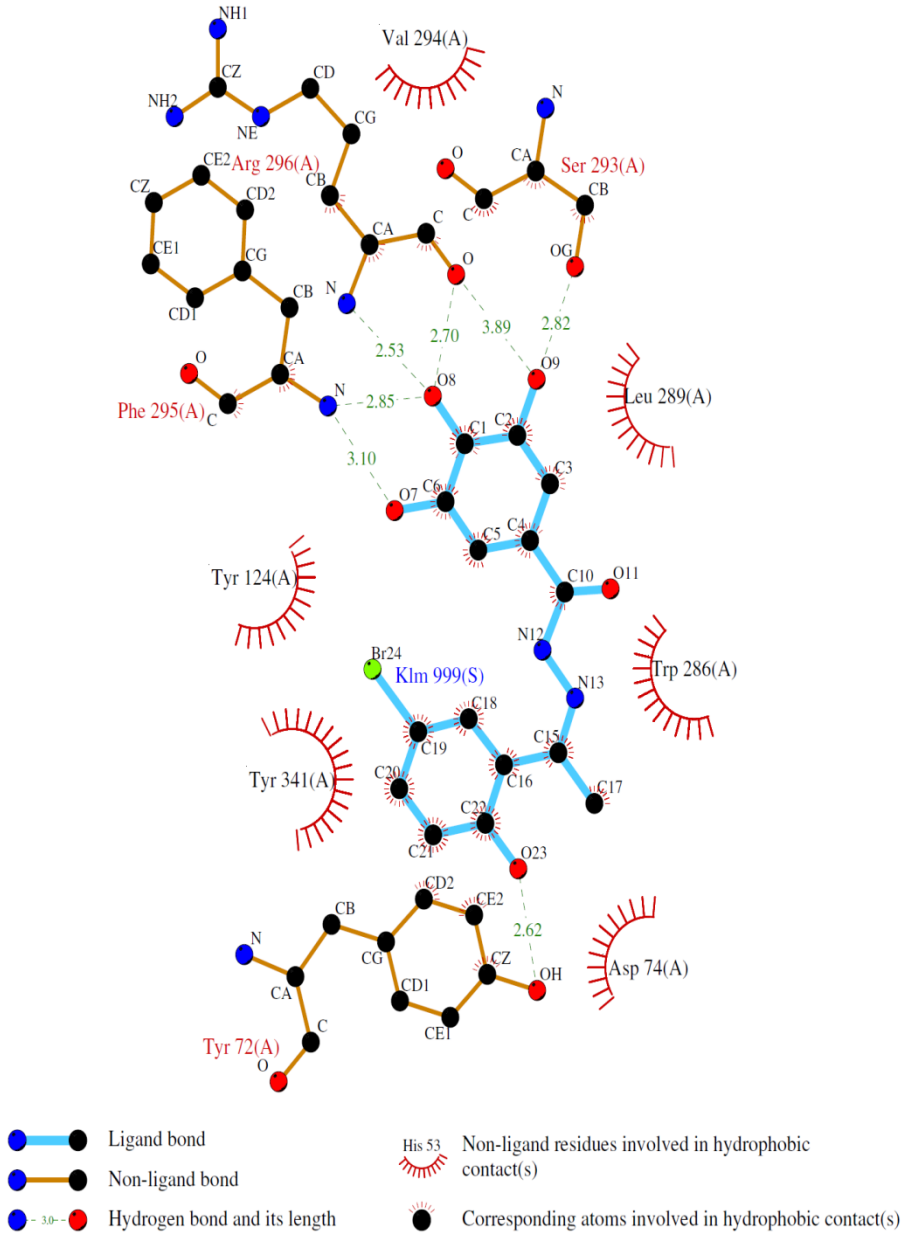

Figure 4.9.2(b): Representations of the molecular model of the complex formed between compound 2 and hAChE. 2D schematic representation of the hydrogen bonding and hydrophobic interactions.

The residues that have been reported to be involved in protein-ligand interactions are Tyr 72, Asp 74, Tyr 124, Ser 125, Trp 286, Tyr 337 and Tyr 341 (PAS); Trp 236, Phe 295, Phe 297 and Phe 338 (ABP); Ser 203, His 447 and Glu 334 (ES); Gly 121, Gly 122 and Ala 204 (OH); and Trp 86, Tyr 133, Glu 202, Glu 448 and Ile 451 (AS) (Wiesner, 2007). The molecular docking simulation of the complex formed between compound **2** and hAChE (Figure 4.9.2 a-c) showed the ligand well positioned in the active-site gorge, with the monohydroxyphenyl and trihydroxyphenyl moieties interacting with residues in the PAS and ABP, respectively.

A closer inspection of the interactions at the PAS showed the presence of a hydrogen bond between the 2-hydroxyl group and Tyr 72, π-π stacking involving the monohydroxyphenyl ring, Trp 286 and Tyr 341 and a cation-π interaction between the protonated nitrogen atom of the amide and Trp 286. Furthermore, hydrophobic interactions between **2** and the rich aromatic residues (Asp 74, Tyr 124, Trp 286, Leu 289 and Tyr 341) along the gorge appear to direct the trihydroxyphenyl moiety into the ABP, thus enabling the phenolic hydroxyl groups to form a network of hydrogen bonds with Ser 293, Phe 295 and Arg 296.Molecular modeling of the complexes formed between the enzyme and compounds **3** and **6** suggested the involvement of a similar set of interactions as for the complex with compound **2** (see Figures 4.9.3 and 4.9.4). In the case of the complex with compound **3**, the model showed, at the PAS, a hydrogen bond between the 2-hydroxyl group and Asp 74, a σ-π interaction between carbon 6 in the aromatic ring and Trp 286, a cation-π interaction between the protonated nitrogen atom of the amide and Tyr 341 and a hydrogen bond between the amide nitrogen atom and Tyr 124 and, in the ABP, hydrogen bonds between two of the hydroxyl groups in the trihydroxyphenyl moiety and Ser 293 and Arg 296. The complex with compound **6** showed, at the PAS, π-π stacking between the pyridinyl ring and Trp 286

and hydrogen bonds between the amide nitrogen atom and the carbonyl group and Arg 296 and, in the ABP, hydrogen bonds between of the hydroxyl groups in the trihydroxyphenyl moiety and Tyr 337 and Phe 338.

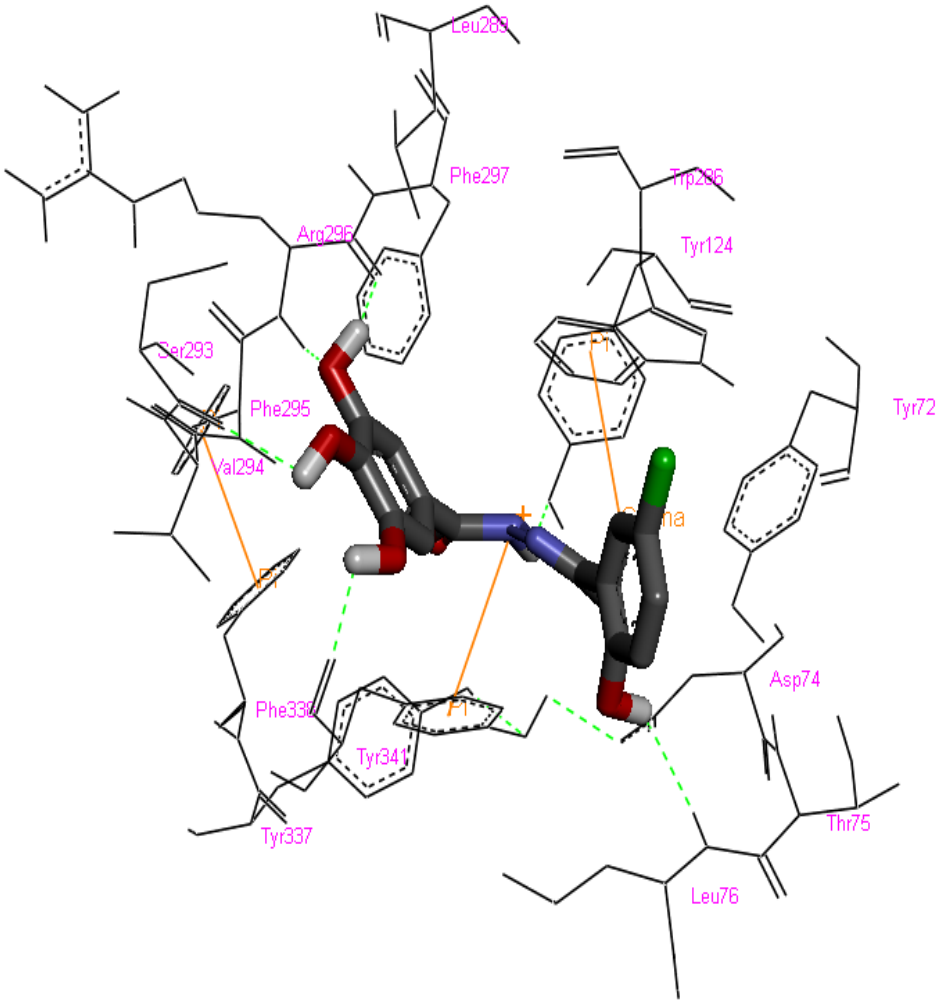

Figure 4.9.3(a). Representations of the molecular model of the complex formed between compound 3 and hAChE. 3D representation of the ligand-enzyme binding interactions. Compound **3** is represented as a dark grey sticks and hydrogen bonds as green dashed lines; (**b**) 2D schematic representation of the hydrogen bonding and hydrophobic interactions.

Figure. *Cont.*

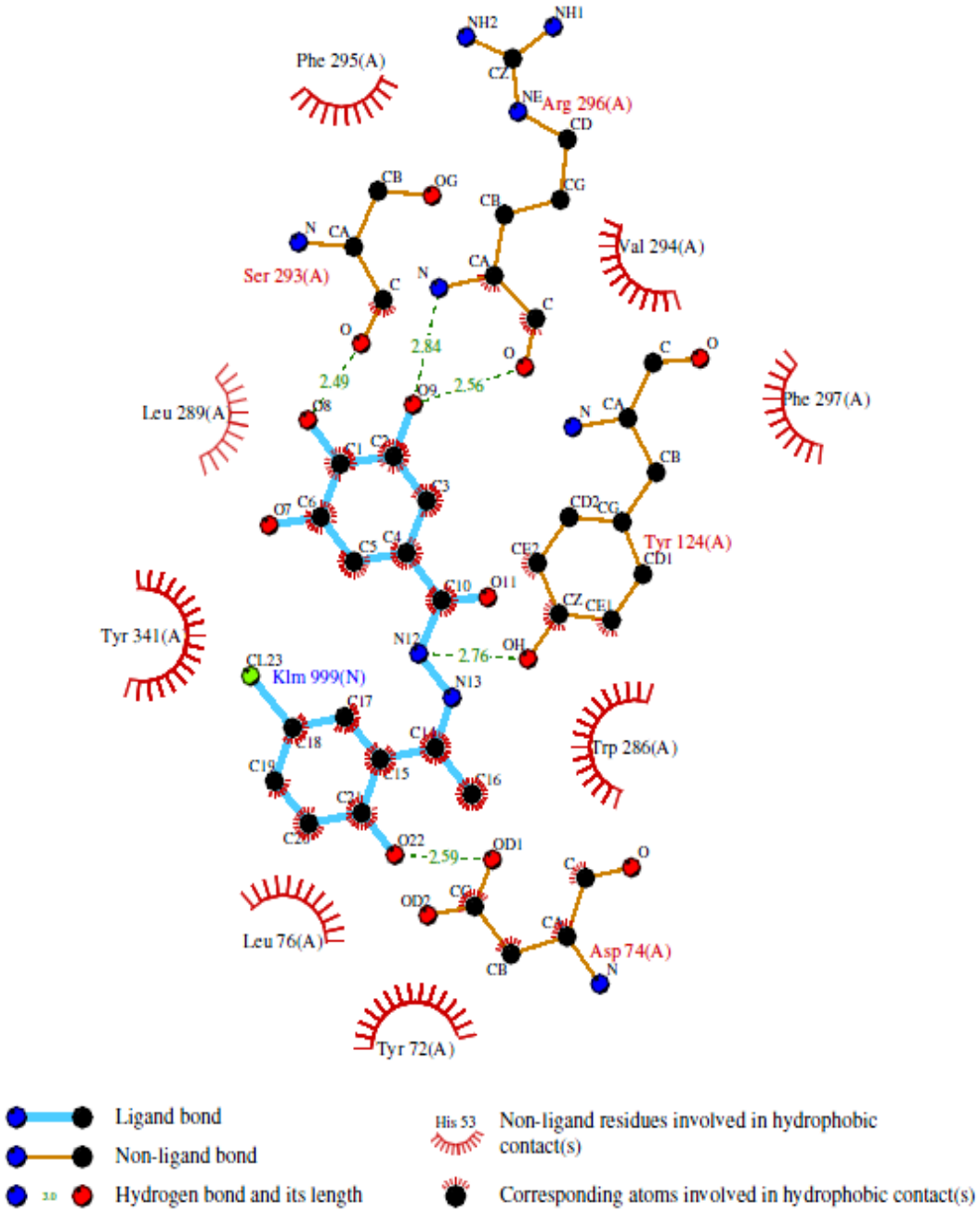

Figure 4.9.3(b). Representations of the molecular model of the complex formed between compound 3 and hAChE. 2D schematic representation of the hydrogen bonding and hydrophobic interactions.

This analysis suggests that the hAChE inhibition activity of compounds **2**, **3** and **6** is probably due to their ability to block the active-site gorge, thus preventing the substrate, acetylcholine, from entering the active site.

Antioxidant Assays: The antioxidant efficacies of the compounds **1–6** were tested and the results obtained (see Table 4.7) revealed different activities in the two assays. This indicates that two mechanisms, operating in different ways, must be responsible for the observed activity. The color change from deep purple to yellow at 515 nm observed in the DPPH assay confirmed the radical scavenging activity of the compounds. A reference curve of absorbance (A) against DPPH concentration in methanol was plotted and used for the calculation of DPPH concentration at various reaction times (R^2 = 0.9999). The compounds showed IC_{50} values in the range of 1.1–2.3 μg/mL. All the compounds tested showed a lower IC_{50} compared to the positive control used (ascorbic acid), except for compound **6**, which showed no significant difference with the IC_{50} of the positive control. The high activity of the compounds in the DPPH assay can be related to the resonance effect of the polyhydroxyl groups attached to the phenolic ring in the compounds, whereupon electron donating substituents increase the electron density in the aromatic ring making it more reactive towards electrophilic attack or mainly due to their redox properties, which can play an important role in the absorption and neutralization of free radicals, the quenching of singlet and triplet oxygen, or the decomposition of peroxides (Heo, 2007 and Khaledi, 2011). This presumably promotes the release of phenolic hydrogen to the (1,1-diphenyl-2-picrylhydrazyl) free radical indicated by a color change from purple to yellow. The second method used for testing the antioxidant activities of these compounds was the FRAP assay. It is considered an accurate method for assessing "antioxidant power". Ferric to ferrous ion reduction at low pH causes a colored ferrous-tripyridyltriazine complex to

form. FRAP values are obtained by comparing the absorbance change at 593 nm in test reaction mixtures with those containing ferrous ions at known concentrations.

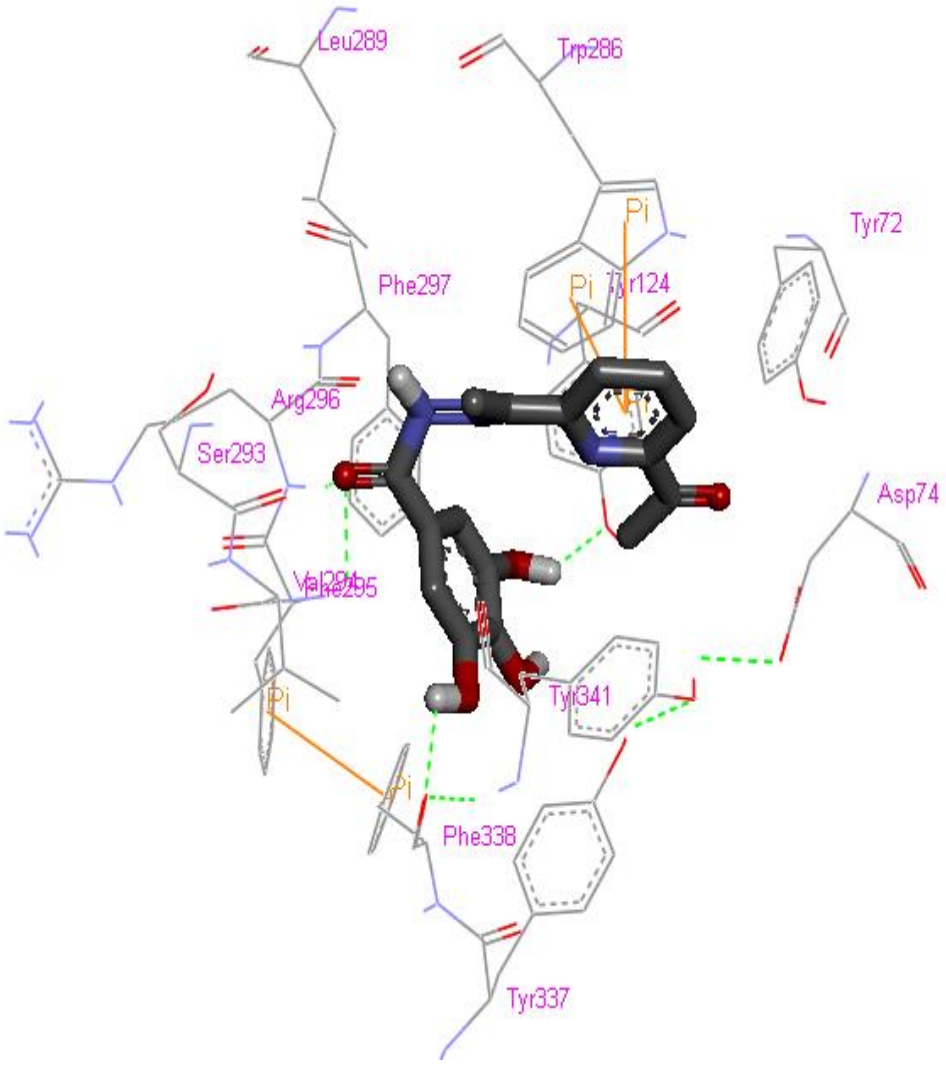

Figure 4.9.4(a). Representations of the molecular model of the complex formed between compound 6 and hAChE._3D representation of the ligand-enzyme binding interactions. Compound 6 is represented as a dark grey sticks and hydrogen bonds as green dashed lines

Figure. *Cont.*

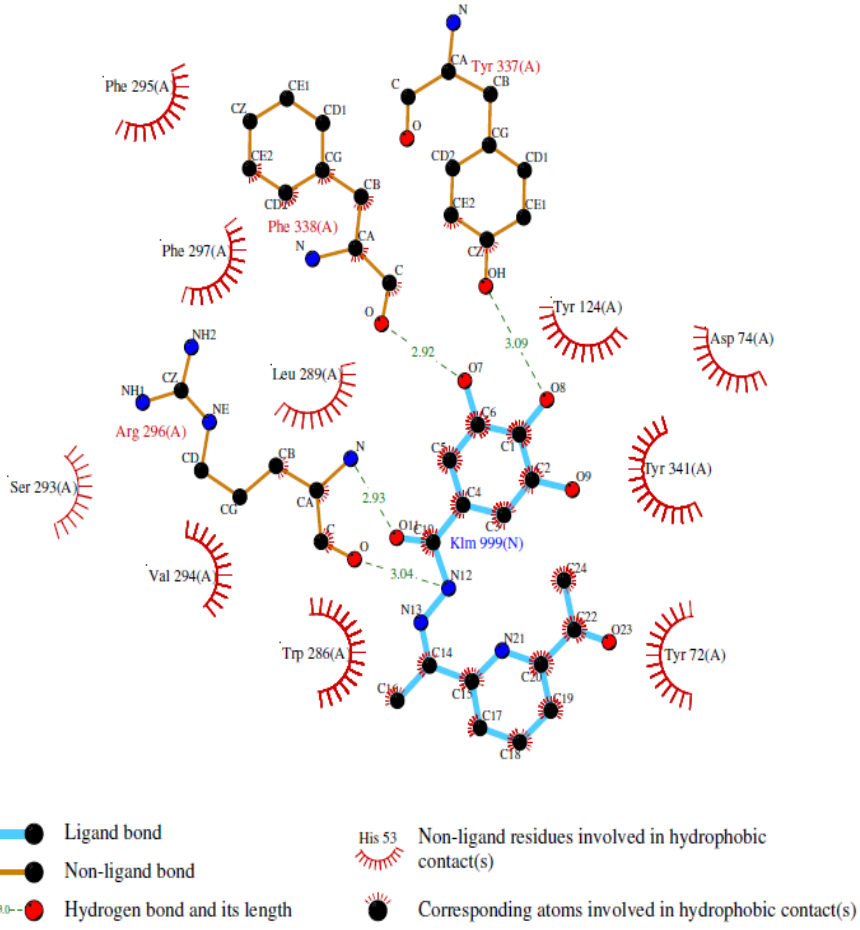

Figure 4.9.4(b). Representations of the molecular model of the complex formed between compound 6 and hAChE. 2D schematic representation of the hydrogen bonding and hydrophobic interactions.

In this study, the compounds showed FRAP values in the range 2,000–9,000 which is above the values shown by BHT and ascorbic acid used as standards. It was observed that compounds **1**–**5** demonstrated the highest activities in the DPPH assay while **1** and **2** showed the highest values in the FRAP assay. This can be attributed to increased π-electron delocalization within the pyridine ring which increases the electron density and causes ferric ion reduction (Stockdale. 1971).

4.10 ANTI-ULCER APPLICATIONS

Peptic ulcer occurs in the parts of the digestive tract that are exposed to gastric juice containing acid and pepsin secreted by the H^+/K^+ATPase or proton pump on the parietal cells (oxyntic cells)of the stomach (Grossman, 1981). Gastric ulcer is one type of peptic ulcer other than duodenal ulcer (Patrick, 2005) and it occurs on the stomach wall. It can be defined as red hemorrhagic bands of erosion on the stomach lining (Patrick, 2005) and this disease is caused by endogenous noxious agents such as hydrochloric acid, proteolytic enzymes and bile. The exogenous agents however, include ingestion of non-steroidal anti-inflammatory drugs for instance nalfon, tolectin, butazolidin, naproxen, ibuprofen and indomethacin (Grossman, 1981; Yamada, 1999), cigarette smoking (Yamada, 1999; Yuan, 2007), steroid ingestion (Grossman, 1981), alcohol consumption, psychological stress, oral biphosphonates, potassium chloride, immunosuppressive medications and decline in prostaglandin levels amongst older people (Yuan, 2007). The pathogenesis pathway of the formation of gastric ulcer is complex and still at the crossroad to be clearly understood (Yuan, 2007). In this study, gastric ulcer was being induced by ethanol and it is found that ethanol produced gastric damage by impairing gastric defensive factors such as mucus and mucosa circulation (Szabo, 198). Copper(II) complexes of amino acids had been discovered to show potent activity in preventing the formation of gastric ulcer induced by ethanol (Franco, 1997).

4.10.1 Acute toxicity study of Zn(BzSO-HAP)

Animals treated with Zn(BzSO-HAP) at a dose of 2 g/kg or 5 g/kg were kept under observation for 14 days. All of the animals remained alive and no animal manifested any significant sign of toxicity at these doses. There were no abnormal signs, behavioral changes, body weight changes, or macroscopic finding at any time of observation. There

was no mortality in the above-mentioned doses at the end of 14 days of observation. Histological examination of the liver and kidney, hematology, and serum biochemistry revealed no significant differences between the different groups as shown in (Figure 4.10.1). All of the data of the acute toxicity tests are listed in Tables 4.8 and 4.9.

Table 4.8: Acute toxicity test result of renal Function test Zn(BzSO-HAP)

Animals Group	**Renal Function test**						
	Sodium (mmol/L)	Pottasium (mmol/L)	Chloride (mmol/L)	CO_2 (mmol/L)	Anion gap (mmol/L)	Urea (mmol/L)	Creatinine (µmol/L)
Control Grp	138.17 ±2.64	5.12 ±0.09	103.33 ±1.91	23.13 ±0.88	18.17 ±0.60	5.73 ±0.37	50.83 ±1.79
L. D(2 g/kg)	137.67 ±1.65	5.30 ±0.05	102.67 ±1.60	20.42 ±0.61	19.17 ±0.40	4.85 ±0.08	47.67 ±1.22
H. D(5 g/kg)	138.50 ±1.59	4.63 ±0.04	102.83 ±1.69	22.9 ±0.36	17.33 ±0.42	5.98 ±0.21	48.00 ±1.16

All values expressed as mean and standards error mean. There is no significant difference between groups

Table 4.9: Acute toxicity test Liver function test of Zn(BzSO-HAP)

Animals Group	**Liver Function test**								
	Total protein (g/L)	**Albumin (g/L)**	**Globulin (g/L)**	**Total bilirubin (µmol/L)**	**Conjugated bilirubin (µmol/L)**	**AP (IU/L)**	**ALT (IU/L)**	**AST (IU/L)**	**G-Glutaml. Transferase (IU/L)**
Control Grp	71.17 ± 0.64	11.33 ± 0.38	59.83±1.10	1.81 ± 0.08	0.83 ± 0.02	134.83±3.00	53.5 ± 0.59	151.5 ± 2.93	4.67 ± 0.13
L.D (2g/kg)	71.50 ± 1.39	11.67 ± 0.13	59.50± 0.70	2.17 ± 0.06	1.00 ± 0.09	133.17±1.87	50.00 ± 1.40	163.67± 2.13	5.00 ± 0.29
HD (5g/kg)	71.83 ± 0.50	11.83 ± 0.39	60.17 ± 0.42	1.50 ± 0.06	1.00 ± 0.04	135.33±0.09	52.17 ± 1.28	155.00± 2.27	5.33 ± 0.10

All values expressed as mean and standards error mean. There is no significant difference between groups

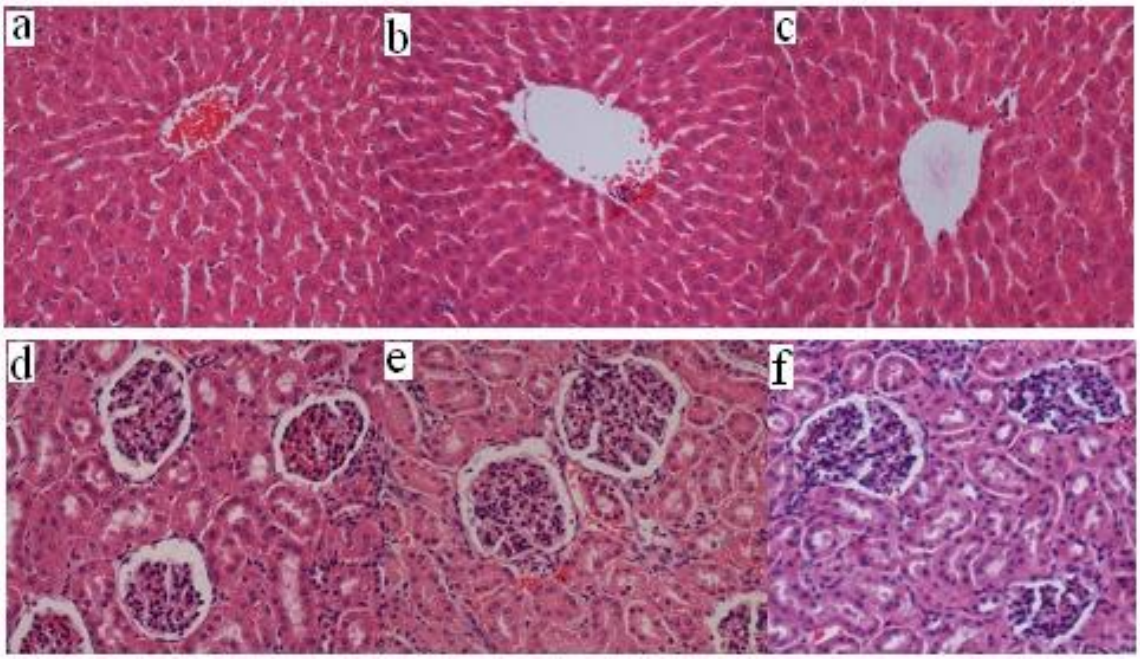

Figure 4.10.1: Histological sections of acute toxicity test. Figure a, b and c (20x) liver section in rats treated with 5 g/kg vehicle, LD and HD compound, respectively. Figure (d, e (20x) and f (10x)).kidney section in rats treated with 5 ml/kg vehicle. There is no significant differences in structures of liver and kidney between treated (LD, HD) and control groups.

4.10.2 Cytoprotective activity

The metal compound in Table 4.10 showed an important cytoprotective activity against ulcers induced by absolute ethanol. The values of ulcer area, percentage of ulcer inhibition and pH compared with those of the cimetidine group showed that the compound is bioactive.

Table 4.10: Observed ulcer area, inhibition (percentage), pH and mucus by Zn(BzSO-HAP)2 in rats

Animal Group	**Pre-treatment (5 ml/kg dose)**	**Ulcer area $(mm)^2$ (Mean ± S.E.M)**	**Inhibition (%)**	**pH of gastric content**	**Mucus weight of gastric content**
1	Tween 20 (Ulcer Control)	840.00 ± 4.60^{a}	-	$3.78 + 0.154^{a}$	$0.73 + 0.065^{a}$
2	Cimetidine (50 mg/kg)	145.00 ± 4.91^{b}	82.74%	$6.20 + 0.491^{b}$	$1.18 + 0.069^{b}$
3	$Zn(BzSO\text{-}HAP)^2$ (50 mg/kg)	85.40 ± 4.43^{c}	89.83%	$5.10 + 0.379^{ab}$	$1.33 + 0.086^{b}$
4	$Zn(BzSO\text{-}HAP)_2$ (100 mg/kg)	00.00 ± 0.00^{d}	100%	$5.54 + 0.415^{b}$	$1.40 + 0.140^{b}$

All values are expressed as mean ± standard error mean. Means with different superscripts are significantly different. The mean difference is significant at the $p<0.05$ level.

The ulcer areas in the benzenesulfanohydrazone treated groups were significantly smaller than the control group. As can be observed in Table 4.10 the oral administration of the metal complex (50 mg/kg and 100mg/kg) at 30 min before ethanol administration markedly reduced the mucosal damage by up to 100% in animals treated with a high dose of the compound. At the same time the compound did not induce any significant changes in the normal gastric mucosa of the rats of any tested group. The results of the present study confirm the known ulcerogenic effects of ethanol. The chemical structure shows that the benzenesulfanohydrazones complexes have hydroxyl coordinated groups. Based on its structure and potentials to generate hydroxyl radicals, benzenesulfanohydrazone complexes can be described as oxidants and appear to increase the load of free radicals. The carbonyl group in the compounds appears to achieve the antioxidant balance and to protect the gastric mucosa from injurious agents. Therefore, this group may play a role as an electrophilic acceptor in the structure. The mechanism of cytoprotective activity has been suggested to be mediated through a reaction between the electrophilic acceptor and the

sulfhydryl-containing groups of the mucosa. Also, compounds with the hydroxyl group can form hydroxyl radicals, which are known to mediate in the pathogenesis of gastric mucosal injury. This result has been reported in a study (Al-Shabanah, 2000) about the effect of ninhydrin on the biochemical and histopathological changes in the gastric mucosa of rats. Further studies are warranted to identify the detailed mechanism of action of these bioactive compounds.

The administration of ethanol to rats produces gastric mucosal lesions and erosions similar to those occurring in gastric ulcer. These lesions are produced because ethanol can affect the protective defense mechanisms at the mucosal layer (Repetto and Liesuy, 2002). This study describes a model to produce extensive gastric necrosis in rats after induction with absolute ethanol. Once administered to rats, the ethanol rapidly penetrates the mucosa layer and causes extensive damage (Rajeshkumar, 2001; Abdulla, 2010). This process supports the finding that only 30 min was needed to produce acute gastric ulceration in rats. Administration of absolute ethanol to fasted rats caused severe gastric damage, which was visible from the outside of the stomach as thick reddish-black lines in the ulcerated control group (Figure 4.10.2). Administration of the zinc(II) metal complex of benzenesulfanohydrazones at 30 min before the administration of absolute ethanol lead to good prevention with reduction or absence of the lesions. This result shown in (Figure 4.10.2) view of the outside of the stomach and (Figure 4.10.3) view of the opened stomach.

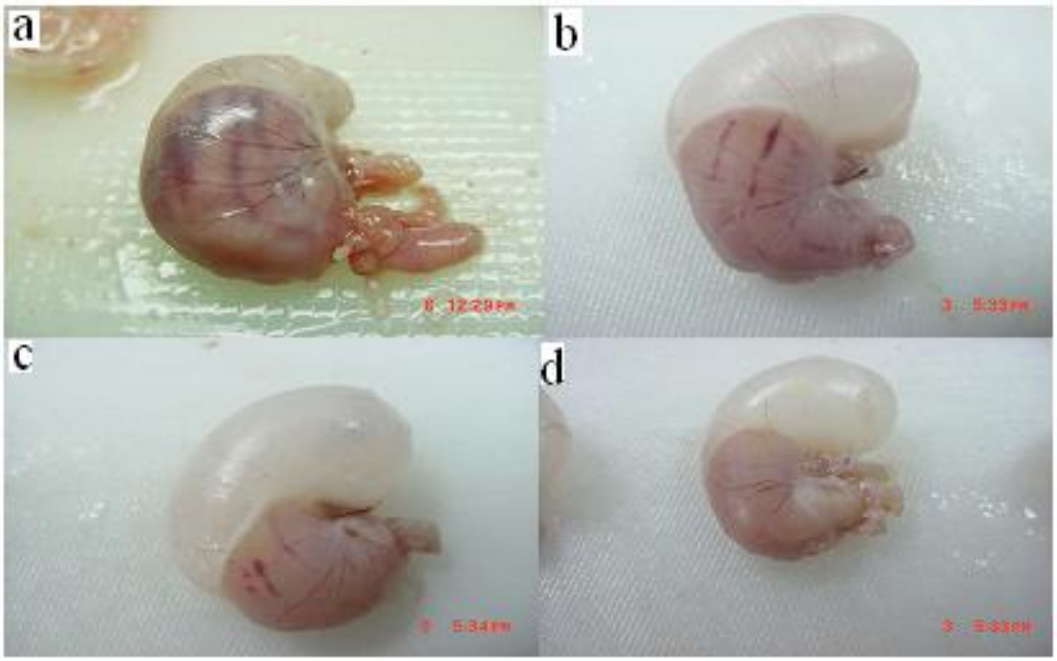

Figure 4.10.2: Macroscopical appearance of gastric mucosa in rats. (**a**) Rats pre-treated with 10% Tween 20. Severe macroscopic necrosis of gastric mucosa. Absolute ethanol produced extensive visible hemorrhagic necrosis of gastric mucosa. **(b)** Rats pre-treated with cimetidine 50 mg kg^{-1}). Mild macroscopic necrosis of gastric mucosa. The drug reduces the formation of gastric lesions induced by absolute ethanol. **(c)** Rats pre-treated with Zn(BzSO-HAP) (50 mg kg^{-1}). Mild macroscopic necrosis of gastric mucosa. The compound reduces the formation of gastric lesions induced by absolute ethanol. **(3d)** Rats pre-treated with Zn(BzSO-HAP) (100 mg kg^{-1}). The compound prevents the formation of gastric lesions induced by absolute ethanol.

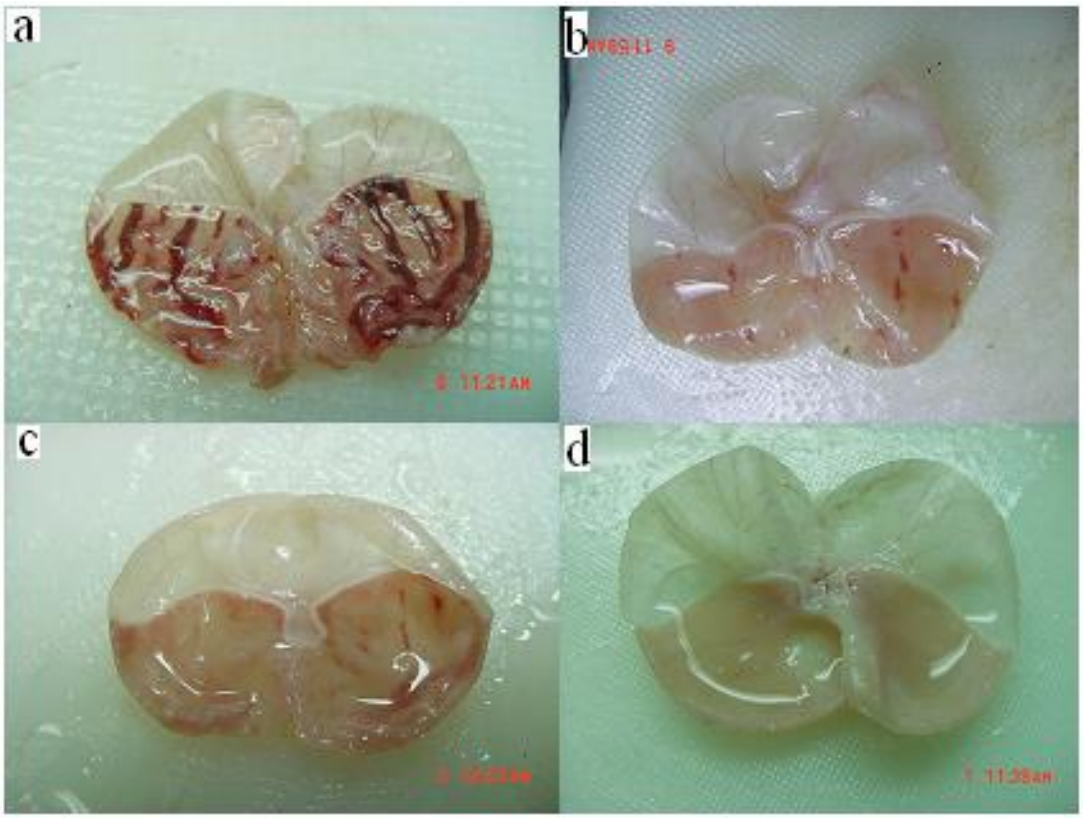

Figure 4.10.3: Macroscopical appearance of gastric mucosa in rats in open stomach. (**a**) Rats pre-treated with 10% Tween 20. Severe macroscopic necrosis of gastric mucosa. Absolute ethanol produced extensive visible hemorrhagic necrosis of gastric mucosa. **(b)** Rats pre-treated with cimetidine 50 mg kg^{-1}). Mild macroscopic necrosis of gastric mucosa. The drug reduces the formation of gastric lesions induced by absolute ethanol. **(c)** Rats pre-treated with Zn(BzSO-HAP) (50 mg kg^{-1}). Mild macroscopic necrosis of gastric mucosa. The compound reduces the formation of gastric lesions induced by absolute ethanol. **(4d)** Rats pre-treated with Zn(BzSO-HAP) (100 mg kg^{-1}). The compound prevents the formation of gastric lesions induced by absolute ethanol.

4.10.3. Histological evaluation of gastric lesions

The histological analysis of ethanol treated and control rat stomachs revealed the presence of necrotic debris in the lamina propria of the mucosa. The lesions extended down the mucosal layer involving the surface epithelium (Figure 4.10.4). The treated groups had less damage along the surface of the epithelium. Mucosal blood flow has been observed to be an

important factor in the damage caused by alcohol and is modulated by prostaglandin (Holander, 1984). The effectiveness of benzenesulfanohydrazones complex in prevention against mucosal damage caused by ethanol may be an indication of its effect on prostaglandin.

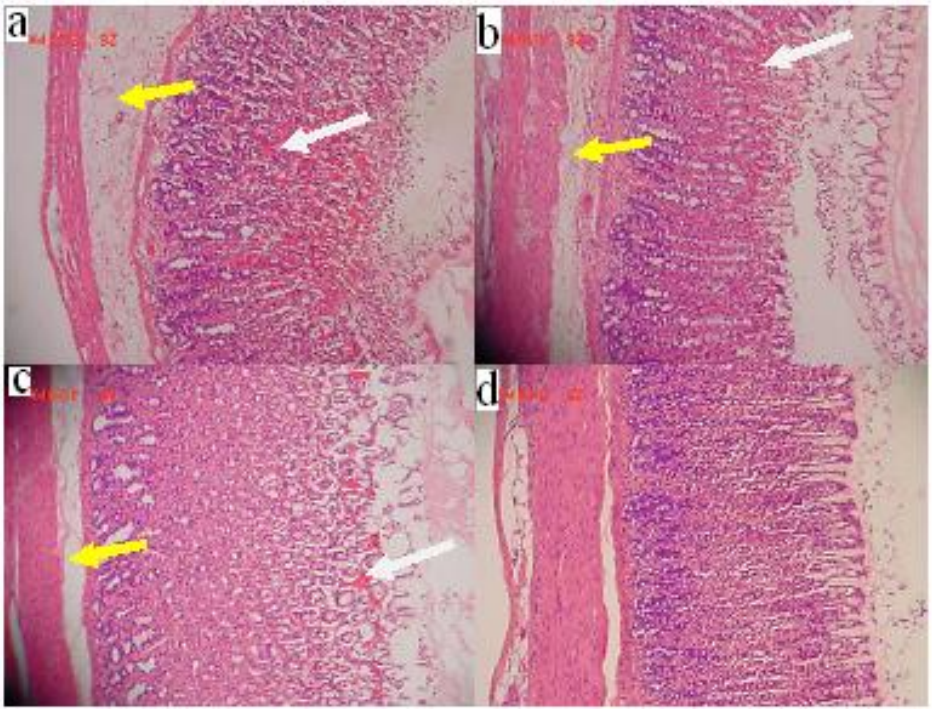

Figure 4.10.4: Histological section of the absolute ethanol-induced gastric mucosal damage in rats. (a) Rats pre-treated with 10% Tween 20 (ulcer control). Severe disruption of the surface epithelium, deep penetration of necrotic lesions into mucosa (arrow) and edema of the sub mucosa layer (yellow arrow) with leukocyte infiltration of ulcerative tissues. (b) Rats pre-treated with cimetidine (50 mg/kg). Moderate disruption of the surface epithelium and edema of the sub mucosal layer (yellow arrow) with leucocytes infiltration. (c) Rats pre-treated with Zn(BzSO-HAP) (50 mg kg^{-}). There is mild disruption of the surface epithelium. (5d). Rats pre-treated with Zn(BzSO-HAP) (100 mg kg^{-1}. No disruption to the surface epithelium (arrow), and no edema and leucocytes infiltration of sub mucosal layer (H&E stain, 10x).

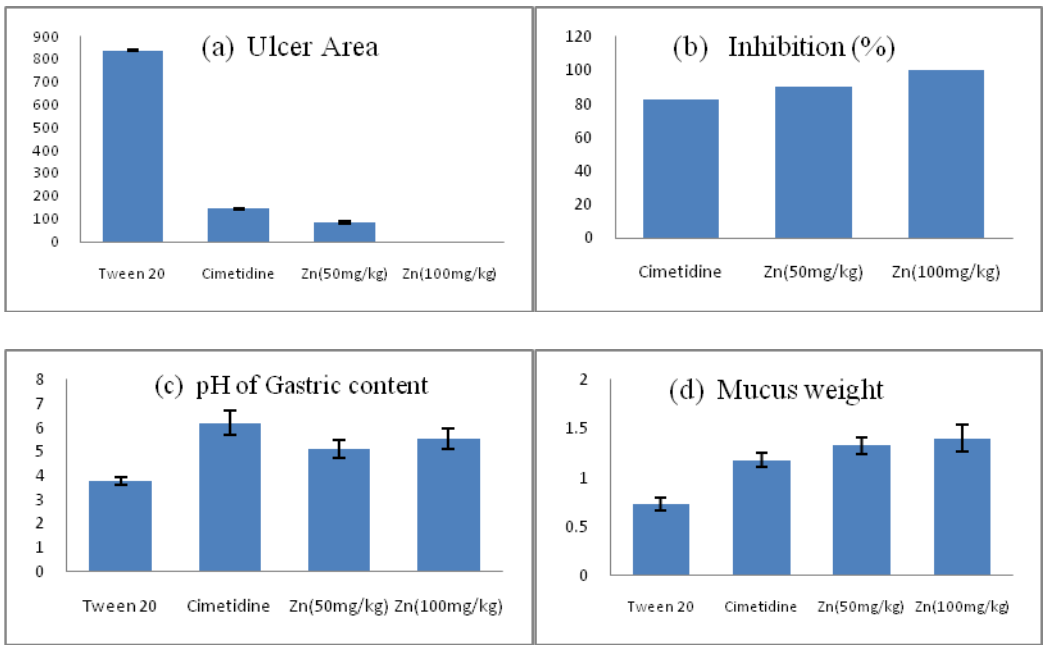

Figure 4.10.5: shows the effect of compound on ethanol induced gastric mucosal lesions in rats **(d)** Summarized the effect of compound on mucosal weight. **(c)** Shows the effect of benzenesulfanohydrazones complex on the acidity of the gastric juice in range of (pH=5.1± 0.04^{c} -5.54±0.03^{d}) compared to the cimetidine group (pH=6.2 ± 0.06b). **(b)** Shows the inhibition of benzenesulfanohydrazones Zinc(II) complex 50 mg kg^{-1} and 100 mg kg^{-1} against the stomach ulcer induced by absolute alcohol and the results are compared to the standard drug, cimetidine **(a)** this shows the Ulcer area for the compound compared with the control group and standard cimetidine. Cimetidine has been reported to decrease acid output but did not decrease the ulcer area. This supported the present study which both doses had indicated better cytoprotective effects in reducing ulcer area formation compared with cimetidine with less gastric secretion.

To determine the safety of drugs and products for human use, toxicological evaluations are carried out in various experimental animals to predict toxicity and to provide guidelines for selecting a safe dose in humans. The hematological, gastrointestinal and cardiovascular adverse effects have the highest overall concordance between animals and humans (Olson,

2000). The liver and kidney of the treated rats showed no significant change compared to the control group. Haematology and clinical biochemistry values were within the range of the control animals tested and were similar to some of the control reference values published by other researchers (Ringler and Dabich 1979; Witthawaskul, 2003). In acute toxicity studies, a product is considered nontoxic if no deaths are registered after 14 days of observation and no clinical signs of toxicity are obsearved at doses $\leq$ 5 g/kg. Because the highest dose of zinc(II) complex that did not cause any toxicity was 5 g/kg body weight, these findings suggest that the compound is relatively nontoxic (Brock, 1995).

The effectiveness of the zinc(II) metal complex with 2'-[1-(2-hydroxyphenyl) ethylidene] benzenesulfanohydrazide in preventing mucosal damage caused by ethanol may indicate its effect on prostaglandin. The treatment with the benzenesulfanohydrazones complex reduced the volume of gastric secretion. In the cimetidine group the gastric contents were around (1.18±0.04) g, while those of the treated groups were in range of (1.33 ± 0.01 -1.40 ± 0.01) g. This characteristic indicates that the benzenesulfanohydrazones of the zinc(II) metal complex acts similar histamine H2 receptor antagonists. Therefore, the cimetidine has been used as standard antiulcer drug in present study as can decrease acid output but does not decrease the ulcer area. This previous observation supports the result of the present study, in which both of doses of zinc(II) complex showed cytoprotective effects, in terms of reducing the ulcerative area, that were similar to the effect of cimetidine, which reduced the gastric secretion. The inhibition activity of the zinc(II) complex with 2'-[1-(2-hydroxyphenyl) ethylidene] benzenesulfanohydrazide against ulcer formation was excellent and was higher than that of the cimetidine group which had a percentage of 89.83% inhibition. As the dosage was increased further, the ulcer inhibition increased to 100%. The reduced gastric acidity measured after pylorus ligation suggests that the cytoprotective

mechanism of action of the extract on gastric mucosa may involve direct inhibition of gastric secretion. The reduction of acidity observed after incubation of the gastric juice with the extract suggests that the cytoprotective mechanism may involve the simple neutralization of the acid secreted in the stomach. Figure 4.10.5 shows the effect of the benzenesulfanohydrazone complex on the acidity of the gastric juice in pH range from 5.1± 0.04 to 5.54±0.03 compared to the cimetidine group (pH=6.2 ± 0.06b). These results agree with previous studies (Mahmood, 2010; Murakamu, 1990). In this study Zn(II) benzenesulfanohydrazone complex was found to reduce gastric lesions induced by ethanol *in vivo*.

In conclusion this paper describes a model to produce extensive gastric necrosis in rats by induction with absolute ethanol. It also describes good prevention of gastric necrosis by administration of zinc(II) complex with benzenesulfanohydrazones 30 min before induction with absolute ethanol which reduced or eliminated lesion formation. The compound was tested for acute toxicity. Haematology and clinical biochemistry values were within the range of the control animals tested and were similar to some of the control reference values. The highest dose of zinc(II) complex that did not cause any toxicity was 5 g/kg body weight, which indicates that the compound is relatively non-toxic.

5.0 CONCLUSION

In the first part of this thesis synthesis, characterization, X-ray structures and biological application was presented for synthesized metal complexes. The Schiff-based complexes were also highly inhibitive only against the Gram positive bacterium. They exhibit significant antimicrobial activities against *Methicillin-resistant Staphylococcus aureus.* Very weak antimicrobial activity was observed with *Acinetobacter baumannii* and *Pseudomonas aeruginosa*. No antimicrobial activity observed with *Klebsiella pneumonia.*

Further study on time-kill assay is needed to confirm if the compound are bactericidal. The study of mechanism of action (MOA) of the compound is suggested to further expand the knowledge on its target organism and application.

Secondly, the anticancer activity of the complexes were analyzed with emphasis to MCF-7 cell line, we have studied the mechanistic interaction of Cobalt(III) Schiff base compound with nucleic acids and analyzed its biochemical effect on human breast cell line. In the cytotoxicity assay the compound showed high *in vitro* cytotoxic properties with significant growth inhibition activity against MCF-7cell line. The data from our present study suggested the efficient capability of the Cobalt(III) compound to inhibit growth activities as anti-cancer compound against human breast MCF-7cell line, and deserves further investigation on other human cell lines as potential new antitumor drug

Lastly, synthesized novel Schiff bases were observed to be potentially useful for acetyl-cholinesterase inhibition and possible treatment for AD. The compounds also showed strong free radical inhibitory activities.

List of Publications

Title: Gastroprotection Studies of Schiff Base Zinc (II) Derivative Complex against Acute Superficial Hemorrhagic Mucosal Lesions in Rats. Author(s): Shahram Golbabapour,Nura Suleiman Gwaram, Pouya Hassandarvish, Maryam Hajrezaie, Behnam Kamalidehghan, Mahmood Ameen Abdulla, Hapipah Mohd Ali, A. Hamid A Hadi, Nazia Abdul Majid Source:PLoS ONE 8(9): e75036. Published: 2013, doi:10.1371/journal.pone.0075036.

Title: Schiff base metal derivatives enhance the expression of HSP70 and suppress BAX proteins in prevention of acute gastric lesion," Author(s): Shahram Golbabapour,Nura Suleiman Gwaram, Mazen M.Jamil Al-Obaidi, Abdoreza Soleimani Farjam, Hapipah Mohd Ali and Nazia Abdul Majid Source: BioMed Research International, Volume 2013, Article ID 703626, 7 pages, September 2013, http://dx.doi.org/10.1155/2013/703626

Title: Acute Toxicity and Gastroprotection Studies of a New Schiff Base Derived Copper (II) Complex against Ethanol-Induced Acute Gastric Lesions in Rats. Author(s): Maryam Hajrezaie, Shahram Golbabapour, Pouya Hassandarvish, Nura Suleiman Gwaram, A. Hamid A. Hadi, Hapipah Mohd Ali, Nazia Majid, Mahmood Ameen Abdulla mail Source: PLoS ONE 7(12): e51537. doi:10.1371/journal.pone.0051537

Title: Antibacterial Evaluation of Some Schiff Bases Derived from 2-Acetylpyridine and Their Metal Complexes. Author(s): Gwaram, Nura Suleiman; Ali, Hapipah Mohd; Khaledi, Hamid; et al. Source: Molecules Volume: 17 Issue: 5 Pages: 5952-5971 Published: 2012 DOI: 10.3390/molecules17055952

Title: Synthesis, Characterization, X-ray Crystallography, Acetyl Cholinesterase Inhibition and Antioxidant Activities of Some Novel Ketone Derivatives of Gallic Hydrazide Derived Schiff Bases. Author(s): Gwaram, Nura Suleiman; Ali, Hapipah Mohd; Abdulla, Mahmood Ameen; et al. Source: Molecules Volume: 17 Issue: 3 Pages: 2408-2427 Published: 2012 DOI: 10.3390/molecules17032408.

Title: Synthesis, characterization, and biological applications of some 2-acetylpyridine and acetophenone derivatives. Author(s):Nura Suleiman Gwaram, Hapipah Mohd Ali, Siti

Munirah Saharin, Mahmood Ameen Abdulla, Pouya Hassandarvish, Thong Kwai Lin, Chai Lay Ching and Cher Lin Ooi. Source Journal of Applied Pharmaceutical Science Vol. 2 (12), pp. 027-038, December, 2012, DOI: 10.7324/JAPS.2012.21206

Title: Synthesis, spectral characterization and biological activity of Zn(II) complex with 2′-[1-(2-hydroxyphenyl)ethylidene]benzenesulfanohydrazide. Author(s): Gwaram, Nura Suleiman; Laila Musalam, Hapipah Mohd. Ali, Mahmood Ameen Abdulla, Shayma A. Shaker. Source: Arabian Journal of Chemistry, *In Press, Corrected Proof, Available online 14 January 2012*

Title: Synthesis of 2 '-(5-Chloro-2-Hydroxybenzylidene) Benzenesulfanohydrazide Schiff Base and its Anti-Ulcer Activity in Ethanol-Induced Gastric Mucosal Lesions in Rats Author(s): Gwaram, Nura S.; Musalam, Laila; Ali, Hapipah M.; et al. Source: Tropical Journal of Pharmaceutical Research Volume: 11 Issue: 2 Pages: 251-257 Published: 2012 DOI: 10.4314/tjpr.v11i2.11.

Title: Two new polymorphs of 2,6-diaminopyrimidin-4(3H)-one monohydrate Author(s): Gwaram, Nura Suleiman; Khaledi, Hamid; Ali, Hapipah Mohd; et al. Source: Acta Crystallographica Section C-Crystal Structure Communications Volume: 67 Pages: O6-O9 Published: 2011. DOI: 10.1107/s0108270110046317

Title: Aqua{2-(morpholin-4-yl)-N- 1-(2-pyridyl)ethylidene ethanamine-kappa N-3,N ',N "}bis(thiocyanato-kappa N)manganese(II). Author(s): Gwaram, Nura Suleiman; Khaledi, Hamid; Ali, Hapipah Mohd. Source: Acta Crystallographica Section E-Structure Reports Online Volume: 67 Pages: M928-U1007 Published: 2011. DOI: 10.1107/s1600536811022124.

Title: Aqua{2-morpholino-N- 1-(2-pyridyl)ethylidene ethanamine-kappa N-3,N ',N "}bis(thiocyanato-kappa N)cobalt(II). Author(s): Gwaram, Nura Suleiman; Hisham, Nurul Azimah Ikmal; Khaledi, Hamid; Ali, Hapipah Mohd Source: Acta Crystallographica Section E-Structure Reports Online Volume: 67 Pages: M205-U885 Published: 2011 DOI: 10.1107/s160053681100136x

Title: Aqua{2-morpholino-N- 1-(2-pyridyl)ethylidene ethanamine-kappa N-3,N ',N "}bis(thiocyanato-kappa N)nickel(II). Author(s): Gwaram, Nura Suleiman; Hisham, Nurul Azimah Ikmal; Khaledi, Hamid; Ali, Hapipah Mohd Source: Acta Crystallographica Section E-Structure Reports Online Volume: 67 Pages: M108-U1116 Published: 2011 DOI: 10.1107/s1600536810052578

Title: Aqua{N,N-dimethyl-N '- 1-(2-pyridyl)ethylidene ethane-1,2-diamine-kappa 3 N,N ',N "}bis(thiocyanato-kappa N)nickel(II). Author(s): Gwaram, Nura Suleiman; Saharin, Siti Munirah; Khaledi, Hamid; et al. Source: Acta Crystallographica Section E-Structure Reports Online Volume: 67 Pages: M513-U1123 Published: 2011. DOI: 10.1107/s1600536811011512

Title: Bis(mu-2-{1- 2-(dimethylamino)ethylimino ethyl}phenolato)bis bromidocopp er(II) monohydrate. Author(s): Gwaram, Nura Suleiman; Khaledi, Hamid; Ali, Hapipah Mohd Source: Acta Crystallographica Section E-Structure Reports Online Volume: 67 Pages: M931-U1039 Published: 2011. DOI: 10.1107/s1600536811022045

Title: Catena-Poly {N,N-dimethyl-N '- 1-(pyridin-2-yl)ethylidene ethane-1,2-diamine-kappa(3) N,N ',N "}(thiocyanato-kappa N)cadmium -mu-thiocyanato-kappa(2) S:N Author(s): Gwaram, Nura Suleiman; Khaledi, Hamid; Ali, Hapipah Mohd Source: Acta Crystallographica Section E-Structure Reports Online Volume: 67 Pages: M480-U835 Published: 2011. DOI: 10.1107/s1600536811010063

Title: Chlorido(2-{1-[(2-morpholinoethyl)imino]ethyl}phenolato-kappa N-3,N ',O)copper(II). Author(s): Hisham, Nurul Azimah Ikmal; Gwaram, Nura Suleiman; Khaledi, Hamid; Ali, Hapipah Mohd Source: Acta Crystallographica Section E-Structure Reports Online Volume: 67 Pages: M57-U651 Published: JAN 2011. DOI: DOI 10.1107/S1600536810051160

Title: Di-mu-thiocyanato-kappa N-2:S;kappa S-2:N-bis({2-morpholino-N- 1-(2-pyridyl)ethylidene ethanamine-kappa N-3,N ',N "}(thiocyanato-kappa N)cadmium)

Author(s): Gwaram, Nura Suleiman; Hisham, Nurul Azimah Ikmal; Khaledi, Hamid; Ali, Hapipah Mohd. Source: Acta Crystallographica Section E-Structure Reports Online Volume: 67 Pages: M251-U1438 Published: 2011. DOI: 10.1107/s1600536811002480

Title: Dibromido{2-(morpholin-4-yl)-N- 1-(2-pyridyl)ethylidene ethanamine-kappa N-3,N ',N "}cadmium. Author(s): Gwaram, Nura Suleiman; Khaledi, Hamid; Ali, Hapipah Mohd Source: Acta Crystallographica Section E-Structure Reports Online Volume: 67 Pages: M347-U634 Published: 2011. DOI: 10.1107/s160053681100554x

Title: Dichloridobis 2-(morpholin-4-yl)ethanamine-kappa N-2,N ' cadmium. Author(s): Gwaram, Nura Suleiman; Khaledi, Hamid; Ali, Hapipah Mohd Source: Acta Crystallographica Section E-Structure Reports Online Volume: 67 Pages: M298-U188 Published: 2011. DOI: 10.1107/s1600536811003709

Title: Dichlorido{2-(morpholin-4-yl)-N-[1-(pyridin-2-yl)ethylidene]ethanamine-kappa N-3,N ',N "}copper(II) monohydrate. Author(s): Gwaram, Nura Suleiman; Khaledi, Hamid; Ali, Hapipah Mohd. Source: Acta Crystallographica Section E-Structure Reports Online Volume: 67 Pages: M334-U503 Published: MAR 2011. DOI: DOI 10.1107/S1600536811004892

Title: Dichlorido{2-morpholino-N- 1-(2-pyridyl)ethylidene ethanamine-kappa N-3,N ',N "}manganese(II). Author(s): Hisham, Nurul Azimah Ikmal; Gwaram, Nura Suleiman; Khaledi, Hamid; Ali, Hapipah Mohd Source: Acta Crystallographica Section E-Structure Reports Online Volume: 67 Pages: M41-U515 Published: 2011. DOI: 10.1107/s1600536810050221

Title: Dichlorido{2-morpholino-N- 1-(2-pyridyl)ethylidene ethanamine-kappa N-3,N ',N "}zinc(II). Author(s): Hisham, Nurul Azimah Ikmal; Gwaram, Nura Suleiman; Khaledi, Hamid; et al. Source: Acta Crystallographica Section E-Structure Reports Online Volume: 67 Pages: M55-U629 Published: 2011. DOI: 10.1107/s1600536810050671

Title: Dichlorido{N,N-dimethyl-N '- 1-(2-pyridyl)ethylidene ethane-1,2-diamine-kappa N-

3,N ',N "}manganese(II). Author(s): Hisham, Nurul Azimah Ikmal; Gwaram, Nura Suleiman; Khaledi, Hamid Ali, Hapipah Mohd Source: Acta Crystallographica Section E-Structure Reports Online Volume: 67 Pages: M229-U1113 Published: 2011 DOI: 10.1107/s1600536811002030

Title: Dichlorido{N,N-dimethyl-N '- 1-(2pyridyl)ethylidene ethane-1,2-diamine-k(3) N,N ',N "}zinc. Author(s): Gwaram, Nura Suleiman; Khaledi, Hamid; Ali, Hapipah Mohd Source: Acta Crystallographica Section E-Structure Reports Online Volume: 67 Pages: M1027-U291 Published: 2011, DOI: 10.1107/s1600536811025669

Title: Dichlorido{N,N-dimethyl-N '- 1-(pyridin-2-yl)ethylidene ethane-1,2-diamine-kappa N-3,N ',N "}cadmium. Author(s): Gwaram, Nura Suleiman; Khaledi, Hamid; Ali, Hapipah Mohd. Source: Acta Crystallographica Section E-Structure Reports Online Volume: 67 Pages: M348-U642 Published: 2011. DOI: 10.1107/s1600536811005538

Title: Dichlorido{N,N-dimethyl-N '-[1-(pyridin-2-yl)ethylidene]ethane-1,2-diamine-kappa *N*-3,*N*',*N*"}cadmium. Author(s): Gwaram, NS; Khaledi, H; Ali, HM Source: Acta Crystallographica Section E-Structure Reports Online Volume: 67 Pages: DOI: DOI 10.1107/S1600536811005538

Title: Diiodido{2-(morpholin-4-yl)-N- 1-(2-pyridyl)ethylidene ethanamine-kappa N-3,N ',N "}zinc. Author(s): Gwaram, Nura Suleiman; Khaledi, Hamid; Ali, Hapipah Mohd Source: Acta Crystallographica Section E-Structure Reports Online Volume: 67 Pages: M628-U1110 Published: 2011. DOI: 10.1107/s1600536811014656

Title: Hexachloridobis{mu(2)-2-(piperazin-1-yl)-N- 1-(2-pyridyl)ethylidene etha namine}trizinc dihydrate. Author(s): Gwaram, Nura Suleiman; Khaledi, Hamid; Ali, Hapipah Mohd. Source: Acta Crystallographica Section E-Structure Reports Online Volume: 67 Pages: M1091-U829 Published: 2011. DOI: 10.1107/s1600536811027437

Title: {2-Morpholino-N- 1-(2-pyridyl)ethylidene ethanamine-kappa N-3,N ',N "}bis(thiocyanato-kappa N)copper(II). Author(s): Gwaram, Nura Suleiman; Hisham, Nurul

Azimah Ikmal; Khaledi, Hamid; et al. Source: Acta Crystallographica Section E-Structure Reports Online Volume: 67 Pages: M58-U661 Published: 2011. DOI: 10.1107/s1600536810050889

Title: {2-Morpholino-N- 1-(2-pyridyl)ethylidene ethanamine-kappa N-3,N ',N "}bis(thiocyanato-kappa N)zinc(II). Author(s): Gwaram, Nura Suleiman; Hisham, Nurul Azimah Ikmal; Khaledi, Hamid; et al. Source: Acta Crystallographica Section E-Structure Reports Online Volume: 67 Pages: M131-U255 Published: 2011. DOI: 10.1107/s1600536810053778

Title: {N,N-Dimethyl-N '- 1-(2-pyridyl)ethylidene ethane-1,2-diamine-kappa N-3,N ',N "}bis(thiocyanato-kappa N)copper(II). Author(s): Gwaram, Nura Suleiman; Khaledi, Hamid; Ali, Hapipah Mohd. Source: Acta Crystallographica Section E-Structure Reports Online Volume: 67 Pages: M930-U1031 Published: 2011. DOI: 10.1107/s1600536811022057

Title: (1S,2S)-2-(1-{ 2-(2-Oxidobenzylideneamino)cyclohexyl imino}-ethyl)pheno lato-kappa O-4,N,N ',O ' copper(II). Author(s): Gwaram, Nura Suleiman; Khaledi, Hamid; Ali, Hapipah Mohd. Source: Acta Crystallographica Section E-Structure Reports Online Volume: 66 Pages: M813-U892 Published: 2010. DOI: 10.1107/s1600536810022889

Title: 2,6-Diamino-4-oxo-3,4-dihydropyrimidin-1-ium chloride dihydrate. Author(s): Gwaram, NS; Khaledi, H; Ali, HM. Source: Acta Crystallographica Section E-Structure Reports Online Volume: 66 Pages: O2294-U216 Published: SEP 2010 DOI: DOI 10.1107/S1600536810031557

Title: Dichlorido{2-morpholino-N- 1-(2-pyridyl)ethylidene ethanamine-kappa N-3,N ',N "}cadmium. Author(s): Hisham, Nurulazimah Ikmal; Gwaram, Nura Suleiman; Khaledi, Hamid; et al. Source: Acta Crystallographica Section E-Structure Reports Online Volume: 66 Pages: M1471-U1246 Published: 2010 DOI: 10.1107/s1600536810043163

Title: N '- 1-(5-Bromo-2-hydroxyphenyl)ethylidene -3,4,5-trihydroxybenzohydrazide

dimethyl sulfoxide solvate trihydrate. Author(s): Gwaram, Nura Suleiman; Khaledi, Hamid; Ali, Hapipah Mohd; et al. Source: Acta Crystallographica Section E-Structure Reports Online Volume: 66 Pages: O721-U5910 Published: 2010 DOI: 10.1107/s1600536810007002.

Title: Nutritional Composition of African Spider Flower, best Journal 2(1):112-119 biological and environmental sciences journal for the tropics June 2005. Author(s).Nura Suleiman Gwaram, Lawal Gusau Hassan et. Al.

List of Conferences:

3rd International Conference for young chemist 2010 (ICYC, 2010) Copthorne Orchid Hotel, Penang, Malaysia, 23rd - 25th June, 2010. Poster Presented: SYNTHESIS AND CHARACTERIZATION OF NEW SCHIFF BASES AND THEIR METAL COMPLEXES OF SOME BENZOYLHYDRAZONE DERIVATIVES.

7th Mathematics and Physical Sciences Graduate Congress, 2011 (7th MPSGC). Hosted by Faculty of Science NAtional University od Singapore (NUS). 12th - 14th December, 2011. Oral Presented: Biological applications and electrochemistry of the newly synthesized *N,N',N''* donor Schiff base transition metal complexes.

17th Malaysian Chemical congress (17MCC) 2012 Held at PWTC Kuala Lumpur Malaysia from 15th - 17th October 2012. Oral Presented: Antioxidant and cytotoxicity studies of some new transition metal complexes derived from 4(2-amioethyl)morpholine and 2-acetylpyridine.

17th Malaysian Chemical congress (17MCC) 2012 Held at PWTC Kuala Lumpur Malaysia from 15th - 17th October 2012. Poster Presented:.

4th International Conference for young chemist 2013 (ICYC, 2013) School of chemical Sciences Universiti Sains Malaysia. Bayview Hotel Georgetown Penang 30th Jan - 1st Feb. 2013. Oral Presentation: Synthesis, characterization, x-ray structures, *in vitro* and *in silico* biological applications some complexes.

University of Malaya-Hydrabad University Bilateral Seminar, held on 26-28 October 2010. Poster Presented: Synthesis and x-ray structures for Asymmetric diamine compounds of Potential Schiff bases and their metal complexes.

Biotechnology and bioproduct Research Cluster (UMBIO) IPS University of Malaya. 2012 Poster Presented: Synthesis, Characterization, X-ray Crystallography, Acetyl Cholinesterase Inhibition and Antioxidant Activities of Some Novel Ketone Derivatives of Gallic Hydrazide-Derived Schiff Bases

REFERENCES

Abdulla MA, Ahmed KAA, Al-Bayaty FH, Masood Y (2010) Gastroprotective effect of Phyllanthus niruri leaf extract against ethanol-induced gastric mucosal injury in rats. *Afric. J.Pharm. Pharm*. 4: 226–230.

Addison, A. W., Rao, T. N., Reedijk, J., Rijn, V. J. & Verschoor, G. C. (1984). Synthesis, structure, and spectroscopic properties of copper(II) compounds containing nitrogen–sulphur donor ligands; the crystal and molecular structure of aqua[1,7-bis(*N*-methylbenzimidazol-2′-yl)-2,6-dithiaheptane]copper(II) perchlorate. *J. Chem. Soc. Dalton Trans,*. 1349-1356.

Ali H.M, Puvaneswary S., Wan J. B., Sharifudin M. Z., Noorlidah A., H.L. Teoh , Loqman P.M. Nazri and Sharifah R. S. O. Synthesis, Characterization, Electrochemistry, Antimicrobial activity and X-ray structures of some Zinc(II) Complexes of some hydrazone Schiff bases. *Malay. J. Sci.,* (2006), 25, 107-114.

Alnemri, E.S. Livingston, D.J. Nicholson, D.W. Salvesen, G. Thornberry, N.A. Wong, W.W. Y. J. (1996). Human ICE/CED-3 Protease Nomenclature. *cell* 87, 171.

Aoyama, Y., Fujisawa, T., Watanabe, T., Toi, H. & Ogoshi, H. (1986). Catalytic reactions of metalloporphyrins. 1. Catalytic modification of borane reduction of ketone with rhodium(III) porphyrin as catalyst, *J. Am. Chem. Soc.* 108**,** 943–947.

Arts, I.C.; Hollman, P.C. (2005). Polyphenols and disease risk in epidemiologic studies1,2,3,4, *Am. J. Clin. Nutr*. 81, 317S–325S.

Bagihalli, G.B.; Avaji, P.G. (2008). Synthesis, spectral characterization, in vitro antibacterial, antifungal and cytotoxic activities of Co(II), Ni(II) and Cu(II) complexes with 1,2,4-triazole Schiff bases. *Eur. J. Med. Chem*, *43*, 2639–2649.

Banerjee, S., Wu, B., Lassahn, P.-G., Janiak, C. & Ghosh, A. (2005). Synthesis, structure and bonding of cadmium(II) thiocyanate systems featuring nitrogen based ligands of different denticity, *Inorg. Chim. Acta*, *358*, 535-544.

Behmer O, Tolosa E, Freitas-Neto A (1976). Manual para histologia normal epatolo´gica. Edart-Edusp, Sa˜o Paulo: 225.

Benzie, I.F.F.; Strain, J.J. (1999). Ferric reducing/antioxidant power assay: *Method Enzymol.*, *299*, 15–27.

Bermejo, E., Carballo, R., Castineiras, A., Dominguez, R., Liberta, A. E., Maichle-Moessmer, C., Salberg, M. M. & West, D. X. (1999). Synthesis, Structural Characteristics and Biological Activities of Complexes of Zn^{II}, Cd^{II}, Hg^{II}, Pd^{II}, and Pt^{II} with 2-Acetylpyridine 4-Methylthiosemicarbazone, *Eur. J. Inorg. Chem.* 965-973.

Bermejo, E., Castineiras, A., Fostiak, L. M., Santos, I. G., Swearingen, J. K. & West, D. X. (2003). Spectral and structural studies of Zn and Cd complexes of 2-pyridineformamide N(4)-ethylthiosemicarbazone. *Polyhedron*, *23*, 2303-2313.

Bharti, S.K.; Nath, G.; Tilak, R.; Singh, S.K. (2010). Synthesis, anti-bacterial and anti-fungal activities of some novel Schiff bases containing 2,4-disubstituted thiazole ring. *Eur. J. Med. Chem.*, *45*, 651–660.

Bhowmik, P., Chattopadhyay, S., Drew, M. G. B., Diaz, D. & Ghosh, A. (2010). Synthesis, structure and magnetic properties of mono- and di-nuclear nickel(II) thiocyanate complexes with tridentate N_3 donor Schiff bases, *Polyhedron*, *29*, 2637-2642**.**

Bourn, D.; Prescott, J. (2002). A Comparison of the Nutritional Value, Sensory Qualities, and Food Safety of Organically and Conventionally Produced Foods. *Crit. Rev. Food Sci. Nutr. 42*, 1–34.

Bradford, M.M., (1976). A rapid and sensitive method for the quantitation of microgram quantities of protein utilizing the principle of protein-dye binding. *Anal Biochem*. 72, 248–254.

Cai, B.-H. (2009). [(2-Morpholinoethyl)(2-pyridylmethylene)amine]dithiocyanato zinc(II). *Acta. Cryst.* E65, m142.

Ceyhan, G.; Çelik, C.; Uruş, S.; Demirtaş, İ.; Elmastaş, M.; Tümer, M. (2011). Antioxidant, electrochemical, thermal, antimicrobial and alkane oxidation properties of tridentate Schiff base ligands and their metal complexes. *Spectrochim. Acta, 81*, 184–198.

Chattopadhyay, T., Ghosh, M., Majee, A., Nethaji, M. & Das, D. (2005). Linkage isomerism in 4-(2-aminoethyl)morpholine (L) complexes of nickel (II) nitrite: X-ray single crystal structure of *trans*-$[NiL_2(NO_2)_2]$. *Polyhedron*, *24*, 1677-1681.

CHEMICALS DOFO (2005) OECD Guideline for testing of chemicals. Available:

http://www.oecd.org/chemicalsafety/testingofchemicals/ oecd guidelines for the testing of chemicals and relateddocuments.htm. Accessed 2012 Nov 13.

Cotton F.A., Wilkinson G. Advanced Inorganic Chemistry (1998). Wiley-Interscience, New York.

Suparna Banerjee, Michael G. B. Drew, Can-Zhong Lu, Javier Tercero, Carmen Diaz, Ashutosh Ghosh. (2005). Dinuclear Complexes of M^{II} Thiocyanate (M = Ni and Cu) Containing a Tridentate Schiff-Base Ligand: Synthesis, Structural Diversity and Magnetic Properties. *Eur. J. Inorg. Chem. 12*, 2376–2383.

Chattopadhyay, T., Mukherjee, M., Banu, K. S., Banerjee, A., Suresh, E., Zangrando, E. & Das, D. (2009). Mono- and dinuclear Zn(II) complexes of Schiff-base ligands: syntheses, characterization and studies of photoluminescence. *J. Coord. Chem. 62*, 967-979.

Chen, G., Bai, Z.-P. & Qu, S.-J. (2005). [*N*,*N*'-Dimethyl-*N*''-(2-pyridylmethylene) ethane-1,2-diamine] dithiocyanatozinc(II). *Acta Cryst.* E61, m2483-m2484.

Chiumia, G. C., Craig, D. C., Phillips, D. J., Rae, A. D. & Zafar Kaifi, F. M. (1999). Terminal S-coordinated thiocyanate in a nickel(II) complex.: X-ray structures of Ni(poph) (H_2O)(SCN)(NCS) and Ni(poqh) (H_2O) $(NCS)_2$ (poph = 2-pyridine carboxaldehyde 1-oxide 2′-pyridinyl hydrazone, poqh = 2-pyridinecarboxaldehyde 1-oxide 2′-quinolynylhydrazone). *Inorg. Chim. Acta, 285*, 297-300.

Chohan, Z.H.; Arif, M.; Akhtar, M.A.; Supuran, C.T. (2006).Metal-Based Antibacterial and Antifungal Agents: Synthesis, Characterization, and In Vitro Biological Evaluation of Co(II), Cu(II), Ni(II), and Zn(II) Complexes with Amino Acid-Derived Compounds. *Bioinorg. Chem. Appl. 2006*, 83131.

Chohan Zahid H, Andrea Scozzafava, Claudiu T. Supuran. (2003). Zinc Complexes of Benzothiazole-derived Schiff Bases with Antibacterial Activity. *J. Enzyme Inhib. Med. Chem. 18*, 259–263.

Chohan, Z. H. Sumrra, S. H. (2010) Synthesis, characterization and biological properties of thienyl derived triazole Schiff bases and their oxovanadium(IV) complexes, 27, 2,187-193.

Choi, W.C.; Kim, S.C.; Hwang, S.S.; Choi, B.K.; Ahn, H.J.; Lee, M.Y.; Park, S.H.; Kim, S.K. (2002). Antioxidant activity and free radical scavenging capacity between Korean medicinal plants and flavonoids by assay-guided comparison. *Plant Sci*. *163*, 1161–1168.

Claudine, M.; Andrzej, M.; Augustin, S.(2005). Polyphenols and prevention of cardiovascular diseases. *Curr. Opin. Lipidol. 16*, 77–84.

Clemetso, C.A.B.; Andersen, L. Edward, M.M., Janet, M.S., Eds. (1966); New York Academy of Sciences: New York, NY, USA,; Volume 136,pp. 341–376.

Clinical and Laboratory Standards Institute (CLSI). (2011) *Performance Standard for Antimicrobial Susceptibility Testing; Twenty-First Information Supplement*; CLSI document M100-S21; CLSI:Wayne, PA, USA.

Cozzi, P.C. (2004) Metal-Salen Schiff base complexes in caalysis: Practical asects. *Chemical society Reviews*, 33: 410-421

Creaven, B.S.; Duff, B.; Egan, D.A.; Kavanagh, K.; Rosair, G.; Thangella, V.R. (2010). Anticancer and antifungal activity of copper(II) complexes of quinolin-2(1*H*)-one-derived Schiff bases, *Inorg. Chim. Acta, 363*, 4048–4058.

Cukurovali, A.; Yilmaz, İ.; Kirbag, S. (2006). Spectroscopic Characterization and Biological Activity of Salicylaldehyde Thiazolyl Hydrazone Ligands and their Metal Complexes, *Trans. Met. Chem. 31*, 207–213.

D.K. Perry, M.J. Smyth, H.R. Stennicke, G.S. Salvesen, P. Duriez, G.G. Poirier, H.Y. A. (1997). Zinc Is a Potent Inhibitor of the Apoptotic Protease, Caspase-3 A NOVEL TARGET FOR ZINC IN THE INHIBITION OF APOPTOSIS, *The J. Biol. Chem. 272* 18530-18533.

da Silva, C.M.; da Silva, D.L.; Modolo, L.V.; Alves, R.B.; de Resende, M.A.; Martins, C.V.B.; de Fatima, A. (2011). Schiff bases: A short review of their antimicrobial activities. *J. Adv. Res. 2*, 1–8.

Deoghoria, S.; Mostafa, G.; Lu, T.H.; Chandra, S.K. (2004). Synthesis, characterisation and properties of manganese(II) complexes having pseudohalide coordination : X-ray crystal

structure of an unusually distorted hexacoordinated [MnL(NCS)](ClO_4) species (L = pentadentate Schiff base ligand) *Ind. J. Chem., 43A*, 329–332

Diao, Y.-P. (2007). Di-μ-thiocyanato-κ^2S:*N*;κ^2N:*S*-bis {[*N*,*N*-dimethyl-*N*'-(2-pyridylmethylene-κN)ethane-1,2-diamine-κ^2N,*N*']nickel(II)} bis(perchlorate), *Acta Cryst. E63*, m1453-m1454.

Drew, M. G. B. & Hollis, S. (1978). A potentially seven-co-ordinate complex that is only five-co-ordinate;crystal and molecular structure of di-iodo (6,7,8,9-tetrahydro-16,22-di-methyl-5,10-dithia-15,23,24-triaza-17,21-methenodibenzo[*a*,*i*]cyclonona-decene-*NN'N''*)zinc(II) *J. Chem. Soc. Dalton Trans.* 511-516.

Drew, M. G. B., Das, D., De, S. & Datta, D. (2009). Effect of H-bonding on the ambivalence of SCN^- towards copper(II). *Inorg. Chim. Acta*, 362, 1501-1505.

Elerman, Y., Kabak, M. & Elmali, A. (2002). Crystal Structure and Conformation of N-(5-Chlorosalicylidene)-2-hydroxy-5-chloroaniline. *Z. Naturforsch. Teil B*, **57**, 651-656.

Elias, H.; Hilms, E.; Paulus, H. (1982). X-Ray structures and spectral properties of 4-coordinate copper(II) and palladium(II) complexes with a tridentate *ONN*-Schiff base ligand. *Naturforsch, Z. Teil B. 37*, 1266–1273.

Esposito, S.; Leone, S. (2007). Antimicrobial treatment for Intensive Care Unit (ICU) infections including the role of the infectious disease specialist, *Int. J. Antimicrob. Agents 29*, 494–500.

Gibson, V. C., McTavish, S., Redshaw, C., Solan, G. A., White, A. J. P. & Williams, D. J. (2003). From monomeric to polymeric manganese complexes bearing bis(imino)pyridine and related ligands. *Dalton Trans.* 221-226.

Goe, G.L. (1982). Pyridine and pyridine derivatives. In: Grayson, M. & Eckroth, D. *Kirk-Othmer Encyclop. of Chemic. Techn.*, 3rd ed., New York, John Wiley & Sons, Vol. 19, p. 474.

Golbabapour, S., Gwaram, N. S., Al-Obaidi, M. M. J., Soleimani, A., Ali, H. M., & Abdul Majid, N. (2013). Schiff Base Metal Derivatives Enhance the Expression of HSP70 and

Suppress BAX Proteins in Prevention of Acute Gastric Lesion. *BioMed Research International, 2013*

Golbabapour, S., Gwaram, N. S., Hassandarvish, P., Hajrezaie, M., Kamalidehghan, B., Abdulla, M. A., Majid, N. A. (2013). Gastroprotection studies of Schiff base zinc (II) derivative complex against acute superficial hemorrhagic mucosal lesions in rats. *PloS one, 8*(9), e75036.

Gwaram, N. S., Ali, H. M., Abdulla, M. A., Buckle, M. J., Sukumaran, S. D., Chung, L. Y., . . .Hadi, A. H. A. (2012). Synthesis, Characterization, X-ray crystallography, acetyl cholinesterase inhibition and antioxidant activities of some novel ketone derivatives of gallic hydrazide-derived Schiff bases. *Molecules, 17*(3), 2408-2427.

Gwaram, N. S., Ali, H. M., Khaledi, H., Abdulla, M. A., Hadi, A. H. A., Lin, T. K., . . . Ooi, C. L. (2012). Antibacterial Evaluation of Some Schiff Bases Derived from 2-Acetylpyridine and Their Metal Complexes. *Molecules, 17*(5), 5952-5971.

Gwaram, N. S., Ali, H. M., Saharin, S. M., Abdulla, M. A., Hassandarvish, P., Lin, T. K., . . . Ooi, C. L. (2012). Synthesis, characterization, and biological applications of some 2-acetylpyridine and acetophenone derivatives. *Journal of Applied Pharmaceutical Science Vol, 2*(12), 027-038.

Gwaram, N. S., Musalam, L., Ali, H. M., & Abdulla, M. A. (2012). Synthesis of 2'-(5-Chloro-2-Hydroxybenzylidene) Benzenesulfanohydrazide Schiff Base and its Anti-Ulcer Activity in Ethanol-Induced Gastric Mucosal Lesions in Rats. *Tropical Journal of Pharmaceutical Research, 11*(2), 251-257.

Gwaram, N. S., Musalam, L., Ali, H. M., Abdulla, M. A., & Shaker, S. A. (2012). Synthesis, spectral characterization and biological activity of Zn (II) complex with 2′-[1-(2-hydroxyphenyl) ethylidene] benzenesulfanohydrazide. *Arabian Journal of Chemistry*.

Hajrezaie, M., Golbabapour, S., Hassandarvish, P., Gwaram, N. S., Hadi, A. H. A., Ali, H. M.,. Abdulla, M. A. (2012). Acute toxicity and gastroprotection studies of a new schiff base

derived copper (II) complex against ethanol-induced acute gastric lesions in rats. PloS one, 7(12), e51537.

Gourbatsis, S., Perlepes, S. P., Butler, I. S. & Hadjiliadis, N. (1999). Zinc(II) complexes derived from the di-Schiff-base ligand *N*,*N*′-bis[1-(pyridin-2-yl) ethylidene]ethane-1,2-diamine (L_A) and its hydrolytic-cleavage product *N*-[1-pyridin-2-yl)ethylidene]ethane-1,2-diamine (L): preparation, characterization and crystal structure of the 5-coordinate species [$ZnLCl_2$]. *Polyhedron*, *18*, 2369-2375.

Guidos, R.J. (2010). The 10×'20 Initiative: Pursuing a Global Commitment to Develop 10 New Antibacterial Drugs by 2020. *Am. Clin. Infect. Dis. 50*, 1081–1083.

Guilhermino, L.; Lopes, M.C.; Carvalho, A.P.; Soares, A.M.V.M. (1996). Inhibition of acetylcholinesterase activity as effect criterion in acute test with juvenile, *liaphnia magna*. *Chemosphere*, *32*, 721-738.

Heo, B.G.; Park, Y.S.; Chon, S.U.; Lee, S.Y.; Cho, J.Y. (2007). Antioxidant activity and cytotoxicity of methanol extracts from aerial parts of Korean salad plants. *Gorinstein, S Biofactors,* 30, 79–89.

Heider, E.M.; Harper, J.K.; Grant, D.M.; Hoffman, A.; Dugan, F.; Tomere, D.P.; O'Neille, K.L. (2006). Unusual antioxidant activity in a benzoic acid erivative: A proposed mechanism for citrinin. *Tetrahedron*, *62*, 1199–1208.

Hisham, N.A.I.; Gwaram, N.S.; Khaledi, H.; Ali, H.M. (2011). Dichlorido {2-morpholino-N-[1-(2-pyridyl)ethylidene] ethanamine- 3N,N',N"}zinc(II). *Acta Crystallogr. 67*, 55.

Jian-Ying Miao, (2011) Synthesis and Crystal Structures of Bromido-Coordinated Zinc(II) and Copper(II) Complexes with Schiff Bases, *Synthesis and Reactivity in Inorganic, Metal-Organic, and Nano-Metal Chemistry,* 41:689–693

Lavrik, I.N. Golks, A. P.H. K. J. (2005). Clin. Investig. Caspases: *pharmacol. Manip. cell death, 115,* 2665-2672.

Lever A.B.P. (1968): Inorganic Electronic Spectroscopy. Elsevier publishing, Amsterdam.

Lippard S J and Berg J M, (1994) Principles of bioinorganic chemistry: pp 411. University Science Books, Mill Valley, California. ISBN 0-935702-73-3

Lindsay Smith, J. R.; McKeer, L. C.; Taylor, J. M. (1993), "4-Chlorination of Electron-Rich Benzenoid Compounds: 2,4-Dichloromethoxybenzene", *Org. Synth.*; *Coll. Vol. 8*, 167

Ispir, E.; Toroglu, S.; Kayraldrz, A. (2008). Syntheses, characterization, antimicrobial and genotoxic activities of new Schiff bases and their complexes. *Transit. Met Chem., 33*, 53–960.

Narula, J. Pandey, P. Arbustini, E. Haider, N. Narula, N. Kolodgie, F.D. Dal, B. Bello, M.J. Semigran, Bielsa-Masdeu, A. Dec, G.W. (1999). *Proceedings of the National Academy of Sciences, 96*, 8144-8149.

Summerton, J.E. (2007) Morpholino, siRNA, and S-DNA compared: impact of structure and mechanism of action on off-target effects and sequence specificity. *Curr. Top. Med. Chem.,* 7(7):651-60.

Kadoma, Y.; Atsumi, T.; Okada, N.; Ishihara, M.; Yokoe, I.; Fujisawa, S. (2007). Radical-scavenging Activity of Natural Methoxyphenols *vs.* Synthetic Ones using the Induction Period Method. *Molecules, 12*, 130–138.

Kalagouda, B.G.; Manjula, S.P.; Ramesh, S.V.; Rashmi, V.S.; Siddappa, A.P. (2006). X-ray crystal structure of the *N*-(2-hydroxy-1-naphthalidene)phenylglycineSchiff base. Synthesis and characterization of its transition metal complexes. *Trans. Met. Chem. 31*, 580–585.

Katunuma, N. Matsu, A. Le, Q.T. Utsumi, K. Salvesen, G. O. A (2001). Novel procaspase-3 activating cascade mediated by lysoapoptases and its biological significances in apoptosis. *Adv. Enzyme Regul. 41,* 237-250.

Khaledi, H.; Alhadi, A.A.; Yehye, W.A.; Ali, H.M.; Abdulla, M.A.; Hassandarvish, P. (2011). Antioxidant, cytotoxic activities, and structure-activity relationship of gallic acid-

based indole derivatives. *Arch. Pharm. 344*, 703–709.

Kim, J.G., Yu, D.S., Moon, S.H., Park, J.I. & Park, W.W. (1993). Reactions ofcyanopyridines with organometallics. *J. Korean Chem. Soc.*, **37**(9), 826-831 [STN Abstract: CA121-108454]

Kuhn, D.J.; Lam, W.H.; Kazi, A.; Daniel, K.G.; Song, S.J.; Chow, L.M.C. (2005) Synthetic peracetate tea polyphenols as potent proteasome inhibitors and apoptosis inducers in human cancer cells. *Front Biosci. 10*, 1010–1023.

Kureshy, R. I.; Khan, N. H.; Abdi, S. H. R.; Patel S.T.; Iyer, P. (1999) Chiral Ru(II) Schiff base complexes catalyzed enantioselective epoxidation of styrene derivatives using iodosyl benzene as oxidant II. *J. Mol. Catal. A: Chem. 150(1-2)*, 175-183.

Lakshmi, B.; Avaji, P.G.; Shivananda, K.N.; Naggella, P.; Manohar, S.H.; Mahendra, K.N. (2011). Synthesis, spectral characterization and in vitro microbiological evaluation of novel glyoxal, biacetyl and benzil bis-hydrazone macrocyclic Schiff bases and their Co(II), Ni(II) and Cu(II) complexes. *Polyhedron 30*, 1507–1515.

Laskar, I.R.; Maji, T.K.; Das, D.; Lu, T.H.; Wong, W.-T.; Okamoto, K.-i.; Chaudhuri, N.R. (2001). Syntheses, characterisation and solid state thermal studies of 1-(2-aminoethyl)piperidine (L), 1-(2-aminoethyl)pyrrolidine (L) and 4-(2-aminoethyl) morpholine (L.) complexes of nickel(II): X-ray single crystal structure analyses of trans-[NiL2(CH3CN)2](ClO4)2, trans-[NiL2(NCS)2] andtrans-[NiL-2(NCS)2]. *Polyhedron, 20*, 2073–208 2.

Laskwoski, R.A. (2001). Summaries and analyses of PDB structure. *Nucleic Acids Res*. *29*, 221–222.

Li P, Nijhawan D, W. X., (2004). Mitochondrial activation of apoptosis. *Cell. 116*, S57-59.

Li, P., Solanki, N. K., Ehrenberg, H., Feeder, N., Davies, J. E., Rawson, J. M. & Halcrow, M. A. (2000). Copper(II) complexes of hydroquinone-containing Schiff bases. Towards a structural model for copper amine oxidases. *J. Chem. Soc. Dalton Trans.* 1559-1565.

Liu, C. Wang, Y. Xie, S. Zhou, Y. Ren, X. Li, X. Cai, Y. (2011). Liquiritigenin induces mitochondria-mediated apoptosis via cytochrome c release and caspases activation in heLa Cells. *Phytother. Res., 25* 277-283.

Mahmood AA, Mariod AA, Al-Bayaty F, Abdel-Wahab SI (2010) Antiulcerogenic activity of Gynura procumbens leaf extract against experimentallyinduced gastric lesions in rats. *Journ. Medic. Plants Res.* 4: 685–691.

Manabu, F.; Hisanobu, W.; Takayuki, M.; Toshiyuki, S. (1990). Preparation of 14-, 18-, and 22-membered tetraaza macrocycles and their complexing ability for copper(ii) and nickel(II) ions. *Bull. Chem. Soc. Jpn. 63*, 3443–3449.

Mandal, S.; Karmakar, T.K.; Ghosh, A.; Fleck, M.; Bandyopadhyay, D. (2011). Synthesis, crystal structure and antibacterial activity of a group of mononuclear manganese(II) Schiff base complexes. *Polyhedron 30*, 790–795.

Mohamed, M.; Hapipah, M.A.; Mahmood, A.A.; Robinson, T.W. (2009). Synthesis, structural characterization, and anti-ulcerogenic activity of Schiff base ligands derived from tryptamine and 5-chloro, 5-nitro, 3,5-ditertiarybutyl salicylaldehyde and their nickel(II), copper(II), and zinc(II) complexes. *Polyhedron*, *28*, 3993–3998.

Mukhopadhyay, S., Mandal, D., Ghosh, D., Goldberg, I. & Chaudhury, M. (2003) Equilibrium Studies in Solution Involving Nickel(II) Complexes of Flexidentate Schiff Base Ligands: Isolation and Structural Characterization of the Planar Red and Octahedral Green Species Involved in the Equilibrium. *Inorg. Chem. 42,* 8439-8445.

Petrovic, N. Comi, A. Ettinger, M.J. (1996). Identification of an Apo-Superoxide Dismutase (Cu,Zn) Pool in Human Lymphoblasts, *J. Biol. Chem., 271*, 28331

Naeimi, H., Safari, J. & Heidarnezhad, A. (2007). Synthesis of Schiff base ligands derived

from condensation of salicylaldehyde derivatives and synthetic diamine. *Dyes Pigments, 73*, 251–253.

Nair, M., Shi, Z., Karwe, M.V., Ho, C.T. & Daun, H. (1994) Collection and characterization of volatile compounds released at the die during twin screw extrusion of corn flour. *ACS Symp. Ser. 543 Thermal. Generat. Flav.*, 334-347 [STN Abstract: CA120-105394].

Noyori, R.; Yokoyama, K.; Hayakawa, Y. (1988), "Cyclopentenones from α,α'-Dibromoketones and Enamines: 2,5-Dimethyl-3-Phenyl-2-Cyclopenten-1-one", *Org. Synth.*; *Coll. Vol.* **6**: 520

Pandeya, S.N.; Sriram, D.; Nath, G.; DeClercq, E. (1999) Synthesis, antibacterial, antifungal and anti HIV activities of Schiff and Mannich bases derived from isatin derivatives and N-[4-(4-chlorophenyl) thiazol-2-yl] thiosemicarbazide. *Eur. J. Pharm. Sci. 9*, 25–31.

Pignatello, R.; Panico, A.; Mazzone, P.; Pinizzotto, M.R.; Garozzo, A.; Fumeri, P.M. (1994). Schiff bases of *N*-hydroxy-*N*′-aminoguanidines as antiviral, antibacterial and anticancer agents. *Eur. J. Med. Chem. 29*, 781–785.

Porter, A.G. Janicke. R.U. (1999). Emerging roles of caspase-3 in apoptosis. *Cell death differentiation, 6*, 99-104.

Prakash, A.; Singh, B.K.; Bhojak, N.; Adhikari, D. (2010). Synthesis and characterization of bioactive zinc(II) and cadmium(II) complexes with new Schiff bases derived from 4-nitrobenzaldehyde and acetophenone with ethylenediamine. *Spectrochim. Acta 76*, 356–362.

Principles of Bioinorganic Chemistry S. J. Lippard, J. M. Berg. University Science Books, 1994 ISBN: 0-935702-72-5

Qiao, X.; Ma, Z.-Y.; Xie, C.-Z.; Xue, F.; Zhang, Y.-W.; Xu, J.-Y. (2011). Study on potential antitumor mechanism of a novel Schiff Base copper(II) complex: Synthesis,

crystal structure, DNA binding, cytotoxicity and apoptosis induction activity. *J. Inorg. Biochem. 105*, 728–737.

Quian Quiroga, R., Nadasdy, N., and Ben-Shaul, Y. (2004). Unsupervised spike sorting with wavelets and super paramagnetic clustering. *Neural Comput. 16*, 1661–1687.

Reardon, D., Aharonian, G., Gambarotta, S. & Yap, G. P. A. (2002). Mono- and Zerovalent Manganese Alkyl Complexes Supported by the α,α‘-Diiminato Pyridine Ligand: Alkyl Stabilization at the Expense of Catalytic Performance. *Organometallics, 21,* 786-788.

Rice-Evans, C. (1999). In Proceedings of the Society for Experimental Biology and Medicine, London, UK, Volume 220, pp. 262–266.

Rigamonti, L., Cinti, A., Forni, A., Pasini, A. & Piovesana, O. (2008). Copper(II) Complexes of Tridentate Schiff Bases of 5-Substituted Salicylaldehydes and Diamines – The Role of the Substituent and the Diamine in the Formation of Mono-, Di- and Trinuclear Species – Crystal Structures and Magnetic Properties. *Eur. J. Inorg. Chem.,* 3633-3647.

Mohan, S. Abdelwahab, S.I. Kamalidehghan, B. Syam, S. May, K.S. Harmal, N.S.M. Shafifiyaz, N. Hadi, A.H.A. Hashim, N.M. Rahmani, M. (2012) GmbH. *Phytomed. Article in Press*, All rights reserved. http://dx.doi.org/10.1016/j.phymed.2012.1005.1012.

Saleh Salga, M., Khaledi, H., Mohd Ali, H. & Puteh, R. (2010). Dichlorido {*N*,*N*-dimethyl-*N*'-[1-(2-pyridyl)ethylidene]ethane-1,2-diamine-κ^3*N*,*N*',*N*''} copper (II). *Acta Cryst.* E66, m508.

Samoylenko, O.; Zaletok, S.; Orlovsky, O.; Gogol, S.; Klenov, O.; Shapochka, D. (2011). P123 Additive antitumor effect of plant polyphenols and a synthetic inhibitors of polyamines biosynthesis. *Breast, 20*, S22–S23.

Schmiege, B. M., Carney, M. J., Small, B. L., Gerlach, D. L. & Halfen, J. A. (2007). Alternatives to pyridinediimine ligands: syntheses and structures of metal complexes supported by donor-modified α-diimine ligands. *Dalton Trans.* 2547-2562.

Sedlak, J., Lindsay, R.H., (1968). Estimation of total, protein-bound, and nonprotein sulfhydryl groups in tissue with Ellman's reagent. *Anal Biochem 25,* 192–205.

Sengupta S. K., O. P. Pandey, B. K. Srivastava and V. K. Sharma (1998) "Synthesis, structural and biochemical aspects of titanocene and zirconocene chelates of acetylferrocenyl thiosemicarbazones," *Transition Metal Chemistry*: 23 (4), 349–353.

Sengupta, P. Ghosh, S. Mak, T.C.W. (2001) A new route for the synthesis of bis(pyridine dicarboxylato)bis(triphenylphosphine) complexes of ruthenium(II) and X-ray structural characterisation of the biologically active *trans*-$[Ru(PPh_3)_2(L^1H)_2]$ (L^1H_2=pyridine 2,3-dicarboxylic acid). *Polyhderon:* Vol 20, 975.

Shahabadi, N.; Kashanian, S. (2010). DNA binding and DNA cleavage studies of a water soluble cobalt(II) complex containing dinitrogen Schiff base ligand: The effect of metal on the mode of binding, *Eur. J. Med. Chem*. *45*, 4239–4245.

Shi, X.-F., Xie, M.-J. & Ng, S. W. (2006). *cis*-Dichloro (2-morpholinoethylamine-κ^2*N*,*N*')platinum(II). *Acta Cryst. E62*, m2719-m2720.

Shayma A.S.,, Yang F., Sadia M., Eskender M. (2010).Synthesis and Characterization of Mixed Ligand Complexes of Caffeine, Adenine and Thiocyanate with Some Transition Metal Ions. *Sains Malays*. 39: 957–962.

Shayma A.S., Yang F., Abbas A.S. (2009). Synthesis and Characterization of Mixed Ligand Complexes of 8-Hydroxyquinoline and o-hydroxybenzylidene-1-phenyl-2,3-dimethyl-4-amino-3-pyrazolin-5-on with Fe(II), Co(II), Ni(II) and Cu(II) ions. *Eur. J. Sci. Res*. 33: 702-709.

Smith, Jerry March (2001) *March's Advanced Organic Chemistry: Reactions, Mechanisms, and Structure* Michael B. Wiley-Interscience, 5th edition, ISBN 0-471-58589-0

Souza, P., Garcia-Vazquez, J. A. & Masaguer, J. R. (1985). Synthesis and characterization of copper(II) and nickel(II) complexes of the Schiff base derived from 2-(2-aminophenyl)benzimidazole and salicylaldehyde. *Transition Met. Chem. 10*, 410–412.

STN International (1996a) STN databases: CHEMLIST. Columbus, OH, Chemical Abstracts Service. STN International (1996b) STN databases: Registry, CA. Columbus, OH, Chemical Abstracts Service.

Sun, Y., Oberley, L.W., Li, Y., (1988). A simple method for clinical assay of superoxide dismutase. *Clin Chem* 34, 497–500.

Syam, S. Abdul, A.B. Sukari, M.A. Mohan, S. Abdelwahab, S.I. Wah, T.S. (2011). The Growth Suppressing Effects of Girinimbine on Hepg2 Involve Induction of Apoptosis and Cell Cycle Arrest, *Molecules 16* 7155-7170.

Syam, S. Abdelwahab, S.I. Al-Mamary, M.A. Mohan, S. (2012). Synthesis of Chalcones with Anticancer Activities. *Molecules. 17,* 6179-6195.

Tansir A., Nahid N., Parveen S. (2008). Synthesis, characterization and anti-microbial studies of a newlydeveloped polymeric Schiff base and its metal-polychelates. *J. Coord. Chem.*; 61: 1963–1972.

Rahaman, S.H. Chowdhury, H. Bose, D. Ghosh, R. Hung, C.-H. Ghosh, B.K. (2005). Synthesis, structure and properties of mononuclear cobalt(II) and cobalt(III) pseudohalide complexes containing N-donor Schiff bases: Synthetic control of metal oxidation levels. *Polyhedron. 24,* 1755-1763.

Sridhar, S.K.; Pandeya, S.N.; Stables, J.P.; Ramesh, A. (2002). Anticonvulsant activity of hydrazones, Schiff and Mannich bases of isatin derivatives. *Eur. J. Pharm. Sci. 16*, 129–132.

Stockdale, M.; Selwyn, M.J. (1971). Effects of Ring Substituents on the Activity of Phenols as Inhibitors and Uncouplers of Mitochondrial Respiration. *Eur. J. Biochem. 21*, 565–574.

Sun, Y.-X. (2005). Dichloro[*N*,*N*-dimethyl-*N*'-(pyridin-2-ylmethylidene) ethane-1,2-diamine] zinc(II). *Acta Cryst. E61,* m373-m374.

Sun-Waterhouse, D.; Chen, J.; Chuah, C.; Wibisono, R.; Melton, L.D.; Laing, W. (2009). Kiwifruit-based polyphenols and related antioxidants for functional foods: kiwifruit extract-

enhanced gluten-free bread. *Int. J. Food Sci. Nutr. 60*, 251–264.

Suo, J. (2008). Bis{μ-4-chloro-2-[(2-pyridylethyl)iminomethyl] phenolato}bis [chloridocopper(II)]. *Acta Cryst.* E64, m1046.

Tajudeen, S.S.; Radha, E. (2009). Synthesis, Characterization and Antimicrobial Activity of Transition Metal Complexes of Schiff Base Derivatives from Isonicotinic Acid Hydrazide. *Asian J. Chem. 21*, 313–316.

Tansir, A.; Nahid, N.; Shadma, P. (2008). Synthesis, characterization and anti-microbial studies of a newly developed polymeric Schiff base and its metal-polychelates. *J. Coord. Chem. 61*, 1963–1972.

Varley, H.A., Gowenlock, H., Bell, M., (1980). *Practical Clinical Biochemistry*, fifth ed. The Whitefrairs Press, London.

Vinayak V. Kane and Maitland Jones Jr (1990). "Spiro[5.7]trideca-1,4-dien-3-one", *Org. Synth.*; *Coll. Vol.* **7**: 473

Walters J., Pop C., Scott F.L., Drag M., Swartz P., Mattos C., Salvesen G.S., A.C. C, (2009). A constitutively active and uninhibitable caspase-3 zymogen efficiently induces apoptosis. *Biochem. J. 424*, 335-345.

Wang, J. & You, Z. (2007). Chlorido{2,4-dichloro-6- [(2-diethylaminoethylimino) methyl]phenolato}copper(II). *Acta Cryst.* E63, m1200-m1201.

Wang, Q., Bi, C.-F., Wang, D.-Q. & Fan, Y.-H. (2009). Dichlorido{*N*-[1- (2-pyridyl)ethylidene]ethane-1,2-diamine}copper(II). *Acta Cryst.* E65, m439.

Wiesner, J.; Kriz, Z.; Kuca, K.; Jun, D.; Koca, J. (2007). Acetylcholinesterases – the structural similarities and differences. *J. Enzyme Inhib. Med. Chem., 22*, 417–424.

Xu, D.; Ma, S.; Du, G.; He, Q.; Sun, D. (2008). Synthesis, characterization, and anticancer properties of rare earth complexes with Schiff base and o-phenanthroline. *J. Rare Earth., 26*, 643–647.

Xu, R.-B., Xu, X.-Y., Wang, M.-Y., Wang, D.-Q., Yin, T., Xu, G.-X., Yang, X.-J., Lu, L.-D., Wang, X. & Lei, Y.-J. (2008). Crystal structure and properties of a Cu(II) complex with

the tridentate Schiff-base ligand, paeonol(2-aminoethylpiperazine), *J. Coord. Chem. 61,* 3306-3313.

Xue, L.-W., Zhao, G.-Q., Han, Y.-J., Chen, L.-H. & Peng, Q.-L. (2010). {*N*,*N*-Dimethyl-*N*'-[1-(2-pyridyl)ethylidene]propane-1,3-diamine}bis(thiocyanato-κ*N*) copper (II). *Acta Cryst.* E66, m1274.

You, Z.-L., Jiao, Q.-Z., Niu, S.-Y. & Chi, J.-Y. (2006). Syntheses, Characterization and Crystal Structures of Three Structurally Similar Dinuclear Schiff Base Cadmium(II) Complexes with Bridging Azide or Thiocyanate Ligands. *Z. Anorg. Allg. Chem. 632,* 2486-2490.

You, Z.-L., Wang, J. & Han, X. (2006). [*N*,*N*-Diethyl-*N*'- (2-pyridylmethylene) ethane-1,2-diamine]dithiocyanatocopper(II). *Acta Cryst. E62,* m860-m861.

You, Z.L.; Chi, J.Y. (2006). Synthesis, crystal structures and antibacterial activities of two Schiff base zinc(II) complexes. *Synth. React. Inorg. Met.-Org., Nano-Met. Chem., 36,* 713–717.

Yousefi, M. (2010). Diiodido(2,3,5,6-tetrapyridin-2-ylpyrazine-κ^3N^2,N^1,N^6)zinc(II). *Acta Cryst. E66,* m1600-m1601.

Yue, G.-R., Xu, X.-J., Shi, Y.-Z. & Feng, L. (2005). [*N*,*N*-Dimethyl-*N*'- (2-pyridylmethylene)ethane-1,2-diamine]dithiocyanatocopper(II). *Acta Cryst. E61,* m693-m694.

Yusnita, J.; Puvaneswary, S.; Ali, H.M.; Robinson, W.T.; Lin, T.K. (2009). Synthesis, structural characterization and antibacterial activity of 2,6-diacetylpyridine bis(benzenesulfonohydrazide) Schiff bases and their copper(II) complexes. *Polyhedron 28,* 3050–3054.

Zahra AA, Kadir FA, Mahmood AA, Al hadi AA, Suzy SM, et al. (2011) Acute toxicity study and wound healing potential of Gynura procumbens leaf extract in rats. *J. Medicin. Plants Res*. 5: 2551–2558.

Zahra, M.A.S.F., A.A. Mahmood, M.A. Hapipah, M.N. Suzita and I. Salmah, (2009). Anti-ulcerogenic activity of aqueous extract of ficusdeltoidea against ethanol-induced gastric mucosal injury in rats. *Res. J. Med. Sci.*, 3(2): 42-46.

Zakrzewski, G.; Lingafelter, E.C. (1970). The crystal and molecular structure of dibromo-1- (2-pyridyl)-2,5-diaza-5-methyl-hexa-1-enezinc(II). *Inorg. Chim. Acta*, *4*, 251–257.

Zhang, J.A.; Pan, M.; Zhang, J.Y.; Kang, B.S.; Su, C.Y. (2009). Syntheses, structures and bioactivities of cadmium(II) complexes with a tridentate heterocyclic N- and S-ligand. *Inorg. Chim. Acta*, *362*, 3519–3525.

Zhao, K., Yin, X.-H., Lin, C.-W., Meng, D.-X. & Wu, F. (2008). Bis[6-(3,5-dimethyl-1*H*-pyrazol-1-yl)picolinato]nickel(II)-aqua[6-(3,5-dimethyl-1*H*-pyrazol-1-yl)picolinic acid]dithiocyanatonickel(II) (1/1). *Acta Cryst.* E64, m84-m85.

Zhong-Lu You, Yong-Ming Cui, Yu-Ping Ma, Che Wang, Xiao-Shuang Zhou, Kun Li, Synthesis, characterization and urease inhibitory activity of oxovanadium(V) complexes with similar Schiff bases. *Inorg. Chem. Comm.* 14(5):636-640.

APPENDICES

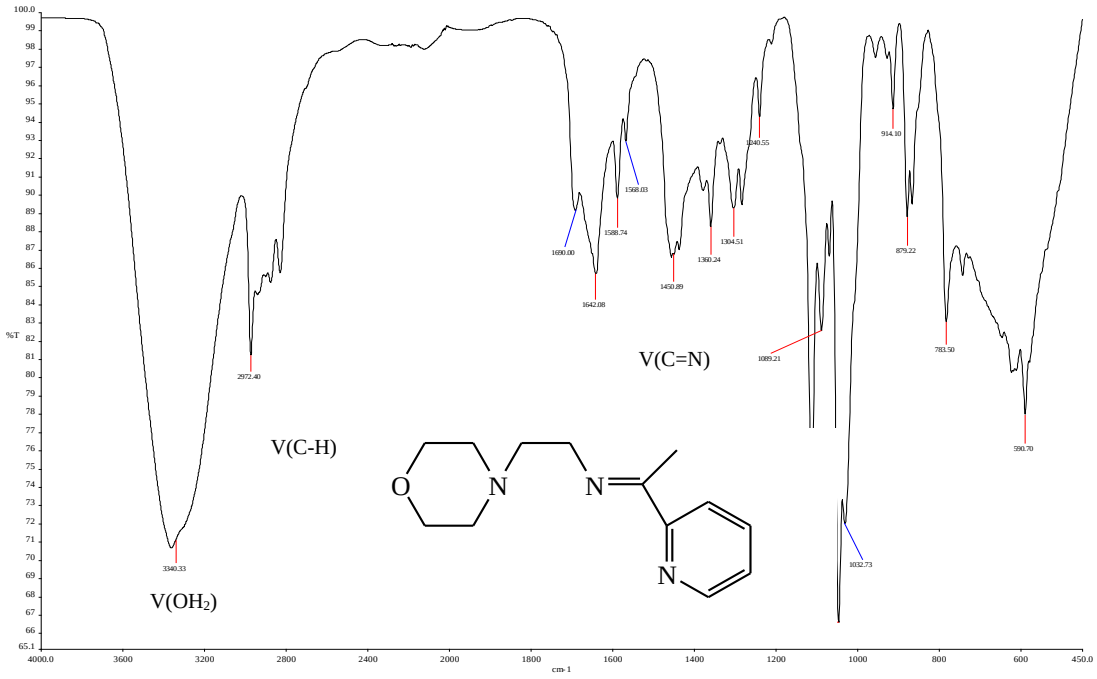

Appendix 1: IR spectra of (LMA)

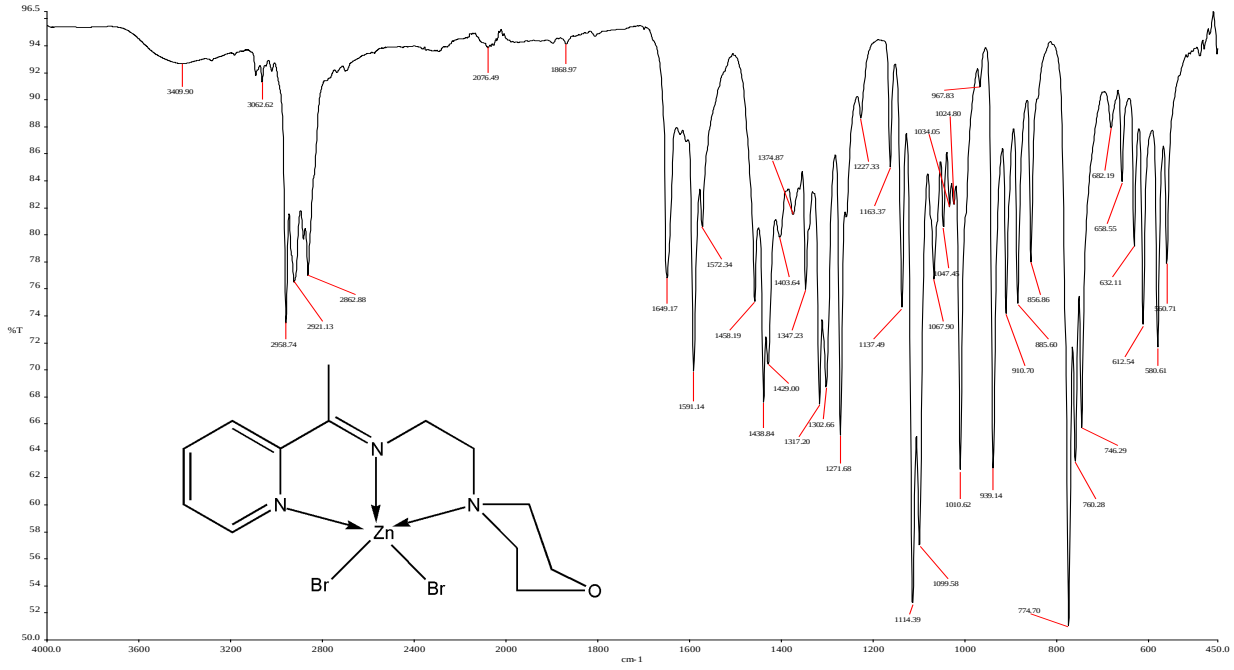

Appendix 2: IR spectra of [Zn(LMA)Br2]

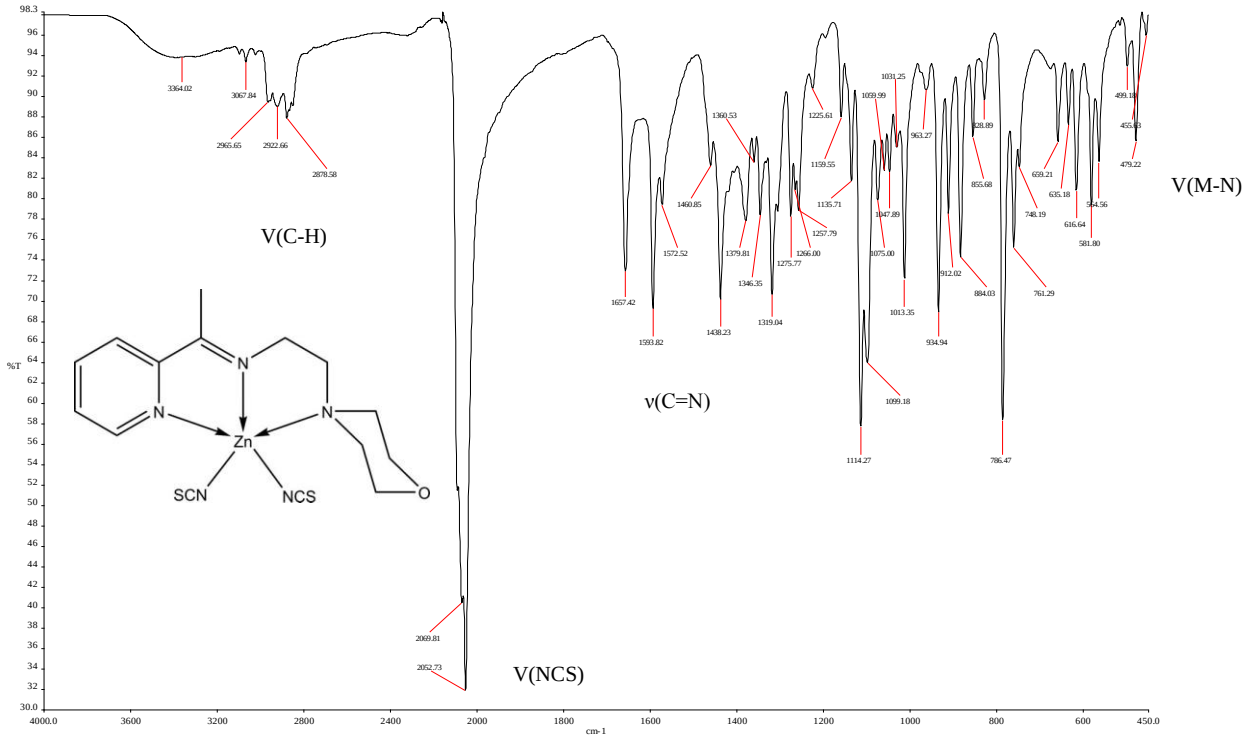

Appendix 3: IR spectra of $Zn(LMA)(NCS)_2$

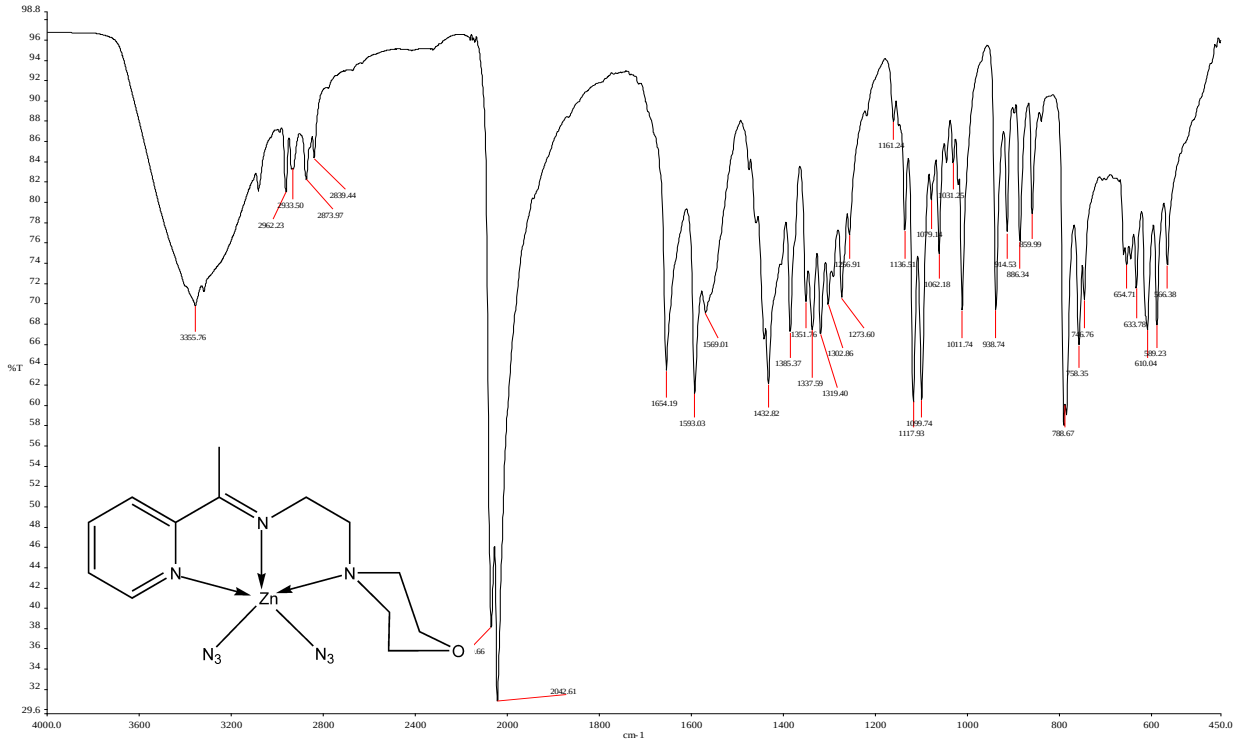

Appendix 4: IR spectra of $[Zn(LMA)(N_3)_2]$

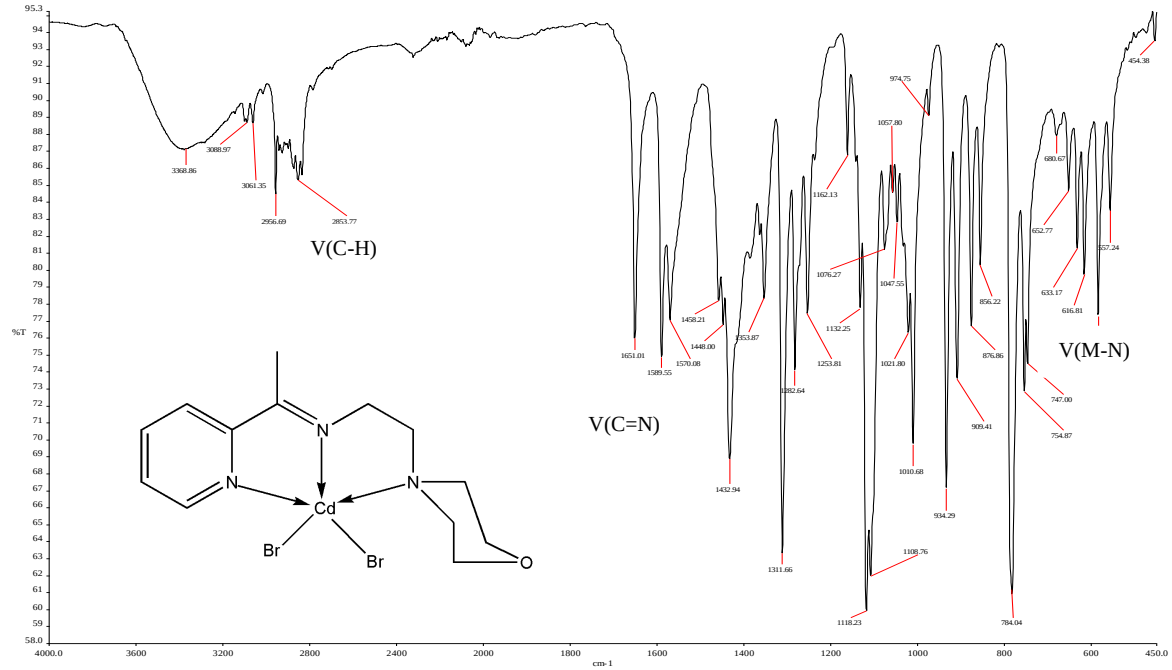

Appendix 5: IR spectra of [Cd(LMA)Br_2]

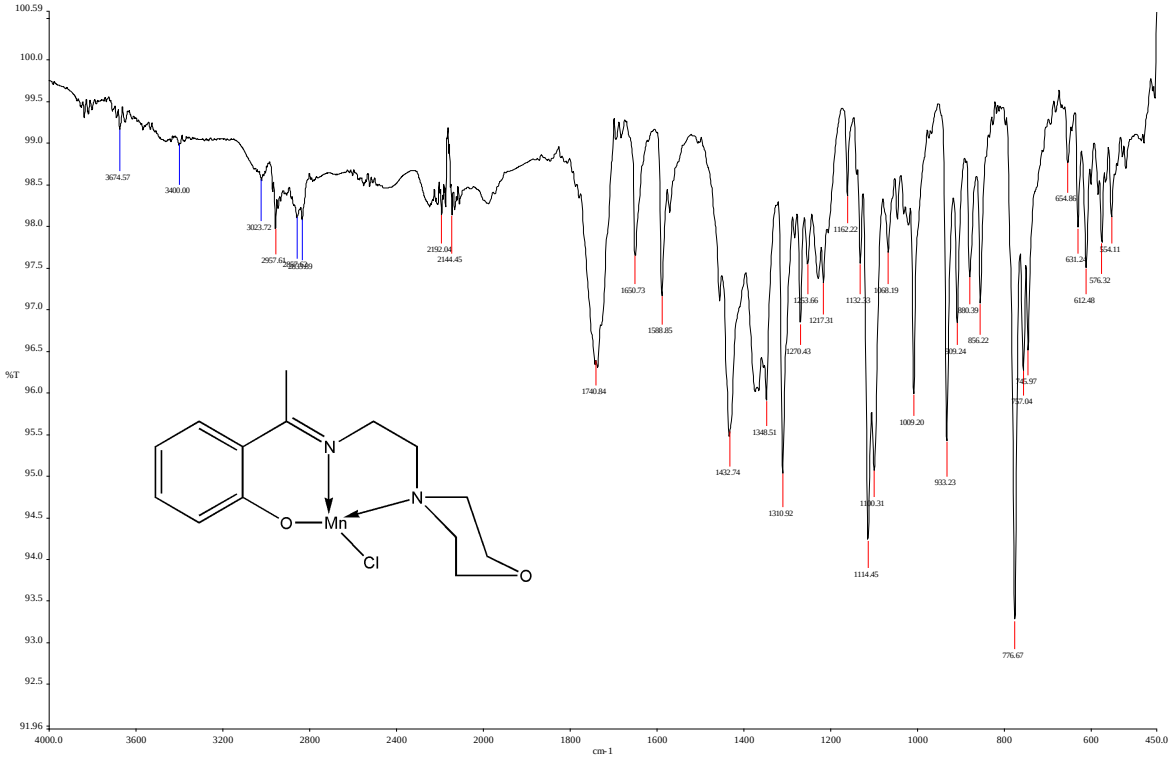

Appendix 6: IR spectra of [Mn(LMH)Cl]

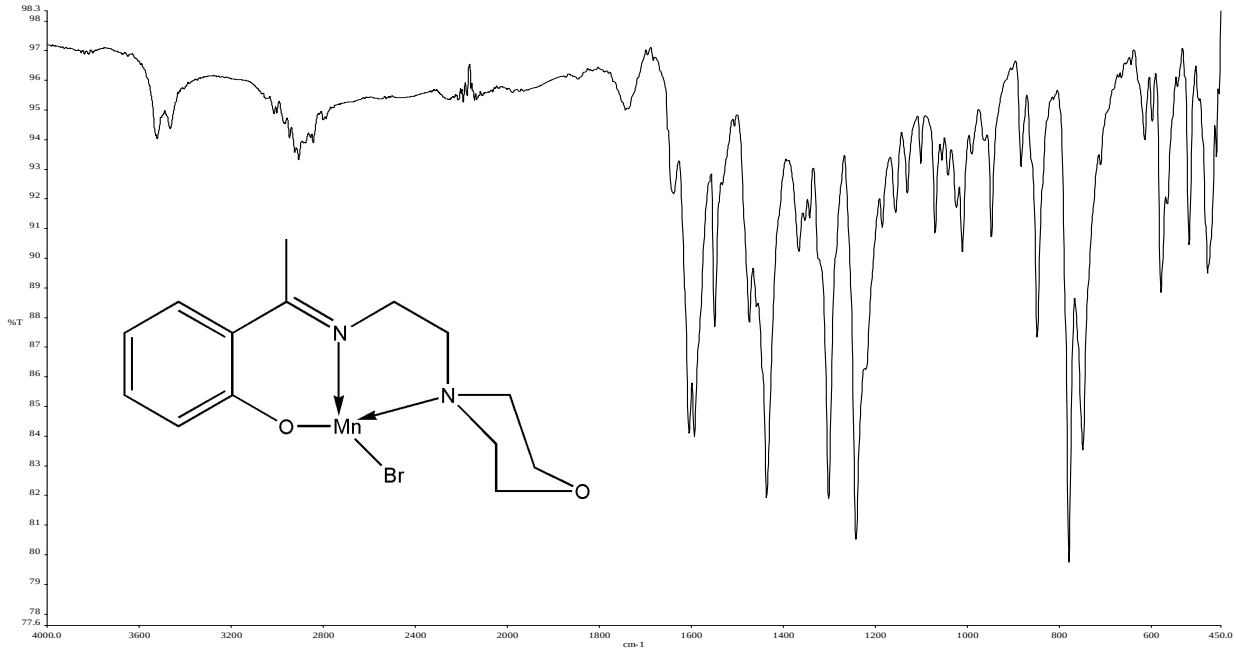

Appendix 7: IR spectra of [Mn(LMH)Br]

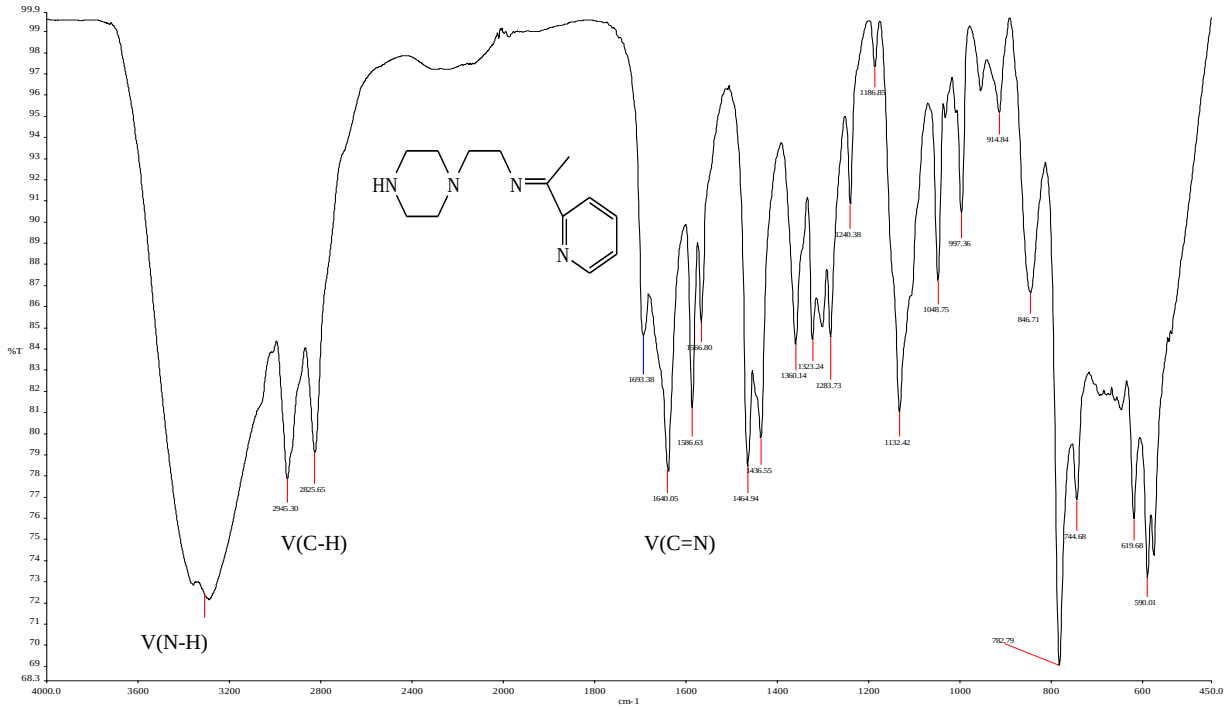

Appendix 8: IR spectra of (LPA)

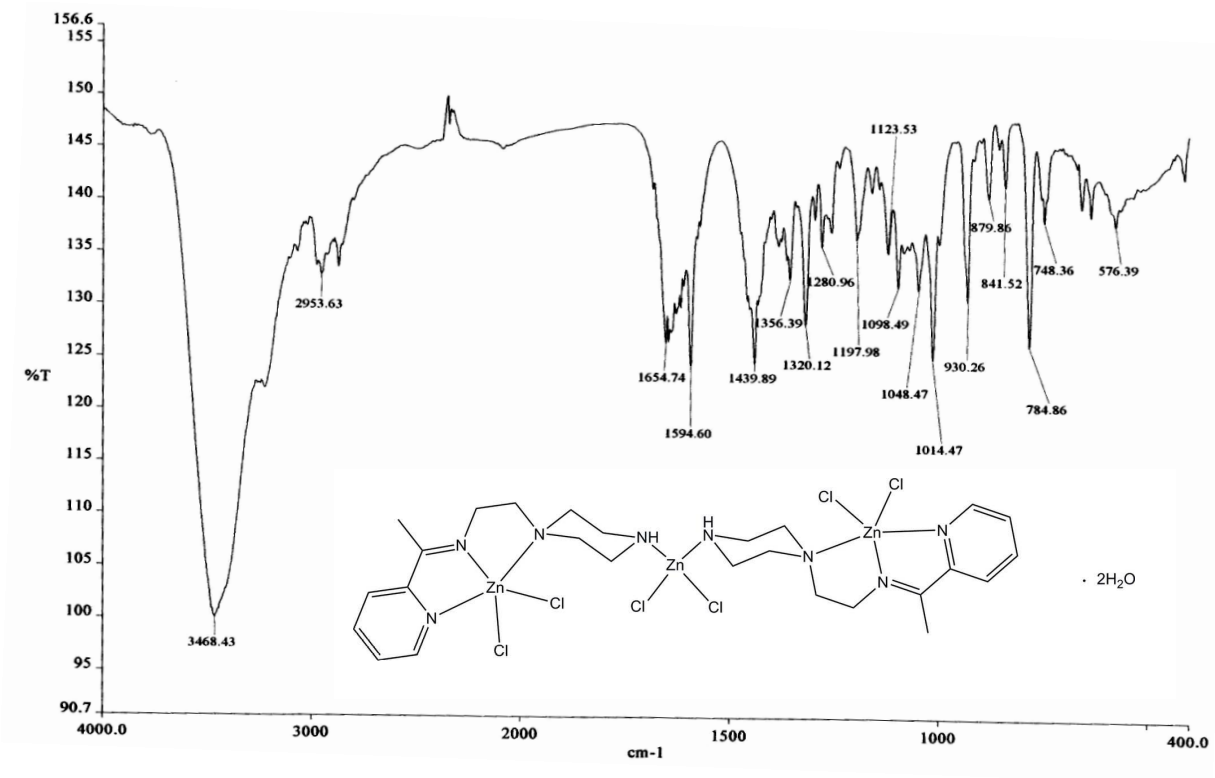

Appendix 9: IR spectra of $[Zn_2(LPA)_2Cl_6]$

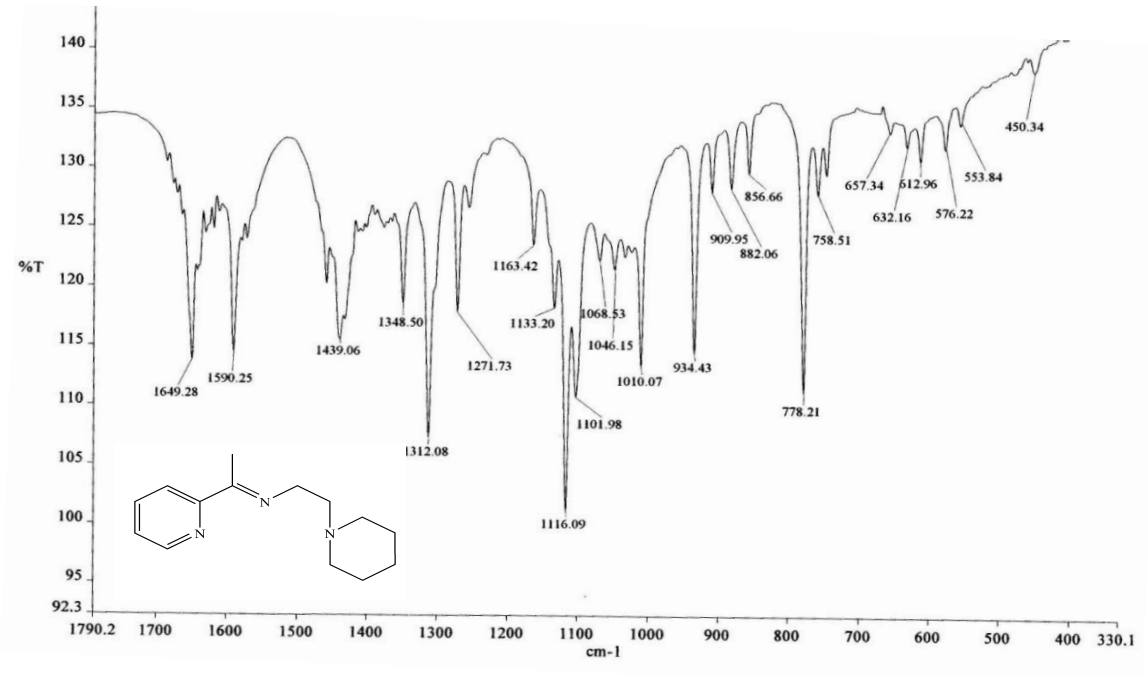

Appendix 10: IR spectra of LPiA

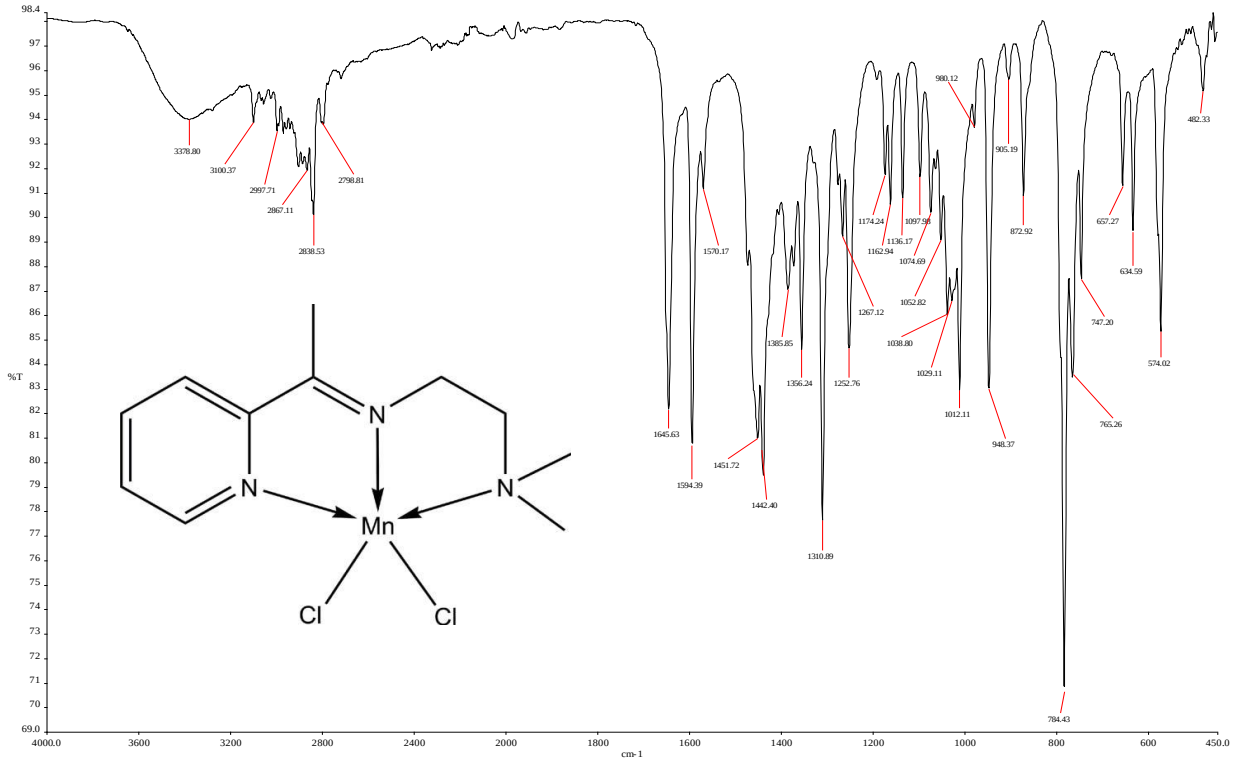

Appendix 11: IR spectra of [Mn(LNA)Cl_2]

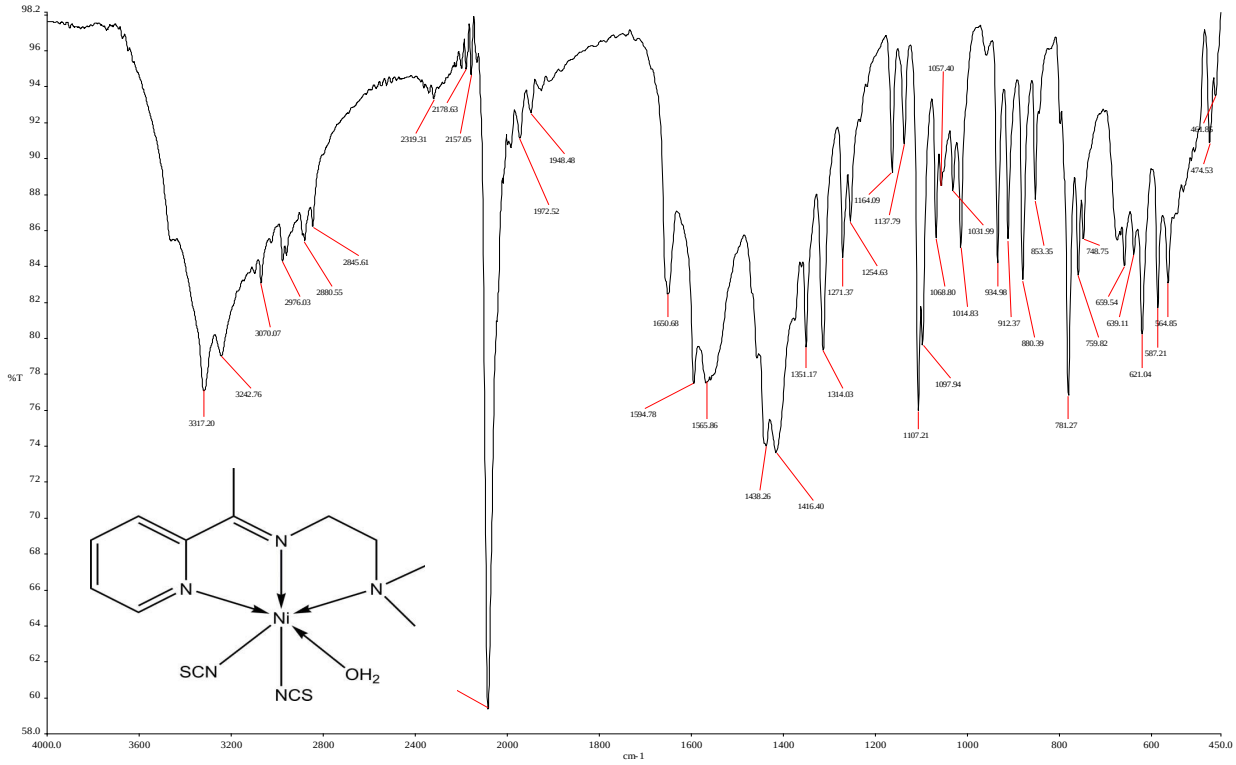

Appendix 12: IR spectra of [Ni(LNA)$(NCS)_2H_2O$]

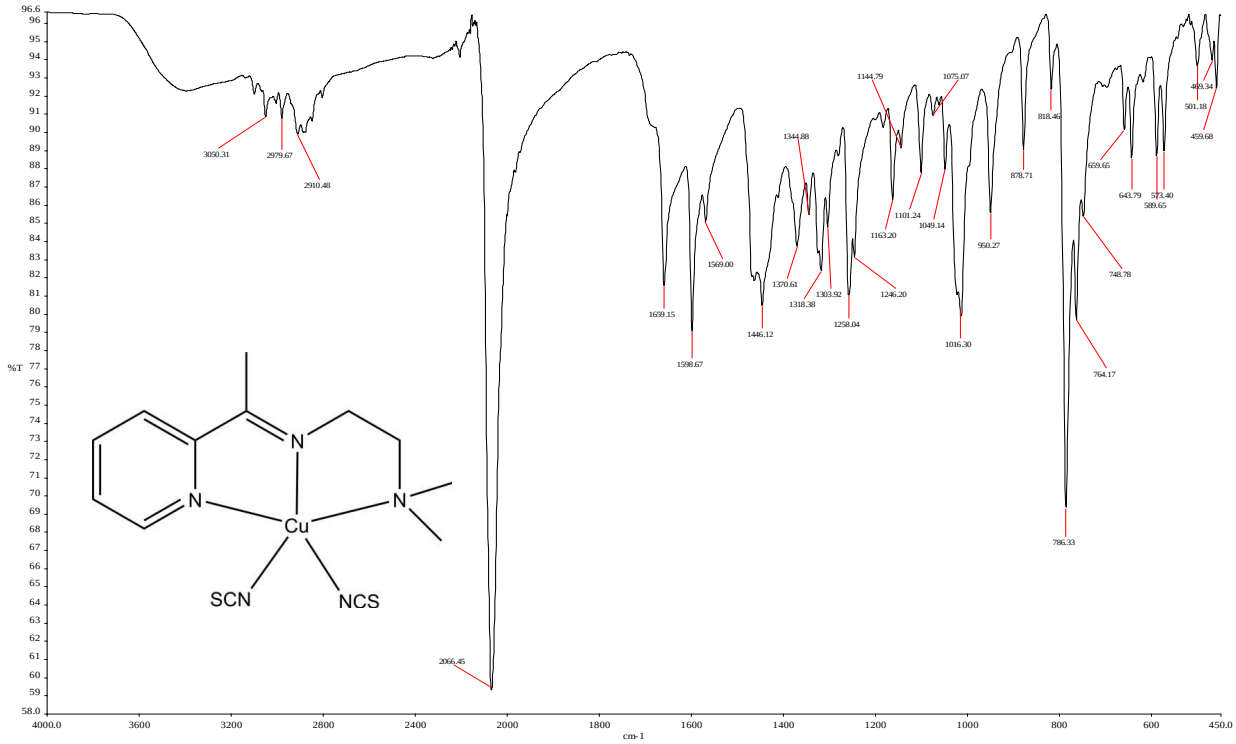

Appendix 13: IR spectra of [Cu(LNA)$(NCS)_2$]

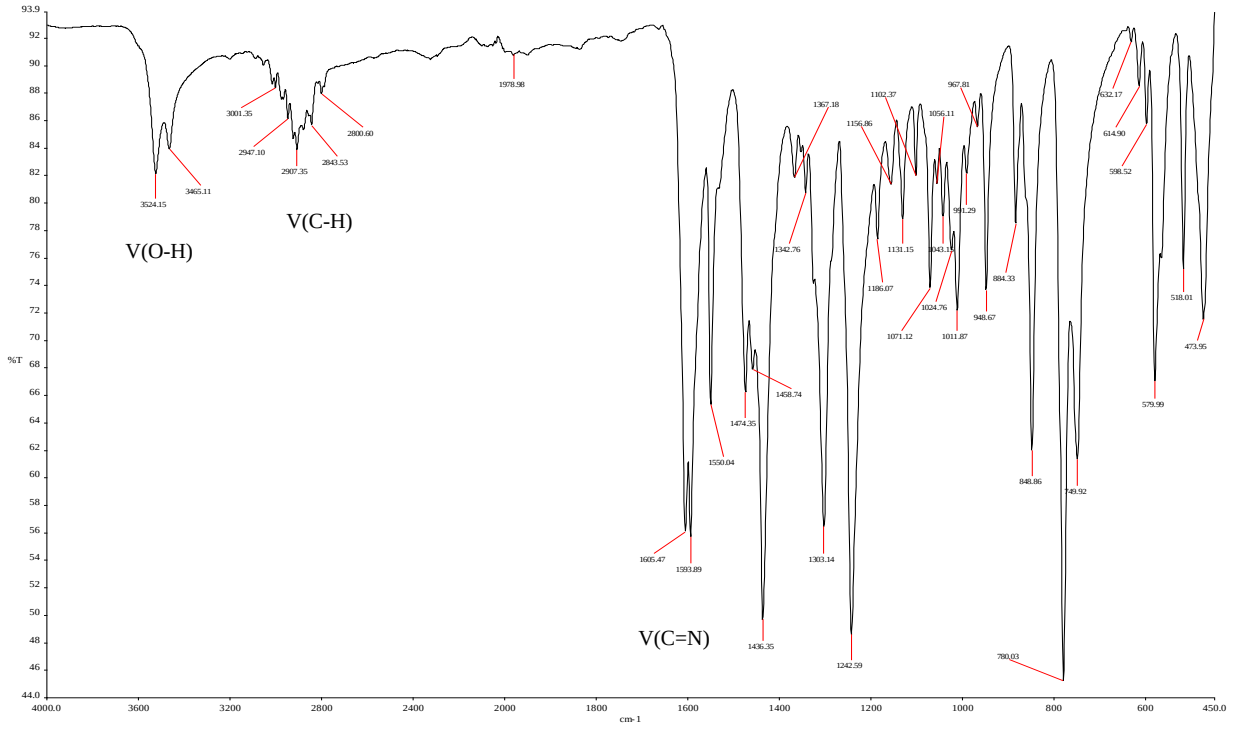

Appendix 14: IR spectra of LNH

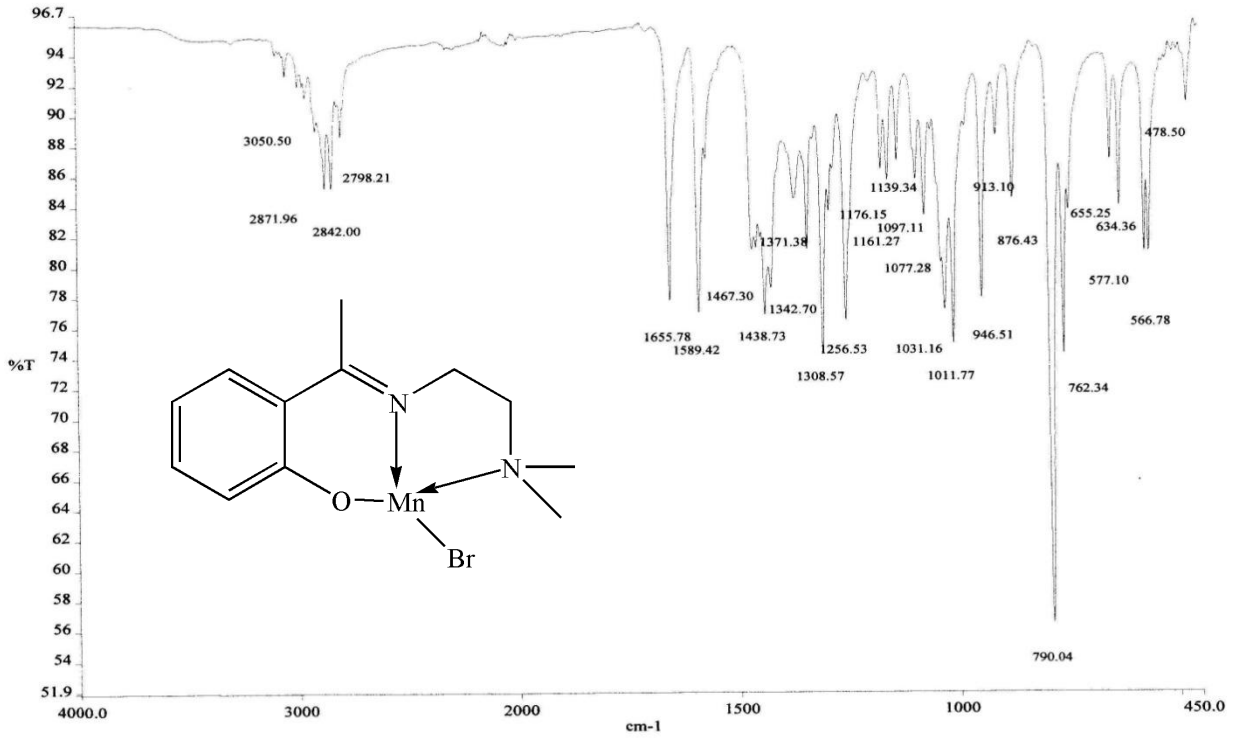

Appendix 15: IR spectra of [Mn(LNH)Br]

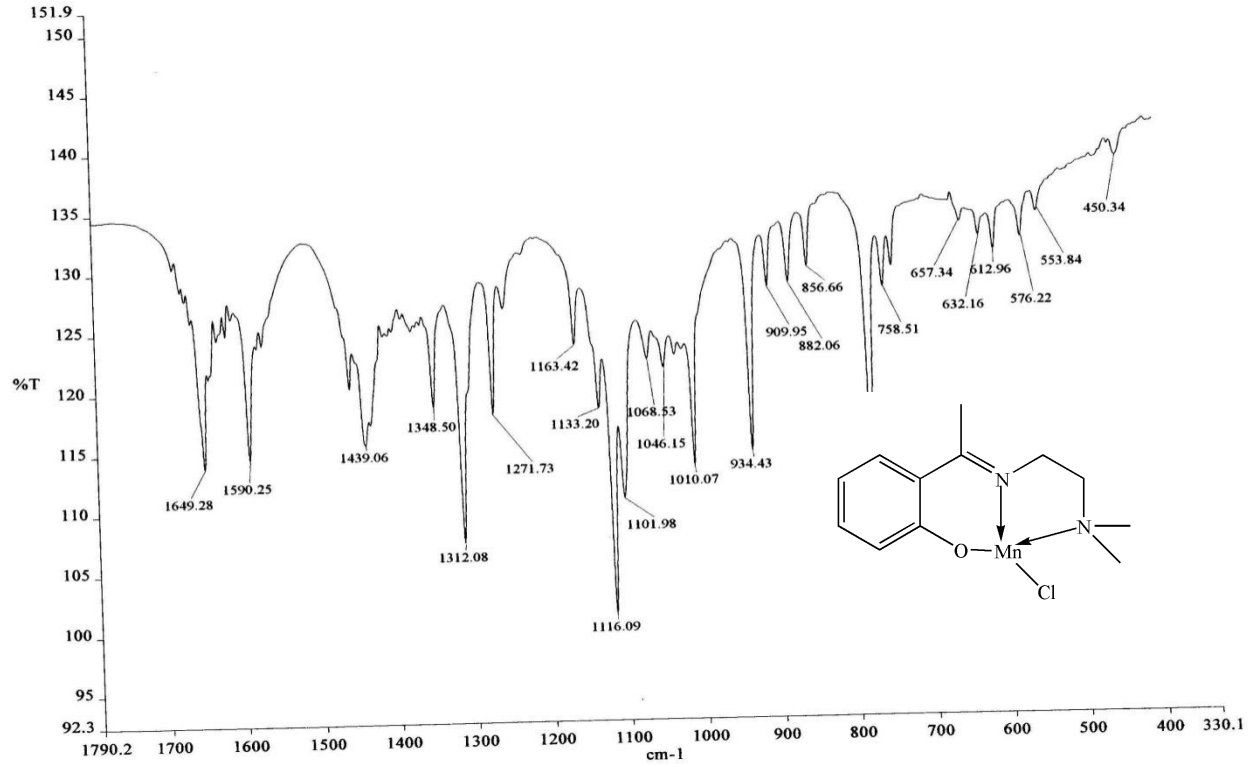

Appendix 16: IR spectra of [Mn(LNH)Cl]

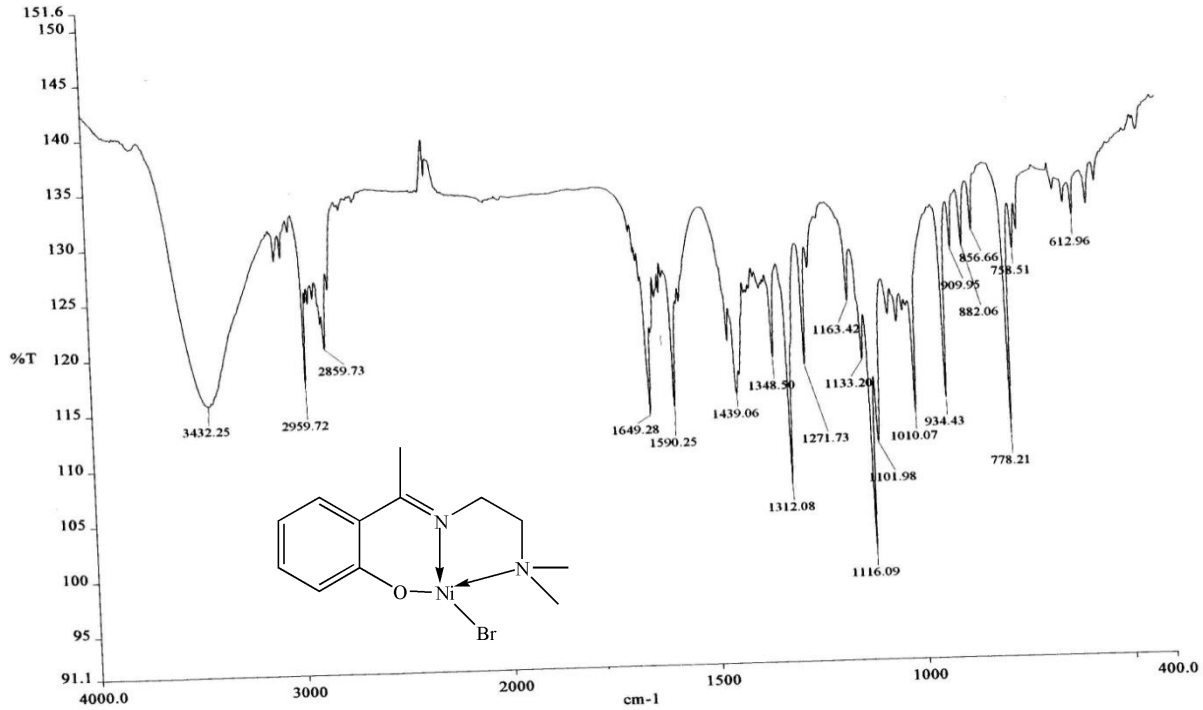

Appendix 17: IR spectra of [Ni(LNH)Br]

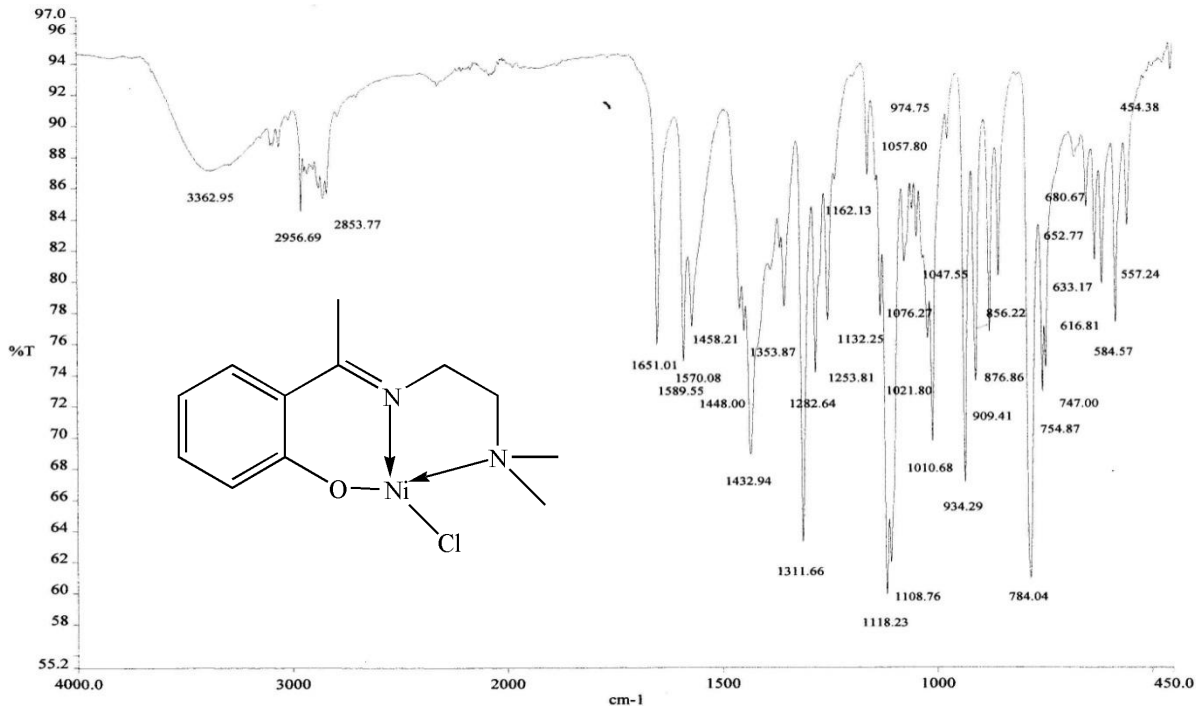

Appendix 18: IR spectra of [Ni(LNH)Cl]

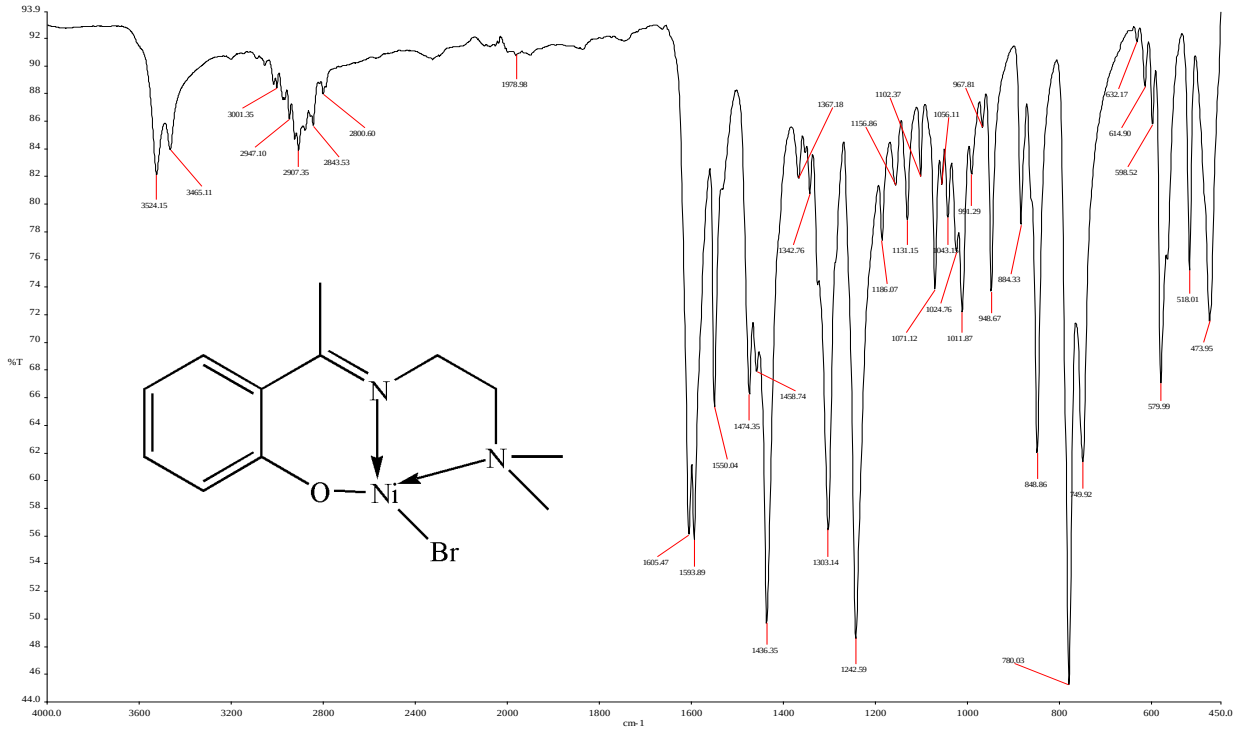

Appendix 19: IR spectra of [Ni(LNH)Br]

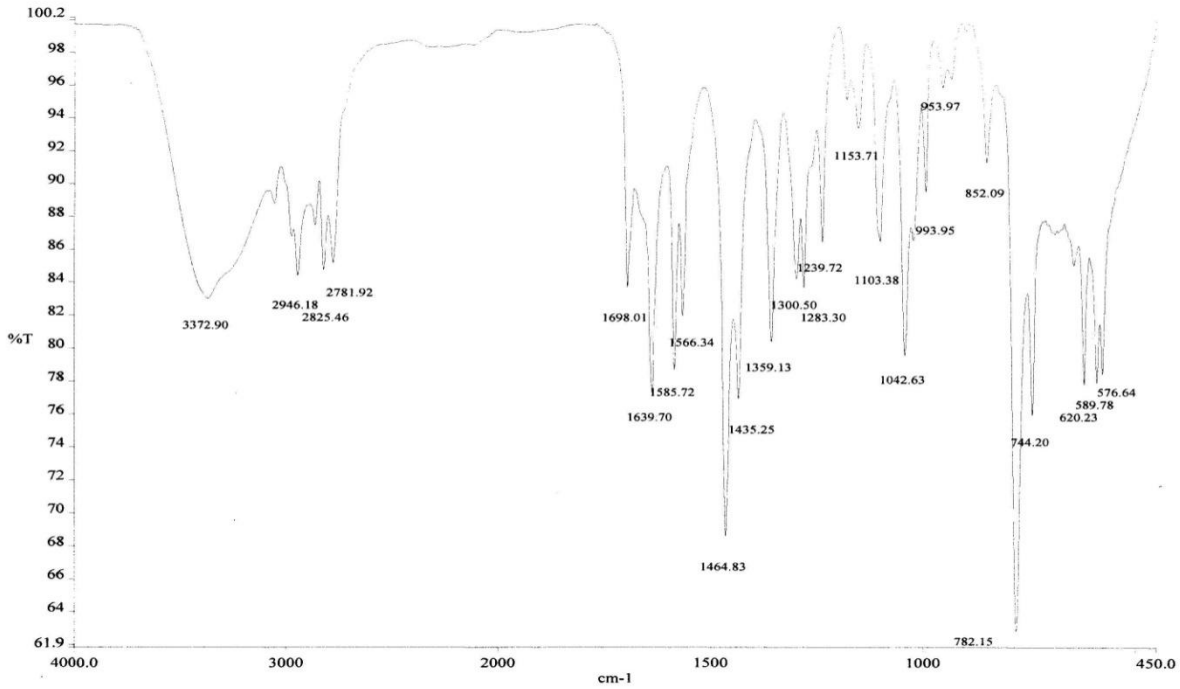

Appendix 20: IR spectra of [Cu(LNH)Cl]

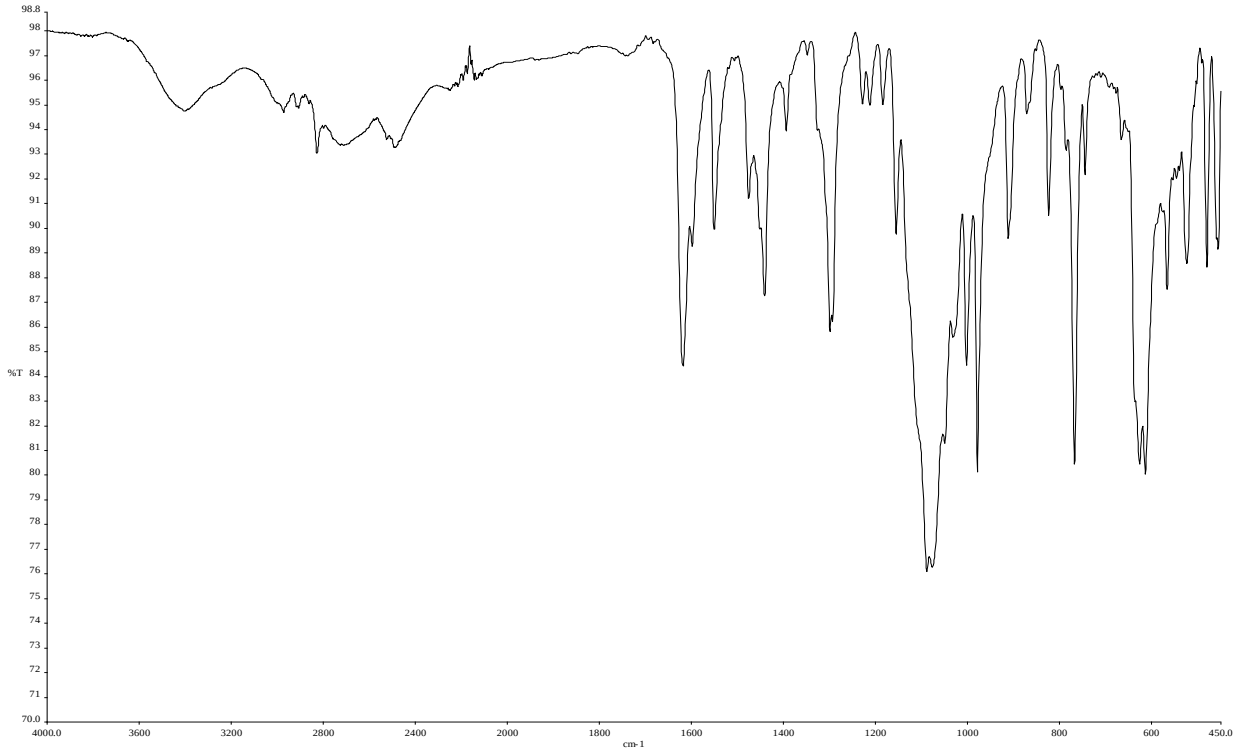

Appendix 21: IR spectra of [Zn(LNH)Br]

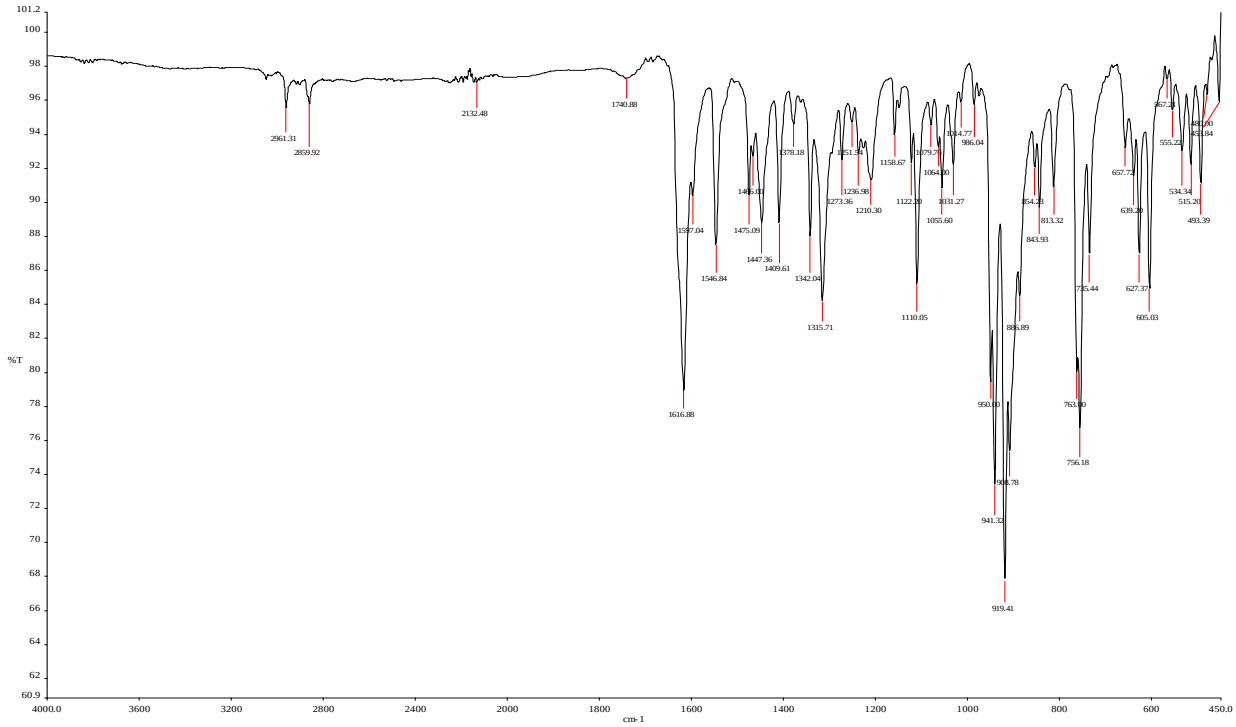

Appendix 22: IR spectra of [Zn(LNH)Cl]

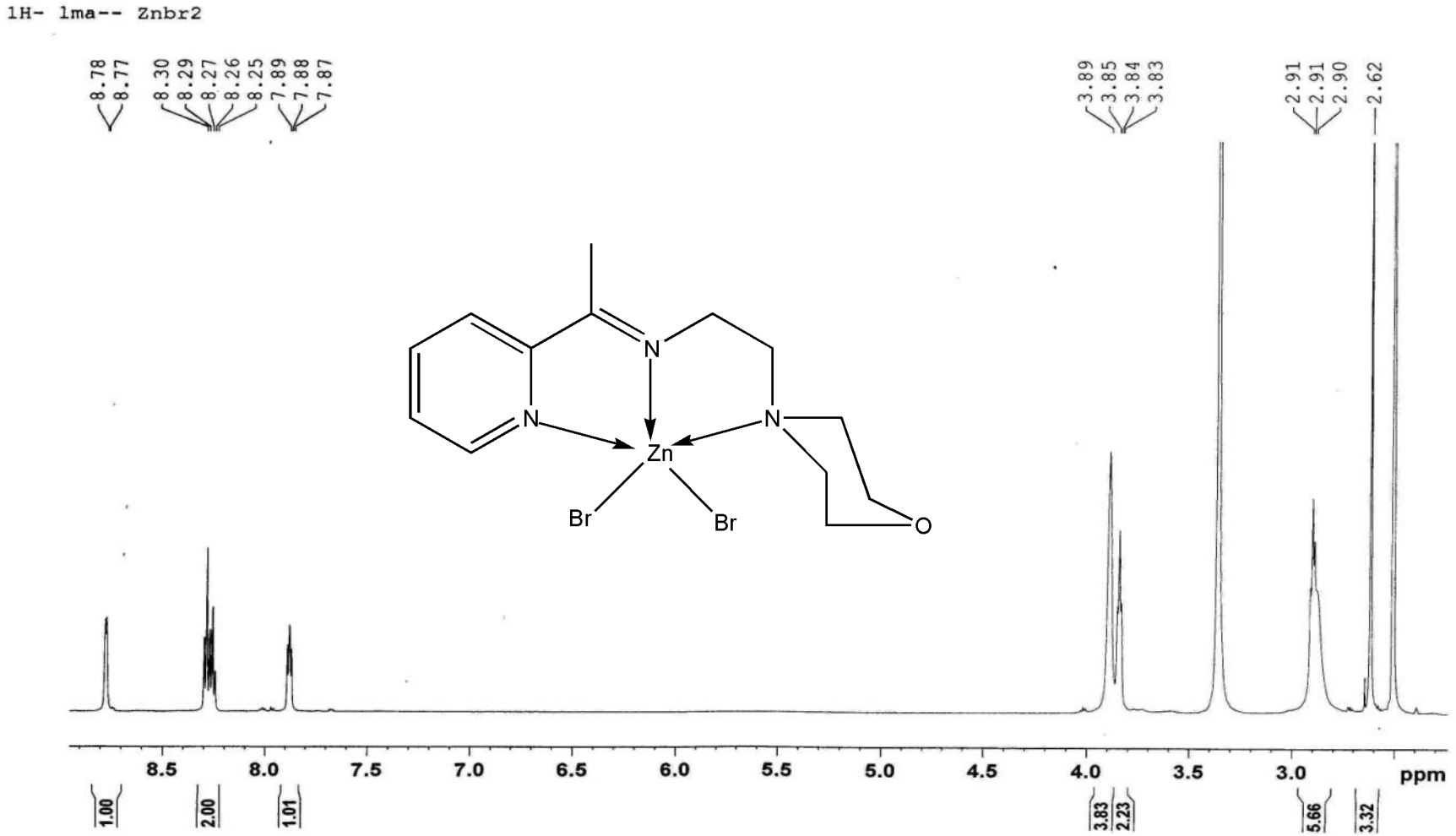

Appendix 23: 1H-NMR spectra of Preparation of [Zn(LMA)Br_2]

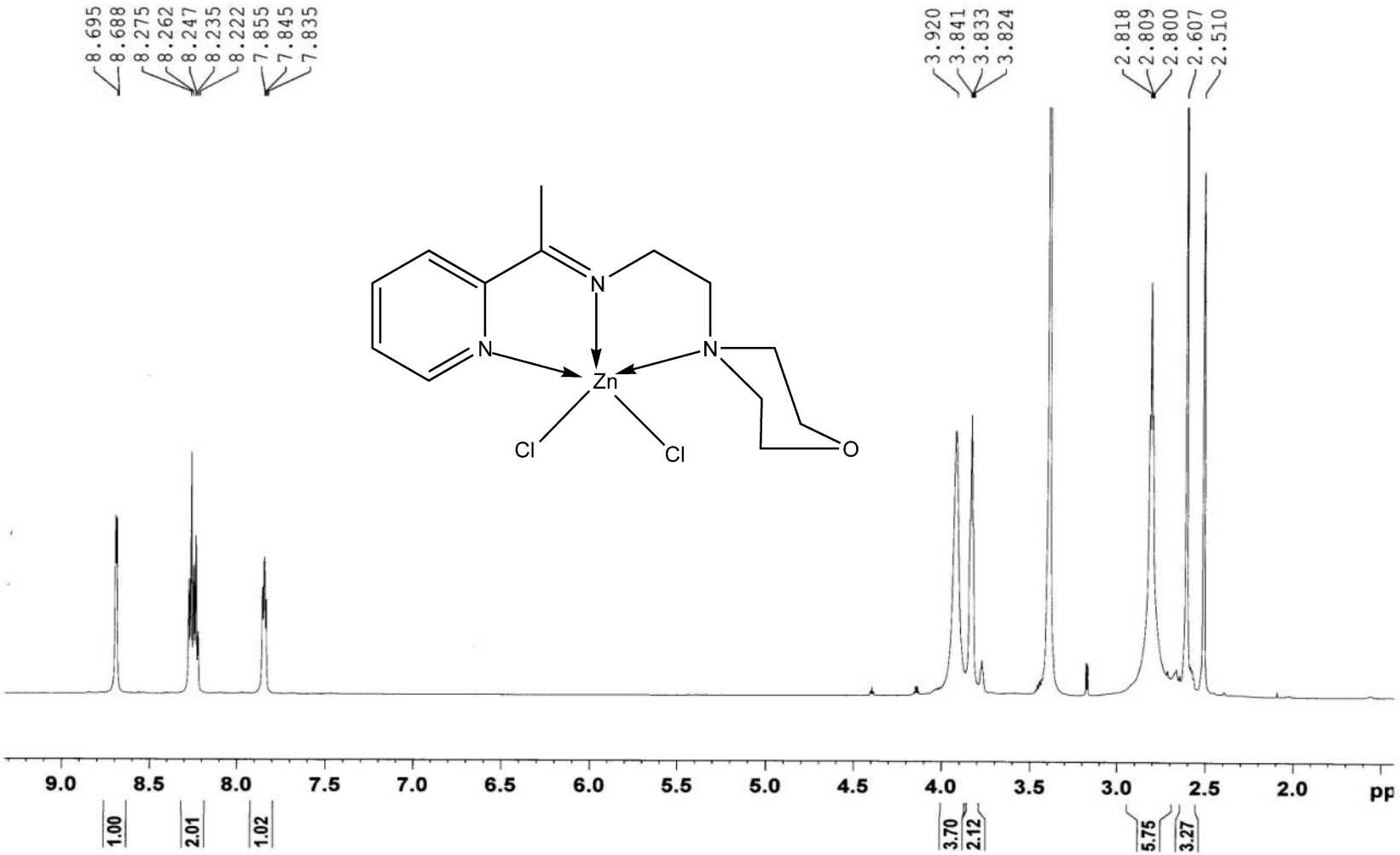

Appendix 24: 1H-NMR spectra of Preparation of $[Zn(LMA)Cl_2]$

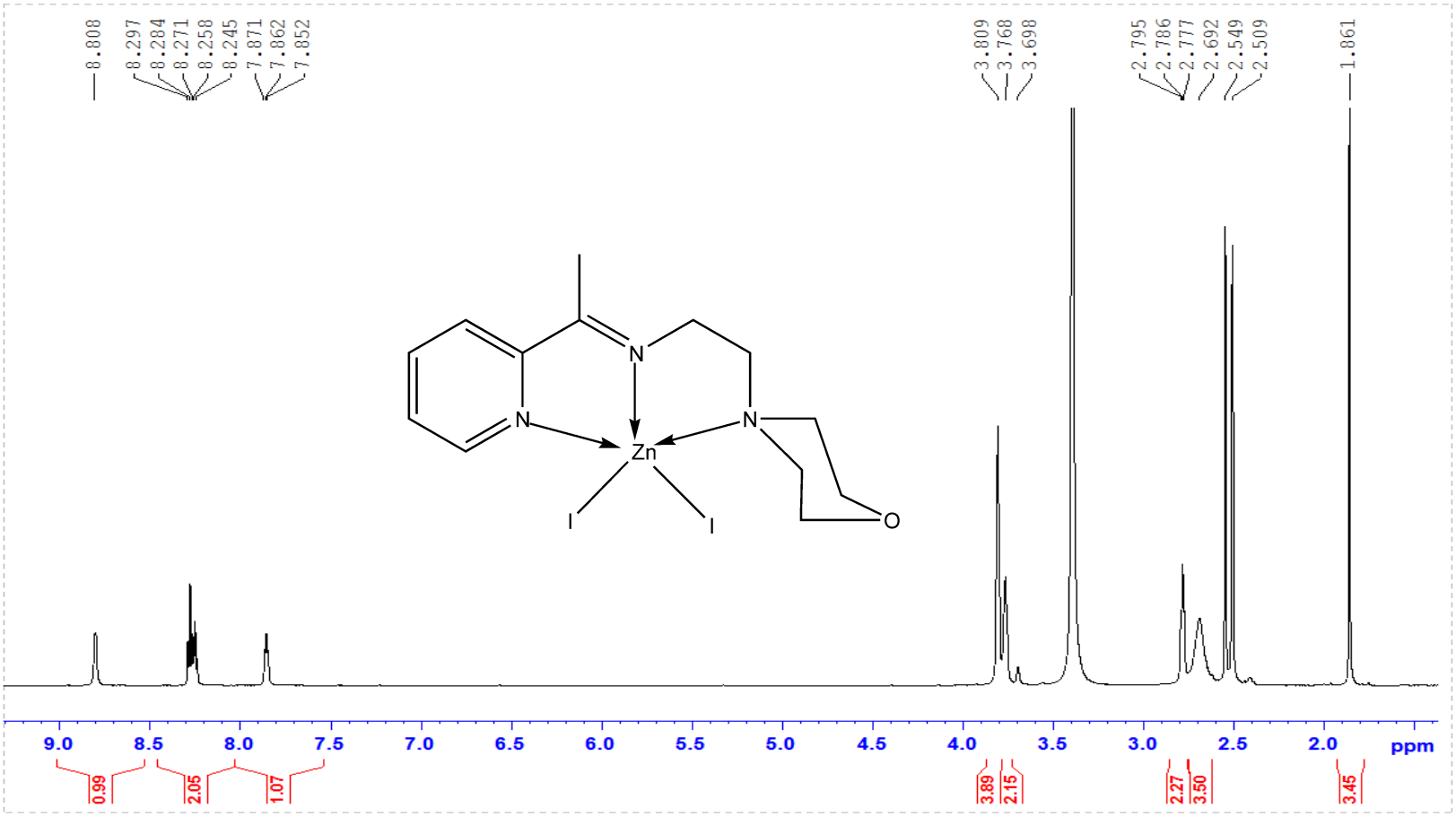

Appendix 25: 1H-NMR spectra of Preparation of $[Zn(LMA)I_2]$

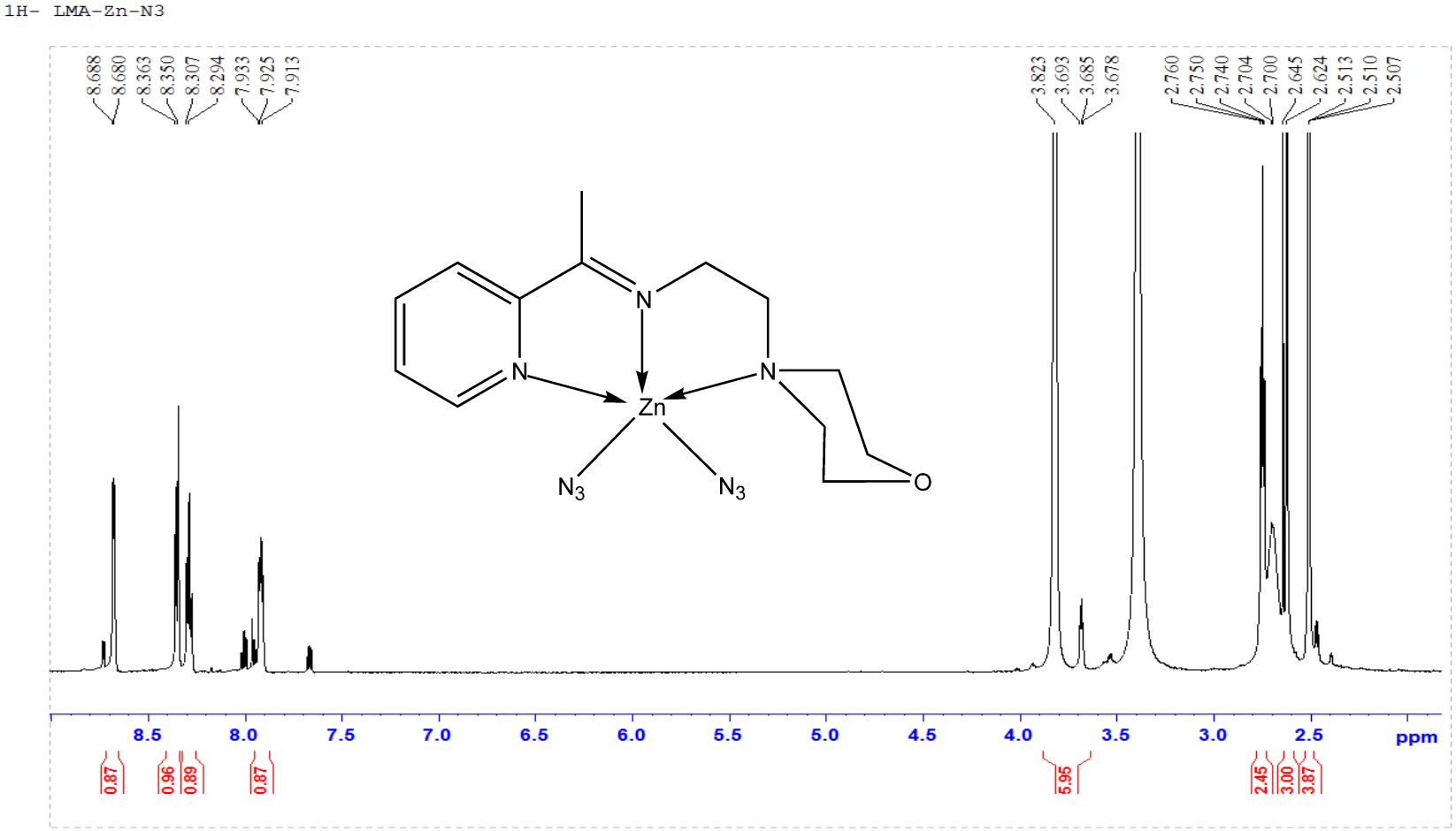

Appendix 25: 1H-NMR spectra of Preparation of $[Zn(LMA)(N_3)_2]$

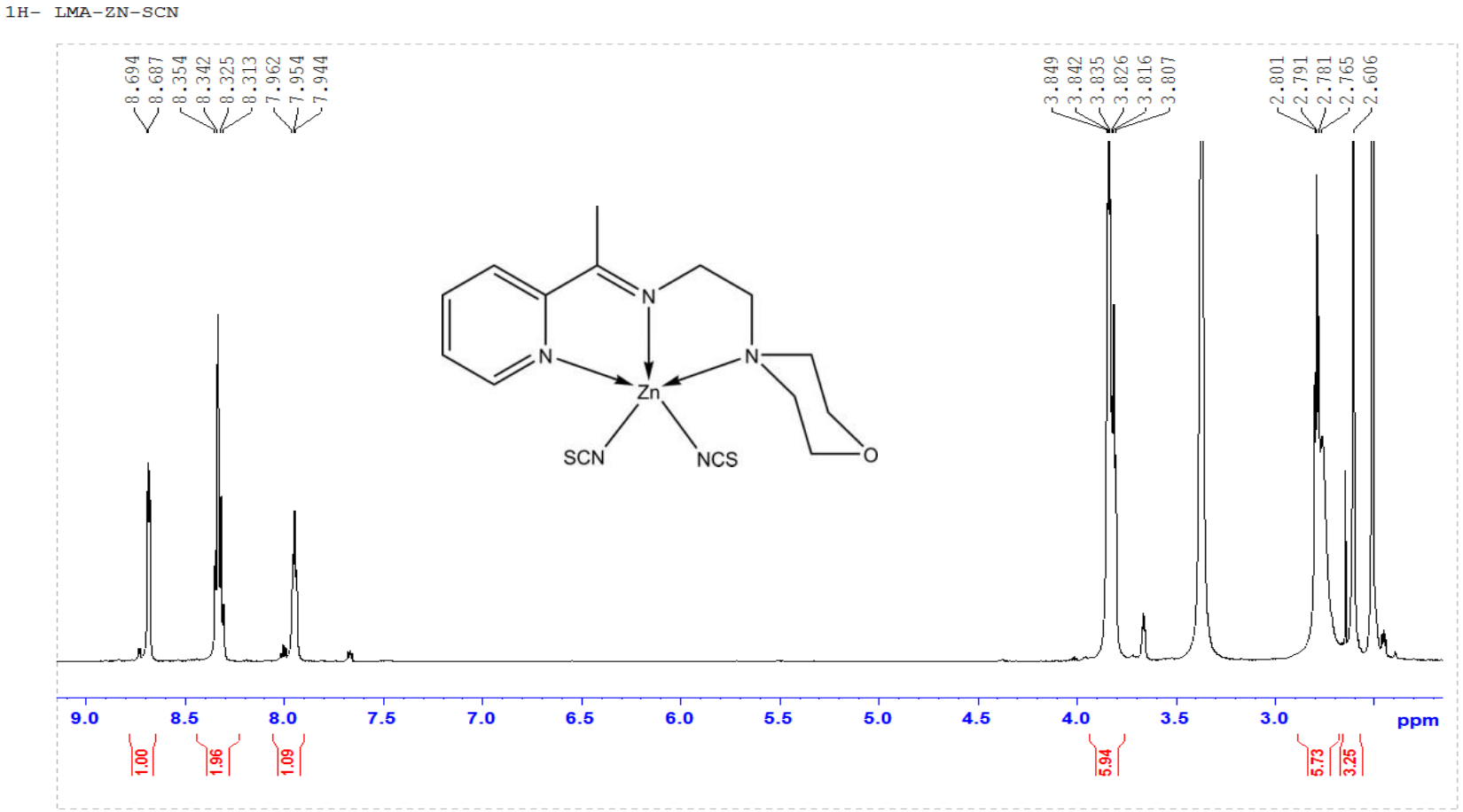

Appendix 26: 1H-NMR spectra of Preparation of [Zn(LMA)$(NCS)_2$]

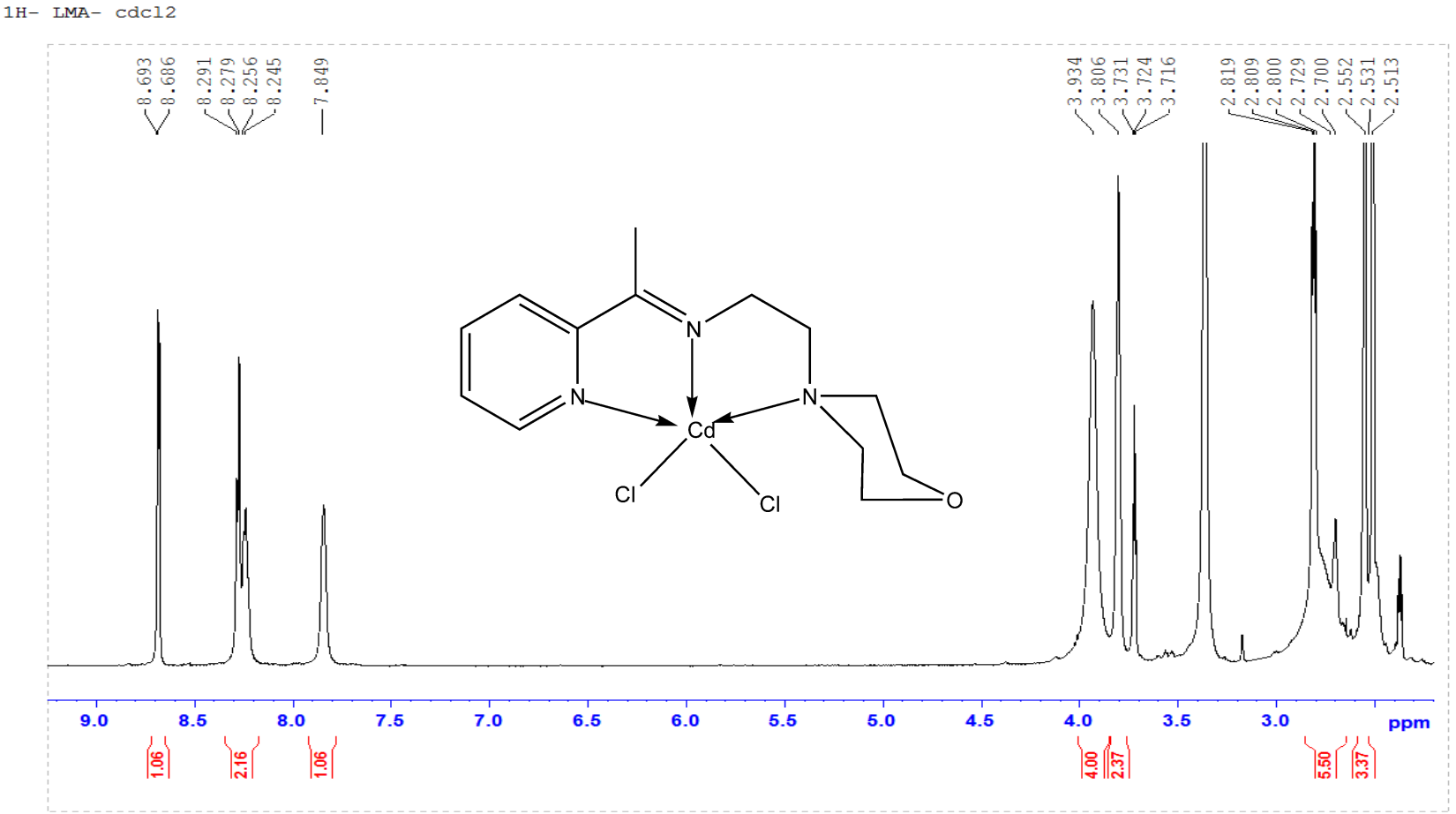

Appendix 27: 1H-NMR spectra of Preparation of [Cd(LMA)Cl_2]

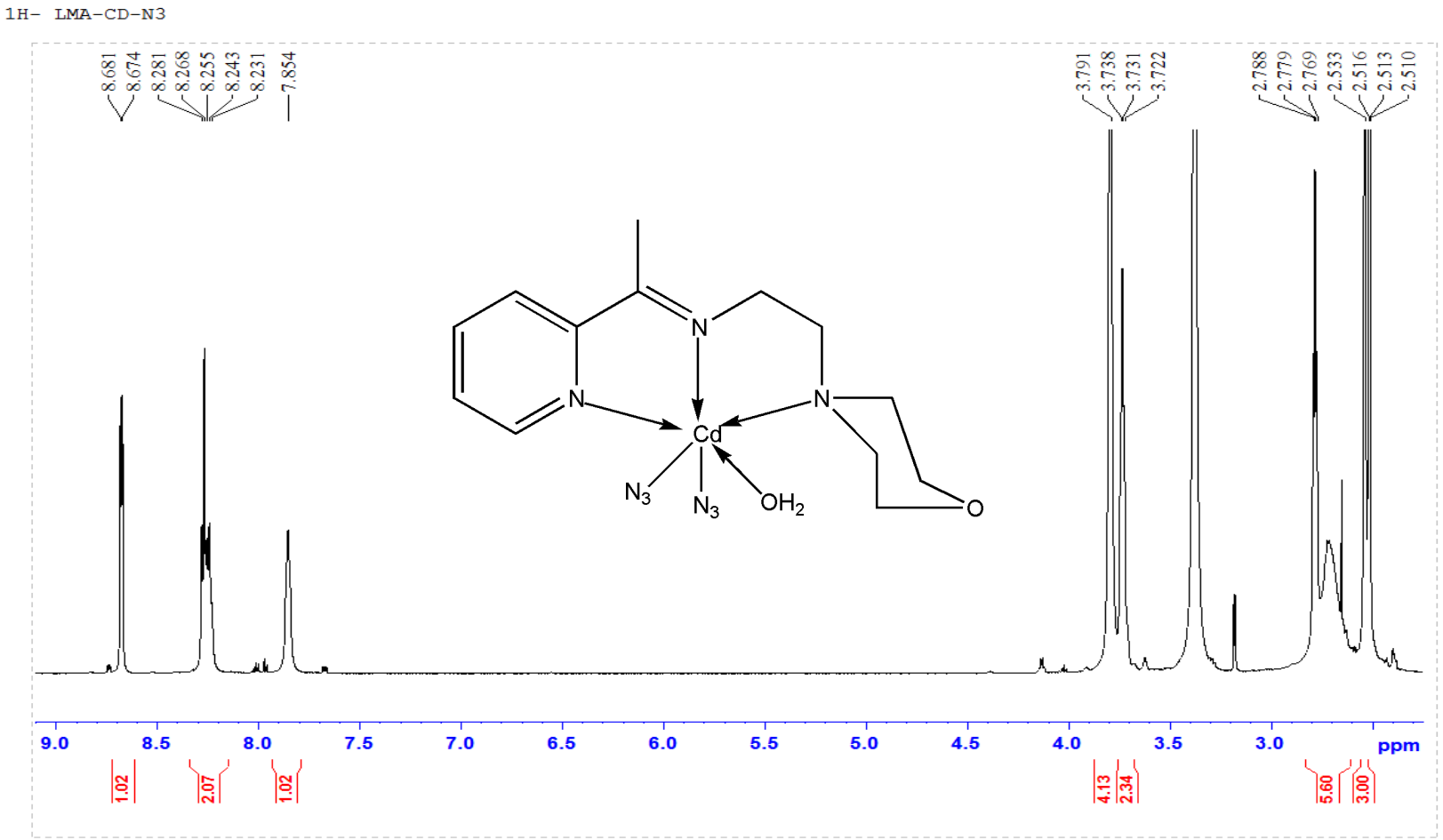

Appendix 28: 1H-NMR spectra of Preparation of [Cd(LMA)$(N_3)_2H_2O$]

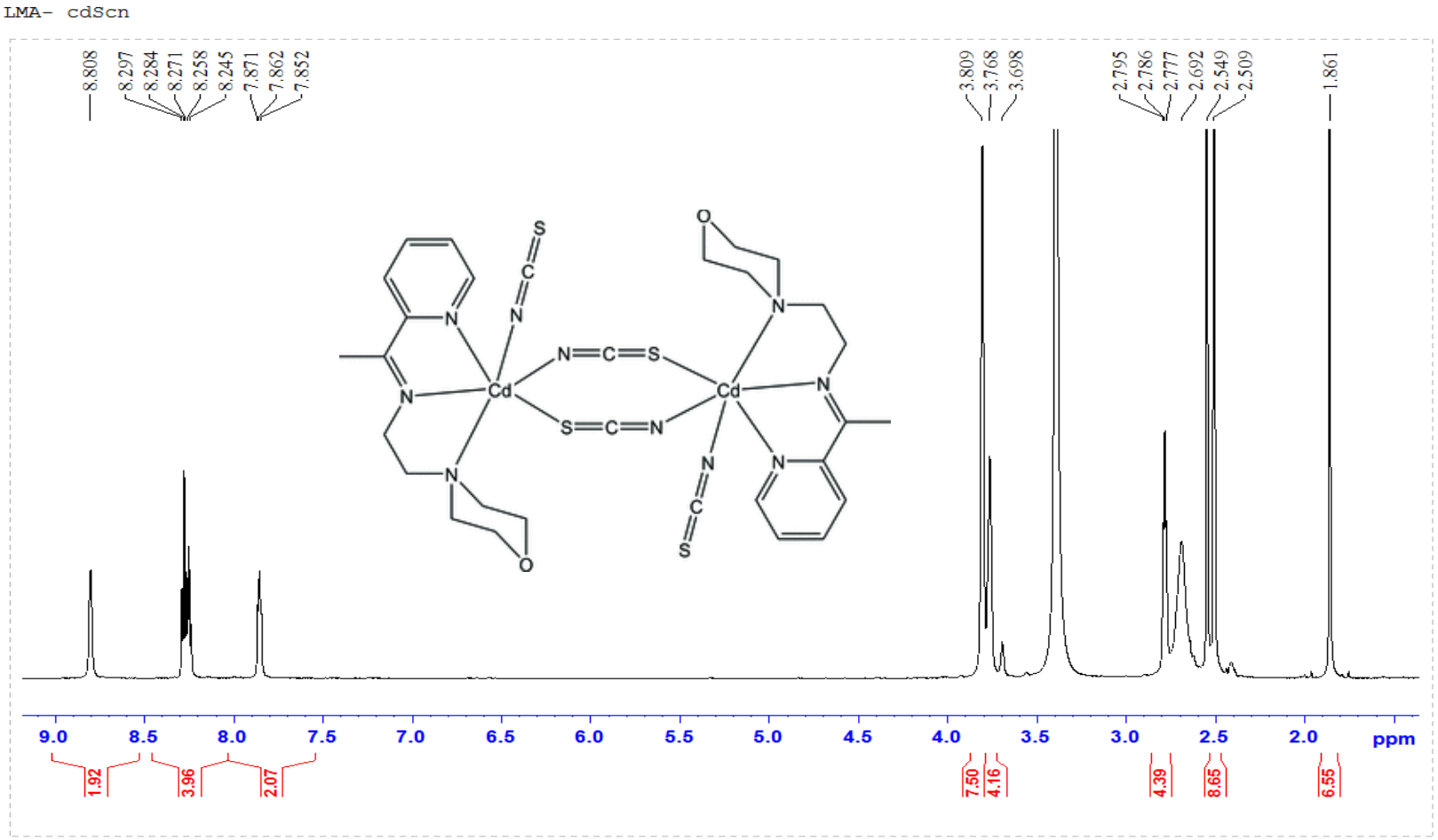

Appendix 29: 1H-NMR spectra of Preparation of $[Cd_2(LMA)_2(NCS)_4]$

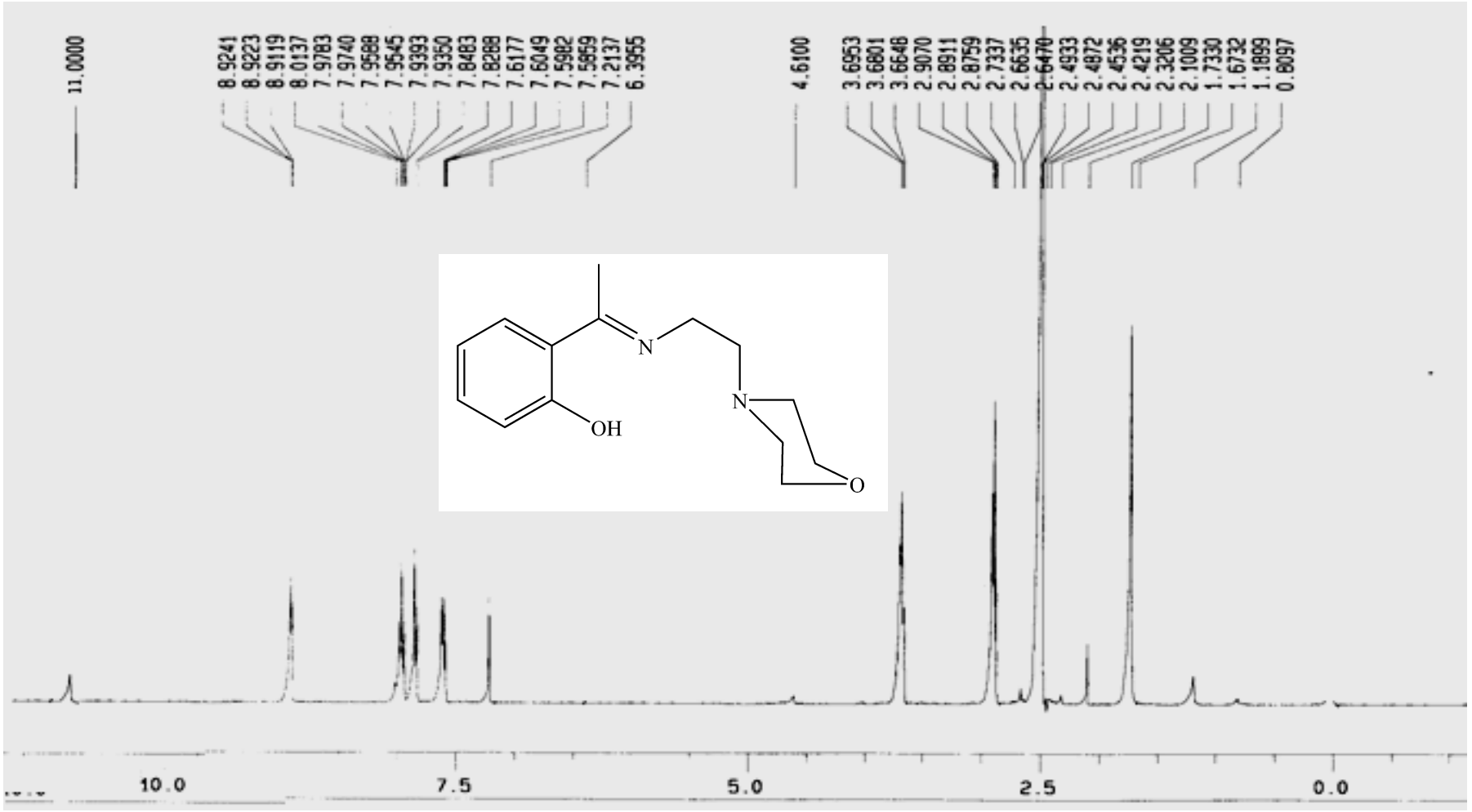

Appendix 30: 1H-NMR spectra of Preparation of LMH

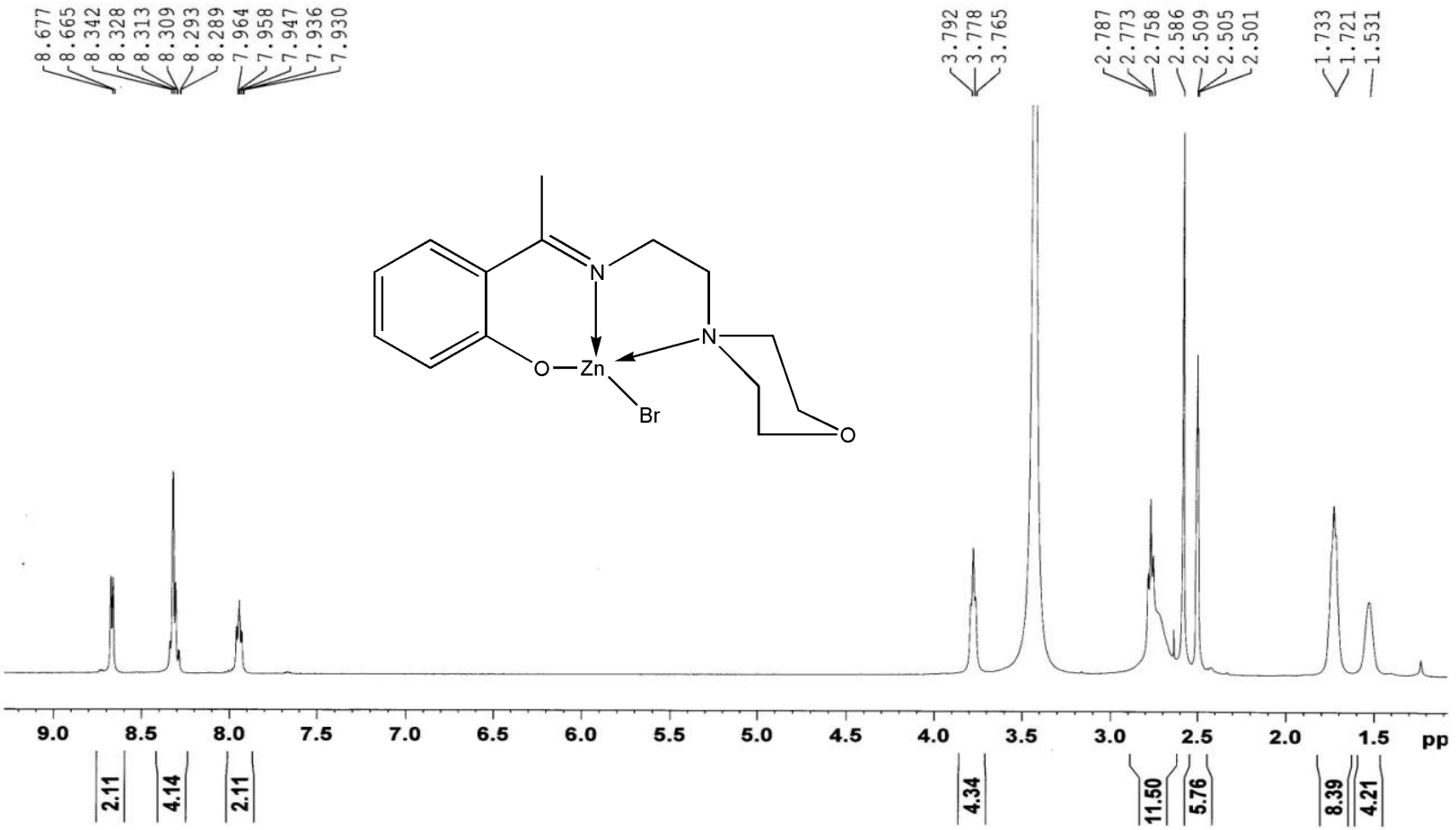

Appendix 31: 1H-NMR spectra of Preparation of [Zn(LMH)Br]

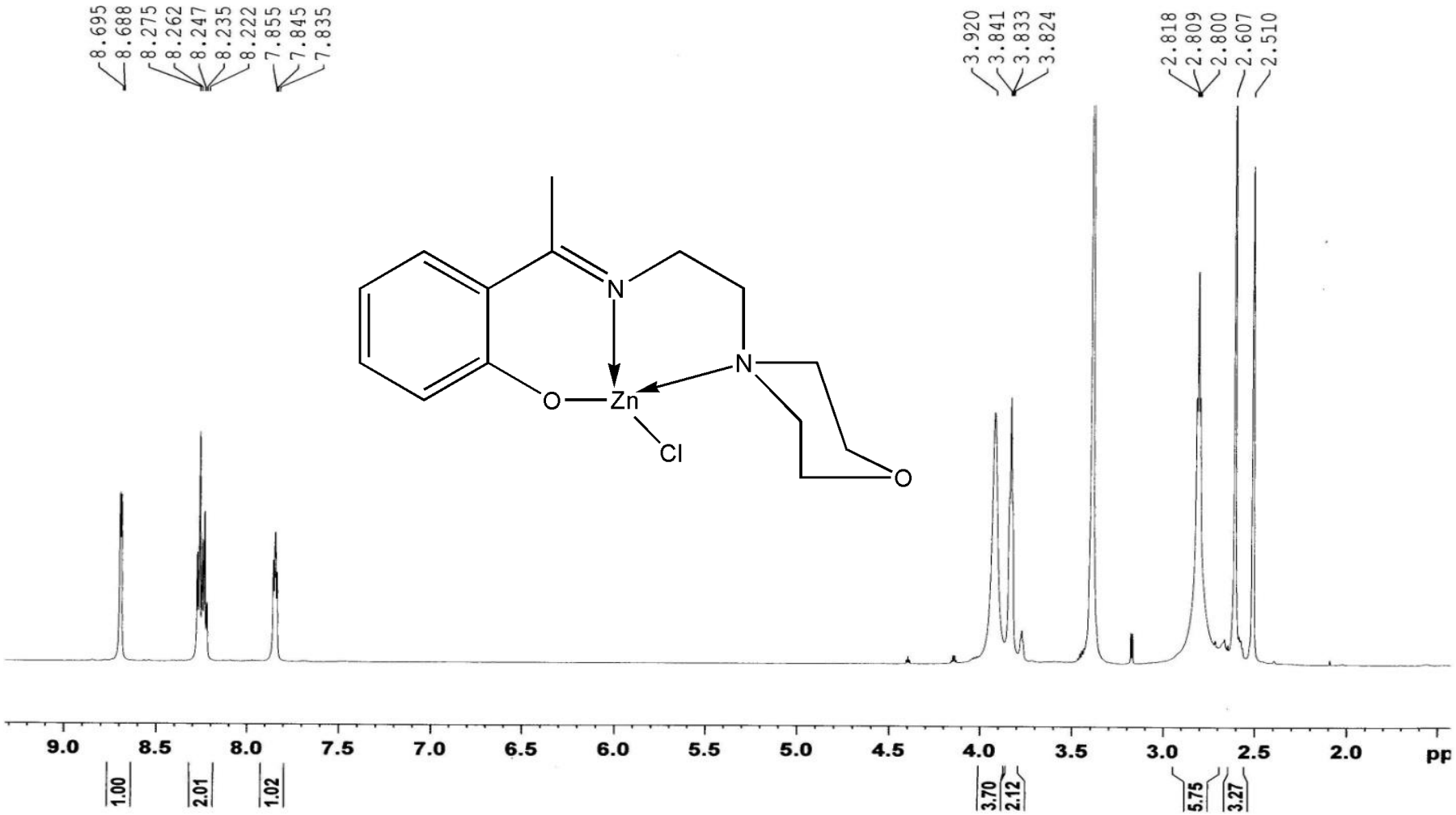

Appendix 32: 1H-NMR spectra of Preparation of [Zn(LMH)Cl]

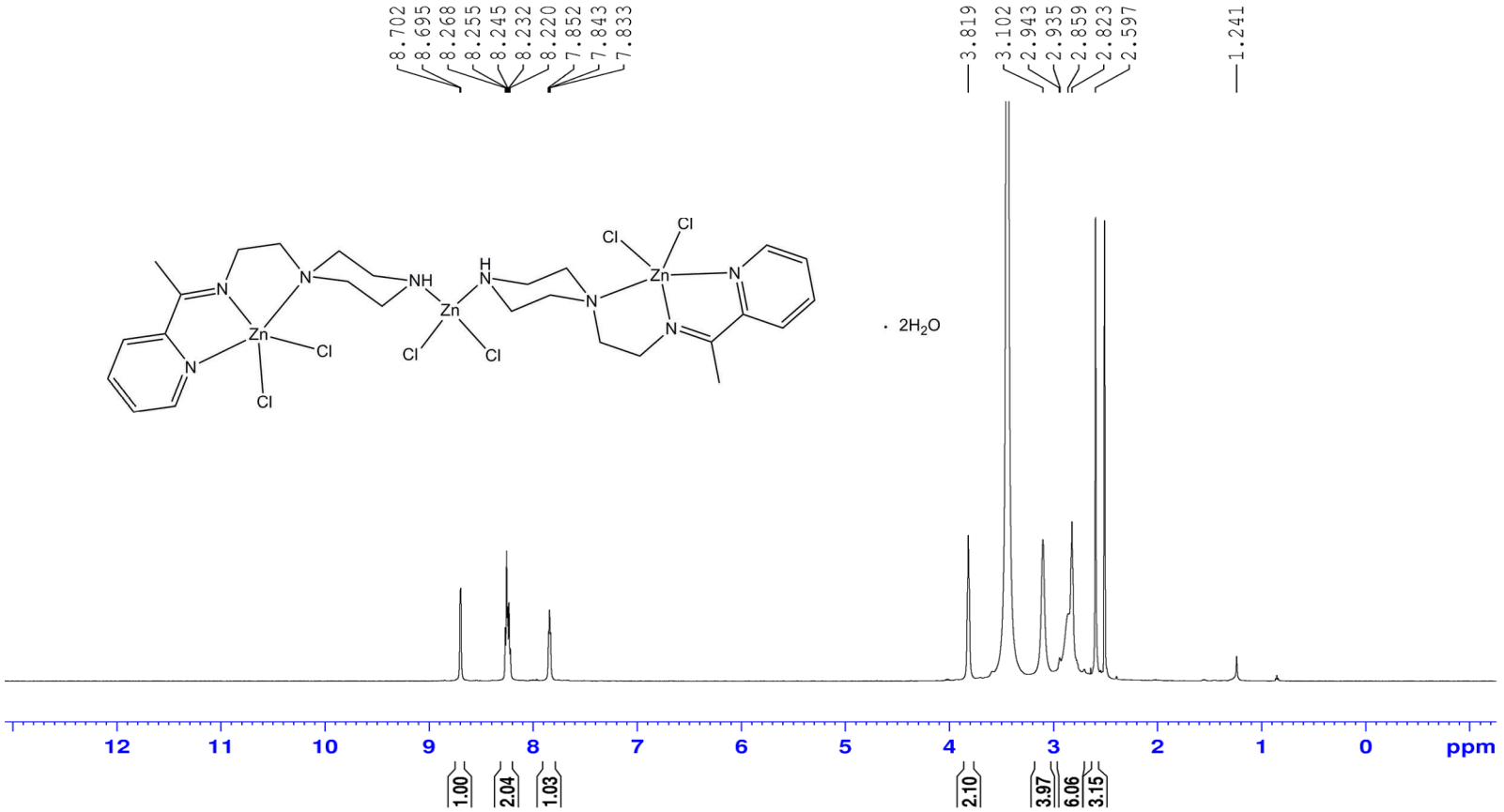

Appendix 33: 1H-NMR spectra of Preparation of $[Zn_3(LPA)_2(Cl)_6]$

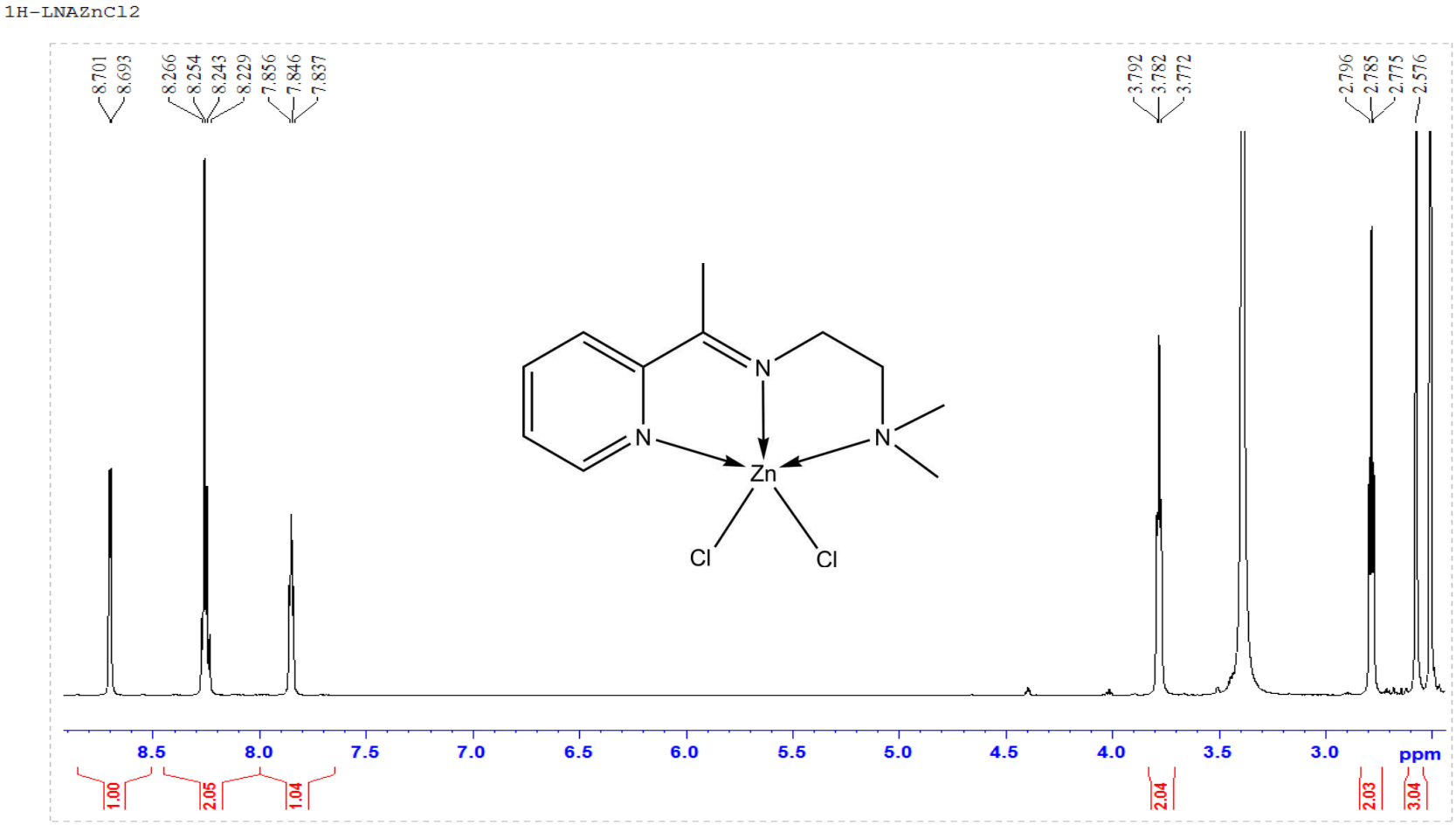

Appendix 34: 1H-NMR spectra of Preparation of [Zn(LNA)Cl_2]

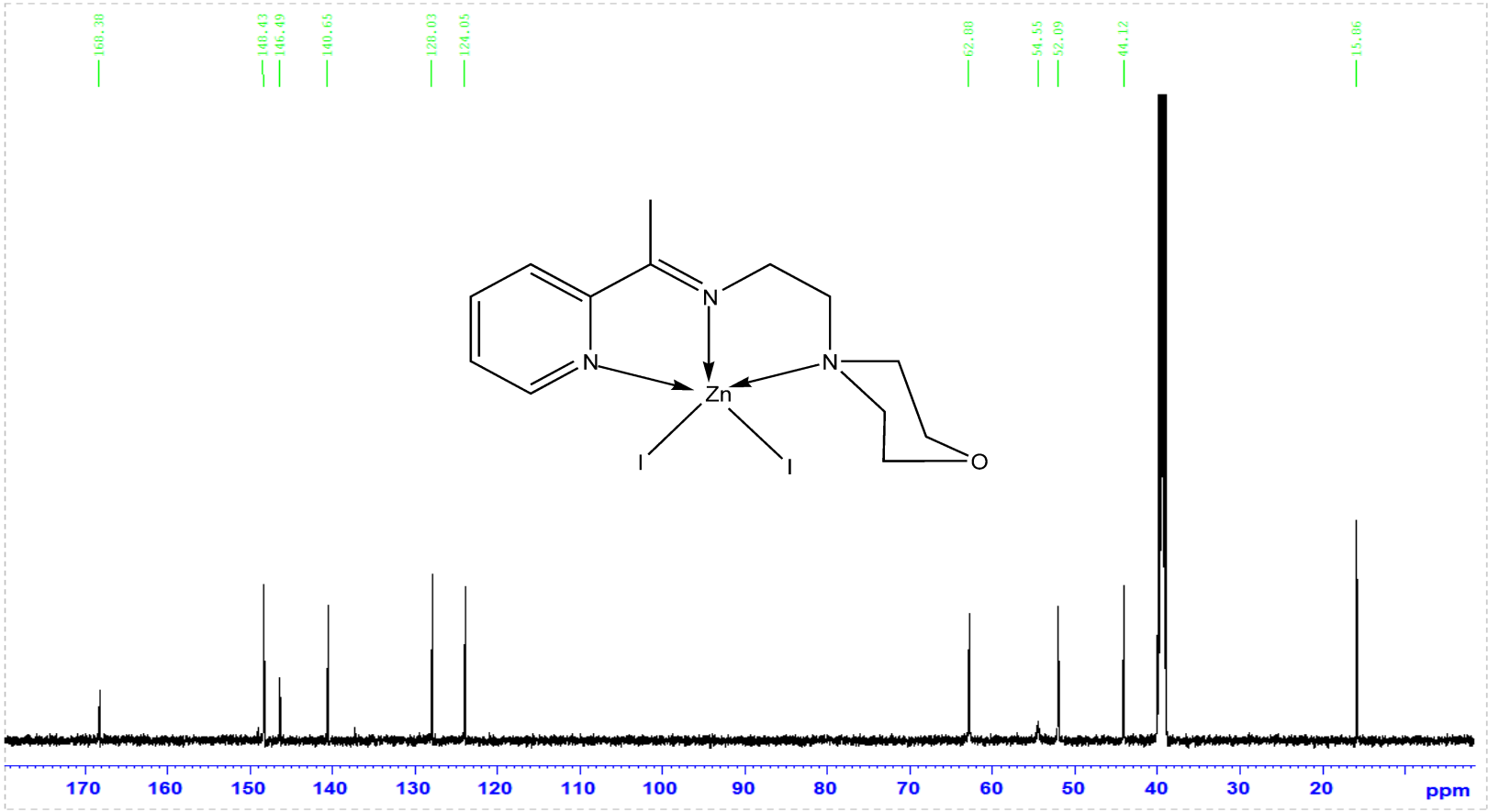

Appendix 35: 13C-NMR spectra of Preparation of [Zn(LMA)I_2]

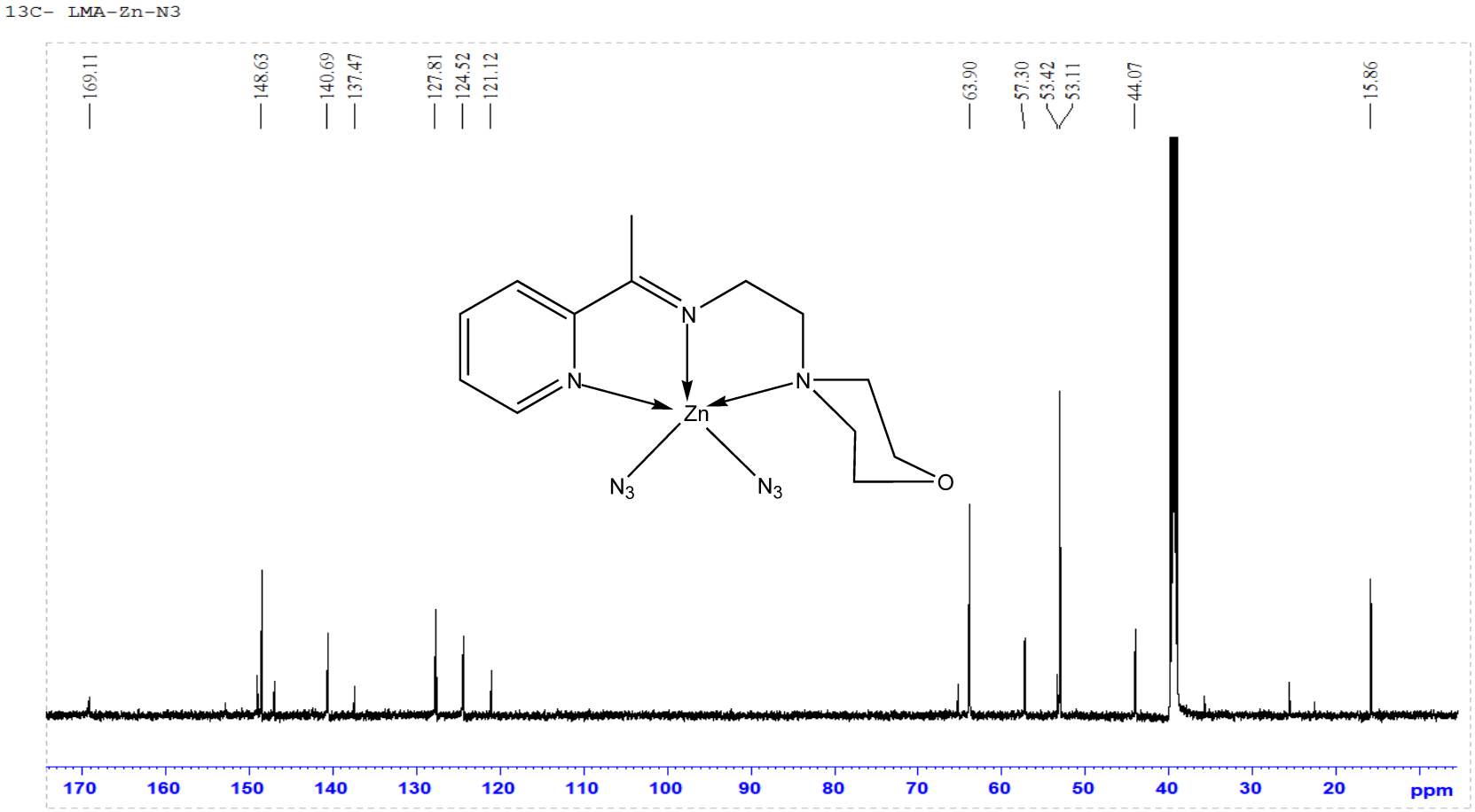

Appendix 36: 13C-NMR spectra of Preparation of $[Zn(LMA)(N_3)_2]$

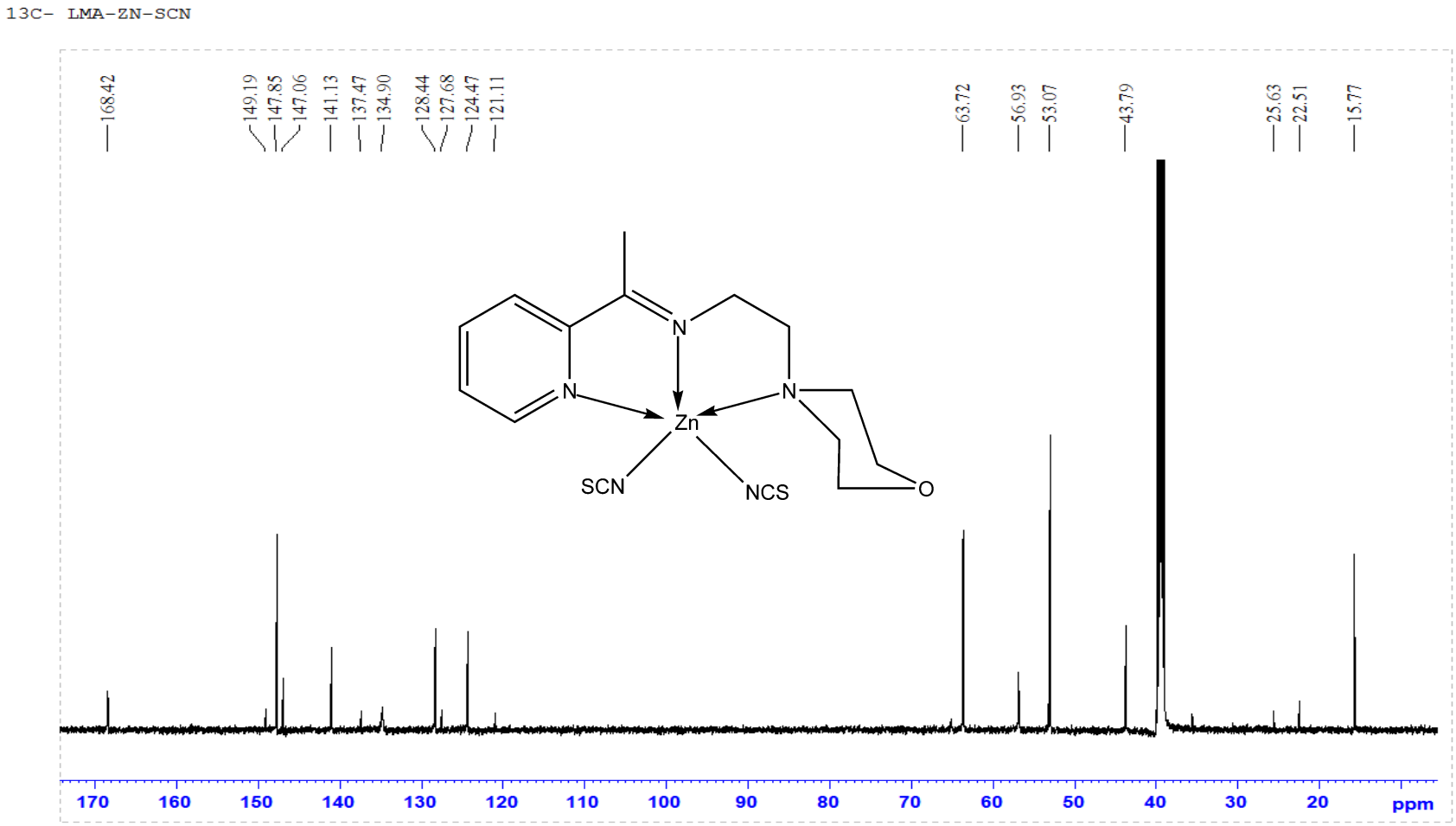

Appendix 37: 13C-NMR spectra of Preparation of $[Zn(LMA)(NCS)_2]$

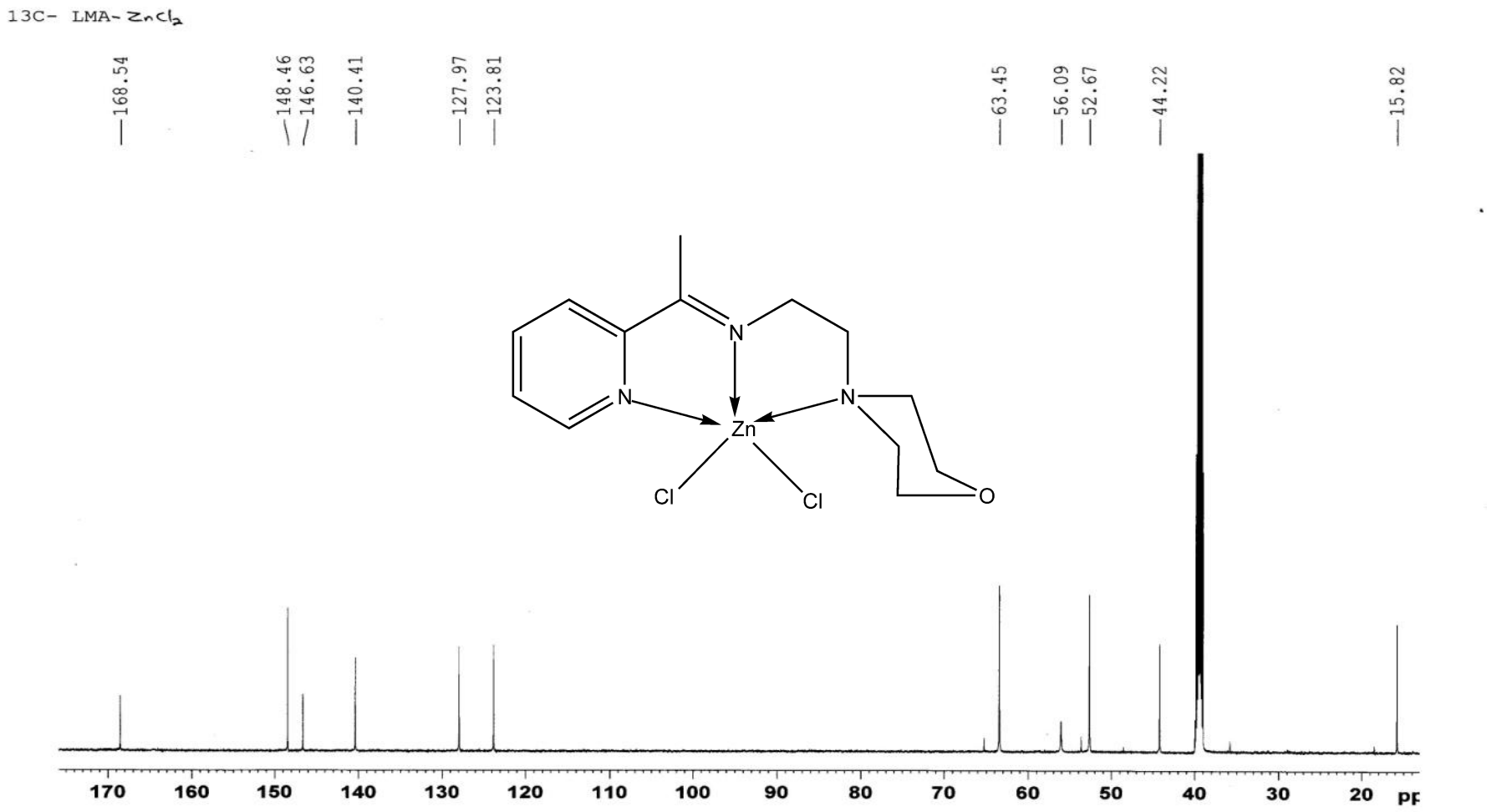

Appendix 38: 13C-NMR spectra of Preparation of [Zn(LMA)Cl_2]

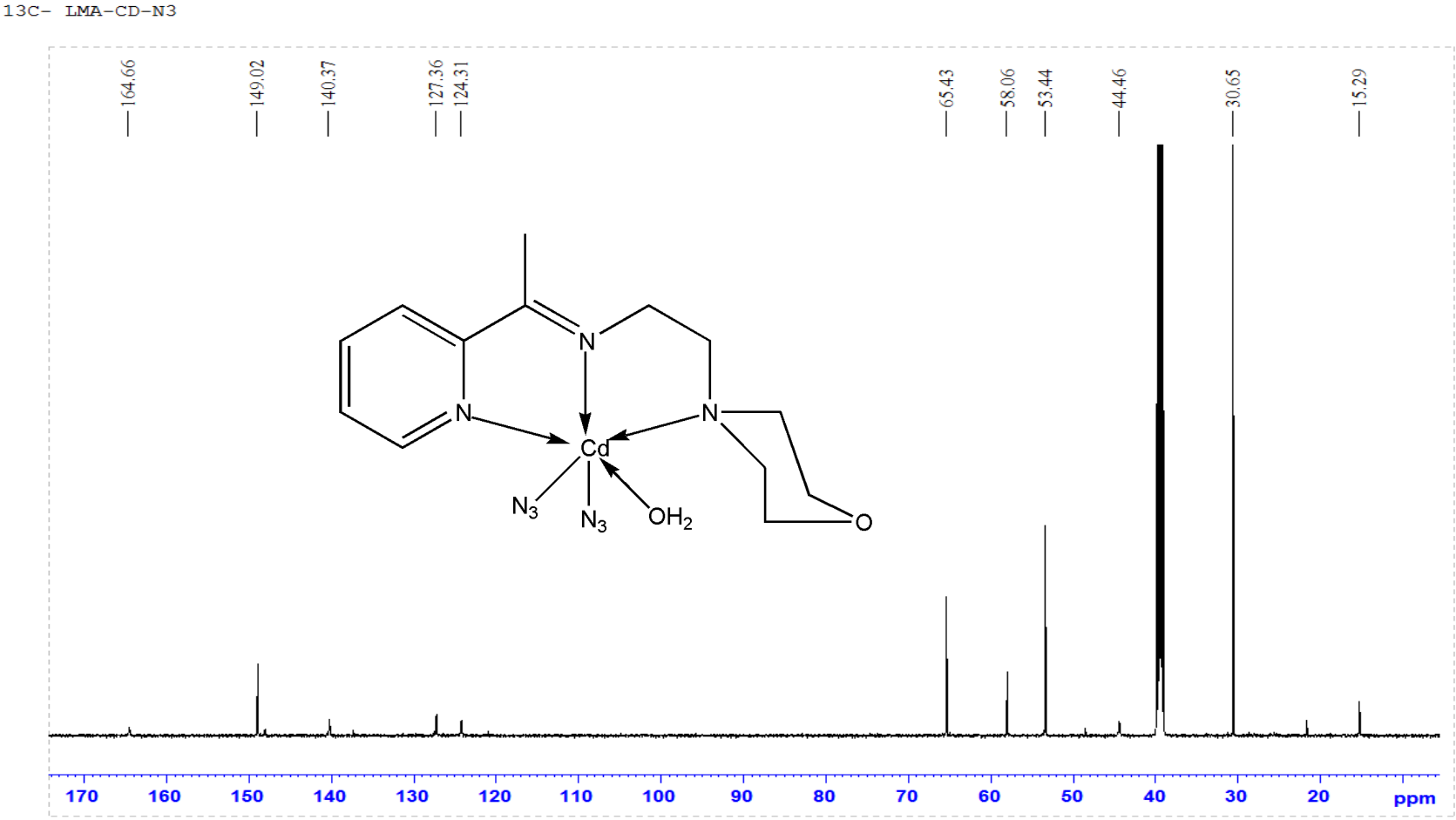

Appendix 39: 13C-NMR spectra of Preparation of $[Cd(LMA)(N_3)_2H_2O]$

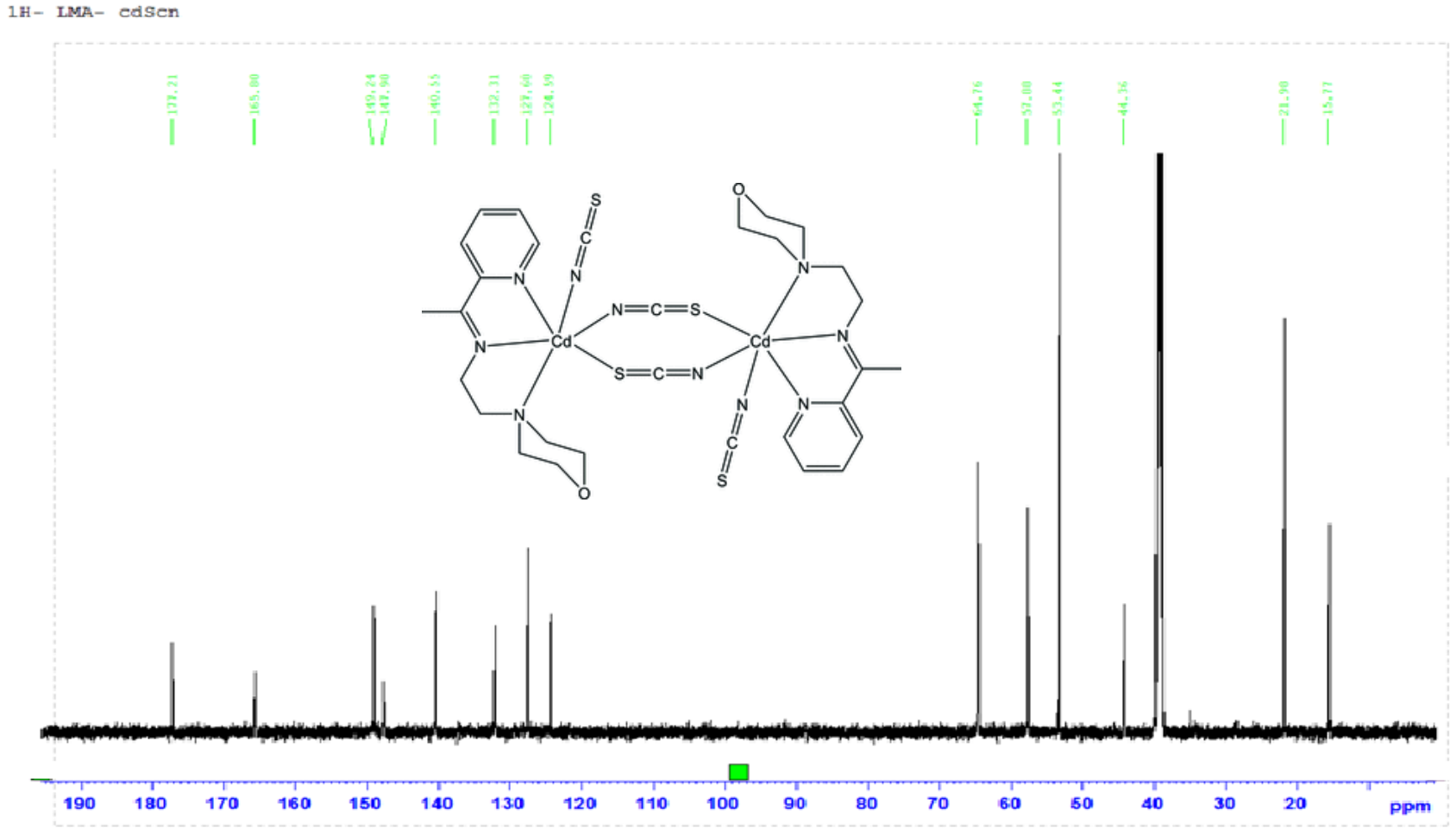

Appendix 40: 13C-NMR spectra of Preparation of $[Cd_2(LMA)_2(NCS)_4]$

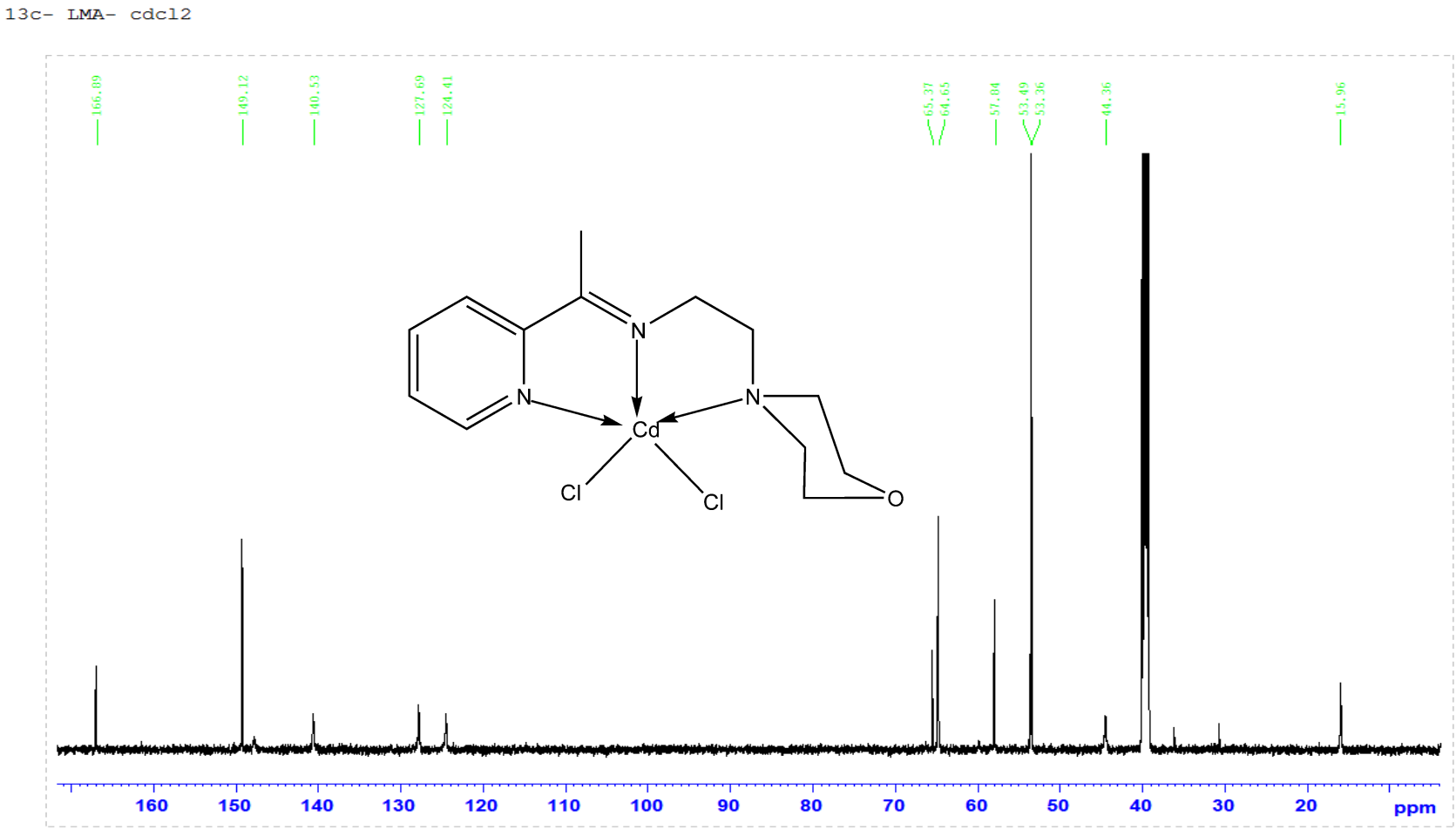

Appendix 41: 13C-NMR spectra of Preparation of [Cd(LMA)Cl_2]

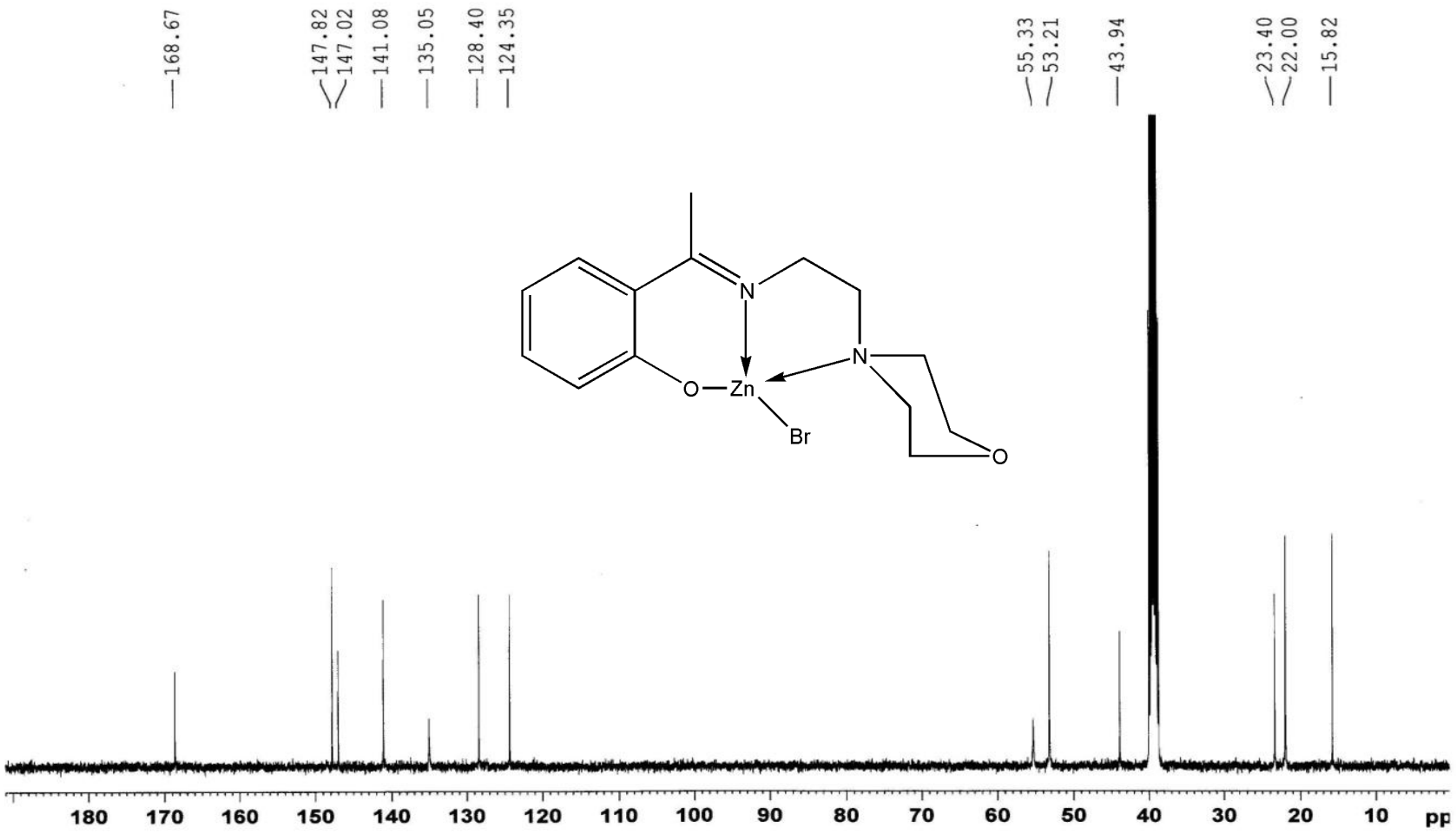

Appendix 42: 13C-NMR spectra of Preparation of [Zn(LMH)Br]

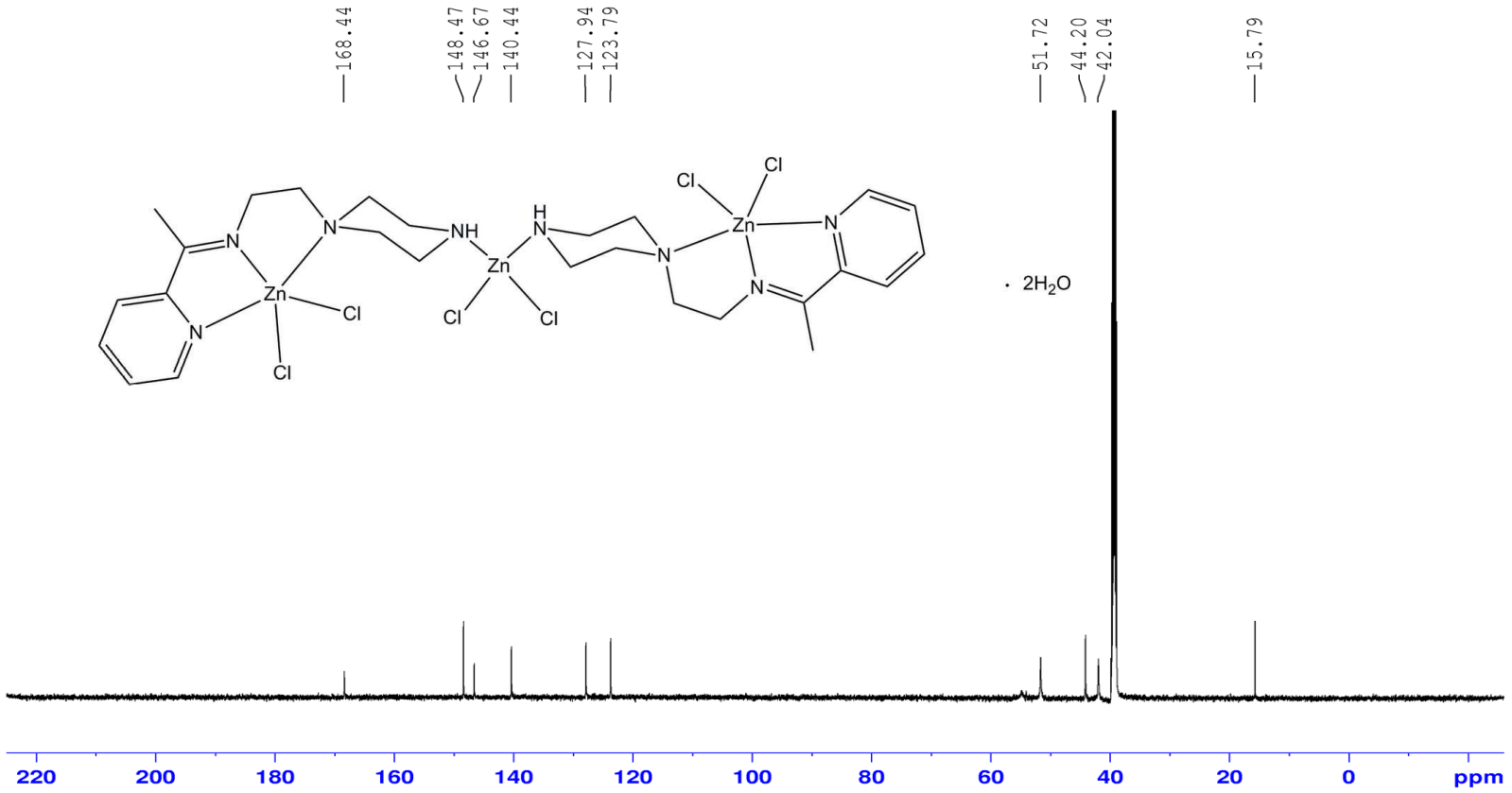

Appendix 43: 13C-NMR spectra of Preparation of $[Zn_3(LPA)_2(Cl)_6]$

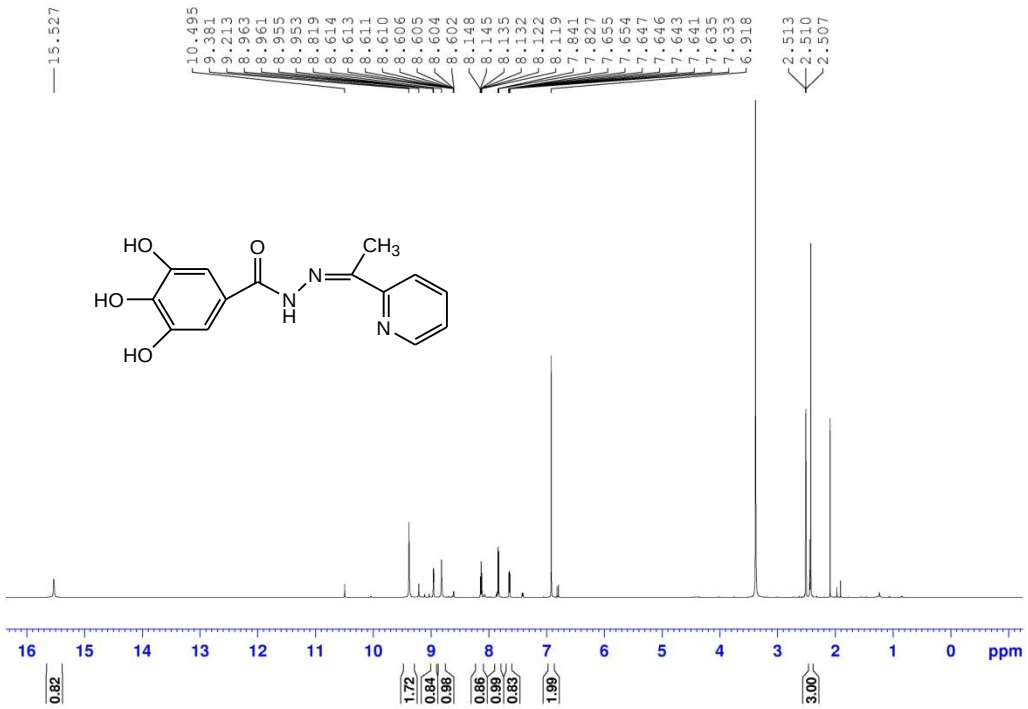

Appendix 44:1H-NMR spectrum for 2-AP

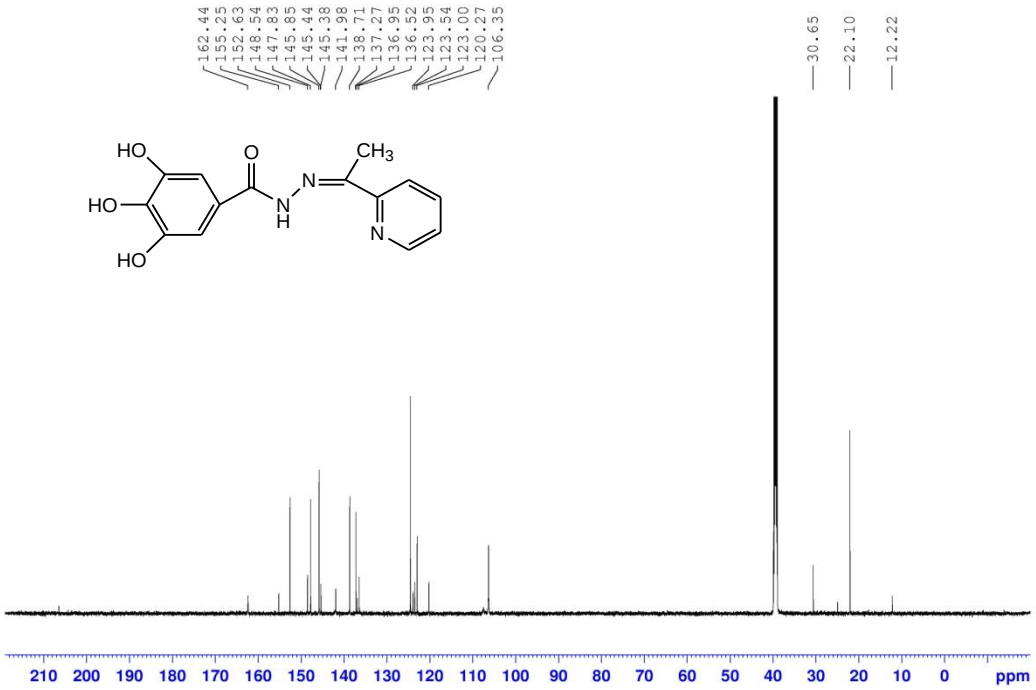

Appendix 45:13C-NMR spectrum for 2-AP

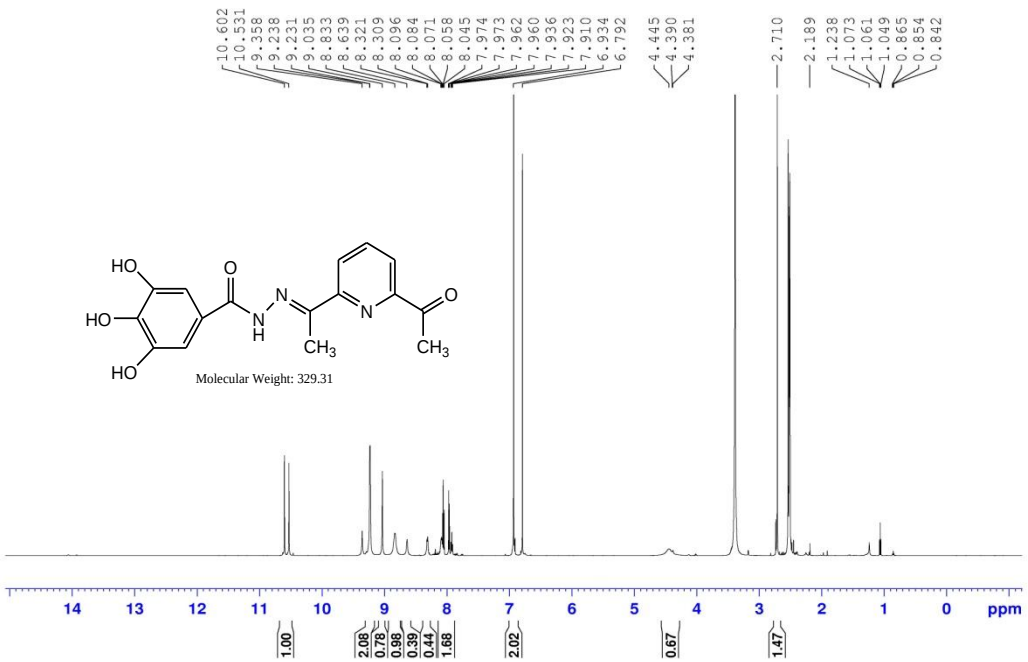

Appendix 46:1H-NMR spectrum for 2,6-DAP

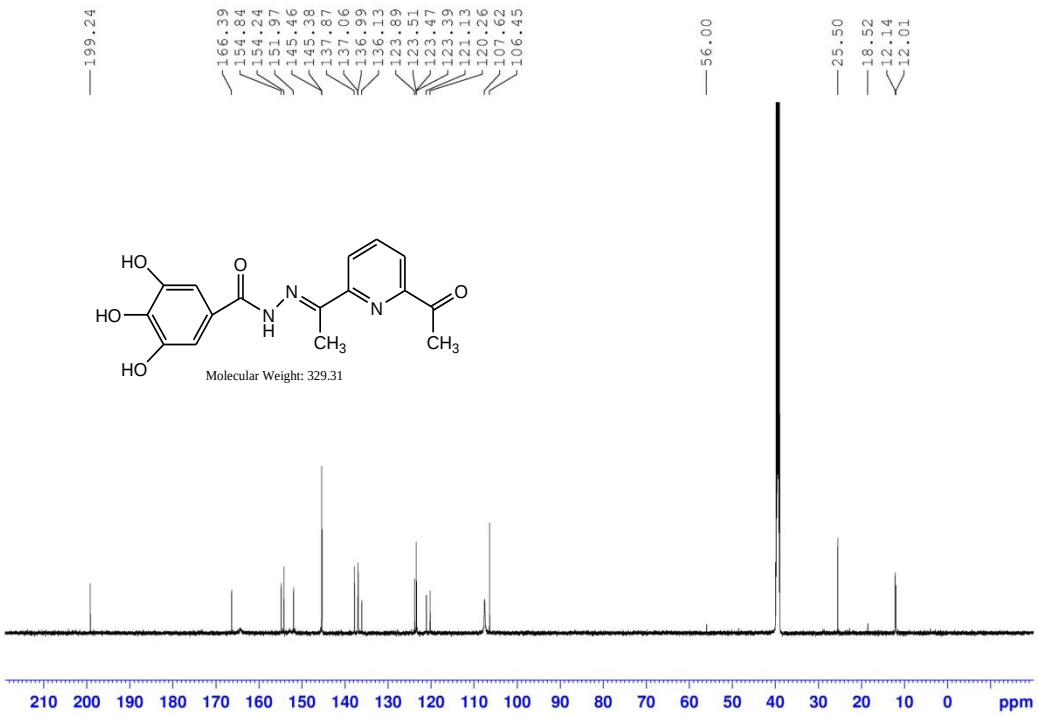

Appendix 47:13C-NMR spectrum for 2,6-DAP

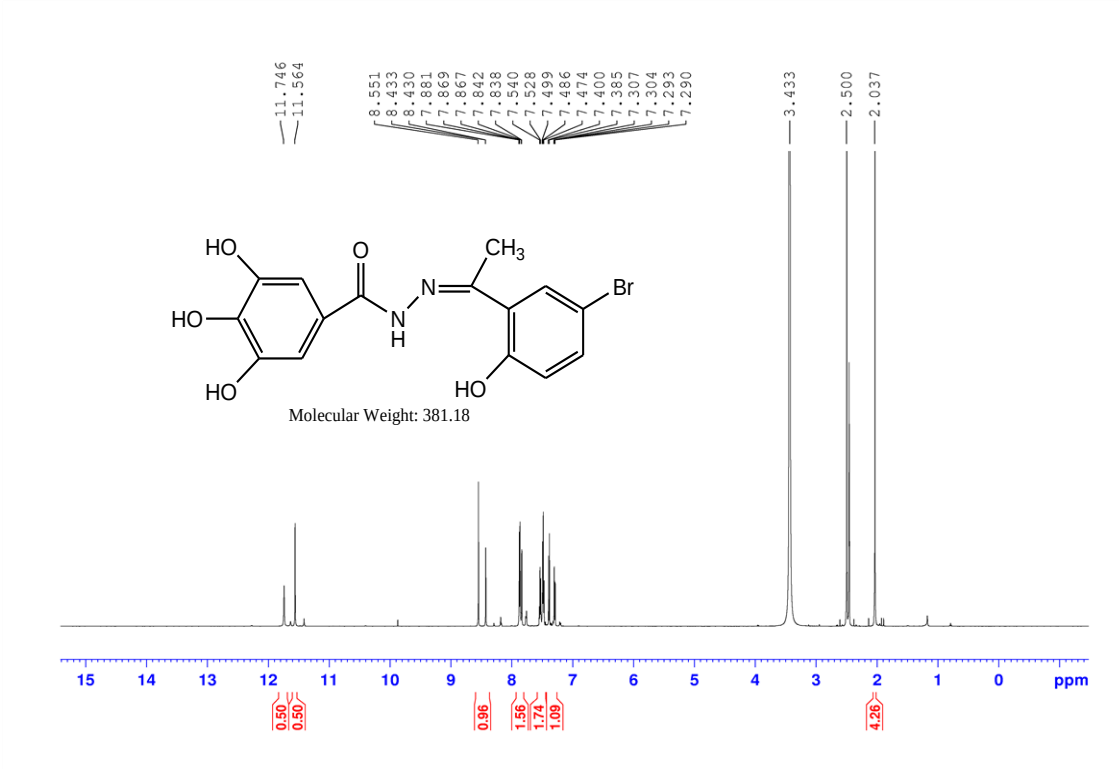

Appendix 48:1H-NMR spectrum for BrAP

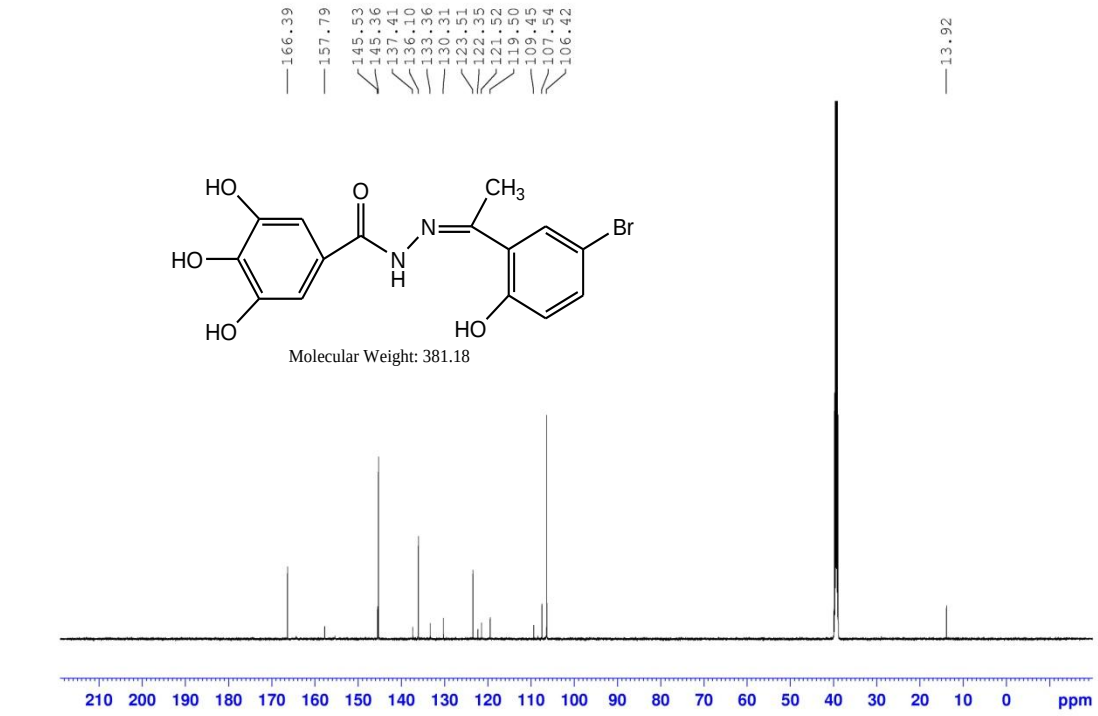

Appendix 49:13C-NMR spectrum for Br-AP

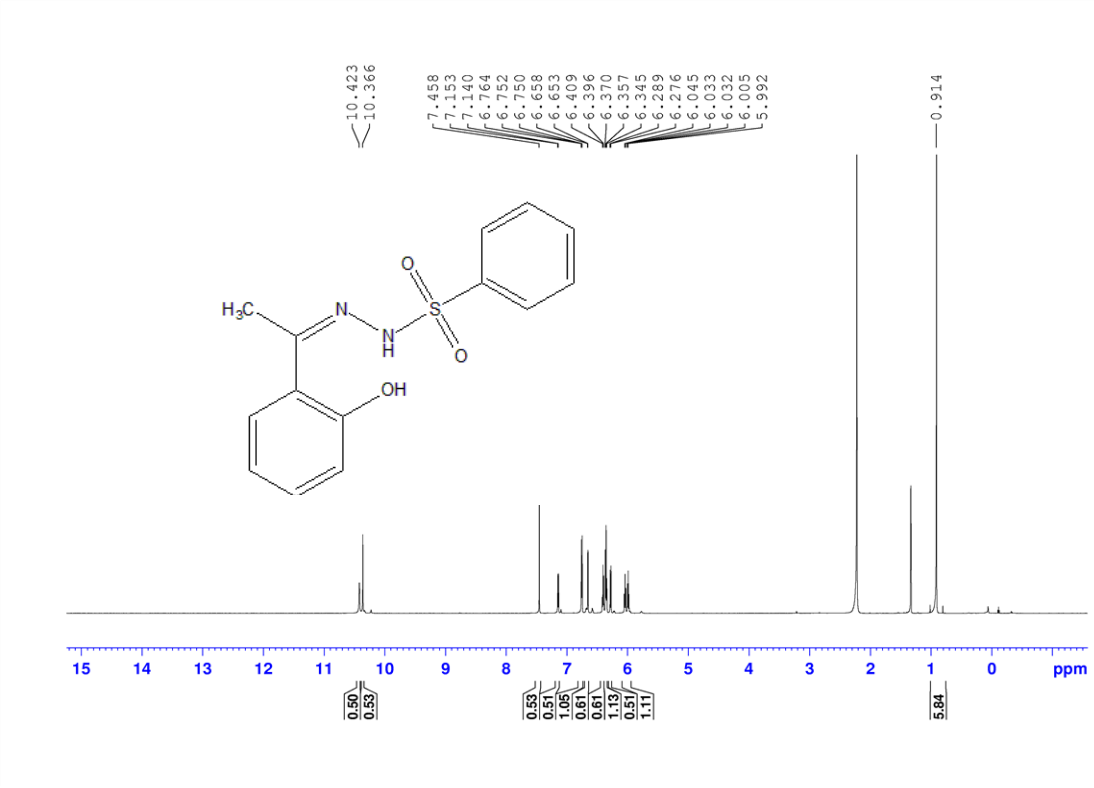

Appendix 50:1H-NMR spectrum for Bs-ZH

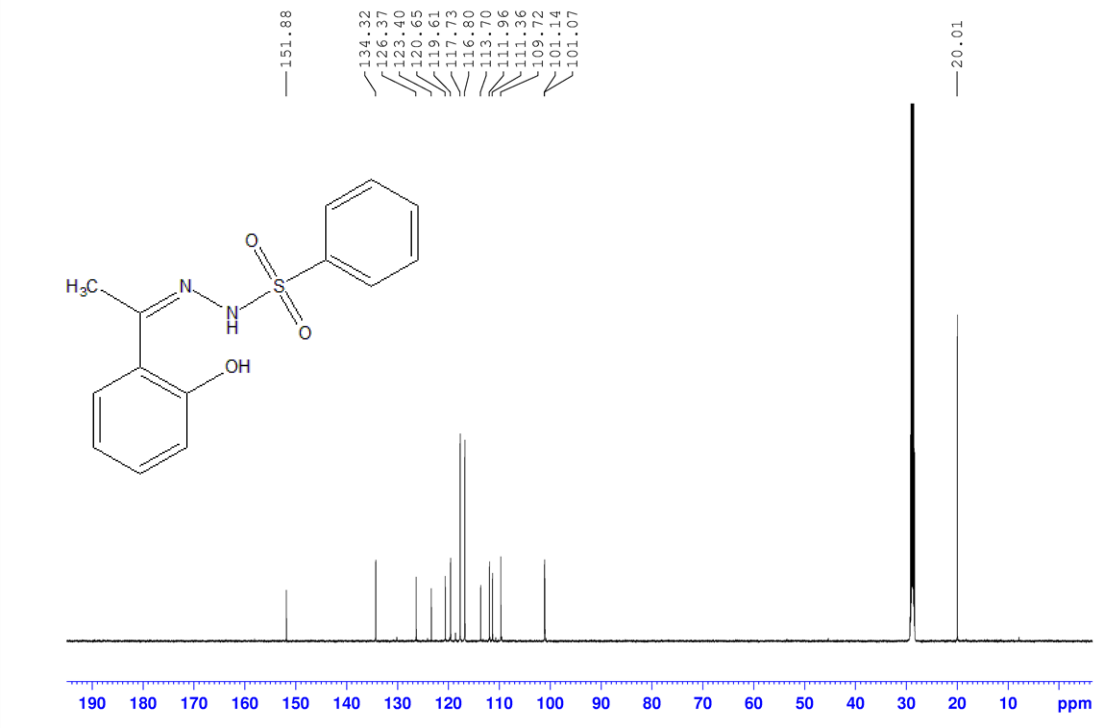

Appendix 51:13C-NMR spectrum for BS-ZH

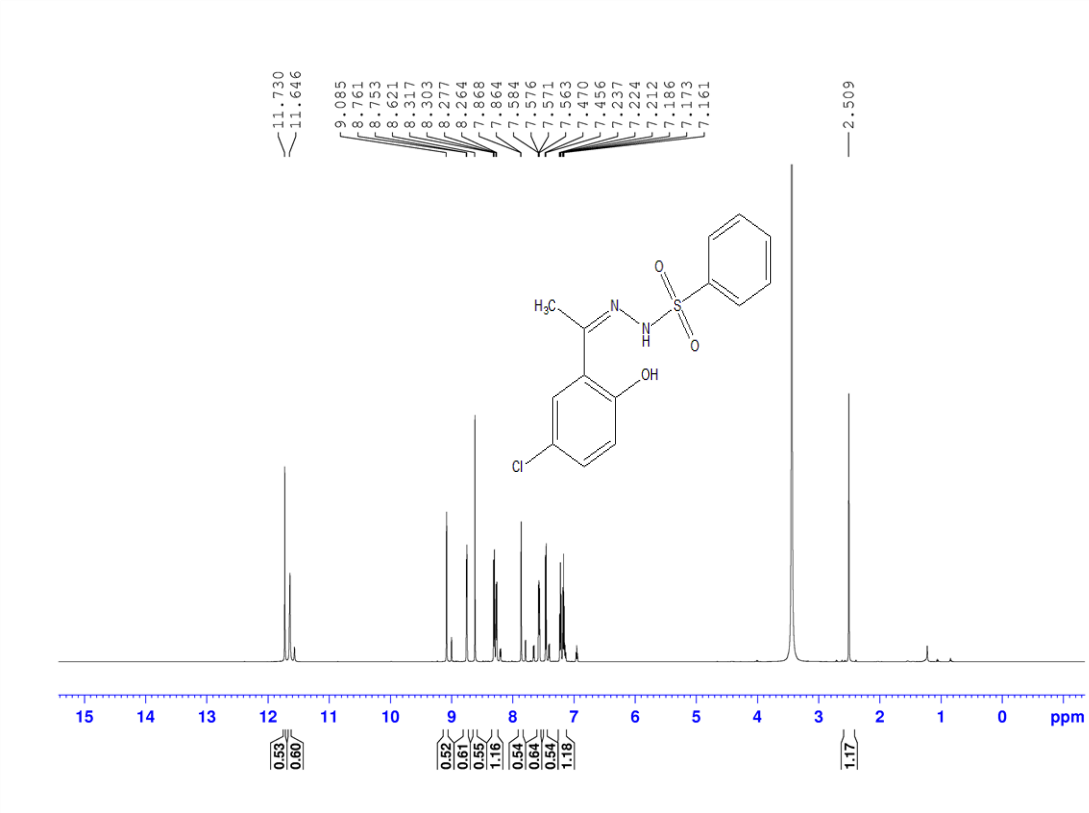

Appendix 52:1H-NMR spectrum for Cl-Bs-ZH

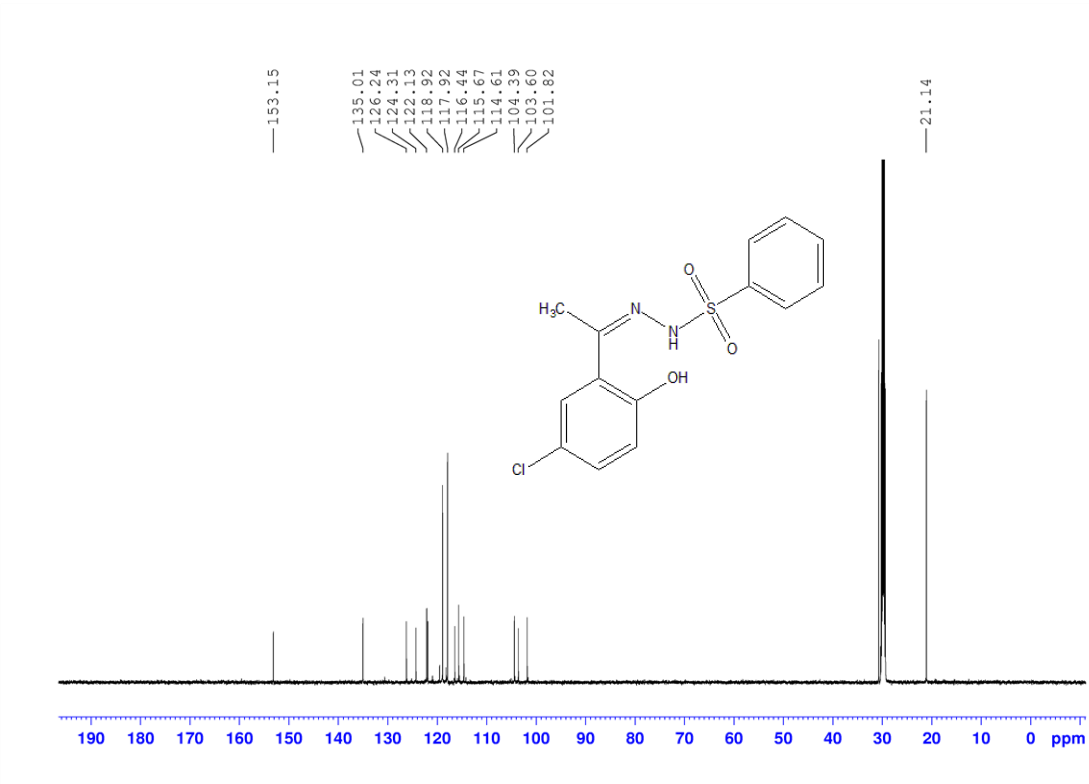

Appendix 53:13C-NMR spectrum for Cl-Bs-ZH

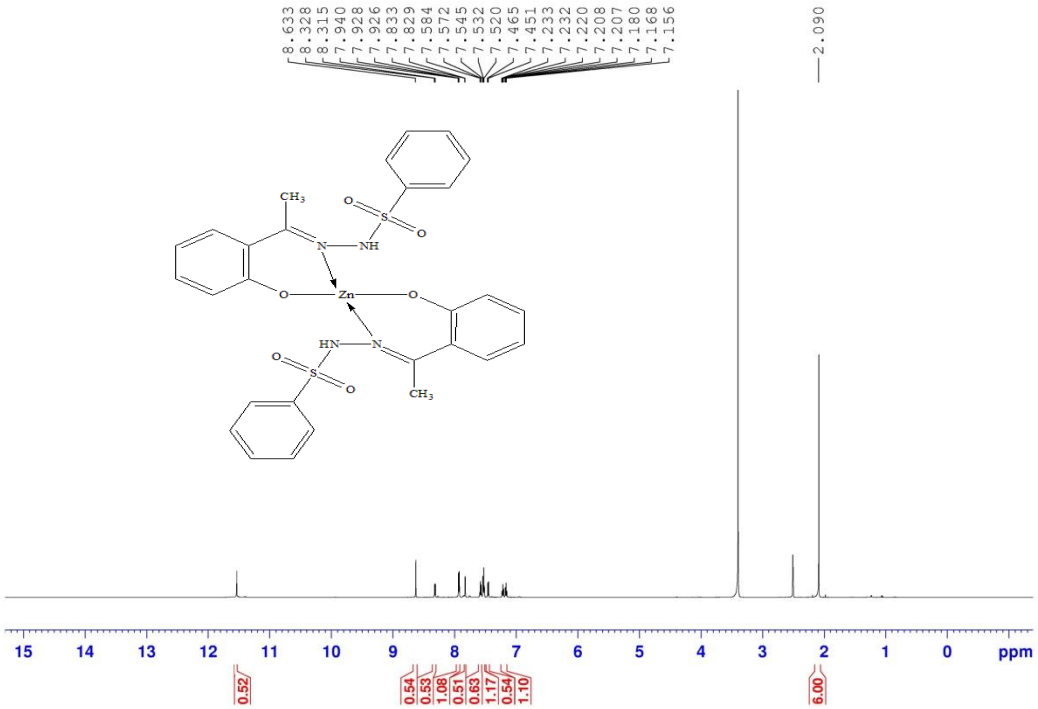

Appendix 54:1H-NMR spectrum for Zn-Bs-ZH

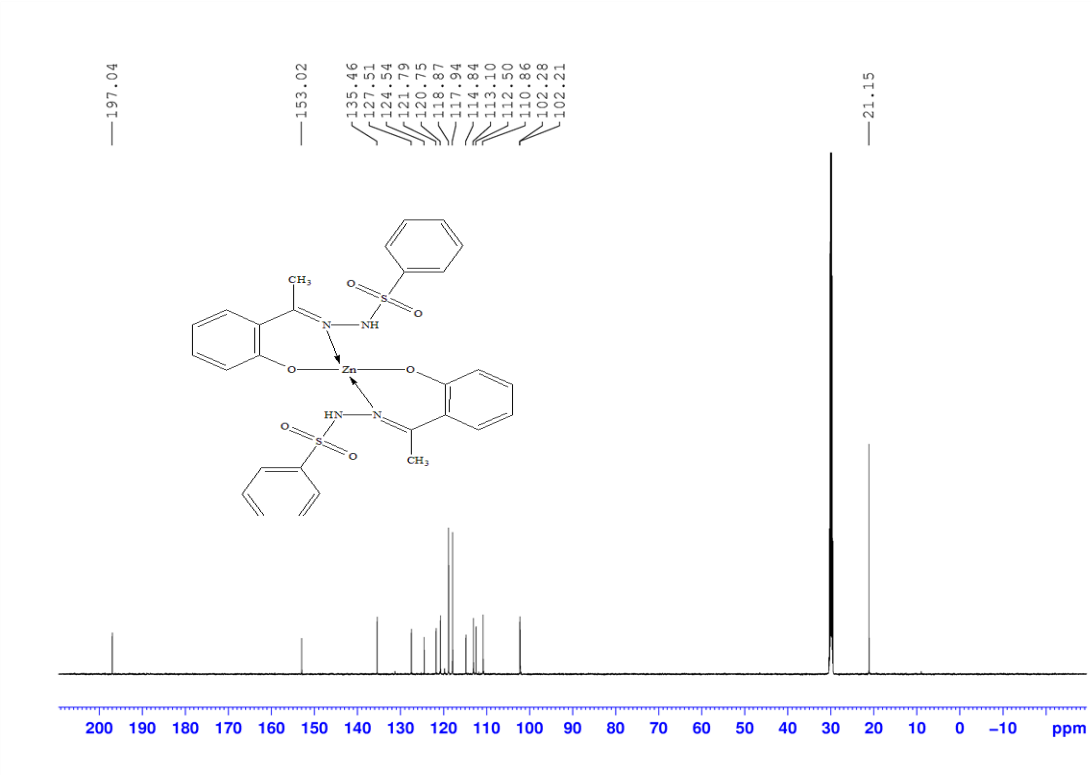

Appendix 55:13C-NMR spectrum for Zn-Bs-ZH

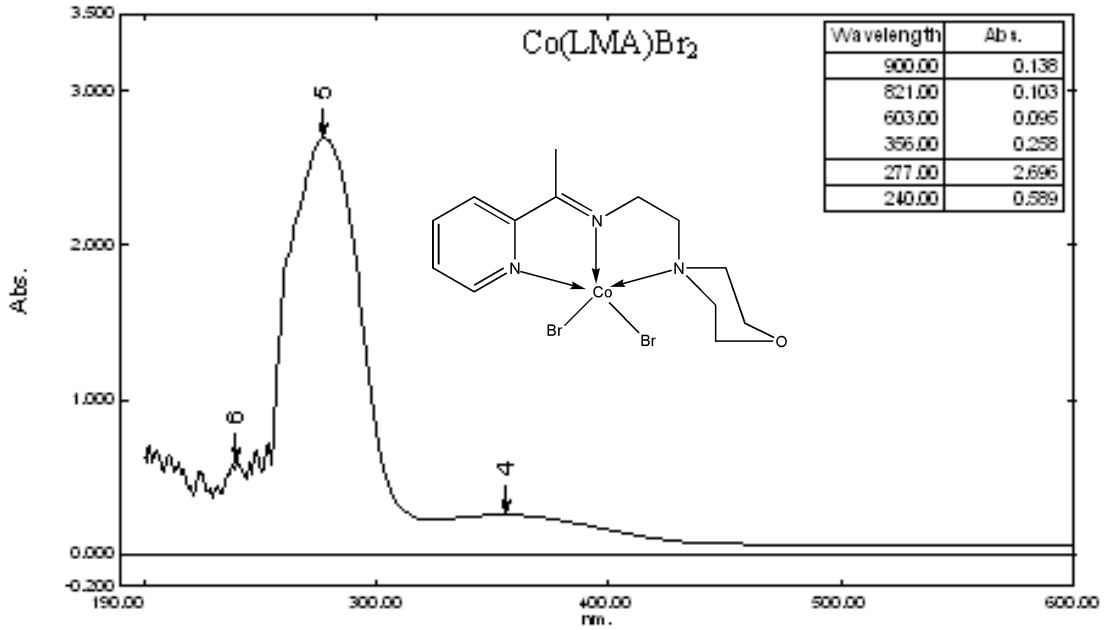

Appendix 56: UV-Visible spectra of [Co(LMA)Br_2]

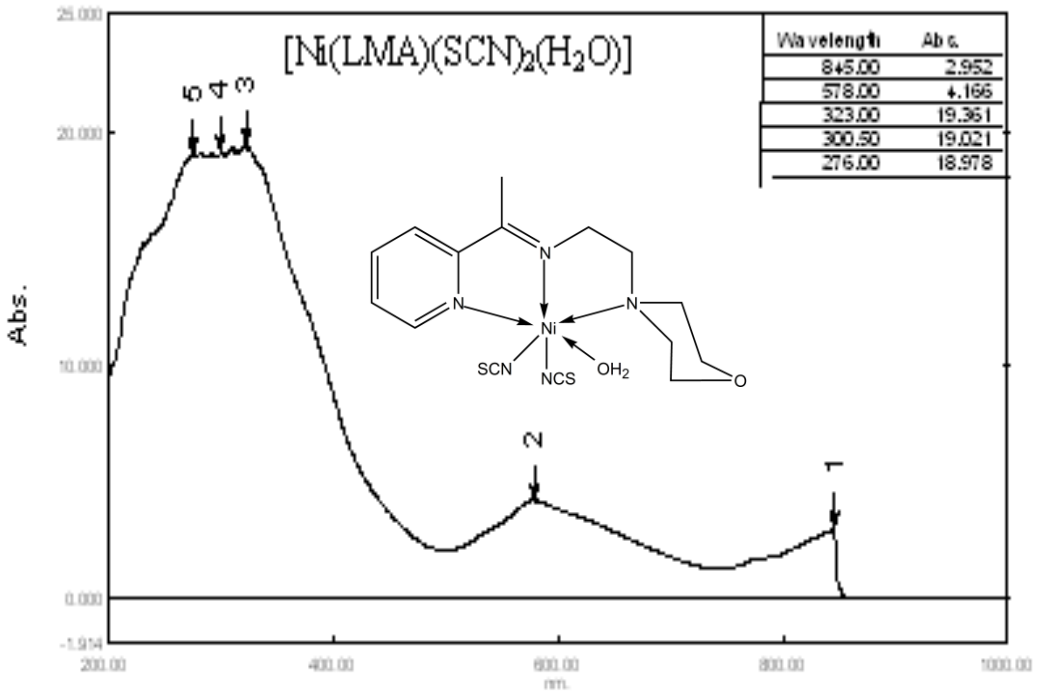

Appendix 57: UV-Visible spectra of [Ni(LMA)(NCS)(H_2O)]

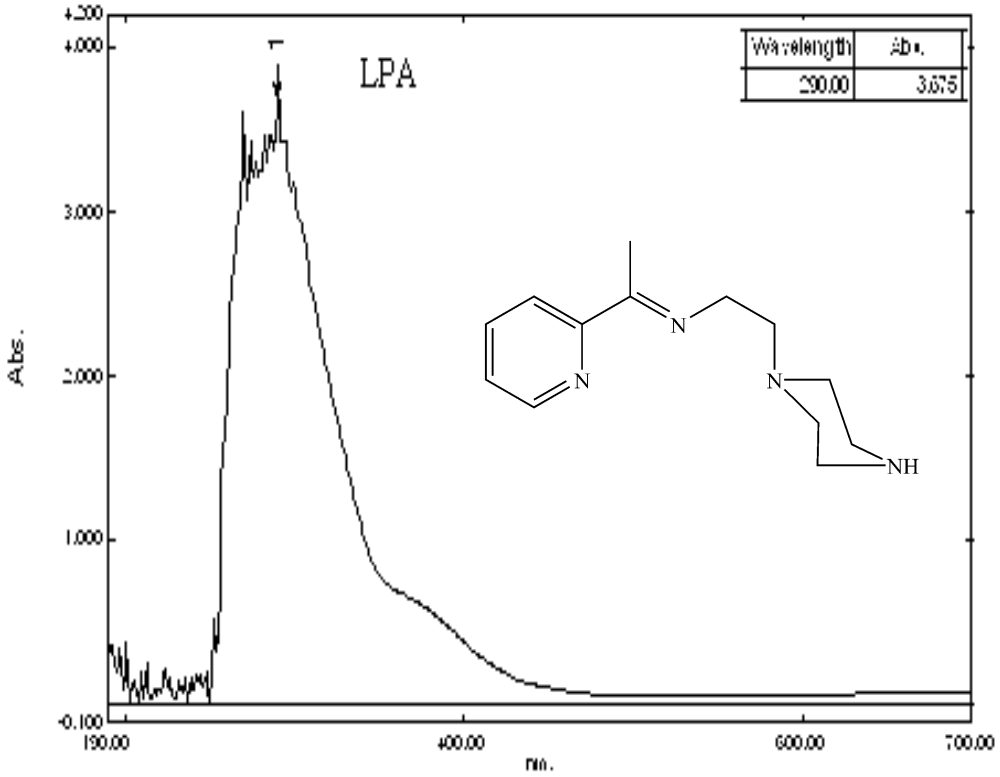

Appendix 58: UV-Visible spectra of LPA

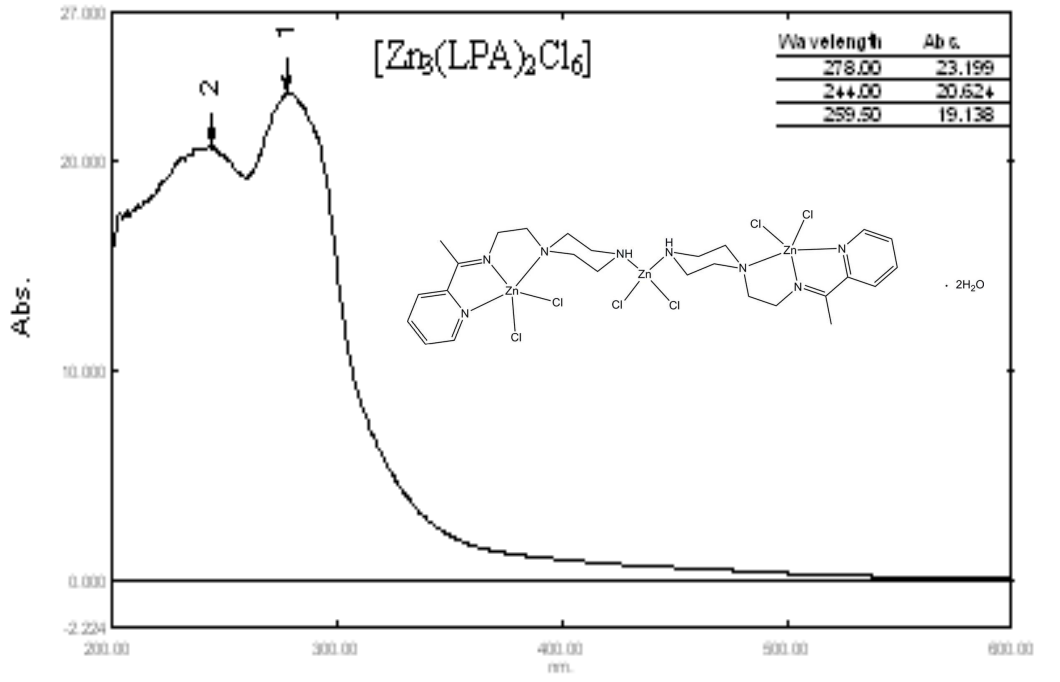

Appendix 59: UV-Visible spectra of $[Zn_3(LPA)_2Cl_6]$

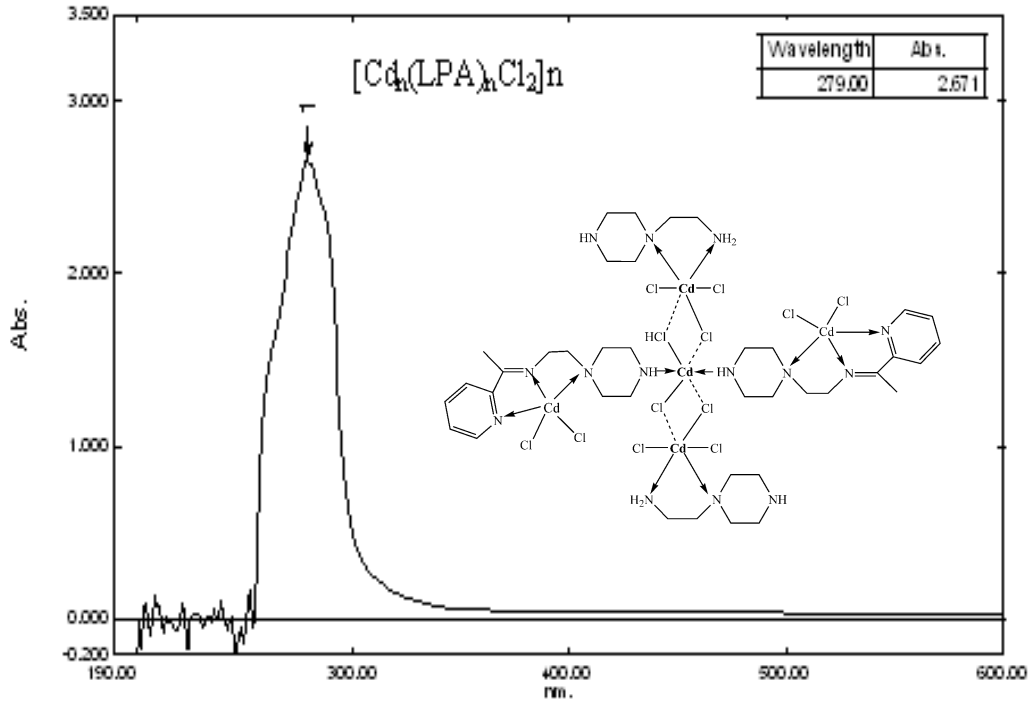

Appendix 60: UV-Visible spectra of [Cdn(LPA)nCl]n

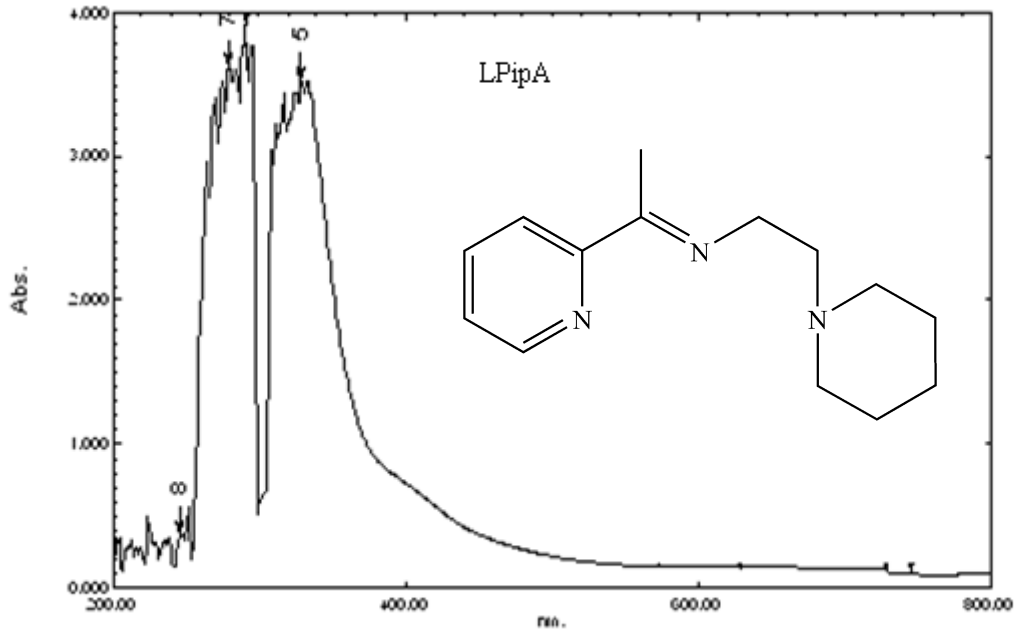

Appendix 61: UV-Visible spectra of LPipA

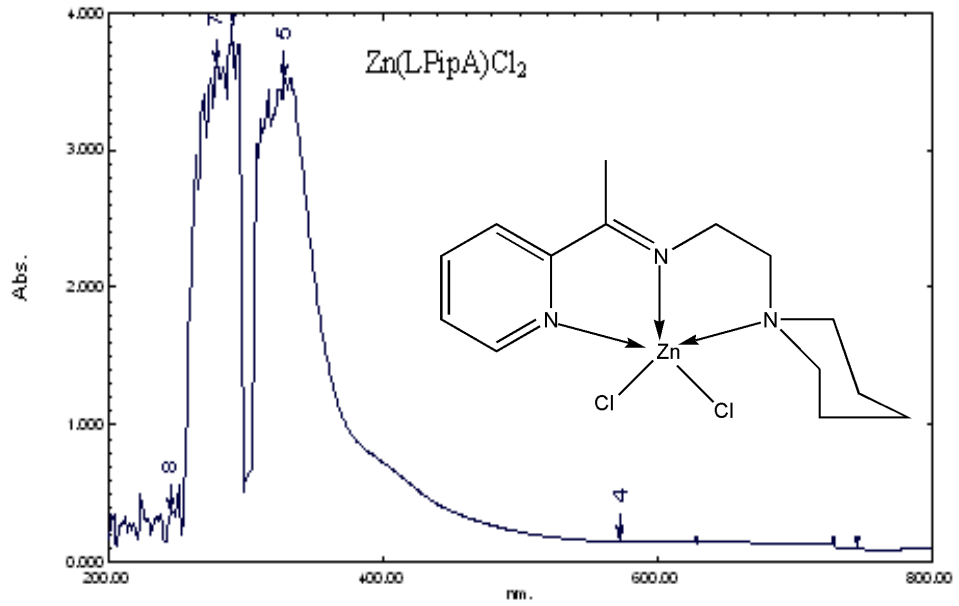

Appendix 62: UV-Visible spectra of [$Zn(LPipA)Cl_2$]

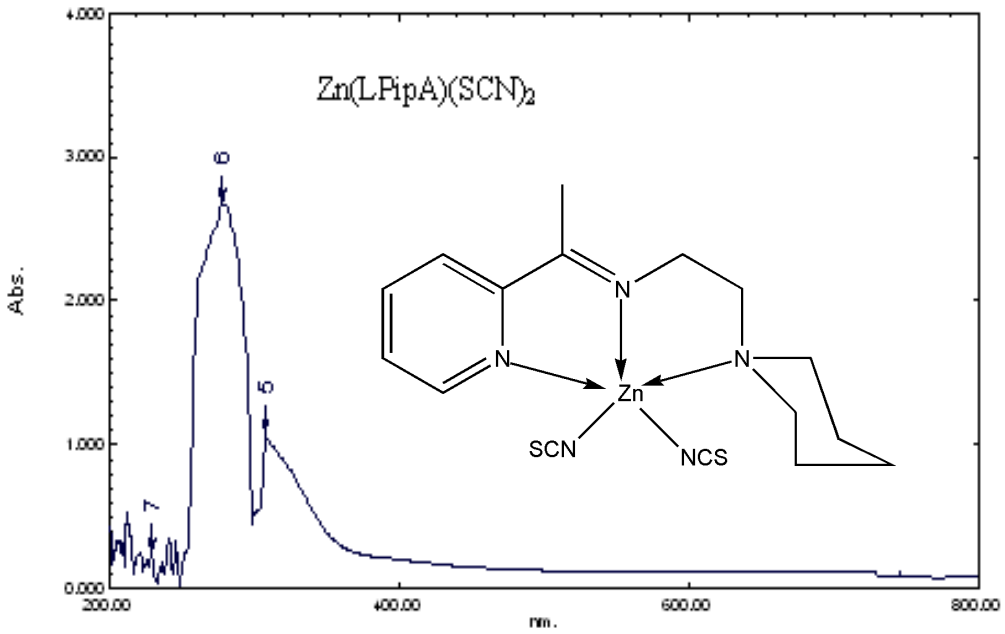

Appendix 63: UV-Visible spectra of [$Zn(LPipA)(NCS)_2$]

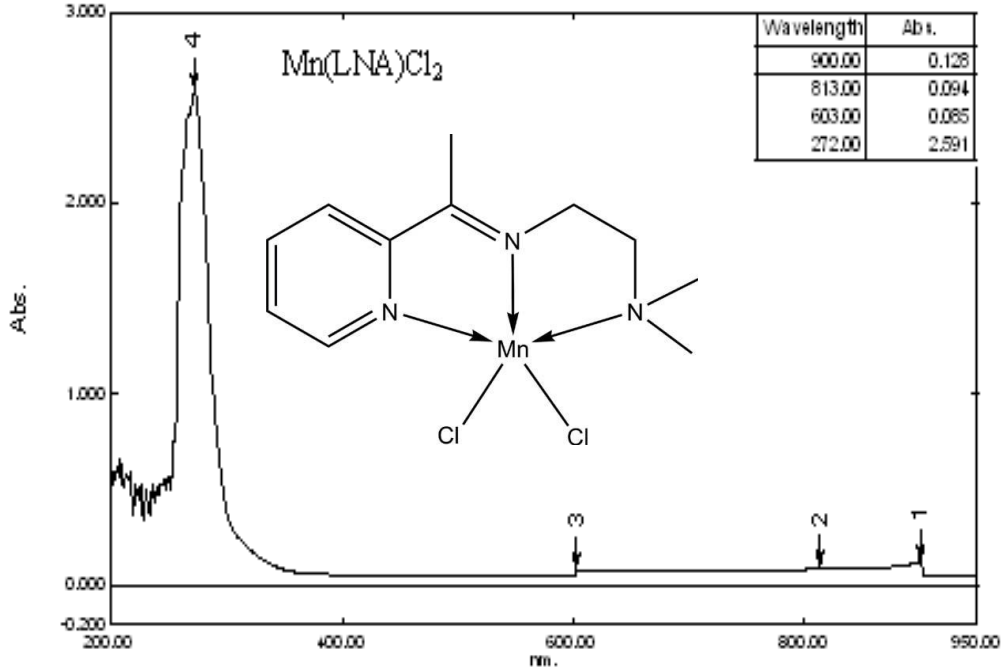

Appendix 64: UV-Visible spectra of [$Mn(LNA)Cl_2$]

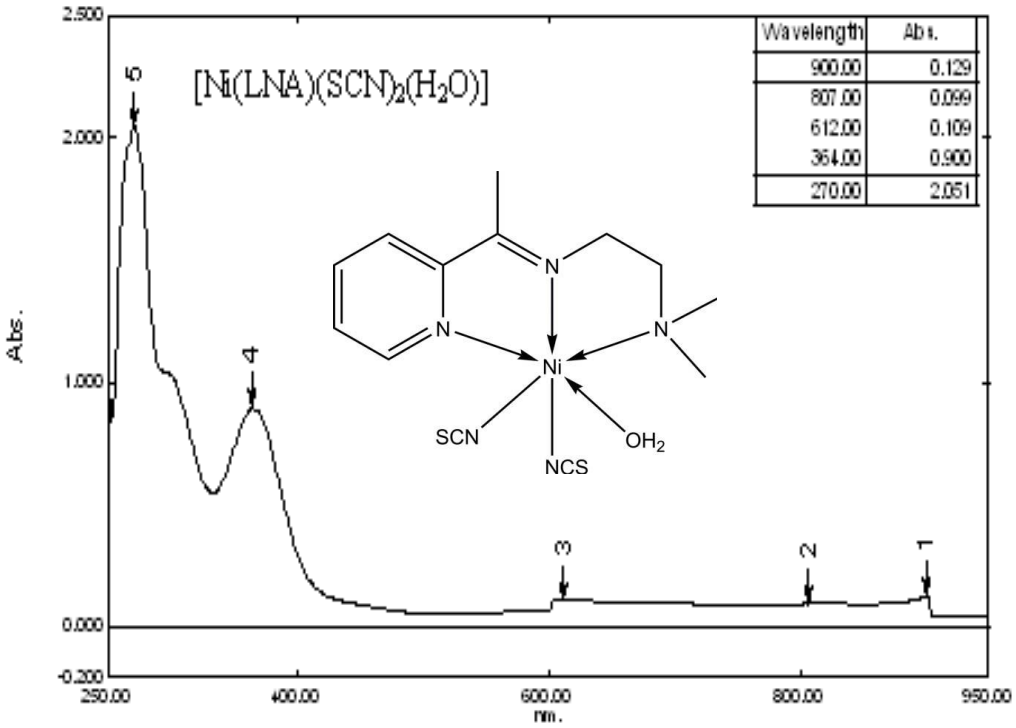

Appendix 65: UV-Visible spectra of [$Ni(LNA)(NCS)_2(H_2O)$]

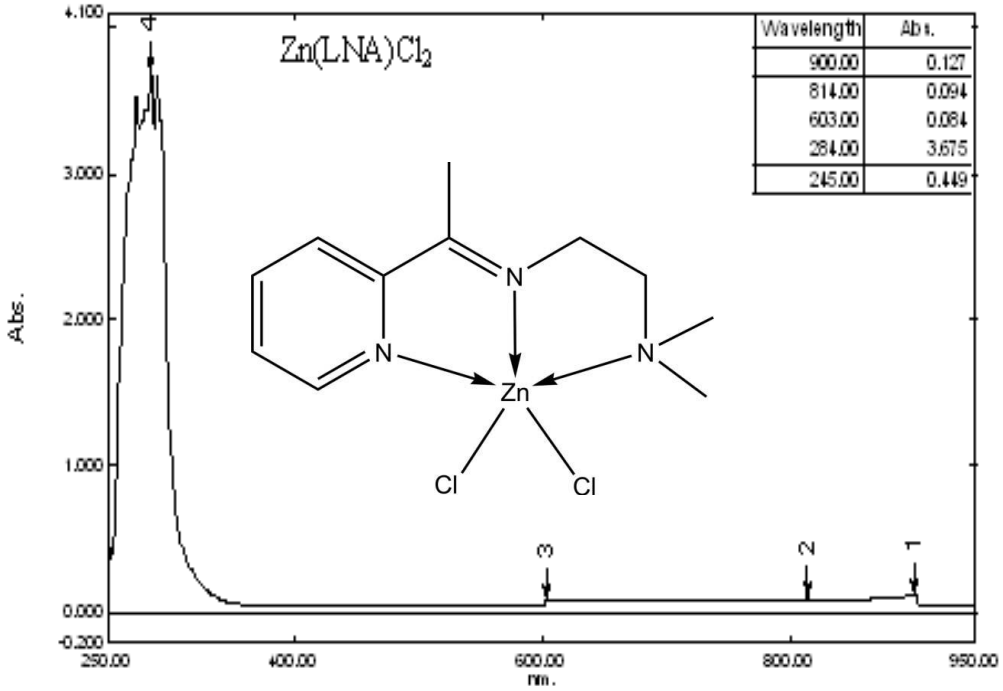

Appendix 66: UV-Visible spectra of [Zn(LNA)Cl_2]

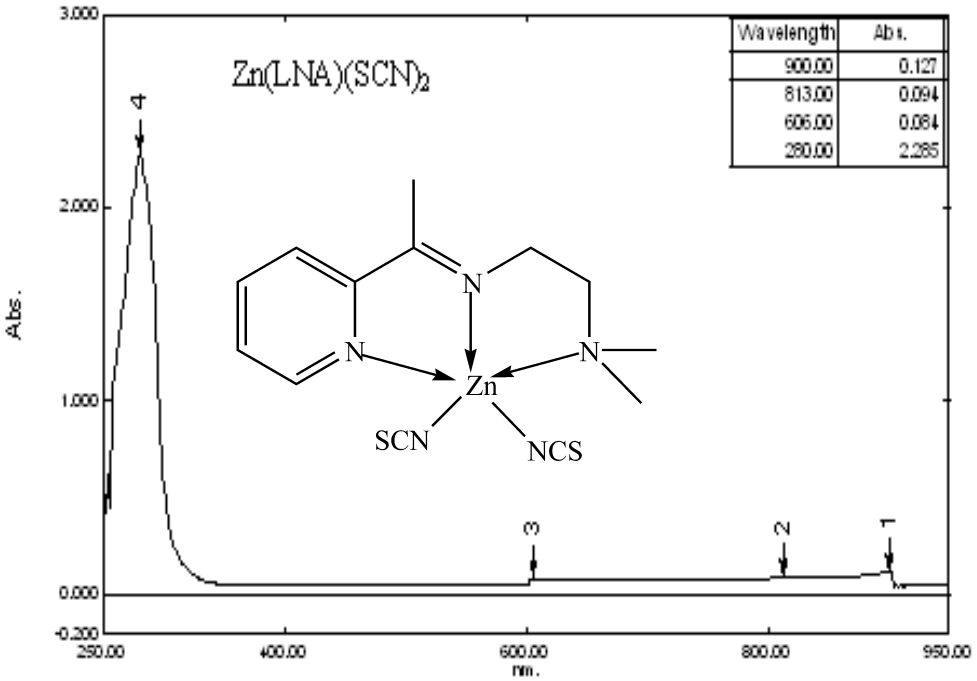

Appendix 67: UV-Visible spectra of [Zn(LNA)$(NCS)_2$]

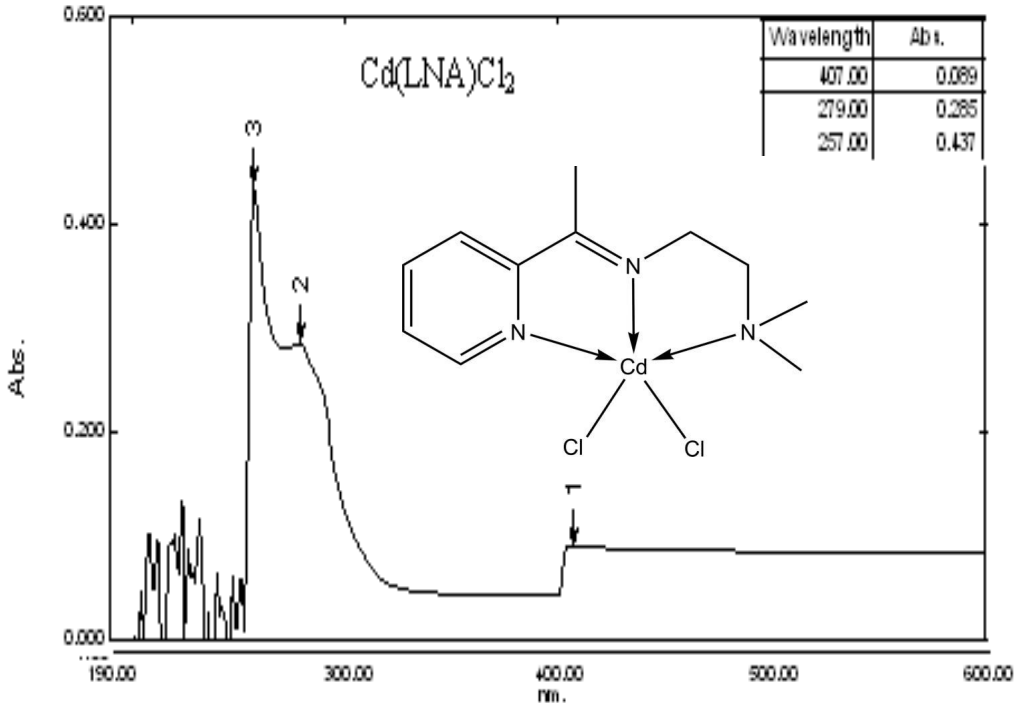

Appendix 68: UV-Visible spectra of [Cd(LNA)Cl_2]

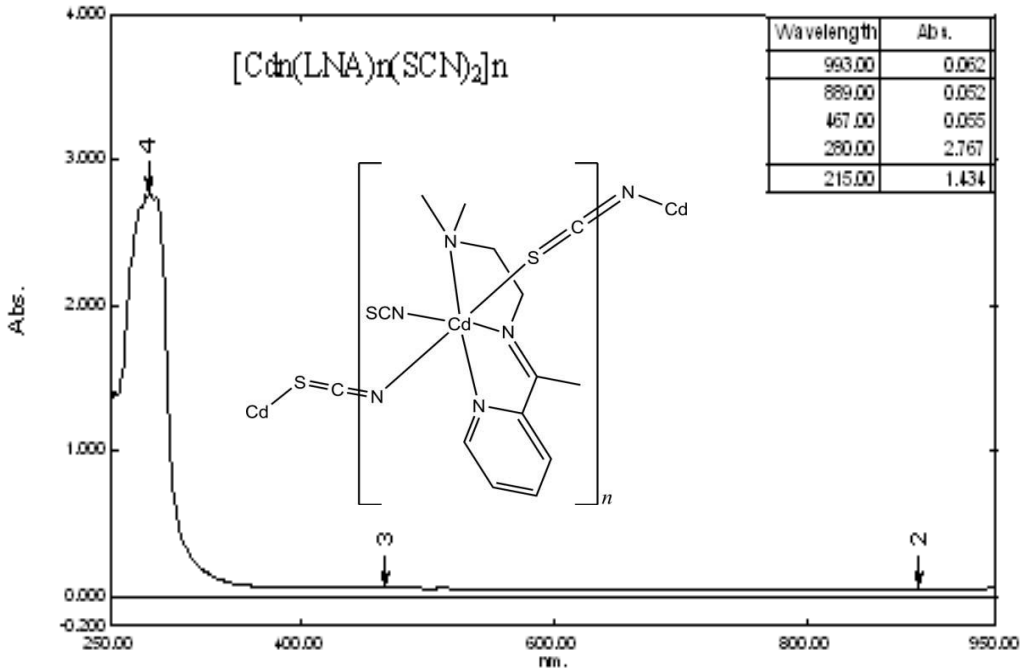

Appendix 69: UV-Visible spectra of [Cdn(LNA)n(NCS)n]n.

OPEN ACCESS Freely available online

PLOS ONE

Gastroprotection Studies of Schiff Base Zinc (II) Derivative Complex against Acute Superficial Hemorrhagic Mucosal Lesions in Rats

Shahram Golbabapour[1,3], Nura Suleiman Gwaram[2], Pouya Hassandarvish[1], Maryam Hajrezaie[1,3], Behnam Kamalidehghan[4], Mahmood Ameen Abdulla[1], Hapipah Mohd Ali[2], A. Hamid A Hadi[2], Nazia Abdul Majid[3]*

1 Department of Biomedical Science, Faculty of Medicine, University of Malaya, Kuala Lumpur, Malaysia, **2** Department of Chemistry, University of Malaya, Kuala Lumpur, Malaysia, **3** Institute of Biological Science, Faculty of Science, University of Malaya, Kuala Lumpur, Malaysia, **4** Department of Pharmacy, Faculty of Medicine, University of Malaya, Kuala Lumpur, Malaysia

Abstract

Background: The study was carried out to assess the gastroprotective effect of the zinc (II) complex against ethanol-induced acute hemorrhagic lesions in rats.

Methodology/Principal Finding: The animals received their respective pre-treatments dissolved in tween 20 (5% v/v), orally. Ethanol (95% v/v) was orally administrated to induce superficial hemorrhagic mucosal lesions. Omeprazole (5.790×10^{-5} M/kg) was used as a reference medicine. The pre-treatment with the zinc (II) complex (2.181×10^{-5} and 4.362×10^{-5} M/kg) protected the gastric mucosa similar to the reference control. They significantly increased the activity levels of nitric oxide, catalase, superoxide dismutase, glutathione and prostaglandin E2, and decreased the level of malondialdehyde. The histology assessments confirmed the protection through remarkable reduction of mucosal lesions and increased the production of gastric mucosa. Immunohistochemistry and western blot analysis indicated that the complex might induced Hsp70 up-regulation and Bax down-regulation. The complex moderately increased the gastroprotectiveness in fine fettle. The acute toxicity approved the non-toxic characteristic of the complex ($<87.241\times10^{-5}$ M/kg).

Conclusion/Significance: The gastroprotective effect of the zinc (II) complex was mainly through its antioxidant activity, enzymatic stimulation of prostaglandins E2, and up-regulation of Hsp70. The gastric wall mucus was also a remarkable protective mechanism.

Citation: Golbabapour S, Gwaram NS, Hassandarvish P, Hajrezaie M, Kamalidehghan B, et al. (2013) Gastroprotection Studies of Schiff Base Zinc (II) Derivative Complex against Acute Superficial Hemorrhagic Mucosal Lesions in Rats. PLoS ONE 8(9): e75036. doi:10.1371/journal.pone.0075036

Editor: David D. Roberts, Center for Cancer Research, National Cancer Institute, United States of America

Received May 1, 2013; **Accepted** August 8, 2013; **Published** September 13, 2013

Funding: This study was funded and supported by the University of Malaya (HIR Grant UM.C/625/1/HIR/151 and PG016/2012B and RG057/11BIO). The funders had no role in study design, data collection and analysis, decision to publish, or preparation of the manuscript.

Competing Interests: The authors have declared that no competing interests exist.

* E-mail: nazia@um.edu.my

Introduction

Zinc, the second most abundant transition metal, is an essential trace element with a variety of biological roles in organisms [1–3]. It stabilizes macromolecules [4] and is critical in storage routines, transcription factors, and replication proteins [5,6]. Involved in various metabolisms of genome [7–10] and proteins [11–13], zinc is a vital biological element (for a review, see [14]). Variation in structural configuration of zinc proteins introduced zinc as the only metal which appears in all six fundamental enzyme classes; oxidoreductases, lyases, hydrolases, transferases, ligases, and isomerases [15]. Zn^{2+} possesses lewis acid properties [16] and redox activity [17]. Zinc based compounds potentially may have a variety of therapeutic activities which makes it an attractive element in drug therapy. Analogous zinc compound has anti-bacterial activity against gram-positive bacteria [1]. Zinc controls bacterial gene expression for instance, bacterial proteins such as the iron responsive regulator fur, alcohol dehydrogenases, hydrolases, lyases, and Cu/Zn superoxide dismutases utilize zinc [18–20]. The effectiveness of the zinc (II) complex in preventing mucosal damage might inhibit pathogenesis activity of bacteria in the gastrointestinal (GI) tract.

Inflammatory reactions are governed by histamine, bradykinin, serotonin, prostaglandins, the blood clotting system, and T cells (lymphokines) [21]. Essential for T-cell proliferation, activation of extracellular signal regulated kinase 2 in response to IL-2 is dependent on zinc [21]. Zinc signals in neutrophil granulocytes are required for the formation of neutrophil extracellular traps [22]. The presence of bromine atoms coordinated to the zinc metal ion seemed a possible active site for the complex and this might be ascribed to the electron donating properties of the halogens by resonance, making the lone pair electrons more available to a plausible electron transfer (for a review, see [23,24]). Similarly, bromine substituted copper complex showed amazing

OPEN ACCESS Freely available online

PLOS ONE

Acute Toxicity and Gastroprotection Studies of a New Schiff Base Derived Copper (II) Complex against Ethanol-Induced Acute Gastric Lesions in Rats

Maryam Hajrezaie[1,3☯], Shahram Golbabapour[1,3☯], Pouya Hassandarvish[1], Nura Suleiman Gwaram[2], A. Hamid A. Hadi[2], Hapipah Mohd Ali[2], Nazia Majid[3], Mahmood Ameen Abdulla[1]*

1 Department of Molecular Medicine, Faculty of Medicine, University of Malaya, Kuala Lumpur, Malaysia, 2 Department of Chemistry, University of Malaya, Kuala Lumpur, Malaysia, 3 Institute of Biological Science, Faculty of Science, University of Malaya, Kuala Lumpur, Malaysia

Abstract

Background: Copper is an essential element in various metabolisms. The investigation was carried out to evaluate acute gastroprotective effects of the Copper (II) complex against ethanol-induced superficial hemorrhagic mucosal lesions in rats.

Methodology/Principal Findings: Rats were divided into 7 groups. Groups 1 and 2 were orally administered with Tween 20 (10% v/v). Group 3 was orally administered with 20 mg/kg omeprazole (10% Tween 20). Groups 4–7 received 10, 20, 40, and 80 mg/kg of the complex (10% Tween 20), respectively. Tween 20 (10% v/v) was given orally to group 1 and absolute ethanol was given orally to groups 2–7, respectively. Rats were sacrificed after 1 h. Group 2 exhibited severe superficial hemorrhagic mucosal lesions. Gastric wall mucus was significantly preserved by the pre-treatment complex. The results showed a significant increase in glutathione (GSH), superoxide dismutase (SOD), nitric oxide (NO), and Prostaglandin E2 (PGE_2) activities and a decrease in malondialdehyde (MDA) level. Histology showed marked reduction of hemorrhagic mucosal lesions in groups 4–7. Immunohistochemical staining showed up-regulation of Hsp70 and down-regulation of Bax proteins. PAS staining of groups 4–7 showed intense stain uptake of gastric mucosa. The acute toxicity revealed the non-toxic nature of the compound.

Conclusions/Significance: The gastroprotective effect of the Copper (II) complex may possibly be due to preservation of gastric wall mucus; increase in PGE_2 synthesis; GSH, SOD, and NO up-regulation of Hsp70 protein; decrease in MDA level; and down-regulation of Bax protein.

Citation: Hajrezaie M, Golbabapour S, Hassandarvish P, Gwaram NS, A Hadi AH, et al. (2012) Acute Toxicity and Gastroprotection Studies of a New Schiff Base Derived Copper (II) Complex against Ethanol-Induced Acute Gastric Lesions in Rats. PLoS ONE 7(12): e51537. doi:10.1371/journal.pone.0051537

Editor: David D. Roberts, Center for Cancer Research, National Cancer Institute, United States of America

Received July 11, 2012; **Accepted** November 8, 2012; **Published** December 10, 2012

Funding: The authors would like to thank the University of Malaya for funding this research, RG373/11HTM and HIR-MOHE (F000009-21001). The funders had no role in study design, data collection and analysis, decision to publish, or preparation of the manuscript.

Competing Interests: The authors have declared that no competing interests exist.

* E-mail: ammeen@um.edu.my

☯ These authors contributed equally to this work.

Introduction

Ulcer is an open sore or lesion, usually found on the skin or mucous membrane of the body. A peptic ulcer is a lesion occurs at the lining of the stomach or duodenum, where hydrochloric acid and pepsin are present. In the past, it was thought that lifestyle factors, such as stress and diet caused ulcers. Later, researchers found that stomach acids (i.e., hydrochloric acid) and pepsin took part in ulcer formation. Many researches have shown that most ulcers (80% of gastric ulcers and 90% of duodenal ulcers) contribute significantly to bacterium *Helicobacter pylori*. Among the three factors (lifestyle, hydrochloric acid and pepsin, and *H. Pylori*) important in ulcer development, *H. pylori* is the primary cause of the gastric ulcer [1,2]. Stress is an important etiological factor in the incidence of gastric ulcer. Free radicals, in stress-involved gastrointestinal injuries, may inactivate synthetize of mucosal prostaglandin (by accumulating H_2O_2, an inhibitor in synthesis of the prostaglandin, which propitiates the generation of reactive oxygen species [3]. Lipid-derived free radicals such as conjugated dienes and lipid hydroperoxides cause oxidative reactions. The process of lipid peroxidation is mediated by the interaction between hydroxyl radicals and the cell membrane, during which the lipid-derived free radicals produce [4]. Recently, a numerous researches have been inclined to find effective synthetic chemical compounds with gastroprotective properties [5,6,7].

Copper is an essential trace element in human metabolism, but does not exist in ionic form in biological systems. The amount of copper in the body is measured in complexes with organic compounds. The process of chelating metals smuggles them to bypass the intestinal wall and to enter into the mainstream of nutrient flow and usage in the body. Copper complexes such as copper aspirinate and copper tryptophanate, remarkably increase healing rate of ulcers and wounds [8]. The Copper complexes shorten the healing period of gastric ulcers for five days and promote the wound healing process at the same time retaining

Molecules **2012**, *17*, 5952-5971; doi:10.3390/molecules17055952

OPEN ACCESS

molecules

ISSN 1420-3049

www.mdpi.com/journal/molecules

Article

Antibacterial Evaluation of Some Schiff Bases Derived from 2-Acetylpyridine and Their Metal Complexes

Nura Suleiman Gwaram [1,*], Hapipah Mohd Ali [1], Hamid Khaledi [1], Mahmood Ameen Abdulla [2], A. Hamid A. Hadi [1], Thong Kwai Lin [3], Chai Lay Ching [3] and Cher Lin Ooi [3]

[1] Chemistry Department, Faculty of Science, University of Malaya, Kuala Lumpur 50603, Malaysia; E-Mails: hapipah@um.edu.my (H.M.A.); khaledi@gmail.com (H.K.)

[2] Molecular Medicine Department, Faculty of Medicine, University of Malaya, Kuala Lumpur 50603, Malaysia; E-Mail: ameen@um.edu.my

[3] Institute of Biological Science, Faculty of Science, University of Malaya, Kuala Lumpur 50603, Malaysia; E-Mails: thongkl@um.edu.my (T.K.L.); lcchai@um.edu.my (C.L.C.)

* Author to whom correspondence should be addressed; E-Mail: nura_suleiman@yahoo.com; Tel.: +603-7967-4246/7155; Fax: +603-7967-4193.

Received: 27 March 2012; in revised form: 13 May 2012 / Accepted: 15 May 2012 / Published: 18 May 2012

Abstract: A series of Schiff bases derived from 2-acetylpyridne and their metal complexes were characterized by elemental analysis, NMR, FT-IR and UV-Vis spectral studies. The complexes were screened for anti-bacterial activity against Methicillin-resistant *Staphylococcus aureus* (MRSA), *Acinetobacter baumanni* (AC), *Klebsiella pneumonie* (KB) and *Pseudomonas aeruginosa* (PA) using the disc diffusion and micro broth dilution assays. Based on the overall results, the complexes showed the highest activities against MRSA while a weak antibacterial activity was observed against *A. baumanii* and *P. aeruginosa*.

Keywords: Schiff bases; metal complexes; x-ray crystallography; anti-bacteria

1. Introduction

Schiff base ligands containing various donor atoms (like N, O, S, *etc*.) show broad biological activities and are of special interest due to variety of ways in which they can bond to metal ions. It is known that the existence of metal ions bonded to biologically active compounds may enhance their activities [1]. Schiff base metal complexes show great diversity in their varied biological activities as

Molecules **2012**, *17*, 2408-2427; doi:10.3390/molecules17032408

OPEN ACCESS

molecules

ISSN 1420-3049

www.mdpi.com/journal/molecules

Article

Synthesis, Characterization, X-ray Crystallography, Acetyl Cholinesterase Inhibition and Antioxidant Activities of Some Novel Ketone Derivatives of Gallic Hydrazide-Derived Schiff Bases

Nura Suleiman Gwaram [1,*], Hapipah Mohd Ali [1], Mahmood Ameen Abdulla [2], Michael J. C. Buckle [3], Sri Devi Sukumaran [3], Lip Yong Chung [3], Rozana Othman [3], Abeer A. Alhadi [3], Wageeh A. Yehye [1], A. Hamid A. Hadi [1], Pouya Hassandarvish [2], Hamid Khaledi [1] and Siddig Ibrahim Abdelwahab [3,*]

[1] Department of Chemistry, Faculty of Science, University of Malaya, Kuala Lumpur 50603, Malaysia

[2] Department of Molecular Medicine, Faculty of Medicine, University of Malaya, Kuala Lumpur 50603, Malaysia

[3] Departments of Pharmacy, Faculty of Medicine, University of Malaya, Kuala Lumpur 50603, Malaysia

* Authors to whom correspondence should be addressed; E-Mails: nura_suleiman@siswa.um.edu.my (N.S.G.); siddigroa@yahoo.com (S.I.A.); Tel.: +60-12-656-5990.

Received: 28 January 2012; in revised form: 21 February 2012 / Accepted: 23 February 2012 / Published: 28 February 2012

Abstract: Alzheimer's disease (AD) is the most common form of dementia among older people and the pathogenesis of this disease is associated with oxidative stress. Acetylcholinesterase inhibitors with antioxidant activities are considered potential treatments for AD. Some novel ketone derivatives of gallic hydrazide-derived Schiff bases were synthesized and examined for their antioxidant activities and *in vitro* and *in silico* acetyl cholinesterase inhibition. The compounds were characterized using spectroscopy and X-ray crystallography. The ferric reducing antioxidant power (FRAP) and 2,2-diphenyl-1-picrylhydrazyl (DPPH) assays revealed that all the compounds have strong antioxidant activities. *N*-(1-(5-bromo-2-hydroxyphenyl)-ethylidene)-3,4,5-trihydroxybenzohydrazide (2) was the most potent inhibitor of human acetyl cholinesterase, giving an inhibition rate of 77% at 100 μM. Molecular docking simulation of the ligand-enzyme complex suggested that the ligand may be positioned in the enzyme's active-site gorge, interacting with residues in the peripheral anionic subsite (PAS) and acyl

Hindawi Publishing Corporation
BioMed Research International
Volume 2013, Article ID 703626, 7 pages
http://dx.doi.org/10.1155/2013/703626

Research Article

Schiff Base Metal Derivatives Enhance the Expression of HSP70 and Suppress BAX Proteins in Prevention of Acute Gastric Lesion

Shahram Golbabapour,[1,2] Nura Suleiman Gwaram,[3] Mazen M. Jamil Al-Obaidi,[4] A. F. Soleimani,[5] Hapipah Mohd Ali,[3] and Nazia Abdul Majid[2]

[1] *Department of Biomedical Science, Faculty of Medicine, University of Malaya, 50603 Kuala Lumpur, Malaysia*
[2] *Institute of Biological Sciences, Faculty of Science, University of Malaya, 50603 Kuala Lumpur, Malaysia*
[3] *Department of Chemistry, Faculty of Science, University of Malaya, 50603 Kuala Lumpur, Malaysia*
[4] *Faculty of Dentistry, Universiti Teknologi MARA, 40450 Shah Alam, Malaysia*
[5] *Institute of Tropical Agriculture, Universiti Putra Malaysia, 43400 Kuala Lumpur, Malaysia*

Correspondence should be addressed to Nazia Abdul Majid; nazia@um.edu.my

Received 26 June 2013; Accepted 22 September 2013

Academic Editor: Ibrahim Banat

Schiff base complexes have appeared to be promising in the treatment of different diseases and disorders and have drawn a lot of attention to their biological activities. This study was conducted to evaluate the regulatory effect of Schiff base metal derivatives on the expression of heat shock proteins (HSP) 70 and BAX in protection against acute haemorrhagic gastric ulcer in rats. Rats were assigned to 6 groups of 6 rats: the normal control (Tween 20 5% v/v, 5 mL/kg), the positive control (Tween 20 5% v/v, 5 mL/kg), and four Schiff base derivative groups named SchiffL1, SchiffL2, SchiffL3, and SchiffL4 (25 mg/kg). After 1 h, all of the groups received ethanol 95% (5 mL/kg) but the normal control received Tween 20 (Tween 20 5% v/v, 5 mL/kg). The animals were euthanized after 60 min and the stomachs were dissected for histology (H&E), immunohistochemistry, and western blot analysis against HSP 70 and BAX proteins. The results showed that the Schiff base metal derivatives enhanced the expression of HSP70 and suppressed the expression of BAX proteins during their gastroprotection against ethanol-induced gastric lesion in rats.

1. Introduction

Wide spectrum applications of the Schiff base in biological systems have opened a new horizon in pharmaceutical researches. Schiff bases are usually synthesized through the condensation process of primary amines and active carbonyl groups. Furthermore, indole derivatives have critical roles in variety of biological activities. In novel therapeutics, the development of hybrid molecules consisting different pharmacophores in one frame may lead to remarkable pharmacological effects. The coadministration of the moieties, acting by different mechanisms, may have a synergistic effect with higher activities [1]. The pharmacological activity of Schiff bases metal complexes is solely attributed to the metal, its ligands, or both. Two important factors such as maximum thermodynamic stability and large degree of selectivity are crucial in the design of Schiff base metal complexes or ligands for pharmaceutical application. Various metal complexes have been introduced for their potential therapeutic applications. Possessing various biological activities, some of the first row transition metals are important in metalloproteins. The chemistry of the metal complexes of Schiff bases containing nitrogen and other donors is well described by Tarafder and colleagues [2]. Various Schiff base complexes have shown variety of properties such as anticancer [3–5], antimicrobial, antifungal [6, 7], antiviral [8] and antioxidant, and anti-inflammatory activity [9]; also see [10]. It is believed that some complexes are more effective in metal complexes

ARTICLE IN PRESS

Arabian Journal of Chemistry (2012) xxx, xxx–xxx

King Saud University

Arabian Journal of Chemistry

www.ksu.edu.sa
www.sciencedirect.com

ORIGINAL ARTICLE

Synthesis, spectral characterization and biological activity of Zn(II) complex with 2′-[1-(2-hydroxyphenyl)ethylidene]benzenesulfanohydrazide

Nura Suleiman Gwaram [a], Laila Musalam [a], Hapipah Mohd. Ali [a], Mahmood Ameen Abdulla [b], Shayma A. Shaker [c,*]

[a] Chemistry Department, Faculty of Science, University of Malaya, 50603 Kuala Lumpur, Malaysia
[b] Molecular Medicine Department, Faculty of Medicine, University of Malaya, 50603 Kuala Lumpur, Malaysia
[c] Department of Engineering Sciences and Mathematics, College of Engineering, Universiti Tenaga Nasional, KM 7 Jalan Kajang-Puchong, 43009 Kajang, Selangor, Malaysia

Received 20 July 2011; accepted 7 January 2012

KEYWORDS
Benzenesulfanohydrazone;
Zinc(II) complex;
Schiff base;
Gastric ulcer;
Histology

Abstract Zinc(II) complex with 2′-[1-(2-hydroxyphenyl) ethylidene] benzenesulfanohydrazide, was synthesized, and structurally characterized by elemental analysis CHN, TGA, UV, FT-IR, ^{1}H NMR and ^{13}C NMR spectroscopy. Its preventive effect on ulcer activity induced by absolute ethanol in Sprague–Dawley rats was studied *in vivo*. Gastric ulcers were induced in rats by administrating absolute ethanol. Twenty four Spragu–Dawley rats (12 males and 12 females) were assigned equally into the following 4 groups ($n = 6$): negative control; positive control; low dose, which received low oral doses of the compound; and high dose, which received high oral doses of the compounds . These animals were subjected to overnight fasting (food but not water) prior to dosing. Gastric wall mucus, ulcer areas and histology of gastric walls were assessed in addition gastric homogenate was determined for superoxide dismutase (SOD), glutathione (GSH) and malondialdehyde (MDA). Pre-treatment of rats with compound significantly prevented ethanol-induced gastric wall depletion and restored non-sulfhydryl (NP-SH) content in glandular stomachs. The Zinc(II) complex also exhibits high levels of SOD, and GSH enzymes as well as a reduced amount of lipid

* Corresponding author. Tel.: +60 3 8921 7241.
E-mail address: drshaimaa611@yahoo.com (S.A. Shaker).

Peer review under responsibility of King Saud University.
doi:10.1016/j.arabjc.2012.01.002

Production and hosting by Elsevier

Please cite this article in press as: Gwaram, N.S. et al., Synthesis, spectral characterization and biological activity of Zn(II) complex with 2′-[1-(2-hydroxyphenyl)ethylidene]benzenesulfanohydrazide. Arabian Journal of Chemistry (2012), doi:10.1016/j.arabjc.2012.01.002

Journal of Applied Pharmaceutical Science Vol. 2 (12), pp. 027-038, December, 2012
Available online at http://www.japsonline.com
DOI: 10.7324/JAPS.2012.21206
ISSN 2231-3354

Synthesis, characterization, and biological applications of some 2-acetylpyridine and acetophenone derivatives

Nura Suleiman Gwaram[*1], Hapipah Mohd Ali[1], Siti Munirah Saharin[1], Mahmood Ameen Abdulla[2], Pouya Hassandarvish[2], Thong Kwai Lin[3], Chai Lay Ching[3] and Cher Lin Ooi[3]

[1]Chemistry Department, Faculty of Science, University of Malaya, 50603 Kuala Lumpur, Malaysia.
[2]Molecular Medicine Department, Faculty of Medicine, University of Malaya, 50603 Kuala Lumpur, Malaysia.
[3]Institute of Biological Science Faculty of science, University of Malaya, 50603 Kuala Lumpur, Malaysia.

ARTICLE INFO

Article history:
Received on: 09/12/2012
Revised on: 21/12/2012
Accepted on: 26/12/2012
Available online: 30/12/2012

Key words:
Schiff bases; Complexes; Anticancer; MCF-7; Antibacterial; MRSA

ABSTRACT

This paper comprises two series of complexes which showed different modes of coordination. The fist series involved an *N,N',N''*-donor Schiff base ligand from the reaction of 2-acetylpridine as carbonyl compound with *N,N'*-dimethylethylenediamine (**L1**), the second series involved *N,N',O*-donor Schiff base from the condensation reaction of 2-hydroxyacetophenone (ketone) as carbonyl compound with *N,N'*-dimethylethylenediamine (**L2**). The ligands and complexes were characterized by using melting point, elemental analysis, FT-IR, NMR, and UV/Visible spectroscopy. The complexes showed very low cytotoxicity towards MCF-7 breast cancer cell line. They also showed moderate zone inhibition against Gram positive bacterium *Methicillin-resistant Staphylococcus aureus*. *Acinetobacter baumannii* and *Pseudomonas aeruginosa*. No antimicrobial activity observed with *Klebsiella pneumonia*.

INTRODUCTION

Many pyridines find application in areas where bioactivity is important, as in medicinal drugs and in agricultural products such as herbicides, insecticides, fungicides, and plant growth regulators (Goe, 1982). 2-Acetylpyridine is used as a chemical intermediate in organic synthetic, pharmaceutical & agricultural chemical manufacture and as an analytical reagent. Also used as a food additive as a flavor enhancer, flavoring agent or adjuvant (Goe, 1982) In the area of bioinorganic chemistry the interest in the imines complexes lies in that they provide synthetic models for the metal-containing sites in metalloproteins/enzymes and also contributed enormously to the development of medicinal chemistry, radio immunotherapy, cancer diagnosis and treatment of tumor (Adoración *et al.,* 2004; Larry, 2003). In addition, some of the complexes containing N and O donor atoms are effective as stereo specific catalysts for oxidation (Kureshy *et al.,* 1999) reduction (Yasuhiro *et al.,* 1986), hydrolysis (Ross *et al.,* 1986), biocidal activity (Parbati *et al.,* 2001) and other transformations of organic and inorganic chemistry. Some of the members of the first row transition metals play major roles in various biological activities on which recently have been included in anticancer agents to exploit their various applications because of the exceptionally wide range of reactivity available and have been particularly attractive (Nenad *et al.,* 1996) these transition metal complexes offer a great diversity in their action; such as anticancer and antiviral properties (Bernadette *et al.,* 2010; Garoufis *et al.,* 2009, Bernadette *et al.,* 2010; Raman *et al.,* 2010 and Shakir *et al.,* 2011), DNA binding and DNA cleavage activities (Shahabadi *et al.,* 2010) and many other biological activities (Mladenova *et al.,* 2002). It is also known that the existence of metal ions bonded to biologically active compounds may enhance their antimicrobial activities (Prakash *et al.,* 2010). Such as anticonvulsant (Sridhar *et al.,* 2002), antifungal (Bharti *et al.,* 2010), anti-HIV (Pandeya *et al.,* 1999), antiviral and anticancer (Zhang *et al.,* 2009) and antimicrobial (Mandal *et al.,* 2011; Yusnita *et al.,* 2009; Pignatello *et al.,* 1994; Nair *et al.,* 2010; Tajudeen *et al.,* 2009 and Ling-Wei *et al.,* 2011).

* *Corresponding Author*
Department of chemistry, Faculty of Science,
University of Malaya, 50603 Kuala lumpur, Malaysia.

Acta Crystallographica Section E
Structure Reports Online
ISSN 1600-5368

Dibromido{2-(morpholin-4-yl)-*N*-[1-(2-pyridyl)ethylidene]ethanamine-κ^3N,N',N''}cadmium

Nura Suleiman Gwaram, Hamid Khaledi* and Hapipah Mohd Ali

Department of Chemistry, University of Malaya, 50603 Kuala Lumpur, Malaysia
Correspondence e-mail: khaledi@siswa.um.edu.my

Received 9 February 2011; accepted 15 February 2011

Key indicators: single-crystal X-ray study; T = 100 K; mean σ(C–C) = 0.005 Å; R factor = 0.021; wR factor = 0.041; data-to-parameter ratio = 20.0.

The Cd^{II} ion in the title compound, $[CdBr_2(C_{13}H_{19}N_3O)]$, is five-coordinated by the *N*,*N*′,*N*′′-tridentate Schiff base ligand and two Br atoms in a distorted square-pyramidal geometry. In the crystal, intermolecular C—H···O and C—H···Br hydrogen bonds link adjacent molecules into layers parallel to the *ab* plane. An intramolecular C—H···Br interaction is also observed.

Related literature

For the crystal structure of the analogous $CdCl_2$ complex, see: Ikmal Hisham *et al.* (2010). For the crystal structures of similar $CdBr_2$ complexes, see: Bermejo *et al.* (1999, 2003). For a description of the geometry of complexes with five-coordinate metal atoms, see: Addison *et al.* (1984).

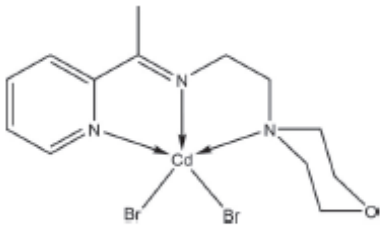

Experimental

Crystal data

$[CdBr_2(C_{13}H_{19}N_3O)]$
M_r = 505.53
Orthorhombic, $P2_12_12_1$
a = 9.1906 (8) Å
b = 12.2604 (10) Å
c = 14.7499 (12) Å
V = 1662.0 (2) Å^3
Z = 4
Mo $K\alpha$ radiation
μ = 6.12 mm^{-1}
T = 100 K
0.33 × 0.27 × 0.19 mm

Data collection

Bruker APEXII CCD diffractometer
Absorption correction: multi-scan (*SADABS*; Sheldrick, 1996)
T_{min} = 0.237, T_{max} = 0.389
20236 measured reflections
3642 independent reflections
3445 reflections with $I > 2\sigma(I)$
R_{int} = 0.032

Refinement

$R[F^2 > 2\sigma(F^2)]$ = 0.021
$wR(F^2)$ = 0.041
S = 1.09
3642 reflections
182 parameters
H-atom parameters constrained
$\Delta\rho_{max}$ = 0.73 e Å^{-3}
$\Delta\rho_{min}$ = −0.54 e Å^{-3}
Absolute structure: Flack (1983), 1556 Friedel pairs
Flack parameter: 0.023 (9)

Table 1
Hydrogen-bond geometry (Å, °).

D—H···A	D—H	H···A	D···A	D—H···A
C3—H3···O1^{i}	0.95	2.42	3.132 (4)	131
C7—H7*B*···Br1^{ii}	0.98	2.92	3.840 (4)	157
C10—H10*A*···O1^{iii}	0.99	2.45	3.383 (4)	156
C11—H11*B*···Br2	0.99	2.91	3.727 (4)	141

Symmetry codes: (i) $x, y+1, z$; (ii) $x+1, y, z$; (iii) $x+\frac{1}{2}, -y-\frac{1}{2}, -z+2$.

Data collection: *APEX2* (Bruker, 2007); cell refinement: *SAINT* (Bruker, 2007); data reduction: *SAINT*; program(s) used to solve structure: *SHELXS97* (Sheldrick, 2008); program(s) used to refine structure: *SHELXL97* (Sheldrick, 2008); molecular graphics: *X-SEED* (Barbour, 2001); software used to prepare material for publication: *SHELXL97* and *publCIF* (Westrip, 2010).

The authors thank University of Malaya for funding this study (FRGS grant No. FP004/2010B).

Supplementary data and figures for this paper are available from the IUCr electronic archives (Reference: BG2390).

References

Addison, A. W., Rao, T. N., Reedijk, J., Rijn, V. J. & Verschoor, G. C. (1984). *J. Chem. Soc. Dalton Trans.* pp. 1349–1356.
Barbour, L. J. (2001). *J. Supramol. Chem.*, **1**, 189–191.
Bermejo, E., Carballo, R., Castineiras, A., Dominguez, R., Liberta, A. E., Maichle-Moessmer, C., Salberg, M. M. & West, D. X. (1999). *Eur. J. Inorg. Chem.* pp. 965–973.
Bermejo, E., Castineiras, A., Fostiak, L. M., Santos, I. G., Swearingen, J. K. & West, D. X. (2003). *Polyhedron*, **23**, 2303–2313.
Bruker (2007). *APEX2* and *SAINT*. Bruker AXS Inc., Madison, Wisconsin, USA.
Flack, H. D. (1983). *Acta Cryst.* A**39**, 876–881.
Ikmal Hisham, N., Suleiman Gwaram, N., Khaledi, H. & Mohd Ali, H. (2010). *Acta Cryst.* E**66**, m1471.
Sheldrick, G. M. (1996). *SADABS*. University of Göttingen, Germany.
Sheldrick, G. M. (2008). *Acta Cryst.* A**64**, 112–122.
Westrip, S. P. (2010). *J. Appl. Cryst.* **43**, 920–925.

Acta Crystallographica Section E
Structure Reports Online
ISSN 1600-5368

Dichlorido{2-morpholino-*N*-[1-(2-pyridyl)ethylidene]ethanamine-κ^3N,N',N''}cadmium

Nurulazimah Ikmal Hisham, Nura Suleiman Gwaram, Hamid Khaledi* and Hapipah Mohd Ali

Department of Chemistry, University of Malaya, 50603 Kuala Lumpur, Malaysia
Correspondence e-mail: khaledi@siswa.um.edu.my

Received 21 October 2010; accepted 22 October 2010

Key indicators: single-crystal X-ray study; T = 100 K; mean σ(C–C) = 0.008 Å; R factor = 0.038; wR factor = 0.117; data-to-parameter ratio = 18.9.

In the title compound, $[CdCl_2(C_{13}H_{19}N_3O)]$, the Cd^{II} ion is five-coordinate, with the N,N',N''-tridentate Schiff base ligand 2-morpholino-*N*-[1-(2-pyridyl)ethylidene]ethanamine and two Cl atoms in a distorted square-pyramidal geometry. In the crystal structure, C—H···Cl hydrogen-bonding interactions connect the molecules into a three-dimensional network.

Related literature

For the crystal structures of similar compounds, see: Ikmal Hisham *et al.* (2009); Cai (2009).

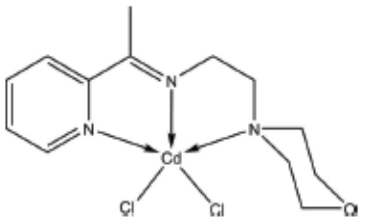

Experimental

Crystal data

$[CdCl_2(C_{13}H_{19}N_3O)]$
M_r = 416.61
Monoclinic, $P2_1/n$
a = 9.6357 (12) Å
b = 13.9300 (18) Å
c = 12.2514 (17) Å
β = 106.776 (2)°
V = 1574.5 (4) Å^3
Z = 4
Mo $K\alpha$ radiation
μ = 1.73 mm^{-1}
T = 100 K
0.23 × 0.10 × 0.04 mm

Data collection

Bruker APEXII CCD diffractometer
Absorption correction: multi-scan (*SADABS*; Sheldrick, 1996)
T_{min} = 0.692, T_{max} = 0.934
9407 measured reflections
3437 independent reflections
2646 reflections with $I > 2\sigma(I)$
R_{int} = 0.043

Refinement

$R[F^2 > 2\sigma(F^2)]$ = 0.038
$wR(F^2)$ = 0.117
S = 1.08
3437 reflections
182 parameters
H-atom parameters constrained
$\Delta\rho_{max}$ = 0.81 e Å^{-3}
$\Delta\rho_{min}$ = −1.16 e Å^{-3}

Table 1
Hydrogen-bond geometry (Å, °).

D—H···A	D—H	H···A	D···A	D—H···A
C4—H4···Cl1^{i}	0.95	2.69	3.603 (6)	161
C7—H7C···Cl2^{ii}	0.98	2.73	3.607 (6)	149
C8—H8A···Cl2^{iii}	0.99	2.82	3.730 (6)	153
C11—H11B···Cl1	0.99	2.80	3.654 (6)	144

Symmetry codes: (i) $-x+1, -y, -z+1$; (ii) $-x+2, -y, -z+1$; (iii) $-x+\frac{1}{2}, y-\frac{1}{2}, -z+\frac{1}{2}$.

Data collection: *APEX2* (Bruker, 2007); cell refinement: *SAINT* (Bruker, 2007); data reduction: *SAINT*; program(s) used to solve structure: *SHELXS97* (Sheldrick, 2008); program(s) used to refine structure: *SHELXL97* (Sheldrick, 2008); molecular graphics: *X-SEED* (Barbour, 2001); software used to prepare material for publication: *SHELXL97* and *publCIF* (Westrip, 2010).

The authors thank the University of Malaya for funding this study (UMRG grant RG024/09BIO).

Supplementary data and figures for this paper are available from the IUCr electronic archives (Reference: PV2344).

References

Barbour, L. J. (2001). *J. Supramol. Chem.* **1**, 189–191.
Bruker (2007). *APEX2* and *SAINT*. Bruker AXS Inc., Madison, Wisconsin, USA.
Cai, B.-H. (2009). *Acta Cryst.* E**65**, m142.
Ikmal Hisham, N. A., Ali, H. M. & Ng, S. W. (2009). *Acta Cryst.* E**65**, m870.
Sheldrick, G. M. (1996). *SADABS*. University of Göttingen, Germany.
Sheldrick, G. M. (2008). *Acta Cryst.* A**64**, 112–122.
Westrip, S. P. (2010). *J. Appl. Cryst.* **43**, 920–925.

Acta Crystallographica Section E
Structure Reports Online
ISSN 1600-5368

Di-μ-thiocyanato-κ^2N:S;κ^2S:N-bis({2-morpholino-N-[1-(2-pyridyl)ethylidene]ethanamine-κ^3N,N',N''}(thiocyanato-κN)cadmium)

Nura Suleiman Gwaram, Nurul Azimah Ikmal Hisham, Hamid Khaledi* and Hapipah Mohd Ali

Department of Chemistry, University of Malaya, 50603 Kuala Lumpur, Malaysia
Correspondence e-mail: khaledi@siswa.um.edu.my

Received 14 January 2011; accepted 18 January 2011

Key indicators: single-crystal X-ray study; T = 100 K; mean σ(C–C) = 0.003 Å; R factor = 0.023; wR factor = 0.047; data-to-parameter ratio = 18.4.

In the title complex, $[Cd_2(NCS)_4(C_{13}H_{19}N_3O)_2]$, the two Cd^{II} ions are bridged by a pair of thiocyanate N:S-bridging ligands around an inversion center. One terminal thiocyanate N atom and one N,N',N'-tridentate Schiff base ligand complete a distorted CdN_5S octahedral geometry about each Cd^{II} atom. In the crystal, the Schiff base aromatic rings of adjacent molecules are arranged above each other into infinite chains along the a axis with alternate centroid–centroid separations of 3.5299 (13) and 3.7857 (13) Å.

Related literature

For the structure of the Cu(II) complex with the same Schiff base and thiocyanate, see: Suleiman Gwaram *et al.* (2011). For the structures of similar cadmium complexes, see: Banerjee *et al.* (2005); You *et al.* (2006).

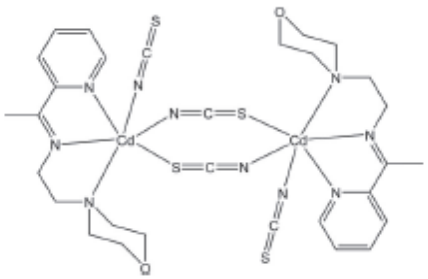

Experimental

Crystal data

$[Cd_2(NCS)_4(C_{13}H_{19}N_3O)_2]$
M_r = 923.74
Monoclinic, $P2_1/c$
a = 7.2934 (2) Å
b = 26.4085 (5) Å
c = 10.0111 (3) Å
β = 107.853 (3)°
V = 1835.02 (9) Å^3
Z = 2
Mo $K\alpha$ radiation
μ = 1.43 mm^{-1}
T = 100 K
0.38 × 0.23 × 0.07 mm

Data collection

Bruker APEXII CCD diffractometer
Absorption correction: multi-scan (*SADABS*; Sheldrick, 1996)
T_{min} = 0.613, T_{max} = 0.907
15344 measured reflections
4008 independent reflections
3638 reflections with $I > 2\sigma(I)$
R_{int} = 0.026

Refinement

$R[F^2 > 2\sigma(F^2)]$ = 0.023
$wR(F^2)$ = 0.047
S = 1.10
4008 reflections
218 parameters
2 restraints
H-atom parameters constrained
$\Delta\rho_{max}$ = 0.39 e Å^{-3}
$\Delta\rho_{min}$ = −0.45 e Å^{-3}

Data collection: *APEX2* (Bruker, 2007); cell refinement: *SAINT* (Bruker, 2007); data reduction: *SAINT*; program(s) used to solve structure: *SHELXS97* (Sheldrick, 2008); program(s) used to refine structure: *SHELXL97* (Sheldrick, 2008); molecular graphics: *X-SEED* (Barbour, 2001); software used to prepare material for publication: *SHELXL97* and *publCIF* (Westrip, 2010).

The authors thank the University of Malaya for funding this study (FRGS grant No. FP004/2010B).

Supplementary data and figures for this paper are available from the IUCr electronic archives (Reference: OM2400).

References

Banerjee, S., Wu, B., Lassahn, P.-G., Janiak, C. & Ghosh, A. (2005). *Inorg. Chim. Acta*, **358**, 535–544.
Barbour, L. J. (2001). *J. Supramol. Chem.* **1**, 189–191.
Bruker (2007). *APEX2* and *SAINT*. Bruker AXS Inc., Madison, Wisconsin, USA.
Sheldrick, G. M. (1996). *SADABS*. University of Göttingen, Germany.
Sheldrick, G. M. (2008). *Acta Cryst.* A**64**, 112–122.
Suleiman Gwaram, N., Ikmal Hisham, N. A., Khaledi, H. & Mohd Ali, H. (2011). *Acta Cryst.* E**67**, m58.
Westrip, S. P. (2010). *J. Appl. Cryst.* **43**, 920–925.
You, Z.-L., Jiao, Q.-Z., Niu, S.-Y. & Chi, J.-Y. (2006). *Z. Anorg. Allg. Chem.* **632**, 2486–2490.

Acta Crystallographica Section E
Structure Reports Online
ISSN 1600-5368

Aqua{2-morpholino-*N*-[1-(2-pyridyl)ethylidene]ethanamine-κ^3N,N',N''}bis(thiocyanato-κN)cobalt(II)

Nura Suleiman Gwaram, Nurul Azimah Ikmal Hisham, Hamid Khaledi* and Hapipah Mohd Ali

Department of Chemistry, University of Malaya, 50603 Kuala Lumpur, Malaysia
Correspondence e-mail: khaledi@siswa.um.edu.my

Received 30 December 2010; accepted 10 January 2011

Key indicators: single-crystal X-ray study; T = 100 K; mean σ(C–C) = 0.007 Å; R factor = 0.055; wR factor = 0.137; data-to-parameter ratio = 14.6.

In the title complex, $[Co(NCS)_2(C_{13}H_{19}N_3O)(H_2O)]$, the Co^{II} ion is six-coordinated by the N,N',N''-tridentate Schiff base, the N atoms of two thiocyanate ligands and one water molecule in a distorted octahedral geometry. Intramolecular C—H···N and C—H···O hydrogen bonds occur. In the crystal, intermolecular O—H···O, O—H···S, C—H···S and S···S [3.5546 (18) Å] interactions result in an infinite three-dimensional network.

Related literature

For the crystal structure of the analogous Ni^{II} complex, see: Suleiman Gwaram *et al.* (2011). For a similar Co(II) complex, see: Sun *et al.* (2007).

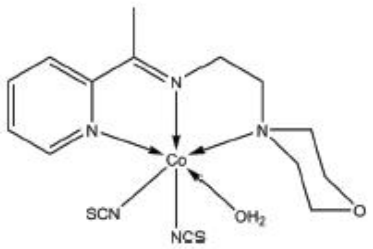

Experimental

Crystal data

$[Co(NCS)_2(C_{13}H_{19}N_3O)(H_2O)]$ M_r = 426.42
Monoclinic, $P2_1/c$
a = 7.1554 (3) Å
b = 22.187 (1) Å
c = 12.1297 (5) Å
β = 91.115 (3)°
V = 1925.31 (14) Å^3
Z = 4
Mo $K\alpha$ radiation
μ = 1.13 mm^{-1}
T = 100 K
0.18 × 0.10 × 0.08 mm

Data collection

Bruker APEXII CCD diffractometer
Absorption correction: multi-scan (*SADABS*; Sheldrick, 1996)
T_{min} = 0.823, T_{max} = 0.915
13017 measured reflections
3401 independent reflections
2662 reflections with $I > 2\sigma(I)$
R_{int} = 0.062

Refinement

$R[F^2 > 2\sigma(F^2)]$ = 0.055
$wR(F^2)$ = 0.137
S = 1.08
3401 reflections
233 parameters
3 restraints
H atoms treated by a mixture of independent and constrained refinement
$\Delta\rho_{max}$ = 0.79 e Å^{-3}
$\Delta\rho_{min}$ = −0.54 e Å^{-3}

Table 1
Hydrogen-bond geometry (Å, °).

D—H···A	D—H	H···A	D···A	D—H···A
O2—H2A···O1^{i}	0.83 (3)	1.88 (3)	2.701 (4)	172 (5)
O2—H2B···S1^{ii}	0.83 (3)	2.36 (3)	3.161 (3)	162 (5)
C11—H11A···O2	0.99	2.40	3.121 (6)	130
C12—H12B···N4	0.99	2.62	3.511 (7)	150
C2—H2···S1^{i}	0.95	2.85	3.774 (6)	165

Symmetry codes: (i) $x, -y+\frac{1}{2}, z+\frac{1}{2}$; (ii) $x-1, y, z$.

Data collection: *APEX2* (Bruker, 2007); cell refinement: *SAINT* (Bruker, 2007); data reduction: *SAINT*; program(s) used to solve structure: *SHELXS97* (Sheldrick, 2008); program(s) used to refine structure: *SHELXL97* (Sheldrick, 2008); molecular graphics: *X-SEED* (Barbour, 2001); software used to prepare material for publication: *SHELXL97* and *publCIF* (Westrip, 2010).

The authors thank the University of Malaya for funding this study (FRGS grant FP004/2010B).

Supplementary data and figures for this paper are available from the IUCr electronic archives (Reference: PV2377).

References

Barbour, L. J. (2001). *J. Supramol. Chem.* **1**, 189–191.
Bruker (2007). *APEX2* and *SAINT*. Bruker AXS Inc., Madison, Wisconsin, USA.
Sheldrick, G. M. (1996). *SADABS*. University of Göttingen, Germany.
Sheldrick, G. M. (2008). *Acta Cryst.* A**64**, 112–122.
Suleiman Gwaram, N., Ikmal Hisham, N. A., Khaledi, H. & Mohd Ali, H. (2011). *Acta Cryst.* E**67**, m108.
Sun, X.-P., Gu, W. & Liu, X. (2007). *Acta Cryst.* E**63**, m1339–m1340.
Westrip, S. P. (2010). *J. Appl. Cryst.* **43**, 920–925.

Acta Crystallographica Section E
Structure Reports Online
ISSN 1600-5368

{2-Morpholino-*N*-[1-(2-pyridyl)ethylidene]ethanamine-κ^3N,N',N''}bis(thiocyanato-κN)copper(II)

Nura Suleiman Gwaram, Nurul Azimah Ikmal Hisham, Hamid Khaledi* and Hapipah Mohd Ali

Department of Chemistry, University of Malaya, 50603 Kuala Lumpur, Malaysia
Correspondence e-mail: khaledi@siswa.um.edu.my

Received 1 December 2010; accepted 4 December 2010

Key indicators: single-crystal X-ray study; T = 100 K; mean σ(C–C) = 0.002 Å; R factor = 0.023; wR factor = 0.061; data-to-parameter ratio = 18.4.

In the title compound, $[Cu(NCS)_2(C_{13}H_{19}N_3O)]$, the Cu^{II} ion is five-coordinated by the N,N',N''-tridentate Schiff base and the N atoms of two isothiocyanate ligands in a square-pyramidal geometry. In the crystal, C—H···N, C—H···O and C—H···S interactions link adjacent molecules into layers parallel to the *ac* plane. A weak intermolecular π–π interaction occurs between the aromatic rings with a centroid–centroid distance of 3.9412 (9) Å.

Related literature

For related structures of Cu(II) complexes, see: Drew *et al.* (2009); You *et al.* (2006); Yue *et al.* (2005).

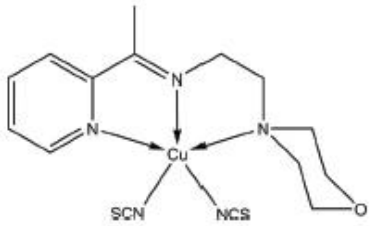

Experimental

Crystal data

$[Cu(NCS)_2(C_{13}H_{19}N_3O)]$
M_r = 413.01
Monoclinic, $P2_1/c$
a = 10.6912 (1) Å
b = 14.0350 (2) Å
c = 12.2530 (2) Å
β = 92.203 (1)°
V = 1837.22 (4) Å^3
Z = 4
Mo $K\alpha$ radiation
μ = 1.43 mm^{-1}
T = 100 K
0.41 × 0.39 × 0.08 mm

Data collection

Bruker APEXII CCD diffractometer
Absorption correction: multi-scan (*SADABS*; Sheldrick, 1996)
T_{min} = 0.592, T_{max} = 0.894
16491 measured reflections
4007 independent reflections
3593 reflections with $I > 2\sigma(I)$
R_{int} = 0.024

Refinement

$R[F^2 > 2\sigma(F^2)]$ = 0.023
$wR(F^2)$ = 0.061
S = 1.08
4007 reflections
218 parameters
2 restraints
H-atom parameters constrained
$\Delta\rho_{max}$ = 0.37 e Å^{-3}
$\Delta\rho_{min}$ = −0.26 e Å^{-3}

Table 1
Hydrogen-bond geometry (Å, °).

D—H···A	D—H	H···A	D···A	D—H···A
C4—H4···O1^{i}	0.95	2.40	3.211 (2)	144
C7—H7B···O1^{i}	0.98	2.33	3.248 (2)	155
C7—H7C···S2^{ii}	0.98	2.83	3.7021 (18)	149
C8—H8B···N5^{iii}	0.99	2.55	3.367 (2)	140
C13—H13A···N4	0.99	2.58	3.181 (2)	119

Symmetry codes: (i) $x+1, y, z$; (ii) $x, -y+\frac{1}{2}, z+\frac{1}{2}$.

Data collection: *APEX2* (Bruker, 2007); cell refinement: *SAINT* (Bruker, 2007); data reduction: *SAINT*; program(s) used to solve structure: *SHELXS97* (Sheldrick, 2008); program(s) used to refine structure: *SHELXL97* (Sheldrick, 2008); molecular graphics: *X-SEED* (Barbour, 2001); software used to prepare material for publication: *SHELXL97* and *publCIF* (Westrip, 2010).

The authors thank the University of Malaya for funding this study (UMRG grant RG024/09BIO).

Supplementary data and figures for this paper are available from the IUCr electronic archives (Reference: IS2639).

References

Barbour, L. J. (2001). *J. Supramol. Chem.* **1**, 189–191.
Bruker (2007). *APEX2* and *SAINT*. Bruker AXS Inc., Madison, Wisconsin, USA.
Drew, M. G. B., Das, D., De, S. & Datta, D. (2009). *Inorg. Chim. Acta*, **362**, 1501–1505.
Sheldrick, G. M. (1996). *SADABS*. University of Göttingen, Germany.
Sheldrick, G. M. (2008). *Acta Cryst.* A**64**, 112–122.
Westrip, S. P. (2010). *J. Appl. Cryst.* **43**, 920–925.
You, Z.-L., Wang, J. & Han, X. (2006). *Acta Cryst.* E**62**, m860–m861.
Yue, G.-R., Xu, X.-J., Shi, Y.-Z. & Feng, L. (2005). *Acta Cryst.* E**61**, m693–m694.

Acta Crystallographica Section E
Structure Reports Online
ISSN 1600-5368

Dichlorido{2-morpholino-*N*-[1-(2-pyridyl)ethylidene]ethanamine-κ^3N,N',N''}manganese(II)

Nurul Azimah Ikmal Hisham, Nura Suleiman Gwaram, Hamid Khaledi* and Hapipah Mohd Ali

Department of Chemistry, University of Malaya, 50603 Kuala Lumpur, Malaysia
Correspondence e-mail: khaledi@siswa.um.edu.my

Received 29 November 2010; accepted 1 December 2010

Key indicators: single-crystal X-ray study; T = 100 K; mean σ(C–C) = 0.002 Å; R factor = 0.020; wR factor = 0.053; data-to-parameter ratio = 19.5.

In the title compound, $[MnCl_2(C_{13}H_{19}N_3O)]$, the Mn^{II} ion is pentacoordinated in a distorted square-pyramidal geometry. The coordination environment is defined by the *N*,*N*′,*N*″-tridentate Schiff base ligand and one Cl atom in the basal positions and one Cl atom in the apical position. In the crystal, intermolecular C—H···Cl hydrogen bonds link the molecules into a three-dimensional network. An intramolecular C—H···Cl hydrogen bond is also observed.

Related literature

For the crystal structure of the analogous Cd^{II} complex, see: Ikmal Hisham *et al.* (2010). For the crystal structure of $[MnCl_2(C_{24}H_{25}N_3)]$, a structurally similar Mn^{II} complex, see: Schmiege *et al.* (2007).

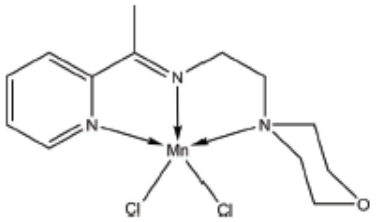

Experimental

Crystal data

$[MnCl_2(C_{13}H_{19}N_3O)]$ M_r = 359.15
Monoclinic, $P2_1/n$
a = 9.6117 (6) Å
b = 13.8507 (8) Å
c = 12.1330 (7) Å
β = 106.738 (1)°
V = 1546.82 (16) Å^3
Z = 4
Mo $K\alpha$ radiation
μ = 1.20 mm^{-1}
T = 100 K
0.40 × 0.35 × 0.25 mm

Data collection

Bruker APEXII CCD diffractometer
Absorption correction: multi-scan (*SADABS*; Sheldrick, 1996)
T_{min} = 0.646, T_{max} = 0.754
15613 measured reflections
3543 independent reflections
3370 reflections with $I > 2\sigma(I)$
R_{int} = 0.019

Refinement

$R[F^2 > 2\sigma(F^2)]$ = 0.020
$wR(F^2)$ = 0.053
S = 1.11
3543 reflections
182 parameters
H-atom parameters constrained
$\Delta\rho_{max}$ = 0.33 e Å^{-3}
$\Delta\rho_{min}$ = −0.23 e Å^{-3}

Table 1
Hydrogen-bond geometry (Å, °).

D—H···A	D—H	H···A	D···A	D—H···A
C4—H4···Cl1^{i}	0.95	2.71	3.6257 (13)	163
C7—H7C···Cl2^{ii}	0.98	2.75	3.6202 (13)	149
C8—H8A···Cl2^{iii}	0.99	2.83	3.7207 (14)	151
C12—H12B···Cl1	0.99	2.77	3.5904 (14)	141

Symmetry codes: (i) $-x+1, -y, -z+1$; (ii) $-x, -y, -z+1$; (iii) $-x+\frac{1}{2}, y-\frac{1}{2}, -z+\frac{1}{2}$.

Data collection: *APEX2* (Bruker, 2007); cell refinement: *SAINT* (Bruker, 2007); data reduction: *SAINT*; program(s) used to solve structure: *SHELXS97* (Sheldrick, 2008); program(s) used to refine structure: *SHELXL97* (Sheldrick, 2008); molecular graphics: *XP* in *SHELXTL* (Sheldrick, 2008); software used to prepare material for publication: *SHELXL97* and *publCIF* (Westrip, 2010).

The authors thank University of Malaya for funding this study (UMRG grant RG024/09BIO).

Supplementary data and figures for this paper are available from the IUCr electronic archives (Reference: IS2637).

References

Bruker (2007). *APEX2* and *SAINT*. Bruker AXS Inc., Madison, Wisconsin, USA.
Ikmal Hisham, N. A., Suleiman Gwaram, N., Khaledi, H. & Mohd Ali, H. (2010). *Acta Cryst.* E**66**, m1471.
Schmiege, B. M., Carney, M. J., Small, B. L., Gerlach, D. L. & Halfen, J. A. (2007). *Dalton Trans.* pp. 2547–2562.
Sheldrick, G. M. (1996). *SADABS*. University of Göttingen, Germany.
Sheldrick, G. M. (2008). *Acta Cryst.* A**64**, 112–122.
Westrip, S. P. (2010). *J. Appl. Cryst.* **43**, 920–925.

Acta Crystallographica Section E
Structure Reports Online
ISSN 1600-5368

Aqua{2-(morpholin-4-yl)-*N*-[1-(2-pyridyl)ethylidene]ethanamine-κ^3N,N',N''}bis(thiocyanato-κN)-manganese(II)

Nura Suleiman Gwaram, Hamid Khaledi* and Hapipah Mohd Ali

Department of Chemistry, University of Malaya, 50603 Kuala Lumpur, Malaysia
Correspondence e-mail: khaledi@siswa.um.edu.my

Received 31 May 2011; accepted 7 June 2011

Key indicators: single-crystal X-ray study; T = 100 K; mean σ(C–C) = 0.003 Å; R factor = 0.037; wR factor = 0.082; data-to-parameter ratio = 18.2.

In the title compound, $[Mn(NCS)_2(C_{13}H_{19}N_3O)(H_2O)]$, the Schiff base acts as an N,N',N''-tridentate ligand, forming two five-membered chelating rings with the Mn^{II} atom. The distorted octahedral geometry around the metal atom is completed by two *cis*-positioned *N*-bound thiocyanate ligands and one water molecule. In the crystal, adjacent molecules are linked through O—H···O, O—H···S and C—H···S hydrogen bonds into a three-dimensional supra-molecular structure. An intramolecular C—H···O hydrogen bond also occurs.

Related literature

For the isostructural Co(II) complex, see: Suleiman Gwaram *et al.* (2011).

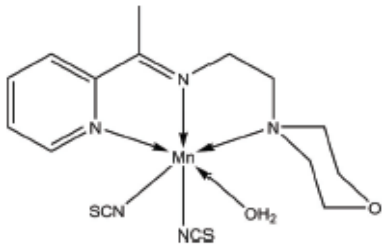

Experimental

Crystal data

$[Mn(NCS)_2(C_{13}H_{19}N_3O)(H_2O)]$
M_r = 422.43
Monoclinic, $P2_1/c$
a = 7.1837 (13) Å
b = 22.408 (4) Å
c = 12.112 (2) Å
β = 91.149 (3)°
V = 1949.3 (6) Å^3
Z = 4
Mo $K\alpha$ radiation
μ = 0.91 mm^{-1}
T = 100 K
0.19 × 0.16 × 0.08 mm

Data collection

Bruker APEXII CCD diffractometer
Absorption correction: multi-scan (*SADABS*; Sheldrick, 1996)
T_{min} = 0.846, T_{max} = 0.931
11816 measured reflections
4235 independent reflections
3197 reflections with $I > 2\sigma(I)$
R_{int} = 0.040

Refinement

$R[F^2 > 2\sigma(F^2)]$ = 0.037
$wR(F^2)$ = 0.082
S = 1.01
4235 reflections
233 parameters
3 restraints
H atoms treated by a mixture of independent and constrained refinement
$\Delta\rho_{max}$ = 0.33 e Å^{-3}
$\Delta\rho_{min}$ = −0.46 e Å^{-3}

Table 1
Selected bond lengths (Å).

Mn1—N1	2.2835 (19)	Mn1—N4	2.137 (2)
Mn1—N2	2.2115 (18)	Mn1—N5	2.145 (2)
Mn1—N3	2.3891 (19)	Mn1—O2	2.2117 (17)

Table 2
Hydrogen-bond geometry (Å, °).

D—H···A	D—H	H···A	D···A	D—H···A
O2—H2A···S1^{i}	0.82 (2)	2.38 (2)	3.1910 (18)	169 (2)
O2—H2B···O1^{ii}	0.82 (2)	1.89 (2)	2.693 (2)	164 (3)
C11—H11A···O2	0.99	2.41	3.179 (3)	134
C12—H12A···S2^{iii}	0.99	2.82	3.674 (2)	145

Symmetry codes: (i) $x+1, y, z$; (ii) $x, -y+\frac{1}{2}, z-\frac{1}{2}$; (iii) $-x, -y+1, -z+2$.

Data collection: *APEX2* (Bruker, 2007); cell refinement: *SAINT* (Bruker, 2007); data reduction: *SAINT*; program(s) used to solve structure: *SHELXS97* (Sheldrick, 2008); program(s) used to refine structure: *SHELXL97* (Sheldrick, 2008); molecular graphics: *X-SEED* (Barbour, 2001); software used to prepare material for publication: *SHELXL97* and *publCIF* (Westrip, 2010).

The authors thank the University of Malaya for funding this study (FRGS grant FP004/2010B).

Supplementary data and figures for this paper are available from the IUCr electronic archives (Reference: XU5237).

References

Barbour, L. J. (2001). *J. Supramol. Chem.* **1**, 189–191.
Bruker (2007). *APEX2* and *SAINT*. Bruker AXS Inc., Madison, Wisconsin, USA.
Sheldrick, G. M. (1996). *SADABS*. University of Göttingen, Germany.
Sheldrick, G. M. (2008). *Acta Cryst.* A**64**, 112–122.
Suleiman Gwaram, N., Ikmal Hisham, N. A., Khaledi, H. & Mohd Ali, H. (2011). *Acta Cryst.* E**67**, m108.
Westrip, S. P. (2010). *J. Appl. Cryst.* **43**, 920–925.

Acta Crystallographica Section E
Structure Reports Online
ISSN 1600-5368

Aqua{2-morpholino-*N*-[1-(2-pyridyl)ethylidene]ethanamine-κ^3N,N',N''}bis(thiocyanato-κN)nickel(II)

Nura Suleiman Gwaram, Nurul Azimah Ikmal Hisham, Hamid Khaledi* and Hapipah Mohd Ali

Department of Chemistry, University of Malaya, 50603 Kuala Lumpur, Malaysia
Correspondence e-mail: khaledi@siswa.um.edu.my

Received 13 December 2010; accepted 15 December 2010

Key indicators: single-crystal X-ray study; T = 100 K; mean σ(C–C) = 0.003 Å; R factor = 0.025; wR factor = 0.058; data-to-parameter ratio = 14.9.

In the title compound, $[Ni(NCS)_2(C_{13}H_{19}N_3O)(H_2O)]$, the Ni^{II} ion is six-coordinated by the N,N',N''-tridentate Schiff base, the N atoms of two thiocyanate ligands and one water O atom in a distorted octahedral geometry. Intramolecular C—H···N and C—H···O hydrogen bonds occur. In the crystal, O—H···S, O—H···O and C—H···S hydrogen bonds link adjacent molecules into layers parallel to the *ac* plane.

Related literature

For the structure of the Cu(II) complex with the Schiff base and thiocyanate, see: Suleiman Gwaram *et al.* (2011). For the structures of related Ni(II) complexes, see: Chiumia *et al.* (1999); Zhao *et al.* (2008).

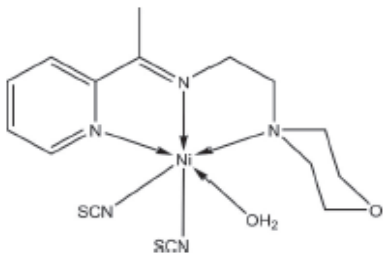

Experimental

Crystal data

$[Ni(NCS)_2(C_{13}H_{19}N_3O)(H_2O)]$
M_r = 426.20
Monoclinic, $P2_1/c$
a = 7.1881 (1) Å
b = 21.9708 (3) Å
c = 12.1438 (2) Å
β = 91.412 (1)°
V = 1917.27 (5) Å^3
Z = 4
Mo $K\alpha$ radiation
μ = 1.25 mm^{-1}
T = 100 K
0.35 × 0.32 × 0.22 mm

Data collection

Bruker APEXII CCD diffractometer
Absorption correction: multi-scan (*SADABS*; Sheldrick, 1996)
T_{min} = 0.669, T_{max} = 0.771
14240 measured reflections
3474 independent reflections
3168 reflections with $I > 2\sigma(I)$
R_{int} = 0.023

Refinement

$R[F^2 > 2\sigma(F^2)]$ = 0.025
$wR(F^2)$ = 0.058
S = 1.09
3474 reflections
233 parameters
4 restraints
H atoms treated by a mixture of independent and constrained refinement
$\Delta\rho_{max}$ = 0.45 e Å^{-3}
$\Delta\rho_{min}$ = −0.36 e Å^{-3}

Table 1
Selected bond lengths (Å).

Ni1—N1	2.1079 (16)	Ni1—N4	2.0270 (16)
Ni1—N2	2.0243 (15)	Ni1—N5	2.0318 (16)
Ni1—N3	2.2317 (16)	Ni1—O2	2.0996 (13)

Table 2
Hydrogen-bond geometry (Å, °).

D—H···A	D—H	H···A	D···A	D—H···A
O2—H2A···S1^{i}	0.83 (1)	2.32 (1)	3.1410 (14)	168 (2)
O2—H2B···O1^{ii}	0.84 (1)	1.89 (1)	2.7023 (19)	163 (2)
C2—H2···S1^{ii}	0.95	2.84	3.769 (3)	167
C11—H11A···N4	0.99	2.53	3.409 (3)	147
C12—H12B···O2	0.99	2.40	3.100 (2)	127

Symmetry codes: (i) $x+1, y, z$; (ii) $x, -y+\frac{1}{2}, z-\frac{1}{2}$.

Data collection: *APEX2* (Bruker, 2007); cell refinement: *SAINT* (Bruker, 2007); data reduction: *SAINT*; program(s) used to solve structure: *SHELXS97* (Sheldrick, 2008); program(s) used to refine structure: *SHELXL97* (Sheldrick, 2008); molecular graphics: *X-SEED* (Barbour, 2001); software used to prepare material for publication: *SHELXL97* and *publCIF* (Westrip, 2010).

The authors thank the University of Malaya for funding this study (FRGS grant FP004/2010B).

Supplementary data and figures for this paper are available from the IUCr electronic archives (Reference: IS2646).

References

Barbour, L. J. (2001). *J. Supramol. Chem.* **1**, 189–191.
Bruker (2007). *APEX2* and *SAINT*. Bruker AXS Inc., Madison, Wisconsin, USA.
Chiumia, G. C., Craig, D. C., Phillips, D. J., Rae, A. D. & Zafar Kaifi, F. M. (1999). *Inorg. Chim. Acta*, **285**, 297–300.
Sheldrick, G. M. (1996). *SADABS*. University of Göttingen, Germany.
Sheldrick, G. M. (2008). *Acta Cryst.* A**64**, 112–122.
Suleiman Gwaram, N., Ikmal Hisham, N. A., Khaledi, H. & Mohd Ali, H. (2011). *Acta Cryst.* E**67**, m58.
Westrip, S. P. (2010). *J. Appl. Cryst.* **43**, 920–925.
Zhao, K., Yin, X.-H., Lin, C.-W., Meng, D.-X. & Wu, F. (2008). *Acta Cryst.* E**64**, m84–m85.

Acta Crystallographica Section E
Structure Reports Online
ISSN 1600-5368

Dichlorido{2-morpholino-*N*-[1-(2-pyridyl)ethylidene]ethanamine-κ^3N,N',N''}zinc(II)

Nurul Azimah Ikmal Hisham, Nura Suleiman Gwaram, Hamid Khaledi* and Hapipah Mohd Ali

Department of Chemistry, University of Malaya, 50603 Kuala Lumpur, Malaysia
Correspondence e-mail: khaledi@siswa.um.edu.my

Received 30 November 2010; accepted 3 December 2010

Key indicators: single-crystal X-ray study; T = 100 K; mean σ(C–C) = 0.004 Å; R factor = 0.034; wR factor = 0.091; data-to-parameter ratio = 16.4.

In the title compound, $[ZnCl_2(C_{13}H_{19}N_3O)]$, the Schiff base ligand acts as an N,N',N''-tridentate chelating agent, making two five-membered rings with the Zn^{II} ion. The metal atom is five-coordinated by the Schiff base ligand and two Cl atoms in a distorted square-pyramidal geometry. An intramolecular C—H···Cl interaction occurs. In the crystal, adjacent molecules are linked together *via* C—H···Cl hydrogen-bonding and long range C—H···O and C—H···Cl interactions into a three-dimensional network.

Related literature

For the crystal structure of an analogous Cd^{II} complex, see: Ikmal Hisham *et al.* (2010). For crystal structures of similar Zn^{II} complexes, see: Chattopadhyay *et al.* (2009); Sun (2005).

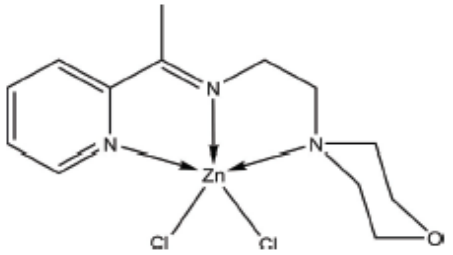

Experimental

Crystal data

$[ZnCl_2(C_{13}H_{19}N_3O)]$ M_r = 369.58
Monoclinic, $P2_1/n$
a = 9.5737 (12) Å
b = 13.7064 (17) Å
c = 12.0766 (15) Å
β = 106.643 (2)°
V = 1518.3 (3) Å^3
Z = 4
Mo $K\alpha$ radiation
μ = 1.97 mm^{-1}
T = 100 K
0.35 × 0.21 × 0.05 mm

Data collection

Bruker APEXII CCD diffractometer
Absorption correction: multi-scan (*SADABS*; Sheldrick, 1996)
T_{min} = 0.546, T_{max} = 0.908
13693 measured reflections
2979 independent reflections
2552 reflections with $I > 2\sigma(I)$
R_{int} = 0.047

Refinement

$R[F^2 > 2\sigma(F^2)]$ = 0.034
$wR(F^2)$ = 0.091
S = 1.08
2979 reflections
182 parameters
H-atom parameters constrained
$\Delta\rho_{max}$ = 1.03 e Å^{-3}
$\Delta\rho_{min}$ = −0.39 e Å^{-3}

Table 1
Hydrogen-bond geometry (Å, °).

D—H···A	D—H	H···A	D···A	D—H···A
C4—H4···Cl1^{i}	0.95	2.71	3.625 (3)	161
C7—H7*C*···Cl2^{ii}	0.98	2.77	3.619 (3)	146
C12—H12*B*···Cl1	0.99	2.73	3.526 (3)	138
C10—H10*A*···O1^{iii}	0.99	2.61	3.408 (3)	137
C9—H9*B*···Cl1^{iv}	0.99	2.88	3.665 (3)	137
C7—H7*B*···Cl1^{i}	0.98	2.85	3.807 (3)	166
C8—H8*A*···Cl2^{v}	0.99	2.87	3.750 (3)	149

Symmetry codes: (i) $-x+2,-y,-z$; (ii) $-x+1,-y,-z$; (iii) $-x+1,-y,-z+1$; (iv) $-x+\frac{1}{2},y-\frac{1}{2},-z+\frac{1}{2}$.

Data collection: *APEX2* (Bruker, 2007); cell refinement: *SAINT* (Bruker, 2007); data reduction: *SAINT*; program(s) used to solve structure: *SHELXS97* (Sheldrick, 2008); program(s) used to refine structure: *SHELXL97* (Sheldrick, 2008); molecular graphics: *XP* in *SHELXTL* (Sheldrick, 2008); software used to prepare material for publication: *SHELXL97* and *publCIF* (Westrip, 2010).

The authors thank University of Malaya for funding this study (UMRG grant RG024/09BIO).

Supplementary data and figures for this paper are available from the IUCr electronic archives (Reference: PV2366).

References

Bruker (2007). *APEX2* and *SAINT*. Bruker AXS Inc., Madison, Wisconsin, USA.
Chattopadhyay, T., Mukherjee, M., Banu, K. S., Banerjee, A., Suresh, E., Zangrando, E. & Das, D. (2009). *J. Coord. Chem.* **62**, 967–979.
Ikmal Hisham, N., Suleiman Gwaram, N., Khaledi, H. & Mohd Ali, H. (2010). *Acta Cryst.* E**66**, m1471.
Sheldrick, G. M. (1996). *SADABS*. University of Göttingen, Germany.
Sheldrick, G. M. (2008). *Acta Cryst.* A**64**, 112–122.
Sun, Y.-X. (2005). *Acta Cryst.* E**61**, m373–m374.
Westrip, S. P. (2010). *J. Appl. Cryst.* **43**, 920–925.

Acta Crystallographica Section E
Structure Reports Online
ISSN 1600-5368

Diiodido{2-(morpholin-4-yl)-*N*-[1-(2-pyridyl)ethylidene]ethanamine-κ^3N,N',N''}zinc

Nura Suleiman Gwaram, Hamid Khaledi* and Hapipah Mohd Ali

Department of Chemistry, University of Malaya, 50603 Kuala Lumpur, Malaysia
Correspondence e-mail: khaledi@siswa.um.edu.my

Received 14 April 2011; accepted 19 April 2011

Key indicators: single-crystal X-ray study; T = 100 K; mean σ(C–C) = 0.004 Å; R factor = 0.018; wR factor = 0.045; data-to-parameter ratio = 19.3.

In the title compound, $[ZnI_2(C_{13}H_{19}N_3O)]$, the Zn^{II} ion is five-coordinated in a distorted square-pyramidal geometry, in which the basal plane is defined by three N atoms from the Schiff base ligand and one iodide ion. A second iodide ligand, situated in the apical position, completes the coordination geometry. In the crystal structure, C—H···O hydrogen bonds link a pair of molecules around an inversion centre into a dimer.

Related literature

For the structure of an analogous $ZnCl_2$ complex, see: Ikmal Hisham *et al.* (2011). For square-pyramidal ZnI_2 complexes with N,N',N''-tridentate ligands, see: Drew & Hollis (1978); Yousefi (2010). For a description of the geometry of complexes with five-coordinated metal ions, see: Addison *et al.* (1984).

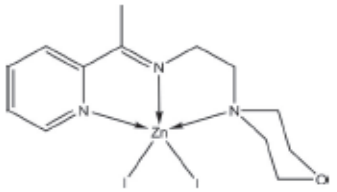

Experimental

Crystal data

$[ZnI_2(C_{13}H_{19}N_3O)]$
M_r = 552.48
Triclinic, $P\overline{1}$
a = 8.8874 (3) Å
b = 10.3117 (4) Å
c = 10.3643 (4) Å
α = 68.8810 (18)°
β = 81.959 (2)°
γ = 66.3990 (17)°
V = 811.91 (6) Å^3
Z = 2
Mo $K\alpha$ radiation
μ = 5.31 mm^{-1}
T = 100 K
0.17 × 0.13 × 0.09 mm

Data collection

Bruker APEXII CCD diffractometer
Absorption correction: multi-scan (*SADABS*; Sheldrick, 1996)
T_{min} = 0.465, T_{max} = 0.646
7292 measured reflections
3517 independent reflections
3260 reflections with $I > 2\sigma(I)$
R_{int} = 0.013

Refinement

$R[F^2 > 2\sigma(F^2)]$ = 0.018
$wR(F^2)$ = 0.045
S = 1.05
3517 reflections
182 parameters
H-atom parameters constrained
$\Delta\rho_{max}$ = 0.85 e Å^{-3}
$\Delta\rho_{min}$ = −1.23 e Å^{-3}

Table 1
Selected bond lengths (Å).

Zn1—N1	2.205 (2)	Zn1—I1	2.6018 (4)
Zn1—N2	2.093 (2)	Zn1—I2	2.6506 (4)
Zn1—N3	2.269 (2)		

Table 2
Hydrogen-bond geometry (Å, °).

D—H···A	D—H	H···A	D···A	D—H···A
C13—H13A···O1^{i}	0.99	2.55	3.491 (3)	159

Symmetry code: (i) $-x+1, -y+2, -z+2$.

Data collection: *APEX2* (Bruker, 2007); cell refinement: *SAINT* (Bruker, 2007); data reduction: *SAINT*; program(s) used to solve structure: *SHELXS97* (Sheldrick, 2008); program(s) used to refine structure: *SHELXL97* (Sheldrick, 2008); molecular graphics: *X-SEED* (Barbour, 2001); software used to prepare material for publication: *SHELXL97* and *publCIF* (Westrip, 2010).

The authors thank the University of Malaya for funding this study (FRGS grant No. FP004/2010B).

Supplementary data and figures for this paper are available from the IUCr electronic archives (Reference: HY2422).

References

Addison, A. W., Rao, T. N., Reedijk, J., Rijn, V. J. & Verschoor, G. C. (1984). *J. Chem. Soc. Dalton Trans.* pp. 1349–1356.
Barbour, L. J. (2001). *J. Supramol. Chem.* **1**, 189–191.
Bruker (2007). *APEX2* and *SAINT*. Bruker AXS Inc., Madison, Wisconsin, USA.
Drew, M. G. B. & Hollis, S. (1978). *J. Chem. Soc. Dalton Trans.* pp. 511–516.
Ikmal Hisham, N. A., Suleiman Gwaram, N., Khaledi, H. & Mohd Ali, H. (2011). *Acta Cryst.* E**67**, m55.
Sheldrick, G. M. (1996). *SADABS*. University of Göttingen, Germany.
Sheldrick, G. M. (2008). *Acta Cryst.* A**64**, 112–122.
Westrip, S. P. (2010). *J. Appl. Cryst.* **43**, 920–925.
Yousefi, M. (2010). *Acta Cryst.* E**66**, m1600–m1601.

Acta Crystallographica Section E
Structure Reports Online
ISSN 1600-5368

{2-Morpholino-*N*-[1-(2-pyridyl)-ethylidene]ethanamine-κ^3N,N',N''}-bis(thiocyanato-κN)zinc(II)

Nura Suleiman Gwaram, Nurul Azimah Ikmal Hisham, Hamid Khaledi* and Hapipah Mohd Ali

Department of Chemistry, University of Malaya, 50603 Kuala Lumpur, Malaysia
Correspondence e-mail: khaledi@siswa.um.edu.my

Received 9 December 2010; accepted 22 December 2010

Key indicators: single-crystal X-ray study; T = 100 K; mean σ(C–C) = 0.003 Å; R factor = 0.027; wR factor = 0.072; data-to-parameter ratio = 16.3.

The asymmetric unit of the title compound, $[Zn(NCS)_2(C_{13}H_{19}N_3O)]$, contains two crystallographically independent molecules. In each molecule, the Zn^{II} ion is five-coordinated by the *N*,*N*′,*N*″-tridentate Schiff base and the N atoms of two thiocyanate ligands in a distorted square-pyramidal geometry. The two molecules differ mainly in the deviations from the ideal geometry, with τ values of 0.14 and 0.33. In the crystal, intermolecular C—H···S hydrogen bonds are observed. An intramolecular C—H···N hydrogen bond occurs in one of the independent molecules.

Related literature

For the crystal structures of similar zinc complexes, see: Cai (2009); Chen *et al.* (2005). For a description of the geometry of complexes with five-coordinate metal atoms, see: Addison *et al.* (1984).

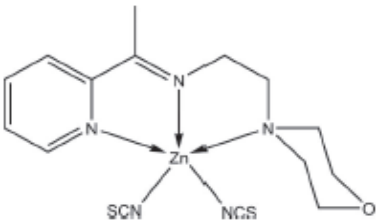

Experimental

Crystal data

$[Zn(NCS)_2(C_{13}H_{19}N_3O)]$
M_r = 414.84
Triclinic, $P\overline{1}$
a = 9.9203 (2) Å
b = 13.5659 (2) Å
c = 14.6957 (2) Å
α = 112.702 (1)°
β = 91.471 (1)°
γ = 94.356 (1)°
V = 1815.97 (5) Å^3
Z = 4
Mo $K\alpha$ radiation
μ = 1.59 mm^{-1}
T = 100 K
0.42 × 0.33 × 0.25 mm

Data collection

Bruker APEXII CCD diffractometer
Absorption correction: multi-scan (*SADABS*; Sheldrick, 1996)
T_{min} = 0.554, T_{max} = 0.691
15347 measured reflections
7111 independent reflections
6171 reflections with $I > 2\sigma(I)$
R_{int} = 0.020

Refinement

$R[F^2 > 2\sigma(F^2)]$ = 0.027
$wR(F^2)$ = 0.072
S = 1.02
7111 reflections
435 parameters
5 restraints
H-atom parameters constrained
$\Delta\rho_{max}$ = 0.63 e Å^{-3}
$\Delta\rho_{min}$ = −0.27 e Å^{-3}

Table 1
Hydrogen-bond geometry (Å, °).

D—H···A	D—H	H···A	D···A	D—H···A
C12—H12A···S1^{i}	0.99	2.84	3.826 (2)	175
C16—H16···S2^{ii}	0.95	2.74	3.670 (2)	168
C27—H27B···N9	0.99	2.55	3.421 (3)	147

Symmetry codes: (i) $-x+1, -y+1, -z+1$; (ii) $-x+1, -y+2, -z+1$.

Data collection: *APEX2* (Bruker, 2007); cell refinement: *SAINT* (Bruker, 2007); data reduction: *SAINT*; program(s) used to solve structure: *SHELXS97* (Sheldrick, 2008); program(s) used to refine structure: *SHELXL97* (Sheldrick, 2008); molecular graphics: *X-SEED* (Barbour, 2001); software used to prepare material for publication: *SHELXL97* and *publCIF* (Westrip, 2010).

The authors thank the University of Malaya for funding this study (UMRG grant RG024/09BIO).

Supplementary data and figures for this paper are available from the IUCr electronic archives (Reference: VM2068).

References

Addison, A. W., Rao, T. N., Reedijk, J., Rijn, V. J. & Verschoor, G. C. (1984). *J. Chem. Soc. Dalton Trans.* pp. 1349–1356.
Barbour, L. J. (2001). *J. Supramol. Chem.* **1**, 189–191.
Bruker (2007). *APEX2* and *SAINT*. Bruker AXS Inc., Madison, Wisconsin, USA.
Cai, B.-H. (2009). *Acta Cryst.* E**65**, m142.
Chen, G., Bai, Z.-P. & Qu, S.-J. (2005). *Acta Cryst.* E**61**, m2483–m2484.
Sheldrick, G. M. (1996). *SADABS*. University of Göttingen, Germany.
Sheldrick, G. M. (2008). *Acta Cryst.* A**64**, 112–122.
Westrip, S. P. (2010). *J. Appl. Cryst.* **43**, 920–925.

Acta Crystallographica Section E
Structure Reports Online
ISSN 1600-5368

Dichlorido{*N*,*N*-dimethyl-*N*′-[1-(pyridin-2-yl)ethylidene]ethane-1,2-diamine-κ^3N,N',N''}cadmium

Nura Suleiman Gwaram, Hamid Khaledi* and Hapipah Mohd Ali

Department of Chemistry, University of Malaya, 50603 Kuala Lumpur, Malaysia
Correspondence e-mail: khaledi@siswa.um.edu.my

Received 9 February 2011; accepted 15 February 2011

Key indicators: single-crystal X-ray study; T = 100 K; mean σ(C–C) = 0.003 Å; R factor = 0.016; wR factor = 0.038; data-to-parameter ratio = 16.9.

In the title compound, $[CdCl_2(C_{11}H_{17}N_3)]$, the Schiff base acts as an *N*,*N*′,*N*′′-tridentate ligand towards the Cd^{II} ion. Two Cl atoms complete a distorted square-pyramidal geometry around the metal atom. In the crystal, a C—H···Cl interaction connects pairs of molecules into centrosymetric dimers.

Related literature

For the structure of a $CuCl_2$ complex of the same Schiff base, see: Saleh Salga *et al.* (2010). For the structure of a similar Cd^{II} complex, see: Bian *et al.* (2003). For a description of the geometry of complexes with five-coordinate metal atoms, see: Addison *et al.* (1984).

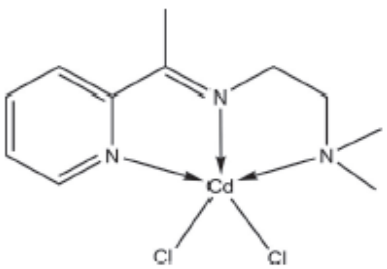

Experimental

Crystal data

$[CdCl_2(C_{11}H_{17}N_3)]$ M_r = 374.58
Triclinic, $P\overline{1}$
a = 8.0276 (2) Å
b = 9.6048 (2) Å
c = 10.0851 (2) Å
α = 102.534 (1)°
β = 103.365 (1)°
γ = 97.850 (1)°
V = 724.09 (3) Å^3
Z = 2
Mo $K\alpha$ radiation
μ = 1.86 mm^{-1}
T = 100 K
0.23 × 0.11 × 0.04 mm

Data collection

Bruker APEXII CCD diffractometer
Absorption correction: multi-scan (*SADABS*; Sheldrick, 1996)
T_{min} = 0.674, T_{max} = 0.929
5023 measured reflections
2652 independent reflections
2547 reflections with $I > 2\sigma(I)$
R_{int} = 0.014

Refinement

$R[F^2 > 2\sigma(F^2)]$ = 0.016
$wR(F^2)$ = 0.038
S = 1.08
2652 reflections
157 parameters
H-atom parameters constrained
$\Delta\rho_{max}$ = 0.29 e Å^{-3}
$\Delta\rho_{min}$ = −0.39 e Å^{-3}

Table 1
Hydrogen-bond geometry (Å, °).

D—H···A	D—H	H···A	D···A	D—H···A
C7—H7*B*···Cl2^{i}	0.98	2.77	3.679 (2)	155

Symmetry code: (i) $-x, -y, -z+1$.

Data collection: *APEX2* (Bruker, 2007); cell refinement: *SAINT* (Bruker, 2007); data reduction: *SAINT*; program(s) used to solve structure: *SHELXS97* (Sheldrick, 2008); program(s) used to refine structure: *SHELXL97* (Sheldrick, 2008); molecular graphics: *X-SEED* (Barbour, 2001); software used to prepare material for publication: *SHELXL97* and *publCIF* (Westrip, 2010).

The authors thank University of Malaya for funding this study (FRGS grant No. FP004/2010B).

Supplementary data and figures for this paper are available from the IUCr electronic archives (Reference: PV2387).

References

Addison, A. W., Rao, T. N., Reedijk, J., Rijn, V. J. & Verschoor, G. C. (1984). *J. Chem. Soc. Dalton Trans.* pp. 1349–1356.
Barbour, L. J. (2001). *J. Supramol. Chem.* **1**, 189–191.
Bian, H.-D., Xu, J.-Y., Gu, W., Yan, S.-P., Liao, D.-Z., Jiang, Z.-H. & Cheng, P. (2003). *Chin. J. Struct. Chem.* **22**, 710–712.
Bruker (2007). *APEX2* and *SAINT*. Bruker AXS Inc., Madison, Wisconsin, USA.
Saleh Salga, M., Khaledi, H., Mohd Ali, H. & Puteh, R. (2010). *Acta Cryst.* E**66**, m508.
Sheldrick, G. M. (1996). *SADABS*. University of Göttingen, Germany.
Sheldrick, G. M. (2008). *Acta Cryst.* A**64**, 112–122.
Westrip, S. P. (2010). *J. Appl. Cryst.* **43**, 920–925.

Acta Crystallographica Section E
Structure Reports Online
ISSN 1600-5368

catena-Poly[[{*N*,*N*-dimethyl-*N*′-[1-(pyridin-2-yl)ethylidene]ethane-1,2-diamine-κ^3N,N',N''}(thiocyanato-κN)-cadmium]-μ-thiocyanato-$\kappa^2S:N$]

Nura Suleiman Gwaram, Hamid Khaledi* and Hapipah Mohd Ali

Department of Chemistry, University of Malaya, 50603 Kuala Lumpur, Malaysia
Correspondence e-mail: khaledi@siswa.um.edu.my

Received 3 March 2011; accepted 17 March 2011

Key indicators: single-crystal X-ray study; T = 100 K; mean σ(C–C) = 0.003 Å; R factor = 0.023; wR factor = 0.056; data-to-parameter ratio = 19.5.

In the title compound, $[Cd(NCS)_2(C_{11}H_{17}N_3)]_n$, the Cd^{II} atom is octahedrally coordinated by the *N*,*N*′,*N*″-tridentate Schiff base ligand and one terminal thiocyanate N atom. Two *trans*-*N*:*S*-bridging thiocyanates complete the N_5S donor set around the Cd atom. In the crystal, adjacent Cd^{II} ions are linked by the thiocyanate *N*:*S*-bridges into polymeric chains along the *c* axis.

Related literature

For the structures of some cadmium thiocyanate complexes with nitrogen-based ligands, see: Banerjee *et al.* (2005). For a singly bridged cadmium thiocyanate complex, see: Bose *et al.* (2004). For a triply bridged cadmium thiocyanate complex, see: Chen *et al.* (2002). For an S-bound terminal thiocyanate cadmium complex, see: Nfor *et al.* (2006).

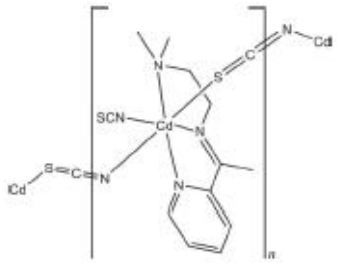

Experimental

Crystal data

$[Cd(NCS)_2(C_{11}H_{17}N_3)]$
M_r = 419.84
Monoclinic, $P2_1/c$
a = 14.602 (2) Å
b = 9.5827 (14) Å
c = 12.8714 (19) Å
β = 107.483 (2)°
V = 1717.9 (4) Å^3
Z = 4
Mo $K\alpha$ radiation
μ = 1.51 mm^{-1}
T = 100 K
0.35 × 0.29 × 0.08 mm

Data collection

Bruker APEXII CCD diffractometer
Absorption correction: multi-scan (*SADABS*; Sheldrick, 1996)
T_{min} = 0.619, T_{max} = 0.889
19975 measured reflections
3756 independent reflections
3298 reflections with $I > 2\sigma(I)$
R_{int} = 0.047

Refinement

$R[F^2 > 2\sigma(F^2)]$ = 0.023
$wR(F^2)$ = 0.056
S = 1.07
3756 reflections
193 parameters
H-atom parameters constrained
$\Delta\rho_{max}$ = 0.54 e Å^{-3}
$\Delta\rho_{min}$ = −0.73 e Å^{-3}

Table 1
Selected bond lengths (Å).

Cd1—N4	2.2406 (18)	Cd1—N1	2.3801 (18)
Cd1—N5	2.3008 (19)	Cd1—N3	2.3820 (19)
Cd1—N2	2.3345 (17)	Cd1—S2	2.7803 (6)

Symmetry code: (i) $x, -y+\frac{1}{2}, z-\frac{1}{2}$.

Data collection: *APEX2* (Bruker, 2007); cell refinement: *SAINT* (Bruker, 2007); data reduction: *SAINT*; program(s) used to solve structure: *SHELXS97* (Sheldrick, 2008); program(s) used to refine structure: *SHELXL97* (Sheldrick, 2008); molecular graphics: *X-SEED* (Barbour, 2001); software used to prepare material for publication: *SHELXL97* and *publCIF* (Westrip, 2010).

The authors thank the University of Malaya for funding this study (FRGS grant No. FP004/2010B).

Supplementary data and figures for this paper are available from the IUCr electronic archives (Reference: OM2412).

References

Banerjee, S., Wu, B., Lassahn, P.-G., Janiak, C. & Ghosh, A. (2005). *Inorg. Chim. Acta*, **358**, 535–544.
Barbour, L. J. (2001). *J. Supramol. Chem.* **1**, 189–191.
Bose, D., Banerjee, J., Rahaman, S. H., Mostafa, G., Fun, H.-K., Walsh, R. D. B., Zaworotko, M. J. & Ghosh, B. K. (2004). *Polyhedron*, **23**, 2045–2053.
Bruker (2007). *APEX2* and *SAINT*. Bruker AXS Inc., Madison, Wisconsin, USA.
Chen, W., Liu, F. & You, X. (2002). *J. Solid State Chem.* **167**, 119–125.
Nfor, E. N., Liu, W., Zuo, J.-L. & You, X.-Z. (2006). *Transition Met. Chem.* **31**, 837–841.
Sheldrick, G. M. (1996). *SADABS*. University of Göttingen, Germany.
Sheldrick, G. M. (2008). *Acta Cryst.* A**64**, 112–122.
Westrip, S. P. (2010). *J. Appl. Cryst.* **43**, 920–925.

Acta Crystallographica Section E
Structure Reports Online
ISSN 1600-5368

Dichlorido{2-(morpholin-4-yl)-*N*-[1-(pyridin-2-yl)ethylidene]ethanamine-κ^3N,N',N''}copper(II) monohydrate

Nura Suleiman Gwaram, Hamid Khaledi* and Hapipah Mohd Ali

Department of Chemistry, University of Malaya, 50603 Kuala Lumpur, Malaysia
Correspondence e-mail: khaledi@siswa.um.edu.my

Received 7 February 2011; accepted 9 February 2011

Key indicators: single-crystal X-ray study; T = 100 K; mean σ(C–C) = 0.003 Å; R factor = 0.025; wR factor = 0.060; data-to-parameter ratio = 17.0.

In the title compound, $[CuCl_2(C_{13}H_{19}N_3O)]\cdot H_2O$, the tridentate Schiff base ligand and the two Cl atoms complete a distorted square-pyramidal coordination geometry around the Cu^{II} ion in which the three N atoms and one Cl atom are located in the basal plane and the other Cl atom is at the apical position. In the crystal, O—H···Cl hydrogen bonds link the complex molecules and the uncoordinated water molecules into infinite chains along the *a* axis. The chains are further connected into a three-dimensional network *via* C—H···O and C—H···Cl interactions.

Related literature

For the structures of $CuCl_2$ complexes with similar ligands, see: Saleh Salga *et al.* (2010); Wang *et al.* (2009). For the structure of a $CdCl_2$ complex with the same Schiff base ligand, see: Ikmal Hisham *et al.* (2010). For a description of the geometry of complexes with a five-coordinate metal atom, see: Addison *et al.* (1984).

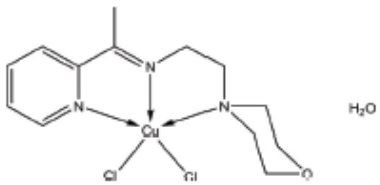

Experimental

Crystal data

$[CuCl_2(C_{13}H_{19}N_3O)]\cdot H_2O$
M_r = 385.77
Monoclinic, $P2_1/n$
a = 7.9194 (8) Å
b = 8.5793 (8) Å
c = 22.925 (2) Å
β = 91.981 (1)°
V = 1556.6 (3) Å^3
Z = 4
Mo $K\alpha$ radiation
μ = 1.75 mm^{-1}
T = 100 K
0.18 × 0.16 × 0.09 mm

Data collection

Bruker APEXII CCD diffractometer
Absorption correction: multi-scan (*SADABS*; Sheldrick, 1996)
T_{min} = 0.743, T_{max} = 0.858
9634 measured reflections
3348 independent reflections
2948 reflections with $I > 2\sigma(I)$
R_{int} = 0.023

Refinement

$R[F^2 > 2\sigma(F^2)]$ = 0.025
$wR(F^2)$ = 0.060
S = 1.05
3348 reflections
197 parameters
2 restraints
H atoms treated by a mixture of independent and constrained refinement
$\Delta\rho_{max}$ = 0.37 e Å^{-3}
$\Delta\rho_{min}$ = −0.34 e Å^{-3}

Table 1
Hydrogen-bond geometry (Å, °).

D—H···A	D—H	H···A	D···A	D—H···A
O2—H2*A*···Cl2^{i}	0.84 (2)	2.35 (2)	3.1829 (16)	173 (2)
O2—H2*B*···Cl1	0.83 (2)	2.48 (2)	3.2841 (18)	164 (2)
C2—H2···O2^{ii}	0.95	2.41	3.307 (2)	156
C3—H3···Cl2^{iii}	0.95	2.82	3.619 (2)	142
C4—H4···O2^{iv}	0.95	2.50	3.445 (2)	172
C7—H7*A*···Cl1^{v}	0.98	2.68	3.6179 (19)	161
C8—H8*A*···O1^{vi}	0.99	2.47	3.336 (2)	146
C10—H10*B*···Cl1	0.99	2.79	3.4496 (19)	124
C10—H10*A*···Cl2	0.99	2.71	3.3566 (19)	123

Symmetry codes: (i) $x-1, y, z$; (ii) $-x+1, -y+1, -z$; (iii) $-x+2, -y+2, -z$; (iv) $-x+1, -y+2, -z$; (v) $x, y+1, z$; (vi) $-x+\frac{1}{2}, y+\frac{1}{2}, -z+\frac{1}{2}$

Data collection: *APEX2* (Bruker, 2007); cell refinement: *SAINT* (Bruker, 2007); data reduction: *SAINT*; program(s) used to solve structure: *SHELXS97* (Sheldrick, 2008); program(s) used to refine structure: *SHELXL97* (Sheldrick, 2008); molecular graphics: *X-SEED* (Barbour, 2001); software used to prepare material for publication: *SHELXL97* and *publCIF* (Westrip, 2010).

The authors thank University of Malaya for funding this study (FRGS grant No. FP004/2010B).

Supplementary data and figures for this paper are available from the IUCr electronic archives (Reference: IS2674).

References

Addison, A. W., Rao, T. N., Reedijk, J., Rijn, V. J. & Verschoor, G. C. (1984). *J. Chem. Soc. Dalton Trans.* pp. 1349–1356.
Barbour, L. J. (2001). *J. Supramol. Chem.* **1**, 189–191.
Bruker (2007). *APEX2* and *SAINT*. Bruker AXS Inc., Madison, Wisconsin, USA.
Ikmal Hisham, N., Suleiman Gwaram, N., Khaledi, H. & Mohd Ali, H. (2010). *Acta Cryst.* E**66**, m1471.
Saleh Salga, M., Khaledi, H., Mohd Ali, H. & Puteh, R. (2010). *Acta Cryst.* E**66**, m508.
Sheldrick, G. M. (1996). *SADABS*. University of Göttingen, Germany.
Sheldrick, G. M. (2008). *Acta Cryst.* A**64**, 112–122.
Wang, Q., Bi, C.-F., Wang, D.-Q. & Fan, Y.-H. (2009). *Acta Cryst.* E**65**, m439.
Westrip, S. P. (2010). *J. Appl. Cryst.* **43**, 920–925.

Acta Crystallographica Section E
Structure Reports Online
ISSN 1600-5368

{*N*,*N*-Dimethyl-*N*′-[1-(2-pyridyl)ethylidene]ethane-1,2-diamine-κ^3N,N',N''}bis(thiocyanato-κN)copper(II)

Nura Suleiman Gwaram, Hamid Khaledi* and Hapipah Mohd Ali

Department of Chemistry, University of Malaya, 50603 Kuala Lumpur, Malaysia
Correspondence e-mail: khaledi@siswa.um.edu.my

Received 20 May 2011; accepted 7 June 2011

Key indicators: single-crystal X-ray study; T = 100 K; mean σ(C–C) = 0.005 Å; R factor = 0.045; wR factor = 0.128; data-to-parameter ratio = 18.6.

The asymmetric unit of the title compound, $[Cu(NCS)_2(C_{11}H_{17}N_3)]$, consists of two crystallographically independent molecules. In each molecule, the Cu^{II} ion is five-coordinated in a distorted square-pyramidal geometry wherein the basal plane is defined by the *N*,*N*′,*N*″-tridentate Schiff base and one *N*-bound thiocyanate ligand. The second *N*-donor thiocyanate group, located at the apical site, completes the coordination environment. In the crystal, intermolecular C—H···S and C—H···N hydrogen bonds link adjacent molecules into infinite layers parallel to the *ac* plane. Intramolecular C—H···N interactions are also observed.

Related literature

For the structures of similar copper(II) isothiocyanate complexes, see: Xue *et al.* (2010); Yue *et al.* (2005). For the structure of the polymeric cadmium thiocyanate complex of the same Schiff base, see: Suleiman Gwaram *et al.* (2011). For a description of the geometry of complexes with five-coordinate metal atoms, see: Addison *et al.* (1984).

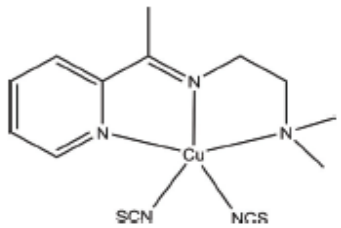

Experimental

Crystal data

$[Cu(NCS)_2(C_{11}H_{17}N_3)]$
M_r = 370.98
Triclinic, $P\overline{1}$
a = 10.9895 (4) Å
b = 11.2172 (4) Å
c = 13.7549 (5) Å
α = 81.222 (2)°
β = 87.121 (2)°
γ = 79.702 (2)°
V = 1648.27 (10) Å^3
Z = 4
Mo $K\alpha$ radiation
μ = 1.58 mm^{-1}
T = 100 K
0.44 × 0.31 × 0.13 mm

Data collection

Bruker APEXII CCD diffractometer
Absorption correction: multi-scan (*SADABS*; Sheldrick, 1996)
T_{min} = 0.544, T_{max} = 0.821
14403 measured reflections
7159 independent reflections
5182 reflections with $I > 2\sigma(I)$
R_{int} = 0.036

Refinement

$R[F^2 > 2\sigma(F^2)]$ = 0.045
$wR(F^2)$ = 0.128
S = 1.00
7159 reflections
385 parameters
H-atom parameters constrained
$\Delta\rho_{max}$ = 1.04 e Å^{-3}
$\Delta\rho_{min}$ = −0.81 e Å^{-3}

Table 1
Hydrogen-bond geometry (Å, °).

D—H···A	D—H	H···A	D···A	D—H···A
C4—H4···N5^{i}	0.95	2.58	3.429 (5)	149
C8—H8B···S4^{ii}	0.99	2.82	3.788 (4)	167
C9—H9A···S4^{iii}	0.99	2.84	3.735 (4)	150
C22—H22A···S2^{iii}	0.99	2.81	3.749 (4)	159
C11—H11B···N5	0.98	2.60	3.156 (5)	116
C21—H21A···S1	0.99	2.84	3.727 (4)	150
C21—H21B···S2	0.99	2.82	3.793 (4)	167
C24—H24B···N10	0.98	2.60	3.198 (5)	119

Symmetry codes: (i) $-x+1,-y+1,-z$; (ii) $x+1,y,z-1$; (iii) $-x+1,-y+1,-z+1$.

Data collection: *APEX2* (Bruker, 2007); cell refinement: *SAINT* (Bruker, 2007); data reduction: *SAINT*; program(s) used to solve structure: *SHELXS97* (Sheldrick, 2008); program(s) used to refine structure: *SHELXL97* (Sheldrick, 2008); molecular graphics: *X-SEED* (Barbour, 2001); software used to prepare material for publication: *SHELXL97* and *publCIF* (Westrip, 2010).

The authors thank the University of Malaya for funding this study (FRGS grant No. FP004/2010B).

Supplementary data and figures for this paper are available from the IUCr electronic archives (Reference: IS2717).

References

Addison, A. W., Rao, T. N., Reedijk, J., Rijn, V. J. & Verschoor, G. C. (1984). *J. Chem. Soc. Dalton Trans.* pp. 1349–1356.
Barbour, L. J. (2001). *J. Supramol. Chem.* **1**, 189–191.
Bruker (2007). *APEX2* and *SAINT*. Bruker AXS Inc., Madison, Wisconsin, USA.
Sheldrick, G. M. (1996). University of Göttingen, Germany.
Sheldrick, G. M. (2008). *Acta Cryst.* A**64**, 112–122.
Suleiman Gwaram, N., Khaledi, H. & Mohd Ali, H. (2011). *Acta Cryst.* E**67**, m480.
Westrip, S. P. (2010). *J. Appl. Cryst.* **43**, 920–925.
Xue, L.-W., Zhao, G.-Q., Han, Y.-J., Chen, L.-H. & Peng, Q.-L. (2010). *Acta Cryst.* E**66**, m1274.
Yue, G.-R., Xu, X.-J., Shi, Y.-Z. & Feng, L. (2005). *Acta Cryst.* E**61**, m693–m694.

Acta Crystallographica Section E
Structure Reports Online
ISSN 1600-5368

Dichlorido{*N*,*N*-dimethyl-*N*′-[1-(2-pyridyl)ethylidene]ethane-1,2-diamine-κ^3N,N',N''}manganese(II)

Nurul Azimah Ikmal Hisham, Nura Suleiman Gwaram, Hamid Khaledi* and Hapipah Mohd Ali

Department of Chemistry, University of Malaya, 50603 Kuala Lumpur, Malaysia
Correspondence e-mail: khaledi@siswa.um.edu.my

Received 10 January 2011; accepted 13 January 2011

Key indicators: single-crystal X-ray study; T = 100 K; mean σ(C–C) = 0.003 Å; R factor = 0.027; wR factor = 0.063; data-to-parameter ratio = 20.5.

The asymmetric unit of the title compound, $[MnCl_2(C_{11}H_{17}N_3)]$, contains two crystallographically independent molecules with slightly different geometries. In each molecule, the Mn^{II} ion is five coordinated by the *N*,*N*′,*N*″-tridentate Schiff base and two Cl atoms in a distorted square-pyramidal geometry. In the crystal, C—H···Cl hydrogen bonds link adjacent molecules into a three-dimensional network.

Related literature

For the structure of a $CuCl_2$ complex of the same Schiff base, see: Saleh Salga *et al.* (2010). For structures of similar Mn^{II} complexes, see: Gibson *et al.* (2003); Reardon *et al.* (2002).

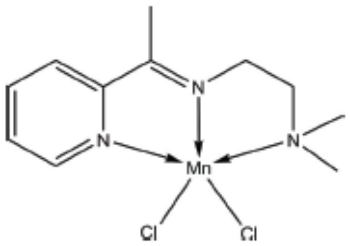

Experimental

Crystal data

$[MnCl_2(C_{11}H_{17}N_3)]$
M_r = 317.12
Monoclinic, $P2_1/c$
a = 17.6157 (8) Å
b = 9.9269 (4) Å
c = 20.4710 (8) Å
β = 124.592 (3)°
V = 2946.9 (2) Å^3
Z = 8
Mo $K\alpha$ radiation
μ = 1.24 mm^{-1}
T = 100 K
0.19 × 0.13 × 0.09 mm

Data collection

Bruker APEXII CCD diffractometer
Absorption correction: multi-scan (*SADABS*; Sheldrick, 1996)
T_{min} = 0.798, T_{max} = 0.897
26611 measured reflections
6426 independent reflections
5326 reflections with $I > 2\sigma(I)$
R_{int} = 0.043

Refinement

$R[F^2 > 2\sigma(F^2)]$ = 0.027
$wR(F^2)$ = 0.063
S = 1.02
6426 reflections
313 parameters
H-atom parameters constrained
$\Delta\rho_{max}$ = 0.32 e Å^{-3}
$\Delta\rho_{min}$ = −0.32 e Å^{-3}

Table 1
Hydrogen-bond geometry (Å, °).

D—H···A	D—H	H···A	D···A	D—H···A
C4—H4···Cl4^{i}	0.95	2.73	3.6815 (18)	155
C7—H7B···Cl3^{i}	0.98	2.75	3.7280 (18)	175
C14—H14···Cl4^{ii}	0.95	2.82	3.7048 (18)	156
C19—H19A···Cl3^{iii}	0.99	2.64	3.5839 (18)	159
C19—H19B···Cl4^{i}	0.99	2.73	3.6579 (19)	156
C22—H22B···Cl4^{i}	0.98	2.78	3.6693 (19)	151

Symmetry codes: (i) $-x+1, y+\frac{1}{2}, -z+\frac{3}{2}$; (ii) $-x+1, -y+1, -z+2$; (iii) $-x+1, y-\frac{1}{2}, -z+\frac{3}{2}$.

Data collection: *APEX2* (Bruker, 2007); cell refinement: *SAINT* (Bruker, 2007); data reduction: *SAINT*; program(s) used to solve structure: *SHELXS97* (Sheldrick, 2008); program(s) used to refine structure: *SHELXL97* (Sheldrick, 2008); molecular graphics: *X-SEED* (Barbour, 2001); software used to prepare material for publication: *SHELXL97* and *publCIF* (Westrip, 2010).

The authors thank the University of Malaya for funding this study (FRGS grant No. FP004/2010B).

Supplementary data and figures for this paper are available from the IUCr electronic archives (Reference: IS2666).

References

Barbour, L. J. (2001). *J. Supramol. Chem.* **1**, 189–191.
Bruker (2007). *APEX2* and *SAINT*. Bruker AXS Inc., Madison, Wisconsin, USA.
Gibson, V. C., McTavish, S., Redshaw, C., Solan, G. A., White, A. J. P. & Williams, D. J. (2003). *Dalton Trans.* pp. 221–226.
Reardon, D., Aharonian, G., Gambarotta, S. & Yap, G. P. A. (2002). *Organometallics*, **21**, 786–788.
Saleh Salga, M., Khaledi, H., Mohd Ali, H. & Puteh, R. (2010). *Acta Cryst.* E**66**, m508.
Sheldrick, G. M. (1996). *SADABS*. University of Göttingen, Germany.
Sheldrick, G. M. (2008). *Acta Cryst.* A**64**, 112–122.
Westrip, S. P. (2010). *J. Appl. Cryst.* **43**, 920–925.

Acta Crystallographica Section E
Structure Reports Online
ISSN 1600-5368

Aqua{*N*,*N*-dimethyl-*N*′-[1-(2-pyridyl)ethylidene]ethane-1,2-diamine-κ^3N,N',N''}bis(thiocyanato-κN)nickel(II)

Nura Suleiman Gwaram, Siti Munirah Saharin, Hamid Khaledi* and Hapipah Mohd Ali

Department of Chemistry, University of Malaya, 50603 Kuala Lumpur, Malaysia
Correspondence e-mail: khaledi@siswa.um.edu.my

Received 24 March 2011; accepted 28 March 2011

Key indicators: single-crystal X-ray study; T = 100 K; mean σ(C–C) = 0.005 Å; disorder in main residue; R factor = 0.031; wR factor = 0.070; data-to-parameter ratio = 15.8.

In the title compound, $[Ni(NCS)_2(C_{11}H_{17}N_3)(H_2O)]$, the Ni^{II} ion is six-coordinated by the *N*,*N*′,*N*″-tridentate Schiff base N atoms, two *cis*-positioned *N*-bound isothiocyanate groups and one water molecule. In the crystal, O—H···S hydrogen bonds link adjacent molecules into infinite layers parallel to the *ac* plane. The layers are further connected into a three-dimensional network *via* C—H···π interactions. The $-CH_2-N(CH_3)_2$ fragment is disordered over two sets of sites in a 0.556 (5):0.444 (5) ratio.

Related literature

For the structure of a similar mononuclear nickel(II) thiocyanate complex, see: Suleiman Gwaram *et al.* (2011). For dimeric nickel(II) thiocyanate complexes with similar Schiff bases, see: Diao (2007); Bhowmik *et al.* (2010).

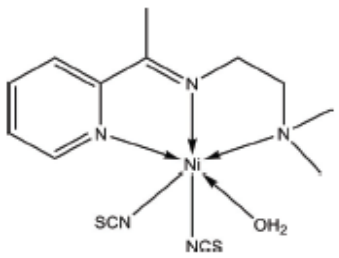

Experimental

Crystal data

$[Ni(NCS)_2(C_{11}H_{17}N_3)(H_2O)]$ M_r = 384.16
Monoclinic, *Cc*
a = 12.8404 (2) Å
b = 14.2623 (3) Å
c = 9.5868 (2) Å
β = 99.467 (1)°
V = 1731.75 (6) Å^3
Z = 4
Mo $K\alpha$ radiation
μ = 1.37 mm^{-1}
T = 100 K
0.22 × 0.19 × 0.11 mm

Data collection

Bruker APEXII CCD diffractometer
Absorption correction: multi-scan (*SADABS*; Sheldrick, 1996)
T_{min} = 0.753, T_{max} = 0.864
7792 measured reflections
3698 independent reflections
3451 reflections with $I > 2\sigma(I)$
R_{int} = 0.026

Refinement

$R[F^2 > 2\sigma(F^2)]$ = 0.031
$wR(F^2)$ = 0.070
S = 1.02
3698 reflections
234 parameters
16 restraints
H atoms treated by a mixture of independent and constrained refinement
$\Delta\rho_{max}$ = 0.58 e Å^{-3}
$\Delta\rho_{min}$ = −0.52 e Å^{-3}
Absolute structure: Flack (1983), 1798 Friedel pairs
Flack parameter: 0.020 (11)

Table 1
Hydrogen-bond geometry (Å, °).

*Cg*1 is the centroid of the N1,C1–C5 ring.

D—H···*A*	*D*—H	H···*A*	*D*···*A*	*D*—H···*A*
O1—H1*B*···S1^{i}	0.82 (2)	2.38 (2)	3.181 (3)	164 (4)
O1—H1*A*···S2^{ii}	0.84 (2)	2.35 (2)	3.190 (3)	178 (4)
C7—H7*C*···*Cg*1^{iii}	0.98	2.88	3.531 (3)	125

Symmetry codes: (i) $x-\frac{1}{2}, -y+\frac{1}{2}, z-\frac{1}{2}$; (ii) $x-\frac{1}{2}, -y+\frac{1}{2}, z+\frac{1}{2}$; (iii) $x, -y+2, z-\frac{1}{2}$.

Data collection: *APEX2* (Bruker, 2007); cell refinement: *SAINT* (Bruker, 2007); data reduction: *SAINT*; program(s) used to solve structure: *SHELXS97* (Sheldrick, 2008); program(s) used to refine structure: *SHELXL97* (Sheldrick, 2008); molecular graphics: *X-SEED* (Barbour, 2001); software used to prepare material for publication: *SHELXL97* and *publCIF* (Westrip, 2010).

The authors thank the University of Malaya for funding this study (FRGS grant No. FP004/2010B).

Supplementary data and figures for this paper are available from the IUCr electronic archives (Reference: GO2008).

References

Barbour, L. J. (2001). *J. Supramol. Chem.* **1**, 189–191.
Bhowmik, P., Chattopadhyay, S., Drew, M. G. B., Diaz, D. & Ghosh, A. (2010). *Polyhedron*, **29**, 2637–2642.
Bruker (2007). *APEX2* and *SAINT*. Bruker AXS Inc., Madison, Wisconsin, USA.
Diao, Y.-P. (2007). *Acta Cryst.* E**63**, m1453–m1454.
Flack, H. D. (1983). *Acta Cryst.* A**39**, 876–881.
Sheldrick, G. M. (1996). *SADABS*. University of Göttingen, Germany.
Sheldrick, G. M. (2008). *Acta Cryst.* A**64**, 112–122.
Suleiman Gwaram, N., Ikmal Hisham, N. A., Khaledi, H. & Mohd Ali, H. (2011). *Acta Cryst.* E**67**, m108.
Westrip, S. P. (2010). *J. Appl. Cryst.* **43**, 920–925.

Acta Crystallographica Section E
Structure Reports Online
ISSN 1600-5368

Dichlorido{*N*,*N*-dimethyl-*N*′-[1-(2-pyridyl)ethylidene]ethane-1,2-diamine-κ^3N,N',N''}zinc

Nura Suleiman Gwaram, Hamid Khaledi* and Hapipah Mohd Ali

Department of Chemistry, University of Malaya, 50603 Kuala Lumpur, Malaysia
Correspondence e-mail: khaledi@siswa.um.edu.my

Received 26 June 2011; accepted 29 June 2011

Key indicators: single-crystal X-ray study; T = 100 K; mean σ(C–C) = 0.003 Å; R factor = 0.021; wR factor = 0.052; data-to-parameter ratio = 20.1.

The asymmetric unit of the title compound, $[ZnCl_2(C_{11}H_{17}N_3)]$, contains two independent pentacoordinate Zn^{II} complex molecules. In each molecule, the metal atom is coordinated by an *N*,*N*′,*N*″-tridenate Schiff base and two Cl atoms in a distorted square-pyramidal geometry. The two molecules differ little in their geometry, but more in their intermolecular interactions. In the crystal, adjacent molecules are connected *via* C—H···Cl interactions into a three-dimensional supramolecular structure. The network is supplemented by π–π interactions formed between the aromatic rings of pairs of the symmetry-related molecules [centroid–centroid distances = 3.6255 (10) and 3.7073 (10) Å]. The crystal lattice contains void spaces with a size of 52 Å^3.

Related literature

For the isotypic Mn(II) complex, see: Ikmal Hisham *et al.* (2011). For the crystal structures of similar $ZnCl_2$ complexes, see: Gourbatsis *et al.* (1999); Sun (2005). For a description of the geometry of five-coordinate metal complexes, see: Addison *et al.* (1984).

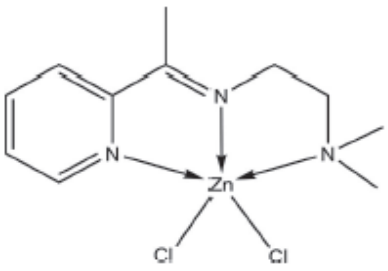

Experimental

Crystal data

$[ZnCl_2(C_{11}H_{17}N_3)]$
M_r = 327.55
Monoclinic, $P2_1/c$
a = 17.4849 (8) Å
b = 9.8161 (4) Å
c = 20.4264 (7) Å
β = 124.578 (3)°
V = 2886.6 (2) Å^3
Z = 8
Mo $K\alpha$ radiation
μ = 2.05 mm^{-1}
T = 100 K
0.27 × 0.23 × 0.15 mm

Data collection

Bruker APEXII CCD diffractometer
Absorption correction: multi-scan (*SADABS*; Sheldrick, 1996)
T_{min} = 0.607, T_{max} = 0.748
20477 measured reflections
6294 independent reflections
5510 reflections with $I > 2\sigma(I)$
R_{int} = 0.022

Refinement

$R[F^2 > 2\sigma(F^2)]$ = 0.021
$wR(F^2)$ = 0.052
S = 1.04
6294 reflections
313 parameters
H-atom parameters constrained
$\Delta\rho_{max}$ = 0.36 e Å^{-3}
$\Delta\rho_{min}$ = −0.28 e Å^{-3}

Table 1
Hydrogen-bond geometry (Å, °).

D—H···A	D—H	H···A	D···A	D—H···A
C3—H3···Cl2^{i}	0.95	2.79	3.6690 (17)	155
C8—H8A···Cl1^{ii}	0.99	2.63	3.5668 (16)	158
C8—H8B···Cl2^{iii}	0.99	2.73	3.6564 (16)	156
C11—H11A···Cl2^{iii}	0.98	2.77	3.6573 (17)	151
C15—H15···Cl2^{iv}	0.95	2.74	3.6347 (17)	157
C18—H18B···Cl1^{iv}	0.98	2.75	3.7227 (17)	175
C19—H19B···Cl4^{v}	0.99	2.82	3.8089 (16)	174

Symmetry codes: (i) $-x, -y+1, -z$; (ii) $-x, y-\frac{1}{2}, -z+\frac{1}{2}$; (iii) $-x, y+\frac{1}{2}, -z+\frac{1}{2}$; (iv) $-x+1, -y+1, -z+1$; (v) $-x+1, y-\frac{1}{2}, -z+\frac{1}{2}$.

Data collection: *APEX2* (Bruker, 2007); cell refinement: *SAINT* (Bruker, 2007); data reduction: *SAINT*; program(s) used to solve structure: *SHELXS97* (Sheldrick, 2008); program(s) used to refine structure: *SHELXL97* (Sheldrick, 2008); molecular graphics: *X-SEED* (Barbour, 2001); software used to prepare material for publication: *SHELXL97* and *publCIF* (Westrip, 2010).

The authors thank the University of Malaya for funding this study (UMRG grant No. RG024/09BIO).

Supplementary data and figures for this paper are available from the IUCr electronic archives (Reference: OM2444).

References

Addison, A. W., Rao, T. N., Reedijk, J., Rijn, V. J. & Verschoor, G. C. (1984). *J. Chem. Soc. Dalton Trans.* pp. 1349–1356.
Barbour, L. J. (2001). *J. Supramol. Chem.*, **1**, 189–191.
Bruker (2007). *APEX2* and *SAINT*. Bruker AXS Inc., Madison, Wisconsin, USA.
Gourbatsis, S., Perlepes, S. P., Butler, I. S. & Hadjiliadis, N. (1999). *Polyhedron*, **18**, 2369–2375.
Ikmal Hisham, N. A., Suleiman Gwaram, N., Khaledi, H. & Mohd Ali, H. (2011). *Acta Cryst.* E**67**, m229.
Sheldrick, G. M. (1996). *SADABS*. University of Göttingen, Germany.
Sheldrick, G. M. (2008). *Acta Cryst.* A**64**, 112–122.
Sun, Y.-X. (2005). *Acta Cryst.* E**61**, m373–m374.
Westrip, S. P. (2010). *J. Appl. Cryst.* **43**, 920–925.

Acta Crystallographica Section E
Structure Reports Online
ISSN 1600-5368

Chlorido(2-{1-[(2-morpholinoethyl)imino]ethyl}phenolato-κ^3N,N',O)copper(II)

Nurul Azimah Ikmal Hisham, Nura Suleiman Gwaram, Hamid Khaledi* and Hapipah Mohd Ali

Department of Chemistry, University of Malaya, 50603 Kuala Lumpur, Malaysia
Correspondence e-mail: khaledi@siswa.um.edu.my

Received 2 December 2010; accepted 6 December 2010

Key indicators: single-crystal X-ray study; T = 100 K; mean σ(C–C) = 0.006 Å; R factor = 0.043; wR factor = 0.096; data-to-parameter ratio = 13.7.

In the title compound, [$CuCl(C_{14}H_{19}N_2O_2)$], the Cu^{II} ion is four-coordinated by one deprotonated N,N',O-tridentate Schiff base and one chloride ion in a distorted square-planar geometry. In the crystal, adjacent molecules are linked *via* C—H···Cl and C—H···O interactions, forming infinite layers parallel to the (100) plane. The structure was determined from a non-merohedrally twined crystal [twin ratio 0.777 (3): 0.223 (3)].

Related literature

For the crystal structures of similar Cu^{II} complexes, see: Elias *et al.* (1982); Ikmal Hisham *et al.* (2009); Wang & You (2007).

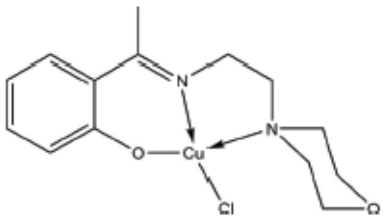

Experimental

Crystal data

$[CuCl(C_{14}H_{19}N_2O_2)]$
M_r = 346.30
Monoclinic, $P2_1/c$
a = 10.7122 (4) Å
b = 17.1657 (7) Å
c = 7.7638 (3) Å
β = 93.493 (3)°
V = 1424.97 (10) Å^3
Z = 4
Mo $K\alpha$ radiation
μ = 1.72 mm^{-1}
T = 100 K
0.31 × 0.22 × 0.07 mm

Data collection

Bruker APEXII CCD diffractometer
Absorption correction: multi-scan (*SADABS*; Sheldrick, 1996)
T_{min} = 0.617, T_{max} = 0.889
10834 measured reflections
2506 independent reflections
2313 reflections with $I > 2\sigma(I)$
R_{int} = 0.034

Refinement

$R[F^2 > 2\sigma(F^2)]$ = 0.043
$wR(F^2)$ = 0.096
S = 1.10
2506 reflections
183 parameters
H-atom parameters constrained
$\Delta\rho_{max}$ = 0.81 e Å^{-3}
$\Delta\rho_{min}$ = −1.15 e Å^{-3}

Table 1
Selected geometric parameters (Å, °).

Cu1—O1	1.877 (3)	Cu1—N2	2.050 (3)
Cu1—N1	1.932 (3)	Cu1—Cl1	2.2565 (11)
O1—Cu1—N1	92.21 (14)	O1—Cu1—Cl1	92.57 (10)
O1—Cu1—N2	162.15 (13)	N1—Cu1—Cl1	158.07 (11)
N1—Cu1—N2	87.14 (14)	N2—Cu1—Cl1	94.66 (10)

Table 2
Hydrogen-bond geometry (Å, °).

D—H···A	D—H	H···A	D···A	D—H···A
C14—H14A···Cl1	0.99	2.75	3.386 (4)	123
C11—H11B···Cl1	0.99	2.78	3.409 (4)	122
C14—H14B···Cl1^{i}	0.99	2.77	3.713 (4)	159
C10—H10B···O1^{ii}	0.99	2.52	3.465 (5)	160
C9—H9B···Cl1^{ii}	0.99	2.83	3.680 (5)	144

Symmetry codes: (i) $x, -y+\frac{1}{2}, z+\frac{1}{2}$ (ii) $-x+1, -y, -z+1$.

Data collection: *APEX2* (Bruker, 2007); cell refinement: *SAINT* (Bruker, 2007); data reduction: *SAINT*; program(s) used to solve structure: *SHELXS97* (Sheldrick, 2008); program(s) used to refine structure: *SHELXL97* (Sheldrick, 2008); molecular graphics: *X-SEED* (Barbour, 2001); software used to prepare material for publication: *SHELXL97* and *publCIF* (Westrip, 2010).

The authors thank University of Malaya for funding this study (UMRG grant RG024/09BIO).

Supplementary data and figures for this paper are available from the IUCr electronic archives (Reference: GK2329).

References

Barbour, L. J. (2001). *J. Supramol. Chem.* **1**, 189–191.
Bruker (2007). *APEX2* and *SAINT*. Bruker AXS Inc., Madison, Wisconsin, USA.
Elias, H., Hilms, E. & Paulus, H. (1982). *Z. Naturforsch. Teil B*, **37**, 1266–1273.
Ikmal Hisham, N. A., Mohd Ali, H. & Ng, S. W. (2009). *Acta Cryst.* E**65**, m870.
Sheldrick, G. M. (1996). *SADABS*. University of Göttingen, Germany.
Sheldrick, G. M. (2008). *Acta Cryst.* A**64**, 112–122.
Wang, J. & You, Z. (2007). *Acta Cryst.* E**63**, m1200–m1201.
Westrip, S. P. (2010). *J. Appl. Cryst.* **43**, 920–925.

Acta Crystallographica Section E
Structure Reports Online
ISSN 1600-5368

Hexachloridobis{μ_2-2-(piperazin-1-yl)-*N*-[1-(2-pyridyl)ethylidene]ethanamine}-trizinc dihydrate

Nura Suleiman Gwaram, Hamid Khaledi* and Hapipah Mohd Ali

Department of Chemistry, University of Malaya, 50603 Kuala Lumpur, Malaysia
Correspondence e-mail: khaledi@siswa.um.edu.my

Received 20 May 2011; accepted 8 July 2011

Key indicators: single-crystal X-ray study; T = 100 K; mean σ(C–C) = 0.007 Å; H-atom completeness 91%; disorder in solvent or counterion; R factor = 0.046; wR factor = 0.127; data-to-parameter ratio = 18.5.

In the trinuclear title compound, $[Zn_3Cl_6(C_{13}H_{20}N_4)_2]\cdot 2H_2O$, each terminal Zn^{II} atom is coordinated by an N_3 donor set from the Schiff base ligands and two Cl atoms in a distorted square-pyramidal geometry. The central Zn^{II} atom is tetrahedrally coordinated by two piperazine N atoms from two Schiff base ligands and two Cl atoms. The piperazine rings adopt chair conformations. In the crystal structure, adjacent complex molecules are linked into a three-dimensional network *via* N—H···O, C—H···Cl and C—H···O hydrogen bonds. The structure includes two water molecules, one of which is disordered over two positions with occupancies of 0.753 (15) and 0.247 (15).

Related literature

For related structures, see: Mukhopadhyay *et al.* (2003); Xu *et al.* (2008). For a description of the geometry of complexes with five-coordinate metal ions, see: Addison *et al.* (1984).

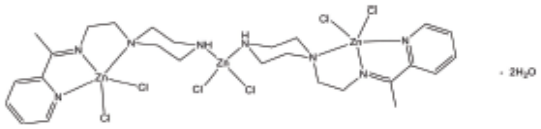

Experimental

Crystal data

$[Zn_3Cl_6(C_{13}H_{20}N_4)_2]\cdot 2H_2O$
M_r = 909.50
Triclinic, $P\overline{1}$
a = 7.6060 (3) Å
b = 14.8850 (5) Å
c = 16.7153 (5) Å
α = 72.570 (2)°
β = 86.834 (2)°
γ = 88.936 (2)°
V = 1802.78 (11) Å^3
Z = 2
Mo $K\alpha$ radiation
μ = 2.46 mm^{-1}
T = 100 K
0.21 × 0.12 × 0.09 mm

Data collection

Bruker APEXII CCD diffractometer
Absorption correction: multi-scan (*SADABS*; Sheldrick, 1996)
T_{min} = 0.626, T_{max} = 0.809
16465 measured reflections
7831 independent reflections
6241 reflections with $I > 2\sigma(I)$
R_{int} = 0.024

Refinement

$R[F^2 > 2\sigma(F^2)]$ = 0.046
$wR(F^2)$ = 0.127
S = 1.04
7831 reflections
424 parameters
8 restraints
H atoms treated by a mixture of independent and constrained refinement
$\Delta\rho_{max}$ = 0.92 e Å^{-3}
$\Delta\rho_{min}$ = −1.31 e Å^{-3}

Table 1
Hydrogen-bond geometry (Å, °).

D—H···A	D—H	H···A	D···A	D—H···A
N4—H4*N*···O2^{i}	0.91 (2)	2.05 (2)	2.953 (7)	170 (5)
N5—H5*N*···O1^{i}	0.92 (2)	2.41 (2)	3.310 (6)	169 (5)
C3—H3···Cl6^{ii}	0.95	2.78	3.563 (4)	140
C7—H7*C*···Cl6^{ii}	0.98	2.79	3.634 (5)	144
C14—H14*A*···Cl3^{iv}	0.99	2.78	3.493 (5)	130
C16—H16*B*···Cl6^{v}	0.99	2.81	3.509 (5)	128
C19—H19*A*···Cl4^{vi}	0.99	2.70	3.689 (6)	174
C11—H11*A*···Cl2	0.99	2.81	3.534 (5)	129
C13—H13*B*···Cl1	0.99	2.63	3.461 (5)	141
C17—H17*A*···Cl5	0.99	2.78	3.491 (5)	129
C14—H14*A*···O2^{i}	0.99	2.59	3.331 (9)	131
C15—H15*B*···O1^{i}	0.99	2.60	3.431 (7)	142

Symmetry codes: (i) $-x+1, -y+1, -z+1$; (ii) $x-1, y+1, z-1$; (iii) $-x+2, -y+1, -z+1$; (iv) $x+1, y, z$; (v) $x-1, y, z$; (vi) $-x+1, -y, -z+1$.

Data collection: *APEX2* (Bruker, 2007); cell refinement: *SAINT* (Bruker, 2007); data reduction: *SAINT*; program(s) used to solve structure: *SHELXS97* (Sheldrick, 2008); program(s) used to refine structure: *SHELXL97* (Sheldrick, 2008); molecular graphics: *X-SEED* (Barbour, 2001); software used to prepare material for publication: *SHELXL97* and *publCIF* (Westrip, 2010).

The authors thank the University of Malaya for funding this study (FRGS grant No. FP004/2010B).

Supplementary data and figures for this paper are available from the IUCr electronic archives (Reference: CI5190).

References

Addison, A. W., Rao, T. N., Reedijk, J., Rijn, V. J. & Verschoor, G. C. (1984). *J. Chem. Soc. Dalton Trans.* pp. 1349–1356.
Barbour, L. J. (2001). *J. Supramol. Chem.*, **1**, 189–191.
Bruker (2007). *APEX2* and *SAINT*. Bruker AXS Inc., Madison, Wisconsin, USA.
Mukhopadhyay, S., Mandal, D., Ghosh, D., Goldberg, I. & Chaudhury, M. (2003). *Inorg. Chem.* **42**, 8439–8445.
Sheldrick, G. M. (1996). *SADABS*. University of Göttingen, Germany.
Sheldrick, G. M. (2008). *Acta Cryst.* A**64**, 112–122.
Westrip, S. P. (2010). *J. Appl. Cryst.* **43**, 920–925.
Xu, R.-B., Xu, X.-Y., Wang, M.-Y., Wang, D.-Q., Yin, T., Xu, G.-X., Yang, X.-J., Lu, L.-D., Wang, X. & Lei, Y.-J. (2008). *J. Coord. Chem.* **61**, 3306–3313.

Acta Crystallographica Section E
Structure Reports Online
ISSN 1600-5368

Bis(μ-2-{1-[2-(dimethylamino)ethylimino]ethyl}phenolato)bis[bromidocopper(II)] monohydrate

Nura Suleiman Gwaram, Hamid Khaledi* and Hapipah Mohd Ali

Department of Chemistry, University of Malaya, 50603 Kuala Lumpur, Malaysia
Correspondence e-mail: khaledi@siswa.um.edu.my

Received 14 April 2011; accepted 7 June 2011

Key indicators: single-crystal X-ray study; T = 100 K; mean σ(C–C) = 0.004 Å; R factor = 0.025; wR factor = 0.060; data-to-parameter ratio = 18.2.

In the centrosymmetric dinuclear copper(II) title complex, $[Cu_2Br_2(C_{12}H_{17}N_2O)_2]\cdot H_2O$, each Cu^{II} ion is five coordinated in a square-pyramidal geometry by the *N*,*N*′,*O*-tridentate Schiff base, one Br atom and the bridging O atom of the centrosymmetrically related Schiff base. In the crystal, the water molecules link the complex molecules into infinite chains along the *b* axis *via* O—H···Br and C—H···O hydrogen bonds.

Related literature

For the structures of some similar doubly bridged copper(II) complexes, see: Li *et al.* (2000); Rigamonti *et al.* (2008); Suo (2008). For a description of the geometry of complexes with five-coordinate metal atoms, see: Addison *et al.* (1984).

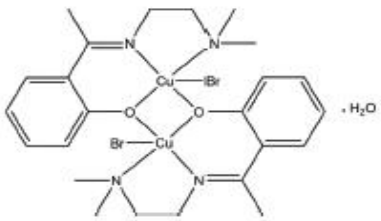

Experimental

Crystal data

$[Cu_2Br_2(C_{12}H_{17}N_2O)_2]\cdot H_2O$
M_r = 715.47
Monoclinic, $C2/c$
a = 20.754 (4) Å
b = 8.2492 (16) Å
c = 18.521 (4) Å
β = 119.528 (2)°
V = 2759.1 (9) Å^3
Z = 4
Mo $K\alpha$ radiation
μ = 4.47 mm^{-1}
T = 100 K
0.19 × 0.14 × 0.09 mm

Data collection

Bruker APEXII CCD diffractometer
Absorption correction: multi-scan (*SADABS*; Sheldrick, 1996)
T_{min} = 0.484, T_{max} = 0.689
10414 measured reflections
3007 independent reflections
2623 reflections with $I > 2\sigma(I)$
R_{int} = 0.042

Refinement

$R[F^2 > 2\sigma(F^2)]$ = 0.025
$wR(F^2)$ = 0.060
S = 1.05
3007 reflections
165 parameters
1 restraint
H atoms treated by a mixture of independent and constrained refinement
$\Delta\rho_{max}$ = 0.36 e Å^{-3}
$\Delta\rho_{min}$ = −0.51 e Å^{-3}

Table 1
Hydrogen-bond geometry (Å, °).

D—H···A	D—H	H···A	D···A	D—H···A
C11—H11*B*···O2^{i}	0.98	2.40	3.299 (3)	152
O2—H2*O*···Br1	0.83 (2)	2.62 (2)	3.4269 (14)	167 (3)

Symmetry code: (i) $x, y-1, z$.

Data collection: *APEX2* (Bruker, 2007); cell refinement: *SAINT* (Bruker, 2007); data reduction: *SAINT*; program(s) used to solve structure: *SHELXS97* (Sheldrick, 2008); program(s) used to refine structure: *SHELXL97* (Sheldrick, 2008); molecular graphics: *X-SEED* (Barbour, 2001; Atwood & Barbour, 2003); software used to prepare material for publication: *SHELXL97* and *publCIF* (Westrip, 2010).

The authors thank the University of Malaya for funding this study (FRGS grant No. FP004/2010B).

Supplementary data and figures for this paper are available from the IUCr electronic archives (Reference: EZ2243).

References

Addison, A. W., Rao, T. N., Reedijk, J., Rijn, V. J. & Verschoor, G. C. (1984). *J. Chem. Soc. Dalton Trans.* pp. 1349–1356.
Atwood, J. L. & Barbour, L. J. (2003). *Cryst. Growth Des.* **3**, 3–8.
Barbour, L. J. (2001). *J. Supramol. Chem.* **1**, 189–191.
Bruker (2007). *APEX2* and *SAINT*. Bruker AXS Inc., Madison, Wisconsin, USA.
Li, P., Solanki, N. K., Ehrenberg, H., Feeder, N., Davies, J. E., Rawson, J. M. & Halcrow, M. A. (2000). *J. Chem. Soc. Dalton Trans.* pp. 1559–1565.
Rigamonti, L., Cinti, A., Forni, A., Pasini, A. & Piovesana, O. (2008). *Eur. J. Inorg. Chem.* pp. 3633–3647.
Sheldrick, G. M. (1996). *SADABS*. University of Göttingen, Germany.
Sheldrick, G. M. (2008). *Acta Cryst.* A**64**, 112–122.
Suo, J. (2008). *Acta Cryst.* E**64**, m1046.
Westrip, S. P. (2010). *J. Appl. Cryst.* **43**, 920–925.